



HAL
open science

On the conflict between mate preference and adaptation: a mathematical approach

Ludovic Maisonneuve

► To cite this version:

Ludovic Maisonneuve. On the conflict between mate preference and adaptation: a mathematical approach. Populations and Evolution [q-bio.PE]. Sorbonne Université, 2022. English. NNT: . tel-04496270v1

HAL Id: tel-04496270

<https://hal.science/tel-04496270v1>

Submitted on 24 Mar 2023 (v1), last revised 8 Mar 2024 (v2)

HAL is a multi-disciplinary open access archive for the deposit and dissemination of scientific research documents, whether they are published or not. The documents may come from teaching and research institutions in France or abroad, or from public or private research centers.

L'archive ouverte pluridisciplinaire **HAL**, est destinée au dépôt et à la diffusion de documents scientifiques de niveau recherche, publiés ou non, émanant des établissements d'enseignement et de recherche français ou étrangers, des laboratoires publics ou privés.



MUSEUM NATIONAL D'HISTOIRE NATURELLE

Ecole Doctorale Sciences de la Nature et de l'Homme – ED 227

Année 2022

N°attribué par la bibliothèque

□□□□□□□□□□

THESE

Pour obtenir le grade de

DOCTEUR DU MUSEUM NATIONAL D'HISTOIRE NATURELLE

Spécialité : Biologie évolutive

Présentée et soutenue publiquement par

Ludovic Maisonneuve

Le 21 septembre 2022

On the conflict between mate preference and adaptation: a mathematical approach

Sous la direction de **Violaine Llaurens** et co-encadré par **Charline Smadi**

JURY :

Michael Kopp	Professeur, Aix Marseille Université	Rapporteur
Andrew Pomiankowski	Professeur, University College London	Rapporteur
Céline Devaux	Maîtresse de conférences, Université de Montpellier	Examinatrice
Richard Merrill	Professeur, Ludwig-Maximilians-Universität München	Examinateur
Violaine Llaurens	Directrice de Recherche CNRS	Directrice de thèse
Charline Smadi	Chargée de Recherche INRAE	Co-encadrante

On the conflict between mate preference and adaptation: a mathematical approach

Sexual preferences play a major role in the process of adaptation and speciation. While preferences for adaptive traits have been extensively studied, but various targets of preference are observed in natural populations, including attractions towards dissimilar or maladaptive traits. During my thesis, I focused on these peculiar forms of sexual preferences. I used mathematical modelling to identify the conditions for the evolution of mate preference targeting locally adaptive *vs.* maladaptive traits. I focused on the evolution of preference targeting warning traits, associated with defence against predators as a case study. Warning colorations reduce predation when they become widespread in a given environment: the local community of predators learns to associate the warning trait with defence and then avoid attacks on prey displaying them. Warning coloration are thus a relevant example of convergent evolution driven by local adaptation. Because these colorations can also be used as a cue during mate choice, they appear as a relevant trait to study the interactions between preference evolution and local selection on the preferred cue in sympatric species. First, I focused on the evolution of disassortative mating in polymorphic populations. I focused on the species *H. numata*, which display polymorphism in warning signals, controlled by a single supergene. Using numerical simulations, I studied how disassortative preferences, leading to preference on locally maladaptive phenotypes can emerge. I showed that the recessive deleterious mutations usually associated with supergenes promotes the evolution of disassortative preference (chapter 1). I also identified the genetic architecture of trait and preference allowing the evolution of disassortative preference. I then used a more general model focusing on polymorphic traits used as mating cues, to identify the conditions on dominance relationships between cues alleles and on their association with deleterious mutations allowing the evolution of disassortative mating (chapter 2). Second, I focused on the effect of reproductive interference between sympatric species on the evolution of preferences. Since local adaptation promotes trait similarity between sympatric species, preference for locally adapted traits may be impaired by reproductive interference. Using quantitative genetics models, I studied the conditions allowing the evolution of preference towards locally non-adapted traits limiting reproductive interference, and its consequences on local adaptation (chapter 3) and sexual dimorphism (chapter 4). Third, I investigated why and when mate preference targets traits involved in local adaptation rather than neutral traits that may diverge between sympatric species (chapter 5). Altogether, this thesis highlights the origin of sexual preferences and shows various conditions where disassortative or maladaptive preference can emerge. I conclude with a critical review highlighting the high prevalence of disassortative mate preference in nature and its peculiar role in the processes of adaptation and speciation.

Étude du conflit entre sélection sexuelle et adaptation: une approche mathématique

Les préférences sexuelles jouent un rôle majeur dans le processus d'adaptation et de spéciation. Alors que les préférences pour les traits adaptés ont été bien étudiées, des préférences envers divers traits sont observées dans les populations naturelles, y compris des préférences envers des traits dissemblables ou inadaptés. Au cours de ma thèse, j'ai étudié ces formes particulières de préférences sexuelles. J'ai utilisé des approches de modélisation mathématique afin d'identifier les conditions menant à l'évolution de préférences sexuelles basées sur des traits adaptés ou, par contraste, mal-adaptés. Je me suis concentré sur l'évolution de préférences ciblant des signaux d'avertissement, associés à des défenses contre les prédateurs. Un signal d'avertissement, réduit la prédation lorsqu'il devient localement répandu : la communauté locale de prédateurs apprend à associer le signal à une défense et évite alors d'attaquer les proies présentant ce signal. Les signaux d'avertissement sont donc un exemple pertinent d'évolution convergente promue par une adaptation locale. Comme ces signaux peuvent également être utilisés lors du choix du partenaire, ils apparaissent comme un trait pertinent pour étudier les interactions entre l'évolution des préférences et la sélection locale chez des espèces sympatriques. Tout d'abord, je me suis concentré sur l'évolution de l'hétérogamie dans les populations polymorphes, en particulier, sur l'espèce *H. numata*, qui présente un polymorphisme de patrons de coloration, contrôlé par un seul supergène. A l'aide de simulations numériques, j'ai étudié l'émergence de préférences hétérogames conduisant à une préférence pour des phénotypes localement inadaptés. J'ai ainsi montré que les mutations délétères récessives habituellement associées aux supergènes favorisent l'évolution de la préférence hétérogame (chapitre 1). J'ai également identifié les architectures génétiques des traits et des préférences permettant l'évolution de préférences hétérogames. J'ai ensuite utilisé un modèle plus général se concentrant sur les traits polymorphes utilisés dans les préférences sexuelles, pour identifier les conditions sur les relations de dominance entre les allèles de trait et sur leur association avec des mutations délétères permettant l'évolution de l'hétérogamie (chapitre 2). Deuxièmement, j'ai étudié l'effet de l'interférence reproductive entre espèces sympatriques sur l'évolution des préférences. Puisque l'adaptation locale favorise la ressemblance des traits entre les espèces sympatriques, la préférence pour les traits adaptés localement peut être altérée par l'interférence reproductive. En utilisant des modèles de génétique quantitative, j'ai étudié les conditions permettant l'évolution de préférences envers des traits localement non-adaptés limitant l'interférence reproductive, et ses conséquences sur l'adaptation locale (chapitre 3) et le dimorphisme sexuel (chapitre 4). Enfin, j'ai étudié pourquoi et quand les préférences sexuelles ciblent des traits impliqués dans l'adaptation locale plutôt que des traits neutres qui peuvent diverger entre espèces sympatriques (chapitre 5). Dans l'ensemble, cette thèse met en lumière l'origine des préférences sexuelles et montre les différentes conditions dans lesquelles des préférences hétérogames ou des préférences envers des traits localement mal-adaptés peuvent émerger. Je conclus par une revue critique soulignant la prévalence des préférences hétérogames dans les populations naturelles et de leurs rôles dans les processus d'adaptation et de spéciation.

Acknowledgments

Aucune réalisation humaine n'est certainement une réalisation individuelle mais presque toujours une réalisation collective. Il est donc nécessaire de remercier ceux qui ont contribué plus ou moins directement à la réalisation de cette thèse, que ce soit par leur aide scientifique, ou simplement pour avoir partagé des bons moments qui rendent la vie plus belle.

J'aimerais commencer par remercier Violaine et Charline qui m'ont supervisé pendant ces trois années de thèse. J'ai beaucoup apprécié votre encadrement, vous avez toujours été très présentes pour moi, tout en me laissant de la liberté sur mes projets. Entrer dans le champ de la biologie évolutive n'est pas forcément facile quand on vient des mathématiques. Grâce à toi Violaine, ces trois années de thèse ont été riches d'enseignements. Merci pour tout ce que tu m'as transmis. J'ai une grande confiance en toi et continuerai à solliciter et écouter tes précieux conseils. Charline, ta rigueur scientifique m'a poussé à être toujours plus exigeant et précis. Il n'y a rien de plus agréable que de travailler avec quelqu'un d'aussi dynamique et motivé. Merci à vous deux de m'avoir aiguillé pendant ces trois années.

I will switch to english for this paragraph to deeply thank Céline Devaux, Michael Kopp, Richard Merrill and Andrew Pomiankowski. Your scientific work has been a source of inspiration for me and I am very happy that you accepted to evaluate this PhD thesis.

Je souhaite aussi remercier les membres du comité de thèse, Tom Van Dooren, Marianne Elias, Manuela López-Villavicencio, Samuel Pavard qui ont pris le temps de m'écouter et de me conseiller. Je tiens à remercier plus particulièrement Sylvain Billiard qui m'a poussé à remettre mon travail en question.

Je souhaite remercier les chercheurs avec qui j'ai eu la chance de discuter, et qui m'ont aidé à clarifier mes idées. Je pense notamment à Marianne Elias, Charline Pinna, Denis Roze, Emmanuelle Porcher, Mathieu Joron, Pierre Lacoste. Plus particulièrement je te remercie Roman : il aura fallu qu'on se donne du courage pour décrypter ces modèles et concepts de génétique des populations. J'aimerais également te remercier Maxime pour m'avoir aidé à m'orienter vers le domaine de l'évolution culturelle, j'espère qu'on aura l'occasion de collaborer à nouveau ensemble. Enfin je tiens à te remercier Thomas pour ton lobbying pro-Lausanne, j'ai hâte qu'on se retrouve à l'UNIL.

Je souhaite également remercier les membres du labo que j'ai côtoyé au cours de ces trois années de thèse. Merci Charline, sûrement celle en qui j'ai le plus confiance, pour toutes ces discussions aussi bien personnelles que scientifiques. Merci Camille, c'était une joie de partager nos débuts en slackline et d'assister à toutes tes cascades. Merci Ariane, la flamme ardente, pour ta bonne humeur, et bien sûr, pour tes conseils capillaires. Merci Léa et ton humour de papa. Merci Julien pour avoir augmenté le nombre de stéphanois dans ma vie. Merci Marianne, véritable puit de science, pour toutes ces discussions stimulantes et ta bienveillance. Je tiens également à remercier Vio, Agathe, Pierre, Joséphine, Erika, Ombeline, Sylvain, Vincent et Arthur.

J'aimerais également remercier ceux avec qui j'ai eu des amitiés fortes. Ces amitiés ont été importantes pour moi et ont contribué à me développer. Merci à toi Dorian, avec qui j'ai parcouru tellement de chemin. Pour reprendre les mots de Bernard Stiegler qui t'es cher, nous nous sommes co-individués. Merci à toi Amaury, cette complicité que nous avons créée à Montceau-les-Mines m'est précieuse. Merci à toi Nilo pour ta gentillesse, c'est toujours un plaisir de discuter avec quelqu'un d'aussi cultivé et pointu.

Durant ces trois années de thèse, j'aurais passé beaucoup de temps en équilibre sur une ligne, entre deux arbres ou entre deux falaises, et à broyer des prises de résine dans des salles d'escalade. Ces moments ont été importants pour moi car ils m'ont permis de décrocher de ma thèse et de faire de belles rencontres. J'aimerais remercier ceux avec qui j'ai partagé ces moments. Je pense notamment à Dorian, Donald l'anarchiste collectiviste (ou communiste libertaire je ne sais pas trop), Tommy, Laure, Arnaud, Solène, Tanguy, Manu, Tom et Thibault.

Merci aux potes du basket X2015. Je suis heureux d'être toujours en contact avec vous. Je pense notamment à Seize, Guillaume, Zhao, Marc, Charly, Chouchou et Romain. Et merci particulièrement à toi Stan, "mon pote de droite", pour ta passion de la politique. J'ai toujours apprécié ton ouverture d'esprit et ta grande honnêteté.

Durant ces trois ans il y a eu de belles rencontres. Je pense notamment à toi Laurent, que j'ai eu la chance de rencontrer durant mon monitorat. Tu es certainement une des personnes les plus curieuses et profondes que je connaisse. Notre amitié compte beaucoup pour moi. Merci pour tous ces moments de discussion, qui ont souvent dérivé en moment d'introspection.

Je souhaite également remercier Raphaël Guilhot et Pierre Pageault, professeurs de mathématiques en CPGE au lycée Etienne Mimard. Vous m'avez appris à aimer les mathématiques et ce que vous m'avez transmis m'est aujourd'hui très précieux.

Merci Anita et Patrice pour votre accueil toujours chaleureux.

Une phrase courte pour toi Clara, qui a pourtant une place immense dans ma vie.
Merci pour ta douceur.

Je tiens également à remercier ma famille qui m'a toujours soutenu. En particulier, je tiens à te remercier Maman, pour m'avoir toujours laissé la liberté de devenir ce que je suis.

Table of Contents

Introduction	3
I When adaptation suppresses recombination: mate preference limiting the expression of genetic deleterious mutations	33
1 Genetic architecture of disassortative mating	35
2 Genetic architecture of mating trait	83
II When adaptation promotes species similarity: mate preference limiting reproductive interference	127
3 When does reproductive interference limits mimicry ?	129
4 Can reproductive interference explain female-limited mimicry ?	209
III Why and when are adaptive traits used in mate choice ?	291
5 Evolution of mate preference towards multiple traits in sympatric species	293
Discussion	335
Bibliography	354
Appendix I: Evolution of conspicuousness in warning traits	391

Introduction

"I feel the bigness of it, but when I speak, I babble like a little child. It is a great task to transmute feeling and sensation into speech, written or spoken, that will, in turn, in him who reads or listens, transmute itself back into the selfsame feeling and sensation. It is a lordly task. See, I bury my face in the grass, and the breath I draw in through my nostrils sets me quivering with a thousand thoughts and fancies."

Jack London
Martin Eden

Making sense of the world

Everybody carefully observing its environment can see how strange and fascinating the world is. For instance, when looking at rock formations called fairy chimney (Figure 1 (a)), I have the strange feeling that they do not belong to their proper place. In everyday life, we often have such feelings. A lot of people can observe ants for a long time, fascinating by their individual and collective behaviors (Figure 1 (b)). The animals with which we interact the most, *i.e.* the other humans, are perhaps the most fascinating for us, because we have trouble to understand the behaviors of our conspecific (Figure 1 (c)). This strangeness is certainly the spice of the world and is calling for explanations. Among human efforts to make sense of the world, there are sciences. We can perfectly explain the formation of fairy chimney by past glacial melting, the water flow resulting and the erosion. But this explanation does not make the fairy chimney less strange because it offers us new sources of strangeness. Indeed, the size of fairy chimney becomes more fascinating with the explanation, because it means that erosion took away a huge mass of soil. It is amazing that such a slow process, that we can not even perceive, can have such a big impact on landscape on a huge time scale.

The world that we try to make sense of is full of living organisms. We live in very close interactions with numerous conspecifics. Our food comes from other organisms and trillion of micro-organisms live within our digestive system and allow us to digest. Our society origins in the domestication of plants, animals and micro-organisms. Viruses parasite us and live among us. Thus, we need to understand the living matter, in order to understand our world. Nowadays, the best understanding of the living matter comes from evolutionary theory. The theory of evolution states that, like fairy chimney, the living organisms that we observe nowadays result from a series of slow processes taking place on a large timescale. These processes are slow at the scale of our lifetime, and most of the time we do not perceive it. The characteristics of living organisms such as their shape, color, behavior can be understood in the light of evolution, *i.e.* using the concepts of evolution to explain how these characteristics may have appeared and persisted.

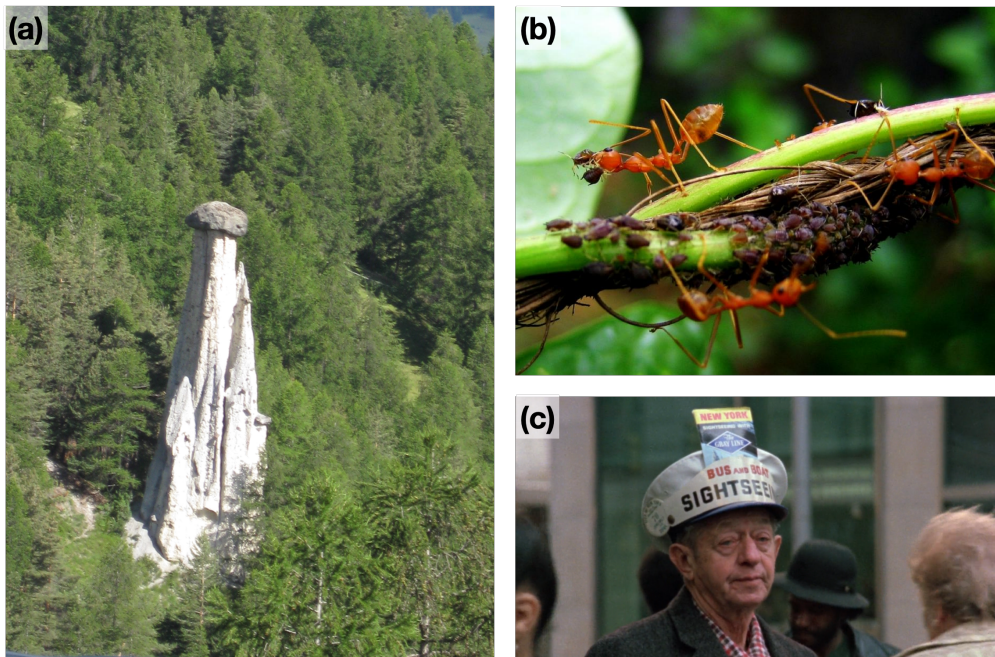


Fig. 1: (a) Fairy chimney near Molines-en-Queyras. ©Meneerke bloem (b) Ants and Aphids. ©Vibha Raj (c) Worker in New York from Reggio, *Koyaanisqatsi*

As we will see below, the main concepts of evolution are simple but they can explain the amazing diversity and complexity observed within living organisms. However, even if we understand very well the main concepts of evolution, understanding evolutionary mechanisms is still challenging.

Understanding evolutionary mechanisms through equations

This thesis aims at participating to a global effort to explain the diversity of living organisms in the light of evolutionary mechanisms. However, this thesis does not report data from any field observations or experiments. How can we shed lights on the mechanisms of evolution without closely looking at any living organisms? This work presented here relies on mathematical equations like this one:

$$\Delta\bar{\phi} = \beta_{\phi^0, \phi} \text{Var}(\phi) \frac{1}{w} \beta_{w, \phi}. \quad (1)$$

However, the link between Equation (1) and living organisms is, at least for the moment, not straightforward. Equation (1) describes the evolution of a discrete ¹ or a continuous value ϕ of a quantitative trait T in a population. This equation can have numerous applications. To illustrate, let us say that T is the beak width of a bird. In a population, of such birds with overlapping generations, Equation (1) describes the change of the mean trait value during a single generation $\Delta\bar{\phi}$. The different analytical expressions composing Equation (1) describe the main concepts of evolution:

1. *Selection and drift* ($\frac{1}{\bar{w}}\beta_{w,\phi}$): $\beta_{w,\phi}$ is the statistical correlation within the population between the bird fitness w and the trait value ϕ , and \bar{w} is the mean fitness observed in the bird population. In natural population, the fitness of an individual depends on numerous traits but also on randomly occurring events. For example, by chance, an individual may escape or not a predator. Therefore assuming that the fitness of each individual (w) is a stochastic variable certainly fits closer the reality. Many models neglect this stochastic effect and assume that the fitness of an individual only depends on his different traits.

The trait values changes ($\Delta\bar{\phi} \neq 0$) if there is a correlation between the fitness and the trait value ($\beta_{w,\phi} \neq 0$). Selection is defined in a broad sense that includes stochastic effect, *i.e.* the variability in individual fitness within the population, is a necessary condition for evolution. Selection can arise when a trait, variable in the population, impacts the fitness. For example, after an environmental change, the bird population might have access only to small resources, individuals with small beak would be better at exploiting such resources, resulting in a higher fitness than large beak individuals. This selection drives the evolution toward small values of beak width ($\frac{1}{\bar{w}}\beta_{w,\phi} < 0$). However even if a trait is unrelated to the survival and to the reproduction, there may be by chance a correlation between the trait value and the fitness

¹For example let us assume a population with red and blue individuals, let $\phi = 1$ (resp. $\phi = 0$) for blue (resp. $\phi = 1$) individuals. Equation (1) then tracks the evolution of the proportion of blue individuals in the population $\bar{\phi}$. Similarly Equation (1) can be used to track the evolution of genotypic frequencies in a population.

leading to the evolution of that trait. Another mechanisms can lead to the evolution of a trait unrelated to the survival and to the reproduction. We assume another trait T' , plumage coloration, which trait value ϕ' is unrelated to the survival and to the reproduction. We assume a statistic correlation within the population between traits value ϕ and ϕ' . For example we assume that individuals with small beak tend to have a blue coloration. In this case there is a correlation between the fitness and the plumage coloration ($\beta_{w,\phi'} \neq 0$) because blue individuals, which have often a small beak, access to more ressources. This leads to the evolution of plumage coloration even if this trait does not impact the survival of individuals. In this case we say that trait T_2 is under indirect selection.

2. *Variability* ($\text{Var}(\phi)$): $\text{Var}(\phi)$ is the variance of the trait value in the population. The trait value evolves ($\Delta\bar{\phi} \neq 0$) only if the trait value is variable ($\text{Var}(\phi) > 0$). Selection generally erodes variability, therefore mechanisms generating trait variability, such as mutations for traits with genetic basis, are essential in the evolutionary process.
3. *Heritability* ($\beta_{\phi^0,\phi}$): $\beta_{\phi^0,\phi}$ is the statistical correlation, between trait values observed in the offsprings (ϕ^0) and in their parents (ϕ). This correlation is usually interpreted as the heritability of the trait (Rice, 2004). For example, a trait can be heritable *via* the transmission of genetic basis of the trait during reproduction. Note that traits can be heritable without genetic basis: for exemple, mother tongue in human is a trait highly heritable.

Equation (1) describes the mechanism leading to phenotypic evolution, with the few main concepts (selection, variability, heritability) of evolution. However, we can also verbally explain how evolution works. And it would certainly be better because most people are more confortable with verbal arguments than equations. Then, we may ask what is the point of using equations to describe evolutionary processes ? Why use mathematics to say what we can say with words ?

The main reason is that verbal arguments can have logical flaws. The living matter is composed of numerous interactions, and then the study of life often leads

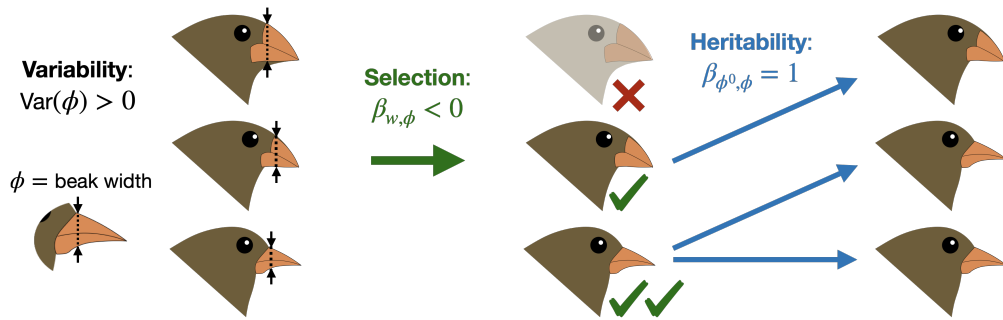


Fig. 2: **Illustration of principles of evolution: selection, variability and heritability.** These principles are linked with mathematical object appearing in Equation (1).

to countless complex verbal arguments. Because of this complexity, we may miss logical flaws. Using mathematics, we translate our argumentation in another language. This language has been rigorously built and defines logic rules. A mathematical model may act as proof-of-concepts, allowing us to test the logical validity of our argumentation (Servedio *et al.*, 2014). Similarly to empiricists making protocols and collecting data to test a hypothesis, theoreticians build and analyse mathematical models, to test the logical soundness of an argument. In a certain sense, Equation (1) is a proof-of-concepts that the main concepts of evolution lead to phenotypic evolution. Indeed, Equation (1) is a simplified version of the Price's theorem (Price, 1970, 1972). Price did not define this equation, this equation results from events defined at the population level (fitness, reproduction). Then, this equation shows that selection acting on a variable and heritable trait leads to the evolution of this trait, within a population.

Proof-of-concept models may sometimes give the feeling to state the obvious. For that reason, van Veelen *et al.* (2012) accuse Equation (1) to be useless, comparing Price's equation to the ironic words of Johan Crujff, a famous Dutch football player, saying that to win a game you need to score more goal that your opponent. During this thesis, I personally sometimes had the feeling of stating the obvious. Even if models have obviously increased our understanding of evolutionary mechanisms (see examples in (Servedio *et al.*, 2014; Otto & Rosales, 2020)), I think there is some truth in models criticisms of stating the obvious. Theoreticians often

want to show that an evolutionary mechanism is logically sound and can explain a pattern observed in a natural population. As theoreticians master everything in their model, they easily create the conditions to observe evolutionary mechanisms leading to an observed pattern. However, I do think this approach has merit: by creating the condition under which a mechanism appears, theoreticians clarify the important conditions for its apparition. This may be particularly useful to understand mechanisms in complex biological systems, where a lot of parameters can potentially influence the outcome. Mathematical modelling allows to identify which parameters importantly influence evolutionary mechanisms, as well as how these parameters influence it.

We can increase our understanding of evolutionary mechanisms by analysing equations. The main reason being that we can work and manipulate the concepts of evolutionary biology through equations. Concepts are very important as they provide a lens to see the world and to understand it better. How could we make sense of evolutionary mechanisms without the concepts of gene, of selection, of individual? By modelling evolutionary mechanisms, we rigorously clarify how key concepts interact and lead to the evolutionary phenomena. For instance Equation (1) clarifies how selection, variability and heritability lead to phenotypic evolution. Because equations perfectly define interactions between objects, I think than mathematics provides, in a sense, clearer explanations of evolutionary mechanisms than verbal arguments. For instance, when I was in a scientific event mixing mathematicians and biologists, I heard a mathematician saying that in order to understand a biological process, she needed to see the equations modelling this process. For someone comfortable with mathematics, it can be a tool to understand biological systems. Studies based on university students found a correlation between skills in statistic and probability and the understanding of evolution (Fiedler *et al.*, 2019; Harms & Fiedler, 2019). That does not mean that we need mathematics to master the concepts of evolution or to study evolutionary biology. That means that mathematics are one amazing tool, among others, to increase our knowledge about evolutionary mechanisms. The famous quote of John Van Neumann may be particularly true applied to biology:

If people do not believe that mathematics is simple, it is only because they do not realize how complicated life is.

Mate preferences are key in evolutionary mechanisms

Evolutionary processes have produced a huge diversity of traits observed among living organisms. However, the evolution of some traits may seem paradoxal, or at least at the first glance. For example, in numerous species, individuals (often males) display extravagant colorful ornaments (see examples in Figure 3). Such ornaments often generate handicap for individuals: in birds, the extravagant tails can impair flight (Balmford *et al.*, 1993), and colorful ornaments generally attract predators and parasites (Zuk & Kolluru, 1998). Such handicapping ornaments should thus have been counter-selected by natural selection. How can we explain their persistence? Darwin suggested that these ornaments might confer an advantage during reproduction because they are preferred by females (Darwin, 1871). Individuals of the opposite sex may mate preferentially with individuals displaying ornaments, where such choice increases their reproductive success. Such difference in reproductive success generates sexual selection acting on traits targeted by preference (Andersson, 1994). Beyond the case of extravagant ornaments, mate preference is central in the theory of evolution. For instance, one of the biggest challenges in evolutionary biology is to identify which process may have produced so many species. Mate preference may have played a key role in the formation of species. Mate preference may generate sexual isolation between two populations, limiting genetic exchange and then promoting sympatric speciation (Bolnick & Fitzpatrick, 2007).

Invoking the role of mate preference in evolutionary processes is often straightforward, however explaining the evolution of such mate preference is challenging. For example, the evolution of preference for handicap ornaments seems paradoxal, as choosers prefer to mate with maladaptive mate. In this section, I detail the evolutionary forces acting on mate preference.

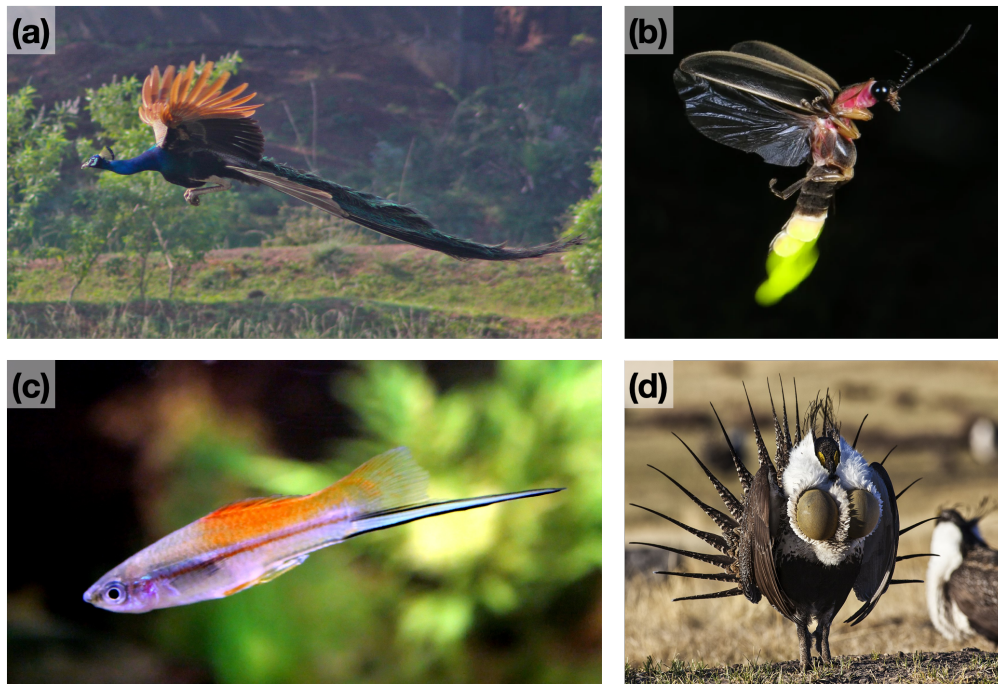


Fig. 3: (a) Peacock with elongated tail flying on rice field, at Karaikudi, Tamilnadu. ©Haribabu Pasupathy (b) Eastern Firefly with a light organ on its abdomen. ©NaturalWorldLover (c) Green swordtail with a elongated caudal fin. ©Usien (d) Greater sage-grouse with its gular sacs inflated. ©Bureau of Land Management

Costs limiting the evolution of mate preference

The evolution of mate preference seems surprising, because many costs have been identified to limit it. These costs generate a direct selection against the evolution of mate preference (see Pomiankowski (1987), for a review of these costs). Several theoretical studies have highlighted the significant role of these costs in the evolution of mate preference (Pomiankowski, 1987; Kopp & Hermisson, 2008; Schneider & Bürger, 2006). For example, mate preference can increase the investment in mate searching, because one needs to sample several mates to find a suitable one. This increased sampling effort can be costly in time (Kruijt & Hogan, 1967), in energy (as empirically estimated in antilopes, Byers *et al.* (2005)) and may increase predation risk, for instance in patrolling animals (Hughes *et al.*, 2012). In addition, the evolution of mate preferences can involve supplementary costs associated

with the rebuttal. In the fly species *Musca domestica*, males jump on the back of females to initiate mating and choosy females have to kick unpreferred males to avoid mating (Sacca, 1964). These costs increase when the preferred males are rare in the population, because it increases mate-searching efforts and the number of males to rebut. We then qualify such cost as relative, because it depends on the distribution of the preferred and non-preferred mating traits in males (Otto *et al.*, 2008). In some plant species the individuals expressing same S-alleles do not mate. Such self-incompatibility limits inbreeding depression, as well as the expression of genetic deleterious mutations associated with S-alleles in the offspring (Llaurens *et al.*, 2009; Stift *et al.*, 2013). The incompatibility system is frequently lost in the expansion range margin of self-incompatible species (Encinas-Viso *et al.*, 2020), where the low diversity of S-alleles reduces the availability of preferred mate (Byers & Meagher, 1992; Vekemans *et al.*, 1998). This highlights the effect of the distribution of traits in the population on relative costs and consequently effect on the evolution of preference. By contrast, fixed costs do not depend on this distribution. The mechanism underlying mate preference may require specialized morphological, physiological and cognitive changes (see Rosenthal (2017) for a review), that may induce specific metabolic costs. For example, in the self-incompatibility system in the genus *Brassica*, mate choice involves a specialized receptor-ligand association (Hiscock & McInnis, 2003), so that the evolution of self-incompatibility is associated with metabolic costs implied by the production of the specific proteins.

Mate preference enhances offspring fitness

Despite the numerous associated costs, mate choice evolved multiple times (see Rosenthal (2017)) suggesting that some positive effects should increase the fitness of choosy individuals. Selection acting on offspring survival indirectly affects the evolution of preference, where preference is promoted when it enhances offspring fitness. Such offspring advantage increases the spread of heritable preferences in the population (Rosenthal, 2017). Empirical studies confirm that preference generally increases offspring fitness (Byers & Waits, 2006; Drickamer *et al.*, 2000)

suggesting that this indirect selection promotes the evolution of preference. Theoretical results suggest that preference based on trait under natural selection often evolves, because it increases the production of adapted offspring (Thibert-Plante & Gavrillets, 2013). In line with this result, a meta-analyse reveals a positive correlation between male survival and the traits targeted by preference (Jennions *et al.*, 2001). Moreover, a growing number of empirical evidence showing that female choice does improve offspring fitness is reported (Welch *et al.*, 1998; Sheldon *et al.*, 1997; Byers & Waits, 2006; Petrie, 1994; Drickamer *et al.*, 2000).

Usually theoretical studies based on population genetic investigate the evolution of preference mediated by indirect selection on offspring, in the light of genetic associations between trait and preference (*e.g.* (Pomiankowski & Iwasa, 1993; Otto *et al.*, 2008; de Cara *et al.*, 2008)). Preference indeed generates association between the loci controlling preference and targeted traits within the offspring (Greenfield *et al.*, 2014): the allele controlling the chosen trait and alleles encoding for the preference towards this specific trait are frequently encountered within the same offspring. Such associations between traits and preferences alleles have been confirmed by subsequent theoretical studies (Kirkpatrick, 1982; Lande, 1981). As a consequence, selection on mating traits acts as indirect selection on preferences. Natural selection acting on mating traits, by generating indirect selection on preferences, has thus a strong indirect effect on their evolution (Fisher, 1930). The effect of natural selection on mating traits on the evolution of mate preferences, first identified by Fisher, has now been confirmed in many theoretical studies (Heisler, 1984, 1985; Kirkpatrick, 1982; O'Donald, 1980a). The indirect selection on offspring may be a major factor shaping the evolution of mate choice.

Sexual selection impacts the evolution of mate preference

Once mate preferences are established in the population, they generate sexual selection on the traits exhibited by individuals during courtship. This sexual selection, acting directly on the mating trait, also indirectly impacts the evolution of preference via the genetic association generated by mating preference. For

example, once a preference is common in a population, the advantage of having this preference may increase because it leads to the production of sexy offspring (Weatherhead & Robertson, 1979). Such sexual selection feedback may drive the evolution of extravagant traits in males, following a fisherian runaway process (Fisher, 1930; Lande, 1981; Kirkpatrick, 1982) (Box 1). Moreover, sexual selection also influences the evolution of mate preference, because it impacts the distribution of mating traits in males, and thus the relative cost of preference. The evolution of mate preferences thus involves complex evolutionary processes, whereby preferences co-evolve with the traits displayed by the chosen individuals. This co-evolution has been observed in natural populations (on the calling song in Hawaiian crickets Grace & Shaw (2011), on the sperm morphology in diving beetles Higginson *et al.* (2012)) and in experimental studies (on the coloration in guppies Brooks & Couldridge (1999), on the sperm morphology in fruit flies Miller & Pitnick (2002)), underpinning the importance of sexual selection feedbacks on the evolution of mate preferences. These sexual selection feedbacks are complex and can lead to surprising results, calling for mathematical framework to identify them.

Box 1: A model of fisherian runaway

To illustrate the importance of genetic correlation between trait and preference on the evolution of mate choice, we summarize the model of R. Lande describing the fisherian runaway (Lande, 1981).

Presentation of the model Let a trait t expressed in males and a preference for this trait p expressed in females take quantitative values. We note \bar{t} and \bar{p} the mean trait and preference values in the population. The change of the mean trait and preference values across one generation follows the equation:

$$\begin{pmatrix} \Delta \bar{t} \\ \Delta \bar{p} \end{pmatrix} = \frac{1}{2} \begin{pmatrix} V_t & C_{tp} \\ C_{tp} & V_p \end{pmatrix} \begin{pmatrix} \beta_t^{ns} + \beta_t^{ss} \\ 0 \end{pmatrix},$$

where V_t and V_p are the genetic variances of trait and preference respectively and C_{tp} is the genetic covariance between trait and preference. β_t^{ns} and β_t^{ss} are selection coefficients on males due to natural and sexual selection respectively.

Dynamics of the model There are an infinite number of equilibrium points given by $\beta_t^{ns} + \beta_t^{ss} = 0$ (see blue line in Figure 4(a) and (b)). The model dynamic depends on the C_{tp}/V_t ratio. When C_{tp}/V_t is low, the mean trait and preference converge to the equilibrium line (Figure 4(a)). The higher C_{tp} , the more extreme are the equilibrium mean trait and preference values. By contrast, when C_{tp}/V_t is higher than a threshold, the mean trait and preference values diverge to infinity (Figure 4(b)).

Interest of the model Lande's model shows that trait and preference can evolve to extreme values or diverge to infinity, despite a fixed adapted trait value is promoted by natural selection in the population. This model highlights that sexual selection generated by preference feedbacks on the evolution of preference, because of the genetic association between trait and preference, leads to unexpected dynamics. This example also illustrates the need to use mathematical model in order to handle the complexity of mate choice evolution.

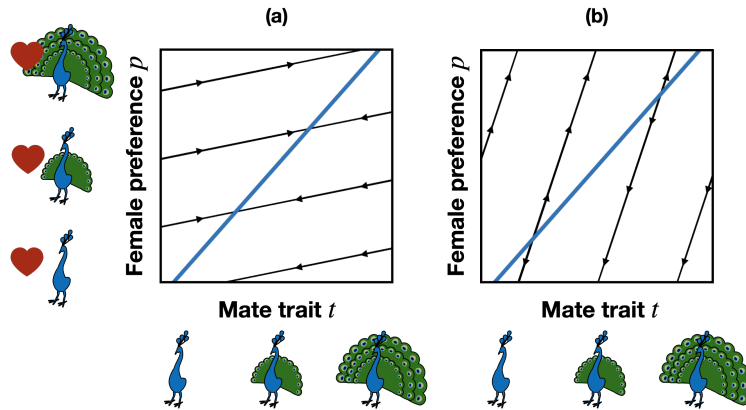


Fig. 4: Illustration of coevolution between trait and preference when the genetic correlation between trait and preference is (a) low or (b) great. The blue line shows the equilibrium point, black arrows show the dynamic of trait and preference.

Note that indirect selection may not be the main driver of the evolution of preference (Kirkpatrick & Barton, 1997). Direct fitness advantages linked to mate choice may also promote its evolution (Wagner, 2011). For example, beneficial sexually transmitted infections may promote preference toward infected individuals (Smith & Mueller, 2015). Another example of direct advantage is observed in comb-footed spiders, where males mate preference reduces the risk of pre-copulatory cannibalism by females (Pruitt & Riechert, 2009).

Mate preference as a species recognition system

So far, we focused on one facet of the scientific literature, dealing with the evolution of mate choice within a population. But species evolve generally in contact with closely related species, and mate preferences are also studied at the light of these interactions. Individuals may not recognise appropriate mates, as males buprestids that attempt to mate with a beer bottle (Gwynne & Rentz, 1983). Individuals may attempt sexual interactions with heterospecifics leading to what Fisher called "the grossest blunder in sexual preference" (Fisher, 1930). Such interactions between species during the process of mate acquisition lead to fitness costs called reproductive interference (Gröning & Hochkirch, 2008). For instance, heterospecific matings may produce maladapted hybrids (Hatfield & Schluter, 1999; Merrill *et al.*, 2012)). The poor fitness of hybrids promotes, by indirect selection, preference for conspecifics, because such preference reduces the production of hybrids (Kirkpatrick & Ravigné, 2002). Sexual interactions with heterospecifics may also be costly even without producing hybrids. For instance, heterospecific mating attempt has been show to reduce females fertility (*e.g.* Takafuji *et al.* (1997); Fujimoto *et al.* (1996)). Moreover, sexual interactions with heterospecifics may be costly, when heterospecifics have an aggressive mating behavior (Gröning & Hochkirch, 2008). Such costs reducing the fitness of the chooser, generate direct selection on preference.

Reproductive interference promotes, by indirect or direct selection, preference for phenotypes common within conspecific and rare within heterospecific. When a

mating trait is shared between sympatric species, reproductive interference promotes preference for the conspecific trait values, that differs the most from heterospecific trait values (McPeck & Gavrillets, 2006; Yamaguchi & Iwasa, 2013). Through the effect of sexual selection, reproductive interference drives reproductive character displacement, *i.e.* the differentiation of mating trait between sympatric species (McPeck & Gavrillets, 2006; Yamaguchi & Iwasa, 2013). Empirical studies report that the traits targeted by preference are more dissimilar between species in sympatric than in allopatric populations (Hinojosa *et al.*, 2020; Yukilevich, 2021), suggesting that reproductive interference is an important selective force acting on the evolution of traits targeted by mate choice in natural population.

Because females invest more resources in reproduction than males, they are generally assumed to be more choosy than males (Trivers, 1972). Sexual selection promoting reproductive character displacement may thus especially act on males. Under weak constraint on sexual differentiation, reproductive interference may trigger the divergence of male trait, while natural selection may promote the evolution of locally adapted female traits, leading to sexual dimorphism. For instance, in two out of the three fruit fly species of the genus *Blepharoneura* that court on the same host plant, a morphometric analysis reveals sexual dimorphism in wing shape, where males, but not females, from the two different species differ in wing shape (Marsteller *et al.*, 2009). In the mexican spadefoot toads *Spea multiplicata*, the level of sexual size dimorphism increases with the proportion of species from the same genus *Spea bombifrons* living in sympatry (Pfennig & Pfennig, 2005), suggesting a link between species interactions and sexual dimorphism.

Note that reproductive interference not always results in reproductive character displacement. Micro-habitat differences among mimetic species may also reduce heterospecific encounters. For example, the two sympatric ladybird species *Harmonia axyridis* and *Harmonia yedoensis* have similar body size and coloration (Sasaji, 1998) and experience reproductive interference (Noriyuki *et al.*, 2012). These species nevertheless have different host specialization (Noriyuki *et al.*, 2011), that may limit reproductive interference (Noriyuki, 2015).

Evolution of mate preference towards multiple traits

As we saw the evolution of preferences depend on the selection regimes acting on the targeted traits within species, but also on interactions with other species living in sympatry. Individuals display a vast number of traits but only a limited number of these traits impact fitness and/or differentiate conspecifics from heterospecifics. However, little is known on the evolutionary factors determining the traits preferentially targeted by preferences, and especially the number of different traits used during mate choice. Such multifactorial selection acting on the different traits may then favor the evolution of preferences targeting several traits. Using multiple mating traits may indeed improve some components of the fitness in the offspring and/or enhance recognition of conspecific males (Candolin, 2003).

Multiple traits preference may then be promoted when targeting traits associated with different components of the indirect fitness benefit (*e.g.* Doucet & Montgomerie (2003); Girard *et al.* (2015); Dale & Slagsvold (1996)). Theoretical modeling shows that preference towards multiple traits providing different indirect fitness benefit can evolve (Iwasa & Pomiankowski, 1994). The evolution of preference towards multiple non-adaptive traits can occur, when these traits provide greater reproductive success in the sons (*sexy sons hypothesis*) (Pomiankowski & Iwasa, 1993), suggesting that sexual selection can also promote the evolution of preference for multiple traits. Furthermore, selection promoting species recognition also promotes the evolution of preference for multiple traits that differentiate closely related species (Hohenlohe & Arnold, 2010; Vortman *et al.*, 2013; Patten *et al.*, 2004). While several sexual and natural selections have been suggested to favor the evolution of multiple traits preference, such evolution is likely to crucially depend on variations and covariation in traits within and among sympatric species. Similar traits may be promoted by natural selection in different sympatric species (*e.g.* in mimetic species, Boussens-Dumon & Llaurens (2021)), in contrast with the classical case of 'magic' traits (Servedio *et al.*, 2011). Indirect fitness benefit may then induce selection on preference conflicting with species recognition (*e.g.* Gumm & Gabor (2005); Higgin & Blows (2007)). For example, in the spadefoot

toad, preference for mating call increases the number of eggs fertilized in choosy females but leads to reproductive interference, because of the similarity of call between sympatric species (Pfennig, 2000). Preferences targeting multiple traits may then allow to improve both offspring fitness through the transmission of adapted alleles and species recognition. For example, in field crickets of the genus *Teleogryllus*, female targets both (1) cuticular hydrocarbons, providing fitness benefits to their offspring (Berson & Simmons, 2019), and (2) male calling song (Hill *et al.*, 1972) that differentiate sympatric species (Moran *et al.*, 2020).

While preference based on multiple traits may be promoted by natural and sexual selection, several constraints might limit the number of traits targeted by preference. Preferences are generally associated with fixed cost generated by mate searching, and these costs might be increased when preference targets multiple traits. Theoretical studies indeed show that the joint fixed costs of preference based on different traits indeed promotes preference based on the trait providing the greatest benefit (Schluter & Price, 1993), especially when the joint fixed costs quickly increase with the strength of preference for each trait (Pomiankowski & Iwasa, 1993; Iwasa & Pomiankowski, 1994). The evolution of preference for multiple traits may also be limited by the number of available partners displaying the preferred combination of traits. Opportunity costs associated with rejection by choosy females indeed increase when the number of targeted traits grows.

The evolution of multiple traits preference may also be limited by the complex cognitive processes involved, explaining the low number of traits used in mate choice in some clades (Candolin, 2003). Multiple traits-based mate choice may thus preferentially evolve in species where multiple sensory systems allow cognitive integration. Evolutionary trade-offs are often thought to limit the evolution of multiple sensory systems: the development of sensory systems is frequently associated with the regression of others (Barton *et al.*, 1995; Nummela *et al.*, 2013). Moreover, physical constraints may generate sensory trade-offs: for example, visual system model of the surfperch reveals trade-off in the performance between luminance and chromatic detection, because of the limited numbers of the different types of cones in the eyes (Cummings, 2004). Neural integration of multiple infor-

mation may also be limited, generating trade-offs in the use of multiple traits in decision. In the swordtail fish *Xiphophorus pygmaeus*, females express preference for a visual and an olfactory traits, when there are exposed to the variation of only one out of their traits within potential mate. However, when both traits vary within potential mates, females do not express preference (Crapon de Caprona & Ryan, 1990), suggesting that sensory trade-off limits the use of multiple traits in preference.

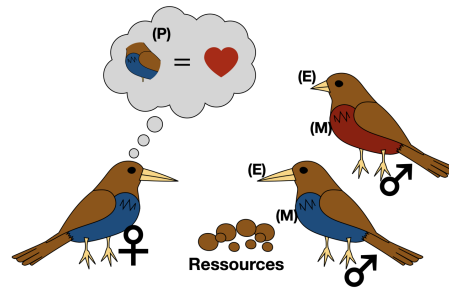
How to model the evolution of preference ?

Mathematical models have often been used to identify complex interactions happening during the evolution of mate choice, such as sexual selection feedback. Here, I describe the usual structure of models investigating mate choice evolution (see also the review of Kopp *et al.* (2018)). Usually, models consider a single choosy sex, assumed to be female, because females generally invest more resources than males in reproduction (Trivers, 1972). Mate choice models consider up to four types of traits, controlled by genetic basis. I illustrate these different types of traits with an example (Figure 5, adapted from Kopp *et al.* (2018)). Note that these traits can be either fixed or allowed to evolve.

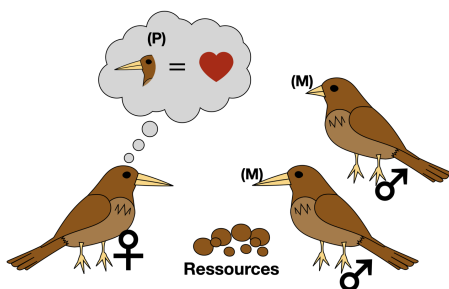
The first category of trait is mating traits (M) that are the target of mate preference. In example (a), females choose their mates according to a single mating trait: plumage coloration (red or blue). In this example, we consider qualitative variations in the traits but note that models can also consider quantitative variations. Models also consider traits that are ecologically selected traits (E). In our example there are two possible beak sizes in the population, small-beaked and large-beaked, with facilitated access to resources for large-beaked individuals. Because of the association between colors and beak sizes in the population (Figure 5(a)), mating with a blue male is advantageous because it produces large-beaked offspring. Note that in many models (*e.g.* Otto *et al.* (2008); Servedio *et al.* (2011)) there is a single trait, under ecological selection targeted by preference (M=E) as illustrated in example (b) (Figure 5(b)).

Categories of trait:
Mating trait (M): trait targeted by mate preference
Preference direction (P): values or states of mating trait preferred by females
Choosiness (C): females discrimination of preferred versus unpreferred males
Ecologically selected trait (E): trait implied in adaptation to the environment

(a) Case 1: general



(b) Case 2: Preference targets a ecologically selected trait (M=E)



(c) Case 3: Matching rule determines preference direction

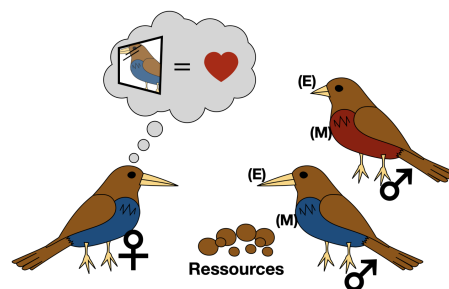


Fig. 5: **Illustration of three main types of models of mate choice evolution.** In the general case (a) four types of traits are considered: (M) mating traits, (E) ecologically selected traits, (P) preference directions and (C) choosiness. In some models the mating trait is also the trait under ecological selection (M=E) (b). Two types of mating rules are considered: preference/trait (a) (b) and matching rule (c).

Female mating behavior is decomposed in preference (P), describing the values or states of mating trait preferred by females (the plumage coloration in example (a)) and in choosiness (C) that describes, how much females discriminate preferred from unpreferred males. Preference (P) does not depend on the phenotype of the female and follow a preference/trait rule assumption. By contrast, many models assumed matching rule, *i.e.* assumes that mate choice depends on a match between the phenotypes of the chooser and the chosen individuals (Kopp *et al.*, 2018). Preference (P) is then not considered, because it is fully determined by the matching rule (see example (c) Figure 5(c)). The matching rule, often used in mathematical models, may be rather uncommon in nature (Kopp *et al.*, 2018).

Testing matching rule is hard, because it requires to manipulate the signal of the chooser, to test whether it modifies the choice. For example, in the brown-headed cowbird *Molothrus ater*, individuals preferred mates with the same plumage coloration and dyeing the plumage of the chooser alters the mating behavior (Hauber *et al.*, 2000).

Mate preference based on adaptive traits: warning traits as a case-study

Among traits that can be used in mate preference, some traits increase survival in a given environment. Mating preference targeting adaptive traits may be particularly advantageous, because it produces offspring adapted to the local environment. In this thesis, I focus on traits involved in aposematism, *i.e.* on conspicuous traits associated with defence against predators (see examples in Figure 6). The emergence of such warning traits is puzzling since they increase detectability by predators (see Appendix I). However when warning traits are common, they play an important role in survival, since they reduce predation.

Warning traits are under positive frequency-dependent selection

Predators aversion for warning traits is generally not innate. However, after some bad experience, predators learn to associate the warning trait with defence (Boydén, 1976; Chai, 1996). Because there are always naive predators, individuals displaying a conspicuous trait can still undergo attacks. Locally common warning traits nevertheless benefit from enhanced protection, because it is likely that most predators already learned to avoid these traits, resulting in a positive frequency-dependent selection (Müller, 1879). Field experiments confirm the advantage of locally abundant warning traits, due to a reduced predation rate (Chouteau *et al.*, 2016; Borer *et al.*, 2010; Mallet & Barton, 1989), in line with the theoretical argument.

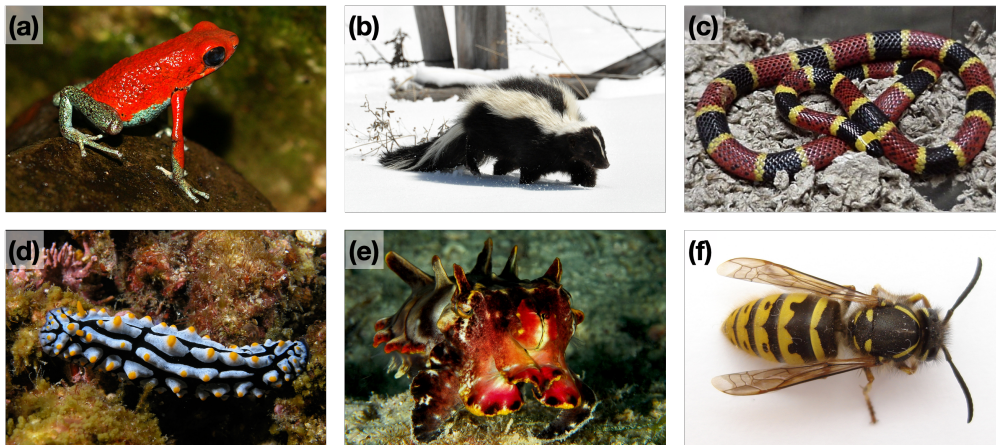


Fig. 6: Aposematic traits are widespread in animals from different clades: (a) The bright coloration signals poisons in granulated poison arrow frogs. ©Patrick Gijssbers (b) The white striped signals defensive musks in striped skunks . ©Dan & Lin Dzurisin (c) The color pattern signals venoms in texas coral snakes. ©LA Dawson (d) The bright coloration signals poisons in nudibranchs. ©Nick Hobgood (e) The bright coloration signals venomous bites in the Flamboyant Cuttlefish. ©Jenny Huang (f) The color pattern signals stings in wasps. ©Trounce

This positive frequency-dependent selection generally promotes the fixation of a single warning signal within a population (Ruxton *et al.*, 2019). Moreover predation pressure acting on warning traits can be applied to different sympatric species and then promotes the fixation of the same warning trait in different sympatric defended species (Chazot *et al.*, 2014). A mimicry ring is then defined as a group of species, where individuals face the same predator community and display a similar warning trait (see an example in mimetic butterflies Figure 7, note that the similarity can be imperfect). Within a mimicry ring, we distinguish Müllerian mimics, *i.e.* species with defence, participating to predator learning (Müller, 1879) and Batesian mimics, *i.e.* species without defence, enjoying the protection provided by the mimicry ring, without participating to predator learning (Bates, 1862). Surprisingly, selection exerted by predators may promote several mimicry rings living in sympatry, each displaying a different well protected warning trait (Briolat *et al.*, 2019; Sherratt, 2008).

Warning traits play an important role in survival, and are frequently targeted

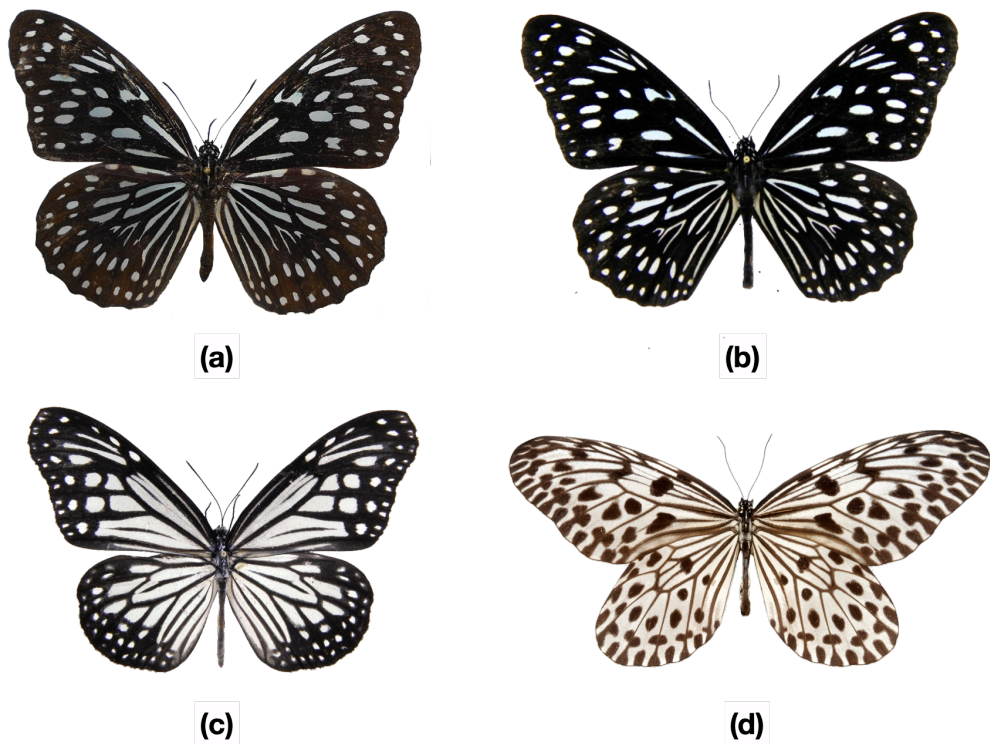


Fig. 7: Butterflies belonging to the *Tirumala* mimicy ring in tropical forests of the Western Ghats, India (Joshi *et al.*, 2017). (a) *Tirumala limniace*. ©Alexander Boldyrev (b) *Tirumala septentrionis*. ©Alexander Boldyrev (c) *Parantica aglea*. ©Alex Dumchus (d) *Idea malabarica*. ©Nick Hobgood. ©Leeds Museums & Galleries.

by mate preference (Jiggins *et al.*, 2001; Naisbit *et al.*, 2001; Kronforst *et al.*, 2006; Merrill *et al.*, 2014). The positive frequency-dependent selection acting on locally mimetic warning trait is thought to indirectly promote the evolution of assortative mating (Otto *et al.*, 2008). Because of positive frequency-dependent selection, most individuals mainly display the locally mimetic warning trait. Then, in the majority of cases, assortative mating preference targets the adaptive most common warning trait, enhancing offspring fitness. However, surprisingly in the mimetic butterfly *Heliconius numata*, disassortative mating based on warning trait is observed (Chouteau *et al.*, 2017). *H. numata* is an unpalatable species, with polymorphic mimetic color patterns (Arias *et al.*, 2016a). In this species, a local

polymorphism of wing patterns, belonging to different mimicry rings, is observed over all its geographical range (Brown & Benson, 1974), in sharp discrepancy with the positive frequency-dependent selection expectation.

Disassortative mating and the genetic architecture of a warning trait

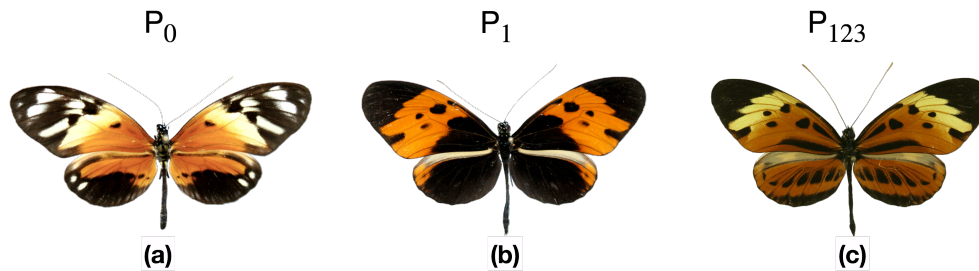


Fig. 8: Three phenotypes present in a *Heliconius numata* population of Tarapoto in northern Peru. (a) *H. n. silvana* associated with the ancestral allele P_0 . (b) *H. n. bicoloratus* associated with the derived allele P_1 . (c) *H. n. tarapotensis* associated with the derived allele P_{123} .

In *H. numata* a single locus controls for the wing pattern variation (Joron *et al.*, 2006b, 2011; Huber *et al.*, 2015). This locus is a supergene created by an inversion P_1 , introgressed from the sister species *H. pardalinus* (Jay *et al.*, 2018). This inversion suppressed recombination between multiple loci controlling wing pattern variations (Jay *et al.*, 2022), where a combination of alleles are locked together within one supergene allele (Joron *et al.*, 2006b, 2011; Huber *et al.*, 2015). Selection exerted by predators might have promoted such a tightly linked combination of alleles. In *H. numata*, the introgressed inversion is associated with a common warning trait in the foothills of the Andes (*H. n. bicoloratus* in Figure 8(b)) (Chouteau *et al.*, 2016). Other inversions, close to the first one, led to the formation of another set of supergene alleles P_{123} (including *H. n. tarapotensis* in Figure 8(c)) (Joron *et al.*, 2011), and is also associated with a mimetic color pattern (Chouteau *et al.*, 2016).

Mimicry is generally assumed to promote the formation of supergene in Batesian species (Charlesworth & Charlesworth, 1975). Because undefended mimics have

a negative impact on predators learning (Lindström *et al.*, 1997; Rowland *et al.*, 2010), the protection provided by a warning trait displayed in a mimicry ring, decreases with the number of undefended mimics in the rings. Such negative frequency-dependent selection often promotes polymorphism in Batesian species, where several phenotypes match with different local mimicry rings (Turner, 1987). Such coexistence of several adaptive variants promotes the formation of supergene (Charlesworth & Charlesworth, 1975). Indeed, a combination of alleles may code for each phenotype that mimics local mimicry rings, breaking those combinations may lead to maladaptive warning trait not common in the mimetic community.

H. numata has similar levels of defence as monomorphic *Heliconius* species, and is thus unlikely to be a Batesian mimic (Arias *et al.*, 2016a). The formation of supergenes might thus also occur in Müllerian species. This is surprising, because a polymorphism of adaptive phenotypes promotes the formation of supergene and the positive frequency-dependent selection acting on warning trait in Müllerian species limits such polymorphism (Turner, 1987). Joron *et al.* (1999) proposed that the spatial distribution of mimicry rings may favor polymorphism in *H. numata* because of selection/migration balance. Even if a warning trait is under positive frequency-dependent selection, different mimicry rings coexist in different localities. For instance, even if the mimetic butterflies *H. erato* and *H. melpomene* are locally monomorphic, their phenotypes vary across localities, exhibiting up to 30 different warning traits (Brower, 1996; Jiggins & McMillan, 1997; Flanagan *et al.*, 2004). If the high mobility is assumed in *H. numata*, migration can maintain local polymorphism of warning traits in this species (Joron *et al.*, 1999). A theoretical study confirms the condition of persistent polymorphism under this selection/migration balance (Joron & Iwasa, 2005). Local adaptation and migration generate balancing selection, promoting the formation of supergene, because recombination between a resident and a migrant haplotype may lead to a phenotype maladaptive (non-mimetic) in all localities (Kirkpatrick & Barton, 2006).

The formation of supergene often involve chromosomal rearrangements, such as inversions, that may be advantageous because they reduce recombination between combination of alleles (Kirkpatrick, 2010). Such a lock of recombination then favors

the capture and accumulation of deleterious recessive mutations (Kirkpatrick & Barton, 2006). In *H. numata*, supergene alleles associated with an inversion are linked to a genetic load, strongly decreasing larval survival in homozygotes (Jay *et al.*, 2021), so that disassortative mating may increase offspring fitness through an increased viability of heterozygotes. The disassortative mating observed in *H. numata* is surprising, because preference often does not target the best adapted warning trait, *i.e.* the trait the most commonly displayed in the local community. However, the genetic basis of the warning trait variation may have promoted the evolution of disassortative mating. The *H. numata* case highlights the importance of considering the genetic architecture of the targeted trait to understand the evolution of mate preference.

When mimetic adaptation conflicts with species recognition

The evolution of preference within a species also depends on interactions with sympatric species. Species interactions may also limit the evolution of preference towards the locally adaptive trait. Warning coloration is indeed frequently involved in mate choice in butterflies (Jiggins *et al.*, 2001; Naisbit *et al.*, 2001; Kronforst *et al.*, 2006; Merrill *et al.*, 2014) and shared between sympatric species (Sherratt, 2008), leading to increased risk of confusion in mimetic species during sexual interactions. Such risk might be even higher between closely-related species, which are more likely to share multiple similar traits because of common ancestry. Species sharing similar warning traits may thus be exposed to substantial reproductive interference, incurring fitness costs during mate acquisition due to interspecific interactions. These interactions include heterospecific courtship and mating, as well as heterospecific male rivalry (Gröning & Hochkirch, 2008). Empirical examples of such reproductive interferences in Müllerian mimetic systems have been reported in the literature (Vasconcellos-Neto & Brown, 1982; Estrada & Jiggins, 2008). However, empirical studies precisely estimating the level of reproductive interference in sympatric species are scarce. Pheromone differences between mimetic species have been documented to limit the rate of erroneous mat-

ings (see Darragh *et al.* (2017); González-Rojas *et al.* (2020) for empirical examples in *Heliconius* butterflies). However, the pheromones of day-flying butterflies usually act as short-distance cues and may thus be perceived during courtship only (Mérot *et al.*, 2015). Females deceived by the color pattern of the heterospecific males may have already spent time and energy or may need to deploy substantial efforts to avoid heterospecific mating. Therefore, females may still suffer from costs associated to reproductive interference, even if they manage to avoid mating with heterospecific males. When females are courted by heterospecific males displaying their preferred cue before rejected them, this also results in increased costs associated with mate searching in males (*i.e.* signal jamming in Gröning & Hochkirch (2008)). Reproductive interference may promote female preference toward non-mimetic males (maladaptive as compared to mimetic males), because such preference reduces sexual interactions with heterospecifics.

Is sexual selection involved in female-limited mimicry ?

Preference toward non-mimetic males may be involved in the evolution of female-limited mimicry. Sexual dimorphism is frequently observed in butterfly species, where Batesian mimicry is sometimes surprisingly limited to females (Ford, 1975; Kunte, 2008; Nishikawa *et al.*, 2015). The evolutionary forces preventing the evolution of mimicry in males are still debated. Sexual selection may limit mimicry in males. In the female-limited Batesian mimic *Papilio glaucus*, females tend to prefer painted non-mimetic traits over artificial mimetic traits (Krebs & West, 1988). Wing colour patterns in mimetic butterflies may therefore modulate male reproductive success, by influencing both male-male competition and mating success with females. In particular, female preference for ancestral trait may generate sexual selection limiting male mimicry (Belt, 1874.; Turner, 1978). Nevertheless, because mimetic coloration is under strong positive selection, female preferences are predicted to favor mimetic coloration in males, as observed in species involved in Müllerian mimicry (Jiggins *et al.*, 2001; Naisbit *et al.*, 2001; Kronforst *et al.*, 2006; Merrill *et al.*, 2014). It is thus unclear what does limit the evolution of

female preferences toward mimetic coloration in males in species involved in Batesian mimicry. As previously highlighted, reproductive interference may promote such preference.

However the role of sexual selection in the evolution of sexual dimorphism is still debated. Alternatively female-limited mimicry could be promoted by natural selection, especially if male and female are submitted to different selective pressures. Because butterfly males and females generally differ in their behavior, the strength of predation pressure might thus differ among sexes (Ohsaki, 1995, 2005): for instance, butterfly females usually spend a lot of time ovipositing on specific host-plants, and thus have a more predictable behavior for predators. Moreover, flight speed is generally lower in females than males: females are heavier because they carry eggs (Gilchrist, 1990), and males have higher relative thorax mass (Karlsson & Wickman, 1990) and muscle mass (Marden & Chai, 1991), resulting in increased flight power (Chai & Srygley, 1990). Predation pressures are thus expected to be stronger in females.

Wing pattern evolution is also shaped by developmental constraints (Van Belleghem *et al.*, 2020), that may impede divergence from the ancestral trait. Such trade-off between developmental constraints favoring the ancestral trait and selection promoting mimicry might differ between sexes: if predation is lower in males, the constraints limiting mimicry may overcome the benefit from mimicry in males, whereas in females the higher predation pressure may promote mimicry. Nevertheless, evidence for the limited predation in males as compared to females is controversial (Wourms & Wasserman, 1985), suggesting that contrasted predation in males and females may thus not be the main driver of female-limited mimicry.

Main questions and objectives

In this thesis, I aim at identifying the conditions for the evolution of mate preference targeting locally adapted *vs* non-adapted traits. While most researches focused on selective regime acting on traits promoting preference towards adap-

tive traits enhancing offspring fitness, I focus on cases where preference towards locally maladapted traits may emerge.

First, I focus on the evolution of disassortative mating in a mimetic species, where such preference leads to non-mimetic offspring. By focusing on the case of *H. numata* I test, using numerical simulations, whether deleterious genetic mutations associated with derived supergene alleles may explain the evolution of disassortative mating, despite the positive frequency-dependent selection acting on warning trait. I also investigate which of genetic architectures of preference allow the evolution of such disassortative mating (**Chapter 1**). Then I develop a general mathematical framework to identify the key mechanisms underlying the evolution of disassortative mating. Using a QLE analytical resolution as well as numerical simulations, I investigate the impact of the genetic architecture of targeted traits, identifying the genetic architecture that allows the evolution of disassortative mating (**Chapter 2**).

Second, I focus on reproductive interference that results from local selection acting on traits in different sympatric species and how such shared selection limits preference towards mimetic mate. In sympatric defended species, trait variation is shaped by similar selective pressure, promoting similar adaptive traits in the different species, usually shared by both sexes. When preference targets warning traits, such similarity between species induce reproductive interference. Such reproductive interference promotes female preference for the scarce males displaying slightly imperfect mimicry. The sexual selection generated by such preference impacts the evolution of locally-adapted traits within sympatric species. Using quantitative genetic models, I study the impacts of reproductive interference on the level of trait convergence between sympatric species (**Chapter 3**). Moreover, such conflict between mimicry and species recognition may explain the female-limited mimicry observed in Batesian species. However, natural selection may also have led to the evolution of female-limited mimicry. I thus compare the evolution of female-limited mimicry, caused by sexual or natural selection, in order to provide testable predictions (**Chapter 4**).

Third, I investigate why and when traits involved in local adaptation are targeted by mate preference. When locally adapted traits are shared between sympatric species, targeting adaptive traits can enhance offspring fitness, but can lead to reproductive interference. Preference may rather target other traits, unlinked to local adaptation, but differing between sympatric species. Multiple traits preference targeting both adaptive traits, as well as additional species recognition traits, may produce adapted offspring, without implying reproductive interference. I investigate the evolution of preference based on multiple traits, when the traits used as cues can be either neutral or submitted to shared selective pressures favoring trait similarity between sympatric species (**Chapter 5**).

Part I

When adaptation suppresses recombination: mate preference limiting the expression of genetic deleterious mutations

The evolution of mate preference towards traits involved in local adaptation depends on the genetic basis of the traits. In *H. numata*, deleterious recessive mutations associated with a supergene controlling the variation in wing patterns may promote the evolution of disassortative mating. However disassortative preference is costly because it leads to non-mimetic offspring. I test, using numerical simulations, whether deleterious genetic mutations associated with derived supergene alleles may explain the evolution of disassortative mating, despite the selective regime acting on wing pattern. I also investigate which of genetic architectures of preference allow the evolution of such disassortative mating (**Chapter 1**). Then I develop a general mathematical framework to identify the key mechanisms underlying the evolution of disassortative mating. Using a QLE analytical resolution as well as numerical simulations, I investigate the impact of the genetic architecture of targeted traits, identifying the genetic architecture that allows the evolution of disassortative mating (**Chapter 2**).

CHAPTER 1

Genetic architecture of disassortative mating

Ludovic Maisonneuve, Mathieu Chouteau, Mathieu Joron
and Violaine Llaurens

Published:

Maisonneuve, L, Chouteau, M, Joron, M, Llaurens, V. (2020) Evolution and genetic architecture of disassortative mating at a locus under heterozygote advantage. *Evolution*, 75:1, 159-165.

doi: 10.1111/evo.14129

Recommended by:

Charles Mullan (2020) Evolutionary insights into disassortative mating and its association to an ecologically relevant supergene.

Peer Community in Evolutionary Biology, 100109.

doi: 10.24072/pci.evolbiol.100109

Abstract

We aim at uncovering the ecological conditions and genetic architecture enabling the puzzling evolution of disassortative mating based on adaptive traits. This rare form of mate choice is observed for some polymorphic traits but theoretical predictions on the emergence and persistence of this behavior are largely lacking. Thus we developed a mathematical model to specifically understand the evolution of disassortative mating based on warning trait in the polymorphic butterfly *Heliconius numata*. We show that heterozygote advantage can promote the evolution of disassortative mating, despite the positive frequency-dependent selection acting on warning trait. We modelled different possible genetic architectures underlying mate choice behaviour, such as self referencing alleles, or specific preference or rejection alleles. Our results showed that each rules enable the emergence of disassortative mating. However, under the more realistic genetic architecture implying attraction or rejection alleles, disassortative mating evolves only when the mating trait and preference loci are tightly linked.

Introduction

Mate preferences often play an important role in shaping trait diversity in natural populations, but the mechanisms responsible for their emergence often remain to be characterized. While the evolution of assortative mating on locally adapted traits is relatively well understood (Otto *et al.*, 2008; de Cara *et al.*, 2008; Thibert-Plante & Gavrillets, 2013), the selective forces involved in the evolution of disassortative mating are still largely unknown. Disassortative mating, *i.e.* the preferential mating between individuals displaying different phenotypes, is a rare form of mate preference (Jiang *et al.*, 2013). In populations where individuals tend to mate with phenotypically distinct partners, individuals with a rare phenotype have a larger number of available mates, resulting in a higher reproductive success. By generating negative frequency-dependent selection on mating cues, disassortative mating is often regarded as a process generating and/or maintaining polymorphism within populations. Obligate disassortative mating leads to the persistence of intermediate frequencies of sexes or mating types (Wright, 1939), and promotes polymorphism (e.g. the extreme case of some Basidiomycete fungi where thousands of mating types are maintained (Casselton, 2002)). Disassortative mating can be based on different traits. Disassortative mating based on odors is known to operate in mice (Penn & Potts, 1999) and humans (Wedekind *et al.*, 1995). Odor profiles are associated with genotype at the MHC loci affecting the immune response, known to be under strong balancing selection (Piertney & Oliver, 2006). Balancing selection on MHC alleles partly stems from heterozygous advantage, whereby heterozygous genotypes might confer an ability to recognize a larger range of pathogens. Such heterozygote advantage may promote the evolution of disassortative mating (Tregenza & Wedell, 2000). Extreme examples of heterozygote advantage are observed for loci with reduced homozygote survival. In the seaweed fly *Coelopa frigida* heterozygotes ($\alpha\beta$) at the locus *Adh* have a higher fitness than homozygotes ($\alpha\alpha$ or $\beta\beta$) (Butlin *et al.*, 1984; Mérot *et al.*, 2020) and females prefer males with a genotype that differs from their own (Day & Butlin, 1987). In the white-throated sparrow *Zonotrichia albicollis*, strong dis-

assortative mating is known to operate with respect to the color of the head stripe and associated with chromosomal dimorphism (Throneycroft, 1975). This plumage dimorphism is associated with a spectacular chromosomal polymorphism (Tuttle *et al.*, 2016), with a complete lack of homozygous individuals for the rearranged chromosome (Horton *et al.*, 2013).

While the fitness advantage of disassortative mating targeting loci with overdominance seems straightforward, the genetic basis of disassortative preferences remains largely unknown. One exception is the self-incompatibility system in *Brassicaceae* where the *S*-locus determines a specific rejection of incompatible pollens (Hiscock & McInnis, 2003). *S*-haplotypes contain tightly linked, co-evolved SCR and SRK alleles, encoding for a protein of the pollen coat and a receptor kinase located in the pistil membrane respectively, preventing fertilization from self-incompatible pollen due to specific receptor-ligand interactions. Self-rejection has also been proposed as an explanation for the disassortative mating associated with odor in humans. Body odors are strongly influenced by genotypes at the immune genes HLA and rejection of potential partners has been shown to be related to the level of HLA similarity, rather than to a particular HLA genotype (Wedekind & Fürti, 1997). In the white-throated sparrow, disassortative mating results from specific preferences for color plumage that differ between males and females; *tan*-striped males are preferred by all females while *white*-striped females are preferred by all males (Houtman & Falls, 1994). Different mechanisms leading to mate preferences and associated genetic architecture can be hypothesized, that may involve the phenotype of the chooser. Based on the categories described by Kopp *et al.* (2018), we assume that disassortative mating can emerge from two main mechanisms. (1) *Self-referencing*, when an individual uses its own signal to choose its mate, which may generate a disassortative mating that depends on the phenotypes of both the choosing and the chosen partners. (2) Preferences for or rejection of a given phenotype in the available partners (*recognition/trait* hypothesis), independently from the phenotype of the choosing partner, may also enable the emergence of disassortative mate preferences. These two mechanisms could involve a two locus architecture where one locus controls the mating cue and the other one the

preference towards the different cues (Kopp *et al.*, 2018). The level of linkage disequilibrium between the two loci could have a strong impact on the evolution of disassortative mating. In models investigating the evolution of assortative mating on locally-adapted traits, theoretical simulations have demonstrated that assortative mating is favored when the preference and the cue loci are linked (Kopp *et al.*, 2018).

Here we explore the evolutionary forces leading to the emergence of disassortative mating. We use as a model system the specific case of the butterfly species *Heliconius numata*, where high polymorphism in wing pattern is maintained within populations (Joron *et al.*, 1999) and strong disassortative mating operates between wing pattern forms (Chouteau *et al.*, 2017). *Heliconius numata* butterflies are chemically-defended (Arias *et al.*, 2016b; Chouteau *et al.*, 2019), and their wing patterns act as warning signals against predators (Chouteau *et al.*, 2016). At a local scale, natural selection on local mimicry usually leads to the fixation of a single warning signal shared by multiple defended species (Müllerian mimicry) (Mallet & Barton, 1989). However, local polymorphism of mimetic color patterns is maintained in certain species for instance under a balance between migration and local selection on mimicry (Joron & Iwasa, 2005). Yet, the level of polymorphism observed within populations of *H. numata* (Joron *et al.*, 1999) would require that the strong local selection is balanced by a very high migration rate. However, disassortative mating based on wing pattern operates in *H. numata*, with females rejecting males displaying the same color pattern (Chouteau *et al.*, 2017). Such disassortative mating could enhance local polymorphism in color pattern within this species. Nevertheless, the mode of evolution of a disassortative mating is unclear, notably because preferences for dissimilar mates should not be favoured if natural selection by predators on adult wing pattern acts against rare morphs (Chouteau *et al.*, 2016). Building on this well-documented case study, we use a theoretical approach to provide general predictions on the evolution of disassortative mating in polymorphic traits, and on expected genetic architecture underlying this behavior.

Variation in wing color pattern in *H. numata* is controlled by a single genomic re-

gion, called the supergene P (Joron *et al.*, 2006b), displaying distinct chromosomal inversion combinations, each associated with a distinct mimetic phenotype (Joron *et al.*, 2011). These inversions have recently been shown to be associated with a significant genetic load, resulting in a strong heterozygote advantage (Jay *et al.*, 2021). We thus investigate whether a genetic load associated with locally adaptive alleles may favor the evolution of mate preference and promote local polymorphism. We then explore two genetic architectures for mate preferences based on (1) *self referencing* and (2) based on a *recognition/trait* rule, and test their respective impacts on the evolution of disassortative mating. Under both hypotheses, we assumed that the mating cue and the mating preference were controlled by two distinct loci, and investigated the effect of linkage between loci on the evolution of disassortative mating.

Methods

Model overview

Based on earlier models of Müllerian mimicry (Joron & Iwasa, 2005; Llaurens *et al.*, 2013), we follow the evolution of mate preferences based on color pattern using ordinary differential equations. We track the density of individuals carrying different genotypes combining the alleles at the locus P controlling mimetic color pattern and at the locus M underlying sexual preference. We assume a diploid species, so that each genotype contains four alleles. All variables and parameters used in the model are summarized in Table 1 and 2 respectively.

The genotype of an individual is thus characterized by the four alleles at locus P and locus M , on the maternal and paternal chromosomes. Therefore the set of all possible four-allele genotypes is defined as $\mathcal{G} = \mathcal{A}_P \times \mathcal{A}_P \times \mathcal{A}_M \times \mathcal{A}_M$ where \mathcal{A}_P , \mathcal{A}_M are the set of alleles at locus P and M respectively. A given genotype is then a quadruplet of the form (p_m, p_f, m_m, m_f) with $p_m \in \mathcal{A}_P$ and $m_m \in \mathcal{A}_M$ (resp. p_f and m_f) being the alleles at loci P and M on the maternal (resp. paternal)

chromosomes. A recombination rate ρ between the color pattern locus P and the preference locus M is assumed.

We consider two geographic patches numbered 1 and 2 where those genotypes can occur. For all $i = (p_m, p_f, m_m, m_f) \in \mathcal{G}$, $n \in \{1, 2\}$, we track down the density of individuals of each genotype i within each patch n , $N_{i,n}$ through time. Following previous models, polymorphism in mimetic color pattern is maintained within each of the two patches, by a balance between (1) local selection on color pattern in opposite directions in the two patches and (2) migration between patches.

The evolution of genotype densities through time, for each patch, is influenced by predation, mortality, migration between patches and reproduction, following the general equations :

$$\forall (i, n) \in \mathcal{G} \times \{1, 2\} \quad \frac{d}{dt} N_{i,n} = \Delta_{i,n}^{pred} + \Delta_{i,n}^{mort} + \Delta_{i,n}^{mig} + \Delta_{i,n}^{rep}, \quad (1.1)$$

where $\Delta_{i,n}^{pred}$, $\Delta_{i,n}^{rep}$, $\Delta_{i,n}^{mig}$, and $\Delta_{i,n}^{mort}$ described the respective contributions of these four processes to the change in density of genotype i within each patch n . The computation of each of these four contributions is detailed in specific sections below.

Since our ordinary differential equations model follows the change in genotype densities at a population level, this amounts to considering that predation, migration, reproduction and survival occur simultaneously (see Equation (1.1)). In a large population, we can assume that predation, migration, reproduction and survival indeed occur in different individuals at the same time. Such a model implies that generations are overlapping and that there is no explicit ontogenic development: each newborn individual instantaneously behaves as an adult individual and can immediately migrate and reproduce. Our deterministic model provides general predictions while ignoring the effects of stochastic processes such as genetic drift.

Mimetic color pattern alleles at locus P

At the color pattern locus P , three alleles are assumed to segregate, namely alleles a , b and c , encoding for phenotypes A , B and C respectively. The set of alleles at locus P is then $\mathcal{A}_P = \{a, b, c\}$. We assume strict dominance among the three alleles with $a > b > c$ in agreement with the strict dominance observed among supergene P alleles within natural populations of *H. numata* (Le Poul *et al.*, 2014) and in other supergenes (Wang *et al.*, 2013; Tuttle *et al.*, 2016; Küpper *et al.*, 2016). The three color pattern phenotypes are assumed to be perceived as categorically different by both mating partners and predators. We note $T_{g \rightarrow cp}$ the function translating each genotype $i = (p_m, p_f, m_m, m_f) \in \mathcal{G}$ into the corresponding color pattern phenotype. For example, for all $(m_m, m_f) \in \mathcal{A}_M \times \mathcal{A}_M$, $T_{g \rightarrow cp}((a, b, m_m, m_f)) = A$ because allele a is dominant over b and the color pattern phenotype depends only on alleles at locus P . Each color pattern allele is also assumed to carry an individual genetic load expressed when homozygous.

Preference modes at locus M

We investigate the evolution of mate preference associated with color patterns, exploring in particular the conditions enabling the evolution of disassortative mating. We assume a single choosy sex: only females can express preferences toward male phenotypes, while males have no preference and can mate with any accepting females. We assume two different models of genetic architecture underlying mate preferences: alleles at locus M determine either (1) a preference toward similar or dissimilar phenotypes, which therefore also depends on the phenotype of the choosing individual, following the *self-referencing* hypothesis or (2) a preference toward a given color pattern displayed by the mating partner, independent of the color pattern of the choosing individual, following the *recognition/trait* hypothesis.

Predation

The probability of predation on individuals depends on their mimetic color patterns controlled by the locus P . Predation is determined in our model by a basic (patch-specific) effect of the local community of prey favouring one of the wing patterns locally (local adaptation through mimicry), itself modulated by positive frequency dependence of the different wing patterns controlled by P , within the focal species population. This is detailed below.

Divergent local adaptation in color pattern

Local selection exerted by predators promotes convergent evolution of wing color patterns among defended species (*i.e.* Müllerian mimicry, (Müller, 1879)), forming mimicry rings composed of individuals from different species displaying the same warning signal within a locality. Mimicry toward the local community of defended prey therefore generates strong local selection on color pattern and the direction of this selection then varies across localities (Sherratt, 2006).

Here we assume two separate populations exchanging migrants of an unpalatable species involved in Müllerian mimicry with other chemically-defended species. Local communities of species involved in mimicry (*i.e.* mimicry rings) differ across localities. We consider two patches occupied by different mimetic communities: population 1 is located in a patch where the local community (*i.e.* other chemically-defended species, not including *H. numata*) mostly displays phenotype A, and population 2 in a patch where the mimetic community mostly displays phenotype B. This spatial variation in mimicry rings therefore generates a divergent selection favouring distinct locally adapted phenotypes. Note that allele c has a disadvantage because the corresponding phenotype C is locally non-mimetic in both patches, *i.e.* different from phenotypes displayed by both mimetic communities. Every individual of the focal (polymorphic) species is exposed to a predation risk modulated by its resemblance to the local mimetic community of butterflies. Each genotype i in population n (with $i = (p_m, p_f, m_m, m_f) \in \mathcal{G}$ and $n \in \{1, 2\}$) suffers

from a basic predation mortality factor $d_{i,n}$. This parameter is lower for individuals displaying the phenotype mimetic to the local community (*i.e.* the phenotype A in population 1 and B in population 2). Individuals displaying phenotype C being locally non-mimetic in both patches, suffer from a high predation risk in both patches.

Here, to simplify, we consider that this basic mortality factor takes the value d_m for the locally mimetic phenotype (A in patch 1, B in patch 2), and d_{n-m} for the locally non-mimetic phenotypes (B and C in patch 1, A and C in patch 2). We therefore introduce parameters d_{n-m} and d_m , with $d_{n-m} > d_m$, as follows: the basic predation mortality factors for individuals not displaying and displaying the same color pattern as the local community respectively. For $i = (p_m, p_f, m_m, m_f) \in \mathcal{G}$, the basic predation mortality factors of individuals with genotype i in patch 1 and 2 are

$$d_{i,1} = \mathbb{1}_{\{T_{g \rightarrow cp}(i)=A\}}d_m + \mathbb{1}_{\{T_{g \rightarrow cp}(i) \neq A\}}d_{n-m}, \quad (1.2)$$

$$d_{i,2} = \mathbb{1}_{\{T_{g \rightarrow cp}(i)=B\}}d_m + \mathbb{1}_{\{T_{g \rightarrow cp}(i) \neq B\}}d_{n-m}, \quad (1.3)$$

where $\mathbb{1}$ is the indicator function which return 1 if the condition under brace is true and 0 else.

Local positive frequency-dependent predation

Predation exerted on a given phenotype depends on its match to the local mimetic environment (taken into account by the parameter $d_{i,n}$ for all $i = (p_m, p_f, m_m, m_f) \in \mathcal{G}$ and for all $n \in \{1, 2\}$, see previous paragraph), but also on its own abundance in the patch as predators learn to associate warning patterns with chemical defense. This learning behavior generates positive frequency-dependent selection on color patterns (Chouteau *et al.*, 2016): displaying a widely shared color pattern decreases the risk of encountering a naive predator (Sherratt, 2006). Number-dependent predator avoidance in the focal species is assumed to depend on its

unpalatability coefficient (λ) and on the density of each phenotype within the population: the protection gained by phenotypic resemblance is greater for higher values of the unpalatability coefficient λ . For $i = (p_m, p_f, m_m, m_f) \in \mathcal{G}, n \in \{1, 2\}$, the change in the density of a genotype i in patch n due to predation thus takes into account both the spatial variation in mimetic communities (using $d_{i,n}$) modulated by the local frequency-dependent selection, and is thus described by the equation:

$$\Delta_{i,n}^{pred} = -\frac{d_{i,n}N_{i,n}}{1 + \lambda \sum_{j \in \mathcal{G}} \mathbb{1}_{\{T_{g \rightarrow cp}(i)=T_{g \rightarrow cp}(j)\}}N_{j,n}}, \quad (1.4)$$

where $\sum_{j \in \mathcal{G}} \mathbb{1}_{\{T_{g \rightarrow cp}(i)=T_{g \rightarrow cp}(j)\}}N_{j,n}$ is the total density, within patch n , of individuals sharing the same color pattern as individuals of genotype i .

Mortality

We assume a baseline mortality rate δ . The recessive genetic loads $\delta_a, \delta_b, \delta_c$ associated with the respective alleles a, b and c limit the survival probabilities of homozygous genotypes at locus P .

For $i = (p_m, p_f, m_m, m_f) \in \mathcal{G}, n \in \{1, 2\}$ the change in density of individuals with genotype i in patch n is given by

$$\Delta_{i,n}^{mort} = -(\delta + (\mathbb{1}_{\{p_m=p_f=a\}}\delta_a + \mathbb{1}_{\{p_m=p_f=b\}}\delta_b + \mathbb{1}_{\{p_m=p_f=c\}}\delta_c))N_{i,n}. \quad (1.5)$$

Migration

We assume a constant symmetrical migration rate m corresponding to a proportion of individuals migrating from one patch to the other, as classically assumed in population genetics models (see for instance Holt (1985); Kuang & Takeuchi (1994); Joron & Iwasa (2005)). The number of individuals of each of the genotypes migrating to the other patch is therefore directly proportional to their density in

their source population. For $i = (p_m, p_f, m_m, m_f) \in \mathcal{G}$, $n \in \{1, 2\}$, $n' \in \{1, 2\}$ with $n \neq n'$, the change in the density of individuals with genotype i in patch n due to migration between patches n and n' is given by the difference between the density of individuals coming into the patch $mN_{i,n'}$ and those leaving the patch $mN_{i,n}$:

$$\Delta_{i,n}^{mig} = mN_{i,n'} - mN_{i,n}. \quad (1.6)$$

where m is the migration coefficient $m \in [0, 1]$.

Reproduction

In the model, the reproduction term takes into account the basic demographic parameter, the effect of mate preference controlled by locus M and the fecundity limitations associated with choosiness.

Local demography

We assume that the populations from both patches have identical carrying capacities K and growth rates r . We name $N_{tot,n}$ the total density in patch n . The change in the total density due to reproduction is given by the logistic regulation function $r(1 - \frac{N_{tot,n}}{K})N_{tot,n}$. Thus for $i = (p_m, p_f, m_m, m_f) \in \mathcal{G}$, $n \in \{1, 2\}$, the change in the density of genotype i in patch n generated by sexual reproduction is given by:

$$\Delta_{i,n}^{rep} = r(1 - \frac{N_{tot,n}}{K})N_{tot,n}F_{i,n}, \quad (1.7)$$

where $(F_{i,n})_{i \in \mathcal{G}}$ are the frequencies of each genotype in the progeny. These frequencies depend on the behavior of the female, controlled by the preference locus M , and on the availability of the preferred partners in the population, as detailed in the following section.

Mate preferences

During sexual reproduction, we assume that only one out of the two sexes expresses a mate preference, as often observed in sexual reproduction where females are usually choosier. Thus we assume females to be the choosy sex. The mate preference of female is then considered strict, implying that choosy individuals never mate with individuals displaying their non-preferred phenotype. Two hypothetical mate preference mechanisms are investigated.

Under the *self-referencing* hypothesis (hyp 1), three alleles are assumed at loci M , coding for (i) random mating r , (ii) assortative mating sim and (iii) disassortative mating dis respectively (see Figure A1.1 for more details), ($\mathcal{A}_M = \{r, sim, dis\}$). We assume that the *self-referencing* preference alleles sim and dis are dominant to the random-mating allele r (see Figure A1.1 for more details). The dominance relationship between the sim and dis alleles is not specified however, because we never introduce these two alleles together. Note that under the *self-referencing* hypothesis (hyp. 1), mate choice depends not only on the color pattern of the male, but also on the phenotype of the female expressing the preference.

The alternative mechanism of mate preference investigated assumes a specific recognition of color patterns acting as mating cue (*recognition/trait*, hyp. 2). Under hyp. 2, four alleles segregate at locus M : allele m_r , coding for an absence of color pattern recognition (leading to random mating behavior), and alleles m_a , m_b and m_c coding for specific recognition of color pattern phenotypes A , B and C ($\mathcal{A}_M = \{m_r, m_a, m_b, m_c\}$). The *no-preference* allele m_r is recessive to all the preference alleles m_a , m_b and m_c , and preference alleles are co-dominant, so that females with heterozygous genotype at locus M may recognize two different color pattern phenotypes. Then, the recognition enabled by preference alleles m_a , m_b and m_c triggers either *attraction* (hyp. 2.a) or *rejection* (hyp. 2.b) toward the recognized color pattern, leading to assortative or disassortative mating depending on the genotype i of the female and the color pattern phenotype of the male (see Figure A1.2 and Figure A1.3 for more details).

Genotype frequencies in the progeny

We assume separate sexes and obligate sexual reproduction, and therefore compute explicitly the Mendelian segregation of alleles during reproduction, assuming a recombination rate ρ between the color pattern locus P and the preference locus M . We assume that the frequency of males and females of a given phenotype is the same. For $i = (p_m, p_f, m_m, m_f) \in \mathcal{G}, n \in \{1, 2\}$, the frequency of genotype i in the progeny in patch n ($F_{i,n}$) then also depends on the frequencies of each genotype in the patch and on the mate preferences of females computed in equation (1.13). We introduce the preference coefficients $(c_{i,J}^{pref})_{(i,J) \in \mathcal{G} \times \{A,B,C\}}$. These coefficients depend on the alleles at locus M as detailed in the next section. For $i = (p_m, p_f, m_m, m_f) \in \mathcal{G}, J \in \{A, B, C\}$ the preference coefficient $c_{i,J}^{pref}$ is defined as $c_{i,J}^{pref} = 1$ when females with genotype i accept males with phenotype J as mating partners and $c_{i,J}^{pref} = 0$ otherwise.

For $i = (p_m, p_f, m_m, m_f) \in \mathcal{G}, n \in \{1, 2\}$, we define $T_{i,n}$ as the probability that a female of genotype i in patch n accepts a male during a mating encounter (see (Otto *et al.*, 2008)):

$$T_{i,n} = c_{i,A}^{pref} P_{A,n} + c_{i,B}^{pref} P_{B,n} + c_{i,C}^{pref} P_{C,n}, \quad (1.8)$$

where for $J \in \{A, B, C\}$, $P_{J,n} = \frac{\sum_{i \in \mathcal{G}} N_{i,n} \mathbb{1}_{\{T_{g \rightarrow cp}(i)=J\}}}{\sum_{i \in \mathcal{G}} N_{i,n}}$ denotes the frequency of phenotype J in patch n .

Because choosy individuals might have a reduced reproductive success due to limited mate availability (Kirkpatrick & Nuismer, 2004; Otto *et al.*, 2008), we also assume a relative fitness cost associated with choosiness. This cost is modulated by the parameter c_r . When this cost is absent ($c_r = 0$), females have access to a large quantity of potential mates, so that their mating rate is not limited when they become choosy ("Animal" model). When this cost is high ($c_r = 1$), females have access to a limited density of potential mates, so that their mating rate tends to decrease when they become choosy ("Plant" model). Intermediate values of c_r imply that females can partially recover the fitness loss due to the encountering of

non-preferred males towards reproduction with other males. This cost of choosiness is known to limit the evolution of assortative mating (Otto *et al.*, 2008) and may thus also limit the emergence of disassortative mating.

Following (Otto *et al.*, 2008) we compute the mating rate $M_{i,n}$ of a female with genotype i in patch n :

$$M_{i,n} = 1 - c_r + c_r T_{i,n}. \quad (1.9)$$

We note \bar{M}_n the average mating rate in patch n defined as

$$\bar{M}_n = \sum_{i \in \mathcal{G}} f_{i,n} M_{i,n}, \quad (1.10)$$

where for $i = (p_m, p_f, m_m, m_f) \in \mathcal{G}$, $n \in \{1, 2\}$, $f_{i,n}$ is the frequency of genotype i in patch n .

For $(j, k) \in \mathcal{G}^2$, the quantity

$$\frac{f_{j,n} M_{j,n}}{\bar{M}_n}, \quad (1.11)$$

is the probability that, given that a female has mated in patch n , this female is of genotype j , and

$$\frac{c_{j, T_{g \rightarrow cp}(k)}^{pref} f_{k,n}}{T_{j,n}} = \frac{c_{j, T_{g \rightarrow cp}(k)}^{pref} f_{k,n}}{c_{j,A}^{pref} P_{A,n} + c_{j,B}^{pref} P_{B,n} + c_{j,C}^{pref} P_{C,n}}, \quad (1.12)$$

is the probability that, given that a female of genotype j has mated in patch n , its mate is a male of genotype k , depending on female preference and availability of males carrying genotype k .

For $i = (p_m, p_f, m_m, m_f) \in \mathcal{G}$, $n \in \{1, 2\}$, the frequency of genotype i in the

progeny of the population living in patch n is

$$F_{i,n} = \sum_{(j,k) \in \mathcal{G}^2} c_{seg}(i, j, k, \rho) \times \underbrace{\frac{f_{j,n} M_{j,n}}{\bar{M}_n}}_{\substack{\text{probability, given that} \\ \text{a female has mated, that this} \\ \text{female is of genotype } j}} \times \underbrace{\frac{c_{j,Tg \rightarrow cp}^{pref} f_{k,n}}{T_{j,n}}}_{\substack{\text{probability, given that a female} \\ \text{of genotype } j \text{ has mated,} \\ \text{that her mate is a male of genotype } k}}, \quad (1.13)$$

where $c_{seg}(i, j, k, \rho)$ controls the mendelian segregation of alleles during reproduction between an individual of genotype j and an individual of genotype k , depending on the recombination rate ρ between the color pattern locus P and the preference locus M (see Appendix A1.1 for detailed expression of $c_{seg}(i, j, k, \rho)$).

Model exploration

The complexity of this two-locus diploid model prevents comprehensive exploration with analytical methods, we therefore used numerical simulations to identify the conditions promoting the evolution of disassortative mating. All parameters and parameter intervals used in the different simulations are summarized in Table 2. The values of the basic predation mortality factor d_m and d_{n-m} , the unpalatability λ and migration rate m are chosen as conditions maintaining balanced polymorphism at the color pattern locus P assuming random mating, taken from (Joron & Iwasa, 2005).

Simulations are performed using Python v.3. and by using discrete time steps as an approximation (Euler method) (see Appendix A1.2 for more details about the numeric resolution). We checked that reducing the magnitude of the time step provided similar dynamics (see Figure A1.4), ensuring that our discrete-time simulations provide relevant outcomes.

Abbreviation	Description
$N_{i,n}$	Density of individuals with genotype i in patch n
$\Delta_{i,n}^{pred}$	Change in the density of individuals with genotype i caused by predation
$\Delta_{i,n}^{rep}$	Change in the density of individuals with genotype i caused by reproduction
$\Delta_{i,n}^{mig}$	Change in the density of individuals with genotype i caused by migration
$\Delta_{i,n}^{mort}$	Change in the density of individuals with genotype i caused by mortality
$T_{g \rightarrow cp}(i)$	Color pattern phenotype of individuals with genotype i
$c_{i,J}^{pref}$	Preference of individuals with genotype i towards individuals with phenotype J
$f_{i,n}$	Frequency of genotype i in patch n
$P_{I,n}$	Frequency of phenotype I in patch n
$T_{i,n}$	Probability that a female of genotype i in patch n accepts a male as mating partner during one mating encounter
$M_{i,n}$	Mating rate of females with genotype i in patch n
\overline{M}_n	Average female mating rate in patch n
$F_{i,n}$	Frequency of genotype i in the progeny of the population living in patch n
P_{s-acc}	Proportion of individuals expressing a self-accepting behavior
P_{s-av}	Proportion of individuals expressing a self-avoidance behavior

Table 1.1: **Description of variables used in the model.**

Abbreviation	Description	Parameter interval
\mathcal{A}_P	Set of all possible alleles at locus P	$\{a, b, c\}$
\mathcal{A}_M	Set of all possible alleles at locus M	$\{r, sim, dis\}$ (hyp. 1) $\{m_r, m_a, m_b, m_c\}$ (hyp. 2)
\mathcal{G}	Set of all possible genotypes	$\mathcal{A}_P \times \mathcal{A}_P \times \mathcal{A}_M \times \mathcal{A}_M$
$N_{tot,n}^0$	Initial population density in patch n	100
d_m	Basic predation mortality factor for individuals displaying the color pattern matching the local community	0.05
d_{n-m}	Basic predation mortality factor for individuals displaying a color pattern different from the local community	0.15
λ	Unpalatability coefficient	0.0002
m	Migration rate	[0,1]
ρ	Recombination rate	[0, 0.5]
r	Growth rate	1
K	Carrying capacity within each patch	2000
δ	Baseline mortality rate	0.1
δ_i	Genetic load linked to allele i	[0, 1]
c_r	Relative cost of choosiness	[0, 1]

Table 1.2: **Description of parameters used in the model and range explored in simulations.**

Introduction of preference alleles

We assume that random mating is the ancestral preference behavior. Before introducing preference alleles, we therefore introduce color pattern alleles in equal proportions, and let the population evolve under random mating until the dynamical system reaches an equilibrium. We assume that a steady point is reached when the variation of genotype frequencies in the numerical solution during one time unit is below 10^{-5} (see Appendix A1.3 for more details). At this steady state, we then introduce the preference allele *dis* in proportion 0.01 (when exploring hyp. 1) or the preference alleles m_a, m_b, m_c in proportion $\frac{0.01}{3}$ (when exploring hyp. 2).

After the introduction of preference alleles, we follow the evolution of disassortative mating and its consequences in the two populations:

- Early dynamic : First, we identify the range of parameters enabling the emergence of disassortative mating, by tracking genotype numbers during the first 100 time steps after the introduction of preference alleles.
- Steady state : Then, we study the long-term evolutionary outcome associated with the changes in mating behavior, by computing genotype numbers at equilibrium, *i.e.* by running simulations until the variation of genotype frequency during one time unit is below 10^{-5} (see Supp. 4 for more details).

Summary statistics

To facilitate the interpretation of our results, we compute a number of summary statistics from the outcomes of our simulations. We define haplotypes as the pairs of alleles in $\mathcal{A}_P \times \mathcal{A}_M$ containing two alleles located on the same chromosome or inherited from the same parent. We then calculate haplotype frequencies in patch n $(f_{p,m,n}^{haplo})_{(p,m) \in \mathcal{A}_P \times \mathcal{A}_M}$ for $n \in \{1, 2\}$. Then for $(p, m, n) \in \mathcal{A}_P \times \mathcal{A}_M \times \{1, 2\}$, the

frequency of haplotype (p, m) in patch n is given by:

$$f_{p,m,n}^{haplo} = \frac{\sum_{i=(p_m,p_f,m_m,m_f) \in \mathcal{G}} N_{i,n} (\frac{1}{2} \mathbb{1}_{\{p_m=p\}} \mathbb{1}_{\{m_m=m\}} + \frac{1}{2} \mathbb{1}_{\{p_f=p\}} \mathbb{1}_{\{m_f=m\}})}{\sum_{i=(p_m,p_f,m_m,m_f) \in \mathcal{G}} N_{i,n}}. \quad (1.14)$$

The estimation of haplotype frequencies allows to characterize the association between color pattern alleles and preference alleles, leading to different mating behaviors among partners with different color patterns, specifically under the *recognition/trait* hypothesis (Hyp.2). To characterize female mating preferences generated by the different genotypes at locus M and the link with their own color pattern phenotype, we then distinguish two main behaviors emerging under hyp. 2 (Figures A1.2 and A1.3) for *attraction* (hyp. 2.a) and *rejection* (hyp. 2.b) hypotheses respectively:

- Self-acceptance : females mate with males displaying their own color pattern phenotype.
- Self-avoidance : females do not mate with males displaying their own color pattern phenotype.

In order to compare the mating behaviors observed under *self-referencing* (hyp. 1) *attraction* (hyp. 2.a) and *rejection* (hyp. 2.b) hypotheses, we compute population statistics, P_{s-acc} (see equation (1.15)) and P_{s-av} (see equation (1.16)) as the proportion of individuals exhibiting respectively a self-acceptance or a self-avoidance behavior throughout both patches. These two inferred behaviors can be directly compared with mate preferences empirically estimated. For example, in experiments where females can choose partners among males displaying different color patterns (Chouteau *et al.*, 2017), the proportion of females mating with males displaying their own phenotype color pattern can be easily scored and compared to the proportion of self-accepting individuals computed in our model.

$$P_{s-acc} = \sum_{i \in \mathcal{G}} f_i c_{i, T_{g \rightarrow cp}(i)}^{pref}, \quad (1.15)$$

$$P_{s-av} = \sum_{i \in \mathcal{G}} f_i (1 - c_{i, T_{g \rightarrow cp}(i)}^{pref}). \quad (1.16)$$

Data and Code Accessibility

Codes are available online: github.com/Ludovic-Maisonneuve/Evolution_and_genetic_architecture_of_disassortative_mating.

Results

Effect of mate choice on polymorphism

The emergence of disassortative mating requires initial polymorphism at the trait used as mating cue. Because the costs associated with mate searching and courting penalize females preferring rare phenotypes, the distribution of color pattern variation in the population may be an important condition for the emergence of disassortative mating. In turn, the evolution of disassortative mating is likely to generate a positive selection on rare phenotypes, therefore enhancing polymorphism at the color pattern locus P . To disentangle the feedbacks between polymorphism of the cue and evolution of disassortative mating, we first investigate the impact of different mating behaviors on the distribution of color pattern phenotypes within populations.

Under random mating, the frequencies of color pattern alleles at equilibrium computed for different migration rates m show that polymorphism can be maintained through an equilibrium between spatially heterogeneous selection and migration (Figure 1.1(a)), consistent with previous results from the literature (Joron & Iwasa, 2005). In the absence of migration however, phenotypes A and B are fixed in the

populations living in patch 1 and 2 respectively, owing to their mimetic advantage within their respective communities. Polymorphism with persistence of phenotypes A and B within each population can only be maintained with migration, but in all cases phenotype C , locally non-mimetic in both patches, is not maintained in any of the two populations (Figure 1.1(a)).

To test the effect of mate choice on this selection/migration equilibrium, we then compare those simulations assuming random mating (*i.e.* with preference alleles r) with simulations where *self-referencing* preference alleles generating either assortative (*sim* allele) or disassortative (*dis* allele) behavior were introduced at the mate choice locus M (hyp. 1), assumed to be fully linked to the color pattern locus P ($\rho = 0$). Assuming assortative mating via *self-referencing* (hyp. 1) the results are similar to those observed under random mating (Figures 1.1(a) and 1.1(b)). Nevertheless, the proportion of locally adapted alleles is higher than under random mating because assortative mating reinforces positive frequency dependent selection on those alleles. In contrast, disassortative mating maintains a higher degree of polymorphism, with the two locally mimetic phenotypes A and B and the locally non-mimetic phenotype C persisting within both populations, for all migration rates (Figure 1.1(c)). The locally non-mimetic phenotype C is rarely expressed because allele c is recessive. Nevertheless, individuals displaying phenotype C benefit from a high reproductive success caused by disassortative mating. Indeed, the strict disassortative preference assumed here strongly increases the reproductive success of individuals displaying a rare phenotype such as C . Negative frequency-dependent selection (FDS hereafter) on color pattern thus generated by disassortative mating counteracts the positive FDS due to predator behavior acting on the same trait. Therefore, disassortative mate preferences can strongly promote polymorphism within the two populations living in patch 1 and 2 respectively. When polymorphism is high, the cost of finding a dissimilar mate may be reduced, therefore limiting selection against disassortative preferences. Our results thus highlight the decreased cost of finding a dissimilar mate once disassortative mating becomes established.

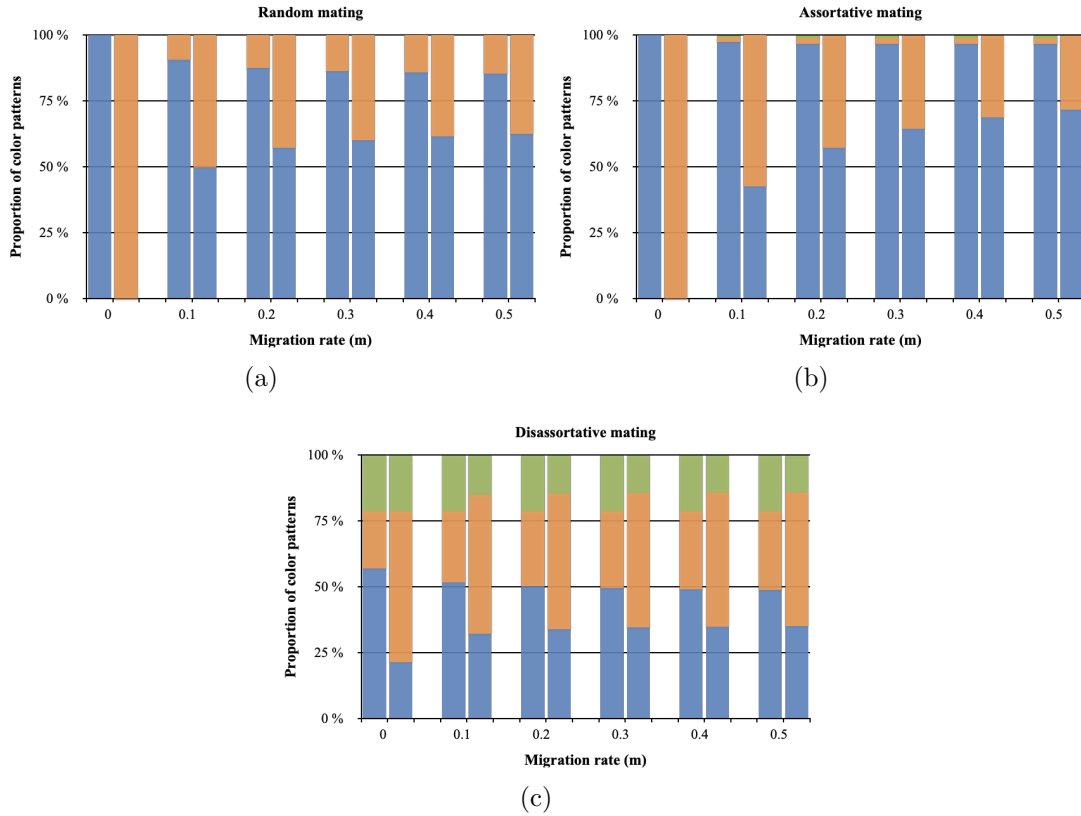


Fig. 1.1: Influence of mate preferences on color pattern diversity within both patches. The equilibrium frequencies of color pattern phenotypes in patches 1 and 2 for different migration rates m are computed assuming different mating behaviors, *i.e.*, random (a), assortative (b) or disassortative (c). The heights of the colored bars indicate the frequencies of color pattern phenotypes A , B and C (blue, orange and green areas respectively) in patches 1 and 2 (on the left and right side respectively, for each migration level). The three alleles at the locus P controlling color pattern variations are introduced in proportion $\frac{1}{3}$ in each patch. The locus M controls for the *self-referencing* based mate preferences (hyp. 1): preferences alleles r , sim and dis were introduced in simulations shown in panel (a), (b) and (c) respectively. Simulations are run assuming $r = 1$, $K = 2000$, $N_{tot,1}^0 = N_{tot,2}^0 = 100$, $\lambda = 0.0002$, $d_m = 0.05$, $d_{n-m} = 0.15$, $\rho = 0$, $c_r = 0.1$, $\delta_a = \delta_b = \delta_c = 0$ and $\delta = 0.1$.

Linked genetic load favors the persistence of maladaptive alleles

In the following simulations, the migration parameter m is set to 0.1, to allow for the persistence of polymorphism of color pattern phenotype A and B when assuming random mating. We then investigate the influence of a genetic load

associated with the different color pattern alleles on polymorphism at the color pattern locus P , under random mating. This allows quantifying the effect of heterozygote advantage, independently of the evolution of mating preferences. We observe that the locally non-mimetic phenotype C is maintained together with phenotypes A and B within both populations, when (i) all three alleles carry a genetic load of similar strength, *i.e.* $\delta_a = \delta_b = \delta_c > 0$ or (ii) when allele c is the only one without any associated genetic load ($\delta_a = \delta_b > 0$ and $\delta_c = 0$) (Figure A1.5). In contrast, phenotype C is not maintained when a genetic load is associated with allele c only ($\delta_a = \delta_b = 0$ and $\delta_c > 0$), or when this load is stronger than the one associated with alleles a and b (Figure A1.5). The heterozygote advantage generated by genetic load associated with the dominant mimetic alleles at locus P therefore favors the persistence of a balanced polymorphism and more specifically promotes the maintenance of allele c in both patches, even though this allele does not bring any benefit through local (mimicry) adaptation.

Evolution of disassortative mating

Because we expect heterozygote advantage at the color pattern locus P to enhance the evolution of disassortative-mating allele at locus M , we first investigate the influence of a genetic load on the evolution of disassortative behavior by testing the invasion of *self-referencing* mutation triggering self-avoidance *dis* (hyp. 1) in a population initially performing random mating with genotype frequencies at equilibrium. We compute the frequency of mutants 100 time units after their introduction, assuming full linkage between loci P and M . Figure 1.2 shows that the genetic load associated with alleles a and b ($\delta_a = \delta_b$), has a strong positive impact on the emergence of disassortative mating. The genetic load associated with the recessive allele c (δ_c) has a weaker positive effect on the evolution of disassortative mating. Simulations assuming different relative cost of choosiness (c_r) show a similar effect of associated genetic loads (Figure 1.2). However the cost of choosiness reduces the range of genetic load values allowing the emergence of disassortative preference. When this cost is high, the invasion of mutant allele *dis*

is prevented, regardless of the strength of genetic load (Figure 1.2(d)). Although an increased cost of choosiness slows down the invasion of the disassortative mating mutant *dis* (Figure 1.2), a genetic load linked to the color pattern locus *P* generally favors the emergence of disassortative mating in both patches.

To investigate the long-term evolution of disassortative mating promoted by the genetic loads associated with color pattern alleles, we then compute the frequency of mutant allele *dis* at equilibrium in conditions previously shown to promote its emergence (*i.e.* assuming limited cost of choosiness). Figure 1.3 shows that the mutant preference allele *dis* is never fixed within populations. This suggests that the heterozygote advantage at locus *P* allowing the emergence of disassortative mating decreases when this behavior is common in the population. The *dis* mutant nevertheless reaches high frequencies when the genetic load associated with the recessive allele *c* is intermediate ($\delta_c \approx 0.35$) and the genetic load associated with dominant alleles *a* and *b* is strong (Figure 1.3). This result seems surprising because the highest level of disassortative mating is not reached when the genetic load is the highest in all the three alleles at locus *P*. On the contrary, disassortative mating is favoured when a genetic load is associated with the dominant alleles only: disassortative mating produces fitter offspring (*i.e.* expressing no genetic load), when the genetic load is associated with dominant alleles. Indeed dominant alleles are always expressed as color pattern phenotypes, and therefore females carrying at least one dominant allele linked with a genetic load avoid mating with males carrying at least the same allele.

How does the genetic architecture of mating preference influence the evolution of disassortative mating ?

To study the impact of the genetic architecture of mate preferences on the evolution of disassortative mating, we then compare the invasion of *self-referencing* alleles *dis* with the invasion of *recognition/trait* alleles (*i.e.* alleles m_r , m_a , m_b and m_c controlling random mating and specific recognition of phenotype *A*, *B* and *C* respectively, hyp. 2). We assume loci *P* and *M* to be fully linked ($\rho = 0$),

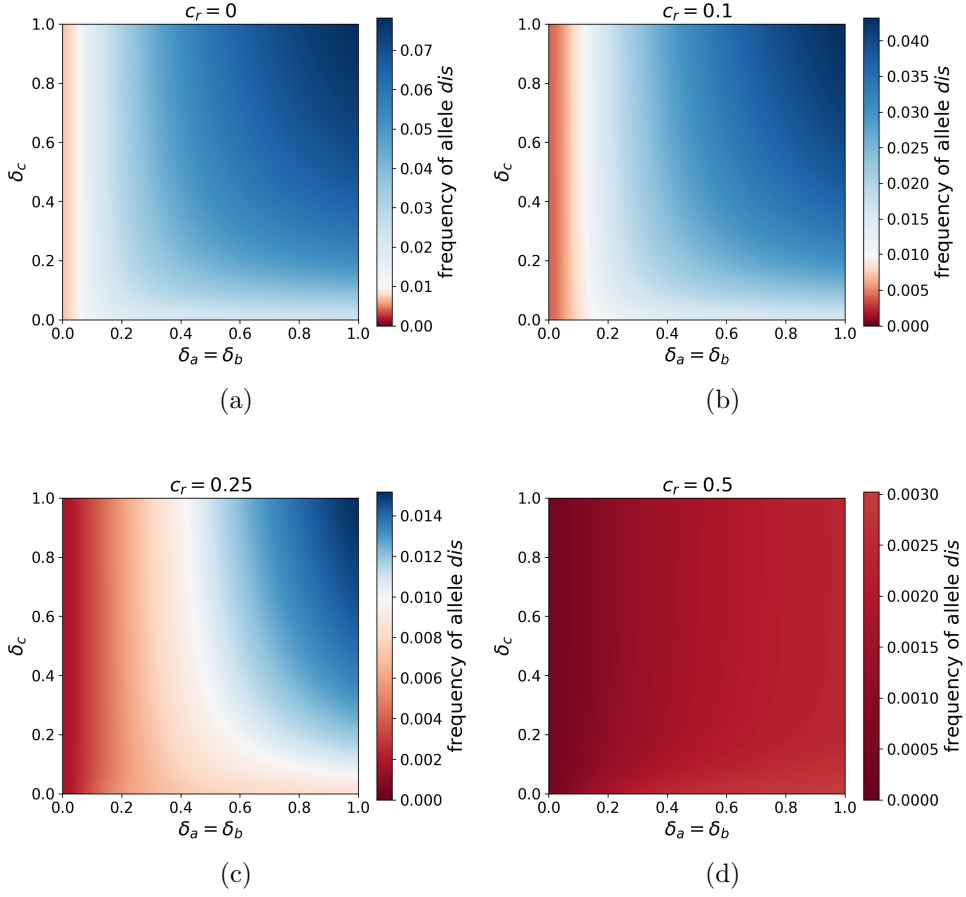


Fig. 1.2: **Influence of a linked genetic load on the emergence of disassortative mating for different costs of choosiness, assuming *self-referencing* (hyp. 1).** The frequency of the mutant disassortative-mating allele *dis* is shown 100 time units after its introduction depending on the strength of genetic load associated with the dominant alleles *a* and *b*, $\delta_a = \delta_b$, and to the recessive allele *c*, δ_c . The initial frequency of allele *dis* was 0.01, the area where mutant allele increase (resp. decrease) is shown in blue (resp. red). Simulations are run assuming either (a) no cost of choosiness $c_r = 0$, (b) a low cost of choosiness $c_r = 0.1$, (c) an intermediate cost of choosiness $c_r = 0.25$ or (d) an elevated cost of choosiness $c_r = 0.5$. Simulations are run assuming $r = 1$, $K = 2000$, $N_{tot,1}^0 = N_{tot,2}^0 = 100$, $\lambda = 0.0002$, $d_m = 0.05$, $d_{n-m} = 0.15$, $m = 0.1$ and $\rho = 0$.

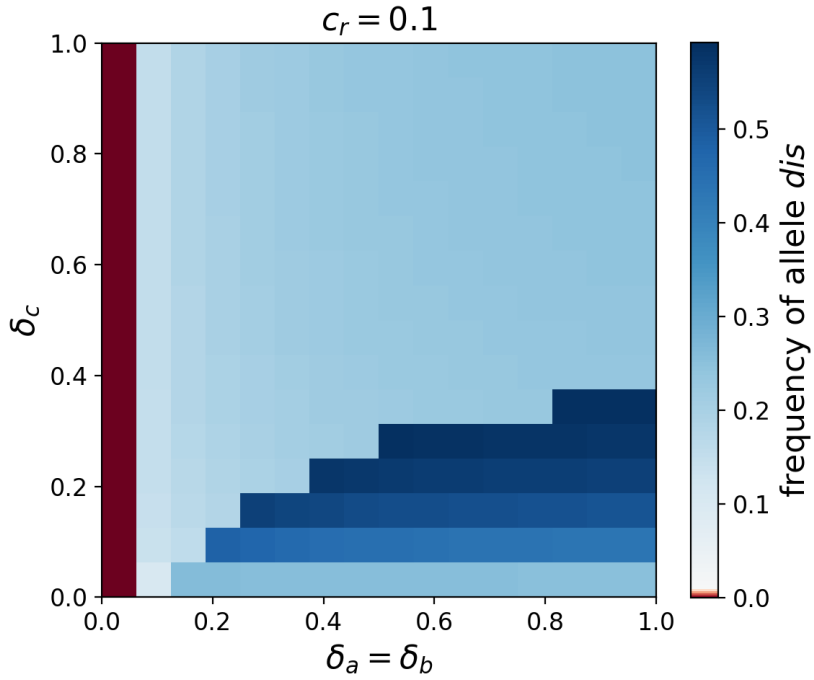


Fig. 1.3: **Influence of a linked genetic load on the level of disassortative mating at equilibrium for low cost of choosiness ($c_r = 0.1$), assuming *self-referencing* (hyp. 1).** The frequency of the mutant disassortative-mating allele *dis* is shown at equilibrium after its introduction depending on the strength of genetic load associated with the dominant alleles *a* and *b* ($\delta_a = \delta_b$) and with the recessive allele *c*, δ_c . The initial frequency of allele *dis* is 0.01. The area where the frequency of the mutant allele increases (resp. decrease) is shown in blue (resp. red). Simulations are run assuming $r = 1$, $K = 2000$, $N_{tot,1}^0 = N_{tot,2}^0 = 100$, $\lambda = 0.0002$, $d_m = 0.05$, $d_{n-m} = 0.15$, $m = 0.1$, $\rho = 0$ and $c_r = 0.1$.

and compare simulations where mate preference alleles trigger either disassortative preference (hyp. 1), *attraction* (hyp. 2.a) or *rejection* (hyp. 2.b) of the recognized color pattern phenotype. We report the frequencies of haplotypes, in order to follow the association of color pattern and preference alleles (Figures 1.4(a), 1.4(b) and 1.4(c) respectively).

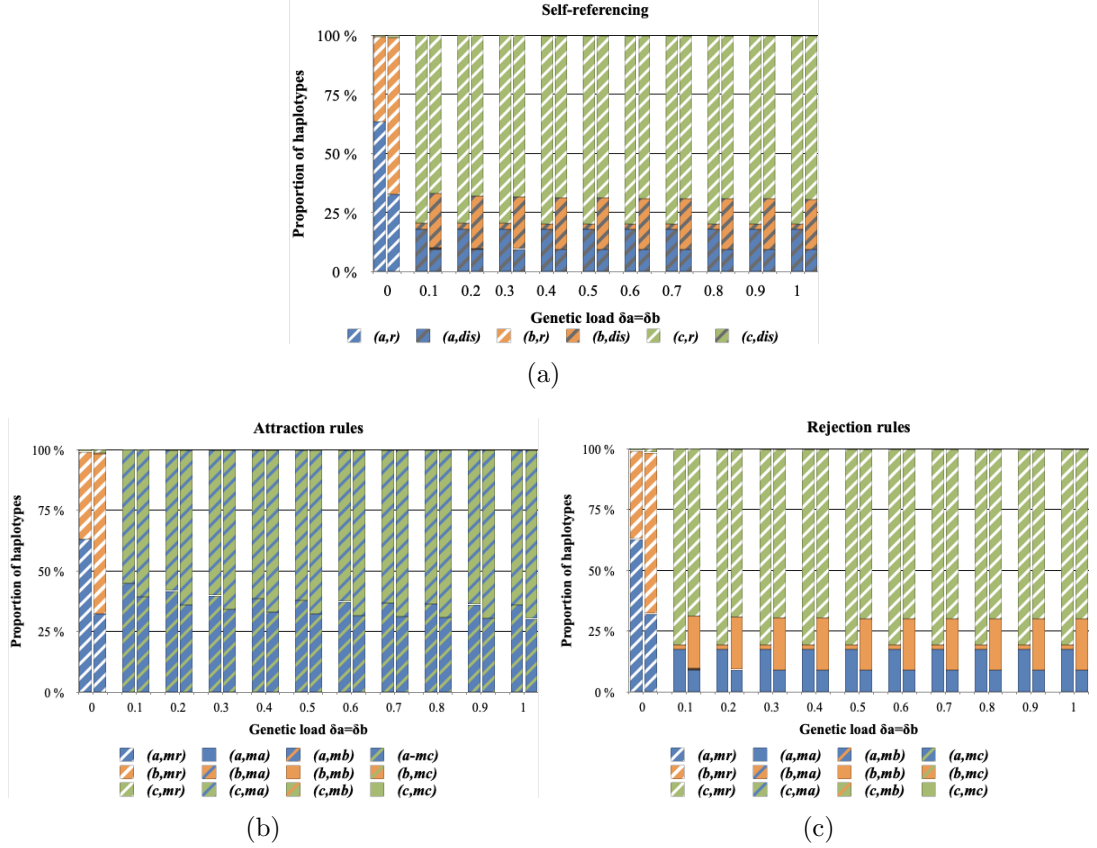


Fig. 1.4: Influence of a genetic load on haplotype diversity, assuming (a) *self-referencing* (hyp. 1), (b) *attraction* rule (hyp. 2.a) or (c) *rejection* rule (hyp. 2.b) at the preference locus (*recognition/trait*). The proportion of haplotypes at equilibrium after the introduction of preference alleles in both patches are shown for different values of genetic load associated with alleles a and b ($\delta_a = \delta_b$). For each value of genetic load ($\delta_a = \delta_b$) the first and second bars show the frequencies of haplotypes in the patches 1 and 2 respectively. Simulations are run assuming $r = 1$, $K = 2000$, $N_{tot,1}^0 = N_{tot,2}^0 = 100$, $\lambda = 0.0002$, $d_m = 0.05$, $d_{n-m} = 0.15$, $\rho = 0$, $m = 0.1$, $\delta_c = 0$, $\delta = 0.1$ and $c_r = 0.1$.

Under a *self-referencing* rule, alleles a and b are associated with preference allele dis when the genetic load associated with the dominant alleles (alleles a and b) is

greater than 0. Indeed disassortative mating favors the production of heterozygotes and reduces the expression of the genetic load in offspring. In contrast, the recessive allele c , not associated with any genetic load, is preferentially linked with the random-mating allele r . This result is surprising because heterozygotes carrying a c allele have a lower predation risk than homozygotes with two c alleles: homozygotes are indeed locally non-mimetic in both patches, while heterozygotes are locally mimetic in one out of the two patches. However, the benefit associated with haplotype (c, dis) through increased production of heterozygous offspring is weak. Because of the genetic load associated with the dominant color alleles a and b , c allele is common in the population, resulting in relatively high frequency of homozygotes with two c alleles, and of heterozygotes with one c allele. Alleles a and b are frequently linked with the disassortative preference allele dis , further promoting the formation of heterozygotes. Since c allele is recessive, disassortative crosses between individuals with phenotype C and either A or B frequently produce progeny with half of the offspring carrying two c alleles, suffering from increased predation. The limited survival of these offspring reduces the benefits associated with the haplotype (c, dis) . Because the dis allele is also associated with a cost of choosiness, linkage between allele c and the random-mating allele r could then be promoted.

When preference alleles cause female attraction to males exhibiting a given phenotype (hyp. 2.a), only haplotypes (a, m_c) and (c, m_a) are maintained in both patches at equilibrium (Figure 1.4(b)). The haplotype (a, m_c) benefits from both positive selection associated with mimicry and limited expression of the genetic load due to the preferential formation of heterozygotes. Haplotype (c, m_a) is maintained because of the benefit associated with the choice of the most frequent mimetic phenotype A , and the limited expression of the locally non-mimetic phenotype C due to c being recessive. The proportion of haplotype (a, m_c) decreases as the genetic load associated with allele a increases. Indeed the mating between two individuals of genotype (a, c, m_c, m_a) becomes more likely and leads to the formation of individuals (a, a, m_c, m_c) suffering from the expression of the genetic load. Allele b is then lost because of the dominance relationships between alleles a and b .

Phenotype A is more commonly expressed than phenotype B : haplotype (c, m_a) is thus favoured over haplotype (c, m_b) , through increased mate availability. Sexual selection caused by disassortative preferences generate a strong disadvantage associate with b allele, ultimately leading to its extinction.

By contrast, when mate preference is based on alleles causing *rejection* behavior (hyp. 2.b) and when a genetic load is associated with the dominant alleles a and b at locus P , these alleles become associated with the corresponding rejection alleles at locus M (*i.e.* (a, m_a) and (b, m_b) have an intermediate frequencies in both patches) (Figure 1.4(c)). Recessive allele c becomes associated with random-mating preference allele r . The three alleles (a , b and c) persist within patches for all positive values of genetic load. This contrasts with the evolutionary outcome observed under attraction rule (hyp. 2.a) where allele b is lost if the genetic load is greater than 0 (Figure 1.4(b)).

We then investigate how these haplotype frequencies translate into individual behaviors in the populations at equilibrium. As highlighted in Figure 1.5, the proportion of each behavior depends more on the existence of a genetic load linked to dominant alleles, than on its strength. The proportion of disassortative mating is similar when assuming *self-referencing* (hyp. 1) and *recognition/trait* leading to rejection (hyp. 2.b) ($P_{s-av} \approx 48\%$) (Figures 1.5(a) and 1.5(c)).

By contrast, when we consider preference alleles leading to *attraction* (hyp. 2.a), the disassortative behavior is scarcer at equilibrium ($P_{s-av} \approx 36\%$) (Figure 1.5(b)). This may seem surprising given that most haplotypes are formed by a color pattern allele linked with an *attraction* allele for a different color pattern (Figure 1.4(b)). Nevertheless, the color pattern allele c is linked to m_a coding for attraction to A . As a consequence, most individuals formed are heterozygous at both the color pattern locus P (with one allele a and one allele c) and at the preference locus M (with one preference allele coding for attraction toward phenotype A and another preference allele triggering attraction toward phenotype C). These double heterozygotes thus benefit from mimicry and avoid the expression of deleterious mutations, and are self-accepting. However, under the *self-referencing* (hyp. 1) or

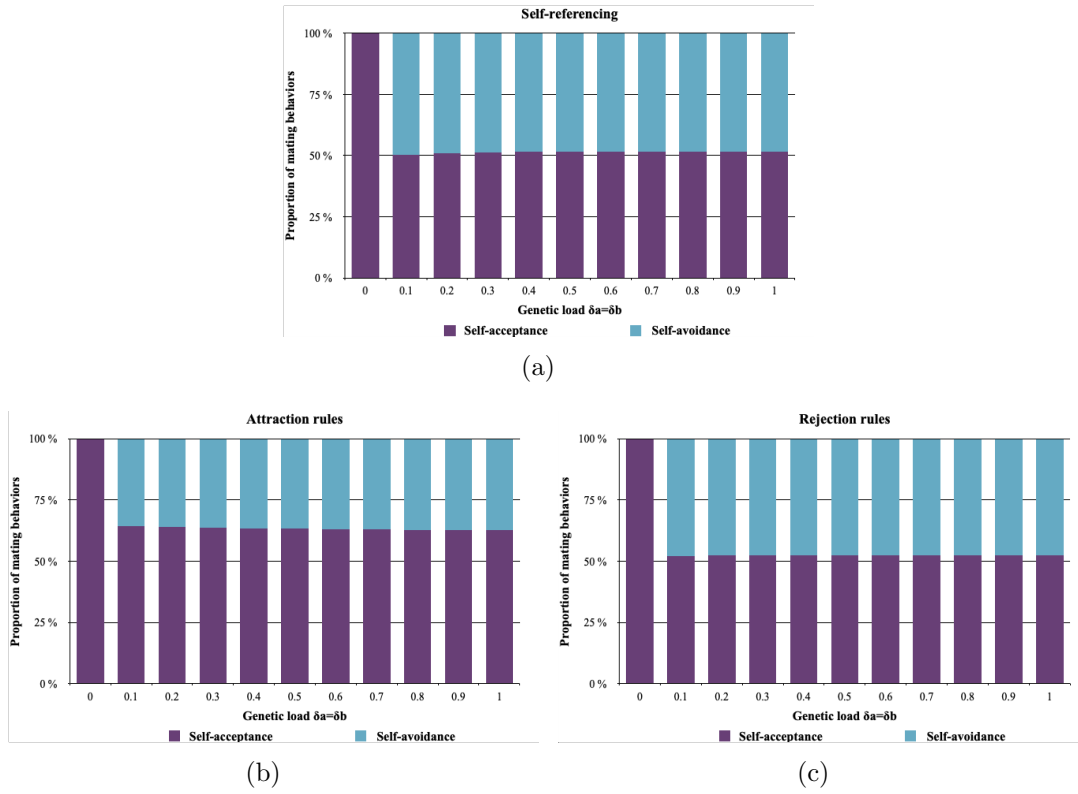


Fig. 1.5: Influence of a genetic load on the distribution of mating behavior observed at the population level, assuming (a) *self-referencing* (hyp. 1), (b) *attraction rule* (hyp. 2.a) or (c) *rejection rule* (hyp. 2.b) at the preference locus (*recognition/trait*). The proportion of individuals displaying self-acceptance P_{s-acc} (in purple) and self-avoidance P_{s-av} (in blue) obtained at equilibrium after the introduction of preference alleles are shown for different values of the level of genetic load of δ_a and δ_b . Simulations are run assuming $r = 1$, $K = 2000$, $N_{tot,1}^0 = N_{tot,2}^0 = 100$, $\lambda = 0.0002$, $d_m = 0.05$, $d_{n-m} = 0.15$, $\rho = 0$, $m = 0.1$, $\delta_c = 0$, $\delta = 0.1$ and $c_r = 0.1$.

rejection (hyp. 2.b) rules disassortative mating is more likely to emerge. Indeed under hyp. 2.b, haplotypes composed by a phenotype allele and its corresponding preference allele ((a, m_a) for example) generally immediately translates into a self-avoiding behavior, whatever the genotypic combinations within individuals. Moreover under hyp. 1 disassortative haplotype, *i.e.* an haplotype where the preference allele is *dis*, always generates a disassortative behavior.

This highlights that the genetic architecture of mate preference plays a key role in the evolution of the mating behavior of diploid individuals: the evolution of

disassortative haplotypes inducing disassortative preferences do not necessarily cause disassortative mating at the population level. At equilibrium, the proportion of self-avoidance behavior in the population hardly depends of the strength of the genetic load (Figure 1.5). However, the strength of the genetic load does increase the speed of evolution of disassortative mating (see Figure A1.6 comparing the invasion dynamics of the self-avoiding behavior when assuming different levels of genetic load), therefore suggesting stronger positive selection on disassortative mating when the genetic load associated with dominant wing color pattern alleles is higher.

Impact of linkage between loci P and M on the evolution of disassortative mating

In previous sections, we observed that the genetic load associated with the two most dominant alleles at the color pattern locus P impacts the evolution of mate choice. Assuming that the color pattern locus P and the preference locus M are fully linked, we also noticed that disassortative mating is more prevalent at equilibrium under the *self-referencing* rule (hyp. 1) and the *rejection rule* (hyp. 2.b) rather than under the *attraction* (hyp. 2.a) rule. We then test the effect of recombination between alleles at the two loci on the evolution of mate choice by performing simulations with different values of the recombination rate ρ .

Assuming *self-referencing* (hyp. 1), increasing recombination rate strongly promotes the self-avoidance behavior ($P_{s-av} \approx 98\%$) (see Figure 1.6(a)). Selection generated by the genetic load associated to color pattern alleles a and b promotes their linkage with the disassortative *self-referencing* allele dis , while the genetic-load free allele c tends to be linked to the random-mating allele r (as observed in simulations assuming no recombination, Figure A1.7(a)). Because allele dis reaches a high frequency in the population, recombination generates a large density of recombinant haplotypes (a, r) , (b, r) , (c, dis) . Haplotypes (a, r) and (b, r) are disfavored because they lead to the production of offspring suffering from the expression of a genetic load, whereas (c, dis) leads to the production of viable off-

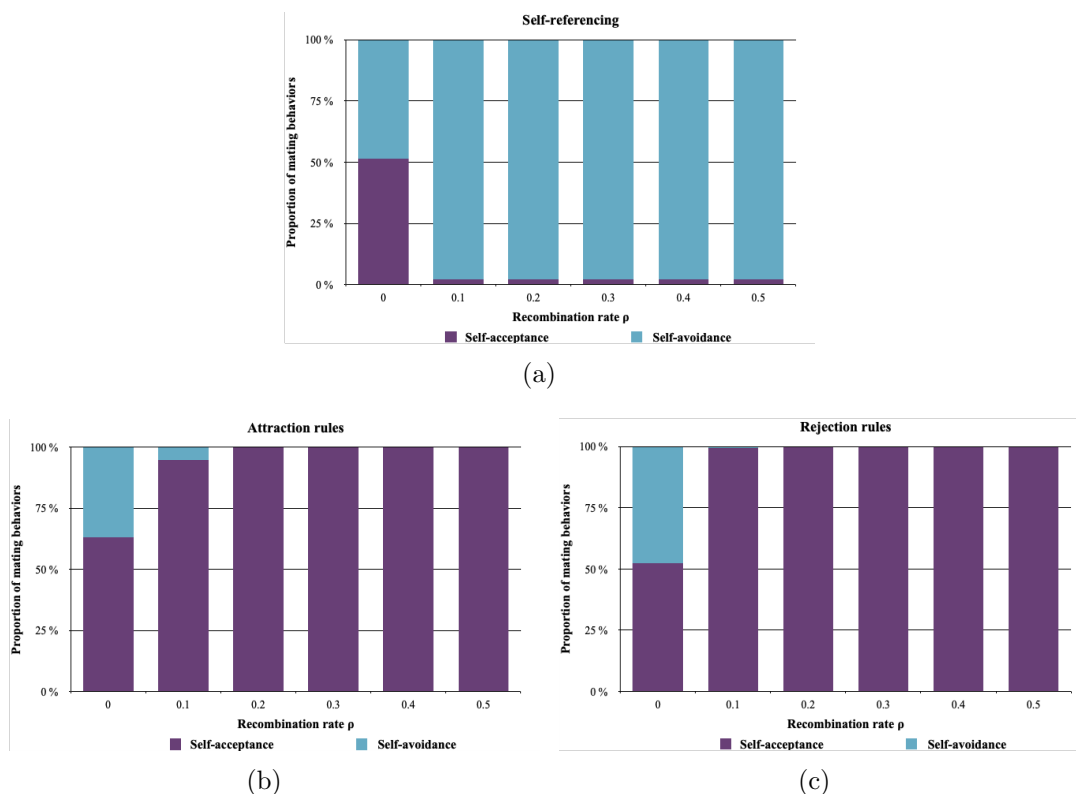


Fig. 1.6: Influence of the recombination rate between color pattern and preference alleles on the distribution of mating behavior observed at the population level, assuming different genetic architectures of mate preferences: either (a) *self-referencing* (hyp. 1), or *recognition/trait* leading to (b) *attraction rule* (hyp. 2.a) or (c) *rejection rule* (hyp. 2.b). The proportion of individuals displaying self-acceptance P_{s-acc} (in purple) and self-avoidance P_{s-av} (in blue) obtained at equilibrium are shown for different values of recombination rate ρ between the preference locus M and the color pattern locus P . Simulations are run assuming $r = 1$, $K = 2000$, $N_{tot,1}^0 = N_{tot,2}^0 = 100$, $\lambda = 0.0002$, $d_m = 0.05$, $d_{n-m} = 0.15$, $m = 0.1$, $\delta_a = \delta_b = 0.5$, $\delta_c = 0$, $\delta = 0.1$ and $c_r = 0.1$.

spring. Therefore, under the *self-referencing* hypothesis (hyp. 1), recombination thus significantly increases the proportion of disassortative mating.

Under *self-referencing* rule (hyp. 1), mate preference depends on the phenotype displayed by the individual, so that allele *dis* always translates into a disassortative behavior. By contrast, when assuming *recognition/trait* for a given color pattern allele (hyp. 2), mating behavior depends only on the genotype at the preference locus M , independently from the color pattern of the female. We therefore expect a stronger effect of recombination rate on mate choice evolution. Figures

1.6(b) and 1.6(c) indeed confirms this prediction. Under *attraction* (hyp. 2.a) and *rejection* (hyp. 2.a) rules, the most striking effect is observed when comparing simulations assuming $\rho = 0$ vs $\rho > 0$: self-avoidance behavior is rarely observed in the population ($P_{s-av} \approx 1\%$) when there is recombination ($\rho > 0$).

Our results suggest that disassortative mating can emerge either (1) under the *self-referencing* rule or (2) under the *recognition/trait* rule assuming a tight linkage between the loci controlling cue and preference. Nevertheless, strict *self-referencing* behaviour, under which preference varies according to the chooser’s phenotype, is rarely observed in natural populations (see Kopp *et al.* (2018) for a review). We thus expect that disassortative mating might emerge when the mating cue and the preference loci are tightly linked or are controlled by a single pleiotropic gene.

Discussion

Genetic architecture of disassortative mating: theoretical predictions

Our model shows that, without recombination between color pattern and preference alleles, disassortative mating is more likely to emerge when the genetic architecture is with *self-referencing* or with color pattern recognition triggering *rejection*. Loci underlying disassortative mating empirically identified are generally consistent with either the *self-referencing* hypothesis (*e.g.* the heterostyly locus in Primulaceae, controlling for different length of style and anthers mechanically preventing assortative mating (Li *et al.*, 2016)), or with the specific *rejection* hypothesis, triggered by molecular recognition (*e.g.* self-incompatibility locus in Brassicaceae (Hiscock & McInnis, 2003) or mating type loci *MAT* in fungi (Billiard *et al.*, 2011)).

Similar mate preference is obtained with some *recognition/trait* genotypes as with some *self-referencing* genotypes: for example, under the *rejection* rule, the genotype (a, a, m_a, m_a) leads to the same mate preference as the genotype (a, a, dis, dis)

under the *self-referencing* genetic architecture. However, our results show that when recombination between the two loci does occur, a *self-referencing* architecture may facilitate the evolution of disassortative mating. Introducing recombination in the *recognition/trait* architecture enables the decoupling of the mating cue and of its corresponding preference alleles, thereby disrupting the self rejection behavior. The evolution of disassortative mating through specific recognition alleles could nevertheless occur, pending their tight linkage with cue alleles, as observed in the well-documented *S*-locus of Brassicaceae. At this *S*-locus, the gene *SCR*, controlling the pollen cue and the gene *SRK* encoding the receptor located in the pistil have been tightly linked over the course of their evolution (Sato *et al.*, 2002). The *S*-locus shows important structural rearrangements that limits the recombination between these two genes (Goubet *et al.*, 2012). This recombination suppression may have favored the evolution of self-incompatibility.

In contrast, the genetic mechanisms involved in disassortative mating are largely unknown in animals. The genetic basis of mate preferences are mostly documented for assortative mating behaviors. Attraction towards specific cues have been documented to trigger assortative mating in *Heliconius* butterflies. The locus controlling preference for yellow *vs.* white in *H. cydno* maps close to the gene *aristaless*, whose expression differences determine the white/yellow switch in this species (Kronforst *et al.*, 2006; Westerman *et al.*, 2018). In *H. melpomene*, a major QTL associated with preference towards red was identified in crosses between individuals displaying a red pattern and individuals with a white pattern (Merrill *et al.*, 2019). This QTL is also located close to the gene *optix* involved in the variation of red patterning in *H. melpomene*. Assortative mating in *Heliconius* thus seems to rely on alleles encoding preference for specific cues, linked to with loci involved in the variation of these cues.

In contrast with the attraction alleles documented in animal species where assortative mating behavior is observed, our results show that alleles coding for rejection of certain cues are more likely to promote the evolution of disassortative mating. Indeed when preference alleles cause *attraction* to males exhibiting a given phenotype, heterozygote advantage favors haplotypes formed by a color pattern

allele linked with an attraction allele for a different color pattern. However, these haplotypes do not necessarily imply a complete self-avoidance behavior in females carrying them. The co-dominance assumed at the preference locus indeed generates preference for two different phenotypes in heterozygotes at the preference locus, favoring self-acceptance. This effect is reinforced by the mate choice, promoting the association between a color allele and the corresponding attraction allele in the offspring, and therefore increasing the emergence of self-accepting genotypes. This might explain the low proportion of self-avoidance behavior observed within populations, when assuming the *attraction* rule.

Altogether, our theoretical model shows that the genetic basis of mate preferences has a strong impact on the evolution of disassortative mating at loci under heterozygote advantage. This emphasizes the need to characterize the genetic basis of mate preference empirically and the linkage disequilibrium with the locus controlling variation in the mating cues.

Evolution of disassortative mating results from interactions between dominance and deleterious mutations

Here, we confirm that the evolution of disassortative mating is promoted by the heterozygote advantage associated with alleles determining the mating cue. As mentioned above, the phenotype of the chosen individuals depends on the dominance relationships at the color pattern locus. Our model highlights that the interaction between dominance and associated genetic load is crucial for the evolution of disassortative mating: when the associated genetic load is low in the recessive cue alleles and large in dominant cue alleles, disassortative mating is favored. Indeed, disassortative mating is advantageous when it favors the production of offspring free from genetic load expression and the dominance allows a direct signalling of the shared deleterious mutations. This theoretical prediction is in accordance with the few documented cases of polymorphism promoted by disassortative mating. In the polymorphic butterfly *Heliconius numata* for instance, the top dominant haplotype *bicoloratus* is associated with a strong genetic load

(Jay *et al.*, 2021). Similarly, in the white throated sparrow, the dominant *white* allele is also associated with a significant genetic load (Tuttle *et al.*, 2016). Again, in the self-incompatibility locus of the *Brassicaceae*, dominant haplotypes carry a higher genetic load than recessive haplotypes (Llaurens *et al.*, 2009). Disassortative mating is beneficial because it increases the number of heterozygous offspring with higher fitness. Once disassortative mating is established within a population, recessive deleterious mutations associated with the dominant haplotype become sheltered because the formation of homozygotes carrying two dominant alleles is strongly reduced, thereby limiting the opportunities for purging via recombination (Llaurens *et al.*, 2009). Falk & Li (1969) proved that disassortative mate choice promotes polymorphism, and therefore limits the loss of alleles under negative selection. Disassortative mating might thus shelter deleterious mutations linked to dominant alleles, and reinforce heterozygote advantage. The sheltering of deleterious mutations is favored by the interaction between two aspects of the genetic architecture: dominance at the mating cue locus and limited recombination. This is likely to happen in polymorphic traits involving chromosomal rearrangements, where recombination is limited. Many rearranged haplotypes are indeed associated with serious fitness reduction as homozygotes (Faria *et al.*, 2019), such as in the derived haplotypes of the supergene controlling plumage and mate preferences in the white-throated sparrow (Thomas *et al.*, 2008). The deleterious elements in the inverted segment can be due to an initial capture by the inversions (Kirkpatrick, 2010), but they could also accumulate through time, resulting in different series of deleterious mutations associated to inverted and non-inverted haplotypes (Berdan *et al.*, 2021).

Here, we assume that mate choice relied purely on a single cue. Nevertheless, mate choice could be based on other cues, controlled by linked loci and enabling discrimination between homozygotes and heterozygotes, thereby further increasing the proportion of heterozygous offsprings with high fitness. We also modelled strict preferences regarding color patterns, but choosiness might be less stringent in the wild, and may limit the evolution of disassortative mating. Depending on the cues and dominance relationships among haplotypes, different mate choice

behaviors may also evolve, which might modulate the evolution of polymorphism within populations. Our model thus stresses the need to document dominance relationships among haplotypes segregating at polymorphic loci, as well as mate choice behavior and cues, to understand the evolutionary forces involved in the emergence of disassortative mating.

Conclusions

Inspired by a well-documented case of disassortative mating based on cues subject to natural selection, our model shows that heterozygote advantage is likely to favor the evolution of disassortative mating. We highlight that disassortative mating is more likely to emerge when loci code for self-referencing disassortative preference or rejection of specific cues. However rejection locus only promotes disassortative mating when they are in tight linkage with the locus controlling mating cue variation.

Acknowledgments

The authors would like to thank Charline Smadi and Emmanuelle Porcher for feedback on the modeling approach developed here. We also thank Thomas Aubier and Richard Merrill and the whole *Heliconius* group for stimulating discussion on mate choice evolution in our favorite butterflies. We are also grateful to Roger Butlin and Tom Van Dooren for their thoughtful review of a previous version of this manuscript. We also thank Sylvain Gerber for his help in improving the English of this article. This work was supported by the Emergence program from Paris City Council to VL. The authors would like to thank the ANR SUPERGENE (ANR-18-CE02-0019) for funding the PhD of LM.

Appendix

A1.1 Mendelian segregation

To compute the proportion of a given genotype in the progeny of the different crosses occurring in the population, we define a function $c_{seg}(g^O, g^M, g^F, \rho)$ summarizing the Mendelian segregation of alleles assuming two diploid loci and a rate of recombination ρ between these loci. Let $g^O = (p_m^O, p_f^O, m_m^O, m_f^O)$, $g^M = (p_m^M, p_f^M, m_m^M, m_f^M)$ and $g^F = (p_m^F, p_f^F, m_m^F, m_f^F)$ be the offspring, maternal and paternal genotypes respectively, all in \mathcal{G} . For $I \in \{O, M, F\}$, p_m^I and m_m^I (resp. p_f^I and m_f^I) are the alleles on the maternal (resp. paternal) chromosomes. $c_{seg}(g^O, g^M, g^F, \rho)$ is the average proportion of genotype g^O in the progeny of a mother of genotype g^M mating with a father of genotype g^F given a recombination rate ρ .

Each diploid mother can produce four types of haploid gametes containing alleles (p_m^M, m_m^M) , (p_f^M, m_f^M) , (p_f^M, m_m^M) or (p_m^M, m_f^M) , in proportion $\frac{1-\rho}{2}$, $\frac{1-\rho}{2}$, $\frac{\rho}{2}$ and $\frac{\rho}{2}$ respectively. Then the proportion of gametes with alleles $(p, m) \in \mathcal{A}_P \times \mathcal{A}_M$ produced by the mother is given by the function $c_{seg-h}(p, m, g^M, \rho)$, where

$$\begin{aligned} c_{seg-h}(p, m, g^M, \rho) &= \frac{1-\rho}{2} \mathbb{1}_{\{p=p_m^M\}} \mathbb{1}_{\{m=m_m^M\}} + \frac{1-\rho}{2} \mathbb{1}_{\{p=p_f^M\}} \mathbb{1}_{\{m=m_f^M\}} \\ &\quad + \frac{\rho}{2} \frac{1-\rho}{2} \mathbb{1}_{\{p=p_f^M\}} \mathbb{1}_{\{m=m_m^M\}} + \frac{\rho}{2} \frac{1-\rho}{2} \mathbb{1}_{\{p=p_m^M\}} \mathbb{1}_{\{m=m_f^M\}}. \end{aligned}$$

Similarly, each diploid father can produce four types of haploid gametes. The proportion of genotype $(p, m) \in \mathcal{A}_P \times \mathcal{A}_M$ in the gametes of a given father is given by the function $c_{seg-h}(p, m, g^F, \rho)$.

The average proportion of genotype g^O in the progeny of a cross between a mother of genotype g^M and a father of genotype g^F given a recombination rate ρ is given by:

$$c_{seg}(g^O, g^M, g^F, \rho) = c_{seg-h}(p_m^O, m_m^O, g^M, \rho) c_{seg-h}(p_f^O, m_f^O, g^F, \rho).$$

A1.2 Numerical resolution

In this study, we used a numerical scheme to simulate our dynamical system. For $(i, n) \in \mathcal{G} \times \{1, 2\}$, let $N_{i,n}^t$ be the numerical approximation of $N_{i,n}(t)$. We use an explicit Euler scheme, therefore we approximate the quantity $\frac{d}{dt}N_{i,n}(t)$ by

$$\frac{N_{i,n}^{t+\Delta t} - N_{i,n}^t}{\Delta t},$$

with Δt being the step time in our simulations.

For $(i, n) \in \mathcal{G} \times \{1, 2\}$, an approximation of equation (1) becomes:

$$\frac{N_{i,n}^{t+\Delta t} - N_{i,n}^t}{\Delta t} = \left(\Delta_{i,n}^{pred}\right)^t + \left(\Delta_{i,n}^{mort}\right)^t + \left(\Delta_{i,n}^{mig}\right)^t + \left(\Delta_{i,n}^{rep}\right)^t.$$

This equation is equivalent to:

$$N_{i,n}^{t+\Delta t} = N_{i,n}^t + \Delta t \left(\left(\Delta_{i,n}^{pred}\right)^t + \left(\Delta_{i,n}^{mort}\right)^t + \left(\Delta_{i,n}^{mig}\right)^t + \left(\Delta_{i,n}^{rep}\right)^t \right).$$

Given $(N_{i,n}^0)_{(i,n) \in \mathcal{G} \times \{1,2\}}$, we can simulate an approximation of the dynamical system.

A1.3 Numerical approximation of equilibrium states

To estimate the equilibrium reached by our dynamical system using simulations assuming different initial conditions, we define the variable V^t quantifying the change in the numerical solution :

$$V^t = \sqrt{\sum_{(i,n) \in \mathcal{G} \in \{1,2\}} \left(\frac{N_{i,n}^{t+\Delta t} - N_{i,n}^t}{\Delta t} \right)^2}.$$

When $\frac{V^t}{N_{tot}} < 10^{-5}$, we assume that the dynamical system has reached equilibrium, with N_{tot} being the total density in both patches.

Figures

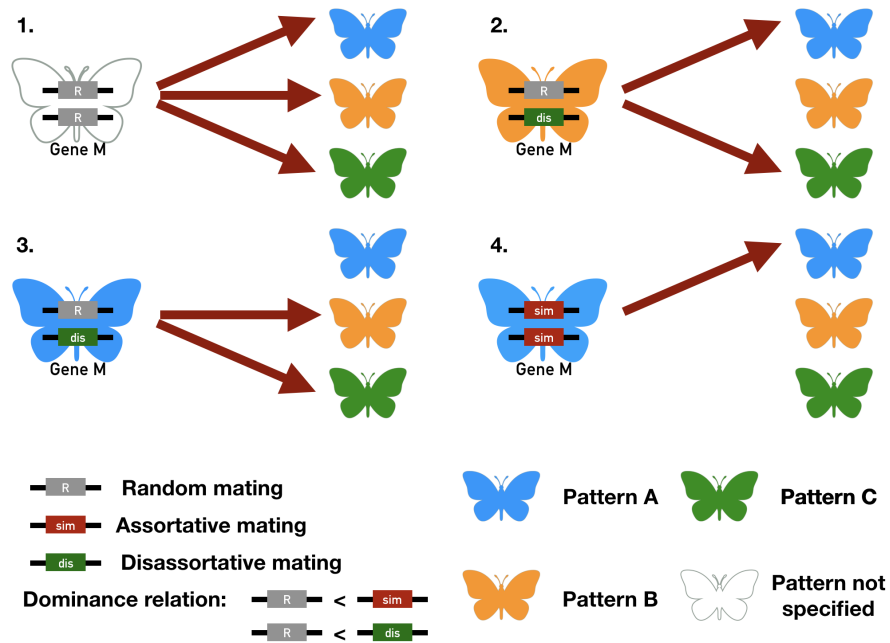


Fig. A1.1: Mate preferences expressed by individuals carrying different genotypes at the preference locus *M*, assuming *self-referencing* (hyp. 1). 1. Butterflies carrying two *r* alleles mate at random, independently of either their own color pattern or the color pattern displayed by mating partners. 2-3. Butterflies carrying a *dis* allele display disassortative mating, and mate preferentially with individuals with a color pattern different from their own. 4. Butterflies carrying a *sim* allele display an assortative mating behavior and therefore preferentially mate with individuals displaying the same color pattern. Cases 1 and 4 therefore lead to *self-acceptance*, while cases 2 and 3 lead to *self-avoidance*.

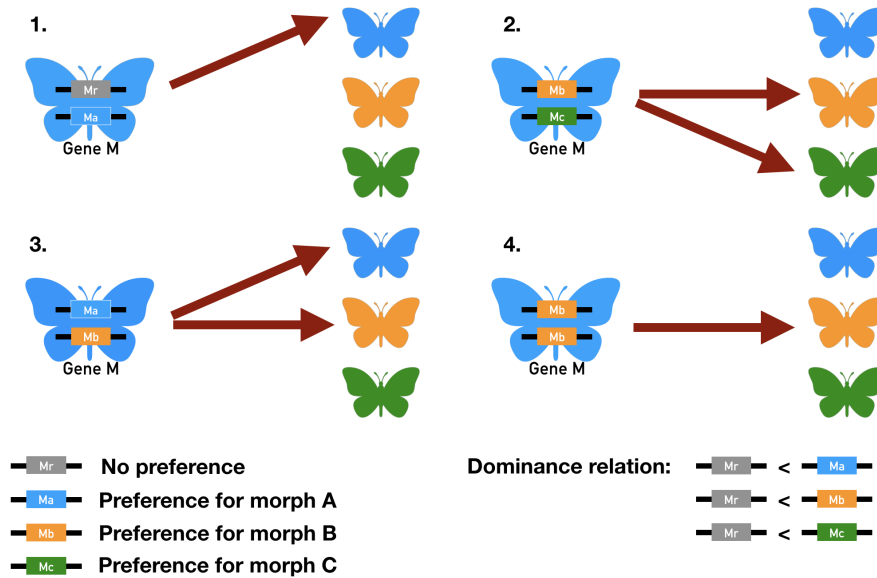


Fig. A1.2: Mate preferences expressed by individuals carrying different genotypes at the preference locus *M*, assuming preference alleles encoding for *attraction of specific color patterns (recognition/trait)* (hyp. 2.a). 1. A butterfly displaying phenotype A (in blue) carries one allele coding for specific attraction toward partners displaying phenotype A (in blue) and the allele coding for random mating at the locus *M* controlling the mate choice. This butterfly will mate preferentially with individuals displaying phenotype A, resulting in assortative mating. 2. A butterfly displaying phenotype A (in blue) carries one allele coding for specific attraction toward partner displaying phenotype B (in orange) and one allele coding for specific attraction toward partners displaying phenotype C (in green). This individual will preferentially mate with individuals displaying phenotype B and C, resulting in disassortative mating. 3. A butterfly displaying phenotype A (in blue) carries one allele coding for specific attraction toward partner displaying phenotype A (in blue) and one allele coding for specific attraction toward partners displaying phenotype B (in orange). This individual will preferentially mate with individuals displaying phenotype A and B. 4. A butterfly displaying phenotype A (in blue) carries two alleles coding for specific attraction toward partner displaying phenotype B (in orange). This individual will preferentially mate with individuals displaying phenotype B, resulting in disassortative mating. Cases 1 and 3 therefore lead to *self-acceptance*, while cases 2 and 4 lead to *self-avoidance*.

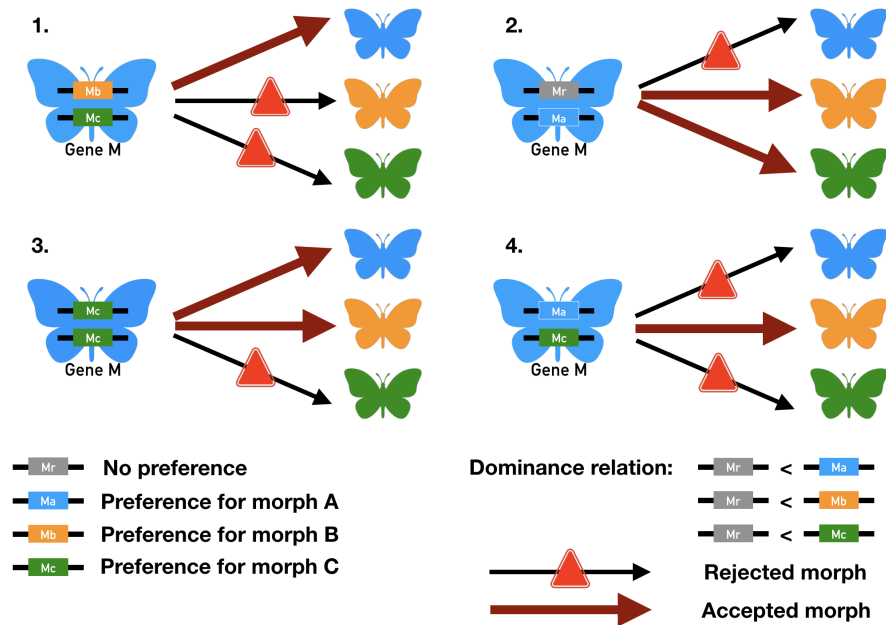


Fig. A1.3: Mate preferences expressed by the different individuals carrying different genotypes at the preference locus *M*, assuming preference alleles encoding for *rejection* of specific color patterns (*recognition/trait*) (hyp. 2.a). 1. A butterfly displaying phenotype A (in blue) carries one allele coding for specific rejection toward partners displaying phenotype B (in orange) and one allele coding for specific rejection toward partners displaying phenotype C (in green). This butterfly will mate preferentially with individuals displaying phenotype A, resulting in assortative mating. 2. A butterfly displaying phenotype A (in blue) carries one allele coding for specific rejection toward partners displaying phenotype A (in orange) and one allele coding for random mating (in grey). This butterfly will mate preferentially with individuals displaying phenotypes B and C, resulting in disassortative mating. 3. A butterfly displaying phenotype A (in blue) carries two alleles coding for specific rejection toward partners displaying phenotype C (in green). This butterfly will mate preferentially with individuals displaying phenotypes A and B. 4. A butterfly displaying phenotype A (in blue) carries one allele coding for specific rejection toward partners displaying phenotype A (in blue) and one allele coding for specific rejection toward partners displaying phenotype C (in green). This butterfly will mate preferentially with individuals displaying phenotype B resulting in disassortative mating. Cases 1 and 3 therefore lead to *self-acceptance*, while cases 2 and 4 lead to *self-avoidance*.

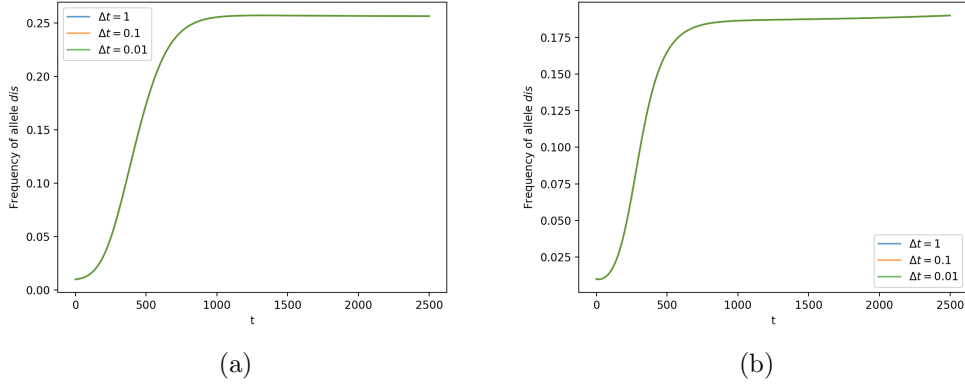
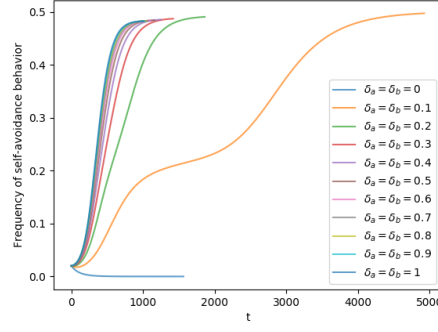


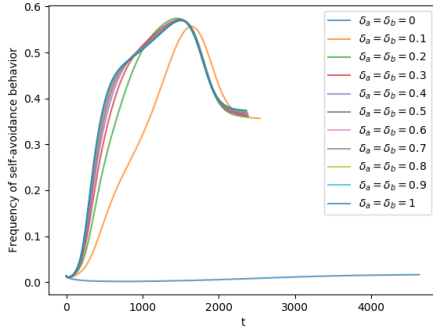
Fig. A1.4: Evolution of the proportion of a mutant *dis* in the population immediately after its introduction, using simulations with three different time units ($\Delta t = 1$ in blue, $\Delta t = 0.1$ in orange or $\Delta t = 0.01$ in green), under the *self-referencing* hypothesis (hyp. 1). All simulations give similar dynamics, assuming (a) $\delta_a = \delta_b = 0.5$, $\delta_c = 0$ or (b) $\delta_a = \delta_b = \delta_c = 0.2$, confirming that using discrete time simulations provides relevant estimations of the evolution of disassortative mating. Simulations are run during 2500 time steps and assuming $r = 1$, $K = 2000$, $N_{tot,1}^0 = N_{tot,2}^0 = 100$, $\lambda = 0.0002$, $d_m = 0.05$, $d_{n-m} = 0.15$, $\rho = 0$, $m = 0.1$, $\delta = 0.1$ and $c_r = 0.1$.

$\delta_1 = \delta_2$	δ_3	Population 1			Population 2		
		Proportion of morph A	Proportion of morph B	Proportion of morph C	Proportion of morph A	Proportion of morph B	Proportion of morph C
0.00	0.00	90.5 %	9.5 %	0.0 %	49.8 %	50.2 %	0.0 %
0.00	0.25	90.5 %	9.5 %	0.0 %	49.8 %	50.2 %	0.0 %
0.00	0.50	90.5 %	9.5 %	0.0 %	49.8 %	50.2 %	0.0 %
0.00	1.00	90.5 %	9.5 %	0.0 %	49.8 %	50.2 %	0.0 %
0.25	0.00	61.8 %	7.7 %	30.6 %	22.3 %	52.1 %	25.6 %
0.25	0.25	78.8 %	17.9 %	3.3 %	36.2 %	57.6 %	6.2 %
0.25	0.50	80.5 %	17.8 %	1.7 %	39.3 %	57.2 %	3.5 %
0.25	1.00	81.6 %	17.6 %	0.8 %	41.5 %	56.6 %	1.8 %
0.50	0.00	54.5 %	5.7 %	39.8 %	18.7 %	49.6 %	31.7 %
0.50	0.25	76.3 %	18.6 %	5.1 %	33.9 %	57.8 %	8.3 %
0.50	0.50	78.7 %	18.7 %	2.6 %	37.5 %	57.7 %	4.8 %
0.50	1.00	80.2 %	18.5 %	1.3 %	40.2 %	57.3 %	2.5 %
1.00	0.00	49.9 %	4.6 %	45.5 %	16.9 %	47.7 %	35.4 %
1.00	0.25	74.6 %	18.9 %	6.5 %	32.7 %	57.4 %	9.8 %
1.00	0.50	77.5 %	19.1 %	3.3 %	36.6 %	57.7 %	5.7 %
1.00	1.00	79.3 %	19.0 %	1.7 %	39.6 %	57.4 %	3.0 %

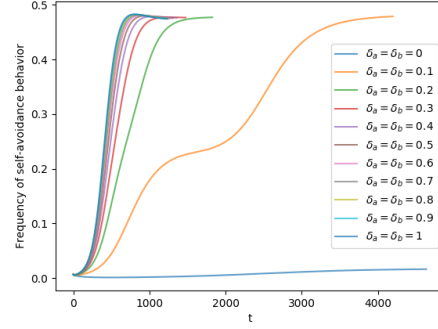
Fig. A1.5: Influence of genetic load on color pattern polymorphism, assuming random mating. The proportions of phenotypes *A*, *B* and *C* in the populations living in patch 1 and 2 respectively at equilibrium depend on the different values of genetic load associated with the dominant allele *a* (δ_a), intermediate-dominant allele *b* (δ_b) and recessive allele *c* (δ_c). Simulations are run assuming $r = 1$, $K = 2000$, $N_{tot,1}^0 = N_{tot,2}^0 = 100$, $\lambda = 0.0002$, $d_m = 0.05$, $d_{n-m} = 0.15$, $\rho = 0$, $m = 0.1$, $\delta = 0.1$ and $c_r = 0.1$.



(a)



(b)



(c)

Fig. A1.6: Frequency of *self-avoidance* behavior at the population level through time for different levels of genetic load, assuming (a) *self-referencing* (hyp. 1), (b) *attraction* rule (hyp. 2.a) or (c) *rejection* rule (hyp. 2.b) at the preference locus (*recognition/trait*). The evolution of the proportion of individuals displaying *self-avoidance* P_{s-av} after the introduction of preference alleles until equilibrium are shown for different values of genetic load δ_a and δ_b . Simulations are run assuming $r = 1$, $K = 2000$, $N_{tot,1}^0 = N_{tot,2}^0 = 100$, $\lambda = 0.0002$, $d_m = 0.05$, $d_{n-m} = 0.15$, $\rho = 0$, $m = 0.1$, $\delta_c = 0$, $\delta = 0.1$ and $c_r = 0.1$.

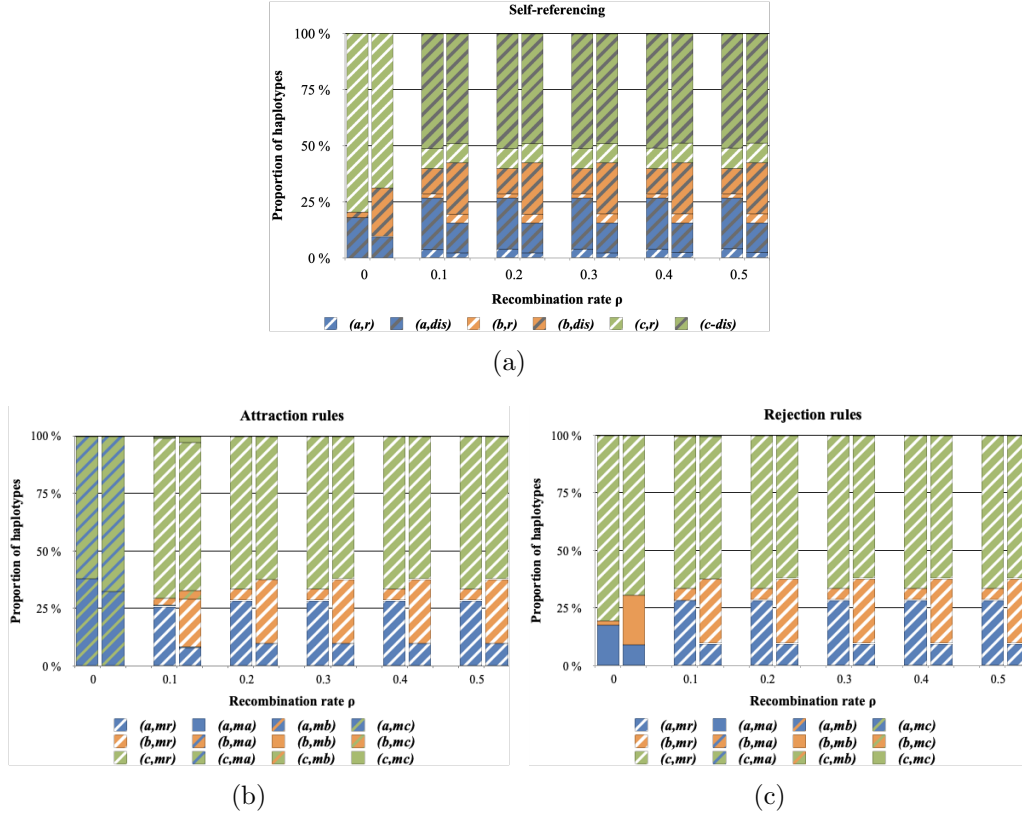


Fig. A1.7: Influence of the recombination between color pattern and preference alleles on haplotype diversity, assuming (a) *self-referencing* (hyp. 1), (b) *attraction rule* (hyp. 2.a) or (c) *rejection rule* (hyp. 2.b) at the preference locus (*recognition/trait*). The proportion of haplotypes at equilibrium after the introduction of preference alleles in both patches are shown for different values of recombination rate ρ between the preference locus M and the color pattern locus P . For each value of recombination rate (ρ) the first and second bars represented haplotype proportions in the populations living in the patch 1 and 2 respectively. Simulations are run assuming $r = 1$, $K = 2000$, $N_{tot,1}^0 = N_{tot,2}^0 = 100$, $\lambda = 0.0002$, $d_m = 0.05$, $d_{n-m} = 0.15$, $m = 0.1$, $\delta_a = \delta_b = 0.5$, $\delta_c = 0$, $\delta = 0.1$ and $c_r = 0.1$.

CHAPTER ONE

CHAPTER 2

Genetic architecture of mating trait

Ludovic Maisonneuve, Thomas Beneteau, Mathieu Joron,
Charline Smadi and Violaine Llaurens

Published:

Maisonneuve, L, Beneteau, T, Joron, M, Smadi, C, Llaurens, V. (2021) When do opposites attract? A model uncovering the evolution of disassortative mating.

The American Naturalist, 198:5, 625-641.

doi: 10.1086/716509

Abstract

Disassortative mating is a form of mate preference that promotes the persistence of polymorphism. While the evolution of assortative mating, and its consequences on trait variation and speciation have been extensively studied, the conditions enabling the evolution of disassortative mating are still poorly understood. From the analysis of a two-locus diploid model, with one locus controlling the mating trait under viability selection and the other locus coding for the level of disassortative preference, we show that heterozygote advantage and negative frequency-dependent viability selection acting at the mating trait locus promote the evolution of disassortative preferences. We also show that disassortative mating generates sexual selection which disadvantages heterozygotes at the mating trait locus, limiting the evolution of disassortative preferences. Our results show that, when one mating trait allele is dominant and rare, it reduces such negative sexual selection feedback as well as opportunity costs associated with disassortative mating. For that reason we show that the genetic architecture of the warning trait in *H. numata*, where alleles carrying genetic deleterious mutation are dominant, promotes the evolution of disassortative mating.

Introduction

The evolution of mate preferences is puzzling because preferences increase the risk of missing mating opportunities, which may incur significant fitness costs. While the evolution of assortative mating has been reported in many species, disassortative mating is more scarcely observed (Jiang *et al.*, 2013; Janicke *et al.*, 2019), suggesting that the ecological conditions enabling its evolution could be more restrictive. Here, using a general approach, we investigate the selection regimes allowing the evolution of disassortative mating using a mathematical model.

The multiple costs associated with mate choice tend to generate direct selection against the evolution of mate preferences (see (Pomiankowski, 1987) for a review), and may further limit the evolution of disassortative mating (see (Pomiankowski, 1987; Schneider & Bürger, 2006; Kopp & Hermisson, 2008; Otto *et al.*, 2008) for theoretical studies). These costs of choosiness are generally separated into fixed and relative costs (Otto *et al.*, 2008). Relative costs depend on the distribution of the mating cue within population. For example, relative costs of choosiness may emerge from the increased investment in mate searching, because an individual needs to investigate several mates to find a suitable one. Increased sampling effort can be costly in time Kruijt & Hogan (1967), in energy (as empirically estimated in antilopes Byers *et al.* (2005)) and may enhance predation risk, for instance in patrolling animals Hughes *et al.* (2012). Evaluation effort increases with the proportion of unpreferred males, implying growing relative costs of choosiness when the preferred cue is rarely displayed in the population. In addition, mate rejection by choosy individuals can also incur relative fitness costs, as in the case of males harassment: in the fly species *Musca domestica*, males jump on females' back to initiate mating and choosy females have to kick unpreferred males to avoid mating (Sacca, 1964). The number of males to kick out decreases with the proportion of preferred males. By contrast, fixed costs associated with mate choice do not depend on the composition of the population. For instance, metabolic costs may emerge from the mechanisms underlying mate choice, requiring specialized morphological, physiological and cognitive changes (see Rosenthal (2017) for a review). For exam-

ple, in the self-incompatibility system in the genus *Brassica*, mate choice involves a specialized receptor-ligand association (Hiscock & McInnis, 2003), so that the evolution of self-incompatibility is associated with metabolic costs induced by the production of the specific proteins.

Despite these costs, mate choice is ubiquitous in nature (Jiggins *et al.*, 2001; Merrill *et al.*, 2014; Backwell & Passmore, 1996; Cisar, 1999; Hiscock & McInnis, 2003; Barrett, 1990; Savolainen *et al.*, 2006) indicating that mate preference evolves readily and that choosy individuals enjoy benefits compensating those costs. Choosy individuals may enjoy direct benefits (Wagner, 2011) (for instance through beneficial sexually transmitted microbes (Smith & Mueller, 2015), or by decreasing risk of pre-copulatory cannibalism (Pruitt & Riechert, 2009)), as well as indirect benefits associated with mate preferences through an enhanced quality of their offspring (Petrie, 1994; Sheldon *et al.*, 1997; Welch *et al.*, 1998; Drickamer *et al.*, 2000; Jiggins *et al.*, 2001; Byers & Waits, 2006).

Viability selection acting on mating cues, by generating indirect selection on preferences, may thus promote their evolution (Fisher, 1930). Such indirect selection is caused by genetic associations between mating preference and mating cues (linkage disequilibrium) (Ewens, 1979; Barton & Turelli, 1991; Kirkpatrick *et al.*, 2002), generated during zygote formation because of mate preferences. The indirect effect of viability selection, that acts directly on mating cues, on the evolution of mate preferences, first identified by Fisher, has now been confirmed in many theoretical studies (O'Donald, 1980a; Heisler, 1984; Barton & Turelli, 1991). Preference based on a selectively neutral mating cue may also evolve if the cue is correlated with an adaptive trait due to linkage disequilibrium between preference and an adaptive trait (Heisler, 1985). A growing number of empirical evidence showing that female choice does improve offspring fitness is reported (Welch *et al.*, 1998; Sheldon *et al.*, 1997; Byers & Waits, 2006; Petrie, 1994; Drickamer *et al.*, 2000), suggesting that preferences generate linkage disequilibria between preference alleles and other combinations of alleles favored by viability selection. The indirect selection may thus be a major driver of the evolution of mate choice.

Once mate preferences are established in the population, they generate sexual selection on the traits exhibited by individuals during courtship, that may drive the evolution of extravagant traits in males, following a Fisherian runaway (Fisher, 1930; O'Donald, 1980b; Lande, 1981; Kirkpatrick, 1982; Veller *et al.*, 2020; Gomulkiewicz & Hastings, 1990; Otto, 1991; Greenspoon & Otto, 2009). The evolution of mate preferences thus involves complex evolutionary processes where preferences co-evolve with the cues displayed by the chosen individuals. This co-evolution has been observed in natural populations (Grace & Shaw, 2011; Higginson *et al.*, 2012) and in experimental studies (Brooks & Couldridge, 1999; Miller & Pitnick, 2002), underpinning the importance of sexual selection feedbacks on the evolution of mate preferences.

The different selection regimes acting on mating cues can therefore drive the evolution of different mating patterns, through indirect selection. Disruptive selection on mating cue has been demonstrated to promote assortative preferences (Kirkpatrick, 2000; Dieckmann, 2004; Gavrillets, 2004; Otto *et al.*, 2008; Bank *et al.*, 2012; de Cara *et al.*, 2008). By contrast, selection conferring fitness advantages to intermediate phenotypes is often thought to promote disassortative mating (Kondrashov & Shpak, 1998; Kirkpatrick & Nuismer, 2004). Nevertheless, the selection regimes enabling the evolution of disassortative mating are much less studied than the selective pressures involved in the evolution of assortative mating, extensively investigated in the context of speciation (Gavrillets, 2004; Kopp *et al.*, 2018).

Disassortative mating has been documented only in a few cases. The best documented cases are the MHC loci in humans and mice, where females prefer males with a genotype different from their own (Wedekind *et al.*, 1995). MHC genes are involved in specific recognition of pathogens, and host-pathogens interactions classically generate negative frequency dependent selection and/or heterozygote advantage (recognition of a larger range of pathogens) (Piertney & Oliver, 2006). Such balancing selection regimes are thought to promote disassortative mating at MHC loci (Slade & McCallum, 1992; Penn & Potts, 1999; Ihara & Feldman, 2003). Using numerical simulations in a haploid model, Howard & Lively (2003, 2004) confirm that host-pathogens interactions at MHC loci promote the emergence of

disassortative mating, although they never observed the fixation of this mating behavior in the population. In a more general model, Nuismer *et al.* (2008) observe that sexual selection due to non-random mating generates indirect selection on preference that hampers the fixation of disassortative mating in the population. Despite this limitation, the frequency of disassortative mating can be high when viability selection strongly promotes this behavior. In an extension of Nuismer *et al.* (2008)'s model, Greenspoon & M'Gonigle (2014) show that maternal transmission of pathogens leads to higher levels of disassortative mating. Since transmitted pathogens tend to be adapted to MHC genotype of the mother, disassortative preferences targeting the MHC locus may be advantageous: the resulting offsprings have MHC genotypes differing from their mother and are thus more likely to efficiently eliminate transmitted pathogens.

Other cases of disassortative mating in traits unlinked to immune functions have been reported, such as disassortative mating based on the plumage coloration in the white throated sparrow (Throneycroft, 1975), or on the wing color pattern in the mimetic butterfly *Heliconius numata* (Chouteau *et al.*, 2017). In both cases, one cue allele is linked to a genetic load (Tuttle *et al.*, 2016; Jay *et al.*, 2021), so that disassortative mating may increase offspring fitness through an increased viability of heterozygotes. In both cases, cue alleles associated with a genetic load are dominant to other alleles, suggesting that dominance among cue alleles may play a role in the evolution of disassortative mating. Numerical simulations matching the specific case of the polymorphic mimicry in the butterfly *Heliconius numata* confirm that selection promoting heterozygotes at the mimicry supergene may favor the emergence of disassortative mating (Maisonneuve *et al.*, 2021).

Other theoretical studies have focused on the effect of disassortative mating on the persistence of variations at the cue locus, illustrating that this mate preference may limit the purging of maladaptive cue alleles, and therefore promotes higher levels of polymorphism at the cue locus (Karlin & Feldman, 1968; Falk & Li, 1969; Ihara & Feldman, 2003). Polymorphism, in turn, maintains conditions favoring this mate preference. These results suggest that the evolution of disassortative preferences is likely to depend on viability selection acting at the cue locus

but also on feedbacks between cue polymorphism and mate choice. These complex interactions between selective pressures, identified in different systems where disassortative mating is observed, are now calling for a mathematical framework providing unifying perspective on the evolution of disassortative preference. Here, we use a modelling approach to draw general predictions on the selection regimes enabling the emergence of this mate preference and to shed light on the feedback generated by sexual selection on the evolution of disassortative mating when this behavior is common.

We thus conduct an analytical exploration of the conditions enabling the evolution of disassortative mating by adapting a previous model of evolution of assortative mating developed by Otto *et al.* (2008). The model assumes a population of diploid individuals with two key loci: the first locus C controls variation in a single mating cue, that may be subject to viability selection. The second locus P controls mate preference based on the cue encoded by locus C . We take into account fixed and relative costs associated with choosiness. Contrary to the original model built to understand the evolution of assortative mating, alleles at preference locus P generate disassortative preference. Moreover, we introduce coefficients that describe the dominance at both loci to identify how the dominance relationships impact the evolution of disassortative mating.

We first analyze the model under a Quasi-linkage Equilibrium (QLE) to derive analytical expressions of changes in genetic frequency at both the cue and preference loci, providing general expectations on the conditions enabling the emergence and persistence of disassortative mating. We then use numerical simulations to explore the evolution of disassortative preferences under strong overdominant selection acting at the cue locus, that does not match the QLE assumptions. We finally compare our theoretical predictions with the few documented cases of disassortative mating and discuss why the evolution of disassortative mating may be limited in natural populations.

Methods

Following the theoretical framework developed by Otto *et al.* (2008), we investigate the evolution of disassortative mating by assuming a diploid sexual species with balanced sex ratio, and considering two loci C and P . The locus C controls for a trait used as a mating cue and the locus P for the mate preference. We consider two different alleles, a and b , at locus C so that $\mathcal{G}_C = \{aa, ab, bb\}$ is the set of possible genotypes at this locus. This locus C can be under different viability selection regimes. At the mating preference locus P , we assume two alleles: a resident allele M and a mutant allele m . The set of possible genotypes at locus P is thus $\mathcal{G}_P = \{MM, Mm, mm\}$. The two loci recombine with probability r at each birth event. We consider a discrete time model and follow the genotypes frequencies over time.

Mating cue locus under viability selection

We define $Res(i, j)$ as the phenotypic resemblance between individuals with genotypes i and j at locus C , for all $(i, j) \in \mathcal{G}_C^2$. Individuals with genotypes aa and bb at locus C display distinct phenotypes, so that $Res(aa, bb) = 0$. Dominance between the cue alleles a and b is controlled by the *dominance coefficient* at locus C , h_a . This coefficient describes the dominance of the focal allele a with the following rule, for every $i \in \mathcal{G}_C$:

$$Res(ab, i) = Res(i, ab) = \frac{1 + h_a}{2} Res(aa, i) + \frac{1 - h_a}{2} Res(bb, i). \quad (2.1)$$

Hence if $h_a = 0$ alleles a and b are codominant and if $h_a = 1$ (resp. -1) the focal allele a is dominant (resp. recessive) to b . If $0 < h_a < 1$ (resp. $-1 < h_a < 0$) allele a is incompletely dominant (resp. recessive) to b .

The cue induced by the genotype at locus C determines mating success but can also be under viability selection. We explore the evolution of disassortative mating under different viability selective regimes acting on the mating cues, specifically

focusing on balancing selection regimes promoting polymorphism at locus C .

Let $f(i, k)$ be the frequency of genotype $(i, k) \in \mathcal{G}_C \times \mathcal{G}_P$. We introduce a selection coefficient $S_i(f, h_a)$ acting on genotype $i \in \mathcal{G}_C$, which may vary depending on genotypic frequencies at locus C and dominance between alleles a and b . This allows exploring different regimes of balancing selection, including negative frequency-dependent selection, that can favor polymorphism at locus C . Let w_i be the fitness of genotype i resulting from viability selection acting at locus C

$$w_i := 1 + S_i(f, h_a). \quad (2.2)$$

We assume that viability selection generating changes in genotype frequencies at locus C acts before reproduction. As a consequence, the changes in frequencies due to sexual selection depend on the frequencies at locus C after viability selection, described below. For $(i, k) \in \mathcal{G}_C \times \mathcal{G}_P$:

$$f'_{i,k} = \frac{w_i}{\bar{w}} f_{i,k}, \quad (2.3)$$

with

$$\bar{w} = \sum_{i \in \mathcal{G}_C} w_i \left(\sum_{k \in \mathcal{G}_P} f_{i,k} \right), \quad (2.4)$$

being the average fitness of the females.

Mate choice and reproduction

Reproduction depends on the mating cues controlled by locus C , but also on mate preferences controlled by locus P . Each genotype $k \in \mathcal{G}_P$ is associated with a coefficient ρ_k , which quantifies how much a female of genotype k tends to reject males with the same cue as her own (*i.e.* the strength of disassortative preference of females). The values of ρ_{MM} and ρ_{mm} are fixed. For the genotype Mm , we introduce a dominance coefficient h_m at locus P . Similarly to the dominance at locus C , this coefficient h_m in $[-1, 1]$ describes the dominance of the mutant allele

m .

We assume females to be the choosy sex (Otto *et al.*, 2008; de Cara *et al.*, 2008; Lande, 1981; Gavrilets & Boake, 1998), so that males can mate with any accepting females. We assume a balanced sex-ratio and consider that the frequencies of females and males with genotype i are equal (Otto *et al.*, 2008; de Cara *et al.*, 2008; Gavrilets & Boake, 1998).

To quantify the mating probability between two individuals we introduce the preference matrix $Pref(\rho_k), k \in \mathcal{G}_P$. For $(i, j) \in \mathcal{G}_C^2, k \in \mathcal{G}_P$, the preference matrix is defined by $Pref_{ij}(\rho_k) = 1 - \rho_k Res(ij)$ that measures the strength of preference of female i with genotype k at locus P for male j . Using (2.1) the preference matrix is given by:

$$Pref(\rho_k) = \begin{pmatrix} & aa & ab & bb \\ \begin{matrix} aa \\ ab \\ bb \end{matrix} & \begin{pmatrix} 1 - \rho_k & 1 - \frac{1+h_a}{2}\rho_k & 1 \\ 1 - \frac{1+h_a}{2}\rho_k & 1 - \rho_k & 1 - \frac{1-h_a}{2}\rho_k \\ 1 & 1 - \frac{1-h_a}{2}\rho_k & 1 - \rho_k \end{pmatrix} \end{pmatrix}. \quad (2.5)$$

With the help of this preference matrix describing disassortative mating behavior in the framework of Otto *et al.* (2008) (initially designed to explore the evolution of assortative mating), we investigate the evolution of disassortative mating.

For $(i, k) \in \mathcal{G}_C \times \mathcal{G}_P$, we define $T_{i,k}$ as the probability that a female of genotype (i, k) accepts a male during a mating encounter:

$$T_{i,k} = \sum_{j \in \mathcal{G}_C} Pref_{ij}(\rho_k) p'_j, \quad (2.6)$$

with

$$p'_j := \sum_{l \in \mathcal{G}_P} f'_{j,l} \quad (2.7)$$

being the proportion of genotype j at the cue locus C in the population after the viability selection step.

Choosy females of genotype k at locus P are assumed to pay a fixed cost $c_f \rho_k$ for their choosiness (the choosier a female is, the higher is this cost). Mating behavior is indeed thought to be more costly for choosy females than for females mating with the first male encountered, regardless of displayed cue. Choosy females also pay a relative cost of choosiness, depending on the proportion of preferred males and on a coefficient $c_r \in [0, 1]$. This relative cost is small if the preferred mates are abundant in the population. When a female rejects a given male because he displays an unpreferred cue, she can still accept another mate with probability $1 - c_r$.

We define the fertility of a female of genotype $(i, k) \in \mathcal{G}_C \times \mathcal{G}_P$ as

$$F_{i,k} = (1 - c_r + c_r T_{i,k})(1 - c_f \rho_k). \quad (2.8)$$

The average fertility in the population is thus:

$$\bar{F} = \sum_{(i,k) \in \mathcal{G}_C \times \mathcal{G}_P} f'_{i,k} F_{i,k}. \quad (2.9)$$

Then changes in genotypes frequencies after reproduction are as follows. For $(i', k') \in \mathcal{G}_C \times \mathcal{G}_P$:

$$f''_{i',k'} = \sum_{(i,k) \in \mathcal{G}_C \times \mathcal{G}_P} \left(f'_{i,k} \frac{F_{i,k}}{\bar{F}} \sum_{(j,l) \in \mathcal{G}_C \times \mathcal{G}_P} \text{coef}_{i',k',i,k,j,l,r} \frac{\text{Pref}_{ij}(\rho_k) f'_{j,l}}{T_{i,k}} \right), \quad (2.10)$$

where coef controls the Mendelian segregation of alleles during reproduction. $\text{coef}_{i',k',i,k,j,l,r}$ describes the proportion of individuals of genotype i' at locus C and k' at locus P in the offspring of a choosing individual of genotype i at locus C and k at locus P and a chosen individual of genotype j at locus C and l at locus P . The Mendelian segregation depends on the recombination probability r between the cue locus C and the preference locus P . All variables and parameters used in the model are summed up in Table 2.1.

Abbreviation	Description
\mathcal{G}_C	Set of possible genotypes at locus C : $\mathcal{G}_C = \{aa, ab, bb\}$
\mathcal{G}_P	Set of possible genotypes at locus P : $\mathcal{G}_P = \{MM, Mm, mm\}$
$f_{i,k}$	Frequency of genotype (i, k) in the population, $(i, k) \in \mathcal{G}_C \times \mathcal{G}_P$
$f_{i,k}^f$	Frequency of genotype (i, k) in the population after viability selection, $(i, k) \in \mathcal{G}_C \times \mathcal{G}_P$
$f_{i,k}^r$	Frequency of genotype (i, k) in the population after reproduction, $(i, k) \in \mathcal{G}_C \times \mathcal{G}_P$
p_α	Proportion of allele α at locus C in the population (with $\alpha \in \{a, b\}$).
p_m	Proportion of allele m at locus P in the population (with $m \in \{m, M\}$).
r	Recombination probability between the loci C and P .
ρ_k	Strength of disassortative mating within a female of genotype $k \in \mathcal{G}_P$ at locus P as described in the preference matrix (2.5).
h_a/h_m	Dominance coefficient at locus C describing the dominance of allele a/m .
$S_i(f, h_a)$	Viability selection coefficient when the allele frequencies are f and the dominance coefficient at locus C is h_a .
c_f/c_r	Fixed/relative cost of choosiness.
D_C	Genetic diversity at locus C , $D_C = p_a p_b$.
D_P	Genetic diversity at locus P , $D_P = p_m p_M$.
P^{HW}	Proportion of heterozygotes at the Hardy-Weinberg equilibrium, $P^{HW} = 2p_a p_b$.
P_{ho}^{HW}	Proportion of homozygotes at the Hardy-Weinberg equilibrium, $P_{ho}^{HW} = p_a^2 + p_b^2$.
H_{ns}/H_{ss}	Heterozygote advantage due to viability/sexual selection.
H	Heterozygote advantage.
$\bar{\rho}$	Average strength of disassortative mating in the population.
Δ_ρ	Effect of allele m on the level of disassortative mating in the population.
D_{am}	Linkage disequilibrium between alleles a and m within chromosome (cis). $D_{am} = p_{am} - p_a p_m$, where p_{am} is the proportion of the association between alleles a and m within the chromosome.
$D_{a,m}$	Linkage disequilibrium between alleles a and m between homologous chromosomes (trans). $D_{a,m} = p_{a,m} - p_a p_m$, where $p_{a,m}$ is the proportion of the association between alleles a and m between homologous chromosomes.
D_{he}	Excess of heterozygotes at locus C , $D_{he} = 1 - p_{aa}^2 - p_{bb}^2$.
$D_{he,m}$	Trigenic disequilibrium measuring the association between allele m and the excess of heterozygotes at locus C .
δ	Fitness reduction in homozygotes in numerical simulations.
μ	Asymmetry in viability selection acting on the two homozygous genotypes in numerical simulations.

Table 2.1: Description of variables and parameters used in the model.

Model exploration

QLE approximation exploring the evolution of weak disassortative preference

We use the QLE analysis results presented in a previous model of evolution of assortative mating (see Appendix B in (Otto *et al.*, 2008)). This approach is valid when the selection coefficients, the strength of choosiness as well as costs of assortment are small relative to recombination; namely, for all $(i, f, h_a) \in \mathcal{G}_C \times \mathcal{F}_{C,P} \times [0, 1]$ (where $\mathcal{F}_{C,P}$ denotes the space of frequencies on $\mathcal{G}_C \times \mathcal{G}_P$) and k in \mathcal{G}_P , $S_i(f, h_a)$, ρ_k , c_r and c_f are of order ϵ with ϵ small and the recombination rate r is of order 1. Under this hypothesis the genetic associations (linkage disequilibria and departures from Hardy-Weinberg) are small (of order ϵ). This approach allows to obtain mathematical expressions of allele frequency changes at the cue and preference loci from the Hardy-Weinberg equilibrium. This method highlights the key evolutionary mechanisms shaping the evolution of allele frequencies at these loci. In particular, we assume that the mutant allele m increases disassortative preference (*i.e.* $\rho_{mm} > \rho_{MM}$), and investigate the evolutionary forces acting on

this allele. The QLE approximation assumes a weak viability selection at the cue locus C and is mostly relevant to explore the evolution of weak tendency to disassortative mating (low values of ρ).

Numerical simulations

We then use numerical simulations to explore the evolutionary stable level of strength of disassortative mating when the hypothesis of weak selection is relaxed. We specifically focus on a realistic case of viability selection promoting polymorphism at the cue locus, assuming overdominance. We explore the effect of variations in key parameters, in the range where the QLE analysis is not relevant.

To explore the evolution of disassortative mating acting on the cue locus submitted to overdominance, we model a viability selection regime favoring heterozygotes. We thus set the selection coefficients associated with the different genotypes at the cue locus as:

$$S_{aa} = -\frac{1+\mu}{2}\delta, \quad S_{ab} = 0 \quad \text{and} \quad S_{bb} = -\frac{1-\mu}{2}\delta, \quad (2.11)$$

where δ is the fitness reduction in homozygotes and μ is the asymmetry in viability selection acting on the two homozygous genotypes. If $\mu = 1$ (resp. -1), the disadvantage is applied to genotype aa (resp. bb) only, and if $\mu = 0$ the disadvantage is the same for both homozygotes. To study the evolutionary stable level of strength of disassortative mating, we numerically compute the invasion gradient. First we consider a population without mutant ($p_m = 0$), for each value of the strength of disassortative mating of the resident ρ_{MM} , we let the initial population evolve until the genotype frequencies at the cue locus C reach equilibrium. At equilibrium, we introduce the mutant allele m with an initial 0.01 frequency. We call $\Delta^{100}p_m$ the change in the mutant frequency after hundred generations. We then numerically estimate

$$D(\rho_{MM}) = \frac{\partial \Delta^{100}p_m}{\partial \rho_{mm}}. \quad (2.12)$$

The evolutionary stable level of strength of disassortative mating is the value ρ for

which $D(\rho) = 0$.

We explore the effect of variations in every key parameter (δ , h_a , μ , c_f and c_r) using independent simulations. The default values for the remaining parameters follow the assumptions: codominance at cue locus $h_a = 0$, $\delta = 1$, pure symmetry in viability selection $\mu = 0$ and low cost of choosiness $c_f = c_r = 0.005$. We assume no recombination $r = 0$ and codominance at preference locus $h_m = 0$.

Data and Code Accessibility

Codes are available online: github.com/Ludovic-Maisonneuve/when-do-opposites-attract.

Results

Sexual selection at the cue locus generated by disassortative mating

Following the QLE approach, the change in frequency of allele a at the locus C controlling mating cue is (see Eq. (B2a) in (Otto *et al.*, 2008)):

$$\Delta p_a = \overbrace{D_C(p_a(S_{aa}(f, h_a) - S_{ab}(f, h_a)) + p_b(S_{ab}(f, h_a) - S_{bb}(f, h_a)))}^{\text{Effect of viability selection}} + \underbrace{\bar{\rho}(1 + c_r)D_C((p_b^4 - p_a^4)/4 + h_a(P_{ho}^{HW} - 2P_{he}^{HW})/4)}_{\text{Effect of sexual selection and opportunity cost}} + O(\epsilon^2), \quad (2.13)$$

where $D_C = p_a p_b$ is the genetic diversity at locus C ,

$$\bar{\rho} = p_M^2 \rho_{MM} + 2p_M p_m \rho_{Mm} + p_m^2 \rho_{mm}, \quad (2.14)$$

is the average disassortative mate preference at locus P,

$$P_{he}^{HW} = 2p_a p_b \quad \text{and} \quad P_{ho}^{HW} = p_a^2 + p_b^2 \quad (2.15)$$

are respectively the proportion of heterozygotes and homozygotes at the Hardy-Weinberg equilibrium. Under the QLE assumption the departure from the Hardy-Weinberg equilibrium is small, hence the proportions of heterozygotes and homozygotes are close to P_{he}^{HW} and P_{ho}^{HW} .

Eq. (2.13) highlights that the dynamics of the mating cue allele a can be affected by viability and sexual selections on males and relative cost of choosiness impacting females. Contrary to assortative mating that generates positive frequency-dependent sexual selection, disassortative preferences generate negative frequency-dependent sexual selection on cue alleles (see arrows C and E in Fig. 2.1). The strength of this sexual selection then depends on the average strength of disassortative preference (\bar{p}). Disassortative mating also generates a relative cost of choosiness on females (see arrow D in Fig. 2.1). Similarly to sexual selection, this cost especially disfavors females displaying a common phenotype because these females tend to prefer males with rare phenotype.

Sexual selection and relative cost of choosiness also tightly depend on dominance at the cue locus C . When $h_a \neq 0$ (departure from co-dominance), the evolutionary fate of alleles is strongly influenced by their dominance. When heterozygotes are frequent at locus C , *i.e.* when allele a is neither rare or common ($P_{ho}^{HW} - 2P_{he}^{HW} < 0$ *i.e.* $p_a \in (0.21, 0.79)$), see details in Appendix A2.1), allele a is favored when recessive ($h_a < 0$), because aa homozygotes then display the rarest phenotype and therefore benefit from an improved reproductive success. By contrast, when heterozygotes are rare at locus C ($2P_{he}^{HW} - P_{ho}^{HW} < 0$), allele a is favored when dominant ($h_a > 0$). Indeed, when allele a is rare ($p_a < 0.21$), bb individuals are numerous and preferentially mate with individuals displaying the phenotype encoded by allele a (the rare phenotype). Therefore, when a is dominant, ab individuals benefit from a greater mating success than bb individuals, thereby in-

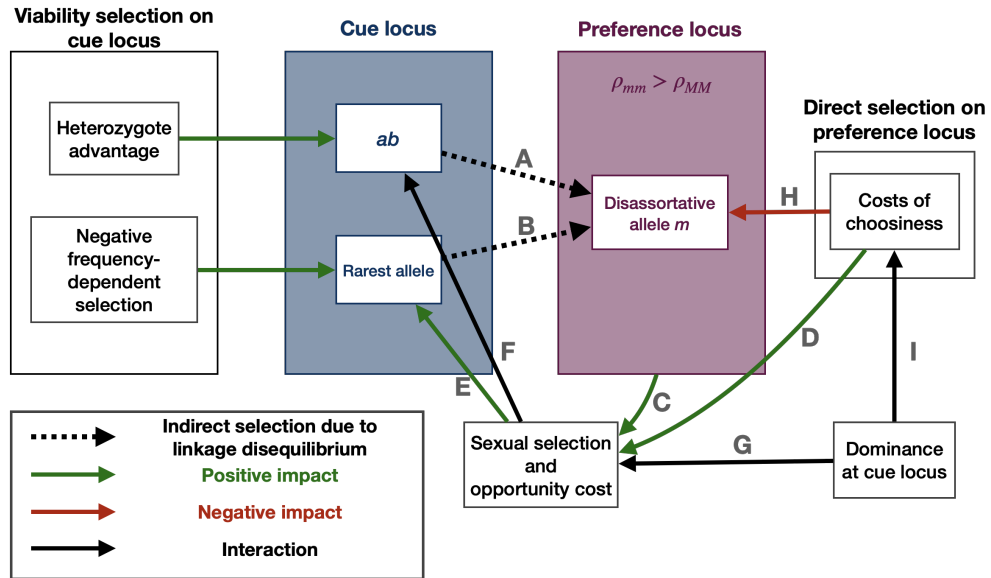


Fig. 2.1: **Selective forces acting on cue and preference loci.** Dashed arrows represent indirect selection due to positive linkage disequilibrium between cue genotype and preference genotype. Green and red arrows represent the positive and negative impact respectively. Black arrows represent an impact that is either positive or negative (see manuscript for details). Disassortative allele is promoted by heterozygote advantage (A) and negative frequency-dependent viability selection (B) at the cue locus via indirect selection due to linkage disequilibrium. Disassortative mating triggers sexual selection on males (C) and opportunity costs on females due to a cost of choosiness (D) that generates negative frequency dependent sexual selection (E) and impacts the fitness of heterozygotes at the cue locus (F). Sexual selection often causes a disadvantage to heterozygotes at the cue locus hampering the fixation of disassortative mating. However the dominance relationship at cue locus impacts sexual selection (G). Under certain conditions sexual selection favors heterozygotes at the cue locus (C), promoting high levels of disassortative mating. The disassortative allele suffers from costs of choosiness (H). These costs depend on the dominance relationship at the cue locus (I).

creasing the frequency of allele a . When the cue allele a is common ($p_a > 0.79$), the dominance of allele a limits the reproductive success of the few remaining heterozygotes ab displaying the frequent phenotype shared with homozygotes aa , as allele b is mostly present in heterozygotes that leads to the gradual elimination of the alternative allele b .

These conclusions are drawn from the QLE approximation, and are relevant for moderate levels of disassortative mating (low values of ρ). Stronger levels of disassortative mating may lead to contrasted outcomes, because some crosses (e.g. $aa \times aa$) will occur at very low frequency.

Evolutionary fate of disassortative mating mutants

To understand the conditions enabling the evolution of disassortative mating, we now approximate the change in frequency of the mutant allele m at the preference locus P , associated with an increased level of disassortative preference as compared to the resident allele M . The QLE analysis highlights that the evolution of disassortative mating depends on (1) the heterozygote advantage, (2) the genetic variation at the cue locus C , and (3) the costs of choosiness, described by the terms $\Delta^{he}p_m$, Δ^Cp_m and $\Delta^{cost}p_m$ respectively. Assuming that ϵ is small, we get (see Eq. (B3a) in (Otto *et al.*, 2008)):

$$\Delta p_m = \Delta^{he}p_m + \Delta^Cp_m + \Delta^{cost}p_m + O(\epsilon^3). \quad (2.16)$$

In the following sections we define these three terms and dissect the evolutionary mechanisms acting on preference alleles.

Disassortative mating is promoted by heterozygote advantage at the cue locus

The impact of heterozygote advantage on the frequency of the mate choice allele m is given by:

$$\Delta^{he} p_m = D_{he,m} H, \quad (2.17)$$

where $D_{he,m}$ (see (2.20)) is the trigenic disequilibrium describing the association between the mutant m at the mate choice locus P and heterozygotes at the cue locus C , and H is the heterozygote advantage at the cue locus C (see (2.18)). The fitness advantage of heterozygotes H can be influenced by both viability and sexual selections, as detailed below:

$$H = \underbrace{2S_{ab}(f) - S_{aa}(f) - S_{bb}(f)}_{\text{Viability selection acting on cues } (H_{ns})} + \underbrace{\frac{1}{2}(p_a^2 H_{aa} + 2p_a p_b H_{ab} + p_b^2 H_{bb})}_{\text{Sexual selection acting on cues } (H_{ss})}. \quad (2.18)$$

The sexual selection promoting heterozygotes at the cue locus C depends on mate preferences for heterozygotes over homozygotes expressed by the different genotypes $i \in \mathcal{G}_C$ at locus C (H_i):

$$H_i = 2Pref(\bar{\rho})_{i,ab} - Pref(\bar{\rho})_{i,aa} - Pref(\bar{\rho})_{i,bb}. \quad (2.19)$$

The effect of heterozygote advantage at the cue locus C on the disassortative mating allele m is then modulated by the association between the mutant m and heterozygotes at the cue locus (i.e. the trigenic disequilibrium $D_{he,m}$), as described by Eq. (2.17). At QLE, the trigenic disequilibrium satisfies:

$$D_{he,m} = \frac{1}{2} D_P \Delta D_{he} + O(\epsilon^2), \quad (2.20)$$

where D_{he} is the excess of heterozygotes at locus C due to allele m and $D_P = p_M p_m$ is the genetic diversity at locus P .

The trigenic disequilibrium depends on the change in the excess of heterozygotes

due to allele m following a single round of mating. This change depends on (1) the fraction of homozygotes at the cue locus C , determined by allele frequencies (p_a and p_b) and dominance relationships (h_a) and (2) the increase in disassortative preferences in the population Δ_ρ (Eq. (2.21)).

$$\Delta D_{he} = D_C^2 \Delta_\rho (P_{ho}^{HW} + h_a(p_b - p_a)) + O(\epsilon^2). \quad (2.21)$$

The increase in disassortative preferences Δ_ρ depends on the effect of the mutant m at the preference locus P and its frequency (Eq. (2.22)).

$$\Delta_\rho = p_m(\rho_{mm} - \rho_{Mm}) + p_M(\rho_{Mm} - \rho_{MM}). \quad (2.22)$$

The change ΔD_{he} has the same sign than the increase in disassortative preferences Δ_ρ (see Appendix A2.1 for details). As the mutant m increases the strength of disassortative preferences (*i.e.* $\rho_{mm} > \rho_{MM}$), $\Delta D_{he} > 0$, meaning that individuals with disassortative preferences tend to produce more heterozygotes at locus C . As a consequence, mutant alleles m , increasing disassortative preferences, are preferentially associated with heterozygotes at the cue locus C . The disassortative mutant m is thus promoted when viability and sexual selections both favor heterozygotes at the mating cue locus C (see arrow A in Fig. 2.1). This contrasts with the assortative mating model of Otto *et al.* (2008), where the assortative allele is preferentially associated with homozygotes at cue locus, suggesting that assortative mating can be promoted when homozygotes are favored.

Dominance relationships affect the change in the frequency of heterozygotes. For instance, when a rare cue allele is dominant, a round of moderate disassortative mating (*i.e.* ρ_{MM} and ρ_{mm} are small) produces more heterozygotes than when the rarer cue allele is recessive. Indeed when the dominant allele is rarer, individuals with disassortative preferences have a higher fecundity because dominance reduces the cost of choosiness (see an explanation for this phenomenon in section *The costs of choosiness limit the fixation of disassortative mating*).

Sexual selection produced by disassortative mating generates a heterozygote disadvantage limiting the evolution of such a behavior

As described above, the disassortative alleles m tend to be preferentially associated with heterozygotes at locus C . Because ab heterozygotes with disassortative preferences (*i.e.* carrying a m allele) mate preferentially with either of the aa or bb homozygotes (depending on the dominance relationship), the evolution of disassortative preferences is likely to generate a sexual selection disfavoring heterozygotes at locus C . This mechanism may hamper the fixation of allele m and limit the evolution of disassortative mating in natural populations. This effect is determined by the mating success of heterozygotes at locus C . From Eq. (2.18), this sexual selection term can be written as:

$$H_{ss} = \bar{\rho} \left(-\frac{P_{he}^{HW}}{2} + \frac{h_a}{2}(p_b - p_a) \right). \quad (2.23)$$

Sexual selection on heterozygotes depends on the strength of disassortative mating ($\bar{\rho}$), the allele frequencies at locus C (p_a and p_b) and the dominance of allele a (h_a). Assuming codominance at cue locus ($h_a = 0$), sexual selection always disfavors heterozygotes at the cue locus (see arrow F in Fig. 2.1). The more common disassortative preferences are in the population, the higher this sexual selection acting against heterozygotes is. Since the disassortative allele m is preferentially associated with heterozygotes at cue locus, it suffers from sexual selection caused by disassortative mating. The spread of a disassortative allele is thus limited by this negative feedback.

However, the sexual selection acting against heterozygotes at the cue locus depends on the dominance relationship at the cue locus (see arrow G in Fig. 2.1). Assuming strict dominance at the cue locus ($h_a = -1$ or $h_a = 1$), heterozygous individuals are indistinguishable from homozygotes, therefore modifying the proportion of phenotypes in the population. Heterozygote advantage at the cue locus due to sexual selection increases when the most common allele is recessive: when allele a is recessive and common heterozygous males ab have the same phenotype

as homozygotes bb . ab males then display the rarest phenotype and benefit from negative frequency-dependent selection. When the dominant cue allele is sufficiently rare, sexual selection favors heterozygotes (see Appendix A2.1), generating a positive feedback loop favoring the evolution of disassortative mating (see arrow F in Fig. 2.1). However, this effect should often be transient because negative frequency-dependent sexual selection rapidly balances phenotypic cue frequencies. In the general case where allele frequencies are balanced at the cue locus, sexual selection is thus expected to limit the evolution of disassortative mating.

Such a negative effect of sexual selection has already been described for the evolution of assortative mating (Otto *et al.*, 2008). Nevertheless, since (1) the assortative allele is preferentially associated with homozygotes at the cue locus, and (2) assortative mating promotes homozygotes, the negative effect of sexual selection on the evolution of assortative mating is expected to be more limited than for disassortative mating where (1) the disassortative allele is preferentially associated with heterozygotes at the cue locus, and (2) disassortative mating disfavors heterozygotes.

Disassortative preferences are favored when the rarer allele is promoted

The change in the frequency of cue alleles impacts the evolution of preference alleles. This impact is described by the term:

$$\Delta^C p_m = (D_{am} + D_{a,m}) \frac{\Delta p_a}{D_C}. \quad (2.24)$$

As highlighted in Eq. (2.24), the invasion of a disassortative mutant m depends on its linkage with the cue allele a (either in *cis* or in *trans*, described by D_{am} and $D_{a,m}$ respectively) and on the variation in the frequency of allele a (Δp_a). If allele m is associated with allele a , the frequency of allele m increases with the rise of frequency of allele a . The QLE approximates the *cis* and *trans* linkage

desequilibria between the mutant allele m and the cue allele a as:

$$D_{am} = D_{a,m} + O(\epsilon^2) = \frac{D_P D_C}{2} \Delta\rho((p_b^A - p_a^A) + \frac{h_a}{2}(P_{ho}^{HW} - P_{he}^{HW})) + O(\epsilon^2). \quad (2.25)$$

D_{am} and $D_{a,m}$ have the same sign as $p_b - p_a$ (see Appendix A2.1 for more details), thus D_{am} and $D_{a,m}$ are positive (resp. negative), when allele a is the rarer (resp. most common). Contrary to assortative alleles preferentially associated with the most common cue allele (Otto *et al.*, 2008), Eq. (2.25) indicates that the disassortative mating allele m tends to be linked with the rarer allele at locus C . This predicts that disassortative mating is likely to emerge when viability selection on the cue provides fitness benefit to rare alleles (see arrow D in Fig. 2.1), while assortative mating is promoted when the most common cue alleles are favored. Disassortative allele m also tends to be more tightly linked either to the dominant cue allele when the frequency of homozygotes is high, or to the recessive allele when the frequency of heterozygotes is high (*i.e.* when $\frac{h_a}{2}(P_{ho}^{HW} - P_{he}^{HW}) \geq 0$), increasing the association between alleles a and m). The effect of dominance can thus modulate the association between allele m and the rarer cue allele.

Given that (1) the disassortative allele m is associated with the rarer cue allele and (2) disassortative mating promotes the rarer allele via sexual selection, the disassortative mating allele m could benefit from a positive feedback loop promoting the evolution of disassortative mating. However, negative frequency-dependent sexual selection rapidly increases the frequency of the initially rare allele, limiting the spread of the m allele in the population. The initially rarer allele may become as common as the other allele breaking the linkage disequilibrium between allele m and alleles at cue locus. Thus this positive effect of sexual selection on the evolution of disassortative mating could be broken with the increase of the initially rarer allele frequency.

The costs of choosiness limit the fixation of disassortative mating

The evolution of mate preferences is generally limited by the costs associated with choosiness. Eq. (2.26) shows that both fixed and relative costs of choosiness indeed limit the fixation of the disassortative mutant m (see arrow H in Fig. 2.1):

$$\Delta^{cost} p_m = -\frac{\Delta\rho}{2} D_P \left(c_f + c_r \left(mate_0 + \frac{1}{2} mate_1 + \frac{h_a}{2} (mate_1^a - mate_1^b) \right) \right) \quad (2.26)$$

where $mate_i$, $i \in \{0, 1\}$ and $mate_1^\alpha$, $\alpha \in \{a, b\}$ describe the proportion of mating partners sharing different numbers of alleles (see Eq. (2.27) and (2.29)). The costs of choosiness disfavor preference alleles increasing disassortative choices (i.e. when $\rho_{mm} > \rho_{MM}$) (see Appendix A2.1 for details). The relative cost of choosiness then crucially depends on the proportion of preferred mates. This effect can be captured by the parameters $mate_k$, $k \in \{0, 1\}$ representing the probability that a female encounters a male differing by k allele at locus C at the Hardy-Weinberg equilibrium:

$$mate_0 = p_a^2 p_a^2 + 2p_a p_b 2p_a p_b + p_b^2 p_b^2, \quad (2.27)$$

$$mate_1 = p_a^2 (2p_a p_b) + 2p_a p_b (p_a^2 + p_b^2) + p_b^2 (2p_a p_b). \quad (2.28)$$

The mating between individuals differing by zero ($mate_0$) or one cue allele ($mate_1$) may be partially avoided when individuals have a disassortative preference, resulting in a cost c_r for the choosy female that may fail to find a suitable male. The term $mate_0 + \frac{1}{2} mate_1$ is minimal when $p_a = p_b$, so that the impact of the relative cost of choosiness is weaker when the cue alleles are in similar proportions in the population, maximizing the opportunities for females to find a male displaying the preferred cue. The dominance at the cue locus C then modulates the crosses at the Hardy-Weinberg equilibrium between individuals carrying at least one allele a

($mate_1^a$) and between individuals carrying at least one allele b ($mate_1^b$)

$$mate_1^a = p_a^2(2p_a p_b) + 2p_a p_b(p_a^2), \quad (2.29)$$

$$mate_1^b = p_b^2(2p_a p_b) + 2p_a p_b(p_b^2). \quad (2.30)$$

When a is dominant ($h_a > 0$), matings between individuals sharing at least one allele a ($mate_1^a$) are limited by disassortative preference, leading to an increased cost of choosiness. By contrast, matings between individuals sharing at least one allele b ($mate_1^b$) are promoted by disassortative preference, therefore limiting the cost of choosiness. The difference between $mate_1^a$ and $mate_1^b$ is thus crucial to understand the impact of the dominance relationship at locus C on the cost of choosiness. This difference is given by:

$$mate_1^a - mate_1^b = 4p_a p_b(p_a - p_b). \quad (2.31)$$

Thus when a is dominant ($h_a > 0$), the relative cost of choosiness is limited when allele a is rare, because bb homozygotes will frequently meet ab heterozygotes displaying their preferred cue. Symmetrically, the cost of choosiness acting on the mutant allele m is higher when the most common cue allele is dominant. The dominance relationship therefore influences the evolution of disassortative mating also by modulating the costs of choosiness (see arrow I in Fig. 2.1).

Recombination rate does not impact the evolution of disassortative mating based on a matching rule under QLE hypothesis

The QLE approximation revealed no effect of the recombination rate r between cue and preference alleles, suggesting that it does not impact the evolution of disassortative mating. Similarly, recombination does not impact the analytical results brought by QLE approach applied to the evolution of assortative mating (Otto *et al.*, 2008). These two models assume mate preferences based on matching rule, *i.e.* that females use their own cue to choose their mate (Kopp *et al.*, 2018). Under this assumption, a mutant allele m immediately translates into disassor-

tative mating in any female carrying it, independently from her genotype at the cue locus. By contrast, assuming a trait/preference rule, *i.e.* when females choose their mate independently of their own cue, any preference allele in a female does not always generate a disassortative behaviour, depending on her genotype at the cue locus. Under such a preference/trait hypothesis, the recombination rate would likely impact the evolution of disassortative preference.

Evolution of disassortative mating assuming strong overdominance at the cue locus

The QLE approximation allows to draw analytic approximations for the change in frequencies at both loci, assuming low levels of selection. Appendix A2.2 shows that QLE approximations are relevant when the parameters $S_i(f, h_a)$ for all $(i, f, h_a) \in \mathcal{G}_C \times \mathcal{F}_{C,P} \times [0, 1]$, ρ_i for all $i \in \mathcal{G}_C$, c_r and c_f are small, but are not valid outside these conditions. Since, we could not perform a local stability analysis using analytical derivation, we run numerical simulations to study ecological situations where viability selection at the cue locus can be strong and/or marked mate preferences lead to high rate of disassortative mating.

Well-documented cases of disassortative mating in natural population present strong heterozygote advantage (Jay *et al.*, 2021; Tuttle *et al.*, 2016). We thus focus on the evolution of disassortative mating acting on a cue locus where strong overdominance is operating (Fig. 2.2).

Recombination between cue and preference loci does not impact the evolution of disassortative mating

We demonstrate using the QLE approach that the recombination rate between cue and preferences alleles does not impact the evolution of disassortative mating. However QLE assumes that recombination is strong compared to the strengths of preference and selection. We numerically evaluate the effect of the recombination rate on the evolutionary stable level of disassortative mating when this assumption

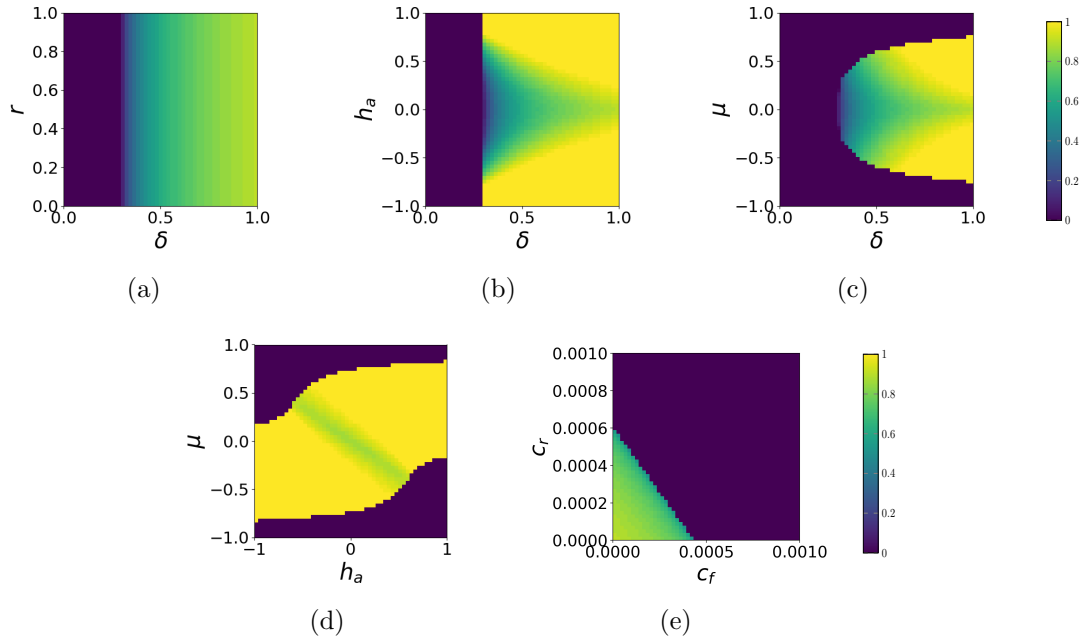


Fig. 2.2: **Evolutionary stable level of strength of disassortative mating ρ acting on a cue locus submitted to overdominance.** We plotted the evolutionary stable level of strength of disassortative mating ρ . The effects of key parameters on the evolution of the disassortative mating acting on the cue loci submitted to overdominance are explored in the different panels: (a) Effect of fitness reduction in homozygotes δ and of dominance coefficient at the cue locus C h_a , (b) Effect of fitness reduction in homozygotes δ and asymmetry in this reduction on the two homozygotes μ , (c) Effect of dominance coefficient at the cue locus C h_a and asymmetry in the fitness reduction on the two homozygotes μ and (d) Effect of fixed cost of choosiness (c_f) and relative cost of choosiness (c_r). The default parameters values are as follows: $h_a = h_m = 0$, $r = 0$, $\delta = 0.9$, $\mu = 0$ and $c_r = c_f = 0.005$.

is violated and find consistent results (Fig. 2.2(a)). These results certainly emerge from the matching-rule used in the model.

Disassortative mating is favored by asymmetrical overdominance

Our simulations show that the difference between the fitness of heterozygotes and homozygotes has a strong effect on the evolution of disassortative mate preferences (Fig. 2.2(b) and 2.2(c)). Higher levels of disassortative mating are favored when heterozygotes at the cue locus are advantaged by viability selection (i.e. when homozygotes suffers from a significant genetic load δ , Fig. 2.2(b) and 2.2(c)), consistent with the predictions brought by the QLE approximation. Interestingly, higher levels of disassortative mating are favored when there is a moderate asymmetry (μ) in the negative selection acting on homozygotes at the cue locus, *i.e.* when one out of the two cue alleles is associated with a stronger genetic load (Fig. 2.2(c)). Selection indirectly acting on mating preference indeed crucially depends on genotypic frequencies at the cue locus C , which become unbalanced under asymmetrical selection. Unbalanced cue allele frequencies tend to increase the frequency of homozygotes compared to the frequency of heterozygotes, increasing the relative advantage of heterozygotes due to viability selection, to sexual selection and to opportunity cost. As disassortative preference tends to be linked with heterozygotes, high levels of disassortative mating are favored by the unbalanced cue allele frequencies.

Because disassortative mating mutants are preferentially associated with the rare allele (carrying the recessive genetic load), once the asymmetrical selection against the rare allele is too strong, it prevents the emergence of the disassortative mating alleles associated with this maladaptive cue allele. When the negative viability selection on the rare allele is lower than a threshold, viability selection allows the emergence of the disassortative mating mutant and even favors the evolution of stronger levels of disassortative mating because as the level of disassortative behavior increases, the disadvantage of being associated with the rarer allele becomes weaker.

Asymmetrical overdominance therefore promotes the evolution of disassortative mating preference, but only when the asymmetry in the genetic load associated with cue alleles is not too high.

Interactions between dominance and fitness of cue alleles determine the evolution of disassortative mate preferences

High levels of disassortative mating are favored when dominance relationships at the cue locus are strict (i.e. when allele a (resp. b) is fully dominant to b ($h_a = 1$) (resp. a ($h_a = -1$))) as highlighted on Fig. 2.2(b). The dominant allele is disfavored by sexual selection generated by disassortative mating. When the dominant allele is rare the association of disassortative preference and cue heterozygosity increases, promoting high levels of disassortative mating. Moreover when the dominant allele is rare, the impact of the costs of choosiness on frequency changes is lower, further promoting high levels of disassortative mating.

When combining both effects leading to unbalanced cue allele frequencies (i.e. dominance and asymmetrical negative selection on cue alleles), we show that high levels of disassortative mating are strongly favored when the fitness reduction in homozygotes is associated with the dominant cue allele (Fig. 2.2(d)). This numerical result is consistent with the prediction drawn from the QLE approximation because the dominant allele is here in low frequency (because of both viability and sexual selections).

The challenging evolution of disassortative mating

Numerical simulations confirm that the evolution of disassortative mating is challenging when moderate overdominance (enhancing the fitness of heterozygotes) is at play at the cue locus. In most cases, strict disassortative mating is not favored. The higher the disassortative preferences, the more sexual selection acts against heterozygotes. When heterozygote advantage is not strong enough, sexual selection caused by mating preferences can overcome heterozygote advantage, favoring

intermediate level of disassortative mating (see green areas on Fig. 2.2(b) and 2.2(c)). By contrast, when viability selection produces strong heterozygote advantage (δ is high) that can compensate sexual selection, complete disassortative preferences can be fixed (see Fig. 2.2(b) and 2.2(c)).

The costs of choosiness may further limit the evolution of the disassortative mutant. Fig. 2.2(e) shows that disassortative mating is under positive selection only when the costs of choosiness are limited (at least inferior to 0.03).

Discussion

Predicted selection regimes promoting disassortative mating match empirical observations

Our results show that disassortative mating is promoted either (1) when heterozygotes at cue locus are in average fitter than homozygotes or (2) when viability selection on cue favors the rarest cue allele. These selection regimes promoting disassortative mating are opposed to the selection regimes promoting assortative mating, such as homozygote advantage at cue locus or viability selection on cue favoring the most common allele (Otto *et al.*, 2008) (see Table 2.2).

Interestingly, our simulations also show that higher levels of disassortative mating are promoted when one cue allele is dominant. The dominance relationship can indeed decrease sexual selection and relative cost of choosiness impairing the evolution of disassortative preferences.

Simulations also highlight that higher levels of disassortative mating are promoted when the dominant allele is disfavored when homozygous. This effect is consistent with the observed cases of disassortative mating. For instance the butterfly *H. numata* displays a strong disassortative mating based on wing-pattern phenotype (in a tetrad experiment, 3/4 of the realized crosses were involving disassortative pairs) (Chouteau *et al.*, 2017). In this species, the variation in wing-pattern morphs

is controlled by a supergene with three main haplotypes (Joron *et al.*, 2011). The dominant haplotypes are associated with a low survival of homozygous larvae (Jay *et al.*, 2021). This case of disassortative mating seems to gather the conditions pinpointed by our model to enable the evolution of higher levels of disassortative mating.

Similarly, in the white-throated sparrow *Zonotrichia albicollis* an almost strict disassortative mating based on plumage morphs (*white* or *tan*) has been reported (Throneycroft, 1975). Two supergene haplotypes, here referred to as *t* and *w*, control this variation in plumage coloration. Individuals with *tt* genotype have a *tan* coloration whereas individuals carrying *tw* and *ww* genotypes have a *white* coloration. However the dominant haplotype *w* is associated with strong genetic load, generating homozygote disadvantage in *ww* individuals (Tuttle *et al.*, 2016). Individuals with *white* coloration may be advantaged over *tan* individuals because they invest less into parental care (Knapton & Falls, 1983), generating an advantage of heterozygotes *tw* over homozygotes *tt*. Here the dominant cue allele is again associated with a strong disadvantage when homozygous, which, according to our results, strongly favors the emergence of disassortative preferences (see Fig 2.3).

Polymorphism at the mating cue has a crucial effect on the evolution of disassortative mating

The number of mating cues within the population is an important parameter in the evolution of mate preference (Otto *et al.*, 2008), because it modulates the opportunity costs generated by choosiness. In our model, we consider only two cue alleles, generating at most three different cue phenotypes in the population. With a higher number of alleles, the number of phenotypes would be greater. Under disassortative mating, these phenotypes should have their frequencies balanced by negative frequency-dependent selection. Thus both females and males would still have sufficient mating opportunities, weakening the relative cost of choosiness and sexual selection. Hence disassortative mating should evolve more easily when the

number of mating cues is higher. This is consistent with the numerical analysis reported in Greenspoon & M'Gonigle (2014), showing that the evolutionary stable level of disassortative preference targeting a MHC locus increases with the number of alleles at this locus. The evolution of disassortative preference at MHC loci may be facilitated by the multiple alleles maintained by selection (de Vries, 1989).

When the mating cue is a quantitative trait (e.g. size-related preferences, (Jiang *et al.*, 2013; Janicke *et al.*, 2019)), variations within populations may be considered as multiple cues, depending on the discrimination rules of the choosy partners. If quantitative variations are perceived as multiple differentiated phenotypes, it would probably promote the evolution of disassortative mating, in a similar manner as high level of discrete polymorphism.

The number of mating cues maintained within a population can also be increased via contacts between populations. The effect of immigration of individuals displaying alternative cues on the evolution of disassortative mating will then depend on viability selection. Cotto & Servedio (2017), show that the contact between populations promotes higher level of assortative mating, because individuals adapted to different habitats produce intermediate offspring maladaptive in each habitat. Contacts between locally adapted populations may thus limit the evolution of disassortative mating because it generates viability selection against hybrids, disfavoring such preferences.

Mating opportunities also depend on the distribution of cues in the population. A more balanced cue distribution within population often increases the negative effect of sexual selection on the evolution of assortative preferences (Otto *et al.*, 2008). For instance, migration between populations has been shown to limit the evolution of further assortative mating because it promotes a more balanced polymorphism within populations and therefore increases the negative effect of sexual selection (Servedio, 2011). Similarly, migration between populations may limit the evolution of disassortative mating, because the resulting more balanced polymorphism increases the negative sexual selection.

Negative feedback in the evolution of disassortative mating contrasts with the evolution of assortative mating

A striking result from our analyses stems from the role of sexual selection generated by disassortative preferences on its evolution, which contrasts with the evolutionary dynamics of assortative mating. Our results confirm that the sexual selection generated by disassortative mating often limits its own spread, as already mentioned by Nuismer *et al.* (2008). Indeed, the disassortative mating allele is generally associated with heterozygotes at the cue locus. Individuals with such allelic combinations tend to preferentially mate with homozygotes, generating sexual selection disfavoring heterozygotes at the cue locus. However, this sexual selection acting against heterozygotes depends on the distribution of cue allele frequency (see more details in Tab. 2.2).

Similarly, the evolution of assortative mating is thought to be limited by sexual selection (Otto *et al.*, 2008) (but sexual selection can promote the evolution of assortative mating in some cases, see more details in Tab. 2.2). However, this negative effect of sexual selection decreases when the proportion of homozygotes at the cue locus is high. Assortative mating usually produces more homozygotes than random mating: a decrease in the level of heterozygosity at the cue locus is thus expected when assortative preferences are spreading within a population. During the evolution of assortative mating, the negative effect of sexual selection on the evolution of assortative mating decreases as the proportion of homozygote increases. The evolution of disassortative mating may therefore be more severely impaired by sexual selection than the evolution of assortative mating.

In two meta-analyses (Jiang *et al.* (2013); Janicke *et al.* (2019)) covering 1,116 and 1,447 measures of strength of assortment respectively, most of the values corresponding to disassortative mating range from -0.5 to 0 (but see below exception), suggesting that high values of strength of disassortative mating are rarely observed. By contrast, most values corresponding to assortative mating behavior range from 0 to 1 , suggesting that the evolution of strict assortative mating is observed in a wide range of organisms.

Jiang *et al.* (2013) and Janicke *et al.* (2019) also show that weak disassortative mating is rare. This observation is unlikely to reflect the negative feedback of sexual selection on the evolution of disassortative preferences, precisely because this effect is weak when preferences are weak. The rarity of weak disassortative mating may instead reflect the effect of a cost of choosiness, which increases with the proportion of heterozygotes in the population, which is itself promoted by the selection regimes that favor disassortative mating.

Alternative genetic architectures of mate preferences may limit the evolution of disassortative mating

The genetic architecture of preference may also have an impact on the evolution of disassortative mating. Theoretical studies on the evolution of assortative mating usually rely on two main types of matching rules Kopp *et al.* (2018): (1) when mate choice of an individual depends on its own phenotype (*matching rule*) and (2) when preference is independent from the phenotype of the chooser (*preference/trait rule*). The evolution of assortative mating is strongly promoted either when assuming the *matching rule*, or when the cue and *preference/trait* loci are tightly linked (Kopp *et al.*, 2018). Here, our results on the evolution of disassortative mating are obtained assuming a *matching rule*, and we expect that assuming a *preference/trait rule* might limit such an evolution, because selection might break the unmatching allelic combinations. In the specific case of polymorphic mimicry, Maisonneuve *et al.* (2021) showed that under *preference/trait* rule, disassortative mating can emerge only if the preference and the cue loci are fully linked.

Moreover, here we only consider a single choosy sex. However, when both sexes are choosy (Servedio & Lande, 2006), the positive selection on the evolution of mate preference in one sex may be relaxed when strong mate preferences are fixed in the other sex (Aubier *et al.*, 2019). Drift then leads to periodic cycles where male and female alternatively become the most choosy sex (Aubier *et al.*, 2019).

Conclusions

Our analytical and numerical results provide a general theoretical framework establishing the conditions enabling the evolution of disassortative mating. Our results pinpoint two selective regimes on mating cue that promote disassortative mating through indirect selection: heterozygote advantage and negative frequency-dependent selection. We also observe that disassortative mating generates sexual selection that often hampers its own fixation, leading to intermediate level of disassortative mating. This sexual selection depends on the dominance at the cue locus: if one type of homozygote at the cue locus is common and if heterozygotes display the same cue as the rare homozygote, sexual selection promotes the evolution of disassortative mating. We also show that this condition reduces the costs associated with choosiness. Interestingly, the favorable selective conditions predicted by our model match with two well-characterized cases of strong disassortative mating.

Acknowledgments

The authors would like to thank the ANR SUPERGENE (ANR-18-CE02-0019) for funding the PhD of LM. This work was partially supported by the Chair “Modélisation Mathématique et Biodiversité” of VEOLIA- Ecole Polytechnique-MNHN-F.X.

Appendix

A2.1 Details of analytic results

We study the evolution of alleles frequencies in a two locus diploid model. One locus controls the mating cue (with two alleles a and b) and the other controls mate preference (with two alleles M and m). The model is described in the main file. We used a QLE analysis to approximate the changes in frequency of the cue allele a and of the preference allele m (see main file for more details). Here, we detail how our analytic results pinpoint some mechanisms explained in the main file.

The dominance relationship at cue locus impacts the action of sexual selection in a way depending on the proportion of heterozygotes

The approximation of the change in frequency of the cue allele a using QLE analysis is given by:

$$\begin{aligned} \Delta p_a = & D_C \left(p_a(S_{aa}(f, h_a) - S_{ab}(f, h_a)) + p_b(S_{ab}(f, h_a) - S_{bb}(f, h_a)) \right) \\ & + \bar{\rho}(1 + c_r) D_C \left(\frac{p_b^4 - p_a^4}{4} + \frac{h_a}{2} (P_{ho}^{HW} - 2P_{he}^{HW}) \right) + O(\epsilon^2), \end{aligned}$$

where we recall that under the QLE approximation, ϵ is a small quantity.

Here we aim to study the impact of the dominance relationship on the variation of allele a frequency. We therefore study the sign of the term

$$A := \frac{h_a}{2} (P_{ho}^{HW} - 2P_{he}^{HW}),$$

describing the effect of the dominance relationship. As $P_{he}^{HW} + P_{ho}^{HW} = 1$ by defini-

tion we have:

$$A = \frac{h_a}{2}(1 - 3P_{he}^{HW}).$$

Thus $A > 0$ when a is partially dominant ($h_a > 0$) (resp. recessive ($h_a < 0$)) and the proportion of heterozygotes is lower (resp. higher) than $1/3$. This entails that when the proportion of heterozygotes is low (resp. high), the dominant (resp. recessive) cue allele is favored.

The condition on P_{he}^{HW} translates in a condition on p_a as follows:

$$\begin{aligned} P_{he}^{HW} > 1/3 &\iff 2p_a p_b > 1/3 \\ &\iff 6p_a(1 - p_a) - 1 > 0 \\ &\iff p_a \in \left(\frac{3 - \sqrt{3}}{6}, \frac{3 + \sqrt{3}}{6}\right). \end{aligned}$$

For the sake of readability we use in the manuscript the approximation $\frac{3 - \sqrt{3}}{6} = 0.21$ and $\frac{3 + \sqrt{3}}{6} = 0.79$.

Disassortative preference promotes heterozygote excess at cue locus

We develop the expression of the change of excess of heterozygotes at cue locus due to the preference allele m , ΔD_{he} :

$$\Delta D_{he} = D_C^2 \Delta \rho(p_a^2 + p_b^2 + \frac{h_a}{2}(p_b - p_a)) + O(\epsilon^2).$$

Thus ΔD_{he} depends on the sign of the term $p_a^2 + p_b^2 + \frac{h_a}{2}(p_b - p_a)$. But the latter can be written as follows:

$$\begin{aligned} p_a^2 + p_b^2 + \frac{h_a}{2}(p_b - p_a) &= p_a^2 + (1 - p_a)^2 + \frac{h_a}{2}(1 - 2p_a), \\ &= 2p_a^2 - (2 + h_a)p_a + \frac{2 + h_a}{2}. \end{aligned}$$

This term is a quadratic function in p_a . The value of its discriminant is:

$$\Delta = h_a^2 - 4 < 0,$$

which entails that this quadratic function is always positive, and that ΔD_{he} has the same sign as $\Delta\rho$. Hence, when allele m is associated with higher disassortative preference ($\Delta\rho$) it promotes heterozygote excess.

Sexual selection generated by disassortative mating can favor or disfavor heterozygotes at cue locus.

The heterozygote advantage due to sexual selection is given by:

$$H_{ss} = \bar{p} \left(-\frac{P_{he}^{HW}}{2} + \frac{h_a}{2}(p_b - p_a) \right).$$

To study the impact of sexual selection on heterozygotes we look at the sign of $-\frac{P_{he}^{HW}}{2} + \frac{h_a}{2}(p_b - p_a)$. The latter can be written as follows:

$$\begin{aligned} -\frac{P_{he}^{HW}}{2} + \frac{h_a}{2}(p_b - p_a) &= -p_a(1 - p_a) + \frac{h_a}{2}(1 - 2p_a), \\ &= p_a^2 - (1 + h_a)p_a + \frac{h_a}{2}. \end{aligned}$$

It is a quadratic function in p_a with discriminant:

$$\Delta = (1 + h_a)^2 - 2h_a = 1 + h_a^2 > 0.$$

Therefore H_{ss} is equal to

$$(p_a - (1 + h_a - \sqrt{1 + h_a^2})/2)(p_a - (1 + h_a + \sqrt{1 + h_a^2})/2).$$

When there is codominance at cue locus (*i.e.* $h_a = 0$), we have $H_{ss} = -\bar{\rho}p_a(1 - p_a) \leq 0$, thus disassortative preference always disfavor heterozygotes at cue locus. A classical functional study yields that $(1 + h_a - \sqrt{1 + h_a^2})/2$ belongs to $[-1, 1]$ and has the sign of h_a , and that $(1 + h_a + \sqrt{1 + h_a^2})/2$ belongs to $[0, 1]$. As a consequence when $h_a \neq 0$, H_{ss} can be either positive or negative depending on the frequency of allele p_a . Therefore when the dominance relationship is unbalanced, sexual selection due to disassortative mating may favor or disfavor heterozygotes at cue locus.

Mutant allele m is always associated with the rarer cue allele.

The associations between allele m and cue alleles are given by the *cis* (D_{am}) and *trans* ($D_{a,m}$) linkage disequilibria. At QLE these linkages can be approximate by:

$$D_{am} = D_{a,m} + O(\epsilon^2) = \frac{D_P D_C}{2} \Delta\rho((p_b^4 - p_a^4) + \frac{h_a}{2}(P_{ho}^{HW} - P_{he}^{HW})) + O(\epsilon^2).$$

To understand the association between allele m and cue alleles we have to look at the sign of $(p_b^4 - p_a^4) + \frac{h_a}{2}(P_{ho}^{HW} - P_{he}^{HW})$. But the latter can be written as follows:

$$\begin{aligned}
(p_b^4 - p_a^4) + \frac{h_a}{2}(P_{ho}^{HW} - P_{he}^{HW}) &= (p_b^2 + p_a^2)(p_b^2 - p_a^2) + \frac{h_a}{2}(p_a^2 + p_b^2 - 2p_a p_b), \\
&= (p_b^2 + p_a^2)(p_b - p_a) + \frac{h_a}{2}(1 - 4p_a p_b), \\
&= (2p_a^2 - 2p_a + 1)(1 - 2p_a) + \frac{h_a}{2}(2p_a - 1)^2, \\
&= (2p_a - 1) \left(-(2p_a^2 - 2p_a + 1) + \frac{h_a}{2}(2p_a - 1) \right), \\
&= (2p_a - 1) \left(-2p_a^2 + (2 + h_a)p_a - 1 - \frac{h_a}{2} \right) \\
&= (2p_a - 1)Q[p_a].
\end{aligned}$$

where Q is a quadratic function, with discriminant:

$$\Delta = (2 + h_a)^2 - 4(2 + h_a) = h_a^4 - 4 < 0.$$

It entails that Q is always negative, and that D_{am} and $D_{a,m}$ have the sign of $1 - 2p_a$ (*i.e.* $p_b - p_a$). As a consequence preference allele m is associated with the rarer allele at cue locus at QLE.

Costs of choosiness penalize the preference allele associated with higher levels of disassortative mating

Here we study the impact of the costs of choosiness on frequencies of preference alleles. We recall that the impact of the costs of choosiness on allele m frequency is given by:

$$-\frac{\Delta\rho}{2}D_P\left(c_f + c_r\left(\text{mate}_0 + \frac{1}{2}\text{mate}_1 + \frac{h_a}{2}(\text{mate}_1^b - \text{mate}_1^a)\right)\right).$$

We are interested in the sign of the term B defined by:

$$\begin{aligned} B &:= mate_0 + \frac{1}{2}mate_1 + \frac{h_a}{2}(mate_1^b - mate_1^a) \\ &= (p_a^4 + 4p_a^2p_b^2 + p_b^4) + 2p_ap_b((1 - h_a)p_a^2 + (1 + h_a)p_b^2). \end{aligned}$$

B is this the sum of two positive terms. Hence when $\Delta\rho$ is positive (*i.e.* when $\rho_{mm} > \rho_{MM}$), the costs of choosiness penalize the preference allele associated with higher disassortative preferences.

A2.2 Comparison of QLE analysis results with numerical simulations

We used a QLE analysis to draw analytic approximations for the changes in frequencies at the cue and preference loci (Δp_a and Δp_m). The results of the QLE analysis are only relevant when for all $(i, f, h_a) \in \mathcal{G}_C \times \mathcal{F}_{C,P} \times [0, 1]$ (where we recall that $\mathcal{F}_{C,P}$ denotes the space of frequencies on $\mathcal{G}_C \times \mathcal{G}_P$), $S_i(f, h_a) = O(\epsilon)$; for all k in \mathcal{G}_P , $\rho_k = O(\epsilon)$, $c_r = O(\epsilon)$ and $c_f = O(\epsilon)$ with ϵ small.

To illustrate that the QLE results provide a good approximation under the QLE hypothesis, we then compare the values of the frequency changes predicted by the QLE analysis ($\Delta^{QLE} p_a$ and $\Delta^{QLE} p_m$) with values from numerical simulations ($\Delta^{num} p_a$ and $\Delta^{num} p_m$). We define $Err \Delta p_a = \left| \frac{\Delta^{QLE} p_a - \Delta^{num} p_a}{\Delta^{num} p_a} \right|$ and $Err \Delta p_m = \left| \frac{\Delta^{QLE} p_m - \Delta^{num} p_m}{\Delta^{num} p_m} \right|$ to quantify the error of the QLE approximation. We assume that the viability selection does not depend on the frequencies distribution and of the dominance at cue locus. Then for all $i \in \mathcal{G}_C$, $S_i(f, h_a) = S_i$. The results are plotted in Figures A2.1 and A2.2 and show that the error of the QLE approximations are low when the hypotheses of the QLE are satisfied *i.e.* the parameters S_{aa} , S_{ab} , S_{bb} , ρ_{MM} , ρ_{mM} , ρ_{mm} , c_r and c_f are small.

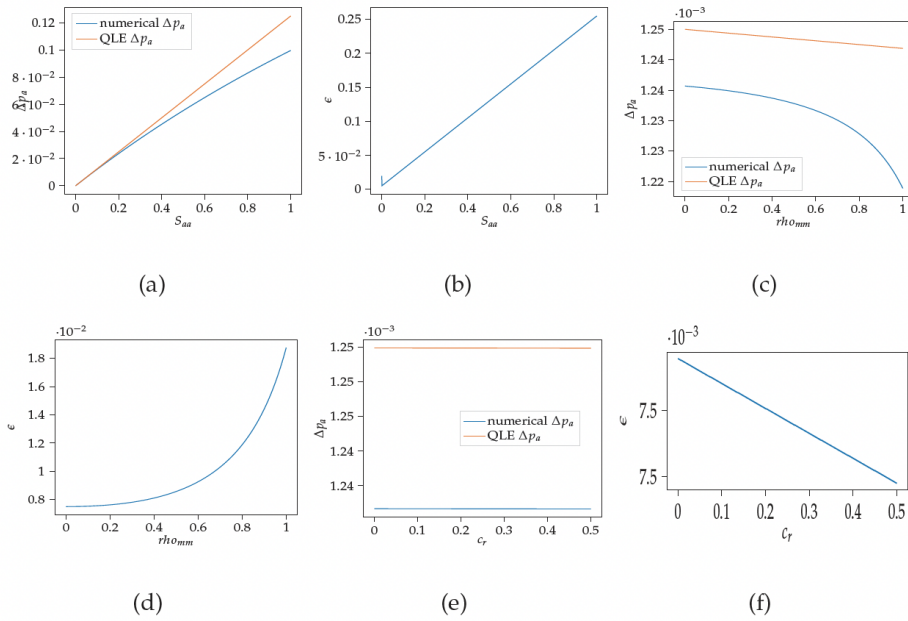


Fig. A2.1: **Change of allele a frequency at cue locus (Δ) after the introduction of mutant predicted by the QLE analysis (orange lines) and by numerical simulations (blue lines).** The effect of key parameters on the evolution of the disassortative mating is explored in the different panels: (a)(b) Effect of the viability selection acting on homozygote aa at cue locus (S_{aa}), (c)(d) Effect of the strength of disassortative mating within an individual of genotype mm at preference locus (ρ_{mm}), (e)(f) Effect of the relative cost of choosiness (c_r). The default parameters values are as follows: $\rho_{MM} = 0$, $\rho_{mm} = 0.01$, $h_a = 1$, $h_m = -1$, $r = 0.1$, $c_r = 0$, $c_f = 0$, $S_{aa} = 0$, $S_{ab} = 0.01$ and $S_{bb} = 0$.

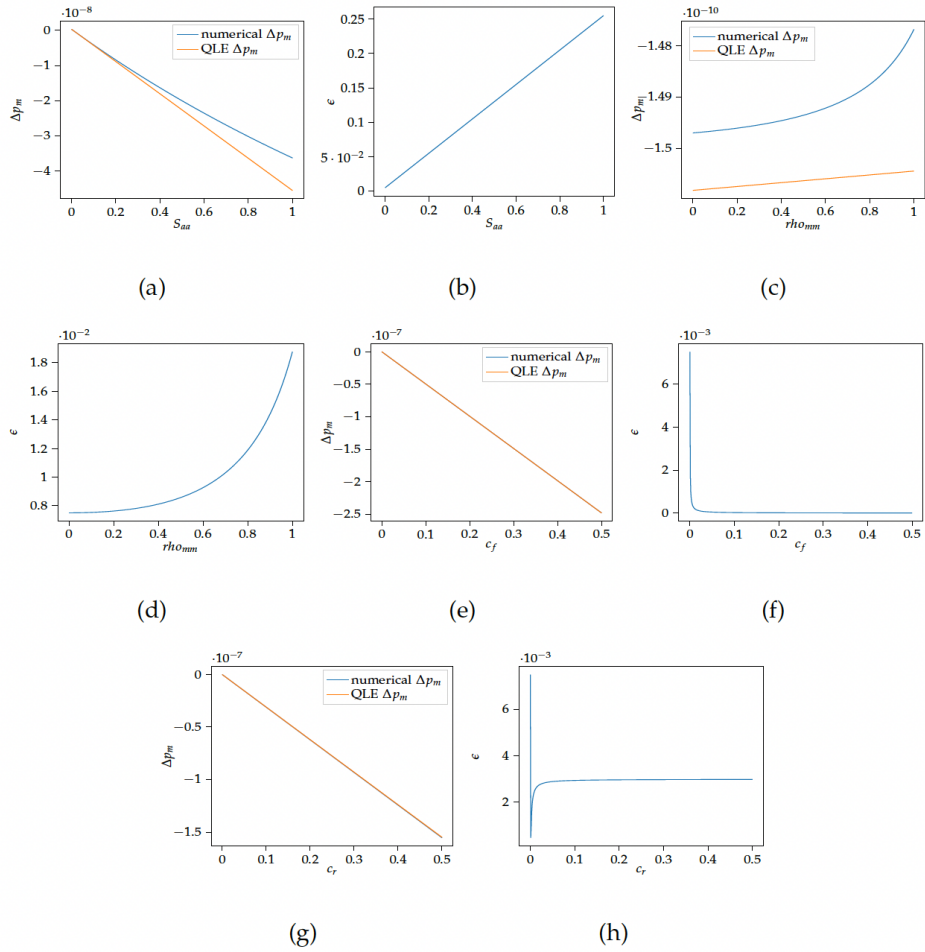


Fig. A2.2: **Change of allele m frequency at preference locus (Δp_m) after the introduction of the mutant predicted by the QLE analysis (orange lines) and by numerical simulations (blue lines).** The effect of key parameters on the evolution of the disassortative mating is explored in the different panels: (a)(b) Effect of the viability selection acting on homozygote aa at cue locus (S_{aa}), (c)(d) Effect of the strength of disassortative mating within an individual of genotype mm at preference locus (ρ_{mm}), (e)(f) Effect of the fixed cost of choosiness (c_f), (g)(h) Effect of the relative cost of choosiness (c_r). The default parameters values are as follows: $\rho_{MM} = 0$, $\rho_{mm} = 0.01$, $h_a = 1$, $h_m = -1$, $r = 0.1$, $c_r = 0$, $c_f = 0$, $S_{aa} = 0$, $S_{ab} = 0.01$ and $S_{bb} = 0$.

Part II

When adaptation promotes species similarity: mate preference limiting reproductive interference

The evolution of preference within a species also depends on interactions with sympatric species. I now focus on reproductive interference that results from local selection promoting traits similarity in different sympatric defended species and how such shared selection limits preference towards mimetic mate. Such reproductive interference promotes female preference for the scarce males displaying slightly imperfect mimicry. The sexual selection generated by such preference impacts the evolution of locally-adapted traits within sympatric species. Using quantitative genetic models, I study the impacts of reproductive interference on the level of trait convergence between sympatric species (**Chapter 3**). Moreover, such conflict between mimicry and species recognition may explain the female-limited mimicry observed in Batesian species. However, natural selection may also have led to the evolution of female-limited mimicry. I thus compare the evolution of female-limited mimicry, caused by sexual or natural selection, in order to provide testable predictions (**Chapter 4**).

CHAPTER 3

When does reproductive interference limits mimicry ?

Ludovic Maisonneuve, Marianne Elias, Charline Smadi and
Violaine Llaurens

Submitted to *The American Naturalist* (major revision):

Maisonneuve, L, Elias, M, Smadi, C, Llaurens, V. (2021) The limits of evolutionary convergence in sympatry: reproductive interference and historical constraints leading to local diversity in warning traits.

bioRxiv.

doi: 10.1101/2021.01.22.427743

Abstract

Mutualistic interactions between defended species represent a striking case of evolutionary convergence in sympatry, driven by the increased protection against predators brought by mimicry in warning traits. However, warning traits are also involved in mate recognition, so that trait convergence might result in heterospecific courtship and mating. Such reproductive interference may drive the evolution of preference towards non-mimetic males, and sexual selection may limit mimicry between sympatric species. Here, we develop a mathematical model to investigate the evolution of a warning trait and of a preference targeting this trait in sympatric defended species. We show that reproductive interference promotes preference for less mimetic males, because such preference reduces interactions with heterospecific. Such preference partially or totally limits the evolution of mimicry, promoting either imperfect mimicry or complete divergence. Our model reveals highlights the importance of female and predator discriminations, as well as historical constraints limiting the warning trait evolution, in the evolution of imperfect mimicry.

Introduction

Mutualistic interactions frequently drive convergent evolution of different traits in sympatric species. For example, avian vocal resemblance has been suggested to allow the formation of mixed-species flocks that may benefit all individuals from the different species (Goodale & Kotagama, 2006); trait similarity between sympatric species may promote pollinator attraction in nectar-rewarding flowers (Schemske, 1981; Benitez-Vieyra *et al.*, 2007). In aposematic species, warning traits are associated with defenses against predators, such as venoms or disgusting tastes. Because predators eventually learn such associations, mimicry among species facing similar communities of predators is often observed (Müllerian mimicry, see Sherratt (2008) for a review). Such convergence in warning trait among defended species is certainly the best documented case of mutualistic interactions driving trait evolution in sympatric species and is observed in a wide range of organisms including plants (Lev-Yadun, 2009), mollusks (Cortesi & Cheney, 2010), vertebrates (Sanders *et al.*, 2006; Springer & Smith-Vaniz, 1972) and insects (Mallet & Gilbert Jr., 1995). Field experiments report the intense selection exerted by predators favoring warning trait convergence in sympatry (Benson, 1972; Mallet & Barton, 1989; Kapan, 2001; Arias *et al.*, 2016c; Chouteau *et al.*, 2016). Surprisingly, despite such intense selection, many sympatric defended species exhibit only imperfect resemblance (*e.g.* (Savage & Slowinski, 1992)) or even different warning traits (*e.g.* (Beccaloni, 1997)) (Briolat *et al.*, 2019).

The level of trait convergence between sympatric species may vary depending on their level of phylogenetic relatedness. For instance, the significant phylogenetic signal observed on the warning trait of mimetic butterflies of the tribe Ithomiini (Elias *et al.*, 2008; Chazot *et al.*, 2014) suggests that historical constraints may limit the convergent evolution of warning traits. Such historical constraints are expected to be more different between distantly related species than closely-related ones, because closely-related species are expected to share similar ancestral trait values. These historical constraints may also imply differences between clades in both (1) the developmental pathway involved in the variation of warning traits or

(2) the selective trade-offs between warning signals and other traits. For example, evolutionary history of different species influences their diet and since diet can influence the warning trait (Grill & Moore, 1998; Ojala *et al.*, 2007), this may lead to different species-specific trade-offs limiting convergence between defended species. Historical constraints thus not only determine ancestral trait values, but also the evolvability of the traits in different species. Theoretical studies suggest that ancestral trait states may play a key role in the evolution of warning traits, because the convergence of trait can be facilitated by an initial resemblance between species (Franks & Noble, 2004; Balogh & Leimar, 2005; Franks & Sherratt, 2007). The initial resemblance between species, in the eyes of predators, depends on predator discrimination capacities, that then determines the strength of selection promoting convergence of warning traits. Other theoretical studies highlight that the level of standing genetic and phenotypic variance within species strongly influences convergence between species (Ruxton *et al.*, 2008). The balance between (1) the shared predation pressure faced by individuals from different sympatric species and (2) the historical constraints within each species may thus strongly shape the level of evolutionary convergence in warning traits. This balance may also modify the direction of evolution of traits within the different defended species living in sympatry. While convergence (Sherratt, 2008) usually assumes a joint evolution of traits in several sympatric species toward resemblance (*e.g.* Symula *et al.* (2001); Flanagan *et al.* (2004)), resemblance might also emerge from advergence, whereby trait evolution occurs in a given species (*i.e.* the 'mimic' species), leading to high similarity to the ancestral trait displayed in another species (*i.e.* the 'model' species) (see (Dalziell & Welbergen, 2016) for the terminology).

Moreover, the convergence of warning traits in different species may entail costs due to behavioral interference, thereby limiting positive selection on trait resemblance. Warning traits are indeed frequently involved in species recognition (Jiggins *et al.*, 2001; Naisbit *et al.*, 2001; Kronforst *et al.*, 2006; Merrill *et al.*, 2014), leading to increased risk of confusion in mimetic species during sexual interactions. Such risk might be even higher between closely-related species, which are more likely to share multiple similar traits because of common ancestry. Species sharing similar warn-

ing traits may thus be exposed to substantial reproductive interference incurring fitness costs during mate acquisition due to interspecific interactions, including heterospecific courtship and mating as well as heterospecific male rivalry (Gröning & Hochkirch, 2008). Empirical examples of such reproductive interferences in Müllerian mimetic systems have been reported in the literature (Vasconcellos-Neto & Brown, 1982; Estrada & Jiggins, 2008). However, empirical studies precisely estimating the level of reproductive interference in sympatric species are scarce. Pheromone differences between mimetic species have been documented to limit the rate of erroneous mating (see Darragh *et al.* (2017); González-Rojas *et al.* (2020) for empirical examples in *Heliconius* butterflies). However, the pheromones of day-flying butterflies usually act as short-distance cues that may be perceived only during courtship (Mérot *et al.*, 2015). Females deceived by the color pattern of the heterospecific males may have already spent time and energy or may need to deploy substantial efforts to avoid heterospecific mating. Therefore, females may still suffer from costs associated to reproductive interference, even if females refuse mating with heterospecific males. When females are courted by heterospecific males displaying their preferred cue before being rejected, this also results in increased costs associated with mate searching in males (*i.e.* signal jamming in (Gröning & Hochkirch, 2008)).

Reproductive interference can generate reproductive character displacement (Gröning & Hochkirch, 2008; Kyogoku, 2015), whereby reproductive traits are more dissimilar between species in sympatric than in allopatric populations (Brown & Wilson, 1956). Such reproductive character displacement may thus impair convergence driven by mutualistic interactions. Theoretical studies have investigated how the evolution of female preferences may promote reproductive character displacement in males (McPeck & Gavrilets, 2006; Yamaguchi & Iwasa, 2013): reproductive interference costs are predicted to favor divergence between female preference and trait displayed by heterospecifics, because this reduces mating attempts with heterospecifics, and therefore promotes the divergence of reproductive traits between conspecific and heterospecific males through sexual selection. Female discrimination then determines the level of divergence between female preference and trait

displayed by heterospecifics necessary to limit the cost of reproductive interference (McPeck & Gavrillets, 2006; Yamaguchi & Iwasa, 2013). Numerical simulations assuming two discrete warning traits and fixed warning trait-based assortative mating show that reproductive interference may impair the convergence of warning traits (Boussens-Dumon & Llaurens, 2021). Nevertheless, understanding the impact of reproductive interference on the evolution of warning trait requires to specifically explore the evolution of female preference towards this trait. Moreover, the outcomes of these antagonistic selective forces might range from trait divergence to full convergence, through limited convergence and cannot be investigated in models assuming only discrete and well-differentiated warning traits, calling for a theoretical framework providing general expectations on the gradual evolution of convergent traits.

Here, we thus investigate the selective pressure limiting the convergence of traits involved in mimetic interactions, by building a mathematical model that describes the evolution of quantitative traits in two sympatric species engaged in mimetic interaction. We specifically study the evolution of (1) the quantitative trait t involved in mimetic interaction, displayed in both males and females and (2) the preference p , which value indicates the male trait value preferred by the female. We assume that individuals from different species gain protection from predators, by sharing similar warning trait values with other defended individuals living in the same environment, whatever species they belong to. However, trait similarity between species generates fitness costs for females *via* reproductive interference (McPeck & Gavrillets, 2006; Yamaguchi & Iwasa, 2013). We neglect fitness costs of reproductive interference acting on males, reflecting the asymmetrical investment in reproduction between sexes observed in numerous species. We assume that a parameter c_{RI} modulates the strength of reproductive interference, and that may reflect the levels of ecological and morphological resemblance between species, likely to increase with their phylogenetic proximity. Because the selective forces acting on warning traits strongly depend on the sensitivity of both females and predators, we test the effect of their discrimination capacity on convergent evolution. We then investigate the interactions between these opposed selective

forces with the effect of historical constraints, reflecting evolutionary history, by assuming different ancestral trait values in the two interacting species, as well as stabilizing selection promoting these ancestral values within each species. Using weak selection approximation (Barton & Turelli, 1991; Kirkpatrick *et al.*, 2002), we obtain equations describing the evolution of the mean trait and mean preference values in both species. We then use analytical results and numerical analyses to investigate the effect of reproductive interference on the convergence of trait, depending on different ecological factors.

Methods

We consider two sympatric species, called species 1 and 2, displaying a warning trait (t_1 and t_2 in species 1 and 2, respectively). We investigate the evolution of the warning trait within each species, influenced by both the learning behavior of shared predators (promoting mimicry between species) and mate choice. In each species $i \in \{1, 2\}$, the trait t_i is expressed in both males and females and we assume that only females express a mating preference for males. The value of female preference p_i indicates the value in male trait triggering the highest attraction of the female. We assume that males and females traits have the same genetic basis, neglecting sexual dimorphism, because sexual dimorphism is rare in mimetic species (Mallet & Joron, 1999). Individuals of both species benefit from increased survival when they display similar trait values, because predators may recognize and associate the warning trait with defense. This resemblance then induces costs for females of each species, because of reproductive interference. We thus assume increasing fitness costs due to reproductive interference, when the traits displayed by males in both species become more similar (see Equation (3.11)).

We assume that in each species the trait and preference are quantitative traits, with an autosomal polygenic basis, and additive effects. We consider discrete and non-overlapping generations. Within each generation, both (1) natural selection

acting on survival and (2) sexual selection acting on reproductive success do occur. Natural selection acting on an individual depends on the trait value it expresses. In each species $i \in \{1, 2\}$, we note $W_{ns}^i(t)$ (defined after in Equation (3.8)) the fitness components due to natural selection acting on an individual displaying the trait value t . To compute the fitness component due to reproduction, we then note $W_r^i(t_m, p_f)$ (defined after in Equation (3.7)) the contribution of a mating between a male with trait t_m and a female with preference p_f of species $i \in \{1, 2\}$ to the next generation. In each species $i \in \{1, 2\}$, we also compute $W_{RI}^i(p_f)$ (defined after in Equation (3.11)) the female fitness component describing fitness reduction due to reproductive interference. Following (Kirkpatrick *et al.*, 2002), the reproductive success $W^i(t_m, t_f, p_f)$ stemming from a mated pair of a male with trait t_m and a female with trait t_f and preference p_f of species i is given by:

$$W^i(t_m, t_f, p_f) = W_{ns}^i(t_m)W_r^i(t_m, p_f)W_{ns}^i(t_f)W_{RI}^i(p_f). \quad (3.1)$$

We assume constant population size (and then constant density) in the two species. We note \bar{W}^i the mean fitness value across all possible mating pairs in species i for $i \in \{1, 2\}$. We assume lottery competition where a mated pair of a male with trait t_m and a female with trait t_f and preference p_f can be chosen as parents with probability $W^i(t_m, t_f, p_f)/\bar{W}^i$.

We assume weak natural and sexual selective pressures (Iwasa *et al.*, 1991; Pomiankowski & Iwasa, 1993) implying that the variance of trait and preference is small relative to the curvature of the fitness function in each species. Using the Price's theorem (see Rice (2004) for instance), we can approximate the change in the mean values of traits (\bar{t}_1, \bar{t}_2) and preferences (\bar{p}_1, \bar{p}_2) in both species, after the natural and sexual selection respectively, by:

$$\begin{pmatrix} \Delta \bar{t}_i \\ \Delta \bar{p}_i \end{pmatrix} = \frac{1}{2} \begin{pmatrix} G_{t_i} & C_{t_i p_i} \\ C_{t_i p_i} & G_{p_i} \end{pmatrix} \begin{pmatrix} \beta_{t_i} \\ \beta_{p_i} \end{pmatrix}, \quad (3.2)$$

where for $i \in \{1, 2\}$ G_{t_i} and G_{p_i} are the additive genetic variances of t_i and p_i and $C_{t_i p_i}$ is the additive genetic covariance between t_i and p_i . β_{t_i} and β_{p_i} describe

the selective forces acting on the trait t_i and the preference p_i respectively and are given by:

$$\beta_{t_i} := \frac{\partial}{\partial t_m} \ln W^i(t_m, t_f, p_f) + \frac{\partial}{\partial t_f} \ln W^i(t_m, t_f, p_f) \Big|_{(t_m, t_f, p_f) = (\bar{t}, \bar{t}, \bar{p})}, \quad (3.3)$$

$$\beta_{p_i} := \frac{\partial}{\partial p_f} \ln W^i(t_m, t_f, p_f) \Big|_{(t_m, t_f, p_f) = (\bar{t}, \bar{t}, \bar{p})}. \quad (3.4)$$

Under weak selection hypothesis, genetic correlations generated by selection and non-random mating quickly reach equilibrium (Nagylaki, 1993) and can thus be approximated by their equilibrium values. Weak selection hypothesis also implies that the variance of trait and preference is low in each species (Iwasa *et al.*, 1991).

Following (Iwasa *et al.*, 1991), we assume that for each $i \in \{1, 2\}$, G_{t_i} and G_{p_i} are positive constants maintained by an equilibrium between selection and recurrent mutations. Under weak selection, for each $i \in \{1, 2\}$, the genetic covariance between t_i and p_i can be approximated by (see Appendix A3.3):

$$C_{t_i p_i} = a_i G_{t_i} G_{p_i}, \quad (3.5)$$

where a_i is the female discrimination in species i (see more details below).

Because under the weak selection hypothesis we assume that a_i is small (weak sexual selection), for each $i \in \{1, 2\}$, $C_{t_i p_i}$ is small in comparison with G_{t_i} and G_{p_i} , allowing us to approximate the change in the mean values of trait and preference in each species $i \in \{1, 2\}$ by:

$$\begin{pmatrix} \Delta \bar{t}_i \\ \Delta \bar{p}_i \end{pmatrix} = \frac{1}{2} \begin{pmatrix} G_{t_i} \beta_{t_i} \\ G_{p_i} \beta_{p_i} \end{pmatrix}. \quad (3.6)$$

Reproduction

In each species $i \in \{1, 2\}$, the contribution to the next generation of a mating between a male with trait t_i and a female with preference p_i is given by

$$W_r^i(t, p) = \exp[-a_i(p_i - t_i)^2], \quad (3.7)$$

where female discrimination $a_i > 0$, assumed constant among conspecific females, quantifies how much females of species i reject males with a non-preferred trait value. Because preference generates sexual selection, we also assume weak female discrimination, in line with the previously-described weak selection hypothesis, *i.e.* $\forall i \in \{1, 2\}$, a_i being of order ε , with ε small.

Ancestral trait value

Phenotypic evolution in both species away from their ancestral trait is limited by historical constraints, specific to each species. The phenotypic evolution thus strongly depends on ancestral trait values in both species t_{a1}, t_{a2} , as well as on the stabilizing selection promoting this ancestral trait value t_{ai} within each species. The strength of the stabilizing selection within each species i depends on the coefficient s_i . The fitness component due to natural selection is thus given by:

$$W_{ns}^i(t_i) = W_{pred}(t_i) \exp[-s_i(t_i - t_{ai})^2], \quad (3.8)$$

where W_{pred} is the fitness component due to predation in species i (see Equation (3.10) below). Because we focus on the interplay between different evolutionary forces, we assume selective coefficients s_1 and s_2 of order ε^2 . This makes selective pressures due to historical constraints, predation and reproductive interference to be of the same order of magnitude (see Appendix A3.2).

Predation depending on the level of mimicry of trait t .

Within each species, the evolution of the trait t , expressed by males and females from the *focal* species, is strongly influenced by the trait displayed in the other species. Müllerian mimicry indeed generates positive density-dependent selection (Benson, 1972; Mallet & Barton, 1989; Chouteau *et al.*, 2016), due to predator learning. This density-dependence is non linear and is often modeled as an hyperbolic decrease in mortality (see (Joron & Iwasa, 2005; Llaurens *et al.*, 2013) for example). The density-dependence is modulated by the individual levels of defense λ_1 and λ_2 , assumed constant among individuals of species 1 and 2, respectively, shaping predator deterrence: the higher the defense, the quicker predators learn. The protection gained against predators then depends on the level of resemblance among defended prey, as perceived by predators, and on the number of individuals sharing similar trait values. The level of protection gained by an individual with trait t because of its resemblance with other individuals is approximated by:

$$\mathcal{D}(t) = \sum_{i=1}^2 \overbrace{\lambda_i n_i \exp[-b(t - \bar{t}_i)^2]}^{\text{protection gained by resemblance with individuals of species } i}, \quad (3.9)$$

because the variance of traits is small relative to the curvature of the fitness function (see Appendix A3.1 for more details). For each $i \in \{1, 2\}$, n_i is the density of individuals in species i . Due to the positive density-dependent selection, $\lambda_i n_i$ is then the defense level in species i . $\exp[-b(t - \tau)^2]$ describes how much predators perceive the trait values t and τ as similar. The predator discrimination coefficient b thus quantifies how much predators discriminate different trait values. We assume that this parameter is of the same order of magnitude as female discrimination a (*i.e.* of order ε). For each $i \in \{1, 2\}$, f_i is the distribution of traits in species i .

We note $d \in (0, 1)$ the basic predation rate and we assume this parameter to be of order ε , with ε small, in line with the weak selection hypothesis. The impact of

predation on the fitness of an individual displaying the trait value t is given by:

$$W_{pred}(t) = 1 - \frac{d}{\mathcal{D}(t)}. \quad (3.10)$$

Cost induced by reproductive interference.

Because heterospecific males may resemble conspecific males, females will suffer from reproductive interference generated by erroneous mating attempts with heterospecific males (see (Gröning & Hochkirch, 2008) for a review of reproductive interference costs). The risk of heterospecific mating depends on the relative densities of heterospecific and conspecific males. We assume a balanced sex-ratio within each species *i.e.* the density of males in species i is $n_i/2$, for $i \in \{1, 2\}$. However, we also consider the capacity of females to recognize conspecific males using alternative cues (pheromones for example). In the model, the investment of females in interspecific mating interaction is captured by the parameter $c_{RI} \in [0, 1]$. This cost of reproductive interference incurred to females can be reduced when female choice is also based on alternative cues differing between mimetic species. Using Equation (1b) in (Yamaguchi & Iwasa, 2013) and that the variance of traits is small relative to the curvature of the fitness function (see Appendix 1 for more details), the fitness of a female of species $i \in \{1, 2\}$ with preference p_i is modulated by:

$$W_{RI}^i(p_i) = \frac{\overbrace{\frac{n_i}{n_i + n_j}}^{\text{probability of encountering a conspecific male with trait } t} \overbrace{\exp[-a_i(p_i - \bar{t}_i)^2]}^{\text{probability of accepting a conspecific male}}}{\exp[-a_i(p_i - \bar{t}_i)^2] \underbrace{\frac{n_i}{n_i + n_j}}_{\text{probability of encountering an heterospecific male with trait } t} + \underbrace{\frac{n_j}{n_i + n_j}}_{\text{probability of encountering an heterospecific male}} \underbrace{c_{RI} \exp[-a_i(p_i - \bar{t}_j)^2]}_{\text{probability of accepting an heterospecific male}}}, \quad (3.11)$$

with $j \in \{1, 2\}$ with $j \neq i$. c_{RI} is the strength of reproductive interference, assumed of order ε , with ε small, in line with the weak selection hypothesis.

Abbreviation	Description
\bar{t}_i/\bar{p}_i	Mean trait/preference value in species i
G_{t_i}/G_{p_i}	Genetic variance of trait t_i /preference p_i
$C_{t_i p_i}$	Genetic covariance between trait t_i and preference p_i
β_{t_i}/β_{p_i}	Selection coefficient on trait t_i /preference p_i
a_i	Female discrimination in species i
s_i	Strength of stabilizing selection due to historical constraints on trait t_i
t_{ai}	Ancestral trait in species i
d	Basic predation rate
b	Predator discrimination
n_i	Density of species i
λ_i	Individuals defense level in species i
$\lambda_i n_i$	Defense level in species i
c_{RI}	Strength of reproductive interference

Table 3.1: Description of variables and parameters used in the model. The subscript $i \in \{1, 2\}$ denotes the identity of the species.

All variables and parameters used in the model are summed up in Table 3.1.

Model exploration.

To specifically test the effect of species interactions on trait convergence, we assume the two species to be initially isolated and explore trait evolution when they become sympatric. Preference for uncommon males leads to opportunity costs (see Equation (A3.3)), promoting mean females preference to be initially equal to mean males trait. We thus assume the initial mean trait and females preference values to equal ancestral trait values within each species. The dynamics of the mean trait and preference values when both species become in contact are then given by Equation (3.6).

Evolution of warning trait in a mimetic species interacting with a fixed *model* species

We first consider the classical case where the species 1 is a *mimic* of the *model* species 2. We thus assume higher abundance ($n_2 \gg n_1$) and greater defense level

in species 2 as compared to species 1. In this case, species 1 weakly impacts the evolution of trait and preferences in species 2, neither through mimicry nor through reproductive interference. We then assume fixed mean trait and preference in species 2, sticking to the ancestral trait value ($\bar{t}_2 = \bar{p}_2 = t_{a2}$). This hypothesis allows a full analytical resolution (see below).

Analytical resolution assuming weak female and predator discriminations ($a_1 = O(\varepsilon)$ and $b = O(\varepsilon)$) Assuming that a_1 and b are of order ε and that s_1 is of order ε^2 , we analytically determine the mean trait and preference values in species 1 at equilibrium (\bar{t}_1^* and \bar{p}_1^*).

Model exploration assuming strong female and predator discriminations ($a_1 = O(1)$ and $b = O(1)$) Because the stringency of the discrimination behavior of female and predator are key drivers of the advergence toward the trait displayed in species 2, we then explore larger values of female and predator discriminations, *i.e.* $a_1 = O(1)$ and $b = O(1)$. Under such assumptions, the effects of predation and reproductive interference on the changes in the mean trait and preference are of order ε . We also assume that s_1 is of order ε , because if s_1 were of order ε^2 the strength of historical constraints would be negligible as compared to the other two selective forces. Assuming strong female discrimination violates the weak selection hypothesis, because strong female discrimination generates strong sexual selection for males and large opportunity cost for females. However, because strong female discrimination leads to higher sexual selection, the discrepancy between preference and trait values ($|\bar{t}_1^* - \bar{p}_1^*|$) becomes limited. Therefore, sexual selection and opportunity cost are actually weak and we can still estimate the matrix of genetic covariance and assume that the genetic variances of traits and preference are low. We assume that the variances of trait and preference are low to keep them small relative to the curvature of the fitness function in each species when ($a_1 = O(1)$ and $b = O(1)$). However, because of the complexity of the model, under strong female and predator discriminations ($a_1 = O(1)$ and $b = O(1)$), we cannot analytically determine the mean trait and preference values at equilibrium

(\bar{t}_1^* and \bar{p}_1^*). We then use numerical simulations of Equation (3.6) to explore cases where a_1 and b are of order 1 and s_1 is of order ε .

Effect of weak or strong female and predator discriminations To investigate the impact of weak or strong female and predator discriminations, we run simulations assuming different values of these parameters. We assumed that $a_1 \propto \tilde{\varepsilon}'$, $b \propto \tilde{\varepsilon}'$, $s_1 \propto \tilde{\varepsilon}\tilde{\varepsilon}'$, $d \propto \tilde{\varepsilon}$ and $c_{RI} \propto \tilde{\varepsilon}$, where \propto means 'proportional to'. Where $\tilde{\varepsilon} = 0.01$ in line with the weak selection hypothesis and $\tilde{\varepsilon}' \in \{1, 0.1, 0.01\}$. The different values of $\tilde{\varepsilon}'$ allows to investigate the intermediate case between weak and strong female and predator discriminations.

The effect of the different parameters on the level of trait divergence $|\bar{t}_1^* - \bar{t}_2^*|$, assuming weak or strong female and predator discriminations, are presented in Appendix A3.4.2.

Joint evolution of warning traits within two interacting species

We then study the joint evolution of trait and preference in both species 1 and 2, accounting for the general case of mimicry between sympatric species with various relative abundances and defense levels, where evolution of traits can occur in both species.

Exploration assuming weak female and predator discriminations ($a_1 = O(\varepsilon)$, $a_2 = O(\varepsilon)$ and $b = O(\varepsilon)$) When we assume that a_1 , a_2 and b are of order ε and s_1 and s_2 are of order ε^2 , we can analytically determine the mean traits and preferences values at equilibrium in most cases. In the few remaining cases, we use numerical analyses to estimate these values (see Appendix A3.5.2). We note \bar{t}_1^* , \bar{t}_2^* , \bar{p}_1^* and \bar{p}_2^* the mean traits and preferences at equilibrium. We follow the quantity $|\bar{t}_1^* - \bar{t}_2^*|$, *i.e.* the mean phenotypic distance between both species at equilibrium, reflecting the level of convergence of traits between species.

Exploration assuming strong female and predator discriminations ($a_1 = O(1)$, $a_2 = O(\varepsilon)$ and $b = O(1)$) Similarly to the previous model exploration, we use numerical simulations to study cases where female and predator discriminations are strong ($a_1 = O(1)$, $a_2 = O(1)$, $b = O(1)$ and $s_1 = O(\varepsilon)$).

The effect of different parameters on the level of trait divergence $|\bar{t}_1^* - \bar{t}_2^*|$, assuming weak or strong female and predator discriminations, are presented in Appendix A3.5.3.

Testable predictions

We use our theoretical model to investigate 3 main questions and to generate predictions that could be then investigated in natural communities of defended species:

What is the impact of reproductive interference on the level of convergence between species ?

To identify the general impact of the strength of reproductive interference c_{RI} on the phenotypic distance between the two species ($|\bar{t}_1^* - \bar{t}_2^*|$), we first look at the analytical resolution assuming that trait and preference are fixed in species 2 ($\bar{t}_2 = \bar{p}_2 = t_{a2}$) and weak female and predator discriminations ($a_1 = O(\varepsilon)$ and $b = O(\varepsilon)$). We then check whether the results obtained in this simplified case still stand when assuming the joint evolution of traits and preference between the two species and strong female and predator discriminations.

What is the impact of the discrimination capacities of predators and choosing females on the level of convergence ?

We assume a fixed level of reproductive interference ($c_{RI} = 0.002$), and that female discrimination is equal in both species ($a_1 = a_2 = a$). We investigate the impact of

female and predator discriminations (a and b) on the phenotypic distance between the two species ($|\bar{t}_1^* - \bar{t}_2^*|$).

What is the impact of relative abundance and defenses levels between species on the direction and strength of convergence ?

We assume that species 2 is well defended ($\lambda_2 = 0.1$, $n_2 = 10$). We investigate the impact of density and of the individual defense level in species 1 (n_1 and λ_1) on the traits displayed in both species and on the phenotypic distance between the two species ($\bar{t}_1^* - \bar{t}_2^*$) with either or not reproductive interference ($c_{RI} = 0$ or $c_{RI} = 0.005$). To determine the direction of advergence, we check whether the trait values observed at equilibrium (*i.e.* \bar{t}_1^* and \bar{t}_2^*) are closer to the ancestral trait value of species 1 or of species 2 (t_{a1} or t_{a2} respectively).

Data and Code Accessibility

Codes are available online: github.com/Ludovic-Maisonneuve/limits-of-ev-conv

Results

Evolution of warning trait in a mimetic species in sympatry with a *model* species

When species 2 is well defended and more abundant than species 1 ($n_2 \gg n_1$), we assumed that trait and preference are fixed in species 2, as in classical *mimic/model* interactions between species (see Method for more details). Assuming weak female and predator discriminations, the mean trait and preference values both converge to the equilibrium values \bar{t}_1^* and \bar{p}_1^* with

$$\bar{t}_1^* = \frac{\frac{2bd\lambda_2 n_2}{(1+\lambda_1 n_1 + \lambda_2 n_2)^2} \bar{t}_2 + 2s_1 t_{a1} - a_1 c_{RI} \frac{n_2}{n_1} \bar{t}_2}{\frac{2bd\lambda_2 n_2}{(1+\lambda_1 n_1 + \lambda_2 n_2)^2} + 2s_1 - a_1 c_{RI} \frac{n_2}{n_1}}, \quad (3.12)$$

and

$$\bar{p}_1^* = \bar{t}_1^* + c_{RI} \frac{n_2}{n_1} (\bar{t}_1^* - \bar{t}_2), \quad (3.13)$$

when

$$a_1 \frac{n_2}{n_1} c_{RI} < \left(\frac{4bd\lambda_2 n_2}{(1 + \lambda_1 n_1 + \lambda_2 n_2)^2} + 4s_1 \right), \quad (3.14)$$

see Appendix A3.4.2.

These analytical expressions allow to predict on the level of resemblance between the trait displayed in species 1 and the fixed trait exhibited in the *model* species 2 ($|\bar{t}_1^* - \bar{t}_2|$) and to study the impact of the different evolutionary forces on the advergence between *mimic* and *model*.

However, when (3.14) is not verified, the distances between mean trait and preference values in species 1 and \bar{t}_2 become very large (not of order 1), and mimicry does not emerge (see Appendix A3.4.2).

Reproductive interference limits mimicry.

Selection exerted by predators favors the advergence of trait in species 1 toward the fixed trait value exhibited in the *model* species 2. When (3.14) is verified, the level of advergence toward \bar{t}_2 is given by:

$$|\bar{t}_1^* - \bar{t}_2| = \frac{2s_1}{\frac{2bd\lambda_2 n_2}{(1 + \lambda_1 n_1 + \lambda_2 n_2)^2} + 2s_1 - a_1 c_{RI} \frac{n_2}{n_1}} |t_{a1} - \bar{t}_2|. \quad (3.15)$$

Hence, if we assume no reproductive interference ($c_{RI} = 0$), we have $|\bar{t}_1^* - \bar{t}_2| < |t_a - \bar{t}_2|$, implying that the trait displayed in species 1 gets closer to the trait displayed in species 2. We then observe different evolutionary outcomes ranging from (a) *mimicry* to (b) *imperfect mimicry*, see Figures 3.1(a) and 3.1(b). The mimicry in the species 1 becomes nearly perfect ($|\bar{t}_1^* - \bar{t}_2|$ close to zero) when the strength of selection due to predation ($2bd\lambda_2 n_2 / (1 + \lambda_1 n_1 + \lambda_2 n_2)^2$) is large enough, as compared to the historical constraints limiting the evolution of the trait in species 1 (s_1) (outcome (a) *mimicry* see Figure 3.1(a)).

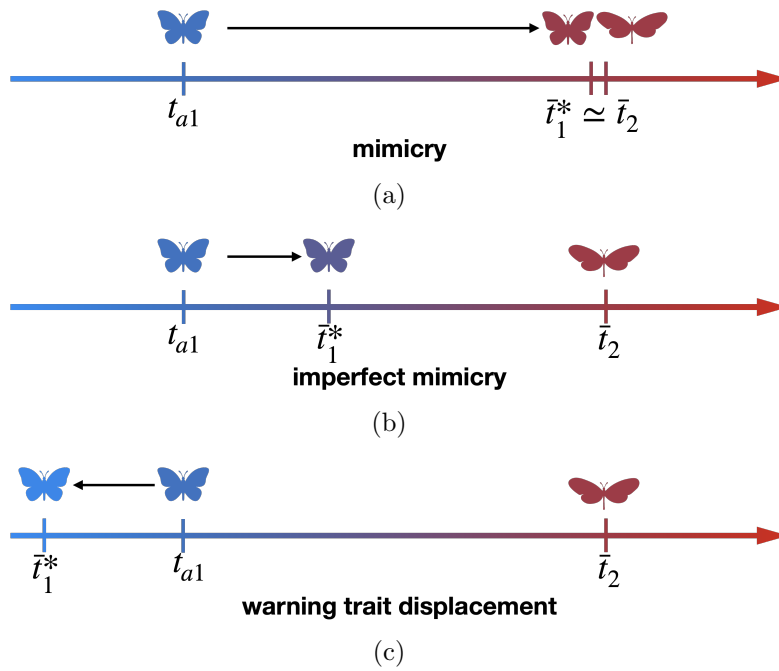


Fig. 3.1: **Illustration of three approximate patterns referred in this paper:** (a) *mimicry*: the value of the trait in species 1 \bar{t}_1 becomes very close to the mean value displayed in species 2 \bar{t}_2 , (b) *imperfect mimicry*: the value of the trait in species 1 \bar{t}_1 gets closer but stays distant from the mean value displayed in species 2 \bar{t}_2 , (c) *warning trait displacement*: the value of the trait species 1 \bar{t}_1 diverges away from the mean value displayed in species 2 \bar{t}_2 .

However, assuming reproductive interference between females from species 1 and males from species 2 impairs advergence. When reproductive interference is non null but has a limited strength, satisfying Inequality (3.14), Equation (3.15) implies that $\partial|\bar{t}_1^* - \bar{t}_2|/\partial c_{RI} > 0$ (see Appendix A3.4.2). Reproductive interference thus increases the distance between the traits displayed in both species, leading to imperfect mimicry in species 1. Reproductive interference promotes the evolution of preference in the opposite direction of the trait displayed by heterospecific males (3.13). Because female preference generates sexual selection on male traits, reproductive interference promotes phenotypic divergence between both species (see Equation (3.13)). Thus reproductive interference limits Müllerian mimicry.

However, when the cost associated with reproductive interference crosses a thresh-

old and (3.14) is verified, *i.e.* when

$$\frac{n_1}{a_1 n_2} \frac{4bd\lambda_2 n_2}{(1 + \lambda_1 n_1 + \lambda_2 n_2)^2} \leq c_{RI} < \frac{n_1}{a_1 n_2} \left(\frac{4bd\lambda_2 n_2}{(1 + \lambda_1 n_1 + \lambda_1 n_1)^2} + 4s_1 \right), \quad (3.16)$$

then

$$|\bar{t}_1^* - \bar{t}_2^*| > |t_{a1} - \bar{t}_2|. \quad (3.17)$$

When assuming such an elevated cost of reproductive interference, imperfect mimicry is thus no longer observed, and reproductive interference rather promotes warning trait displacement. The trait in species 1 diverges away from the trait displayed in species 2 \bar{t}_2 (see Figure 3.1(c) for an illustration).

When inequality (3.14) is not satisfied, the phenotypic distance between both species becomes very large. This very large divergence is biologically unrealistic but suggests that reproductive interference can promote phenotypic divergence between defended species living in sympatry. This unrealistic divergence stems from the weak female discrimination ($a_1 = O(\varepsilon)$) assumed: since females have low discrimination (because a_1 is low), females almost always accept heterospecific males, except when the difference between female preference in species 1 and the trait displayed in species 2 is very high. Reproductive interference promotes females preference that limits fitness costs due to reproductive interference, and therefore promotes a large distance between females preference value in species 1 and the value of the trait displayed in species 2. Relaxing the weak female and predator discriminations hypothesis, *i.e.* assuming that $a_1 = O(1)$ and $b = O(1)$, confirms that reproductive interference limits mimicry in species 1 (see Figure 3.2). However, in this case, when a strong divergence is favored, this divergence becomes high but stays of order $O(1)$. Indeed, as female discrimination is high, this divergence strongly reduces fitness cost due to reproductive interference. Therefore, stabilizing historical constraints on the trait become more important than reproductive interference, thereby preventing very large divergence. Figure 3.2 shows that numerical simulations with parameter values matching weak female and predator discriminations provide similar predictions than the analytical approximation obtained under the same hypotheses.

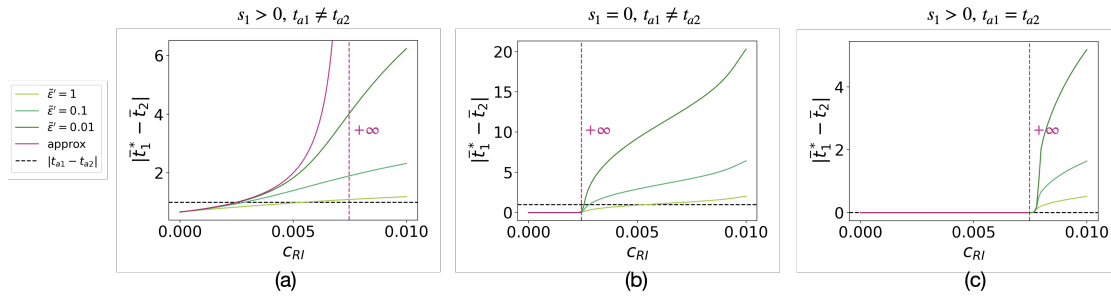


Fig. 3.2: Influence of the strength of reproductive interference c_{RI} on the phenotypic distances between the two species $\bar{t}_1^* - \bar{t}_2$ when trait in species 2 is fixed ($\bar{t}_2 = t_{a2}$), using the analytical approximation (purple curve) or numerical simulations (green curves). We assume (a) $s_1 = 0.5\tilde{\epsilon}\tilde{\epsilon}'$, $t_{a1} = 0$, $t_{a2} = 1$, (b) $s_1 = 0$, $t_{a1} = 0$, $t_{a2} = 1$, and (c) $s_1 = 0.5\tilde{\epsilon}\tilde{\epsilon}'$, $t_{a1} = t_{a2} = 1$ with $\tilde{\epsilon} = 0.01$. We also assume: $G_{t_1} = G_{p_1} = 0.01$, $a_1 = \tilde{\epsilon}'$, $b = \tilde{\epsilon}'$, $d = 2\tilde{\epsilon}$, $\lambda_1 = 0.1$, $\lambda_2 = 0.1$, $n_1 = 10$, $n_2 = 20$. Analytical approximation curves are obtained with $\tilde{\epsilon}' = 0.01$.

These results are maintained when traits and preferences jointly evolve in the two sympatric species (see Figure A3.11).

Historical constraints promoting ancestral trait values allow the evolution of imperfect mimicry

Our previous results highlight that reproductive interference limits the convergence of warning traits. However, the effect of reproductive interference on trait divergence strongly depends on the historical constraints (s_1) promoting the ancestral trait value (t_{a1}). In particular, the effect of historical constraints depends on the distances between the ancestral trait values in species 1 and 2. When species ancestrally display different traits, historical constraints limit the convergence of trait between both species, when predator pressure exceeds reproductive interference (see Appendix A3.4.2). By contrast, historical constraints may limit the divergence of trait between both species when reproductive interference exceeds predator pressure and promotes warning trait displacement (see Appendix A3.4.2). Assuming historical constraints ($s_1 > 0$) and when the ancestral trait values of the

two species differ ($t_{a1} \neq t_{a2}$), an increase in strength of reproductive interference leads to a progressive increase in the phenotypic distance between both species until the phenotypic distance between both species becomes very large (see purple curve in Figure 3.2(a)).

Surprisingly, without historical constraints ($s_1 = 0$) or when the ancestral trait values are the same in both species ($t_{a1} = t_{a2}$), \bar{t}_1 is either equal to \bar{t}_2 when (3.14) is verified, or is very large, when (3.14) is not verified (see purple curve in Figures 3.2(b) and 3.2(c)). Therefore an increase in the strength of reproductive interference (c_{RI}) has no effect on the phenotypic distance between both species, as long as this strength remains below a threshold. This effect is also observed assuming strong female and predator discriminations (see green curves in Figures 3.2(b) and 3.2(c)).

However, when the strength of reproductive interference (c_{RI}) is greater than this threshold, assuming weak female and predator discriminations, the phenotypic distance between both species becomes instantaneously very large. A similar trend is observed when female and predator discriminations are strong: the phenotypic distance is null when the strength of reproductive interference remains below a threshold, but it quickly increases to a high value when the strength of reproductive interference crosses the threshold (see green curves in Figures 3.2(b) and 3.2(c)). This pattern is also observed when traits jointly evolve in both species (see Figure A3.20).

Our results highlight that historical constraints promoting ancestral traits strongly modulate the effect of reproductive interference on the convergence of warning traits. Surprisingly, drastic divergence might be promoted by a strong strength of reproductive interference, even when the ancestral phenotypes are the same in the two interacting species.

Overall, our analytical results reveal the mechanisms underlying trait and preference evolution. However, these analytical results are obtained under restrictive hypotheses: we assumed fixed trait and preference in species 2 and weak female and predator discrimination. To relax those hypotheses, we then study the joint

evolution of traits and preference in both species and study the effect of strong female and predator discrimination using numerical simulations in the following sections.

Higher female than predator discrimination not always favors the convergence of warning traits between two interacting species.

The joint evolution of the traits in both species is shaped by two antagonistic evolutionary forces, generated by reproductive interference and Müllerian mimicry, respectively. Reproductive interference indirectly limits mimicry by impacting females' preference. Therefore, female discrimination a_1 and a_2 may be a key feature to understand the evolution of the trait within each species. The selection exerted by predation also depends on animal behavior through predator learning. We thus investigate the impact of the strength of female discrimination, assumed equal in both species $a_1 = a_2 = a$, and of predator discrimination coefficient b on the evolution of the warning trait.

When female and predator discriminations are low (a and b approximately lower than 3), higher predator than female discrimination favors the convergence of warning traits. Indeed, when female and predator discriminations are low, selections due to predation and reproductive interference are limited and increase with female and predator discriminations respectively. Females are not discriminant (a is low) and tend to accept all encountered males, including heterospecific males, whatever the direction of their preference. The difference in fitness cost due to reproductive interference between females with different preferences is then low, leading to poor divergent selection generated by reproductive interference. With a higher level of female discrimination, fitness cost due to reproductive interference depends more on the direction of preference, leading to higher selection caused by reproductive interference. A similar reasoning on the difference in fitness cost due to predation between individuals displaying different traits explain that selection

promoting convergence, due to predation, increases with the strength of predator discrimination. Therefore, higher predator than female discrimination implies higher selection due to predation than selection due to reproductive interference and promotes mimicry.

By contrast, with higher female discrimination (a approximately greater than 3) and lower predator discrimination (b approximately lower than 3), mimicry becomes more likely (Figure 3.3). Higher levels of female discrimination allow females to accurately distinguish between conspecific and heterospecific males even when they display similar traits. Accurate choice by females allows both species to harbor similar traits from the point of view of predators, without entailing heterospecific mating, relaxing divergent selection generated by reproductive interference.

Surprisingly, when predator discrimination increases above a certain threshold, increased discrimination no longer promotes accurate mimicry (see sharp transition in Figure 3.3). When b is approximately greater than 5.5, mimicry is limited, even without reproductive interference ($c_{RI} = 0$), because of historical constraints (see Figure A3.21). For intermediate predator discrimination ($b \approx 5$), mimicry is limited when reproductive interference is strong and makes similarity too costly for females ($a \approx 1$) (Figure 3.3).

When reproductive interference limits mimicry, it generally leads to warning trait displacement ($|\bar{t}_1^* - \bar{t}_2^*| > |t_{a1} - t_{a2}|$), when female discrimination is low. Under low female discrimination, reproductive interference promotes a large distance between female preference value in species 1 and the value of the trait displayed in species 2, therefore increasing phenotypic distance between the two species.

Reproductive interference can modify the *model/mimic* relationship.

The defense levels in both species, *i.e.* $\lambda_i n_i, i \in \{1, 2\}$, are likely to impact the joint evolution of traits in both species. To investigate how the relative defense

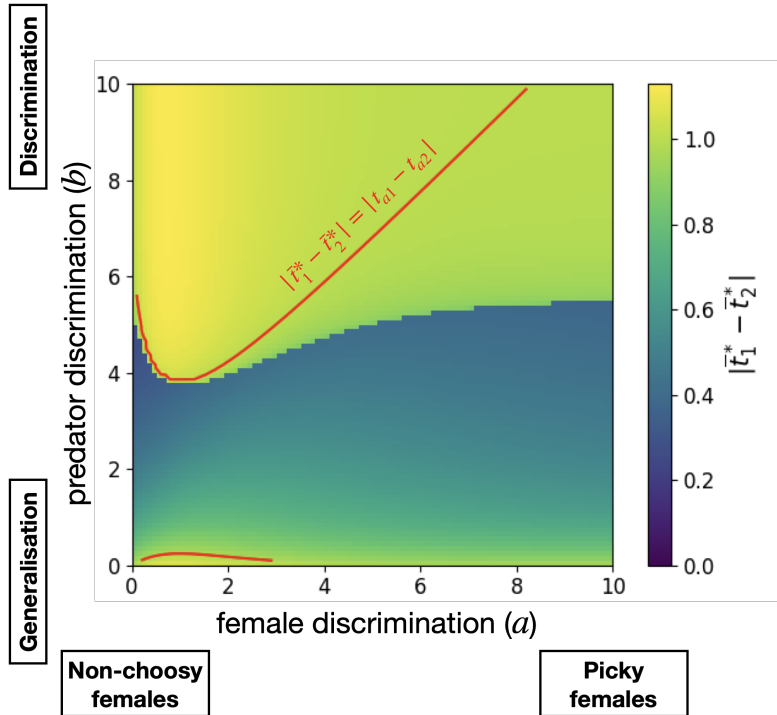


Fig. 3.3: **Influence of female and predator discriminations** ($a_1 = a_2 = a$ and b) on the phenotypic distance between the two species $|\bar{t}_1^* - \bar{t}_2^*|$. The red solid line shows the case where the phenotypic distance between the two species is equal to the ancestral phenotypic distance ($|\bar{t}_1^* - \bar{t}_2^*| = |t_{a1} - t_{a2}|$). We assume: $G_{t_1} = G_{p_1} = G_{t_2} = G_{p_2} = 0.01$, $c_{RI} = 0.002$, $d = 0.02$, $\lambda_1 = \lambda_2 = 0.1$, $n_1 = n_2 = 20$, $s_1 = s_2 = 0.005$, $t_{a1} = 0$, $t_{a2} = 1$.

levels of the two species affect the joint evolution of traits, we study the phenotype at equilibrium in both species and also the phenotypic distance between the two species, for different values of the two components of the defense level of species 1: the individual defense level (λ_1) and the density (n_1). Here we assumed that species 2 is already well protected ($\lambda_2 = 0.1$, $n_2 = 10$).

When assuming no reproductive interference ($c_{RI} = 0$), species traits converge toward the ancestral trait initially displayed in the most defended species. In Figures 3.4(a) and 3.4(b), individuals from the poorly defended species 1 (*i.e.* when $\lambda_1 n_1$ is low) get weak protection from conspecific individuals and thus have a greater advantage to look similar to individuals of species 2. Convergence of

warning traits is thus more likely to happen when species 1 is weakly defended ($\lambda_1 n_1$ small) (see Figure 3.4(c)). The more species 1 is defended, *i.e.* the greater $\lambda_1 n_1$ is, the closer its mean trait value is to the ancestral trait value t_{a1} (see Figure 3.4(a)). Such increase in the defense level of species 1 also impacts the evolution of trait in the sympatric species 2 (see Figure 3.4(b)): when the individual defense level in species 1 (λ_1) is below a threshold, the more individuals from species 1 are protected, the more the mean trait value in species 2 moves away from its ancestral trait (t_{a2}). Surprisingly, above this threshold, the better protected species 1 is, the closer the mean trait value in species 2 gets to its ancestral trait value (t_{a2}). As the mean trait value in species 1 becomes very close to the ancestral trait value t_{a1} , trait values in species 2 leading to protection from heterospecific matings necessitate a great departure from the ancestral trait t_{a2} . Nevertheless, historical constraints still prevent the trait in species 2 to evolve too far away from its ancestral trait value t_{a2} .

When assuming positive strength of reproductive interference ($c_{RI} > 0$), advergence in species 1 toward the trait displayed in species 2 is observed when the individual defense level in species 1 is low (λ_1 approximately lower than 0.1) and when the density in species 1 is sufficiently large (n_1 approximately greater than 2). In this case, the defense level of species 1 ($\lambda_1 n_1$) is low, the protection gained by positive frequency-dependent selection within species is low, and the advergence toward species 2 is thus strongly promoted. Surprisingly, advergence is impaired for similar values of defense level, when the density of species 1 is low (n_1 approximately lower than 2). When the density of species 1 is low, females pay higher fitness costs due to reproductive interference, because they encounter more often heterospecific than conspecific males. Altogether, our results suggest that advergence of the warning traits is likely to happen for low level of individual defense in species 1 (*i.e.* Batesian ($\lambda_1 = 0$) or quasi-Batesian ($\lambda_1 > 0$ but small) mimicry) and when the density of species 1 is high.

The trait value of species 1 does not always converge toward the trait value initially displayed in species 2 (t_{a2}). On the contrary, individuals of species 2 can mimic individuals of species 1 (see blue zone in Figure 3.4(e)), when the defense level of

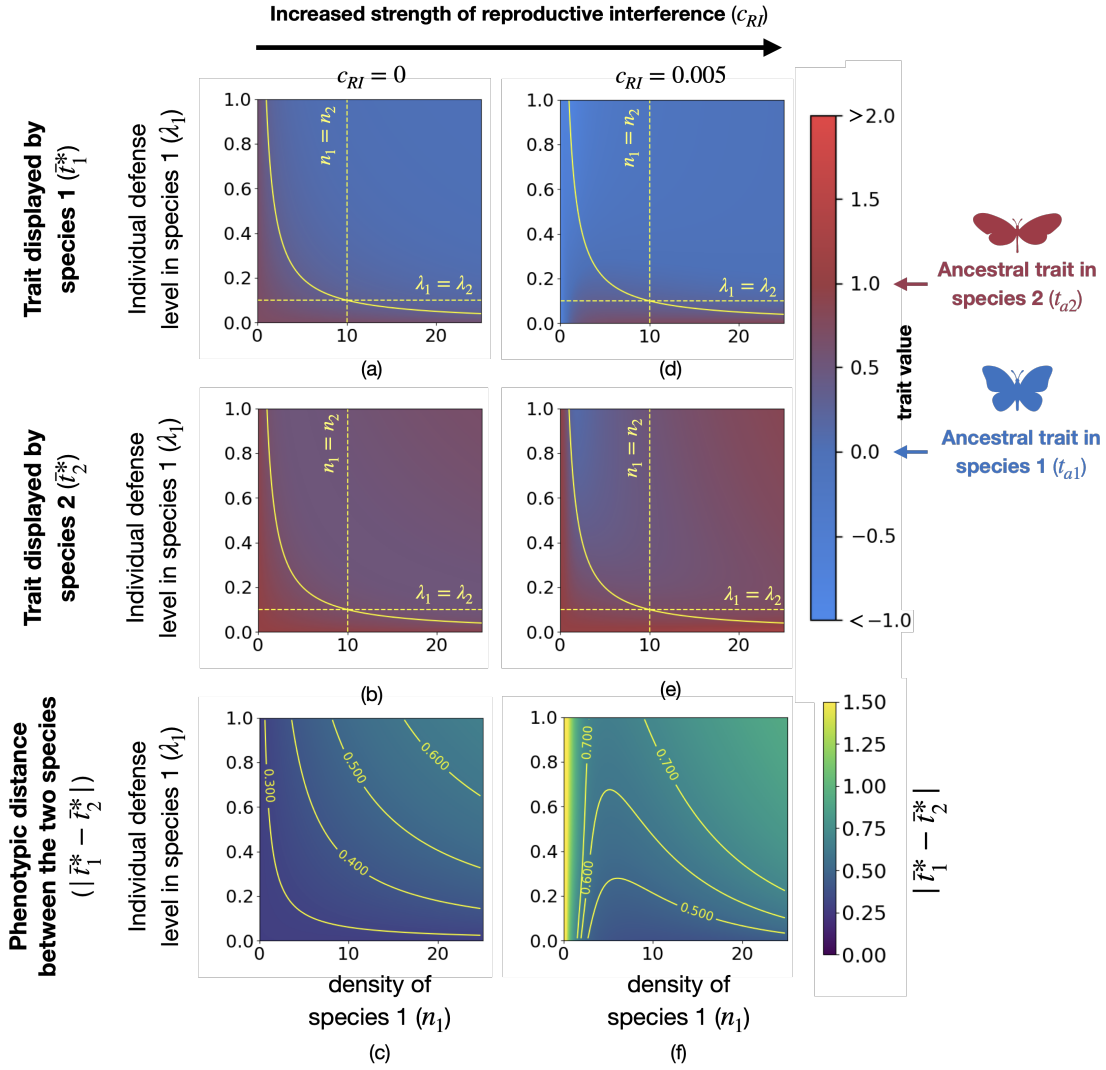


Fig. 3.4: Influence of the density and of the individual defense level in species 1 (n_1 and λ_1) on the traits displayed in both species and on the phenotypic distance between the two species $\bar{t}_1^* - \bar{t}_2^*$, for different strengths of reproductive interference (c_{RI}). (a)(b)(d)(e) Trait values greater than 2 (resp. lower than -1) are shown in red (resp. blue). The yellow solid line shows the case where both species have the same level of defense ($\lambda_1 n_1 = \lambda_2 n_2$). Below (resp. above) this line species 1 has a lower (resp. higher) level of defense than species 2. (c)(f) Phenotypic distances greater than 1.5 are shown in yellow. Yellow lines indicate equal levels of $\bar{t}_1^* - \bar{t}_2^*$. Different values of strengths of reproductive interference are assumed: (a), (b) and (c) $c_{RI} = 0$, (d), (e) and (f) $c_{RI} = 0.005$. We assume: $G_{t_1} = G_{p_1} = G_{t_2} = G_{p_2} = 0.01$, $a_1 = a_2 = 1$, $d = 0.05$, $b = 1$, $\lambda_2 = 0.1$, $n_2 = 10$, $s_1 = s_2 = 0.005$, $t_{a1} = 0$, $t_{a2} = 1$.

individuals of species 1 is high and when species 1 is rare. Because individuals from both species are well defended (high λ_1 and λ_2), individuals of both species benefit from looking similar. However, when species 1 is rarer, this leads to an increased

cost of reproductive interference in species 1, inhibiting convergence towards the ancestral trait value displayed in the alternative species (t_{a2}) (see Figure 3.4(d)). Since predation pressure promotes convergence of traits of both species, the mean trait in species 2 becomes closer to species 1 ancestral trait value t_{a1} . Surprisingly assuming weak female and predator discriminations, such advergence also happens when individuals of species 2 are more defended than individuals from species 1, *i.e.* $\lambda_2 n_2 > \lambda_1 n_1$ (see blue zones in Figures A3.22 (c) and (d) below the yellow solid line). By contrast, when the density in species 1 exceeds the density in species 2, individuals from both species exhibit traits close to their ancestral traits. Both species are well-protected and then gain little from mimicry. Because unbalanced relative density ratio leads to strong cost of reproductive interference in the scarcest species limiting mimicry, mimicry is more likely to be observed between species of similar density (see Figure 3.4(f)).

Our results highlight that reproductive interference impacts the evolution of warning traits, and may even reverse the expected *model/mimic* relationship, depending on the relative abundances and individual defense levels of sympatric species.

Discussion

Reproductive interference alone can not explain imperfect mimicry

Our results show that reproductive interference and historical constraints promoting ancestral traits can generate a continuous range of phenotypic distances from quasi perfect mimicry to warning trait displacement. Our study suggest that reproductive interference alone is unlikely to promote imperfect mimicry, in contradiction with previous predictions (Pfennig & Kikuchi, 2012). When sympatric species share the same ancestral trait, or in absence of historical constraints, we indeed observe either perfect mimicry or strong trait divergence, depending on the strength of reproductive interference. In our model, imperfect mimicry is

observed only when interacting species have different ancestral traits. The contrasted historical constraints undergone by the different species may thus play an important role in imperfect mimicry. These different constraints may be strongly correlated with the phylogenetic distances between species: closely-related species are likely to share similar genetic bases and developmental pathway leading to the warning trait and to also share similar environments, due to niche conservatism (Chazot *et al.*, 2014; Joshi *et al.*, 2017; Elias *et al.*, 2008), likely to limit departure from ancestral trait values. Our results suggest that imperfect mimicry could not be promoted among closely-related species experiencing high levels of reproductive interference but limited differences in ancestral traits. Imperfect mimicry may rather be observed between phylogenetically-distant species, subject to more strikingly different historical constraints, where reproductive interference might be more limited. Distantly-related species indeed might have diverged in other traits, facilitating mate recognition through different cues.

For similar historical constraints, mimicry between defended species can then either be promoted or limited depending on predator discrimination. Low predator discrimination allows the evolution of imperfect mimicry, since imperfect mimics are seen as similar by predators, allowing mutualistic relationship without implying strong cost of historical constraints. By contrast under high predator discrimination, mutualistic mimetic relationships necessitate a strong similarity between species, which is limited by historical constraints. Empirical studies based on vertebrates or on insects show that predators do not perceive difference between Batesian mimics and their models, or at least this difference does not entail a difference in behavior (Dittrich *et al.*, 1993; Kikuchi & Pfennig, 2010; Morris & Reader, 2016). Loose predator discrimination may therefore play a key role in the evolution of imperfect mimicry.

How important are historical constraints in the evolution of warning trait?

Estimating the level of historical constraints potentially shaping the evolution of warning traits is not straightforward. Genetic studies, reviewed in Joron *et al.* (2006a), show that *Heliconius* species share the same 'toolkit' of genes, repeatedly recruited during both convergent and divergent evolutions of warning traits within and between species. This important lability in color patterns observed in this genus suggests a limited level of developmental constraints, facilitating the evolution of mimicry, even between species from different sub-clades within this genus (Hines *et al.*, 2011). By contrast, in butterflies from the tribe ithomiines and in butterflies in tropical forests of the Western Ghats, India, a strong phylogenetic signal on the warning trait is observed (Elias *et al.*, 2008; Chazot *et al.*, 2014; Joshi *et al.*, 2017), suggesting that historical constraints may limit the evolution of mimicry among distantly related species.

Evolution of female preferences limiting the reproductive interference costs generated by mimicry

When considering reproductive interference, the relationship between female and predator discriminations is crucial to understand the evolution of warning traits. Surprisingly, when female and predator discriminations are low, higher predator than female discrimination promotes convergence of warning traits because selection due to predation and reproductive interference increase with predator and female discrimination respectively. By contrast, when female and predator discriminations are high, imperfect mimicry can evolve despite reproductive interference. When female discrimination is high, successful species recognition might occur without decreasing the protection brought by mimicry. Such situation arises when predators largely generalize, and therefore do not discriminate imperfect mimics. Some studies report similar female and predator discriminations (Finkbeiner *et al.*, 2014; McClure *et al.*, 2019), suggesting that reproductive interference may act on

mimetic species. On the other hand, differences in the discrimination of color patterns between prey and predators may exist in the wild. For instance, Llaurens *et al.* (2014) showed that the variations in color pattern between co-mimetic species from the distantly related genera *Heliconius* and *Melinaea* might be better perceived by the *Heliconius* butterflies themselves but not by avian predators. The evolution of visual perception in females could also enhance species discrimination without impairing mimicry. The evolution of vision in females from the *Heliconius* butterflies indeed coincides with the evolution of the yellow pigments 3-OH-kinurenin displayed on their wings (Bybee *et al.*, 2012). The evolution of high discrimination capacities in mimetic prey, as well as the evolution of mating cues undetected by predators could thus limit the cost of reproductive interference in mimetic prey. In butterflies, mate choice indeed often relies on pheromones that may strongly differ among closely-related mimetic species (Darragh *et al.*, 2017; González-Rojas *et al.*, 2020). Similarly, in non-mimetic species, chemical cues may reduce reproductive interference without entailing reproductive character displacement on a trait under natural selection. Females of the swordtails *Xiphophorus pygmaeus* prefer larger mate leading to reproductive interference with males of the *Xiphophorus nigrensis* species. However *X. pygmaeus* females avoid mating with heterospecific on the basis of chemical cues (Crapon de Caprona & Ryan, 1990). Micro-habitat differences among mimetic species may also allow reducing heterospecific encounters, while still benefiting mimicry by sharing the same predator community (Estrada & Jiggins, 2002). For example the two sympatric ladybird species *Harmonia axyridis* and *Harmonia yedoensis* have similar body size and coloration (Sasaji, 1998) and experience reproductive interference (Noriyuki *et al.*, 2012). These species nevertheless have different host specialization (Noriyuki *et al.*, 2011), that may limit reproductive interference (Noriyuki, 2015). Likewise, in three *Morpho* butterfly species displaying local convergence in wing patterns (Llaurens *et al.*, 2021), temporal segregation in patrolling activity has been observed between species sharing similar color patterns (Le Roy *et al.*, 2021), which may strongly limit heterospecific rivalry.

The levels of reproductive interference among mimetic species might thus be mod-

ulated by the evolution of the converging traits themselves, as well as the evolution of other traits involved in species interactions.

Reproductive interference strongly impacts species with low relative density.

Our model shows that the effect of reproductive interference strongly depends on the relative abundances of interacting species, leading to surprising evolutionary outcomes. For example, in rare defended species, selection favoring mimicry towards a defended *model* species is expected to be strong. Nevertheless, our model shows that an elevated cost of reproductive interference prevents the evolution of mimicry in the rarest species, because females then encounter much more heterospecific than conspecific males.

Reproductive interference may particularly promote the emergence and persistence of a distinct warning trait in low-density populations of warning species coming into contact with a local mimicry ring that exhibits a different warning trait. Nevertheless, our model does not take into account the dynamics of population density, and therefore ignores the extinction risk of low-density populations. Such non-mimetic populations with low density might nevertheless persist in the wild, when the level of individual defense is sufficiently high.

Because undefended mimics have a negative impact on predator learning (Lindström *et al.*, 1997), they are expected to be scarce compare to their models (Kunte *et al.*, 2021). In line with this prediction, empirical studies report low density of undefended mimics compared to their defended models (Long *et al.*, 2015; Prusa & Hill, 2021). Reproductive interference may act strongly on Batesian mimics because of their low density with respect to the *model* species. Our model thus suggests that Batesian mimicry among closely related species may be limited by strong reproductive interference acting on Batesian mimics due to phylogenetic proximity and unbalanced density. By contrast, Batesian mimicry may evolve between distantly-related species despite unbalanced density, because high phylo-

genetic distance reduces risk of reproductive interference. This is supported by the pattern of convergence observed in tropical forests of the Western Ghats in India: Müllerian mimicry is observed between closely related species whereas Batesian mimicry involves more distantly related species (Joshi *et al.*, 2017).

Reproductive interference does not always promote divergence of reproductive character (here the warning trait) but can also provoke spatial segregation between species (Gröning & Hochkirch, 2008). The strong reproductive interference acting on scarce mimetic species may limit their coexistence with more abundant mimetic species displaying similar warning signals. Reproductive interference may then restrict the spatial distribution of mimetic species with low abundance to the edges of the range occupied by more abundant co-mimetic species.

Our model also brings new insights to the ecological processes driving the direction of advergence in warning traits. In the absence of reproductive interference, warning traits are expected to evolve in the less defended species (*e.g.* low density populations and/or low level of individual defense) and become mimetic of better-defended species living in sympatry (Balogh & Leimar, 2005; Franks & Sherratt, 2007). When considering the cost of reproductive interference, however, this general trend does not always hold. Our results show that warning traits in the most defended species can evolve toward the warning trait of the less abundant one.

Our model therefore highlights the interplay between mutualism and reproductive interference in sympatric species, which determines the strength and the direction of traits evolution involved in these ecological interactions.

Reproductive interference can explain the emergence of mimetic diversity

In our model, we consider the evolution of warning trait between two interacting species. In the wild however, natural communities involve a variable number of mimetic species, with mimicry ring size ranging from 2 to a dozens of species (Kunte *et al.*, 2021). Assuming reproductive interference, species richness within a

mimicry ring may influence warning trait evolution. We hypothesize that mimicry rings with high species richness are more likely to contain closely related species. The evolution of mimicry in a species may be limited if a closely related species is abundant in the ring because of the strong cost of reproductive interference generated. However, in a mimicry ring with high species richness, species distantly related from the focal species and belonging to the mimicry ring do not imply cost (or at least weak) of reproductive interference but do increase protection against predators promoting mimicry in the focal species. This increased advantage of mimicry towards mimicry ring with high species richness may counterbalance costs due to reproductive interference, increasing the likelihood of having closely related species within large mimicry rings.

Our results shed light not only on the persistence of distinct warning traits within local communities of defended species in the wild, but also on the emergence of these distinct warning traits in the first place. Mimetic diversity is an apparent paradox but several hypotheses have been suggested to promote the persistence of different warning signals, such as the segregation of predators within microhabitats (Beccaloni, 2008; Devries *et al.*, 1999; Elias *et al.*, 2008; Willmott *et al.*, 2017). The spread of distinct warning traits has then frequently been shown to be promoted by demographic stochasticity, as in shifting balance models (Mallet & Joron, 1999; Sherratt, 2006) or in other models combining predator behaviors, such as neophobia, to stochastic effects (Aubier & Sherratt, 2015). However, these models do not provide any selective mechanism explaining the emergence of warning signal with different levels of divergence, contributing to mimetic diversity. By contrast, reproductive interference selects for different levels of divergence in warning traits, and could be a major driver of the diversity of mimetic traits. Note that other mechanisms may generate gradual departure from the ancestral trait value and may also contribute to the diversity of mimetic traits: the evolution of aposematic signals in defended species away from those exhibited in Batesian mimics has been theoretically shown to be promoted (Franks *et al.*, 2009). Artificial modification of the warning trait of mated females has also been demonstrated to reduce harassment by males in the butterfly *H. erato*, and would therefore allow them to lay

more eggs, suggesting that evolution of slightly divergent trait could be promoted in females (Merrill *et al.*, 2018).

We hope our theoretical work will encourage experimental approaches investigating the impact of reproductive interference on mimicry. Such studies may shed lights on the actual role of reproductive interference on mimetic diversity.

Conclusion

Our analytical and numerical results show that reproductive interference and phylogenetic constraints can explain a wide range of levels of convergence, and even explain divergence of warning trait between sympatric species. Our results suggest that reproductive interference alone cannot explain imperfect mimicry, highlighting the role of historical constraints in the evolution of imperfect mimicry. Our study also highlights the importance of female and predator discriminations in the evolution of warning traits.

Acknowledgments

LM would like to thank Dorian Ni for feedbacks on the mathematical part of the study. LM and VL would like to thank Charline Pinna and the whole ‘Evolution and Development of Phenotypic Variations’ team for stimulating discussions on the evolution of the warning traits. The authors would like to thank the ANR SUPERGENE (ANR-18-CE02-0019) for funding the PhD of LM, and the Emergence program from Paris city council for supporting the team of VL. This work was also supported by the Chair “Modélisation Mathématique et Biodiversité” of VEOLIA- Ecole Polytechnique-MNHN-F.X.

Appendix

In Section 1 we detail how some components of fitness can be approximated using that the genetic covariances of traits and preference are low. In Section 2 we detail the computation of the selection vector describing the impact of the selective forces on the evolution of traits and preference. In Section 3, in line with the weak selection hypothesis we suppose that the genetic correlation between trait and preference is at equilibrium and estimate this quantity. In Section 4 we derive results assuming higher abundance in species 2 compared to species 1, allowing to consider fixed trait and preference in species 2. In Section 5 we derive results in the general case.

A3.1 Relative small variance approximation

Because we assume that the variance of traits and preferences is small relative to the curvature of the fitness function we may use approximations in Equations (3.9) and (3.11). Here we detail how we obtained these approximations. \mathcal{D} is defined by

$$\mathcal{D}(t) = \sum_{i=1}^2 \int_{\tau} \overbrace{\lambda_i n_i f_i(\tau) \exp[-b(t-\tau)^2]}^{\text{protection gained by resemblance with individuals of species } i} d\tau, \quad (\text{A3.1})$$

Let $i \in \{1, 2\}$, we have

$$\int_{\tau} f_i(\tau) \exp[-b(t-\tau)^2] d\tau \exp[-b(t-\bar{t}_i)^2] \int_{\tau} f_i(\tau) \exp[b(2t-\tau-\bar{t}_i)(\tau-\bar{t}_i)] d\tau.$$

Using a Taylor expansion of $\exp[b(2t-\tau-\bar{t}_i)(\tau-\bar{t}_i)]$ we have

$$\exp[-b(t-\bar{t}_i)^2] \int_{\tau} f_i(\tau) (1 + b(2t-\tau-\bar{t}_i)(\tau-\bar{t}_i) + O(b(\tau-\bar{t}_i)^2)) d\tau,$$

which is equal to

$$\exp [-b(t - \bar{t}_i)^2] (1 - b\text{Var}(t_i) + O(b\text{Var}(t_i))).$$

Hence when the variance of t_i is small relative to the curvature of the fitness function (implying that $b\text{Var}(t_i)$ is low) the first term of \mathcal{D} can be approximated by

$$\sum_{i=1}^2 \lambda_i n_i \exp [-b(t - \bar{t}_i)^2].$$

The reasoning is similar for each approximation so for $i \in \{1, 2\}$, Equation (3.11) is an approximation of $W_{RI}^i(p_i)$ defined by

$$W_{RI}^i(p_i) = \tag{A3.2}$$

$$\frac{\int_t \overbrace{\frac{n_i}{n_i + n_j} f_i(t)}^{\text{probability of encountering a conspecific male with trait } t} \overbrace{\exp [-a_i(p_i - t)^2]}^{\text{probability of accepting a conspecific male with trait } t} dt}{\int_t \frac{n_i}{n_i + n_j} f_i(t) \exp [-a_i(p_i - t)^2] dt + \int_t \underbrace{\frac{n_j}{n_i + n_j} f_j(t)}_{\text{probability of encountering an heterospecific male with trait } t} \underbrace{c_{RI} \exp [-a_i(p_i - t)^2]}_{\text{probability of accepting an heterospecific male with trait } t} dt}.$$

A3.2 Selection coefficients

In this section we detail how we obtain the expressions for the selection vectors.

For $i \in \{1, 2\}$, the selection coefficients are defined by:

$$\beta_{t_i} := \frac{\partial}{\partial t_m} \ln W^i(t_m, t_f, p_f) + \frac{\partial}{\partial t_f} \ln W^i(t_m, t_f, p_f) \Bigg|_{(t_m, t_f, p_f) = (\bar{t}, \bar{t}, \bar{p})},$$

$$\beta_{p_i} := \frac{\partial}{\partial p_f} \ln W^i(t_m, t_f, p_f) \Bigg|_{(t_m, t_f, p_f) = (\bar{t}, \bar{t}, \bar{p})},$$

where W^i are the fitness of a mated pair of a male with trait t_m and a female with trait t_f and preference p_f of species i , and write

$$W^i(t_m, t_f, p_f) = W_{ns}^i(t_m) W_r^i(t_m, p_f) W_{ns}^i(t_f) W_{RI}^i(p_f).$$

Here W_{ns}^i is the impact of natural selection on fitness and W_{RI}^i is the impact of reproductive interference on fitness of individuals of species i .

A3.2.1 Computation of β_{t_1} and β_{t_2}

For $i \in \{1, 2\}$ the selective forces acting on the trait value in species i write:

$$\begin{aligned} \beta_{t_i} &= \frac{\partial}{\partial t_m} \ln W^i(t_m, t_f, p_f) + \frac{\partial}{\partial t_f} \ln W^i(t_m, t_f, p_f) \Bigg|_{(t_m, t_f, p_f) = (\bar{t}_i, \bar{t}_i, \bar{p}_i)} \\ &= \frac{\partial}{\partial t_m} \left\{ -a_i(p_f - t_m)^2 + \ln W_{pred}(t_m) - s_i(t_m - t_{a_i})^2 \right\} \Bigg|_{(t_m, t_f, p_f) = (\bar{t}_i, \bar{t}_i, \bar{p}_i)} \\ &\quad + \frac{\partial}{\partial t_f} \left\{ \ln W_{pred}(t_f) - s_i(t_f - t_{a_i})^2 \right\} \Bigg|_{(t_m, t_f, p_f) = (\bar{t}_i, \bar{t}_i, \bar{p}_i)} \\ &= -2a_i(\bar{t}_i - \bar{p}_i) + 2 \frac{\partial}{\partial t} \ln(W_{pred}(t)) \Bigg|_{t=\bar{t}_i} - 4s_i(\bar{t}_i - t_{a_i}). \end{aligned}$$

Recall the definition of W_{pred} in (10). The second term of the right hand side equals

$$2 \frac{\partial}{\partial t} \ln (W_{pred}(t)) = -4b \left((t - \bar{t}_2) \lambda_2 n_2 \exp [-b(t - \bar{t}_2)^2] + (t - \bar{t}_1) \lambda_1 n_1 \exp [-b(t - \bar{t}_1)^2] \right) \left(\frac{1}{1 + \lambda_1 n_1 \exp [-b(t - \bar{t}_1)^2] + \lambda_2 n_2 \exp [-b(t - \bar{t}_2)^2]} - d - \frac{1}{1 + \lambda_1 n_1 \exp [-b(t - \bar{t}_1)^2] + \lambda_2 n_2 \exp [-b(t - \bar{t}_2)^2]} \right).$$

When the parameters b and d are of order ε , we obtain

$$\beta_{t_i} = -2a_i(\bar{t}_i - \bar{p}_i) - \frac{4bd(\bar{t}_i - \bar{t}_j)\lambda_j n_j}{(1 + \lambda_1 n_1 + \lambda_2 n_2)^2} - 4s_i(\bar{t}_i - t_{ai}) + O(\varepsilon^3). \quad (\text{A3.3})$$

A3.2.2 Computation of β_{p_i}

For $i \in \{1, 2\}$ the selective forces acting on the preference value in species i write:

$$\begin{aligned} \beta_{p_i} &= \frac{\partial}{\partial p_f} \ln W^i(t_m, t_f, p_f) \Big|_{(t_m, t_f, p_f) = (\bar{t}_i, \bar{t}_i, \bar{p}_i)} \\ &= \frac{\partial}{\partial p_f} \left\{ -a(p_f - t_m)^2 + \ln W_{RI}^i(p_f) \right\} \Big|_{(t_m, t_f, p_f) = (\bar{t}_i, \bar{t}_i, \bar{p}_i)}. \end{aligned}$$

The last term of the right hand side equals

$$\begin{aligned} \frac{\partial}{\partial p_f} \ln (W_{RI}^i(p_f)) &= -\ln \left(1 + c_{RI} \exp [a_i(\bar{t}_i - \bar{t}_j)(\bar{t}_i + \bar{t}_j - 2p_f)] \frac{n_j}{n_i} \right) \\ &\quad - \frac{-2c_{RI} a_i(\bar{t}_i - \bar{t}_j) \exp [a_i(\bar{t}_i - \bar{t}_j)(\bar{t}_i + \bar{t}_j - 2p_f)] \frac{n_j}{n_i}}{1 + c_{RI} \exp [a_i(\bar{t}_i - \bar{t}_j)(\bar{t}_i + \bar{t}_j - 2p_f)] \frac{n_j}{n_i}} \\ &= \frac{2c_{RI} a_i(\bar{t}_i - \bar{t}_j)}{c_{RI} + \exp [a_i(\bar{t}_i - \bar{t}_j)(2p_f - \bar{t}_i - \bar{t}_j)] \frac{n_j}{n_i}}, \end{aligned}$$

with $j \in \{1, 2\}, j \neq i$.

When the parameters a_1, a_2 and c_{RI} are of order ε , we finally obtain

$$\beta_{p_i} = -2a_i(\bar{p}_i - \bar{t}_i) + 2c_{RI}a_i(\bar{t}_i - \bar{t}_j)\frac{n_j}{n_i} + O(\varepsilon^3). \quad (\text{A3.4})$$

A3.3 Computation of the matrix of correlation

In this part we approximate the genetic covariance between trait and preference $C_{t_i p_i}$ in species i for $i \in \{1, 2\}$, using the results from (Kirkpatrick *et al.*, 2002). Trait and preference are controlled by different sets of unlinked loci with additive effects, denoted T_i and P_i , respectively. For each j in T_i (resp. P_i), we note ξ_j^t (resp. ξ_j^p) the contribution of the locus j on trait (resp. preference) value. The trait and preference values of an individual are then given by

$$t_i = \sum_{j \in T_i} \xi_j^t \quad \text{and} \quad p_i = \sum_{j \in P_i} \xi_j^p. \quad (\text{A3.5})$$

As in (Lande, 1981) we assume that the distributions of ξ_j^t and ξ_j^p are multivariate Gaussian. Let C_{jk} be the genetic covariance between loci j and k . Then the elements of the matrix of correlation are given by:

$$G_{t_i} = \sum_{j, k \in T_i} C_{jk}, \quad G_{p_i} = \sum_{j, k \in P_i} C_{jk} \quad \text{and} \quad C_{t_i p_i} = \sum_{k \in T_i, k \in P_i} C_{jk}. \quad (\text{A3.6})$$

To compute the change on genetic correlation we need to identify various selection coefficients (see (Barton & Turelli, 1991; Kirkpatrick *et al.*, 2002)). These coefficients are obtained using the fitness of a mated pair of a male with trait t_m , and a female with trait t_f , and preference p_f $W^i(t_m, t_f, p_f)$, defined in Equation (3.1).

For simplicity we consider only leading terms in the change in genetic correlation. For $(j, k) \in T_i \times P_i$, combining Equations (9), (12), (15) from Kirkpatrick *et al.* (2002) gives the change in the genetic covariance between loci j and k :

$$\begin{aligned}
\Delta C_{jk} = & -\frac{C_{jk}}{2} + \frac{1}{4}\tilde{a}_{t_m t_m}^i \sum_{l,m \in T_i} (C_{jl}C_{km} + C_{jm}C_{kl}) + \frac{1}{4}\tilde{a}_{p_f p_f}^i \sum_{l,k \in P_i} (C_{jl}C_{km} + C_{jm}C_{kl}) \\
& + \frac{1}{4}\tilde{a}_{t_m p_f}^i \sum_{l \in T_i, m \in P_i} C_{jl}C_{km} + \frac{1}{4}\tilde{a}_{t_m p_f}^i \sum_{l \in T_i, m \in P_i} C_{jm}C_{kl} + O(\varepsilon^2) \quad (\text{A3.7})
\end{aligned}$$

with $\tilde{a}_{\mu\rho}^i$ for $(\mu, \rho) \in \{t_m, t_f, p_f\}^2$ being the leading term of

$$a_{\mu\rho}^i := \frac{1}{2} \frac{\partial^2}{\partial \mu \partial \rho} \ln(W^i(t_m, t_f, p_f)) \Big|_{(t_m, t_f, p_f) = (\bar{t}_i, \bar{t}_i, \bar{p}_i)},$$

the selection coefficient calculated from the fitness of a mated pair of a male with trait t_m and a female with trait t_f and preference p_f . The expressions of these coefficients are:

$$a_{p_f p_f}^i = -a_i - \frac{2c_{RI}a_i^2(\bar{t}_i - \bar{t}_j)^2 \frac{n_i}{n_j} \exp[a_i(\bar{t}_i - \bar{t}_j)(2\bar{p}_i - \bar{t}_i - \bar{t}_j)]}{\left(c_{RI} + \frac{n_i}{n_j} \exp[a_i(\bar{t}_i - \bar{t}_j)(2\bar{p}_i - \bar{t}_i - \bar{t}_j)]\right)^2},$$

$$\begin{aligned}
a_{t_m t_m}^i = & -a_i - s_i + 2b^2 (\lambda_j n_j (1 + (\bar{t}_i - \bar{t}_j)^2) \exp[b(\bar{t}_i - \bar{t}_j)^2] + \lambda_i n_i) \\
& \times \left(\frac{1}{1 + \lambda_i n_i + \lambda_j n_j \exp[b(\bar{t}_i - \bar{t}_j)^2]} - \frac{1}{1 + \lambda_i n_i + \lambda_j n_j \exp[b(\bar{t}_i - \bar{t}_j)^2]} \right) \\
& + (2b\lambda_j n_j (\bar{t}_i - \bar{t}_j) \exp[b(\bar{t}_i - \bar{t}_j)^2])^2 \\
& \times \left(\frac{1}{(1 + \lambda_i n_i + \lambda_j n_j \exp[b(\bar{t}_i - \bar{t}_j)^2] - d)^2} - \frac{1}{(1 + \lambda_i n_i + \lambda_j n_j \exp[b(\bar{t}_i - \bar{t}_j)^2])^2} \right),
\end{aligned}$$

and

$$a_{t_m p_f}^i = 2a_i.$$

A Taylor expansion gives $\tilde{a}_{p_f p_f}^i = -a_i$, $\tilde{a}_{t_m t_m}^i = -a_i$ and $\tilde{a}_{t_m p_f}^i = 2a_i$.

By summing Equations (A3.7) over each j, k in T_i and P_i we obtain:

$$\Delta C_{t_i p_i} = -\frac{C_{t_i p_i}}{2} - \frac{1}{2}a_i G_{t_i} C_{t_i p_i} - \frac{1}{2}a_i G_{p_i} C_{t_i p_i} + \frac{1}{2}a_i G_{t_i} G_{p_i} + \frac{1}{2}a_i C_{t_i p_i}^2 + O(\varepsilon^2). \quad (\text{A3.8})$$

For the sake of simplicity we assumed that the genetic correlations between traits and preference are at equilibrium (as in (Barton & Turelli, 1991; Pomiankowski & Iwasa, 1993)). We obtain from (A3.8) that the value at equilibrium is given by

$$C_{t_i p_i}^* = \frac{1 + a_i(G_{p_i} + G_{t_i}) - \sqrt{-4a_i^2 G_{p_i} G_{t_i} + (1 + a_i(G_{p_i} + G_{t_i}))^2}}{2a_i}.$$

Because the genetic variances of trait and preference are low we have

$$C_{t_i p_i}^* \approx a G_{t_i} G_{p_i}.$$

When we relax the hypothesis $a_i = O(\varepsilon)$ and $b = O(\varepsilon)$ the previous calculation still stands, except that $\tilde{a}_{p_f p_f}^i$, $\tilde{a}_{t_m t_m}^i$ and $\tilde{a}_{t_m p_f}^i$ are of order 1 instead of being of order ε .

A3.4 Evolution of warning trait toward a fixed defended species

We assume higher abundance in species 2 compared to species 1 ($n_2 \gg n_1$). We also assume a great defense level in species 2. In this case species 1 weakly impacts the evolution of trait and preferences in species 2 through mimicry and reproductive interference. We assume fixed mean trait and preference in species 2 equal to the ancestral trait value ($\bar{t}_2 = \bar{p}_2 = t_{a2}$). This hypothesis, which we will relax later, allows a full analytical resolution (see below).

In Section 4.1 we compute the values of trait and preference that cancel the leading term of the selection vector. In Section 4.2 we study when trait and preference converge toward the point found in the previous section. In Section 4.3 we study the impact of weak or strong female discrimination hypothesis on the phenotypic distance between the two species. In Section 4.4 we detail the impact of each parameter of the phenotypic distance between the two species.

A3.4.1 Quasi equilibria

We search mean values of trait and preference at equilibrium \bar{t}_1^* and \bar{p}_1^* such as the leading terms of $\Delta\bar{t}_1$ and $\Delta\bar{p}_1$ are null. We remind that we assume weak female and predator discriminations. The leading terms of $\Delta\bar{t}_1^*$ and $\Delta\bar{p}_1^*$ are thus $\tilde{\beta}_{t_1} = \tilde{\beta}_{p_1} = 0$ with

$$\tilde{\beta}_{t_1} = -2a_1(\bar{t}_1^* - \bar{p}_1^*) - \frac{4bd(\bar{t}_1^* - \bar{t}_2)\lambda_2 n_2}{(1 + \lambda_1 n_1 + \lambda_2 n_2)^2} - 4s_1(\bar{t}_1^* - t_{a1}), \quad (\text{A3.9})$$

$$\tilde{\beta}_{p_1} = -2a_1(\bar{p}_1^* - \bar{t}_1^*) + 2c_{RI}a_1(\bar{t}_1^* - \bar{t}_2)\frac{n_2}{n_1}. \quad (\text{A3.10})$$

We call such points quasi equilibria because they are not equilibrium point of Equation (3.6) but only cancel the term of leading order.

Lemma 1 *If*

$$\frac{2bd\lambda_2n_2}{(\lambda_1n_1 + \lambda_2n_2 + 1)^2} + 2s_1 - \frac{a_1c_{RI}n_2}{n_1} \neq 0, \quad (\text{A3.11})$$

there is one quasi equilibrium point $(\bar{t}_1^, \bar{p}_1^*)$, where*

$$\bar{t}_1^* = \frac{\frac{2bd\lambda_2n_2}{(1+\lambda_1n_1+\lambda_2n_2)^2}\bar{t}_2 + 2s_1t_{a1} - \frac{a_1c_{RI}n_2}{n_1}\bar{t}_2}{\frac{2bd\lambda_2n_2}{(1+\lambda_1n_1+\lambda_2n_2)^2} + 2s_1 - \frac{a_1c_{RI}n_2}{n_1}} \quad \text{and} \quad \bar{p}_1^* = \bar{t}_1^* + c_{RI}(\bar{t}_1^* - \bar{t}_2)\frac{n_2}{n_1}. \quad (\text{A3.12})$$

Proof 1 *Assume that $a_1 \neq 0$. From the definitions of $\tilde{\beta}_{t_1}$ and $\tilde{\beta}_{p_1}$ in (A3.9) and (A3.10), we deduce that the values of trait and preference $(\bar{t}_1^*, \bar{p}_1^*)$ for which the selections on trait and preference are null satisfy:*

$$\tilde{\beta}_{t_1} = 0 \iff a_1(\bar{p}_1^* - \bar{t}_1^*) = \frac{2bd(\bar{t}_1^* - \bar{t}_2)\lambda_2n_2}{(1 + \lambda_1n_1 + \lambda_2n_2)^2} + 2s_1(\bar{t}_1^* - t_{a1}), \quad (\text{A3.13})$$

and

$$\tilde{\beta}_{p_1} = 0 \iff a_1(\bar{p}_1^* - \bar{t}_1^*) = a_1c_{RI}(\bar{t}_1^* - \bar{t}_2)\frac{n_2}{n_1}. \quad (\text{A3.14})$$

From (A3.13) and (A3.14) we derivate:

$$\frac{2bd(\bar{t}_1^* - \bar{t}_2)\lambda_2n_2}{(1 + \lambda_1n_1 + \lambda_2n_2)^2} + 2s_1(\bar{t}_1^* - t_{a1}) = a_1c_{RI}(\bar{t}_1^* - \bar{t}_2)\frac{n_2}{n_1}.$$

By factorizing by \bar{t}_1^ we get:*

$$\bar{t}_1^* \left(\frac{2bd\lambda_2n_2}{(1 + \lambda_1n_1 + \lambda_2n_2)^2} + 2s_1 - a_1c_{RI}\frac{n_2}{n_1} \right) = \bar{t}_2 \left(\frac{2bd\lambda_2n_2}{(1 + \lambda_1n_1 + \lambda_2n_2)^2} - a_1c_{RI}\frac{n_2}{n_1} \right) + 2s_1t_{a1}. \quad (\text{A3.15})$$

Using (A3.11), we obtain the value of \bar{t}_1^ given in (A3.12). From (A3.14) we deduce the associated mean preference and conclude the proof.*

A3.4.2 Fast and slow dynamics.

In this section we study when trait and preference in species 1 converge towards the quasi equilibrium point.

We suppose that the parameters are such as $\frac{2bd\lambda_2n_2}{(\lambda_1n_1+\lambda_2n_2+1)^2} + 2s_1 - \frac{a_1c_{RI}n_2}{n_1}$ is not of an order inferior to ε^2 . We may have two long term behaviours. In case of convergence (case 1. of Lemma 2), the trajectories quickly approach the line $\bar{t} = \bar{p}$, before evolving according to a slower dynamic along this line (see the proof of Lemma 2 and Figures A3.1 and A3.2).

Lemma 2 1. *If*

$$\frac{2bd\lambda_2n_2}{(\lambda_1n_1 + \lambda_2n_2 + 1)^2} + 2s_1 - \frac{a_1c_{RI}n_2}{n_1} > 0,$$

the quantities $(\bar{t}_1 - \bar{t}_1^)$ and $(\bar{p}_1 - \bar{p}_1^*)$ become of order $\sqrt{\varepsilon}$ when the number of generations goes to infinity, where the values of \bar{t}_1^* and \bar{p}_1^* have been given in (A3.12).*

2. *If*

$$\frac{2bd\lambda_2n_2}{(\lambda_1n_1 + \lambda_2n_2 + 1)^2} + 2s_1 - \frac{a_1c_{RI}n_2}{n_1} < 0,$$

trait and preference become very large.

Proof 2 *As we have said, we can then decompose the dynamics into two steps. In the first one the leading order terms of the selection coefficient are the terms describing sexual selection and cost of choosiness. In this case we can approximate*

$$\Delta(\bar{t}_1 - \bar{p}_1)^2.$$

$$\begin{aligned} \Delta(\bar{t}_1 - \bar{p}_1)^2 &= (\bar{t}_1 + \Delta\bar{t}_1 - \bar{p}_1 - \Delta\bar{p}_1)^2 - (\bar{t}_1 - \bar{p}_1)^2 \\ &= 2(\bar{t}_1 - \bar{p}_1)(\Delta\bar{t}_1 - \Delta\bar{p}_1) + (\Delta\bar{t}_1 - \Delta\bar{p}_1)^2 \\ &= 2(\bar{t}_1 - \bar{p}_1)\left(\frac{1}{2}G_{t_1}\beta_{t_1} - \frac{1}{2}G_{p_1}\beta_{p_1}\right) + \left(\frac{1}{2}G_{t_1}\beta_{t_1} - \frac{1}{2}G_{p_1}\beta_{p_1}\right)^2 \\ &= -(\bar{t}_1 - \bar{p}_1)\left(2a_1(G_{t_1} + G_{p_1})(\bar{t}_1 - \bar{p}_1) - a_1^2(G_{p_1} + G_{t_1})^2(\bar{t}_1 - \bar{p}_1)\right. \\ &\quad \left.- 2\left(\frac{a_1 c_{RI} G_{p_1} n_2 (\bar{t}_2 - \bar{t}_1)}{n_1} + \frac{2bdG_{t_1}\lambda_2 n_2 (\bar{t}_2 - \bar{t}_1)}{(\lambda_1 n_1 + \lambda_2 n_2 + 1)^2} + G_{t_1} s_1 (t_{a1} - \bar{t}_1)\right)\right) + O(\varepsilon^3), \end{aligned}$$

where we used (6) for the third equality and (A3.3) and (A3.4) for the last one. As by assumption, a_1, c_{RI}, b and d are of order ε , and s of order ε^2 , we obtain

$$\Delta(\bar{t}_1 - \bar{p}_1)^2 = -(\bar{t}_1 - \bar{p}_1)\left(2a_1(G_{t_1} + G_{p_1})(\bar{t}_1 - \bar{p}_1) + O(\varepsilon^2)\right) + O(\varepsilon^3). \quad (\text{A3.16})$$

Denote by r_n the value of $(\bar{t}_1 - \bar{p}_1)^2$ at generation n . We will prove the following statement:

$$\text{There exists } \alpha > 0 \text{ such that for } n \text{ large enough, } r_n \leq 2\alpha\varepsilon^2. \quad (\text{A3.17})$$

If we introduce the parameter

$$\mathcal{A} := 1 - 2a_1(G_{t_1} + G_{p_1}),$$

Equation (A3.16) may be rewritten:

$$r_{n+1} = \mathcal{A}r_n + \sqrt{r_n}f_n(1, \varepsilon) + f_n(2, \varepsilon),$$

for every $n \in \mathbb{N}$ $|f_n(1, \varepsilon)| \leq c_1\varepsilon^2$, $|f_n(2, \varepsilon)| \leq c_2\varepsilon^3$ where c_1 and c_2 are finite constants. Now introduce the variable

$$\rho_n := r_n - r_0\mathcal{A}^n.$$

As a_1 is of order ε , and G_{t_1} and G_{p_1} of order one, there exists a positive and finite constant $C_{\mathcal{A}}$ such that for ε small enough,

$$0 < \mathcal{A} < 1 - C_{\mathcal{A}}\varepsilon.$$

We will choose in the sequel a positive real number α satisfying

$$\sqrt{\frac{2}{\alpha}}c_1 + \frac{c_2}{\alpha} < C_{\mathcal{A}} \quad (\text{A3.18})$$

and

$$\frac{c_1}{\sqrt{\alpha}} + \frac{\sqrt{\alpha}c_1 + c_2}{\alpha} < C_{\mathcal{A}}. \quad (\text{A3.19})$$

As $0 < \mathcal{A} < 1$, we see that for n large enough, $r_0\mathcal{A}^n \leq \alpha\varepsilon^2$. Thus to prove (A3.17), it is enough to prove that for n large enough, $|\rho_n| \leq \alpha\varepsilon^2$. We obtain for ρ the recurrence equation

$$\rho_{n+1} = \mathcal{A}\rho_n + \sqrt{\rho_n + r_0\mathcal{A}^n}f_n(1, \varepsilon) + f_n(2, \varepsilon). \quad (\text{A3.20})$$

Assume first that $|\rho_n| \leq \alpha\varepsilon^2$. In this case,

$$\begin{aligned} |\rho_{n+1}| &\leq \mathcal{A}\alpha\varepsilon^2 + \sqrt{2\alpha\varepsilon^2}c_1\varepsilon^2 + c_2\varepsilon^3 \\ &= \alpha\varepsilon^2 \left(\mathcal{A} + \sqrt{\frac{2}{\alpha}}c_1\varepsilon + \frac{c_2}{\alpha}\varepsilon \right) \leq \alpha\varepsilon^2 \end{aligned}$$

thanks to (A3.18) provided that ε is small enough. Hence it is enough to prove that there exists one n such that $\rho_n \leq \alpha\varepsilon^2$, and the inequality will hold for later generations.

Now assume that $\rho_n > \alpha\varepsilon^2$. Using that

$$\sqrt{\rho_n + r_0\mathcal{A}^n} \leq \sqrt{|\rho_n|} + \sqrt{r_0\mathcal{A}^n} \leq \sqrt{|\rho_n|} + \sqrt{\alpha}\varepsilon$$

for n large enough, we obtain from (A3.20)

$$\begin{aligned} |\rho_{n+1}| &\leq \mathcal{A}|\rho_n| + \sqrt{|\rho_n|}c_1\varepsilon^2 + (\sqrt{\alpha}c_1 + c_2)\varepsilon^3 \\ &\leq \mathcal{A}|\rho_n| + \sqrt{|\rho_n|}c_1\sqrt{\frac{|\rho_n|}{\alpha}}\varepsilon + (\sqrt{\alpha}c_1 + c_2)\frac{|\rho_n|}{\alpha}\varepsilon \\ &= |\rho_n| \left(\mathcal{A} + \frac{c_1}{\sqrt{\alpha}}\varepsilon + \frac{\sqrt{\alpha}c_1 + c_2}{\alpha}\varepsilon \right). \end{aligned}$$

Due to (A3.19), the term in bracket belongs to $(0, 1)$ if ε is small enough. We conclude that there exists n_0 such that $|\rho_n| \leq \alpha\varepsilon^2$ for any $n \geq n_0$. This concludes the proof of (A3.17) and of the fast convergent phase.

We now want to prove that \bar{t}_1 becomes close to \bar{t}_1^* , and \bar{p}_1 to \bar{p}_1^* . To this aim, we look at the variation of

$$\frac{(\bar{t}_1 - \bar{t}_1^*)^2}{G_{t_1}} + \frac{(\bar{p}_1 - \bar{p}_1^*)^2}{G_{p_1}},$$

where the values of \bar{t}_1^* and \bar{p}_1^* are the ones defined in (A3.12). By definition,

$$\Delta \left(\frac{(\bar{t}_1 - \bar{t}_1^*)^2}{G_{t_1}} + \frac{(\bar{p}_1 - \bar{p}_1^*)^2}{G_{p_1}} \right) = \frac{2\Delta\bar{t}_1(\bar{t}_1 - \bar{t}_1^*) + (\Delta\bar{t}_1)^2}{G_{t_1}} + \frac{2\Delta\bar{p}_1(\bar{p}_1 - \bar{p}_1^*) + (\Delta\bar{p}_1)^2}{G_{p_1}}.$$

When $\bar{t}_1 - \bar{p}_1$ is of order ε , $\Delta\bar{t}_1$ and $\Delta\bar{p}_1$ are of order ε^2 . We then neglect the terms proportional to $(\Delta\bar{t}_1)^2$ and $(\Delta\bar{p}_1)^2$. This yields

$$\begin{aligned} \Delta \left(\frac{(\bar{t}_1 - \bar{t}_1^*)^2}{G_{t_1}} + \frac{(\bar{p}_1 - \bar{p}_1^*)^2}{G_{p_1}} \right) &= \frac{2\Delta\bar{t}_1(\bar{t}_1 - \bar{t}_1^*)}{G_{t_1}} + \frac{2\Delta\bar{p}_1(\bar{p}_1 - \bar{p}_1^*)}{G_{p_1}} + O(\varepsilon^4) \\ &= \beta_{t_1}(\bar{t}_1 - \bar{t}_1^*) + \beta_{p_1}(\bar{p}_1 - \bar{p}_1^*) + O(\varepsilon^4), \end{aligned}$$

where we used (6). Now notice that

$$\bar{t}_1 - \bar{t}_1^* = \bar{t}_1 - \bar{p}_1 + \bar{p}_1 - \bar{p}_1^* + \bar{p}_1^* - \bar{t}_1^* = \bar{p}_1 - \bar{p}_1^* + O(\varepsilon) = \frac{\bar{t}_1 - \bar{t}_1^*}{2} + \frac{\bar{p}_1 - \bar{p}_1^*}{2} + O(\varepsilon), \quad (\text{A3.21})$$

as $\bar{p}_1 - \bar{t}_1$ is of order ε and $\bar{p}_1^* - \bar{t}_1^*$ of order ε . We can make the same computation

for $\bar{p}_1 - \bar{p}_1^*$. Adding that β_{t_1} and β_{p_1} are of order ε^2 , we obtain:

$$\Delta \left(\frac{(\bar{t}_1 - \bar{t}_1^*)^2}{G_{t_1}} + \frac{(\bar{p}_1 - \bar{p}_1^*)^2}{G_{p_1}} \right) = (\beta_{t_1} + \beta_{p_1}) \frac{\bar{t}_1 - \bar{t}_1^*}{2} + (\beta_{t_1} + \beta_{p_1}) \frac{\bar{p}_1 - \bar{p}_1^*}{2} + O(\varepsilon^3). \quad (\text{A3.22})$$

Using (A3.3) and (A3.4) and simplifying, we get:

$$\beta_{t_1} + \beta_{p_1} = -\frac{4bd(\bar{t}_1 - \bar{t}_2)\lambda_2 n_2}{(1 + \lambda_1 n_1 + \lambda_2 n_2)^2} - 4s_1(\bar{t}_1 - t_{a1}) + 2c_{RI}a_1(\bar{t}_1 - \bar{t}_2)\frac{n_2}{n_1} + O(\varepsilon^3).$$

By subtracting $-\frac{4bd(\bar{t}_1^* - \bar{t}_2)\lambda_2 n_2}{(1 + \lambda_1 n_1 + \lambda_2 n_2)^2} - 2s_1(\bar{t}_1^* - t_{a1}) + 2c_{RI}a_1(\bar{t}_1^* - \bar{t}_2)\frac{n_2}{n_1}$, which is equal to zero because $\beta_{t_1}|_{(t,p)=(\bar{t}_1^*, \bar{p}_1^*)} = 0$ and $\beta_{p_1}|_{(t,p)=(\bar{t}_1^*, \bar{p}_1^*)} = 0$, we get:

$$\beta_{t_1} + \beta_{p_1} = -\left(\frac{2bd\lambda_2 n_2}{(1 + \lambda_1 n_1 + \lambda_2 n_2)^2} + 2s_1 - a_1 c_{RI} \frac{n_2}{n_1} \right) 2(\bar{t}_1 - \bar{t}_1^*) + O(\varepsilon^3) \quad (\text{A3.23})$$

$$= -\left(\frac{2bd\lambda_2 n_2}{(1 + \lambda_1 n_1 + \lambda_2 n_2)^2} + 2s_1 - a_1 c_{RI} \frac{n_2}{n_1} \right) 2(\bar{p}_1 - \bar{p}_1^*) + O(\varepsilon^3), \quad (\text{A3.24})$$

where we used (A3.21). Replacing $\beta_{t_1} + \beta_{p_1}$ using (A3.23) and (A3.24) into (A3.22) yield:

$$\Delta \left(\frac{(\bar{t}_1 - \bar{t}_1^*)^2}{G_{t_1}} + \frac{(\bar{p}_1 - \bar{p}_1^*)^2}{G_{p_1}} \right) = -A \left((\bar{t}_1 - \bar{t}_1^*)^2 + (\bar{p}_1 - \bar{p}_1^*)^2 \right) + O(\varepsilon^3), \quad (\text{A3.25})$$

with

$$A := \left(\frac{2bd\lambda_2 n_2}{(1 + \lambda_1 n_1 + \lambda_2 n_2)^2} + 2s_1 - a_1 c_{RI} \frac{n_2}{n_1} \right). \quad (\text{A3.26})$$

First case: $A > 0$

We suppose that the parameters are such that A is not of an order inferior to ε^2 . Using computations similar to the ones derived to prove (A3.17), we may prove that after a number of generations large enough, $(\bar{t}_1 - \bar{t}_1^*)^2$ and $(\bar{p}_1 - \bar{p}_1^*)^2$ become of order ε , and thus $\bar{t}_1 - \bar{t}_1^*$ and $\bar{p}_1 - \bar{p}_1^*$ become of order $\varepsilon^{1/2}$.

To illustrate this result we simulated two trajectories of the system (6) $((\bar{t}_n, \bar{p}_n))_{n \in \mathbb{N}}$ and $((\bar{t}_n^2, \bar{p}_n^2))_{n \in \mathbb{N}}$ for two different initial conditions: (t^{i1}, p^{i1}) and (t^{i2}, p^{i2}) . The trajectories are shown in Figure A3.1 and the parameter values are given in the caption. The parameter values correspond to the weak selection hypothesis and are such that $A > 0$.

The fast and slow dynamics are visible in Figure 3.1(a) where the trajectories quickly become close to the line defined by $\bar{t}_1 = \bar{p}_1$ and then slowly converge toward the quasi equilibrium points. We noted $(\bar{t}_1^{eq}, \bar{p}_1^{eq})$ the equilibrium point reached by the two simulated trajectories.

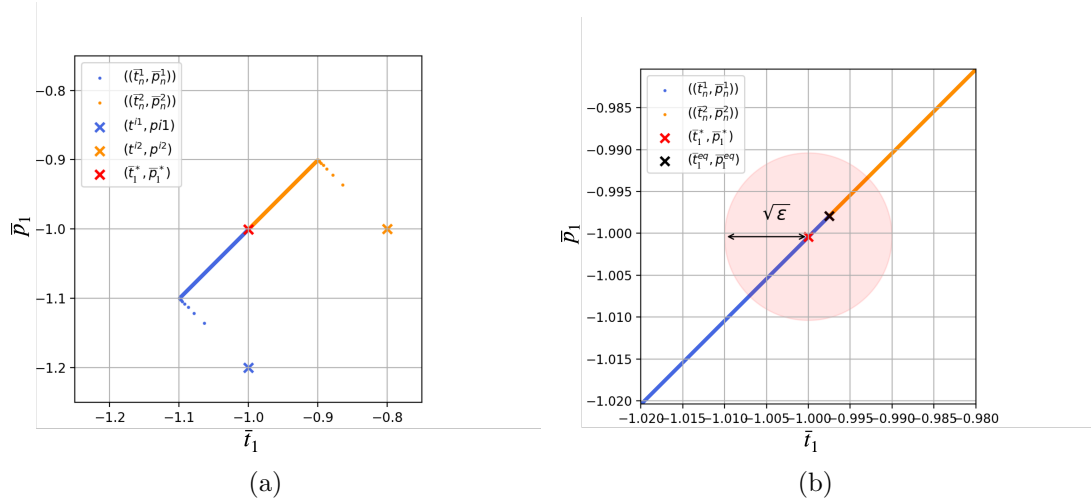


Fig. A3.1: (a) Evolution of mean trait value \bar{t}_1 and mean females preference value \bar{p}_1 for two different initial conditions. The blue (resp. orange) points represent the numerical trajectories for the initial condition (t^{i1}, p^{i1}) (resp. (t^{i2}, p^{i2})) (b) Zoom on the previous figure. The red circle has for center the quasi equilibrium point $(\bar{t}_1^*, \bar{p}_1^*)$ and for radius $\sqrt{\epsilon}$. This illustrates that the numerical steady point $(\bar{t}_1^*, \bar{p}_1^*)$ is at a distance of order $\sqrt{\epsilon}$. The trajectories were obtained with the parameter values: $(t^{i1}, p^{i1}) = (-1, -1.2)$, $(t^{i2}, p^{i2}) = (-0.8, -1)$, $G_{t_1} = G_{p_1} = 0.01$, $a_1 = 10^{-4}$, $b = 2 \times 10^{-4}$, $d = 2 \times 10^{-4}$, $\lambda_1 = 0.1$, $\lambda_2 = 0.1$, $n_1 = 10$, $n_2 = 20$, $c_{RI} = 10^{-4}$, $s_1 = 10^{-8}$, $t_{a1} = 0$ and $t_{a2} = 1$. The trajectories are computed over 1,000,000 generations.

Second case: $A < 0$.

Recall (A3.25) and that we assumed that A is not of order inferior to ε^2 . This entails that $(\bar{t}_1 - \bar{t}_1^*)^2/G_{t_1} + (\bar{p}_1 - \bar{p}_1^*)^2/G_{p_1}$ goes to infinity. However when $\bar{t}_1 - \bar{t}_2$ or $\bar{p}_1 - \bar{p}_2$ becomes high (for example of order $1/\varepsilon$) the approximation made in section 2 does not stand. Therefore from a certain number of generations the approximation does not correctly describe the evolution of trait and preference. We can only conclude that trait and preference become very large. This is illustrated by Figure A3.2 which shows a simulation of two trajectories when $A < 0$.

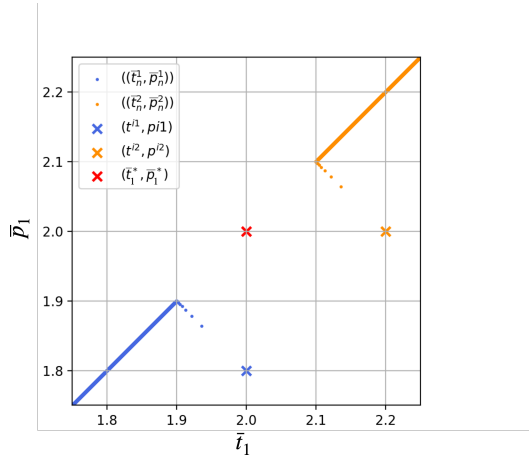


Fig. A3.2: Evolution of mean trait value \bar{t}_1 and mean females preference value \bar{p}_1 for two different initial conditions. The blue (resp. orange) points represent the numerical trajectories for the initial condition (t^{i1}, p^{i1}) (resp. (t^{i2}, p^{i2})). The trajectories were obtained with the parameter values: $(t^{i1}, p^{i1}) = (-1, -1.2)$, $(t^{i2}, p^{i2}) = (-0.8, -1)$, $G_{t_1} = G_{p_1} = 0.01$, $a_1 = 10^{-4}$, $b = 2 \times 10^{-4}$, $d = 2 \times 10^{-4}$, $\lambda_1 = 0.1$, $\lambda_2 = 0.1$, $n_1 = 10$, $n_2 = 20$, $c_{RI} = 10^{-4}$, $s_1 = 0.25 \times 10^{-8}$, $t_{a1} = 0$ and $t_{a2} = 1$. The trajectories are computed over 1,000,000 generations.

A3.4.3 Effect of weak or strong female discrimination on the phenotypic distances between the two species

Previously we obtained an analytic approximation of the phenotypic distance between the two species when the strengths of female and predator discriminations

(a_1 and b) were weak (*i.e.* $a_1 = O(\varepsilon)$ and $b = O(\varepsilon)$). To obtain this approximation we also assumed that the strength of historical constraints has the same order of magnitude as selection coefficients due to predation and reproductive interference (*i.e.* $s_1 = O(\varepsilon^2)$). Under this assumption, the phenotypic distance between the two species becomes very large (see Figure A3.3) when

$$c_{RI} \geq \frac{2n_1}{a_1n_2} \left(\frac{bd\lambda_2n_2}{(1 + \lambda_1n_1 + \lambda_2n_2)^2} + s_1 \right). \quad (\text{A3.27})$$

As explained in the main manuscript, this unrealistic divergence (under the weak female discrimination hypothesis ($a_1 = O(\varepsilon)$)) suggests that reproductive interference promotes strong phenotype divergence between the two species. Under weak female discrimination, only a large distance between females preference and the trait displayed by species 2 leads to a reduction of fitness cost generated by reproductive interference. Because females preference generates sexual selection on males trait, the phenotype divergence between the two species becomes high. When we relax the weak female discrimination hypothesis and use numerical simulations, then a great cost of reproductive interference provokes large but still of order 1 phenotypic distance between the two species (see Figure A3.3). However, we observe that the lower female discrimination, the higher is phenotypic distance when the cost of reproductive interference increases. As explained above, when females are not very choosy, reproductive interference favors the evolution of larger phenotypic distances limiting heterospecific mating.

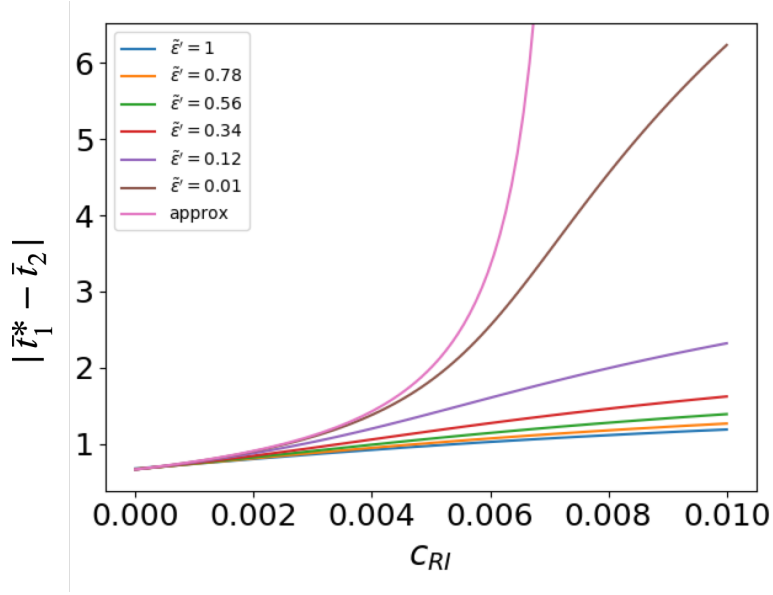


Fig. A3.3: **Influence of the cost generated by reproductive interference c_{RI} on the phenotypic distances between the two species, using the analytical approximation ('approx' curve) or numerical simulations.** Different values of female and predator discriminations coefficient (a_1 and b) and strength of historical constraints (s) are assumed for numerical simulations. This illustrate that curves obtained by numerical simulations tend to look similar to those using the analytical approximation where parameters values tends to satisfy weak female and predator discriminations. We assume: $G_{t_1} = G_{p_1} = 0.01$, $a_1 = \tilde{\epsilon}'$, $b = \tilde{\epsilon}'$, $s = 0.5\tilde{\epsilon}\tilde{\epsilon}'$, $d = 2\tilde{\epsilon}$, $\lambda_1 = 0.1$, $\lambda_2 = 0.1$, $n_1 = 10$, $n_2 = 20$, $t_{a_1} = 0$ and $t_{a_2} = 1$.

A3.4.4 Effect of different parameters on the level of trait divergence $|\bar{t}_1^* - \bar{t}_2|$

We then aim at disentangling the effects of the different parameters of the model on trait divergence. We thus focus on the case where $A > 0$ (recall definition (A3.26)). In this case, assuming weak female and predator discriminations, we know that the phenotypic distance between the two species, $|\bar{t}_1^* - \bar{t}_2|$, equals

$$|\bar{t}_1^* - \bar{t}_2| = \frac{2s_1|t_{a_1} - \bar{t}_2|}{\frac{2bd\lambda_2n_2}{(1+\lambda_1n_1+\lambda_2n_2)^2} + 2s_1 - a_1c_{RI}\frac{n_2}{n_1}},$$

allowing to investigate the relative impact of the different parameters on trait divergence. We also run numerical simulations to investigate the effect of the different parameters assuming strong females preference and predator discrimination (*i.e.* $a_1 = O(1)$ and $b = O(1)$).

Effect of reproductive interference

Assuming weak female and predator discriminations, the impact of the strength of reproductive interference on the phenotypic distance between the two species is given by the sign of $\partial|\bar{t}_1^* - \bar{t}_2|/\partial c_{RI}$. In our case,

$$\frac{\partial|\bar{t}_1^* - \bar{t}_2|}{\partial c_{RI}} = \frac{2s_1 a_1 \frac{n_2}{n_1} |t_{a1} - \bar{t}_2|}{\left(\frac{2bd\lambda_2 n_2}{(1+\lambda_1 n_1 + \lambda_2 n_2)^2} + 2s_1 - a_1 c_{RI} \frac{n_2}{n_1} \right)^2} > 0.$$

Hence the level of divergence increases with the strength of reproductive interference. A similar effect is observed assuming strong female and predator discriminations (see Figure A3.4(a)). Similarly, assuming weak female and predator discriminations

$$\frac{\partial|\bar{t}_1^* - \bar{t}_2|}{\partial a_1} = \frac{2s_1 c_{RI} \frac{n_2}{n_1} |t_{a1} - \bar{t}_2|}{\left(\frac{2bd\lambda_2 n_2}{(1+\lambda_1 n_1 + \lambda_2 n_2)^2} + 2s_1 - a_1 c_{RI} \frac{n_2}{n_1} \right)^2} > 0,$$

thus the phenotypic distance (along with the strength of selection due to reproductive interference) increases with the strength of female discrimination. However, when female discrimination is strong and exceeds a threshold, females are able to distinguish males from their own species from individuals from species 2, which limits divergence of the trait in species 1 (see Figure A3.4(b)). Accurate females choice allows a quasi-similarity of the traits of species 1 and of species 2, without implying heterospecific mating, relaxing the divergent selection exerted by reproductive interference.

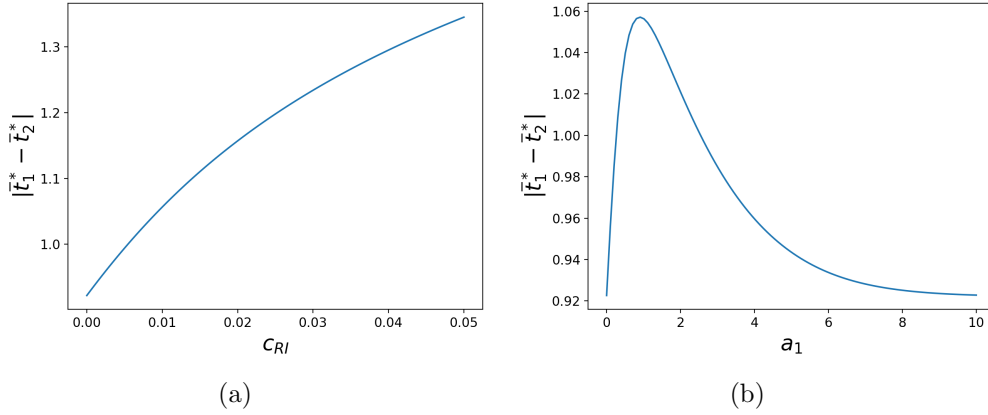


Fig. A3.4: **Influence of the strength of (a) reproductive interference c_{RI} and of (b) female discrimination a_1 on the phenotypic distances between the two species, assuming strong female and predator discriminations.** The default parameters values are as follows: $G_{t_1} = G_{p_1} = 0.01$, $a_1 = 1$, $c_{RI} = 0.01$, $b = 1$, $d = 0.02$, $\lambda_1 = 0.1$, $\lambda_2 = 0.1$, $n_1 = 10$, $n_2 = 20$, $s_1 = 0.0025$, $t_{a1} = 0$ and $t_{a2} = 1$.

Effect of predation

When a_1 and b are of order ε ,

$$\frac{\partial |\bar{t}_1^* - \bar{t}_2|}{\partial d} = \frac{-2b\lambda_2 n_2}{(1 + \lambda_1 n_1 + \lambda_2 n_2)^2} \frac{2s_1 |t_{a1} - \bar{t}_2|}{\left(\frac{2bd\lambda_2 n_2}{(1 + \lambda_1 n_1 + \lambda_2 n_2)^2} + 2s_1 - a_1 c_{RI} \frac{n_2}{n_1} \right)^2} < 0,$$

hence the phenotypic distance decreases with the basic predation rate d . Assuming strong female and predator discriminations leads to similar effect (Figure A3.5(a)).

When a_1 and b are of order ε ,

$$\frac{\partial |\bar{t}_1^* - \bar{t}_2|}{\partial b} = \frac{-2d\lambda_2 n_2}{(1 + \lambda_1 n_1 + \lambda_2 n_2)^2} \frac{2s_1 |t_{a1} - \bar{t}_2|}{\left(\frac{2bd\lambda_2 n_2}{(1 + \lambda_1 n_1 + \lambda_2 n_2)^2} + 2s_1 - a_1 c_{RI} \frac{n_2}{n_1} \right)^2} < 0.$$

An increase on predator discriminating ability b thus also promotes phenotypic convergence as it increases the positive selection on mimicry generated by predation. Surprisingly, when a_1 and b are of order 1 and predator discrimination exceeds a certain threshold, increased discrimination no longer promotes accurate

mimicry (Figure A3.5(b)). When b is high, individuals from species 1 benefit from protection gained by mimicry only when they look very similar to the individuals of species 2. Reproductive interference makes such high similarity too costly, and therefore divergence of the trait in species 1 becomes promoted (Figure A3.5(b)).

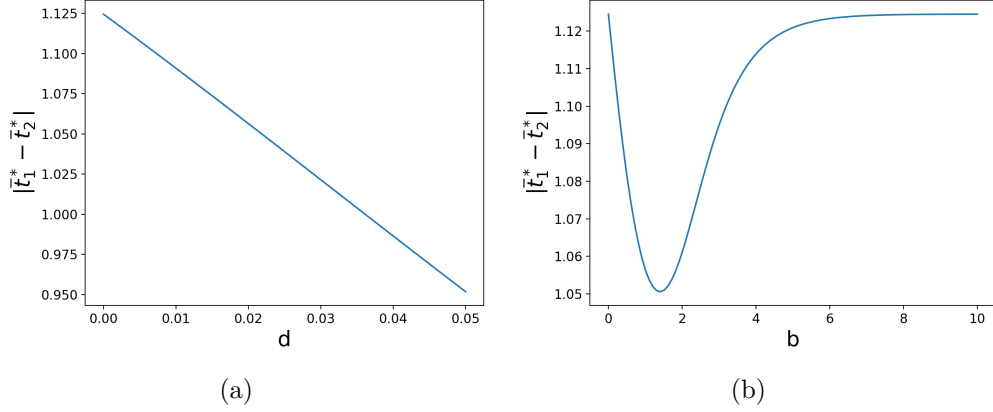


Fig. A3.5: **Influence of the strength of predation d (a) and of predator discrimination b (b) on the phenotypic distances between the two species, assuming strong female and predator discriminations.** The default parameters values are as follows: $G_{t_1} = G_{p_1} = 0.01$, $a_1 = 1$, $c_{RI} = 0.01$, $b = 1$, $d = 0.02$, $\lambda_1 = 0.1$, $\lambda_2 = 0.1$, $n_1 = 10$, $n_2 = 20$, $s_1 = 0.0025$, $t_{a1} = 0$ and $t_{a2} = 1$.

Effect of the defence level of species 1

Without reproductive interference ($c_{RI} = 0$) and when a_1 and b are of order ε , we have

$$\frac{\partial |\bar{t}_1^* - \bar{t}_2|}{\partial \lambda_1 n_1} = \frac{2s_1 |t_{a1} - \bar{t}_2|}{\left(\frac{2bd\lambda_2 n_2}{(1 + \lambda_1 n_1 + \lambda_2 n_2)^2} + 2s_1 \right) (1 + \lambda_1 n_1 + \lambda_2 n_2)^3} > 0.$$

Therefore, the more defended species 1 is, the greater is the phenotypic distance between the two species.

Assuming reproductive interference generates cost ($c_{RI} > 0$), the density of species 1 then modulates the fitness cost incurred by reproductive interference. Therefore, we study the effect of the two components of the level of defence of species 1: the

individual defence level λ_1 and the density n_1 .

$$\frac{\partial |\bar{t}_1^* - \bar{t}_2|}{\partial \lambda_1} = \frac{2bd\lambda_2 n_2 N}{(1 + \lambda_1 n_1 + \lambda_2 n_2)^3} \frac{2s_1 |t_{a1} - \bar{t}_2|}{\left(\frac{2bd\lambda_2 n_2}{(1 + \lambda_1 n_1 + \lambda_2 n_2)^2} + 2s_1 - a_1 c_{RI} \frac{n_2}{n_1} \right)^2} > 0,$$

indicates that the individual defence level increases the phenotypic distance. Assuming strong female and predator discriminations leads to similar effect (Figure A3.6).

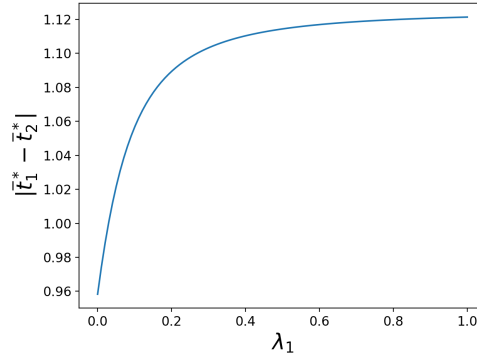


Fig. A3.6: **Influence of the individual defence level λ_1 on the phenotypic distances between the two species, assuming strong female and predator discriminations.** The default parameters values are as follows: $G_{t_1} = G_{p_1} = 0.01$, $a_1 = 1$, $c_{RI} = 0.01$, $b = 1$, $d = 0.02$, $\lambda_1 = 0.1$, $\lambda_2 = 0.1$, $n_1 = 10$, $n_2 = 20$, $s_1 = 0.0025$, $t_{a1} = 0$ and $t_{a2} = 1$.

We also have

$$\frac{\partial |\bar{t}_1^* - \bar{t}_2|}{\partial n_1} = -\frac{1}{n_1} \left(a_1 c_{RI} \frac{n_2}{n_1} - \frac{4bd(\lambda_1 n_1)(\lambda_2 n_2)}{(1 + \lambda_1 n_1 + \lambda_2 n_2)^3} \right) \frac{2s_1 |t_{a1} - \bar{t}_2|}{\left(\frac{2bd\lambda_2 n_2}{(1 + \lambda_1 n_1 + \lambda_2 n_2)^2} + 2s_1 - a_1 c_{RI} \frac{n_2}{n_1} \right)^2}.$$

While strong divergence is promoted when species 1 has a low abundance, for larger abundances, the effect of the density on the phenotypic distance between the two species depends on the strength of reproductive interference and predation (Figure A3.7). When fitness cost due to reproductive interference is great compared to fitness cost due to predation, an increase in the density of species 1 decreases the phenotypic distance, because it reduces the fitness cost due to reproductive interference (similar effect observed assuming strong female and predator

discriminations (Figure A3.7(a)). By contrast, when fitness cost due to reproductive interference is low compared to fitness cost due to predation, an increase in the density of species 1 increases the phenotypic distance because species 1 is better defended (similar effect observed assuming strong female and predator discriminations (see right part of Figure A3.7(b))).

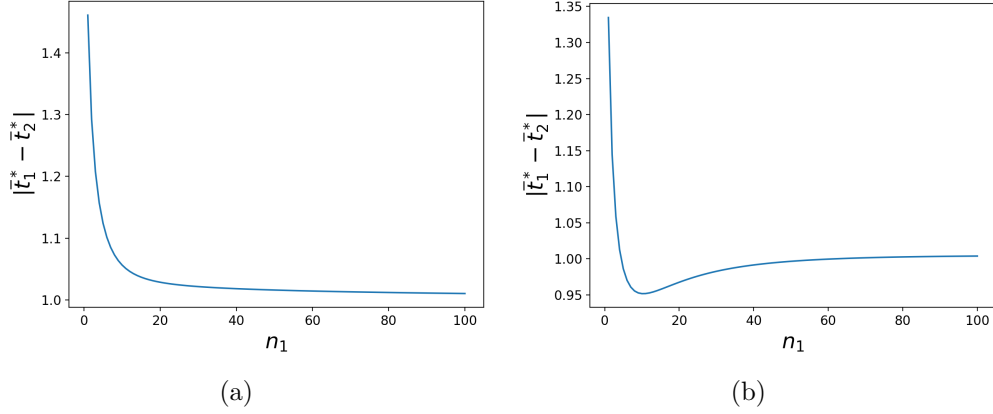


Fig. A3.7: **Influence of the density of species 1 n_1 on the phenotypic distances between the two species, when (a) predation is low compared to reproductive interference and (b) when predation is high compared to reproductive interference, assuming strong female and predator discriminations.** Simulations were run assuming: (a) $d = 0.02$ or (b) $d = 0.05$. The default parameters values are as follows: $G_{t_1} = G_{p_1} = 0.01$, $a_1 = 1$, $c_{RI} = 0.01$, $b = 1$, $\lambda_1 = 0.1$, $\lambda_2 = 0.1$, $n_1 = 10$, $n_2 = 20$, $s_1 = 0.0025$, $t_{a1} = 0$ and $t_{a2} = 1$.

Effect of historical constraints promoting the ancestral trait value t_{a1} .

When a_1 and b are of order ε ,

$$\frac{\partial |\bar{t}_1^* - \bar{t}_2|}{\partial s_1} = \frac{2|t_{a1} - \bar{t}_2| \left(\frac{2bd\lambda_2 n_2}{(1+\lambda_1 n_1 + \lambda_2 n_2)^2} - a_1 c_{RI} \frac{n_2}{n_1} \right)}{\left(\frac{2bd\lambda_2 n_2}{(1+\lambda_1 n_1 + \lambda_2 n_2)^2} + 2s_1 - a_1 c_{RI} \frac{n_2}{n_1} \right)^2}.$$

Thus when selection due to predation is stronger than selection due to reproductive interference (i.e. $\frac{2bd\lambda_2 n_2}{(1+\lambda_1 n_1 + \lambda_2 n_2)^2} > a_1 c_{RI} \frac{n_2}{n_1}$), historical constraints promotes the divergence of trait between the two species (similar effect observed assuming strong

female and predator discriminations (Figure A3.8(b)). By contrast, when the selection due to reproductive interference is stronger than selection due to predation (i.e. $a_1 c_{RI} \frac{n_2}{n_1} > \frac{2bd\lambda_2 n_2}{(1+\lambda_1 n_1 + \lambda_2 n_2)^2}$), historical constraints limits the trait divergence due to reproductive interference (similar effect observed assuming strong female and predator discriminations (Figure A3.8(a))).

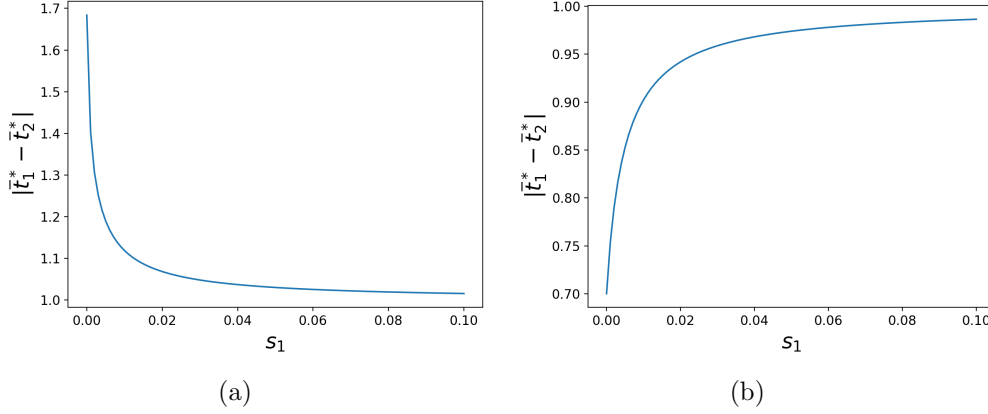


Fig. A3.8: **Influence of the strength of selective constraints s_1 on the phenotypic distances between the two species, when (a) predation is low compared to reproductive interference and (b) when predation is great compared to reproductive interference, assuming strong female and predator discriminations.** Simulations were run assuming: (a) $d = 0.02$ or (b) $d = 0.05$. The default parameters values are as follows: $G_{t_1} = G_{p_1} = 0.01$, $a_1 = 1$, $c_{RI} = 0.01$, $b = 1$, $\lambda_1 = 0.1$, $\lambda_2 = 0.1$, $n_1 = 10$, $n_2 = 20$, $s_1 = 0.0025$, $t_{a1} = 0$ and $t_{a2} = 1$.

Effect of the defence level of species 2.

Finally, we investigate the impact of the composition of species 2 (density n_2 and defense level λ_2) on trait divergence. When a_1 and b are of order ε , we have:

$$\frac{\partial |\bar{t}_1^* - \bar{t}_2|}{\partial \lambda_2} = \frac{2bdn_2(\lambda_2 n_2 - 1 - \lambda_1 n_1)}{(1 + \lambda_1 n_1 + \lambda_2 n_2)^3} \frac{2s_1 |t_{a1} - \bar{t}_2|}{\left(\frac{2bd\lambda_2 n_2}{(1 + \lambda_1 n_1 + \lambda_2 n_2)^2} + 2s_1 - a_1 c_{RI} \frac{n_2}{n_1} \right)^2},$$

and

$$\frac{\partial |\bar{t}_1^* - \bar{t}_2|}{\partial n_2} = \left(\frac{2bd\lambda_2(\lambda_2 n_2 - 1 - \lambda_1 n_1)}{(1 + \lambda_1 n_1 + \lambda_2 n_2)^3} + \frac{a_1 c_{RI}}{n_1} \right) \frac{2s_1 |t_{a1} - \bar{t}_2|}{\left(\frac{2bd\lambda_2 n_2}{(1 + \lambda_1 n_1 + \lambda_2 n_2)^2} + 2s_1 - a_1 c_{RI} \frac{n_2}{n_1} \right)^2}.$$

Thus, when the defence level of species 2 ($\lambda_2 n_2$) is lower than the defence level of species 1 plus one ($\lambda_2 n_2 < 1 + \lambda_1 n_1$), an increase in the defence level of individuals of species 2 promotes phenotypic similarity between the two species (similar effect observed assuming strong but moderate female and predator discriminations (Figure A3.9(a))). Indeed, an increase of $\lambda_2 n_2$ increases the advantage of looking similar to individuals of species 2. More surprisingly, when the defence level of species 2 is greater ($\lambda_2 n_2 > 1 + \lambda_1 n_1$), the phenotypic distance increases with $\lambda_2 n_2$ (similar effect observed assuming strong but moderate female and predator discriminations (Figure A3.9(a))). Under weak ($b = O(\varepsilon)$) or strong but moderate (*e.g.* $b = 1$) predator discrimination, predators tend to generalize mimetic trait. Then individuals of species 1 gain at least a little protection from species 2, even when displaying a imperfectly mimetic trait. When the level of protection of species 2 is high, the fitness costs linked to predation is low compared to the reproductive interference and decreases with the defence level of individuals of species 2. This decrease in selection pressure generated by predation decreases the phenotype similarity between the two species. When predator discrimination is strong and high (*e.g.* $b = 10$), there is no generalization of imperfect mimics by predators, this effect is no longer observed (see Figure A3.9(b)).

The density n_2 and the individual defence level of species 2 λ_2 have the same effect on the overall defence level of species 2 (function of the parameter $\lambda_2 n_2$), and therefore have a similar effect on the phenotypic distance. However, the density of species 2 n_2 also plays a role on the fitness costs generated by reproductive interference. When the strength of reproductive interference is high as compared to predation, the phenotypic distance increases with the density of species 2 (n_2), because it increases the cost of reproductive interference (similar effect observed assuming strong female and predator discriminations (Figure A3.10(a))). When the strength of reproductive interference is low compared to predation, the den-

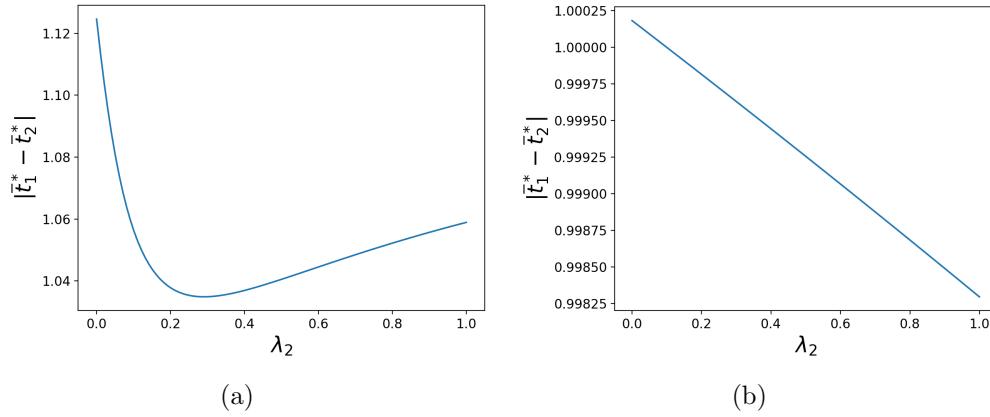


Fig. A3.9: **Influence of the mean defence level of individuals of species 2 λ_2 on the phenotypic distances between the two species for (a) moderate ($b = 1$) and (b) high ($b = 10$) predator discrimination, assuming strong female and predator discriminations (*i.e.* $a_1 = O(1)$ and $b = O(1)$).** Simulations were run assuming: (a) $a_1 = 1$ and (b) $a = 10$. The default parameters values are as follows: $G_{t_1} = G_{p_1} = 0.01$, $a_1 = 1$, $c_{RI} = 0.01$, $d = 0.02$, $\lambda_1 = 0.1$, $\lambda_2 = 0.1$, $n_1 = 10$, $n_2 = 20$, $s_1 = 0.0025$, $t_{a1} = 0$ and $t_{a2} = 1$.

sity of species 2 (n_2) has a similar effect than the defence level of individuals of species 2 λ_2 on the phenotypic distance (similar effect observed assuming strong but moderate female and predator discriminations (Figure A3.10(b))).

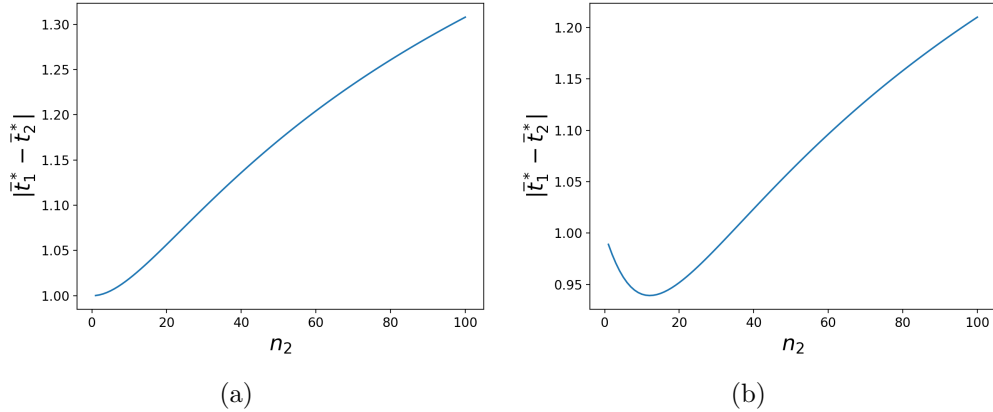


Fig. A3.10: **Influence of the density of species 2 n_2 on the phenotypic distances between the two species, when (a) predation is low compared to reproductive interference and (b) when predation is high compared to reproductive interference, assuming strong female and predator discriminations.** Simulations were run assuming: (a) $d = 0.02$ or (b) $d = 0.05$. The default parameters values are as follows: $G_{t_1} = G_{p_1} = 0.01$, $a_1 = 1$, $c_{RI} = 0.01$, $b = 1$, $\lambda_1 = 0.1$, $\lambda_2 = 0.1$, $n_1 = 10$, $n_2 = 20$, $s_1 = 0.0025$, $t_{a1} = 0$ and $t_{a2} = 1$.

A3.5 Evolution of mimicry between two interacting species

In this section we focus on the general case where traits and preference co-evolve in the two species. In Section 5.1 we compute the values of trait and preference that cancel the leading term of the selection vectors in both species. In Section 5.2 we study when trait and preference converge toward the point found in the previous section. In Section 5.3 we detail the impact of each parameter of the interspecific phenotypic distance. In Section 5.4 we study the impact of historical constraints on phenotypic divergence. In section 5.5 we study the impact of predator discrimination without reproductive interference. In section 5.5 we study the impact of the relative defence level on traits co-evolution.

A3.5.1 Quasi equilibria

We search mean values of traits and preferences at equilibrium \bar{t}_1^* , \bar{p}_1^* , \bar{t}_2^* and \bar{p}_2^* such as the leading terms of $\Delta\bar{t}_1^*$, $\Delta\bar{p}_1^*$, $\Delta\bar{t}_2^*$ and $\Delta\bar{p}_2^*$ are null, or equivalently, $\tilde{\beta}_{t_1} = \tilde{\beta}_{p_1} = \tilde{\beta}_{t_2} = \tilde{\beta}_{p_2} = 0$ with

$$\tilde{\beta}_{t_1} = -2a_1(\bar{t}_1^* - \bar{p}_1^*) - \frac{4bd(\bar{t}_1^* - \bar{t}_2^*)\lambda_2 n_2}{(1 + \lambda_1 n_1 + \lambda_2 n_2)^2} - 4s_1(\bar{t}_1^* - t_{a1}), \quad (\text{A3.28})$$

$$\tilde{\beta}_{p_1} = -2a_1(\bar{p}_1^* - \bar{t}_1^*) + 2c_{RI}a_1(\bar{t}_1^* - \bar{t}_2^*)\frac{n_2}{n_1}, \quad (\text{A3.29})$$

$$\tilde{\beta}_{t_2} = -2a_2(\bar{t}_2^* - \bar{p}_2^*) - \frac{4bd(\bar{t}_2^* - \bar{t}_1^*)\lambda_1 n_1}{(1 + \lambda_1 n_1 + \lambda_2 n_2)^2} - 4s_2(\bar{t}_2^* - t_{a2}), \quad (\text{A3.30})$$

$$\tilde{\beta}_{p_2} = -2a_2(\bar{p}_2^* - \bar{t}_2^*) + 2c_{RI}a_2(\bar{t}_2^* - \bar{t}_1^*)\frac{n_1}{n_2}. \quad (\text{A3.31})$$

Lemma 3 *Let us introduce for $i \neq j \in \{1, 2\}^2$,*

$$A_i = \frac{2bd\lambda_j n_j - a_i c_{RI} \frac{n_j}{n_i} (1 + \lambda_1 n_1 + \lambda_2 n_2)^2}{2bd\lambda_j n_j + (2s_i - a_i c_{RI} \frac{n_j}{n_i}) (1 + \lambda_1 n_1 + \lambda_2 n_2)^2}, \quad (\text{A3.32})$$

$$B_i = \frac{2s_i t_{ai} (1 + \lambda_1 n_1 + \lambda_2 n_2)^2}{2bd\lambda_j n_j + (2s_i - a_i c_{RI} \frac{n_j}{n_i}) (1 + \lambda_1 n_1 + \lambda_2 n_2)^2}. \quad (\text{A3.33})$$

If $2bd\lambda_j n_j + (2s_i - a_i c_{RI}(n_j/n_i)) (1 + \lambda_1 n_1 + \lambda_2 n_2)^2 \neq 0$ for $i \in \{1, 2\}$ and if $A_1 A_2 \neq 1$ there is a unique quasi equilibrium point given for $i \in \{1, 2\}$ by

$$\bar{t}_i^* = \frac{B_i + A_i B_j}{1 - A_1 A_2}, \quad \bar{p}_i^* = \bar{t}_i^* + c_{RI}(\bar{t}_i^* - \bar{t}_j^*)\frac{n_j}{n_i}, \quad (\text{A3.34})$$

Remark. We do not give the quasi equilibrium traits and preferences when one of the following conditions is verified:

- $2bd\lambda_2 n_2 + (2s_1 - a_1 c_{RI}(n_2/n_1)) (1 + \lambda_1 n_1 + \lambda_2 n_2)^2 = 0$,
- $2bd\lambda_1 n_1 + (2s_2 - a_2 c_{RI}(n_1/n_2)) (1 + \lambda_1 n_1 + \lambda_2 n_2)^2 = 0$,
- $A_1 A_2 = 1$.

Indeed investigating those cases leads to a long enumeration of subcases with different quasi equilibrium points, and those cases are negligible compared with all the possible combinations of parameters. We thus choose to not give this enumeration.

Proof 3 Let $2bd\lambda_j n_j + (2s_i - a_i c_{RI}(n_j/n_i))(1 + \lambda_1 n_1 + \lambda_2 n_2)^2 \neq 0$ for $i \neq j \in \{1, 2\}^2$. Using the results of the model with fixed species 2 we have

$$\bar{t}_1^* = \frac{\frac{2bd\lambda_2 n_2}{(1+\lambda_1 n_1 + \lambda_2 n_2)^2} \bar{t}_2^* + 2s_1 t_{a1} - a_1 c_{RI} \frac{N_2}{N_1} \bar{t}_2^*}{\frac{2bd\lambda_2 n_2}{(1+\lambda_1 n_1 + \lambda_2 n_2)^2} + 2s_1 - a_1 c_{RI} \frac{n_2}{n_1}},$$

and

$$\bar{t}_2^* = \frac{\frac{2bd\lambda_1 n_1}{(1+\lambda_1 n_1 + \lambda_2 n_2)^2} \bar{t}_1^* + 2s_2 t_{a2} - a_2 c_{RI} \frac{N_1}{N_2} \bar{t}_1^*}{\frac{2bd\lambda_1 n_1}{(1+\lambda_1 n_1 + \lambda_2 n_2)^2} + 2s_2 - a_2 c_{RI} \frac{n_1}{n_2}},$$

which can be rewritten

$$\bar{t}_1^* = A_1 \bar{t}_2^* + B_1, \quad \bar{t}_2^* = A_2 \bar{t}_1^* + B_2,$$

where $(A_i, B_i), i \in \{1, 2\}$ have been defined in (A3.32)-(A3.33).

If $A_1 A_2 \neq 1$ there are unique values for traits at quasi equilibrium given by \bar{t}_1^* and \bar{t}_2^* defined in (A3.34). Using previous results we have the associated mean preferences at quasi equilibrium \bar{p}_1^* and \bar{p}_2^* defined in (A3.34).

A3.5.2 Fast and slow dynamics.

In this section we study when trait and preference in the both species converge towards the quasi equilibrium point.

Lemma 4 *Let us introduce*

$$\begin{aligned} B_{pred} &= \frac{2bd}{(1 + \lambda_1 n_1 + \lambda_2 n_2)^2}, \\ C_1 &= 2\lambda_2 n_2 B_{pred} + 4s_1 - 2c_{RI} a_1 \frac{n_2}{n_1}, \\ C_2 &= 2\lambda_1 n_1 B_{pred} + 4s_2 - 2c_{RI} a_2 \frac{n_1}{n_2}, \end{aligned}$$

and recall the definitions of A_1 and A_2 in (A3.32).

1. If $C_1 > 0$, $C_2 > 0$ and $C_1 C_2 (1 - A_1 A_2) - \frac{1}{4} (A_1 C_1 - A_2 C_2)^2 > 0$ the quantities $\bar{t}_1 - \bar{t}_1^*$, $\bar{t}_2 - \bar{t}_2^*$, $\bar{p}_1 - \bar{p}_1^*$ and $\bar{p}_2 - \bar{p}_2^*$ become of order $\sqrt{\varepsilon}$ when the number of generation goes to infinity, with \bar{t}_1^* , \bar{t}_2^* , \bar{p}_1^* and \bar{p}_2^* defined by (A3.34).
2. If $C_1 < 0$, $C_2 < 0$ and $C_1 C_2 (1 - A_1 A_2) - \frac{1}{4} (A_1 C_1 - A_2 C_2)^2 > 0$, traits and preferences become very large.

Remark. When $C_1 C_2 (1 - A_1 A_2) - \frac{1}{4} (A_1 C_1 - A_2 C_2)^2 > 0$ or $C_1 C_2 < 0$ we are not able to analytically determine the convergence or the divergence of traits and preferences. To infer such information we simulate the dynamic of traits and preferences considering the leading term of the selection coefficients.

Proof 4 *As previously, we can decompose the dynamics into two steps. In the first one the leading order terms of the selection coefficient are the terms describing sexual selection and cost of choosiness. Using computations similar to the ones in the previous model we can approximate $\Delta(\bar{t}_i - \bar{p}_i)^2$ for $i \in \{1, 2\}$ by*

$$\Delta(\bar{t}_i - \bar{p}_i)^2 = -(\bar{t}_i - \bar{p}_i) \left(2a_i (G_{t_i} + G_{p_i}) (\bar{t}_i - \bar{p}_i) + O(\varepsilon^2) \right) + O(\varepsilon^3).$$

Using the same reasoning that in the previous model we may prove that above a certain number of generations $t_1 - p_1$ and $t_2 - p_2$ are of order ε .

We now look at the variation of

$$\mathcal{A} := \frac{(\bar{t}_1 - \bar{t}_1^*)^2}{G_{t_1}} + \frac{(\bar{t}_2 - \bar{t}_2^*)^2}{G_{t_2}} + \frac{(\bar{p}_1 - \bar{p}_1^*)^2}{G_{p_1}} + \frac{(\bar{p}_2 - \bar{p}_2^*)^2}{G_{p_2}},$$

with \bar{t}_1^* , \bar{t}_2^* , \bar{p}_1^* and \bar{p}_2^* defined by (A3.34).

By definition,

$$\begin{aligned} \Delta\mathcal{A} = & \frac{2\Delta\bar{t}_1(\bar{t}_1 - \bar{t}_1^*) + (\Delta\bar{t}_1)^2}{G_{t_1}} + \frac{2\Delta\bar{t}_2(\bar{t}_2 - \bar{t}_2^*) + (\Delta\bar{t}_2)^2}{G_{t_2}} \\ & + \frac{2\Delta\bar{p}_1(\bar{p}_1 - \bar{p}_1^*) + (\Delta\bar{p}_1)^2}{G_{p_1}} + \frac{2\Delta\bar{p}_2(\bar{p}_2 - \bar{p}_2^*) + (\Delta\bar{p}_2)^2}{G_{p_2}}. \end{aligned}$$

When $\bar{t}_1 - \bar{p}_1$ and $\bar{t}_2 - \bar{p}_2$ are of order ε , $\Delta\bar{t}_1$, $\Delta\bar{t}_2$, $\Delta\bar{p}_1$ and $\Delta\bar{p}_2$ are of order ε^2 . We then neglect the terms proportional to $(\Delta\bar{t}_1)^2$, $(\Delta\bar{t}_2)^2$, $(\Delta\bar{p}_1)^2$ or $(\Delta\bar{p}_2)^2$:

$$\Delta\mathcal{A} = \frac{2\Delta\bar{t}_1(\bar{t}_1 - \bar{t}_1^*)}{G_{t_1}} + \frac{2\Delta\bar{t}_2(\bar{t}_2 - \bar{t}_2^*)}{G_{t_2}} + \frac{2\Delta\bar{p}_1(\bar{p}_1 - \bar{p}_1^*)}{G_{p_1}} + \frac{2\Delta\bar{p}_2(\bar{p}_2 - \bar{p}_2^*)}{G_{p_2}} + O(\varepsilon^4).$$

By replacing the terms $\Delta\bar{t}_1$, $\Delta\bar{t}_2$, $\Delta\bar{p}_1$ and $\Delta\bar{p}_2$ using (12) and simplifying, we obtain:

$$\Delta\mathcal{A} = \beta_{t_1}(\bar{t}_1 - \bar{t}_1^*) + \beta_{p_1}(\bar{p}_1 - \bar{p}_1^*) + \beta_{t_2}(\bar{t}_2 - \bar{t}_2^*) + \beta_{p_2}(\bar{p}_2 - \bar{p}_2^*) + O(\varepsilon^4).$$

Using that for $i \in \{1, 2\}$, $\bar{t}_i - \bar{p}_i$ and $\bar{t}_i^* - \bar{p}_i^*$ are of order ε , we obtain similarly as in (A3.22)

$$\Delta\mathcal{A} = (\beta_{t_1} + \beta_{p_1}) \left(\frac{\bar{t}_1 - \bar{t}_1^*}{2} + \frac{\bar{p}_1 - \bar{p}_1^*}{2} \right) + (\beta_{t_2} + \beta_{p_2}) \left(\frac{\bar{t}_2 - \bar{t}_2^*}{2} + \frac{\bar{p}_2 - \bar{p}_2^*}{2} \right) + O(\varepsilon^3). \quad (\text{A3.35})$$

Using (A3.3) and (A3.4) and simplifying, we obtain:

$$\beta_{t_1} + \beta_{p_1} = -\frac{4bd(\bar{t}_1 - \bar{t}_2)\lambda_2 n_2}{(1 + \lambda_1 n_1 + \lambda_2 n_2)^2} - 4s_1(\bar{t}_1 - t_{a1}) + 2c_{RI}a_1(\bar{t}_1 - \bar{t}_2)\frac{n_2}{n_1} + O(\varepsilon^3).$$

By subtracting $-\frac{4bd(\bar{t}_1 - \bar{t}_2)\lambda_2 n_2}{(1 + \lambda_1 n_1 + \lambda_2 n_2)^2} - 4s_1(\bar{t}_1^* - t_{a1}) + 2c_{RI}a_1(\bar{t}_1^* - \bar{t}_2^*)\frac{n_2}{n_1}$ which is equal to

zero (because $\beta_{t_1}|_{(t_1, t_2, p_1, p_2)=(\bar{t}_1^*, \bar{t}_2^*, \bar{p}_1^*, \bar{p}_2^*)} = 0$ and $\beta_{p_1}|_{(t_1, t_2, p_1, p_2)=(\bar{t}_1^*, \bar{t}_2^*, \bar{p}_1^*, \bar{p}_2^*)} = 0$, we get:

$$\begin{aligned} (\beta_{t_1} + \beta_{p_1}) &= \left(-\frac{4bd\lambda_2 n_2}{(1 + \lambda_1 n_1 + \lambda_2 n_2)^2} - 4s_1 + 2c_{RI}a_1 \frac{n_2}{n_1} \right) (\bar{t}_1 - \bar{t}_1^*) \\ &\quad - \left(-\frac{4bd\lambda_2 n_2}{(1 + \lambda_1 n_1 + \lambda_2 n_2)^2} + 2c_{RI}a_1 \frac{n_2}{n_1} \right) (\bar{t}_2 - \bar{t}_2^*) + O(\varepsilon^3) \\ &= -C_1(\bar{t}_1 - \bar{t}_1^*) + A_1 C_1(\bar{t}_2 - \bar{t}_2^*) + O(\varepsilon^3). \end{aligned}$$

Because for $i \in \{1, 2\}$, $\bar{t}_i - \bar{t}_i^* = \bar{p}_i - \bar{p}_i^* + \bar{t}_i - \bar{p}_i + \bar{p}_i^* - \bar{t}_i^* = \bar{p}_i - \bar{p}_i^* + O(\varepsilon)$ we also have

$$(\beta_{t_1} + \beta_{p_1}) = -C_1(\bar{p}_1 - \bar{p}_1^*) + A_1 C_1(\bar{p}_2 - \bar{p}_2^*) + O(\varepsilon^3).$$

We thus get

$$(\beta_{t_1} + \beta_{p_1})(\bar{t}_1 - \bar{t}_1^*) = -C_1(\bar{t}_1 - \bar{t}_1^*)^2 + A_1 C_1(\bar{t}_1 - \bar{t}_1^*)(\bar{t}_2 - \bar{t}_2^*) + O(\varepsilon^3),$$

and

$$(\beta_{t_1} + \beta_{p_1})(\bar{p}_1 - \bar{p}_1^*) = -C_1(\bar{p}_1 - \bar{p}_1^*)^2 + A_1 C_1(\bar{p}_1 - \bar{p}_1^*)(\bar{p}_2 - \bar{p}_2^*) + O(\varepsilon^3).$$

Hence using (A3.35), the symmetry of the model between populations 1 and 2, and that for $i \in \{1, 2\}$, $\bar{t}_i - \bar{p}_i$ and $\bar{t}_i^* - \bar{p}_i^*$ are of order ε , we obtain:

$$\begin{aligned} 2\Delta\mathcal{A} &= -C_1(\bar{t}_1 - \bar{t}_1^*)^2 + (A_1 C_1 + A_2 C_2)(\bar{t}_1 - \bar{t}_1^*)(\bar{t}_2 - \bar{t}_2^*) - C_2(\bar{t}_2 - \bar{t}_2^*)^2 \\ &\quad - C_1(\bar{p}_1 - \bar{p}_1^*)^2 + (A_1 C_1 + A_2 C_2)(\bar{p}_1 - \bar{p}_1^*)(\bar{p}_2 - \bar{p}_2^*) - C_2(\bar{p}_2 - \bar{p}_2^*)^2, \end{aligned}$$

with can be rewritten in matrix form

$$2\Delta\mathcal{A} = -T^t M T - P^t M P + O(\varepsilon^3),$$

with

$$M = \begin{pmatrix} C_1 & -\frac{A_1C_1+A_2C_2}{2} \\ -\frac{A_1C_1+A_2C_2}{2} & C_2 \end{pmatrix}, \quad T = \begin{pmatrix} \bar{t}_1 - \bar{t}_1^* \\ \bar{t}_2 - \bar{t}_2^* \end{pmatrix}, \quad P = \begin{pmatrix} \bar{p}_1 - \bar{p}_1^* \\ \bar{p}_2 - \bar{p}_2^* \end{pmatrix},$$

and T^t and P^t being the transposed of T and P respectively.

First case: $C_1 > 0$, $C_2 > 0$ and $C_1C_2(1 - A_1A_2) - \frac{1}{4}(A_1C_1 - A_2C_2)^2 > 0$.

According to the Sylvester's criterion the matrix M is positive-definite. Using computations similar to the ones derived to prove (A3.17), we may prove that after a number of generations large enough, $\bar{t}_1 - \bar{t}_1^*$, $\bar{t}_2 - \bar{t}_2^*$, $\bar{p}_1 - \bar{p}_1^*$ and $\bar{p}_2 - \bar{p}_2^*$ become of order $\varepsilon^{1/2}$.

Second case: $C_1 < 0$, $C_2 < 0$ and $C_1C_2(1 - A_1A_2) - \frac{1}{4}(A_1C_1 - A_2C_2)^2 > 0$.

According to the Sylvester's criterion the matrix $-M$ is positive-definite. Therefore \bar{t}_1 , \bar{t}_2 , \bar{p}_1 and \bar{p}_2 become very large.

A3.5.3 Effect of different parameters on the level of trait divergence $|\bar{t}_1^* - \bar{t}_2^*|$ assuming weak or strong female and predator discriminations

We want to verify that the different parameters have similar effect on phenotypic distance between species in this model than in the first. To this aim we plot the effect of different parameters on the level of trait divergence assuming whether (using the analytical approximation when possible or numerical simulations) or (using numerical simulations). The following plots confirm that the parameters have a similar effect on the phenotypic distance.

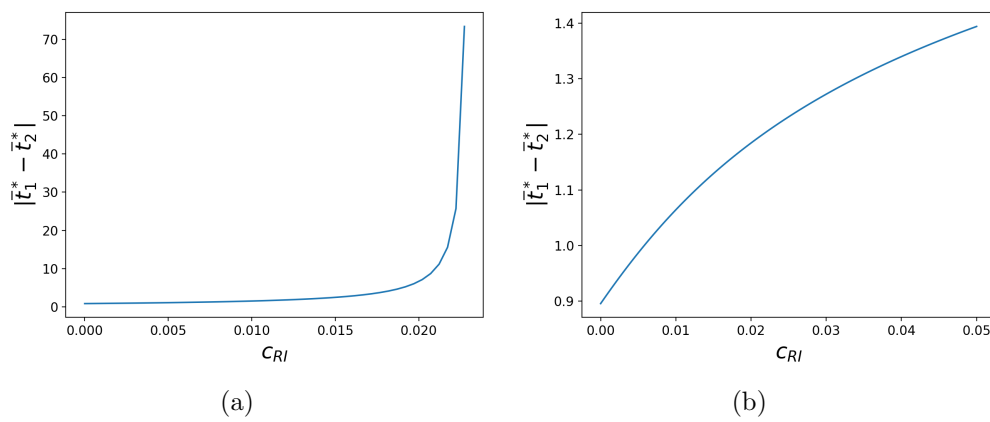


Fig. A3.11: **Influence of the strength of reproductive interference c_{RI} on the phenotypic distances between the two species, assuming (a) weak or (b) strong female and predator discriminations.** Simulations were run assuming (a) $a_1 = a_2 = b = 0.01$ or (b) $a_1 = a_2 = b = 1$. The default parameters values are as follows: $G_{t_1} = G_{p_1} = G_{t_2} = G_{p_2} = 0.01$, $d = 0.02$, $\lambda_1 = 0.1$, $\lambda_2 = 0.1$, $n_1 = 10$, $n_2 = 20$, $s_1 = 0.0000025$, $s_2 = 0.0000025$, $t_{a1} = 0$, $t_{a2} = 1$.

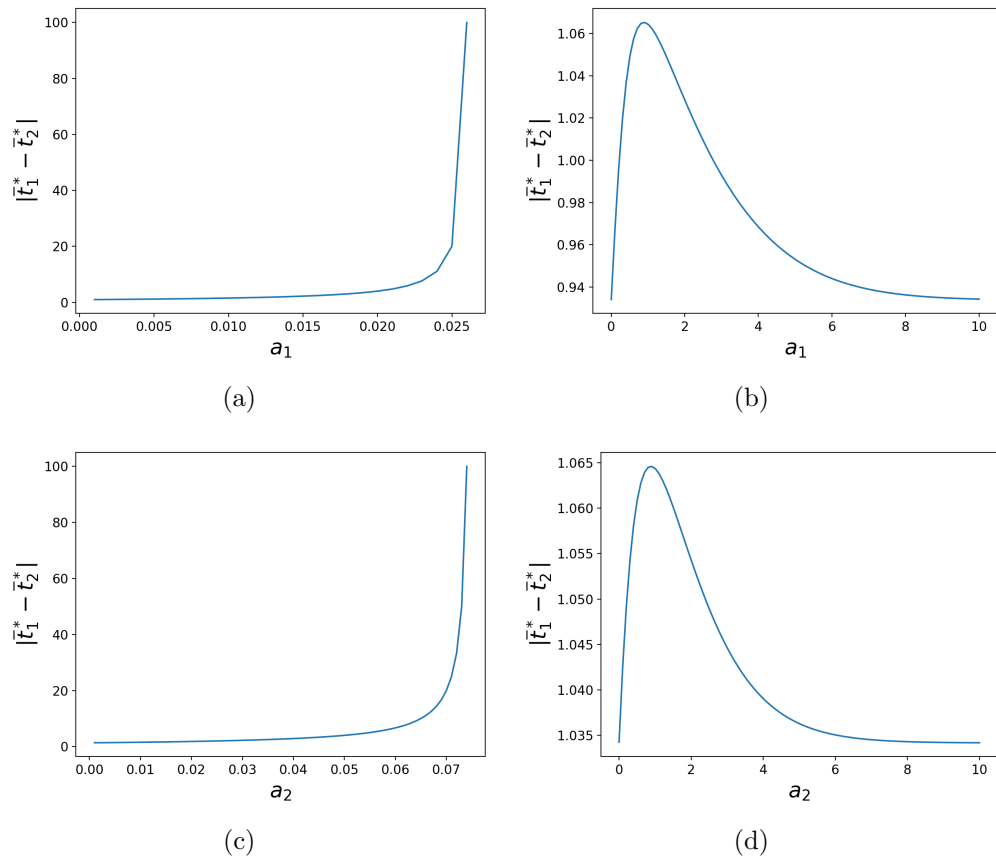


Fig. A3.12: **Influence of female discrimination in species (a)(b) 1 a_1 and (c)(d) 2 a_1 on the phenotypic distances between the two species, assuming (a)(c) weak or (b)(d) strong female and predator discriminations.** Simulations were run assuming (a) $a_2 = b = 0.01$, (b) $a_2 = b = 1$, (c) $a_1 = b = 0.01$ or (d) $a_1 = b = 1$. The default parameters values are as follows: $G_{t_1} = G_{p_1} = G_{t_2} = G_{p_2} = 0.01$, $c_{RI} = 0.01$, $d = 0.02$, $\lambda_1 = 0.1$, $\lambda_2 = 0.1$, $n_1 = 10$, $n_2 = 20$, $s_1 = 0.0000025$, $s_2 = 0.0000025$, $t_{a_1} = 0$, $t_{a_2} = 1$.

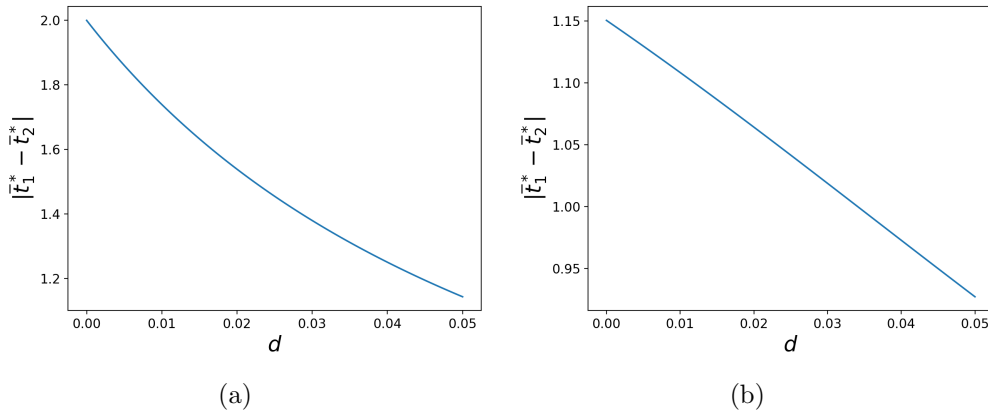


Fig. A3.13: **Influence of the strength of predation d on the phenotypic distances between the two species, assuming (a) weak or (b) strong female and predator discriminations.** Simulations were run assuming (a) $a_1 = a_2 = b = 0.01$, (b) $a_1 = a_2 = b = 1$. The default parameters values are as follows: $G_{t_1} = G_{p_1} = G_{t_2} = G_{p_2} = 0.01$, $c_{RI} = 0.01$, $\lambda_1 = 0.1$, $\lambda_2 = 0.1$, $n_1 = 10$, $n_2 = 20$, $s_1 = 0.0000025$, $s_2 = 0.0000025$, $t_{a1} = 0$, $t_{a2} = 1$.

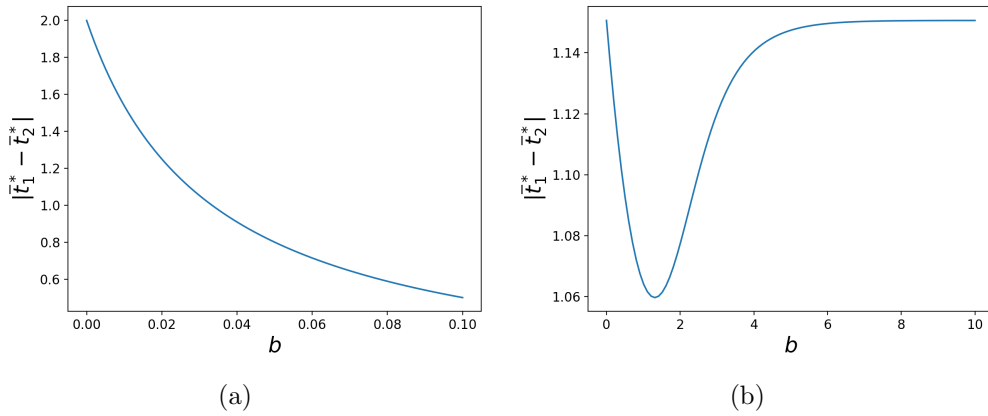


Fig. A3.14: **Influence of predator discrimination b on the phenotypic distances between the two species, assuming (a) weak or (b) strong female and predator discriminations.** Simulations were run assuming (a) $a_1 = a_2 = 0.01$, (b) $a_1 = a_2 = 1$. The default parameters values are as follows: $G_{t_1} = G_{p_1} = G_{t_2} = G_{p_2} = 0.01$, $c_{RI} = 0.01$, $d = 0.02$, $\lambda_1 = 0.1$, $\lambda_2 = 0.1$, $n_1 = 10$, $n_2 = 20$, $s_1 = 0.0000025$, $s_2 = 0.0000025$, $t_{a1} = 0$, $t_{a2} = 1$.

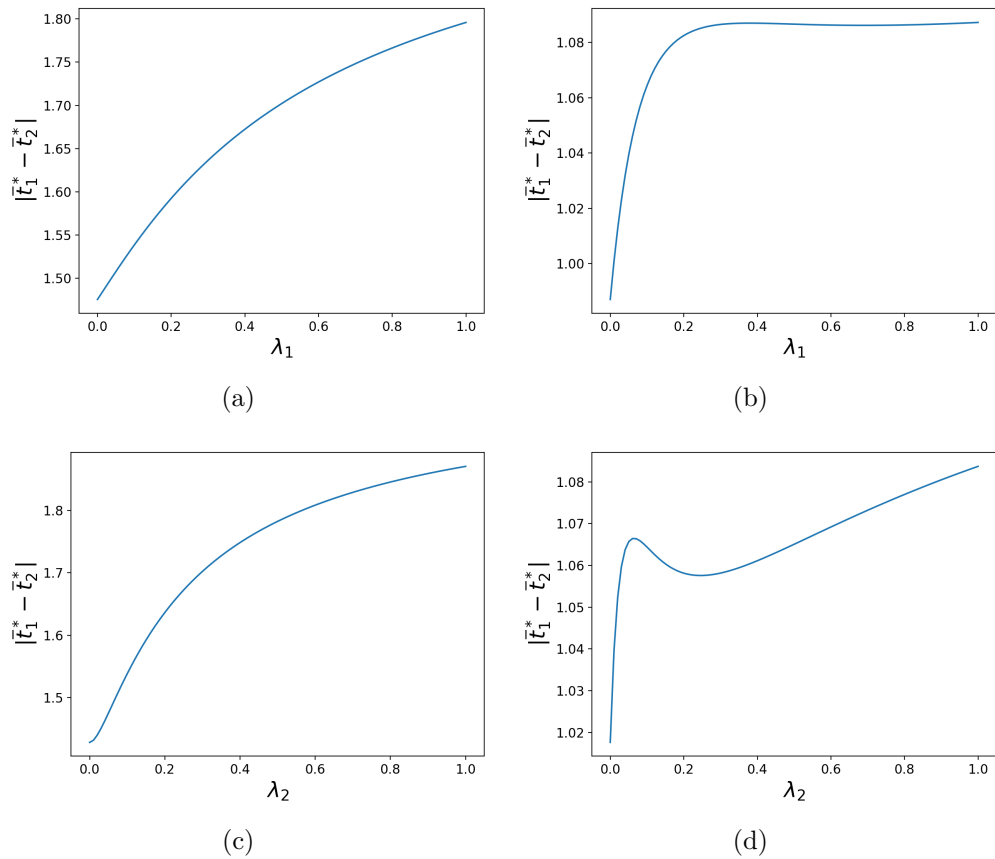


Fig. A3.15: Influence of the defence level of (a)(b) species 1 λ_1 and of (c)(d) species 2 λ_2 on the phenotypic distances between both species, assuming (a)(c) weak or (b)(d) strong female and predator discriminations. Simulations were run assuming (a)(c) $a_1 = a_2 = b = 0.01$, (b)(d) $a_1 = a_2 = b = 1$. The default parameters values are as follows: $G_{t_1} = G_{p_1} = G_{t_2} = G_{p_2} = 0.01$, $c_{RI} = 0.01$, $d = 0.02$, $\lambda_1 = 0.1$, $\lambda_2 = 0.1$, $n_1 = 10$, $n_2 = 20$, $s_1 = 0.0000025$, $s_2 = 0.0000025$, $t_{a1} = 0$, $t_{a2} = 1$.

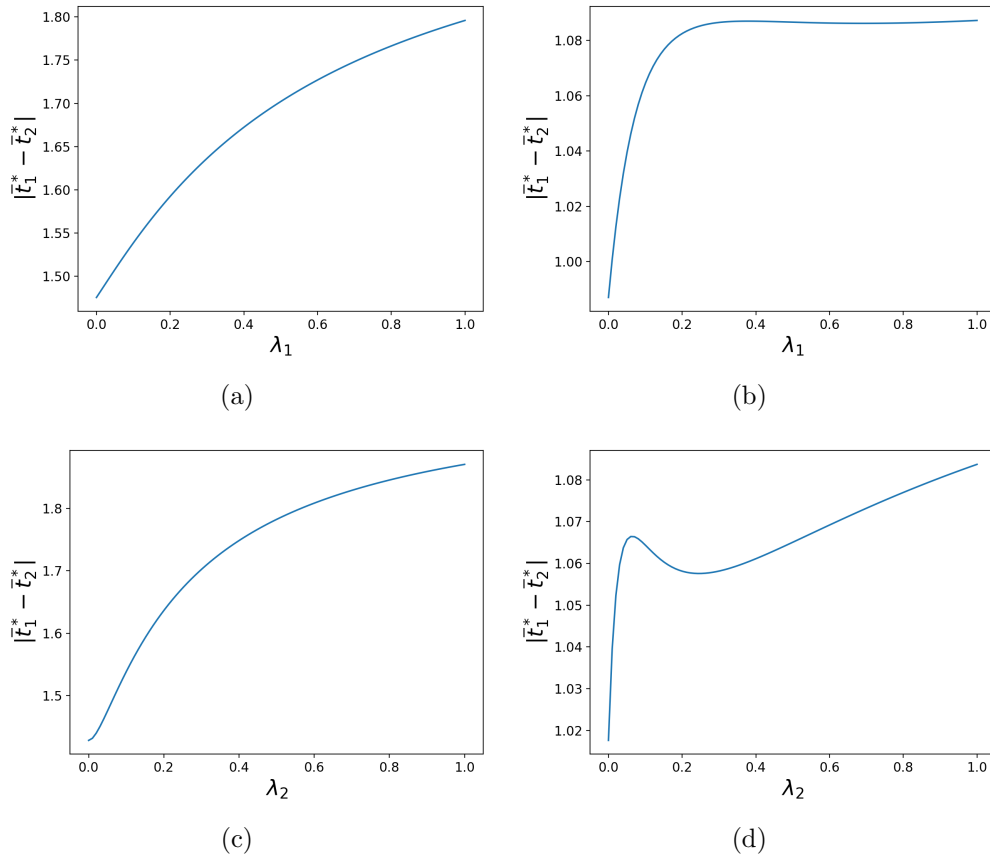


Fig. A3.16: **Influence of the defence level of (a)(b) species 1 λ_1 and of (c)(d) species 2 λ_2 on the phenotypic distances between both species, assuming (a)(c) weak or (b)(d) strong female and predator discriminations.** Simulations were run assuming (a)(c) $a_1 = a_2 = b = 0.01$, (b)(d) $a_1 = a_2 = b = 1$. The default parameters values are as follows: $G_{t_1} = G_{p_1} = G_{t_2} = G_{p_2} = 0.01$, $c_{RI} = 0.01$, $d = 0.02$, $\lambda_1 = 0.1$, $\lambda_2 = 0.1$, $n_1 = 10$, $n_2 = 20$, $s_1 = 0.0000025$, $s_2 = 0.0000025$, $t_{a1} = 0$, $t_{a2} = 1$.

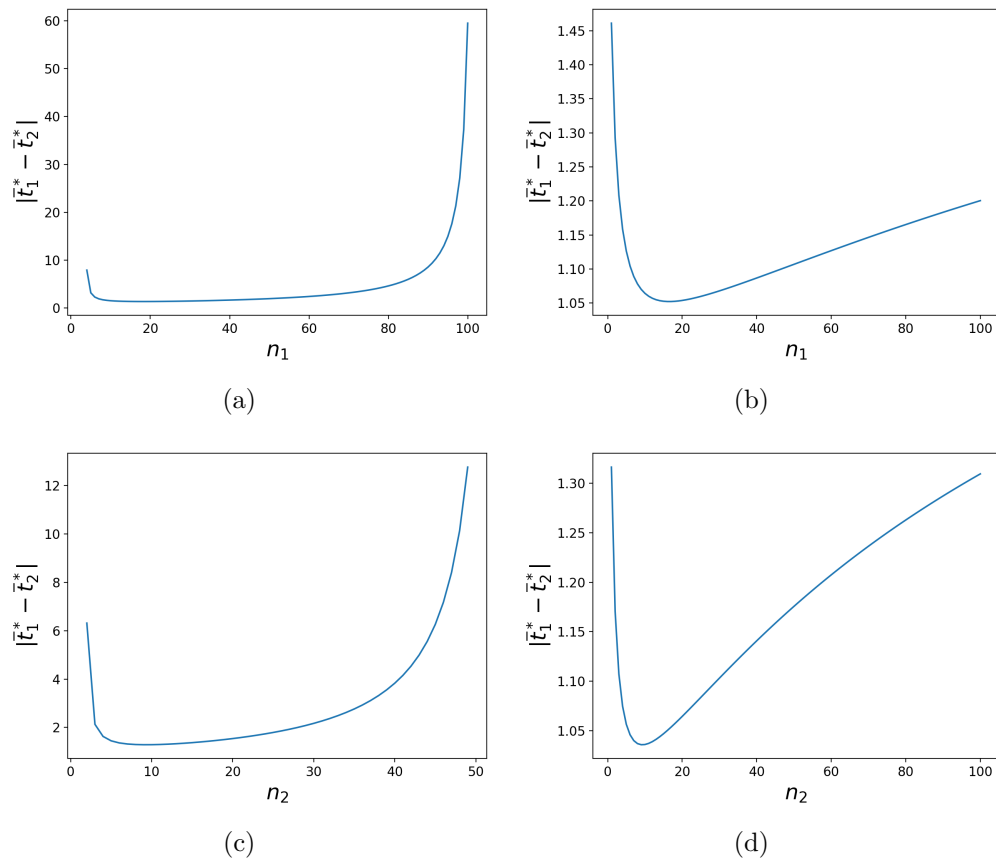


Fig. A3.17: **Influence of the density of (a)(b) species 1 n_1 and of (c)(d) species 2 n_2 on the phenotypic distances between the two species, assuming (a)(c) weak or (b)(d) strong female and predator discriminations.** Simulations were run assuming (a) $a_1 = a_2 = b = 0.01$, (b) $a_1 = a_2 = b = 1$. The default parameters values are as follows: $G_{t_1} = G_{p_1} = G_{t_2} = G_{p_2} = 0.01$, $c_{RI} = 0.01$, $d = 0.02$, $\lambda_1 = 0.1$, $\lambda_2 = 0.1$, $n_1 = 10$, $n_2 = 20$, $s_1 = 0.0000025$, $s_2 = 0.0000025$, $t_{a1} = 0$, $t_{a2} = 1$.

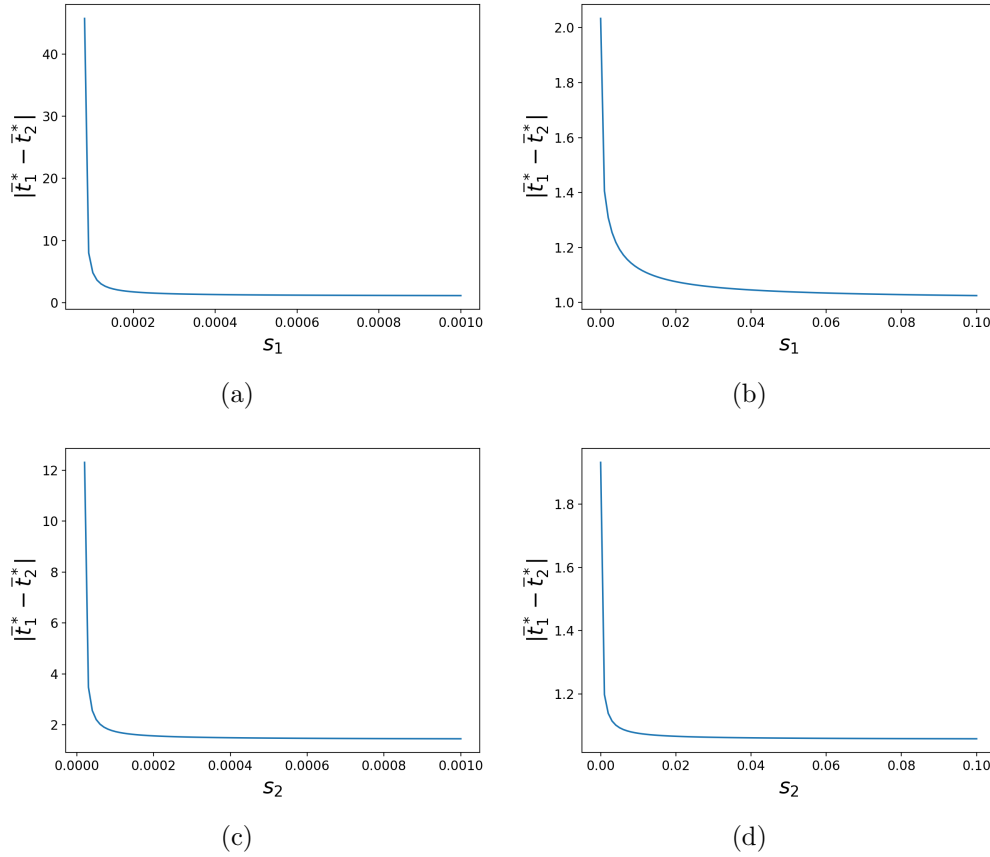


Fig. A3.18: Influence of the strength of selective constraints in (a)(b) species 1 s_1 and in (c)(d) species 2 s_2 on the phenotypic distances between the two species, assuming (a)(c) weak or (b)(d) strong female and predator discriminations. Simulations were run assuming (a)(c) $a_1 = a_2 = b = 0.01$, (b)(d) $a_1 = a_2 = b = 1$. The default parameters values are as follows: $G_{t_1} = G_{p_1} = G_{t_2} = G_{p_2} = 0.01$, $c_{RI} = 0.01$, $d = 0.02$, $\lambda_1 = 0.1$, $\lambda_2 = 0.1$, $n_1 = 10$, $n_2 = 20$, $s_1 = 0.0000025$, $s_2 = 0.0000025$, $t_{a1} = 0$, $t_{a2} = 1$.

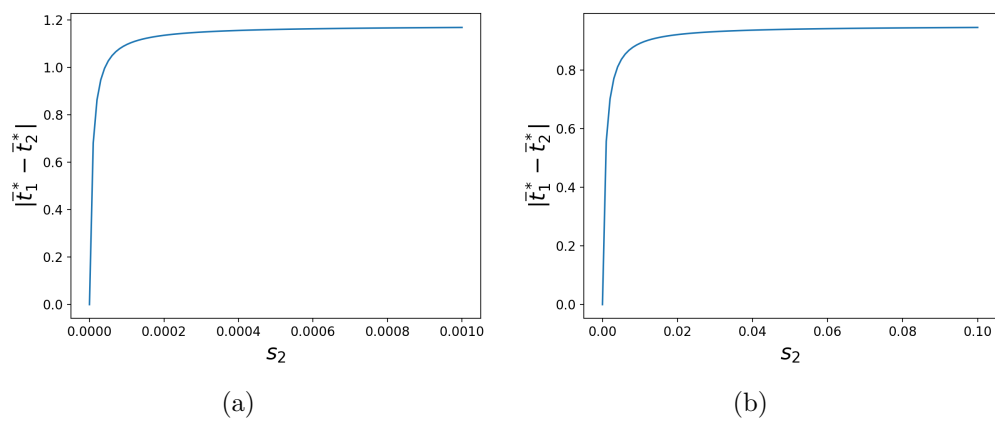


Fig. A3.19: **Influence of the strength of selective constraints in species 2 s_2 on the phenotypic distances between the two species, when predation is great compare to reproductive interference, assuming (a) weak or (b) strong female and predator discriminations.** Simulations were run assuming (a) $a_1 = a_2 = b = 0.01$, (b) $a_1 = a_2 = b = 1$. The default parameters values are as follows: $G_{t_1} = G_{p_1} = G_{t_2} = G_{p_2} = 0.01$, $c_{RI} = 0.01$, $d = 0.05$, $\lambda_1 = 0.1$, $\lambda_2 = 0.1$, $n_1 = 10$, $n_2 = 20$, $s_1 = 0.0000025$, $s_2 = 0.0000025$, $t_{a1} = 0$, $t_{a2} = 1$.

A3.5.4 Historical constraints promoting ancestral trait values strongly modulate phenotypic divergence driven by reproductive interference.

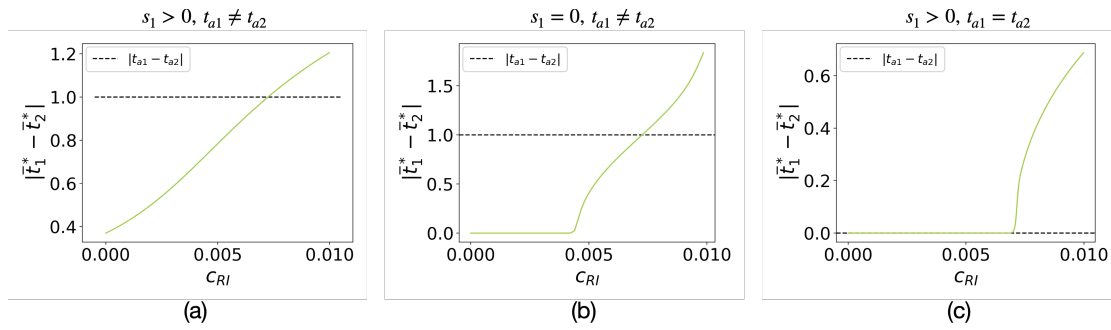


Fig. A3.20: Influence of the cost of reproductive interference c_{RI} on the phenotypic distances between the two species $\bar{t}_1^* - \bar{t}_2^*$ assuming strong female and predator discriminations. We assume (a) $s_1 = s_2 = 0.005$, $t_{a1} = 0$, $t_{a2} = 1$, (b) $s_1 = s_2 = 0$, $t_{a1} = 0$, $t_{a2} = 1$, and (c) $s_1 = s_2 = 0.005$, $t_{a1} = t_{a2} = 1$. We also assume: $G_{t_1} = G_{p_1} = G_{t_2} = G_{p_2} = 0.01$, $a_1 = a_2 = b = 1$, $b = 1$, $d = 0.02$, $\lambda_1 = \lambda_2 = 0.1$, $n_1 = n_2 = 10$.

A3.5.5 Impact of predator discrimination without reproductive interference.

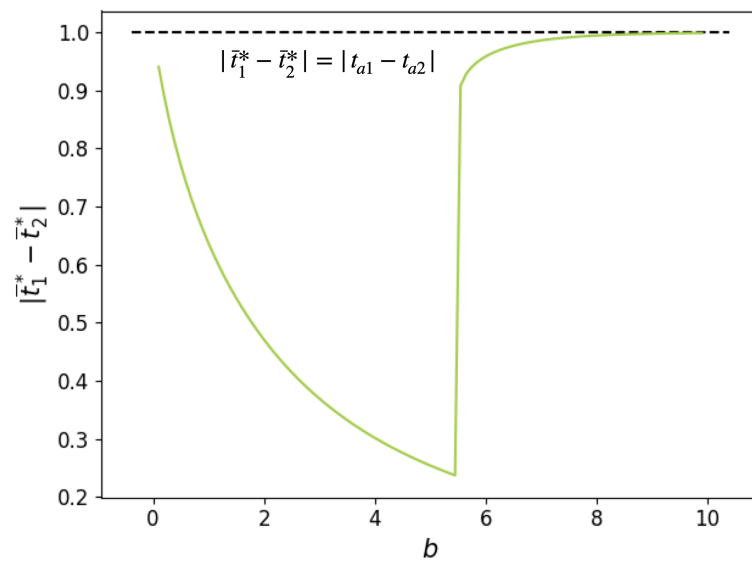


Fig. A3.21: Influence of predator discrimination b on the phenotypic distances between the two species $\bar{t}_1^* - \bar{t}_2^*$ assuming no reproductive interference ($c_{RI} = 0$). We assume: $G_{t_1} = G_{p_1} = G_{t_2} = G_{p_2} = 0.01$, $a_1 = a_2 = b = 1$, $b = 1$, $d = 0.02$, $\lambda_1 = \lambda_2 = 0.1$, $n_1 = n_2 = 10$, $s_1 = s_2 = 0.005$, $t_{a1} = 0$, $t_{a2} = 1$.

A3.5.6 Impact of the relative defence level on traits co-evolution

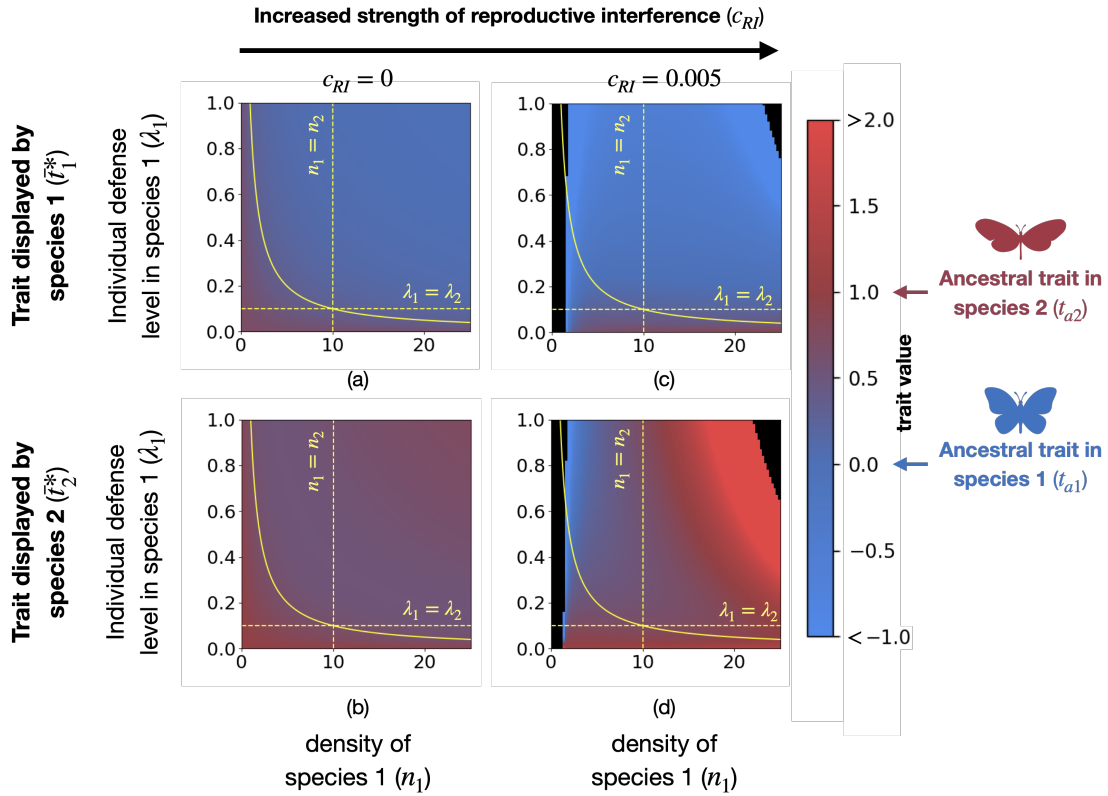


Fig. A3.22: Influence of the density and of the individual defense level in species 1 (n_1 and λ_1) on the traits displayed in both species, for different strengths of reproductive interference (c_{RI}). Plots report values obtained with the analytic approximation, assuming weak female and predator discriminations. Mean trait values can become very large (black zone). Trait values greater than 2 (resp. lower than -1) are shown in red (resp. blue). The yellow solid line shows the case where both species have the same level of defense ($\lambda_1 n_1 = \lambda_2 n_2$). Below (resp. above) this line species 1 has a lower (resp. higher) level of defense than species 2. Different values of strengths of reproductive interference are assumed: (a) and (b) $c_{RI} = 0$, (c) and (d) $c_{RI} = 0.005$. We assume: $G_{t_1} = G_{p_1} = G_{t_2} = G_{p_2} = 0.01$, $a_1 = a_2 = 0.01$, $d = 0.05$, $b = 0.01$, $\lambda_2 = 0.1$, $n_2 = 10$, $s_1 = s_2 = 0.000005$, $t_{a1} = 0$, $t_{a2} = 1$.

CHAPTER THREE

CHAPTER 4

Can reproductive interference explain female-limited mimicry ?

Ludovic Maisonneuve, Charline Smadi and Violaine
Llaurens

Submitted to *Evolution* (minor revision):

Maisonneuve, L, Smadi, C, Llaurens, V. (2021) Evolutionary origins of sexual dimorphism : Lessons from female-limited mimicry in butterflies.

bioRxiv.

doi: 10.1101/2021.07.09.451774

Abstract

The striking female-limited mimicry observed in some butterfly species is a textbook example of sexually-dimorphic trait submitted to intense natural selection. The evolution of mimicry in males could be limited by female preference for non-mimetic males. However, the evolutionary origin of female preference for non-mimetic males remains unclear. Here, we hypothesise that costly sexual interactions between individuals from distinct sympatric species might intensify because of mimicry, therefore promoting female preference for non-mimetic trait. Also natural selection may explain the evolution of female-limited mimicry. Predation pressure favouring mimicry toward defended species could be higher in females because of their slower flight, and thus overcome developmental constraints favouring the ancestral trait that limits the evolution of mimicry in males but not in females. Using a mathematical model, we compare the evolution of female-limited mimicry when assuming either alternative selective hypotheses. We show that the patterns of divergence of male and female trait from the ancestral traits can differ between these selection regimes. We specifically highlight that divergence in female trait is not a signature of the effect of natural selection. Our results also evidence why female-limited mimicry is more frequently observed in Batesian mimics.

Introduction

The evolutionary forces involved in the emergence of sexual dimorphism in different animal species are still debated. As highlighted by Wallace (1865), divergent natural selection could drive the evolution of strikingly different phenotypes in males and females, because they may occupy different ecological niches. Sexual selection exerted by females is also a powerful force leading to the emergence of elaborated traits in males only, therefore leading to sexual dimorphism (Darwin, 1871). The relative contributions of natural and sexual selection to the evolution of sexually dimorphic traits has generated important controversies. The evolution of sexual dimorphism in wing colour patterns in butterflies has been central to

this debate because wing colour patterns are under strong natural selection by predators and are also involved in mate choice and species recognition (Turner, 1978). Quantifying phenotypic divergence in males and females from the ancestral trait may allow one to identify the main evolutionary factors involved in the evolution of sexual dimorphism. Using a phylogenetic approach on European butterflies, van der Bijl *et al.* (2020) recently showed that the wing colour pattern dimorphism is mainly driven by the divergence of male phenotype from the ancestral trait, in line with the sexual selection hypothesis. In contrast to this general trend, sexual dimorphism where females exhibit a derived colour pattern is frequently observed in butterfly species involved in Batesian mimicry (Kunte, 2008). In these palatable species, the evolution of colour patterns looking similar to the phenotype displayed in chemically-defended species living in sympatry is strongly promoted: because predators associate conspicuous colouration to defences, individuals displaying mimetic colouration in palatable species have a reduced predation risk (Bates, 1862; Ruxton *et al.*, 2019). Despite predation affecting individuals from both sexes, mimicry is sometimes surprisingly limited to females (Ford, 1975; Kunte, 2008; Long *et al.*, 2014; Nishikawa *et al.*, 2015), therefore begging the question of the evolutionary forces preventing the evolution of mimicry in males (*i.e.* female-limited mimicry, named FLM hereafter).

Because butterfly males and females generally differ in their behaviour, the strength of predation pressure might differ among sexes (Ohsaki, 1995, 2005): for instance, females usually spend a lot of time ovipositing on specific host-plants, and thus have a more predictable behaviour for predators. Moreover, flight speed is generally higher in males than females: females are heavier because they carry eggs (Gilchrist, 1990), and males have higher relative thorax mass (Karlsson & Wickman, 1990) and muscle mass (Marden & Chai, 1991), resulting in increased flight power (Chai & Srygley, 1990). Predation pressures are thus expected to be stronger in females. In line with this expectation Su *et al.* (2015) show that in a mimetic butterflies where males and females mimic the same species, females are more perfect mimics than males, suggesting also that some constraints limits perfect mimicry in males. Wing pattern evolution is also shaped by developmental con-

straints (Van Belleghem *et al.*, 2020) that may impede divergence from the ancestral trait. Phylogenetic analyses show that FLM derived from sexually monomorphic non-mimetic ancestors (Kunte, 2009; Timmermans *et al.*, 2017) suggesting that mimicry in FLM species is associated with a costly displacement from an ancestral non-mimetic phenotype. In the female-limited polymorphic butterfly *Papilio polytes*, where both mimetic and non-mimetic females co-exist, the mimetic allele reduces the pre-adult survival rate (Komata *et al.*, 2020; Katoh *et al.*, 2020) (but see (Komata *et al.*, 2018) in the FLM butterfly *Papilio memnon*), highlighting cost associated with mimicry. Such trade-off between developmental constraints favouring the ancestral trait and selection promoting mimicry might differ between sexes: if predation is lower in males, the constraints limiting mimicry may overcome the benefit from mimicry in males, whereas in females the higher predation pressure may promote mimicry. In line with this idea, in mimetic Asian pitvipers, where males suffer for a greater predation pressure, females are rarely mimetic, strengthening the role of sexually contrasted predation in promoting sex-limited mimicry (Sanders *et al.*, 2006). Nevertheless, evidence for the limited predation in males as compared to females is controversial in butterflies (Wourms & Wasserman, 1985) therefore questioning whether contrasted predation in males and females is actually the main driver of FLM.

Other constraints triggered by sexual selection might limit mimicry in males. In the female-limited Batesian mimic *Papilio polyxenes asterius*, experimental alteration of male colour pattern into female colour pattern leads to lower success during male-male encounters and increased difficulty in establishing a territory, therefore reducing mating opportunities (Lederhouse & Scriber, 1996). Furthermore, in the female-limited Batesian mimic *Papilio glaucus*, females prefer control painted non-mimetic males over painted mimetic males (Krebs & West, 1988) (but see (Low & Monteiro, 2018) in the FLM butterfly *Papilio polytes*). Wing colour patterns in mimetic butterflies may therefore modulate male reproductive success, by influencing both male-male competition and mating success with females. In particular, female preference for ancestral trait may generate sexual selection limiting male mimicry (Belt, 1874.; Turner, 1978). Nevertheless, because mimetic colouration

is under strong positive selection, females are predicted to prefer mimetic males because it leads to adapted mimetic offspring, favouring mimetic colouration in males, as observed in species involved in Müllerian mimicry, *i.e.* when co-mimetic species are all chemically-defended (Jiggins *et al.*, 2001; Naisbit *et al.*, 2001; Kronforst *et al.*, 2006; Merrill *et al.*, 2014). It is thus unclear what does limit the evolution of female preference towards mimetic colouration in males from mimetic species.

Female preference for mimetic males may be disadvantageous because this behaviour may lead to mating interactions with unpalatable 'model' species. Therefore reproductive interference, *i.e.* costly interactions between different species during mate acquisition (see (Gröning & Hochkirch, 2008) for a definition), may impair the evolution of female preference towards mimetic colour patterns displayed by other sympatric species. The evolution of mimetic colouration in males may indeed increase costs linked to reproductive interference in females, and therefore promote the evolution of preference for non-mimetic traits in males. Such reproductive interference has been observed between species sharing similar aposematic traits (in *Heliconius* and *Mechanitis* species (Estrada & Jiggins, 2008)). The rate of erroneous mating may be limited by the difference in male pheromones between mimetic species (see Darragh *et al.* (2017); González-Rojas *et al.* (2020) for empirical examples in *Heliconius* butterflies). However, females may still suffer from cost associated to reproductive interference, even if they refuse mating with heterospecific males: females may allow courting by heterospecific males displaying their preferred cue, resulting in increased investment in mate searching (see signal jamming in (Gröning & Hochkirch, 2008)). Pheromones may not limit this increase of investment in mate searching, because they act as short-distance cue that may be perceived only during the courtship (Mérot *et al.*, 2015). Females deceived by the colour pattern then need to deploy substantial efforts to avoid the heterospecific mating.

Theoretical studies highlight that the reproductive interference between sympatric species influence the evolution of traits used as mating cues. Reproductive interference indeed promotes the evolution of female preference towards traits differing

from the phenotype displayed in other sympatric species, because it reduces the number of costly sexual interactions (McPeck & Gavrilets, 2006; Yamaguchi & Iwasa, 2013). However these studies do not consider the independent evolution male and female traits. Under weak constraint on sex differentiation, reproductive interference may impede divergence of male trait, while natural selection may promote the evolution of female trait, leading to sexual dimorphism. For instance, in two of the three fruit fly species of the genus *Blepharoneura* that court on the same host plant, a morphometric analysis reveals sexual dimorphism in wing shape where males, but not females, from the two different species differ in wing shape Marsteller *et al.* (2009). In the mexican spadefoot toads *Spea multiplicata*, the level of sexual size dimorphism increases with the proportion of species from the same genus *Spea bombifrons* living in sympatry (Pfennig & Pfennig, 2005) suggesting a link between species interactions and sexual dimorphism. In species exhibiting FLM, reproductive interference may thus inhibit natural selection in males, while females become mimetic. A theoretical study show that reproductive interference can totally impair the evolution of mimicry (Boussens-Dumon & Llaurens, 2021) therefore suggesting that reproductive interference might indeed be a relevant ecological interaction preventing mimicry in males. In the model investigating the effect of reproductive interference on mimicry described in Boussens-Dumon & Llaurens (2021), colour-patten based assortative mating was assumed, preventing the study of the evolution of disassortative preferences in females. Therefore understanding the impact of reproductive interference on the evolution of FLM requires to specifically explore the evolution of female preference, and to assume a genetic architecture enabling mating cues to evolve in different directions in males and females.

Interestingly, the two main hypotheses usually explaining FLM, *i.e.* (1) sexually contrasted predation and (2) sexual selection on males, are both equally relevant for palatable, as well as unpalatable mimetic species. Indeed, sympatric unpalatable species frequently display a common mimetic trait (Sherratt, 2008), suggesting a strong selection promoting mimicry. However, FLM is considered to be widespread in palatable species but rare in unpalatable ones (Mallet & Joron, 1999) (but see

(Nishida, 2017)). This suggests that the evolution of sexual dimorphism in mimetic species might depend on the level of defences.

Here, we investigate how (1) reproductive interference and (2) sexually contrasted predation may promote the evolution of FLM, using a mathematical model. Firstly we pinpoint the specific evolutionary outcomes associated with the emergence of FLM driven by reproductive interference or sexually contrasted predation, therefore providing relevant predictions for comparisons with empirical data. Secondly, we study the impact of unpalatability levels on the emergence of sexual dimorphism, to test whether FLM may be restricted to palatable species. Our model describes the evolution of quantitative traits, following the framework established by Lande & Arnold (1985) in a *focal* species, living in sympatry with a defended *model* species exhibiting a fixed warning trait. We specifically study the evolution of (1) the quantitative traits displayed in males t_m and females t_f involved in mimetic interactions, (2) the preference of females for the different values of males trait p_f . We assume that individuals in the *focal* species gain protection against predators from the similarity of their warning trait towards the trait displayed by the unpalatable *model* species. However, trait similarity between species generates fitness costs of reproductive interference paid by females from the *focal* species (McPeck & Gavrillets, 2006; Yamaguchi & Iwasa, 2013). We assume that a mating between individuals from the *focal* and the *model* species never produce any viable hybrid. We also consider constraints limiting mimicry promoting the ancestral trait value in the *focal* species, by assuming selection promoting the ancestral trait value t_a . Using a weak selection approximation (Barton & Turelli, 1991; Kirkpatrick *et al.*, 2002), we obtain equations describing the evolution of the mean trait and preference values. We then use numerical analyses to investigate (1) the role of reproductive interference in FLM and (2) the effect of the level of unpalatability in the *focal* species on the emergence of FLM.

Model

We consider a single *focal* species living in sympatry with a defended species displaying a fixed warning trait (referred to as the *model* species hereafter). Within the *model* species, all individuals display the same warning trait. We investigate the evolution of the warning trait expressed in the *focal* species, influenced by both (1) predators behaviour promoting mimicry towards the *model* species and (2) mate choice exerted by females on the trait expressed by males. We assume that female is the choosy sex, implying an asymmetry in the selection pressure exerted on male and female traits, potentially favouring the emergence of a sexual dimorphism. We thus study the traits t_m and t_f expressed in males and females respectively, as well as the mate preference expressed by females towards males displaying trait value p_f . In contrast, both males and females of the *model* species display traits close to the mean value \bar{t}' , assumed to be fixed. Individuals of the *focal* species then benefit from increased survival when they display a trait similar to the trait expressed in the *model* species (\bar{t}'), because of the learning behaviour of predators. This resemblance towards the *model* species then induces costs for individuals from the *focal* species, caused by reproductive interference. These reproductive interference costs depend on the discrimination capacities and mate preferences of females and on the phenotypic distances between (1) the traits displayed by males from the *focal* species and (2) the traits expressed in males from the *model* species.

We assume that the traits and preference in the *focal* species are quantitative traits, with an autosomal, polygenic basis with additive effects (Iwasa *et al.*, 1991). We assume that the distribution of additive effects at each locus is a multivariate Gaussian (Lande & Arnold, 1985). We consider discrete and non-overlapping generations. Within each generation, natural selection acting on survival and sexual selection acting on reproductive success occur. Natural selection acting on an individual depends on the trait t expressed. We note $W_{ns}^{\sigma}(t_m)$ and $W_{ns}^{\varphi}(t_f)$ (defined after in equations (4.6) and (4.7)) the fitness components due to natural selection acting on a male of trait t_m and a female of trait t_f respectively. To compute the

fitness component due to reproduction, we then note $W_r(t_m, p_f)$ (defined after in equation (4.21)) the contribution of a mating between a male with trait t_m and a female with preference p_f to the next generation. This quantity depends on (1) female mating preference, (2) male trait and (3) reproductive interference with the *model* species. The fitness of a mated pair of a male with trait t_m and a female with trait t_f and preference p_f is given by:

$$W(t_m, t_f, p_f) = W_{ns}^{\sigma}(t_m)W_r(t_m, p_f)W_{ns}^{\varphi}(t_f). \quad (4.1)$$

We assume that the variance of traits and preference is small relative to the curvature of the fitness function, which is a weak selection assumption (Iwasa *et al.*, 1991; Pomiankowski & Iwasa, 1993). Using the Price's theorem (Rice, 2004), we can approximate the change in the mean values of traits \bar{t}_m, \bar{t}_f and preference \bar{p}_f in the *focal* species after the natural and sexual selection respectively by:

$$\begin{pmatrix} \Delta \bar{t}_m \\ \Delta \bar{t}_f \\ \Delta \bar{p}_f \end{pmatrix} = \frac{1}{2} \begin{pmatrix} G_{t_m t_m} & G_{t_m t_f} & G_{t_m p_f} \\ G_{t_m t_f} & G_{t_f t_f} & G_{t_f p_f} \\ G_{t_m p_f} & G_{t_f p_f} & G_{p_f p_f} \end{pmatrix} \begin{pmatrix} \beta_{t_m} \\ \beta_{t_f} \\ \beta_{p_f} \end{pmatrix}, \quad (4.2)$$

where for $i \in \{t_m, t_f, p_f\}$, G_{ii} is the genetic variance of i and for $i, j \in \{t_m, t_f, p_f\}$ with $i \neq j$ G_{ij} , is the genetic covariance between i and j and with

$$\begin{pmatrix} \beta_{t_m} \\ \beta_{t_f} \\ \beta_{p_f} \end{pmatrix} = \begin{pmatrix} \frac{d}{dt_m} \log(W(t_m, t_f, p_f)) \\ \frac{d}{dt_f} \log(W(t_m, t_f, p_f)) \\ \frac{d}{dp_f} \log(W(t_m, t_f, p_f)) \end{pmatrix} \Bigg|_{(t_m, t_f, p_f) = (\bar{t}_m, \bar{t}_f, \bar{p}_f)}, \quad (4.3)$$

being the selection vector describing the effect of natural and sexual selection on mean traits and preference (see Appendix 1).

Under the weak selection assumption, genetic correlations generated by selection and non-random mating quickly reach equilibrium (Nagylaki, 1993) and can thus be approximated by their equilibrium values.

Following (Iwasa *et al.*, 1991), we assume that for $i \in \{t_m, t_f, p_f\}$, G_{ii} is a positive

constant maintained by an equilibrium between selection and recurrent mutations. We assume $G_{t_m t_f}$ to be constant: because neither selection nor nonrandom mating generate association between t_m and t_f this quantity depends only on the genetic architecture coding for traits expressed in males and females. For example $G_{t_m t_f} = 0$ would describe a situation where t_m and t_f are controlled by different sets of loci. Non-null value of $G_{t_m t_f}$ would mean that t_m and t_f have (at least partially) a common genetic basis.

We assume that traits t_m and t_f have different genetic bases than preference p_f . Thus only nonrandom mating generates genetic association between t_m and p_f . Under weak selection assumption $G_{t_m p_f}$ is assumed to be at equilibrium. This quantity is given by (see Appendix 2):

$$G_{t_m p_f} = a G_{t_m t_m} G_{p_f p_f}, \quad (4.4)$$

where a quantifies how frequently females reject males displaying non-preferred trait (see hereafter).

Because neither selection nor nonrandom mating generate association between t_f and p_f , following equation (4a) in Lande & Arnold (1985), we have

$$G_{t_f p_f} = \frac{G_{t_m t_f} G_{t_m p_f}}{G_{t_m t_m}}. \quad (4.5)$$

Ancestral trait value t_a

To investigate the effect of reproductive interference on the evolution of sexual dimorphism, we study the evolution of male and female traits (t_m and t_f) in the *focal* species, from an ancestral trait value initially shared between sexes (t_a). This ancestral trait value t_a represents the optimal trait value in the *focal* species, without interaction with the *model* species. This optimal value is assumed to be shaped by developmental as well as selective constraints, specific to the *focal* species. The natural selection exerted on males and females then depends on (1) departure from the ancestral trait value t_a , inducing a selective cost s , as well as

(2) protection against predators brought by mimicry, captured by the term W_{pred}^{σ} and W_{pred}^{φ} for males and females respectively. It is thus given by:

$$W_{ns}^{\sigma}(t_m) = W_{pred}^{\sigma}(t_m) \exp[-s(t_m - t_a)^2], \quad (4.6)$$

$$W_{ns}^{\varphi}(t_f) = W_{pred}^{\varphi}(t_f) \exp[-s(t_f - t_a)^2]. \quad (4.7)$$

We assume s to be of order ε , with ε small, therefore enabling to apply the weak selection assumption.

Predation pressure exerted on warning trait

Predators exert selection on individual trait promoting resemblance to the *model* species, resulting in an effect on fitness W_{pred} . Müllerian mimicry indeed generates positive density-dependent selection (Benson, 1972; Mallet & Barton, 1989; Chouteau *et al.*, 2016), due to predators learning. The density-dependence is modulated by the individual defence level λ , shaping predator deterrence: the higher the defence, the higher the defended individual contributes to the learning of predators. We note λ' the defence level of an individual in the *model* species. We assume that harmless individuals ($\lambda = 0$) neither contribute to predators learning, nor impair it. The protection gained against predators then depends on the level of resemblance (as perceived by predators) among defended prey only, and on the number of defended individuals sharing the same signal. We note N and N' the densities of individuals in the *focal* species and in the *model* species, respectively, and we assume a balanced sex ratio. The level of protection gained by an individual with trait t because of resemblance with other individuals is given by:

$$\begin{aligned}
\mathcal{D}(t) = & \underbrace{\int_{\tau_m} \lambda \frac{N}{2} f^{\sigma}(\tau_m) \exp[-b(t - \tau_m)^2] d\tau_m}_{\text{protection gained by resemblance with males of the focal species}} + \underbrace{\int_{\tau_f} \lambda \frac{N}{2} f^{\varphi}(\tau_f) \exp[-b(t - \tau_f)^2] d\tau_f}_{\text{protection gained by resemblance with females of the focal species}} \\
& + \underbrace{\int_{t'} \lambda' N' g(t') \exp[-b(t - t')^2] dt'}_{\text{protection gained by resemblance with individuals of the model species}}, \tag{4.8}
\end{aligned}$$

where $\exp[-b(t - \tau)^2]$ describes how much predators perceive the trait values t and τ as similar. The predator discrimination coefficient b thus quantifies how much predators discriminate different trait values displayed by prey. f^{σ} , f^{φ} and g are the distribution of traits in males and females of the *focal* species and in the *model* species respectively.

Because we assume that traits variance is small relative to the curvature of the fitness function within both the *focal* and the *model* species we can approximate (4.8) by (see Appendix 3):

$$\mathcal{D}(t) \approx \lambda \frac{N}{2} \exp[-b(t - \bar{t}_m)^2] + \lambda \frac{N}{2} \exp[-b(t - \bar{t}_f)^2] + \lambda' N' \exp[-b(t - \bar{t}')^2]. \tag{4.9}$$

Because males and females can display different traits, the protection brought by mimicry might differ between sexes. Moreover, because males and females may have different behaviours and morphologies the strength of predation pressure can also vary between sexes. We note $d_m, d_f \in (0, 1)$ the basic predation rates for males and females respectively. We assume these parameters to be of order ε , with ε small. The impacts of predation on the fitness of a male and a female displaying the trait value t_m and t_f are given by:

$$W_{pred}^{\sigma}(t_m) = \exp\left\{\frac{-d_m}{1 + \mathcal{D}(t_m)}\right\} \quad \text{and} \quad W_{pred}^{\varphi}(t_f) = \exp\left\{\frac{-d_f}{1 + \mathcal{D}(t_f)}\right\}. \tag{4.10}$$

Mating success modulating the evolution of female preference and male trait

The evolution of trait and preference also depends on the contribution to the next generation of crosses between males with trait t_m and females with preference p_f , $W_r(t_m, p_f)$. Because predators behaviour favours mimicry between sympatric species, substantial reproductive interference may occur in the *focal* species, because of erroneous species recognition during mate searching. Such reproductive interference depends on (1) female preference towards the warning trait displayed by males, (2) the distribution of this warning trait in males from both the *focal* and the *model* species and (3) the capacity of females to recognise conspecific males using alternative cues (pheromones for example). In the model, the investment of females in interspecific mating interaction is captured by the parameter $c_{RI} \in [0, 1]$. This cost of reproductive interference incurred to the females can be reduced when female choice is also based on alternative cues differing between mimetic species. We assume c_{RI} to be of order ε , with ε small. When a female with preference p_f encounters a male displaying the trait value t_m , the mating occurs with probability

$$\exp[-a(p_f - t_m)^2], \quad (4.11)$$

when the encountered male is a conspecific or

$$c_{RI} \exp[-a(p_f - t_m)^2], \quad (4.12)$$

when the encountered male belongs to the *model* species. Female choosiness a , assumed constant among females, quantifies how frequently females reject males displaying a non-preferred trait.

During an encounter, the probability that a female with preference p_f accepts a

conspecific male is then given by (Otto *et al.*, 2008):

$$T(p_f) = \int_{t_m} \overbrace{\frac{N}{N+N'} f^\sigma(t_m)}^{\text{probability of encountering a conspecific male with trait } t_m} \overbrace{\exp[-a(p_f - t_m)^2]}^{\text{probability of accepting a conspecific male with trait } t_m} dt_m. \quad (4.13)$$

A female with preference p_f may also accept an heterospecific male with probability:

$$T_{RI}(p_f) = \int_{t'} \overbrace{\frac{N'}{N+N'} g(t')}^{\text{probability of encountering an heterospecific male with trait } t'} \overbrace{c_{RI} \exp[-a(p_f - t')^2]}^{\text{probability of accepting an heterospecific male with trait } t'} dt'. \quad (4.14)$$

Because the variance of traits within both the *focal* and the *model* species is small relative to the curvature of fitness function we have the following approximations:

$$T(p_f) \approx \frac{N}{N+N'} \exp[-a(p_f - \bar{t}_m)^2], \quad (4.15)$$

and

$$T_{RI}(p_f) \approx \frac{N'}{N+N'} c_{RI} \exp[-a(p_f - \bar{t}')^2]. \quad (4.16)$$

We assume that heterospecific crosses never produce any viable offspring, and that females engaged in such matings cannot recover this fitness loss (see Figure 4.1). Only crosses between conspecifics produce viable offspring (see Figure 4.1). Knowing that a female with preference p_f has mated with a conspecific male, the probability that this male displays the trait t_m is given by:

$$\phi(p_f, t_m) = \frac{\exp[-a(p_f - t_m)^2] f^\sigma(t_m)}{\int_{\tau_m} \exp[-a(p_f - \tau_m)^2] f^\sigma(\tau_m) d\tau_m}. \quad (4.17)$$

Using again the assumption that the trait distribution has a low variance, this can

be approximated by

$$\phi(p_f, t_m) \approx \frac{\exp[-a(p_f - t_m)^2] f^{\sigma}(t_m)}{\exp[-a(p_f - \bar{t}_m)^2]}. \quad (4.18)$$

Considering that females only encounter one male, the proportion of crosses between a female with preference p_f and a conspecific male with trait t_m would be

$$\mathcal{P}^1(p_f, t_m) = h(p_f) T(p_f) \frac{\exp[-a(p_f - t_m)^2] f^{\sigma}(t_m)}{\exp[-a(p_f - \bar{t}_m)^2]}, \quad (4.19)$$

where h is the distribution of preferences in the population.

However, we assume that females refusing a mating opportunity can encounter another male with probability $1 - c$ (see Figure 4.1). We interpret $c \in [0, 1]$ as the cost of choosiness (similar to the coefficient c_r in (Otto *et al.*, 2008)). The proportion of matings between a female with preference p_f and a conspecific male with trait t_m is thus given by

$$\begin{aligned} \mathcal{P}(p_f, t_m) &= \sum_{i=0}^{+\infty} ((1 - T(p_f) - T_{RI}(p_f)) (1 - c))^i \mathcal{P}^1(p_f, t_m) \\ &= \frac{\mathcal{P}^1(p_f, t_m)}{c + (1 - c)(T(p_f) + T_{RI}(p_f))}, \end{aligned} \quad (4.20)$$

where $((1 - T(p_f) - T_{RI}(p_f)) (1 - c))^i$ is the probability that a female with preference p_f rejects the i males she first encounters and then encounters an $(i + 1)$ -th male.

The contribution to the next generation of a mating between a male with trait t_m and a female with preference p_f , $W_r(t_m, p_f)$ is thus given by (see Figure 4.1)

$$W_r(t_m, p_f) = \frac{T(p_f)}{c + (1 - c)(T(p_f) + T_{RI}(p_f))} \times \frac{\exp[-a(p_f - t_m)^2]}{\exp[-a(p_f - \bar{t}_m)^2]} \quad (4.21)$$

All variables and parameters used in the model are summed up in Table 4.1.

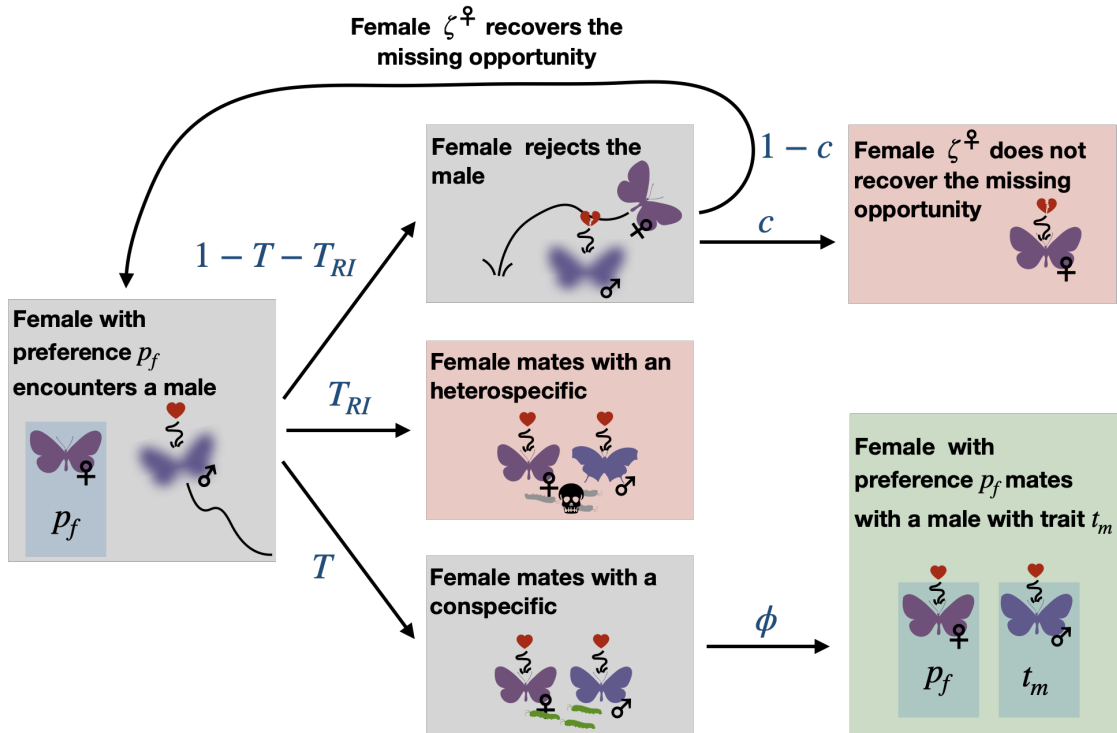


Fig. 4.1: **Computation of the contribution to the next generation of a mating.** During an encounter, a female expresses her preference towards the warning trait displayed by the male and other cues that may differ between conspecific and heterospecific males. A female accepts a conspecific (resp. heterospecific) male with probability $T(p_f)$ (resp. $T_{RI}(p_f)$) (see Equation (4.13) (resp. (4.14))). A mating with an heterospecific male produces no viable offspring and the female cannot mate anymore. When the female mates with a conspecific of trait t_m , the cross occurs with probability $\phi(p_f, t_m)$. During an encounter the female may refuse a mating opportunity with a male displaying a trait value t_m distant from her preference p_f and can subsequently encounter other males with probability $1 - c$. Alternatively, she may not recover the fitness loss with probability c , resulting in an opportunity cost. The contribution to the next generation of a mating between a male with trait t_m and a female with preference p_f is thus given by $W_r(t_m, p_f)$ (see Equation (4.21)). Expressions in blue represent the probabilities associated with each arrow. In red, the female does not produce any offspring. In green, the mating between a male with trait t_m and a female with preference p_f happens and produces progeny.

Abbreviation	Description
\bar{t}_m/\bar{t}_f	Mean trait value displayed in the <i>focal</i> species by males and females respectively
\bar{p}_f	Mean female preference value in the <i>focal</i> species
G	matrix of genetic covariance
a	Female choosiness in the <i>focal</i> species
s	Strength of developmental constraints in the <i>focal</i> species
t_a	Ancestral trait favoured by developmental constraints in the <i>focal</i> species
t'	Trait displayed in the <i>model</i> species
d_m/d_f	Basic predation rate in males and females respectively
b	Predator discrimination
λ/λ'	Defence level of individuals of the <i>focal</i> and <i>model</i> species respectively
N/N'	Density of the <i>focal</i> and <i>model</i> species respectively
c_{RI}	Strength of reproductive interference
c	Cost of choosiness

Table 4.1: Description of variables and parameters used in the model.

Model exploration.

We assume that the *focal* species is ancestrally not in contact with the *model* species, and therefore the initial mean trait values displayed by males and females are equal to the optimal trait t_a . We also assume that the mean female preference value is initially equal to the mean trait value displayed by males. At the initial time, we assume that the *focal* species enters in contact with the *model* species. The dynamics of traits and preference values then follow Equation (4.2). In Appendix 4, we explore two alternative scenarios: where the *focal* and the *model* species (1) ancestrally share common predators promoting mimicry before entering sexually in contact or (2) ancestrally interact sexually before sharing a common predator promoting mimicry.

Numerical simulations of the quantitative model

We use numerical simulations to estimate the traits and preference values at equilibrium $(\bar{t}_m^*, \bar{t}_f^*, \bar{p}_f^*)$. Numerically, we consider that the traits and preference are at equilibrium when

$$\left\| \begin{pmatrix} \Delta \bar{t}_m \\ \Delta \bar{t}_f \\ \Delta \bar{p}_f \end{pmatrix} \right\|_2 < 3 \times 10^{-11}. \quad (4.22)$$

Individual-centred simulations

We also run individual-centred simulations with explicit genetic architecture to study the evolution of FLM with strong selection, as well as with high and fluctuating genetic variance of traits and preference. We assume two genetic architectures in an haploid population:

- Independent genetic basis of male and female trait: we assume three loci T_m , T_f and P_f , coding respectively for male trait, female trait and preference. We assume a large number of alleles at each locus, where each allele is associated with a real number, corresponding to the value of the trait or of the preference. We assume recombination rate between each loci $r_{T_m T_f}$ and $r_{T_f P_f}$.
- Partially common genetic basis of male and female trait: we assume four loci T_1 , T_2 , T_3 and P_f . Locus T_2 controls the trait variations shared by males and females and loci T_1 and T_2 (resp. T_2 and T_3) codes for specific male (resp. female) trait value with additive effect. P_f codes for female preference value. We assume a large number of alleles at each locus, where each allele is associated with a real number. We assume recombination rate between each loci $r_{T_1 T_2}$, $r_{T_2 T_3}$ and $r_{T_3 P_f}$.

We assume non-overlapping generations and constant population size. At each generation, we first model the effect of natural selection. The survival of an individual follows a Bernoulli distribution, where the probability of surviving is given by the fitness component due to natural selection (see Equations (4.6) and (4.6)).

Second, females and males meet uniformly at random. Female acceptance of a potential male follows a Bernoulli distribution, where the acceptance probability is given by Equation (4.11) (resp. (4.12)) if the potential male is a conspecific (resp. heterospecific). Females pay a fertility cost when attempting mating with an heterospecific male. Females may also pay a fertility cost when refusing a mating opportunity, depending on cost of choosiness c .

Third, a mutation appears at each allele in the new generation. Each mutation follows a normal distribution centred on the value associated with the allele. We model the mutation effect across all loci using a constant standard deviation μ . We also assume an initial genetic variance of trait and preference G_0 , and no genetic covariance. We run individual-centred simulations across 10,000 generations. Final trait and preference values are given by the mean value across the 1,000 last generations. We run replicates for each parameter value and we provide the number of replicate runs in the caption of each figure.

Scripts are available online at github.com/Ludovic-Maisonneuve/evo-flm.

Comparing alternative mechanisms inducing female-limited mimicry

First, we compare the evolutionary outcomes when assuming two alternative mechanisms generating FLM in an harmless species ($\lambda = 0$): (1) sexual selection generated by reproductive interference (c_{RI} and $a > 0$) and (2) sexually contrasted predation ($d_f > d_m$). We thus compute the equilibrium traits and preference (\bar{t}_m^* , \bar{t}_f^* , \bar{p}_f^*) for different strengths of reproductive interference ($c_{RI} \in [0, 0.1]$) or different basic predation rate sexual ratios between males and females $d_m/d_f \in [0, 1]$. Note that the two mechanisms are not mutually exclusive in natural populations. However here we investigate them separately to identify the specific evolutionary trajectories they generate. We then determine the range of key parameters enabling the evolution of FLM, under each mechanism assumed. We specifically follow the evolution of sexual dimorphism generated by each mechanism by comparing the level of sexual dimorphism at equilibrium defined by $|\bar{t}_m^* - \bar{t}_f^*|$.

Differential divergence from ancestral traits in male and female causing sexual dimorphism

To investigate whether the evolution of sexual dimorphism stems from increased divergence of traits from the ancestral states of one of the two sexes, we then

compute the sexual bias in phenotypic divergence defined by

$$\phi = |\bar{t}_m^* - t_a| - |\bar{t}_f^* - t_a|.$$

When $\phi < 0$ we have $|\bar{t}_f^* - t_a| > |\bar{t}_m^* - t_a|$ thus the trait diverged more in females than in males (see an illustration in Figure 4.2(a) and Figure 4.2(b)). By contrast $\phi > 0$ indicates that the trait diverged more in males than in females (see an illustration in Figure 4.2(c)). We compare this sexual bias in phenotypic divergence under the two hypothetical mechanisms of FLM, to determine whether this criterium could be used to infer the actual evolutionary pressures involved in the emergence of FLM in natural populations.

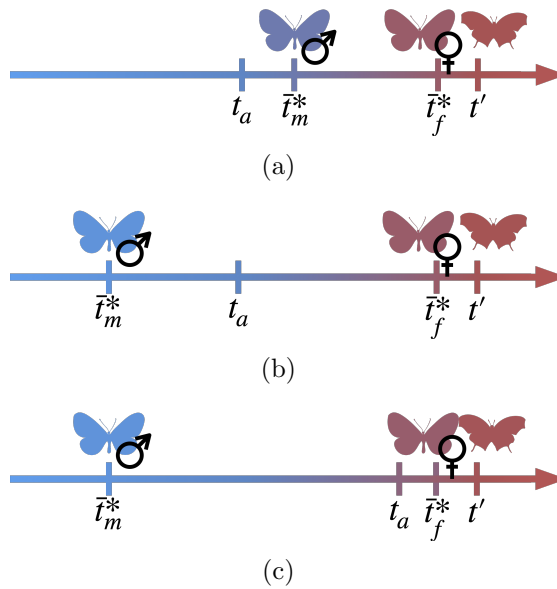


Fig. 4.2: **Illustration of the three main outcomes:** (a) male trait value in the *focal* species gets closer to the value displayed in the *model* species t' , (b) male trait value in the *focal* species diverges away from the value displayed in the *model* species t' , (c) when the ancestral and the mimetic trait are close and male trait value in the *focal* species diverges away from the value displayed in the *model* species t' then the phenotypic distance with the ancestral trait is higher in males than in females.

We first study the values of sexual bias in phenotypic divergence when reproductive interference causes FLM ($c_{RI} = 0.01$), using numerical simulations. We investigate

the effect of two key parameters: female choosiness a modulating cost of reproductive interference and the phenotypic distance between the ancestral trait t_a and the mimetic trait t' . To investigate the impact of the phenotypic distance between the ancestral and the mimetic traits, we fixed the mimetic trait value to 1 ($t' = 1$) and vary the ancestral trait value ($t_a \in [0, 1]$) (see illustration in Figures 4.2(b) and 4.2(c)). We then study the sexual bias in phenotypic divergence when FLM stems from sexually contrasted predation ($d_f > d_m$), by deriving analytical results standing for all parameters value (see Appendix 5).

Investigating the impact of the defence level on the evolution of female-limited mimicry

Because FLM is usually reported for Batesian mimics, we then investigate the impact of the defence level ($\lambda \in [0, 0.1]$) on equilibrium traits (\bar{t}_m^* , \bar{t}_f^*) and the level of sexual dimorphism ($\bar{t}_m^* - \bar{t}_f^*$). Because males and females in the *focal* species can display different traits, the level of protection gained by individuals of one sex through mimicry depends on males and females resemblance to the *model* species but also on the density of individuals of that sex within the *focal* species, modulated by the individual level of defence in the *focal* species (λ). When males from the *focal* species are non-mimetic, their defence level is given by the individual level of defence λ and the density of males $N/2$. To investigate the impact of defence level on the emergence of FLM, we thus explore not only the effect of the individual defence level λ but also of the density of the *focal* species ($N \in [0, 20]$).

The effects of all explored parameters and evolutionary forces on the evolution of FLM are summed up in Figure 4.3.

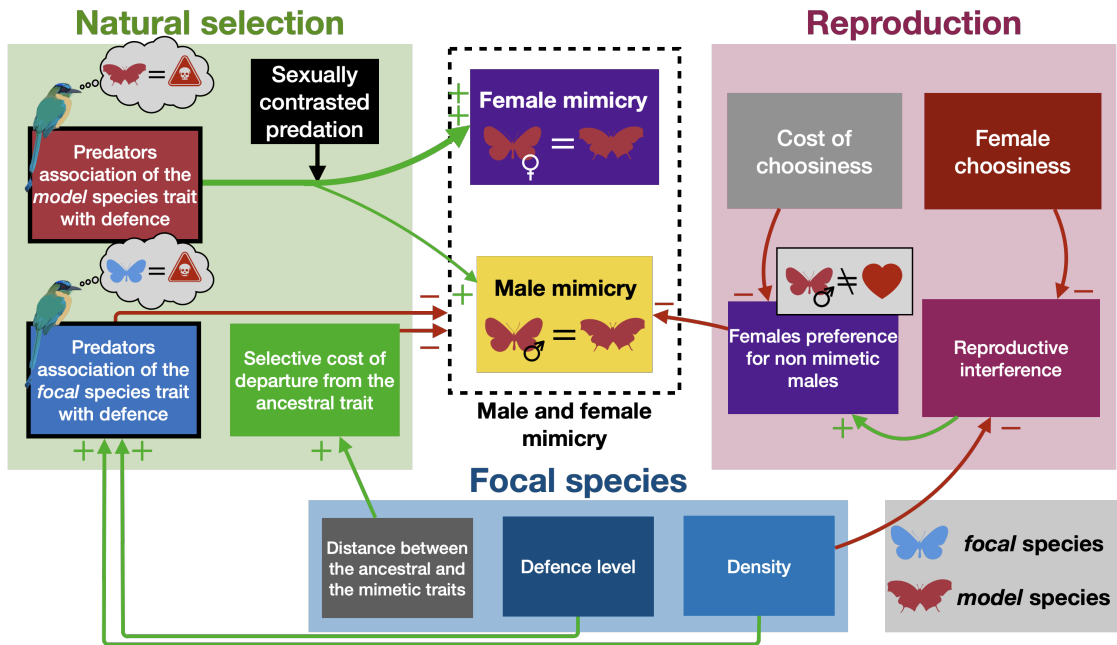


Fig. 4.3: Summary of the impact of selective forces and parameters on the evolution of female-limited mimicry. Green and red arrows represent the positive and negative impact respectively.

Results

Reproductive interference promotes female-limited mimicry in palatable species

We first test whether reproductive interference can generate FLM in a harmless species ($\lambda = 0$). We thus investigate the impact of the strength of reproductive interference (c_{RI}) on the evolution of male trait (\bar{t}_m^*), female trait and preference (\bar{t}_f^* and \bar{p}_f^*), for different levels of female choosiness (a) modulating the costs generated by the strength of reproductive interference (Figure 4.4(a)). Without reproductive interference ($c_{RI} = 0$), both males and females in the *focal* species are mimetic at equilibrium and the sexual dimorphism therefore does not emerge (Figure 4.4(a)). By contrast, when assuming reproductive interference ($c_{RI} > 0$), FLM evolves in the *focal* species (Figure 4.4(a), see temporal dynamics in Figure A4.5(a)). Repro-

ductive interference promotes a greater distance between final female preference \bar{p}_f^* and the trait of the *model* species t' . Such female preference for non-mimetic males reduces costly sexual interactions with heterospecific males of the *model* species and generates sexual selection on male trait, inhibiting mimicry in males. Reproductive interference also promotes FLM in alternative scenarios when the *focal* and the *model* species (1) ancestrally share common predators promoting mimicry before entering sexually in contact or (2) ancestrally interact sexually before sharing a common predator promoting mimicry (see Appendix 4). Because FLM strongly depends on the evolution of female preference for potentially scarce non-mimetic males, it emerges only when the cost of choosiness (c) is low (see Appendix 7 for more details). FLM also evolves only when male and female traits have at least partially different genetic basis, allowing divergent evolution between sexes. The genetic covariance between male and female trait $G_{t_m t_f}$ then only impacts the time to reach the equilibrium (see Appendix 8 for more details).

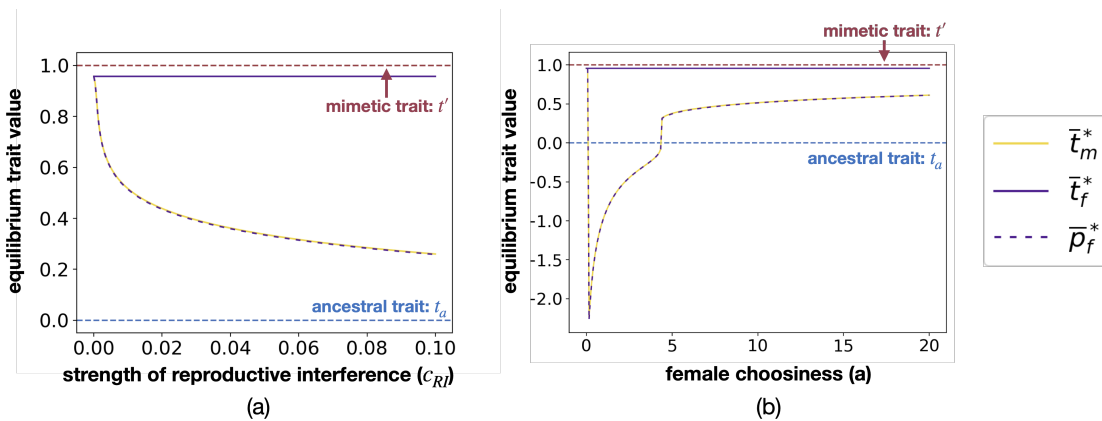


Fig. 4.4: Influence of (a) the strength of reproductive interference c_{RI} and (b) female choosiness a on the equilibrium values of male trait \bar{t}_m^* (yellow solid line), female trait \bar{t}_f^* (purple solid line) and female preference \bar{p}_f^* (purple dashed line). By default we assume: $G_{t_m} = G_{t_f} = G_{p_f} = 0.01$, $G_{t_m t_f} = 0.001$, $c_{RI} = 0.01$, $c = 0.1$, $a = 10$, $b = 5$, $d_m = d_f = 0.05$, $\lambda = 0$, $N = 100$, $\lambda' = 0.01$, $N' = 200$, $s = 0.0025$, $t_a = 0$, $\bar{t}' = 1$.

We also investigate the impact of female choosiness (a) (modulating the stringency of sexual selection and cost of reproductive interference) on FLM, when there is reproductive interference ($c_{RI} > 0$) (Figure 4.4(b)). The relationship between the

final male trait value and the parameter a is sometimes discontinuous because for close value of parameters, the evolutionary dynamics can take different paths. When a is close to 0, both males and females become mimetic to the *model* species (Figure 4.4(b)). In this case, non-choosy females tend to accept almost all males, despite their preference p_f . Thus selection on female preference p_f is low because a change on preference hardly changes the mating behaviour and the resulting cost of reproductive interference. When a is higher than 0 and approximately lower than 5, selection due to reproductive interference on preference is important and reproductive interference promotes FLM. Furthermore, our results show that sexual selection does not only inhibit mimicry in males but may further promote divergence away from the ancestral trait t_a (Figure 4.4(b), see Figure 4.2(b) for an illustration and Figure A4.5(b) for temporal dynamics). Such divergence from the ancestral trait in males does not occur when female choosiness is higher ($a \gtrsim 5$ in Figure 4.4(b) see Figure 4.2(a) for an illustration): when females are more picky, a small difference between female preference and the mimetic trait sufficiently reduces the cost of reproductive interference (Figure 4.4(b)). All results described in this section are confirmed in individual-centred simulations assuming simple genetic architecture of traits and preference (Figures A4.10 and A4.11), highlighting that the weak selection, constant and low genetic variance assumptions does not preclude obtaining relevant analytical predictions.

Sexually contrasted predation promotes female-limited mimicry in palatable species

Higher predation pressure acting on females has been proposed to explain FLM. Here we investigate the impact of the ratio of basic predation rate on males and females (d_m/d_f) on the evolution on FLM (Figure 4.5(a)) in case without reproductive interference and preference ($c_{RI} = 0, a = 0$). When predation pressures are largely lower in males than in females (*i.e.* $d_m/d_f \lesssim 0.2$), sexually contrasted predation promotes FLM (Figure 4.5(a), and see temporal dynamics in Figure A4.5(c)). Limited predation pressure in males implies low advantage to mimicry

that is overcome by developmental constraints. By contrast, predation pressure is higher on females, resulting in a greater advantage to mimicry that overcomes costs of departure from ancestral trait value. However, when the predation ratio increases (*i.e.* $d_m/d_f \gtrsim 0.2$), sexual dimorphism is low, because advantage to mimicry in males becomes greater as compared to costs generated by developmental constraints (Figure 4.5(a)). When males and females suffer from similar predation pressure (*i.e.* $d_m/d_f = 1$), both sexes become mimetic (Figure 4.5(a)).

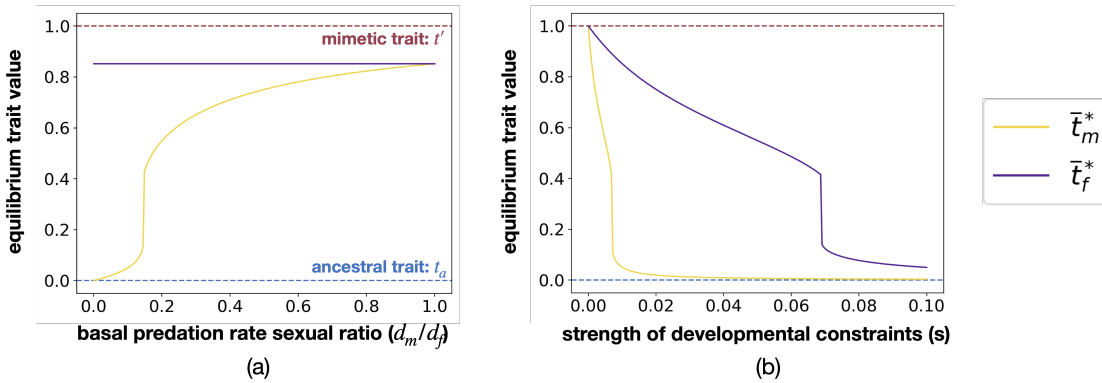


Fig. 4.5: Influence of (a) the ratio of basic predation rate on males and females d_m/d_f and (b) the strength of developmental constraints s on the equilibrium values of male trait \bar{t}_m^* (yellow solid line), and female trait \bar{t}_f^* (purple solid line). By default we assume: $G_{t_m} = G_{t_f} = G_{p_f} = 0.01$, $G_{t_m t_f} = 0.001$, $c_{RI} = 0$, $c = 0$, $a = 0$, $b = 5$, $d_m = 0.005$, $d_f = 0.05$, $\lambda = 0$, $N = 100$, $\lambda' = 0.01$, $N' = 200$, $s = 0.01$, $t_a = 0$, $\bar{t}' = 1$.

Because developmental constraints are a major factor limiting mimicry, we then investigate the impact of the strength of developmental constraints (s) on FLM generated by a sexually contrasted predation ($d_m/d_f = 0.1$). When there is no developmental constraints ($s = 0$), FLM does not evolve, because males become mimetic even if they suffer for low predation (Figure 4.5(b)). By contrast, in individual-centred simulations, male trait becomes highly variable due to a lack of selection, whereas female trait under strong predation pressure, has a low variance (Figure A4.13). Relaxed selection on males may allow trait values leading to poor mimicry to emerge in males, while the stronger selection on females favours their accurate mimicry. This sexually-different selection regime thus increases sexual

dimorphism. However, higher developmental constraints ($0.1 \lesssim s \lesssim 0.7$) limit mimicry in males, but not in females because of sexually contrasted predation (see previous paragraph) (Figure 4.5(b)). Important developmental constraints ($s \gtrsim 0.7$) overcome the advantages provided by mimicry in both sexes, and prevent the evolution of sexual dimorphism (Figure 4.5(b)). Beside the case previously mentioned, all results shown in this section still hold in our individual-centred simulations (Figures A4.12 and A4.13)

Different hypothetical causes of female-limited mimicry lead to different predictions

Here, we use our mathematical model to compare the effect of (1) reproductive interference and (2) sexually contrasted predation on the evolution of FLM. We specifically investigate in which sex the trait evolves away from the ancestral trait, depending on the selective mechanism causing FLM.

First, we focus on the evolution of FLM caused by reproductive interference via sexual selection ($a > 0$ and $d_f = d_m$). We specifically estimate how (1) the distance between the ancestral trait and the mimetic trait $|t_a - t'|$ and (2) the female choosiness a modulate sexual selection and shape the relative divergence of males and females from the ancestral trait value $|\bar{t}_m^* - t_a| - |\bar{t}_f^* - t_a|$. Figure 4.6 highlights that divergence from the ancestral trait can be stronger in males (yellow zone on figure 4.6(c)) or in females (purple zone on Figure 4.6(c)) depending on these parameters.

The evolution of female trait only depends on the distance between the ancestral trait t_a and the mimetic trait t' : because selection always promotes mimicry in females, divergence from the ancestral trait increases with the initial distance from the mimetic trait (Figure 4.6(b)). The level of mimicry in females slightly decreases with the ancestral level of mimicry because it increases the costs of developmental constraints. However, such costs are still overcome by the advantage of being mimetic. By contrast, the evolution of male trait depends on the interplay between

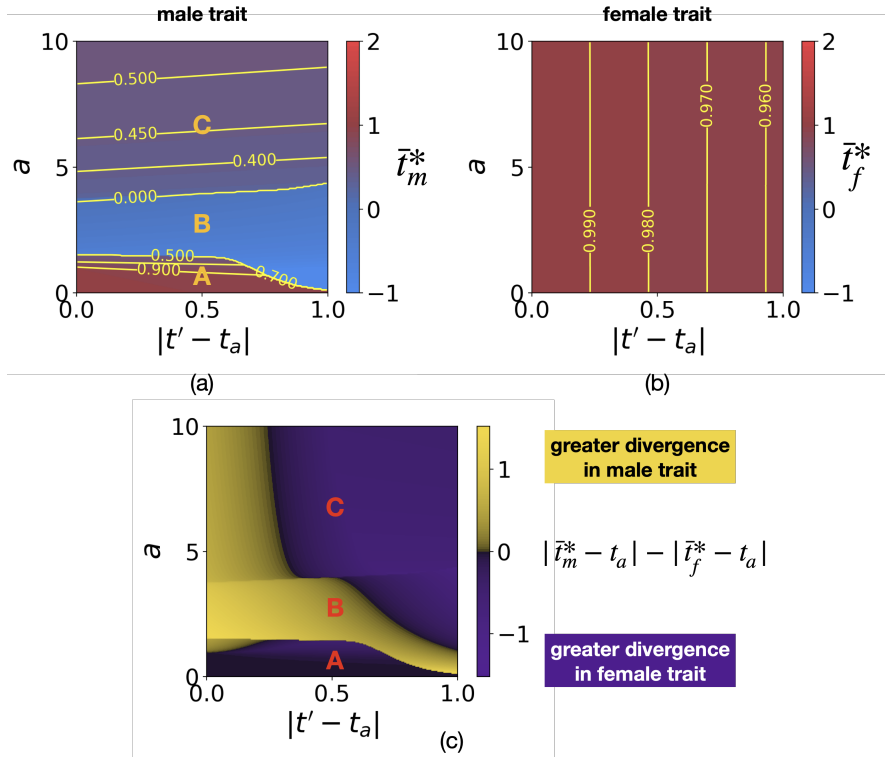


Fig. 4.6: **Influence of the distance between the ancestral and the mimetic traits $|t' - t_a|$ and of female choosiness a on (a) final male trait \bar{t}_m^* , (b) final female trait \bar{t}_f^* and (c) the difference between the level of divergence in males and females $|\bar{t}_m^* - t_a| - |\bar{t}_f^* - t_a|$.** Note that **Figure 4.6(c)** results from **Figures 4.6(a) and 4.6(b)**. Yellow lines indicate equal levels of trait value. We assume: $G_{t_m} = G_{t_f} = G_{p_f} = 0.01$, $G_{t_{mf}} = 0.001$, $c_{RI} = 0.01$, $c = 0.1$, $b = 5$, $d_m = d_f = 0.05$, $\lambda = 0$, $N = 100$, $\lambda' = 0.01$, $N' = 200$, $s = 0.0025$, $t' = 1$.

the sexual selection generated by female preferences and the ancestral level of mimicry (Figure 4.6(a)).

The relationship between the final male trait and the parameters is discontinuous as previously highlighted, leading to three zones within where male trait vary continuously. When female choosiness is low (zone A, $a \lesssim 1.8$), the selection caused by reproductive interference is mild: females are not very choosy and thus tend to accept almost all males despite their preference p_f , therefore relaxing selection on female preference, and favouring the evolution of mimetic trait in males. Mimicry is nevertheless more accurate in females than in males, and males

phenotype tends to stay closer to the ancestral trait value, and to display a so-called "imperfect" mimicry. When the ancestral level of mimicry is poor ($|t_a - t'| \sim 1$), the slight advantage in sexual selection can then overcome the advantage of imperfect mimicry, resulting to divergence in male trait, even for low values of female choosiness ($a \lesssim 1.8$).

However, when female choosiness has intermediate values ($1.8 \lesssim a \lesssim 4$, zone B), enhanced female choosiness increases selection due to reproductive interference and thus reduces mimicry in males. Nevertheless, when the distance between the ancestral and the mimetic trait is already large, divergence in male trait is limited, and the sexual dimorphism mainly stems from the evolution of mimicry in females. Using individual-centred simulations, we then show that stochastic variations may result in the divergence of male trait away from the ancestral trait, when the initial distance between the ancestral trait and the mimetic trait is low ($|t_a - t'| \simeq 0$), (see Figure A4.19).

Contrastingly, high levels of choosiness in females ($a \gtrsim 4$, zone C) promote the evolution of more mimetic males because even a slight difference between the female preference and the mimetic trait allows to reduce cost of reproductive interference. Male divergence is then observed only when the ancestral level of resemblance between the *focal* and the *model* species is very high (*i.e.* low $|t_a - t'|$), and therefore induced cost of reproductive interference, despite the high pickiness (*i.e.* high a) of females.

The evolution of FLM caused by reproductive interference therefore leads to different divergence patterns, including divergence of male phenotypes away from the ancestral trait value. In contrast when FLM is caused by sexually contrasted predation ($d_f > d_m$ and $a = 0$), sexual dimorphism always stems from the evolution of female phenotypes away from the ancestral trait, *i.e.* $|\bar{t}_f^* - t_a| > |\bar{t}_m^* - t_a|$ (see Appendix 5 and see Figure 4.2(a) for an illustration). Individual-centred simulations confirm this pattern, except when the distance between the ancestral trait and the mimetic trait is low ($|t_a - t'| \simeq 0$) (Figure A4.17). In this case, developmental constraints and predation promote the same trait value ($t_a \simeq t'$). The higher sta-

bilising selection in females, caused by a higher predation pressure, implies that female trait diverge less from the ancestral trait than males (Figure A4.19).

While both the reproductive interference and the sexually-contrasted predation may result in FLM, the evolutionary pathways causing the sexual dimorphism are strikingly different. These results are generally maintained when relaxing the weak selection, constant and low genetic variance assumptions (see Appendix 11).

The evolution of FLM depends on defence level

We then investigate the impact of the individual defence level (λ) and the density (N) in the *focal* species on the evolution of sexual dimorphism, when FLM is generated either (1) by sexually contrasted predation (Figure 4.7) or (2) by reproductive interference via sexual selection (Figure 4.8).

Surprisingly, when FLM is caused by sexually-contrasted predation ($d_f > d_m$), the level of sexual dimorphism can either increase or decrease with defence levels in both males and females ($\lambda N/2$), depending on the strength of developmental constraints (Figure 4.7). In both sexes, the increase in defence levels indeed reduces selection favouring mimicry, while the developmental and selective constraints favour ancestral trait value. Great strength of developmental constraints ($s = 0.02$) then totally limits mimicry in males for every defence levels (Figure A4.21(a)). An increase in defence levels reduces mimicry in females (Figure A4.21(b)) but not in males that always displays the ancestral trait resulting in a decrease of the level of sexual dimorphism (Figure 4.7(b)). By contrast, low strength of developmental constraints ($s = 0.01$) allow the evolution of imperfect mimicry in males. However, the evolution of such mimicry in males is strongly impaired when defence level increases. In this range of mild levels of defence, mimicry is nevertheless advantageous in heavily-attacked females (Figure A4.20(b)), resulting in high level of sexual dimorphism (Figure 4.7(a)). However, when the defence level becomes very high, both males and females display the ancestral trait, and sexual dimorphism is no longer observed (Figures A4.20 and A4.21 at the top right). Because of the high

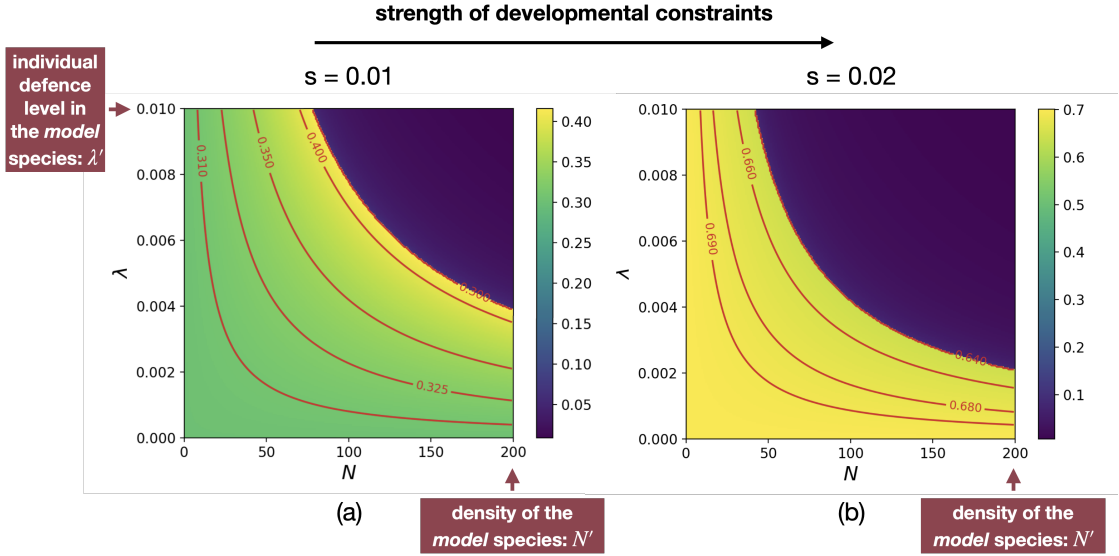


Fig. 4.7: Influence of the density N and of the individual defence level λ in the *focal* species on the equilibrium values of the level of sexual dimorphism ($|\bar{t}_m^* - \bar{t}_f^*|$) for different strength of developmental constraints ((a) $s = 0.01$ (b) $s = 0.02$) when female-limited mimicry is caused by sexually contrasted predation ($d_f > d_m$, $a = 0$). Red lines indicate equal levels of sexual dimorphism. We assume: $G_{t_m} = G_{t_f} = G_{p_f} = 0.01$, $G_{t_m t_f} = 0.001$, $c_{RI} = 0$, $c = 0$, $a = 0$, $b = 5$, $d_m = 0.01$, $d_f = 0.05$, $\lambda' = 0.01$, $N' = 200$, $t_a = 0$, $t' = 1$.

level of defence, individuals of both sexes gain sufficient protection from similarity with their conspecifics, relaxing selection promoting mimicry towards the *model* species. Individual-centred simulations provide the same patterns. Interestingly, the only discrepancy is observed for the effect of the density of the *focal* species when developmental constraints are low: in this case, the level sexual dimorphism no longer increases with with density of the *focal* species (see Appendix 13), contrary to what was observed in the deterministic model (A4.21(a)). Stochasticity of population mean male and female trait values that is likely to increase sexual dimorphism. The amplitude of this stochastic effect reduce with population density that decrease the level of sexual dimorphism because when traits evolves randomly it is likely to produce sexual dimorphism (see figure A4.27).

Similarly, when FLM is caused by reproductive interference ($c_{RI} > 0$) *via* sexual se-

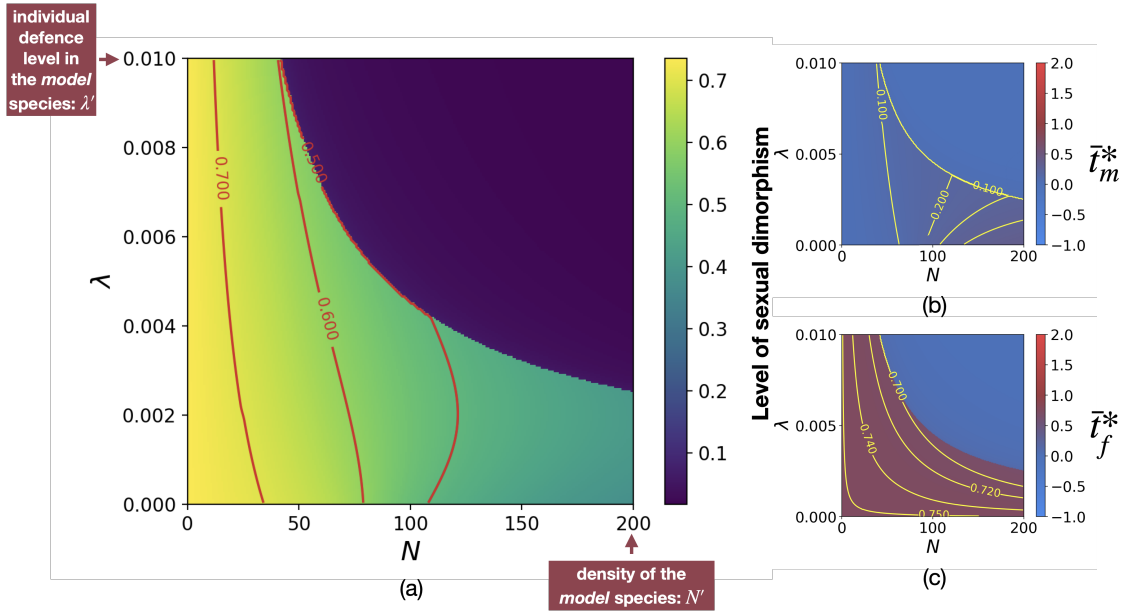


Fig. 4.8: Influence of the density N and of the individual defence level λ in the *focal* species on the equilibrium values of (a) the level of sexual dimorphism $|\bar{t}_m^* - \bar{t}_f^*|$, (b) male trait \bar{t}_m^* and (c) female trait \bar{t}_f^* when female-limited mimicry is generated by sexual selection caused by reproductive interference (c_{RI} , $a > 0$ and $d_f = d_m$). Red and yellow lines indicate equal levels of sexual dimorphism and trait value respectively. We assume: $G_{t_m} = G_{t_f} = G_{p_f} = 0.01$, $G_{t_m t_f} = 0.001$, $c_{RI} = 0.01$, $c = 0.1$, $a = 5$, $b = 5$, $d_m = d_f = 0.05$, $\lambda' = 0.01$, $N' = 200$, $s = 0.02$, $t_a = 0$, $t' = 1$.

lection, the level of sexual dimorphism can also either increase or decrease with the individual defence level λ depending on the strength of developmental constraints (Figures 4.8(a) and A4.22(a)). In contrast with predation differences between sexes, sexual selection induced by reproductive interference generates markedly higher sexual dimorphism for low values of density of the *focal* species ($N < \frac{N'}{4}$) (Figure 4.8(a)). The relative density of the *focal* and the *model* species indeed determines the probability that a female of the *focal* species encounters a conspecific rather than an heterospecific male and thus modulates the costs of reproductive interference. Therefore, when the density of the *focal* species N is low, costs of reproductive interference are great, generating higher selection promoting sexual dimorphism. The density of the *focal* species therefore impacts much more the

level of sexual dimorphism than the individual defence level λ .

Under both hypotheses explaining female limited-mimicry, when developmental constraints totally inhibit mimicry in males, sexual dimorphism decrease with the level of defence. Under the assumption of sexual selection generated by reproductive interference however, sexual dimorphism is higher when the *focal* species is rarer than the *model* species.

Under both selective hypotheses, mimicry toward the sympatric defended *model* species is no longer promoted in either sexes, when the level of defence within the *focal* species is high (Figures A4.20, A4.21 and 4.8(b)(c)) leading to sexual monomorphism. The distance between the ancestral and the mimetic traits $|t' - t_a|$ limits mimicry in both sexes (Figure A4.23) highlighting the important role of the initial advantage and disadvantage of mimicry. Using individual-centred simulations, we nevertheless observed that male and female trait can get closer to the mimetic trait by stochasticity, enabling mimicry to be promoted, when the level of defence within the *focal* species is high (Figures A4.24, A4.26 and A4.28).

Discussion

Ancestral levels of resemblance, sexually-contrasted divergences and the evolution of female-limited mimicry

Our model highlights that both (1) sexually contrasted predation and (2) female preference generated by reproductive interference can favour the evolution of FLM. By explicitly studying how these contrasted selective pressures influence the divergence of male and female trait from a common ancestral trait, our model sheds light on contrasted evolutionary pathways towards sexual dimorphism. Empirical studies based on the estimation of the level of divergence in male and female trait usually interpret elevated divergence in male trait as compared to female trait, as a signature of sexual selection, causing sexual dimorphism (van der Bijl *et al.*, 2020). Focusing on FLM in *Papilio* butterflies, Kunte (2008) shows that sexual

dimorphism is correlated with divergence in female trait, and concluded that FLM is caused by natural selection. However, our results show that when reproductive interference induces female preference, FLM can also stem from an increased divergence in female trait. Our results therefore highlight that higher divergence in female trait is not a reliable evidence of sexually-contrasted selection promoting FLM.

Contrary to reproductive interference, sexually-contrasted predation can generate FLM only when the *focal* and the *model* species have different ancestral traits. Such mechanism would thus be especially relevant for distantly-related co-mimetic species, that are more likely to have divergent ancestors. In contrast, the role of reproductive interference in generating FLM is probably more important in cases where mimetic and model species are more closely related. Our results also show that a non-mimetic ancestral state favour the emergence of FLM under sexually-contrasted selection. Therefore, the FLM observed in *Papilio garamas*, which likely derived from a sexually monomorphic and mimetic ancestor (Kunte, 2009), might be a good candidate to investigate the potential origin of FLM due to reproductive interference. Our results thus stress the need to infer the for ancestral levels of mimicry, as well as the phylogenetic distances between mimetic species and their co-mimics or model species to empirically investigate the effect of reproductive interference on the evolution of FLM.

The level of investment of males in reproduction and the evolution of FLM caused by reproductive interference

Our results show that reproductive interference can generate female preference for non-mimetic males and therefore may cause FLM. Some studies already suggested that sexual selection may generate FLM (Belt, 1874.; Turner, 1978), but the origin of females' preferences for non-mimetic males was unidentified. Our model highlights that reproductive interference could be the driver of such females' preferences.

Nevertheless, the emergence of sexual dimorphism stems from the assumption that female is the only choosy sex. This assumption is relevant when females invest much more in reproduction than males (Trivers, 1972; Balshine *et al.*, 2002). However, this asymmetrical investment in offspring between males and females can vary in different Lepidoptera species. In some species, butterfly males provide a nuptial gift containing nutriment during mating (Boggs & Gilbert, 1979). Such elevated cost of mating in males could promote the evolution of choosiness in males. If the asymmetry in reproductive investment between sexes is limited, the evolution of FLM would then be impaired. Moreover, the investment of males in reproduction impacts the cost of choosiness for females, because females refusing a mating opportunity would be denied access to the nuptial gift. In Lepidoptera, females mating more than once have higher lifetime fecundity than females that mate only once, because nuptial gifts provide important metabolic resources (Wiklund *et al.*, 1993; Lamunyon, 1997). Such elevated cost of rejecting a potential mate may limit the evolution of preference in females, as highlighted by our model: our results indeed show that reproductive interference promotes FLM only when cost of choosiness is low. The evolution of female-mimicry is thus likely to be impaired when the costs of mating are elevated in males, and therefore (1) inducing male choosiness and (2) increasing the opportunity costs generated by female choosiness.

Even when females are the choosy sex, they can still have preference based on multiple cues reducing cost of reproductive interference. Butterflies express preference for pheromones that may strongly differ between closely related species (Darragh *et al.*, 2017; González-Rojas *et al.*, 2020) thus limiting cost of reproductive interference. Moreover, different micro-habitat preference may reduce interspecific interactions and then female probability of accepting a heterospecific male (Estrada & Jiggins, 2002). In our model, the probability to reject an heterospecific male based on other trait than the warning trait is captured by the parameters c_{RI} . Our results show that reproductive interference can promote FLM even when c_{RI} is low. As soon as c_{RI} is non-null, reproductive interference lead to selection on female preference and the evolution of FLM depends on the relative importance of each evolutionary forces.

Because few studies investigate the sexual selection origin of FLM, empirical studies estimating the reproductive costs and benefits in both sexes are strongly lacking. Here, we explicit a mechanism by which sexual selection can generate FLM. We thus hope our theoretical work will encourage experimental approaches investigating the link between reproductive costs and FLM. Such studies may shed light on the actual role of sexual selection generated by RI on the evolution of FLM.

Relative species abundances and defences and the evolution of female-limited mimicry

Our results show that, for both causes of FLM (reproductive interference or sexually contrasted predation), the level of sexual dimorphism decreases with the individual level of defence when developmental constraints totally inhibit mimicry in males. This prediction is consistent with the empirical observation reporting FLM mostly in Batesian mimics, although FLM has still been reported in a few defended species (Nishida, 2017). Our model stresses the need to precisely quantify the level of defences carried out by individuals from different species: important variations in the levels of defences within species have been documented in Müllerian mimics (*e.g.* in *Heliconius* butterflies, Sculfort *et al.* (2020)), as well as in Batesian mimics (*e.g.* viceroy butterfly, Prudic *et al.* (2019)). Empirical quantification of the level of deterrence induced by individuals from co-mimetic species would shed light on the evolutionary conditions favouring the evolution of FLM.

Our model also predicts that the emergence of FLM is strongly linked to the relative density between mimics and models, and our theoretical approach neglects the dynamics of population densities of the *focal* and the *model* species, that may depend on their individual defence level. Empirical studies usually report that the density of undefended mimics is low compared to those of the defended models (Long *et al.*, 2015; Prusa & Hill, 2021). Undefended mimics can have a negative effect predator's learning (Rowland *et al.*, 2010; Lindström *et al.*, 1997), suggesting that Batesian mimicry could evolve and be maintained only in species with a

low density compared to the *model* species. Moreover, a high abundance of the *model* species compared to the potential mimics also increases the protection of imperfect mimics allowing the evolution of gradual Batesian mimicry (Kikuchi & Pfennig, 2010). The relative density between the *focal* and the *model* species is especially important when assuming reproductive interference, because the costs generated by heterospecific interactions depend on the proportion of heterospecific males encountered by females. Our results show that reproductive interference strongly promotes sexual dimorphism when the density of the *focal* species is low as compared to the *model* species. Considering that FLM is caused by reproductive interference, the lower relative density of undefended species may promote FLM, and therefore explain why FLM could be especially favoured in Batesian mimics is reserved to undefended species.

The reported difference in phenology between defended *models* emerging sooner than undefended *mimics* may further enhance the difference in relative abundances between *models* and *mimics*, therefore increasing the cost of reproductive interference for undefended females. Batesian mimics often emerge after their models, when the models warning trait is well known by predators (Prusa & Hill, 2021), and this might reinforce the evolution of FLM caused by reproductive interference in Batesian *mimics*. Overall, our theoretical study stresses the need of ecology studies quantifying relative densities of mimetic defended and palatable species through time. Such field studies, as well as chemical ecology studies quantifying defence variations, are now crucial needed to understand the evolution of FLM, in Batesian and Müllerian mimics.

Sexual conflict limiting males adaptation

Our study highlight that different fitness optima among sexes, due to natural and sexual selection, drives the evolution of sexual dimorphism in both hypothesis explaining FLM. Different fitness optima may stem from sexually dimorphic morphology, leading to different flight ability and to sexually contrasted predation risk. But different sexual roles, such as different levels of physiological investments in

offspring, may also leads to contrasted effect of trait variations on female and male fitness, generating so-called sexual conflicts (Parker, 2006). Sexual conflicts classically involves the evolution of traits enhancing male mating success with multiple females, and of traits enhancing the rejection of non-preferred males in females (*e.g.* conflicting coevolution of genitalia in males and females Brennan *et al.* (2010). FLM driven by reproductive interference provide an original example of sexual conflict: while mimicry would enhance survival in males, female preferences generated by reproductive interference and by their greater reproductive investment, prevent the evolution of mimetic trait in males. This is thus a relevant case-study of sexual conflict driving the evolution of sexual dimorphism. Similarly, costly exaggerated trait in males may be regarded as a results of sexual conflicts: female prefer this expensive trait sign of mate quality (handicap principle (Zahavi, 1975)) leading to maladaptive trait disfavoured by natural selection (Johnstone, 1995b). In black scavenger flies *Sepsis cynipsea* and *Sepsis neocynipsea* species differentiation of exaggerated male forelegs is higher in sympatric population (Baur *et al.*, 2020), suggesting than species interactions may indeed be a key evolutionary force involved in the evolution of exaggerated trait in males. Reproductive interference is indeed expected to promote male exaggerated trait improving species recognition in females. However, evidences of the role of reproductive interference in the evolution of sexual dimorphism are still scarce. Our theoretical work on FLM highlights that conflict between natural selection promoting the same trait in different species and reproductive interference may generate sexual dimorphism. We thus hope our results will stimulate new research on the effect of ecological interactions between closely-related species on the evolution of sexual dimorphism.

Conclusion

Our model show that both sexually contrasted predation and reproductive interference (by promoting preference for non-mimetic males) may generate FLM. Our results therefore show that the patterns of divergence of male and female trait from ancestral state should be interpreted in light from the selection regime involved.

Our model also reveals the important role of ecological interactions between sympatric species on the evolution of sexual dimorphism, highlighting the need to consider the role of reproductive interference in the phenotypic diversification in sympatry.

Acknowledgments

The authors would like to thank the ANR SUPERGENE (ANR-18-CE02-0019) for funding the PhD of LM. This work was partially supported by the Chair “Modélisation Mathématique et Biodiversité” of VEOLIA-Ecole Polytechnique-MNHN-F.X.

Appendix

A4.1 Selection vectors

In this part we detail the calculations to obtain the selection vector (Equation (4.2)).

A4.1.1 Selection acting on male trait β_{t_m}

We compute the first component of the selection vector β_{t_m} describing the selection acting on male trait. This coefficient is given by

$$\beta_{t_m} = \left. \frac{d}{dt_m} \log (W(t_m, t_f, p_f)) \right|_{(t_m, t_f, p_f) = (\bar{t}_m, \bar{t}_f, \bar{p}_f)}.$$

Using (4.1) and (4.6) we have

$$\beta_{t_m} = -2s(\bar{t}_m - t_a) + \left. \frac{d}{dt_m} \log (W_{pred}^{\sigma}(t_m)) \right|_{t_m = \bar{t}_m} + \left. \frac{d}{dt_m} \log (W_r(t_m, p_f)) \right|_{(t_m, p_f) = (\bar{t}_m, \bar{p}_f)}.$$

Selection due to predation

First we compute the part of the selection coefficient due to predation. Using (4.10) we have:

$$\begin{aligned} \left. \frac{d}{dt_m} \log \left(W_{pred}^{\sigma}(t_m) \right) \right|_{t_m=\bar{t}_m} &= \left. \frac{d}{dt_m} \left(\frac{-d_m}{1 + \mathcal{D}(t_m)} \right) \right|_{t_m=\bar{t}_m}, \\ &= \left. \left(\frac{d_m \frac{d}{dt_m} \mathcal{D}(t_m)}{(1 + \mathcal{D}(t_m))^2} \right) \right|_{t_m=\bar{t}_m}. \end{aligned}$$

Using (4.9) we have

$$\begin{aligned} \frac{d}{dt} \mathcal{D}(t) &= -b(t - \bar{t}_m) \lambda N \exp[-b(t - \bar{t}_m)^2] - b(t - \bar{t}_f) \lambda N \exp[-b(t - \bar{t}_f)^2] \\ &\quad - 2b(t - \bar{t}') \lambda' N' \exp[-b(t - \bar{t}')^2]. \end{aligned}$$

Selection due to reproduction

We now compute the part of the selection coefficient due to reproduction. Using (4.21) we have:

$$\left. \frac{d}{dt_m} \log (W_r(t_m, p_f)) \right|_{(t_m, p_f) = (\bar{t}_m, \bar{p}_f)} = -2a(\bar{t}_m - \bar{p}_f).$$

Therefore we have

$$\beta_{t_m} = -2s(\bar{t}_m - t_a) + \frac{d_m \frac{d}{dt_m} \mathcal{D}(t_m) \Big|_{t_m=\bar{t}_m}}{(1 + \mathcal{D}(\bar{t}_m))^2} - 2a(\bar{t}_m - \bar{p}_f).$$

A4.1.2 Selection acting on female trait β_{t_f}

The second component of the selection vector β_{t_f} is given by

$$\beta_{t_f} = \left. \frac{d}{dt_f} \log (W(t_m, t_f, p_f)) \right|_{(t_m, t_f, p_f) = (\bar{t}_m, \bar{t}_f, \bar{p}_f)}.$$

Using (4.1) and (4.7) we have

$$\beta_{t_f} = -2s(\bar{t}_f - t_a) + \frac{d}{dt_f} \log \left(W_{pred}^{\ominus}(t_f) \right) \Big|_{t_f=\bar{t}_f}.$$

Similarly than with male traits we have

$$\frac{d}{dt_f} \log \left(W_{pred}^{\ominus}(t_f) \right) \Big|_{t_f=\bar{t}_f} = \left(\frac{d_f \frac{d}{dt_f} \mathcal{D}(t_f)}{(1 + \mathcal{D}(t_f))^2} \right) \Big|_{t_f=\bar{t}_f}.$$

Thus we have

$$\beta_{t_f} = -2s(\bar{t}_f - t_a) + \frac{d_f \frac{d}{dt_f} \mathcal{D}(t_f) \Big|_{t_f=\bar{t}_f}}{(1 + \mathcal{D}(\bar{t}_f))^2}.$$

A4.1.3 Selection acting on female preference β_{p_f}

The last component of the selection vector β_{t_f} is given by

$$\beta_{p_f} = \frac{d}{dp_f} \log (W(t_m, t_f, p_f)) \Big|_{(t_m, t_f, p_f) = (\bar{t}_m, \bar{t}_f, \bar{p}_f)}.$$

Using (4.1) we have

$$\beta_{p_f} = \frac{d}{dp_f} \log (W_r(t_m, p_f)) \Big|_{(t_m, p_f) = (\bar{t}_m, \bar{p}_f)}.$$

Using (4.21) we have

$$\begin{aligned} \beta_{p_f} &= \frac{d}{dp_f} \log (T(p_f)) \Big|_{p_f=\bar{p}_f} \\ &\quad - \frac{d}{dp_f} \log (c + (1 - c)(T(p_f) + T_{RI}(p_f))) - 2a(p_f - t_m) + 2a(p_f - \bar{t}_m) \Big|_{(t_m, p_f) = (\bar{t}_m, \bar{p}_f)}. \end{aligned}$$

Using (4.15) and (4.16) we have

$$\left. \frac{d}{dp_f} \log(T(p_f)) \right|_{p_f=\bar{p}_f} = -2a(\bar{p}_f - \bar{t}_m),$$

and

$$\begin{aligned} & \left. \frac{d}{dp_f} \log(c + (1-c)(T(p_f) + T_{RI}(p_f))) \right|_{p_f=\bar{p}_f} \\ &= \frac{(1-c) \left(-2a(\bar{p}_f - \bar{t}_m)T(\bar{p}_f) - 2a(\bar{p}_f - \bar{t}')T_{RI}(\bar{p}_f) \right)}{c + (1-c)(T(\bar{p}_f) + T_{RI}(\bar{p}_f))}. \end{aligned}$$

Thus

$$\begin{aligned} \beta_{p_f} &= -2a(\bar{p}_f - \bar{t}_m) \\ &+ 2a \frac{(1-c) \left((\bar{p}_f - \bar{t}_m)T(\bar{p}_f) + (\bar{p}_f - \bar{t}')T_{RI}(\bar{p}_f) \right)}{c + (1-c)(T(\bar{p}_f) + T_{RI}(\bar{p}_f))}. \end{aligned}$$

A4.2 Computation of the matrix of correlation

In this part we approximate the genetic covariance between male trait and female preference $G_{t_m p_f}$, using the results from (Kirkpatrick *et al.*, 2002). Trait and preference are controlled by different sets of unlinked loci with additive effects, denoted T and P , respectively. We note $T_m \subseteq T$ and $T_f \subseteq T$ the loci controlling trait in males and in females respectively. For each i in T (resp. P), we note ξ_i^t (resp. ξ_i^p) the contribution of the locus i on trait (resp. preference) value. The trait t_m of a male is then given by

$$t_m = \sum_{i \in T_m} \xi_i^t. \tag{A4.1}$$

The trait t_f and preference p_f values of a female are given by

$$t_f = \sum_{i \in T_f} \xi_i^t \quad \text{and} \quad p_f = \sum_{i \in P} \xi_i^p. \quad (\text{A4.2})$$

As in (Lande, 1981) we assume that the distributions of ξ_i^t and ξ_i^p are multivariate Gaussian. Let G_{ij} be the genetic covariance between loci i and j . Then the elements of the matrix of correlation are given by:

$$G_{t_m t_m} = \sum_{i,j \in T_m} G_{ij}, \quad G_{t_f t_f} = \sum_{i,j \in T_f} G_{ij}, \quad G_{p_f p_f} = \sum_{i,j \in P} G_{ij} \quad \text{and} \quad G_{t_m p_f} = \sum_{i \in T_m, j \in P} G_{ij}. \quad (\text{A4.3})$$

To compute the change on genetic correlation we need to identify various selection coefficients (see (Barton & Turelli, 1991; Kirkpatrick *et al.*, 2002)). These coefficients are obtained using the contribution to the next generation of a mating between a male with trait t_m and a female with trait t_f and preference p_f due to natural selection and mating preference (see equation 4.1).

For simplicity we consider only leading terms in the change in genetic correlation, computed with a Mathematica script (available online at <https://github.com/Ludovic-Maisonneuve/evo-flm>). For $(i, j) \in T_m \times P_f$, combining Equations (9), (12), (15) from Kirkpatrick *et al.* (2002) gives the change in the genetic covariance between loci i and j :

$$\begin{aligned} \Delta G_{ij} = & -\frac{G_{ij}}{2} + \frac{1}{4} \tilde{a}_{t_m t_m} \sum_{k,l \in T_m} (G_{ik} G_{jl} + G_{il} G_{jk}) + \frac{1}{4} \tilde{a}_{p_f p_f} \sum_{k,l \in P} (G_{ik} G_{jl} + G_{il} G_{jk}) \\ & + \frac{1}{4} \tilde{a}_{t_m p_f} \sum_{k \in T_m, l \in P} G_{ik} G_{jl} + \frac{1}{4} \tilde{a}_{t_m p_f} \sum_{k \in T_m, l \in P} G_{il} G_{jk} + O(\varepsilon^2) \end{aligned} \quad (\text{A4.4})$$

with $\tilde{a}_{\mu\rho}$ for $(\mu, \rho) \in \{t_m, t_f, p_f\}^2$ being the leading term of the selection coefficients

$a_{\mu\rho}$ calculated from the contribution to the next generation:

$$a_{\mu\rho} := \frac{1}{2} \frac{\partial^2}{\partial\mu\partial\rho} \log(W(t_m, t_f, p_f)) \Big|_{(t_m, t_f, p_f) = (\bar{t}_m, \bar{t}_f, \bar{p}_f)}.$$

The expressions of $\tilde{a}_{p_f p_f}$, $\tilde{a}_{t_m t_m}$ and $\tilde{a}_{t_m p_f}$ are given in the Mathematica script.

By summing Equations (A4.4) over each i, j in T_m and P we obtain:

$$\begin{aligned} \Delta G_{t_m p_f} = & -\frac{G_{t_m p_f}}{2} - \frac{1}{2} \tilde{a}_{t_m t_m} G_{t_m t_m} G_{t_m p_f} - \frac{1}{2} \tilde{a}_{p_f p_f} G_{p_f p_f} G_{t_m p_f} \\ & + \frac{1}{4} \tilde{a}_{t_m p_f} G_{t_m t_m} G_{p_f p_f} + \frac{1}{4} \tilde{a}_{t_m p_f} G_{t_m p_f}^2 + O(\varepsilon^2). \end{aligned} \quad (\text{A4.5})$$

Under weak selection genetic correlations quickly reach equilibrium (Nagylaki, 1993). For the sake of simplicity we assumed that the genetic correlations between traits and preferences are at equilibrium (as in (Barton & Turelli, 1991; Pomiankowski & Iwasa, 1993)). We obtain from (A4.5) that the two possible values at equilibrium are given in the Mathematica file. Only one of the two equilibrium values checks the Cauchy–Schwarz inequality ($G_{t_m p_f} \leq \sqrt{G_{t_m t_m} G_{p_f p_f}}$). Because the genetic variance of traits and preference is small relative to the curvature of the fitness function $aG_{t_m t_m}$ and $aG_{p_f p_f}$ are low. A Taylor expansion of the genetic covariance between male trait and female preference at equilibrium gives:

$$G_{t_m p_f}^* \approx aG_{t_m t_m} G_{p_f p_f}.$$

A4.3 Small relative variance approximation

Because we assume that the variance of traits and preference is small relative to the curvature of the fitness function we may use approximation in Equations (4.9), (4.15), (4.16) and (4.18). Here we detail how we obtained these approximations. The reasoning is similar for each approximation so we only explain how we get an

approximation of \mathcal{D} in (4.9). We recall that \mathcal{D} is defined by

$$\begin{aligned} \mathcal{D}(t) &= \int_{\tau_m} \lambda \frac{N}{2} f^{\sigma}(\tau_m) \exp[-b(t - \tau_m)^2] d\tau_m + \int_{\tau_f} \lambda \frac{N}{2} f^{\varrho}(\tau_f) \exp[-b(t - \tau_f)^2] d\tau_f \\ &\quad + \int_{t'} \lambda' N' g(t') \exp[-b(t - t')^2] dt'. \end{aligned}$$

We first approximate the first term of \mathcal{D} . We have

$$\begin{aligned} &\int_{\tau_m} \lambda \frac{N}{2} f^{\sigma}(\tau_m) \exp[-b(t - \tau_m)^2] d\tau_m \\ &= \lambda \frac{N}{2} \exp[-b(t - \bar{t}_m)^2] \int_{\tau_m} f^{\sigma}(\tau_m) \exp[b(2t - \tau_m - \bar{t}_m)(\tau_m - \bar{t}_m)] d\tau_m. \end{aligned}$$

Using a Taylor expansion of $\exp[b(2t - \tau_m - \bar{t}_m)(\tau_m - \bar{t}_m)]$ we have

$$\lambda \frac{N}{2} \exp[-b(t - \bar{t}_m)^2] \int_{\tau_m} f^{\sigma}(\tau_m) (1 + b(2t - \tau_m - \bar{t}_m)(\tau_m - \bar{t}_m) + O(b(\tau_m - \bar{t}_m)^2)) d\tau_m,$$

which is equal to

$$\lambda \frac{N}{2} \exp[-b(t - \bar{t}_m)^2] (1 - b\text{Var}(t_m) + O(b\text{Var}(t_m))).$$

Hence when the variance of t_m is small relative to the curvature of the fitness function, implying that $b\text{Var}(t_m)$ is low, the first term of \mathcal{D} can be approximated by

$$\lambda \frac{N}{2} \exp[-b(t - \bar{t}_m)^2].$$

Similar computations for the other terms give the approximation in Equation (4.9).

A4.4 Alternative scenarios

In the main document, we highlighted how the joint action of reproductive interference and predation may promote the evolution of FLM. We assumed that when

the *focal* species enter in contact with *model*, reproductive interference and predation simultaneously exerted selection on individuals of the *focal* species (scenario 1). Here, we investigate the evolution of FLM under two other alternative scenarios. In scenario 2, we assume that the *focal* and the *model* species ancestrally shared common predators promoting mimicry, before sexual interactions happen between heterospecific individuals. In scenario 3, we assume the opposite sequences of events, whereby heterospecific sexual interactions occur before the two species start to share the same predators.

We compare the evolution of FLM under the three different scenarios using both the deterministic quantitative model (Figure A4.1) and individual-centred simulations assuming either independent genetic basis of male and female trait (Figure A4.2) or common genetic basis of male and female trait (Figure A4.3). Under scenario 2 (resp. 3) we let the traits in the *focal* species evolve with predation only ($d_m = d_f > 0$ and $c_{RI} = 0$) (resp. reproductive interference only ($d_m = d_f = 0$ and $c_{RI} > 0$)), until equilibrium using the deterministic quantitative model or after 10,000 generations using individual-centred simulations. Starting from the equilibria reached under each scenario, we assume that reproductive interference and predation then jointly influence the dynamics of traits in the *focal* species ($d_m = d_f > 0$ and $c_{RI} > 0$). We compare the evolutionary outcomes observed when assuming either (1) that reproductive interference limits mimicry in males ($a = 10$) (Figure A4.1(a)(b)(c), Figure A4.2(a)(b)(c), Figure A4.3(a)(b)(c)) or (2) that reproductive interference promotes divergent evolution of male trait away from the ancestral value ($a = 2.5$) (Figure A4.1(d)(e)(f), Figure A4.2(d)(e)(f), Figure A4.3(d)(e)(f)).

Using the deterministic quantitative model, the three different scenarios leads to the same final male trait and female trait and preference values (Figure A4.1). Similarly, using individual-centred simulations male trait and female trait and preference values generally oscillate around the same value under the three scenarios (Figure A4.2 and A4.3), with few notable exceptions (Figure A4.4). When mimicry evolve first (scenario 2) male trait and female trait and preference values first oscillates around the trait displayed in the *model* species. If species enter

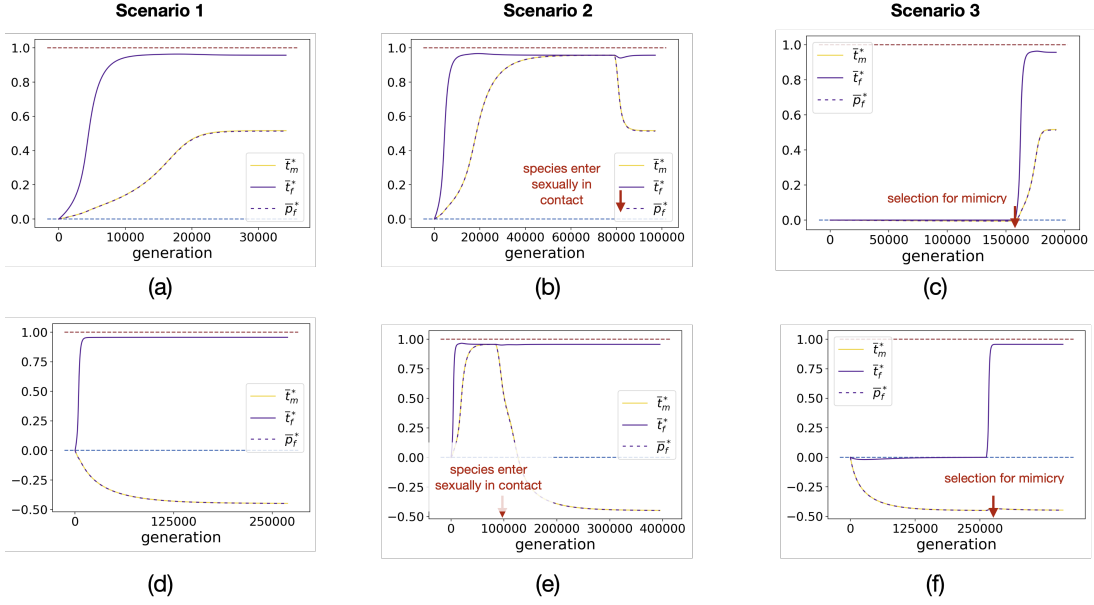


Fig. A4.1: **Effect of the history of species interactions on the dynamics of the mean male trait and female trait and preference values across generations given by the deterministic quantitative model.** Different scenarios ((a)(d) simultaneous heterospecific sexual interactions and mimicry, (b)(e) initial mimicry, (c)(f) initial heterospecific sexual interactions) are explored when (a)(b)(c) reproductive interference limits mimicry in males ($a = 10$) and when (d)(e)(f) reproductive interference promotes divergent evolution of male trait away from the ancestral value ($a = 2.5$). We assume: $G_{t_m} = G_{t_f} = G_{p_f} = 0.01$, $G_{t_m t_f} = 0.001$, $c = 0.1$, $c_{RI} = 0.01$, $b = 5$, $d_m = d_f = 0.05$, $\lambda = 0$, $N = 100$, $\lambda' = 0.01$, $N' = 200$, $s = 0.0025$, $t_a = 0$, $\bar{t}' = 1$.

sexually in contact when male trait is superior to the trait displayed in the *model* species, male trait increases and oscillates around a trait value that differs from the value observed under the other scenarios (Figure A4.4(b)).

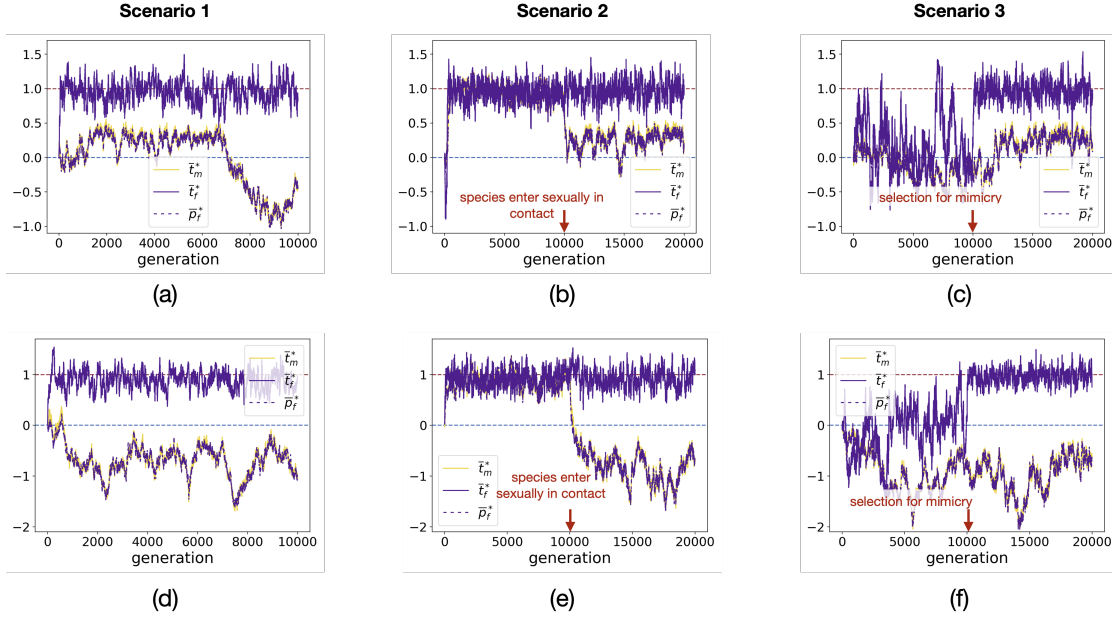


Fig. A4.2: Effect of the history of species interactions on the dynamics of the mean male trait and female trait and preference values across generations. Each plot shows the dynamics obtained from a single simulation of individual-centred model in a given scenario, assuming independent genetic basis of male and female trait. The scenarios used here imply: (a)(d) simultaneous heterospecific sexual interactions and mimicry, (b)(e) initial mimicry, (c)(f) initial heterospecific sexual interactions) are explored when (a)(b)(c) reproductive interference limits mimicry in males ($a = 10$) and when (d)(e)(f) reproductive interference promotes divergent evolution of male trait away the ancestral value ($a = 2.5$). We assume: $G_0 = 0.0025$, $\mu = 0.05$, $r_{T_m T_f} = 0.25$, $r_{T_f P_f} = 0.25$, $c = 0.1$, $c_{RI} = 0.5$, $b = 5$, $d_m = d_f = 0.5$, $\lambda = 0$, $N = 100$, $\lambda' = 0.01$, $N' = 200$, $s = 0.025$, $t_a = 0$, $\bar{t}' = 1$.

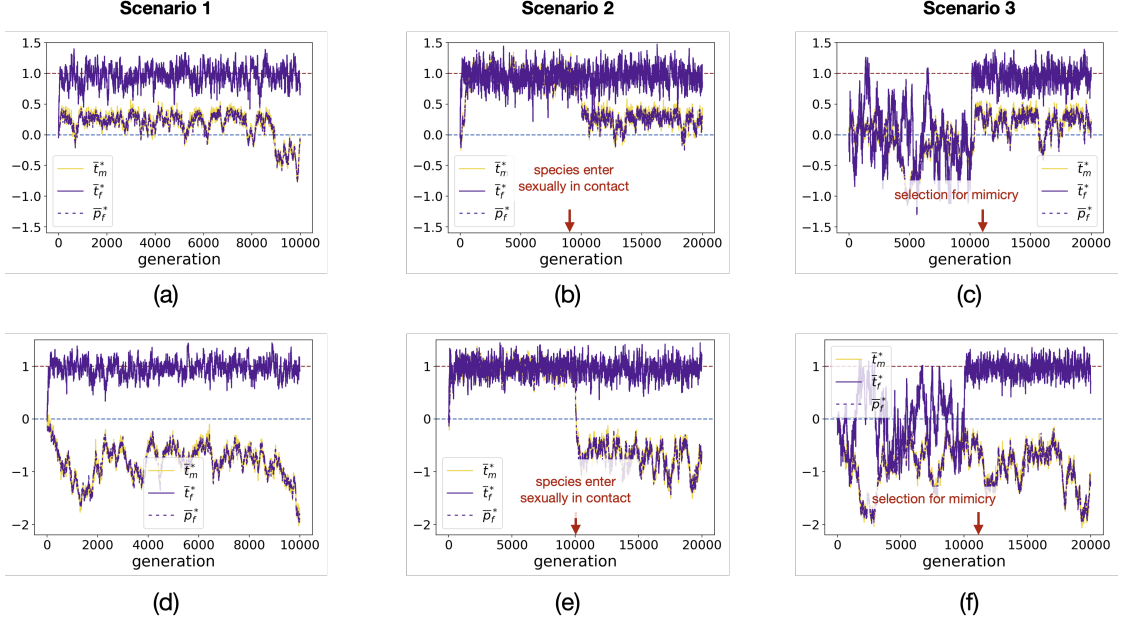


Fig. A4.3: Effect of the history of species interactions on the dynamics of the mean male trait and female trait and preference values across generations. Each plot shows the dynamics obtained from a single simulation of individual-centred model in a given scenario, assuming independent genetic basis of male and female trait. The scenarios used here imply: ((a)(d) simultaneous heterospecific sexual interactions and mimicry, (b)(e) initial mimicry, (c)(f) initial heterospecific sexual interactions) are explored when (a)(b)(c) reproductive interference limits mimicry in males ($a = 10$) and when (d)(e)(f) reproductive interference promotes divergent evolution of male trait away the ancestral value ($a = 2.5$). We assume: $G_0 = 0.0025$, $\mu = 0.05$, $r_{T_1T_2} = 0.25$, $r_{T_2T_3} = 0.25$, $r_{T_3P_f} = 0.25$, $c = 0.1$, $c_{RI} = 0.5$, $b = 5$, $d_m = d_f = 0.5$, $\lambda = 0$, $N = 100$, $N' = 0.01$, $N' = 200$, $s = 0.025$, $t_a = 0$, $\bar{t}' = 1$.

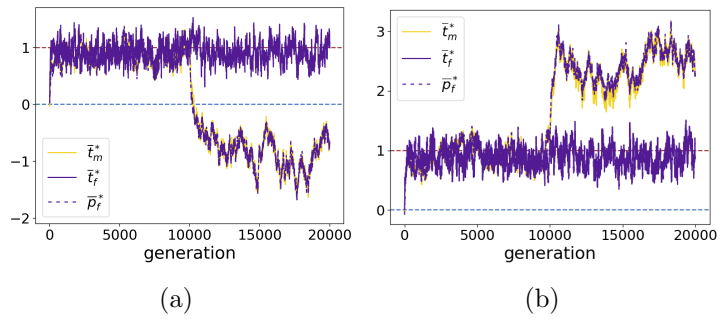


Fig. A4.4: Two independent replicate runs of the dynamics of the mean male trait and female trait and preference values across generations given by individual-centred simulations assuming independent genetic basis of male and female trait when mimicry evolves first (scenario 2). We assume: $G_0 = 0.0025$, $\mu = 0.05$, $r_{T_m T_f} = 0.25$, $r_{T_f P_f} = 0.25$, $c = 0.1$, $a = 2.5$, $c_{RI} = 0.5$, $b = 5$, $d_m = d_f = 0.5$, $\lambda = 0$, $N = 100$, $\lambda' = 0.01$, $N' = 200$, $s = 0.025$, $t_a = 0$, $\bar{t}' = 1$.

A4.5 Sexually contrasted predation promotes higher trait divergence in females

In this part, we show that if FLM in a palatable species ($\lambda = 0$) is not caused by sexual selection ($a = 0$) but by sexually contrasted predation ($d_f > d_m$) then at the final state female trait (\bar{t}_f^*) diverges more from the ancestral trait than male trait (\bar{t}_m^*). In mathematical terms, we prove that if $a = 0$ and $d_f > d_m$ we have

$$|\bar{t}_f^* - t_a| > |\bar{t}_m^* - t_a|. \quad (\text{A4.6})$$

For simplicity we assume that $t' > t_a$, the other case being obtained by symmetry.

At final state we have $\beta_{t_m}(\bar{t}_m^*) = 0$ (β_{t_m} is given in Equation (4.3)). Because we have

$$\beta_{t_m}(t_a) = \frac{-2b(t_a - t')d_m\lambda'N'\exp[-b(t_a - t')^2]}{(1 + \lambda'N'\exp[-b(t_a - t')^2])^2} > 0,$$

and

$$\beta_{t_m}(t') = -2s(t' - t_a) < 0,$$

\bar{t}_m^* is bounded by t_a and t' . Similar arguments give that final female trait is bounded by t_a and t' .

Because \bar{t}_m^* is the final trait we have $\forall \tau \in [t_a, \bar{t}_m^*[, \beta_{t_m}(\tau) > 0$.

For all trait τ we have

$$\beta_{t_f}(\tau) = \beta_{t_m}(\tau) - (d_f - d_m) \frac{2(\tau - t')\lambda'N'\exp[-b(\tau - t')^2]}{(1 + \lambda'N'\exp[-b(\tau - t')^2])^2},$$

which implies that $\forall \tau \in [t_a, t'[, \beta_{t_f}(\tau) > \beta_{t_m}(\tau)$. Then $\forall \tau \in [t_a, \bar{t}_m^*], \beta_{t_f}(\tau) > 0$. Therefore $\bar{t}_f^* > \bar{t}_m^*$ and then we have (A4.6).

A4.6 Temporal dynamics of sexual dimorphism

Here, we illustrate the temporal dynamics of sexual dimorphism when

- reproductive interference limits mimicry in males (Figure A4.5(a)).
- reproductive interference promotes divergence from the ancestral trait in males (Figure A4.5(b)).
- sexually contrasted predation promotes mimicry in females only (Figure A4.5(c)).

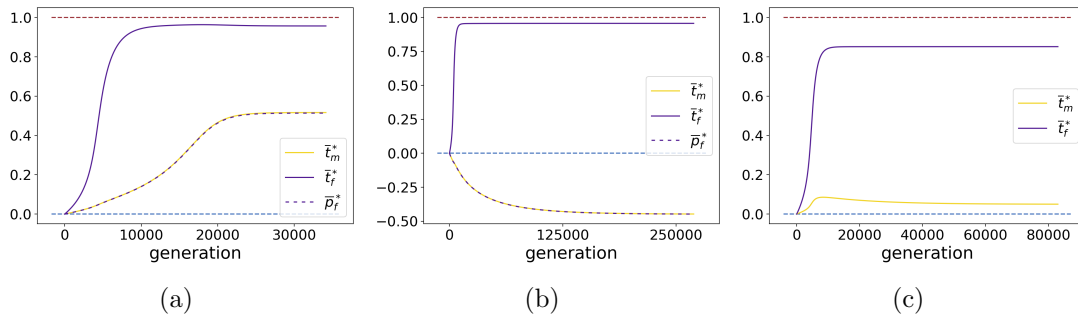


Fig. A4.5: **Evolution of the mean male trait and female trait and preference values across generations (a)(b) when reproductive interference or (c) sexually contrasted predation promotes sexual dimorphism.** We assume: (a) $c_{RI} = 0.01$, $a = 10$, $s = 0.0025$, $d_m = 0.05$, (b) $c_{RI} = 0.01$, $a = 2.5$, $s = 0.0025$, $d_m = d_f = 0.05$ (c) $c_{RI} = 0$, $a = 0$, $s = 0.01$, $d_m = 0.005$. We assume for the other parameters: $G_{t_m} = G_{t_f} = G_{p_f} = 0.01$, $G_{t_m t_f} = 0.001$, $c = 0.1$, $b = 5$, $d_f = 0.05$, $\lambda = 0$, $N = 100$, $\lambda' = 0.01$, $N' = 200$, $t_a = 0$, $\bar{t}' = 1$. The curves stop when the male trait and female trait and preference values reach equilibrium.

A4.7 Reproductive interference promotes female-limited mimicry in palatable species when females have sufficiently low cost of choosiness

The evolution of FLM strongly depends on the evolution of female preference. As we have already seen the evolution of female preference depends on reproductive

interference promoting preferences for non-mimetic males. However such preferences may cause females to seek for rarer males in the population. The evolution of preference limiting the cost of reproductive interference may thus be limited by the cost of choosiness described by the parameter c . We thus investigate the impact of the strength of reproductive interference (c_{RI}) promoting FLM and the cost of choosiness (c) on the final level of sexual dimorphism given by $|\bar{t}_m^* - \bar{t}_f^*|$ (Figure A4.6(a)) and on final female preference \bar{p}_f^* (Figure A4.6(b)). Cost of choosiness limits the evolution of sexual dimorphism due to reproductive interference (Figure A4.6(a)) because it limits the evolution of female preference (Figure A4.6(b)). In natural population, reproductive interference may explain FLM in populations where females have low cost of choosiness.

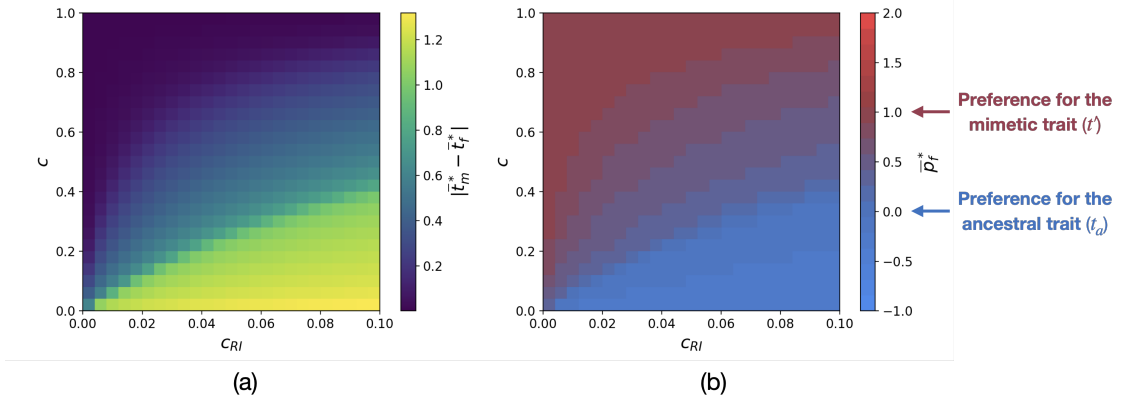


Fig. A4.6: Influence of the strength of reproductive interference c_{RI} and of the cost of choosiness c on the final level of sexual dimorphism $|\bar{t}_m^* - \bar{t}_f^*|$ and final preference \bar{p}_f^* . We assume: $G_{t_m} = G_{t_f} = G_{p_f} = 0.01$, $G_{t_m t_f} = 0.001$, $a = 5$, $b = 5$, $d_m = d_f = 0.05$, $\lambda = 0$, $N = 100$, $\lambda' = 0.01$, $N' = 200$, $s = 0.0025$, $t_a = 0$, $\bar{t}' = 1$.

A4.8 Impact of the genetic correlation between male and female trait $C_{t_m t_f}$

The evolution of the mean male and female trait values (\bar{t}_m and \bar{t}_f) depends on the genetic covariance between male and female trait ($G_{t_m t_f}$) (see equation (4.2)). We

investigate the impact of this genetic covariance and of the strength of reproductive interference (c_{RI}) on the level of sexual dimorphism (Figure A4.7). The level of sexual dimorphism is not impacted by the genetic covariance unless this quantity is at its maximum value ($G_{t_m t_f} = \sqrt{G_{t_m t_m} G_{t_f t_f}}$). Indeed when the genetic covariance is at its maximum value male and female trait have the same genetic basis, therefore the evolution of sexual dimorphism is not possible. By contrast when male and female trait have at least partially different genetic basis ($G_{t_m t_f} < \sqrt{G_{t_m t_m} G_{t_f t_f}}$) the non-shared genetic basis allows the level of sexual dimorphism to increase.

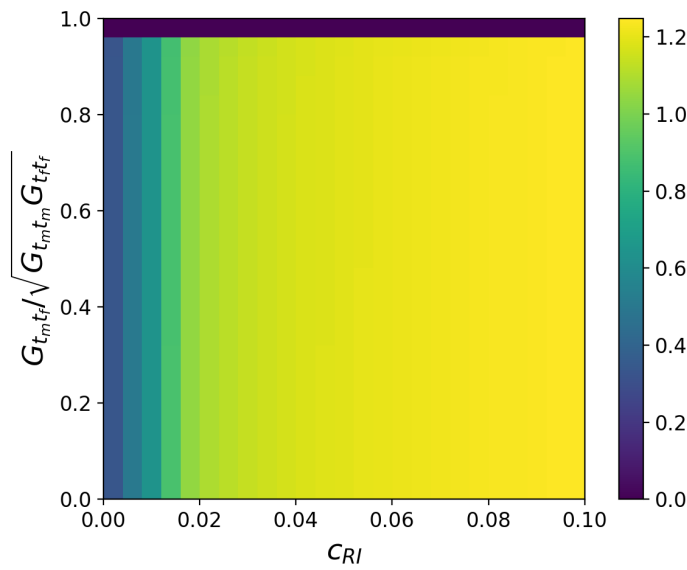


Fig. A4.7: **Influence of the strength of reproductive interference c_{RI} and of the genetic covariance between male and female trait normalized by its maximum value $\frac{G_{t_m t_f}}{\sqrt{G_{t_m t_m} G_{t_f t_f}}}$ on the final level of sexual dimorphism $|\bar{t}_m^* - \bar{t}_f^*|$.** We assume: $G_{t_m} = G_{t_f} = G_{p_f} = 0.01$, $c = 0.1$, $a = 5$, $b = 5$, $d_m = d_f = 0.05$, $\lambda = 0$, $N = 100$, $\lambda' = 0.01$, $N' = 200$, $s = 0.0025$, $t_a = 0$, $\bar{t}' = 1$.

However $G_{t_m t_f}$ impacts the speed at which the equilibrium is reached. When male trait in the *focal* species gets closer to the mimetic trait the genetic correlation increases the speed of convergence because selection on female trait also favours mimicry and also acts on male trait. By contrast when male trait diverges away from the mimetic trait the genetic correlation decreases the speed of convergence.

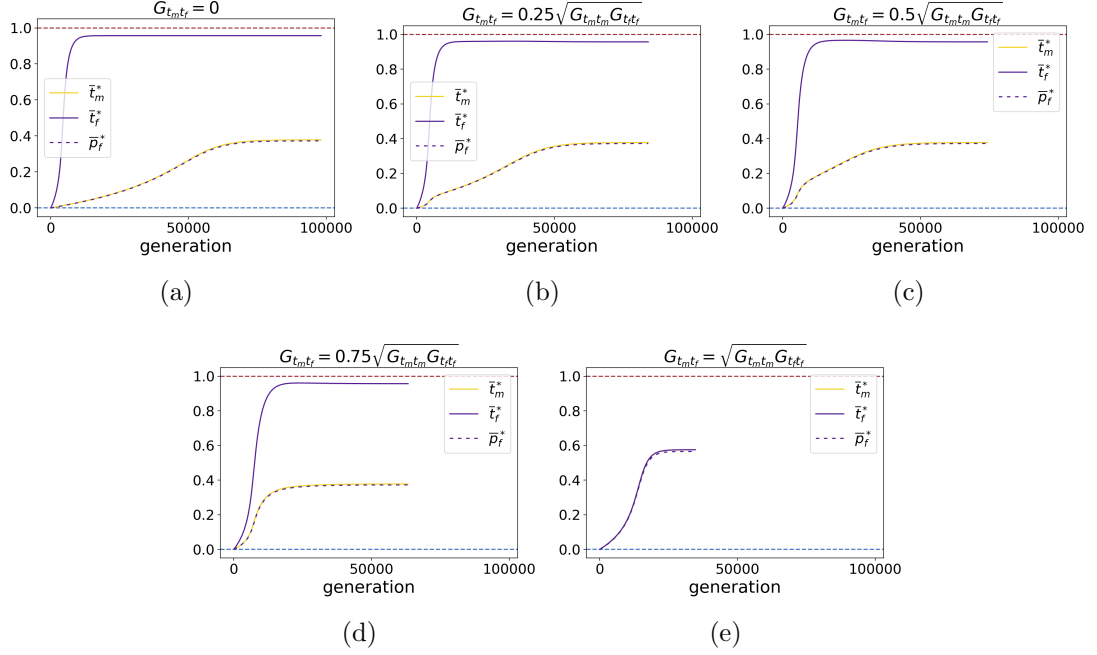


Fig. A4.8: **Evolution of the mean male trait and female trait and preference values across generations for different genetic covariances between male and female trait $G_{t_m t_f}$ when male trait gets closer to the mimetic trait.** We assume different values of the genetic covariance between male and female traits: (a) $G_{t_m t_f} = 0$, (b) $G_{t_m t_f} = 0.25\sqrt{G_{t_m t_m} G_{t_f t_f}}$, (c) $G_{t_m t_f} = 0.5\sqrt{G_{t_m t_m} G_{t_f t_f}}$, (d) $G_{t_m t_f} = 0.75\sqrt{G_{t_m t_m} G_{t_f t_f}}$, (e) $G_{t_m t_f} = \sqrt{G_{t_m t_m} G_{t_f t_f}}$. We assume: $G_{t_m} = G_{t_f} = G_{p_f} = 0.01$, $G_{t_m t_f} = 0.001$, $c_{RI} = 0.01$, $c = 0.1$, $a = 5$, $b = 5$, $d_m = d_f = 0.05$, $\lambda = 0$, $N = 100$, $\lambda' = 0.01$, $N' = 200$, $s = 0.0025$, $t_a = 0$, $\bar{t}' = 1$. The curves stop when the male trait and female trait and preference values reach equilibrium.

We also investigate the impact of the genetic architecture of trait on the evolution of FLM, using individual-centred simulations. We assume either independent genetic basis, or partially common genetic basis of male and female trait. Both genetic architectures lead to similar equilibrium values (see Figures A4.10, A4.11, A4.12, A4.13, A4.14, A4.17, A4.26, A4.24 and A4.28). This confirms that genetic correlation between male and female trait does not impact the level of sexual dimorphism at equilibrium.

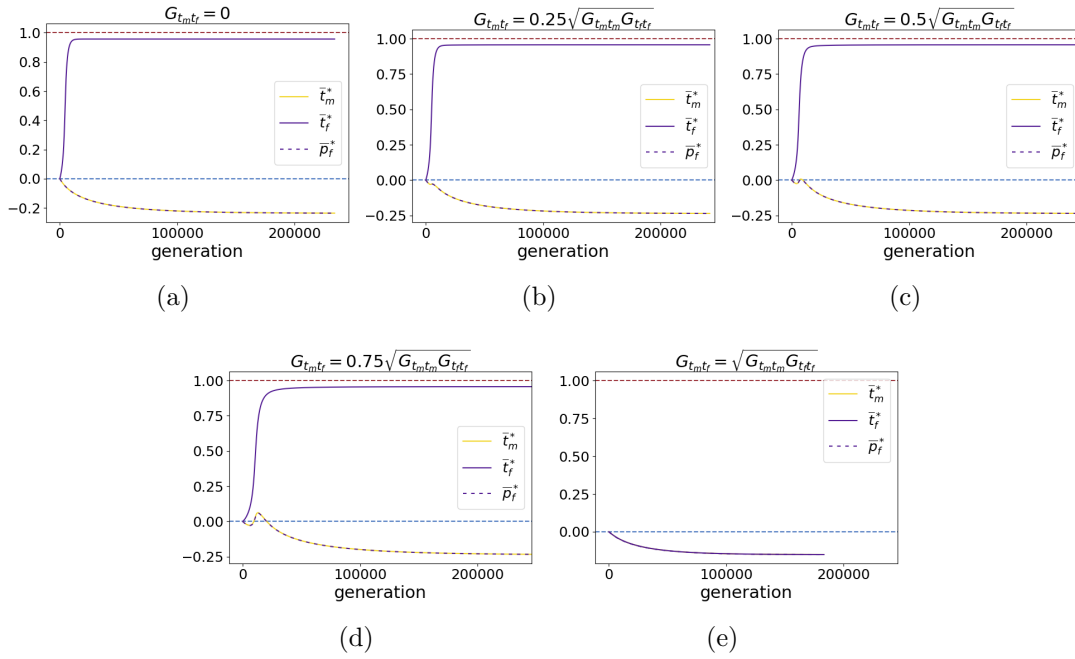


Fig. A4.9: Evolution of the mean male trait and female trait and preference values across generations for different genetic covariances between male and female traits $G_{t_m t_f}$ when reproductive interference promotes divergence of male trait away from the mimetic trait. We assume different value of the genetic covariance between of male and female trait: (a) $G_{t_m t_f} = 0$, (b) $G_{t_m t_f} = 0.25\sqrt{G_{t_m t_m} G_{t_f t_f}}$, (c) $G_{t_m t_f} = 0.5\sqrt{G_{t_m t_m} G_{t_f t_f}}$, (d) $G_{t_m t_f} = 0.75\sqrt{G_{t_m t_m} G_{t_f t_f}}$, (e) $G_{t_m t_f} = \sqrt{G_{t_m t_m} G_{t_f t_f}}$. We assume: $G_{t_m} = G_{t_f} = G_{p_f} = 0.01$, $G_{t_m t_f} = 0.001$, $c_{RI} = 0.05$, $c = 0.1$, $a = 5$, $b = 5$, $d_m = d_f = 0.05$, $\lambda = 0$, $N = 100$, $\lambda' = 0.01$, $N' = 200$, $s = 0.0025$, $t_a = 0$, $\bar{t}' = 1$.

A4.9 Investigation of the effect of reproductive interference on the evolution of FLM using individual-centred simulations

Similarly to the result given by the deterministic quantitative model (shown in Figure 4.4(a)), the level of sexual dimorphism increases with the strength of reproductive interference (c_{RI}) in the individual-centred simulations (Figure A4.10).

As highlighted in the main text, reproductive interference promotes female preference towards non-mimetic males, limiting mimicry in males. The deterministic quantitative model highlights the key role of female choosiness that reduces sexual dimorphism (Figure 4.4(b)). When female choosiness is high, females can easily distinguish conspecifics, even when they are almost mimetic. In line with this result, individual-centred simulations reveal that female choosiness reduces sexual dimorphism (Figure A4.11).

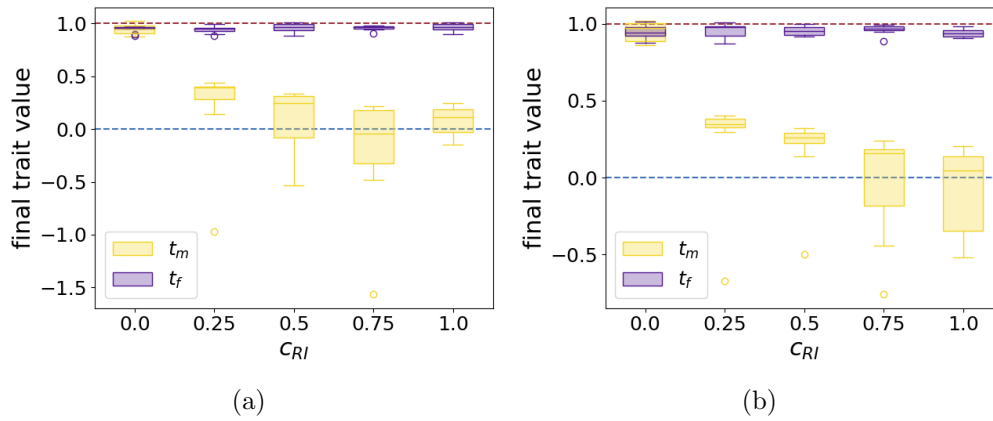


Fig. A4.10: **Boxplots of final mean male (yellow) and female (purple) traits values for different strength of reproductive interference c_{RI} using individual-centred simulations assuming (a) independent genetic basis or (b) partially common genetic basis of male and female trait.** We assume: (a) $r_{T_m T_f} = 0.25$, $r_{T_f P_f} = 0.25$ and (b) $r_{T_1 T_2} = 0.25$, $r_{T_2 T_3} = 0.25$, $r_{T_3 P_f} = 0.25$. We also assume: $G_0 = 0.0025$, $\mu = 0.05$, $c = 0.1$, $a = 10$, $b = 5$, $d_m = d_f = 0.5$, $\lambda = 0$, $N = 100$, $\lambda' = 0.01$, $N' = 200$, $s = 0.025$, $t_a = 0$, $\bar{t}' = 1$. We explored 5 different values of the parameter c_{RI} and we launched 10 replicate runs for each parameter set.

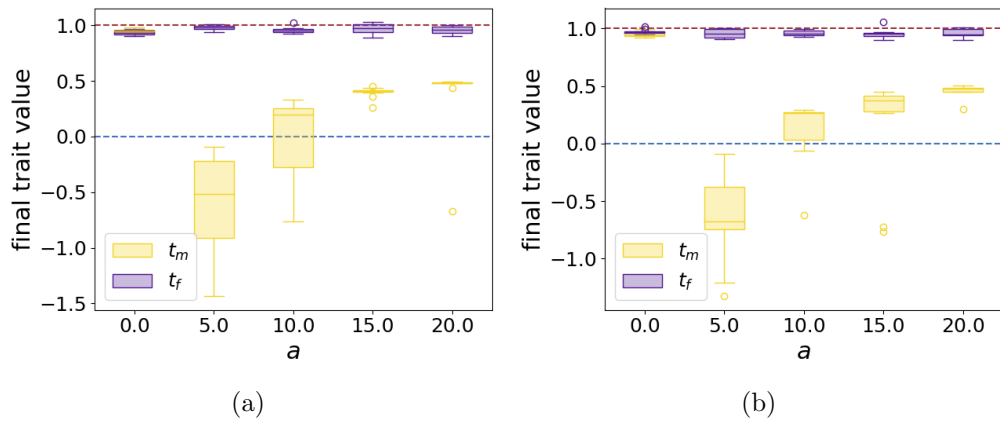


Fig. A4.11: **Boxplots of final mean male (yellow) and female (purple) traits values for different female choosiness a using individual-centred simulations assuming (a) independent genetic basis or (b) partially common genetic basis of male and female trait.** We assume: (a) $r_{T_m T_f} = 0.25$, $r_{T_f P_f} = 0.25$ and (b) $r_{T_1 T_2} = 0.25$, $r_{T_2 T_3} = 0.25$, $r_{T_3 P_f} = 0.25$. We also assume: $G_0 = 0.0025$, $\mu = 0.05$, $c = 0.1$, $c_{RI} = 0.5$, $b = 5$, $d_m = d_f = 0.5$, $\lambda = 0$, $N = 100$, $\lambda' = 0.01$, $N' = 200$, $s = 0.025$, $t_a = 0$, $\bar{t}' = 1$. We explored 5 different values of the parameter a and we launched 10 replicate runs for each parameter set.

A4.10 Investigation of the effect of sexually contrasted predation on the evolution of FLM using individual-centred simulations

In line with the result given by the deterministic quantitative model shown in Figure 4.5(a), the level of sexual dimorphism decreases with the ratio of basic predation rate on males and females (d_m/d_f) in individual-centred simulations (Figure A4.12). This confirms that sexually contrasted predation can drive the evolution of FLM.

The deterministic quantitative model also highlights that only intermediate values of developmental constraints allow the evolution of FLM (Figure 4.5(b)). Studying the mean male and female trait values in the individual-centred simulations allows to confirm this result (Figure A4.13). However, without developmental constraints ($s = 0$), male trait became highly variable, due to a lack of selection. By contrast, female trait, under strong predation pressure, has a low variance. Relaxed selection on males may allow to trait values leading to poor mimicry to emerge in males, while the stronger selection on females favours their accurate mimicry. This sexually-different selection regime thus increases sexual dimorphism.

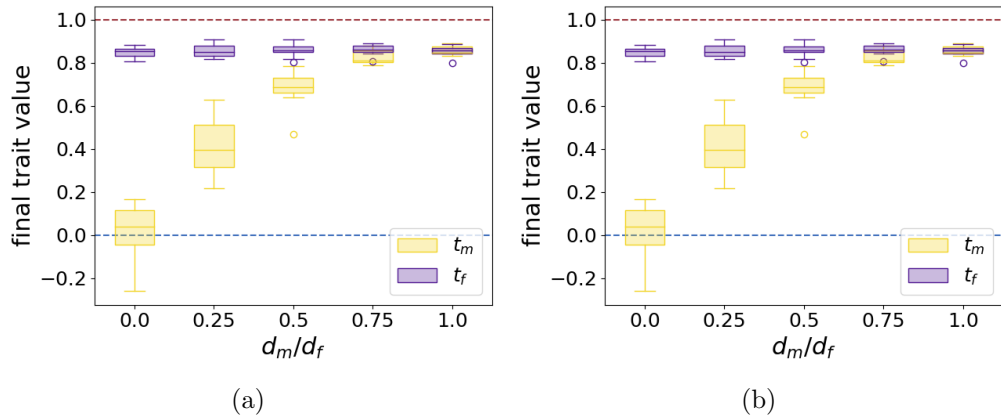


Fig. A4.12: **Boxplots of final mean male (yellow) and female (purple) traits values for different ratio of basic predation rate on males and females d_m/d_f using individual-centred simulations assuming either (a) independent genetic basis or (b) partially common genetic basis of male and female trait.** We assume: (a) $r_{T_m T_f} = 0.25$, $r_{T_f P_f} = 0.25$ and (b) $r_{T_1 T_2} = 0.25$, $r_{T_2 T_3} = 0.25$, $r_{T_3 P_f} = 0.25$. We also assume: $G_0 = 0.0025$, $\mu = 0.05$, $c = 0$, $a = 0$, $c_{RI} = 0$, $b = 5$, $d_f = 0.5$, $\lambda = 0$, $N = 100$, $\lambda' = 0.01$, $N' = 200$, $s = 0.1$, $t_a = 0$, $\bar{t}' = 1$. We explored 5 different values of the parameter d_m/d_f and we launched 10 replicate runs for each parameter set.

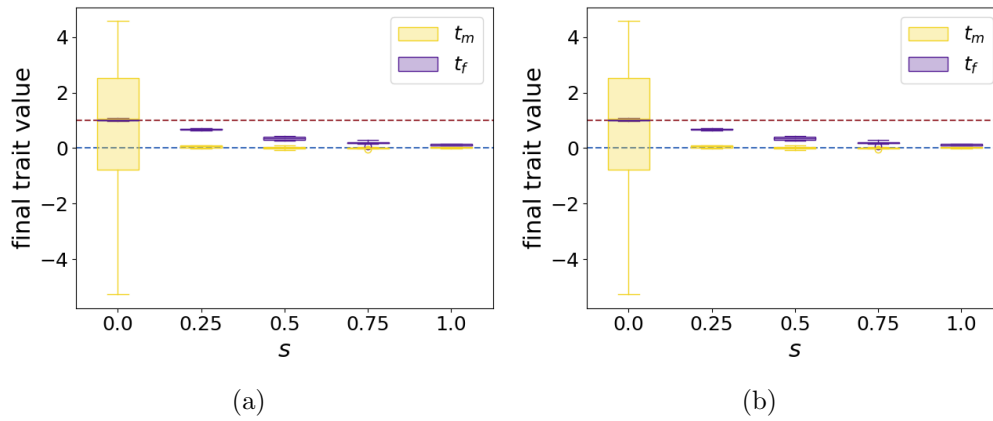


Fig. A4.13: **Boxplots of final mean male (yellow) and female (purple) traits values for different strength of developmental constraints s using individual-centred simulations assuming either (a) independent genetic basis or (b) partially common genetic basis of male and female trait.** We assume: (a) $r_{T_m T_f} = 0.25$, $r_{T_f P_f} = 0.25$ and (b) $r_{T_1 T_2} = 0.25$, $r_{T_2 T_3} = 0.25$, $r_{T_3 P_f} = 0.25$. We also assume: $G_0 = 0.0025$, $\mu = 0.05$, $c = 0$, $a = 0$, $c_{RI} = 0$, $b = 5$, $d_m = 0.05$, $d_f = 0.5$, $\lambda = 0$, $N = 100$, $\lambda' = 0.01$, $N' = 200$, $t_a = 0$, $\bar{t}' = 1$. We explored 5 different values of the parameter s and we launched 10 replicate runs for each parameter set.

A4.11 Exploring the relative divergence of males and females from the ancestral trait using individual-centred simulations

A4.11.1 FLM caused by reproductive interference

The deterministic quantitative model and individuals-centred simulations show the same impact of the distance between the ancestral and the mimetic traits $|t' - t_a|$ and of female choosiness a on (a)(d) the difference between the level of divergence in males and females $|\bar{t}_m^* - t_a| - |\bar{t}_f^* - t_a|$ (Figures 4.6(c) and A4.14(a)(d)). The individual-centred simulations confirm that low distance between the ancestral and the mimetic traits ($|t' - t_a|$), as well as intermediate values of female choosiness (a), both leads to a higher trait divergence in male (Figure A4.14(a)(d)). However, when the ancestral trait is close to the trait displayed in the *model* species ($t_a = 0.99, t' = 1$), the different models then predict a different evolution of mean male trait value:

- Using the deterministic quantitative model, male traits value diverge from the mimetic trait towards the ancestral trait value (Figure 4.6(a)).
- Using individuals-centred simulations, final male trait values are centred around the mimetic trait (Figure A4.14(b)(e)). Male traits also diverge but not necessarily toward the ancestral trait because stochasticity allows male trait to reach higher values than the mimetic trait value (Figure A4.16).

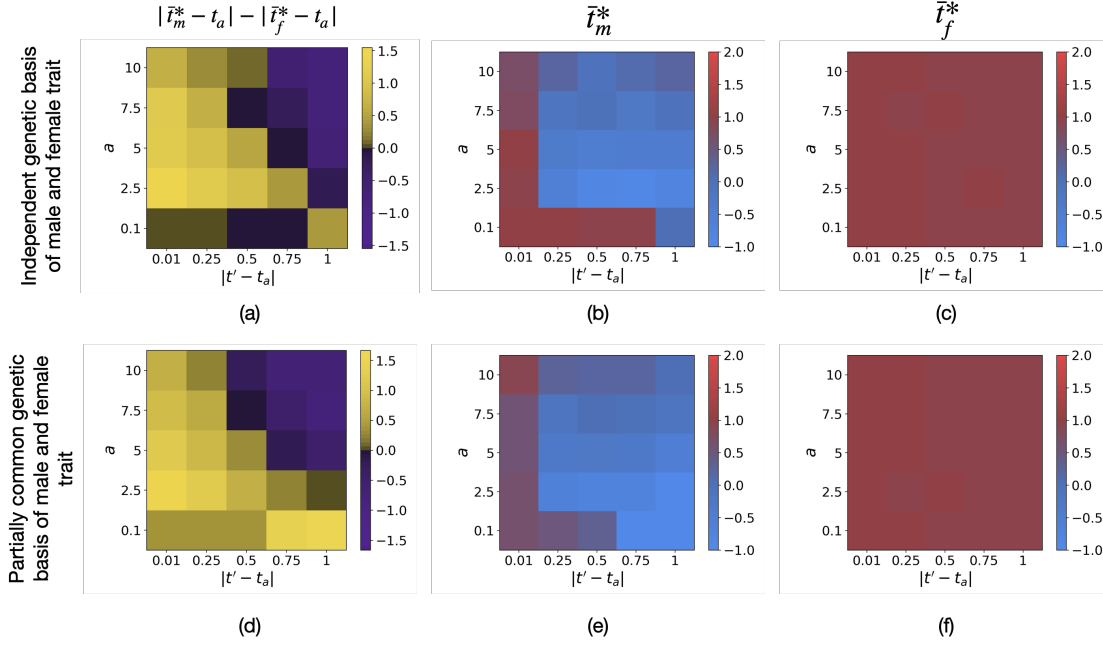


Fig. A4.14: Influence of the distance between the ancestral and the mimetic traits $|t' - t_a|$ and of female choosiness a on (a)(d) the difference between the level of divergence in males and females $|\bar{t}_m^* - t_a| - |\bar{t}_f^* - t_a|$, (b)(e) final male trait \bar{t}_m^* and (c)(f) final female trait \bar{t}_f^* using individual-centred simulations assuming either (a)(b)(c) independent genetic basis or (d)(e)(f) partially common genetic basis of male and female trait. We assume: (a) $r_{T_m T_f} = 0.25$, $r_{T_f P_f} = 0.25$ and (b) $r_{T_1 T_2} = 0.25$, $r_{T_2 T_3} = 0.25$, $r_{T_3 P_f} = 0.25$. We also assume: $G_0 = 0.0025$, $\mu = 0.05$, $c = 0.1$, $c_{RI} = 0.5$, $b = 5$, $d_m = d_f = 0.5$, $\lambda = 0$, $N = 100$, $\lambda' = 0.01$, $N' = 200$, $s = 0.025$, $\bar{t}' = 1$. We explored 5 different values of each parameter a and t_a and we launched 10 replicate runs for each parameter set.

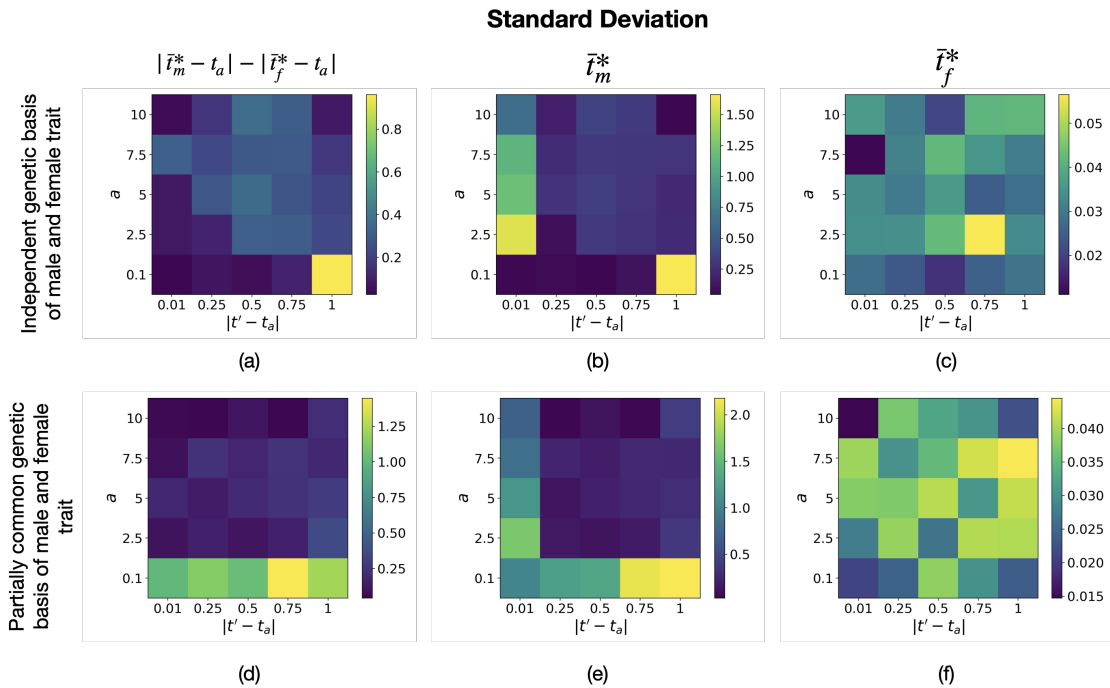


Fig. A4.15: Standard deviation associated with Figure A4.14 of (a)(d) the difference between the level of divergence in males and females $|\bar{t}_m^* - t_a| - |\bar{t}_f^* - t_a|$, (b)(e) final male trait \bar{t}_m^* and (c)(f) final female trait \bar{t}_f^* using individual-centred simulations assuming (a)(b)(c) independent genetic basis or (d)(e)(f) partially common genetic basis of male and female trait.

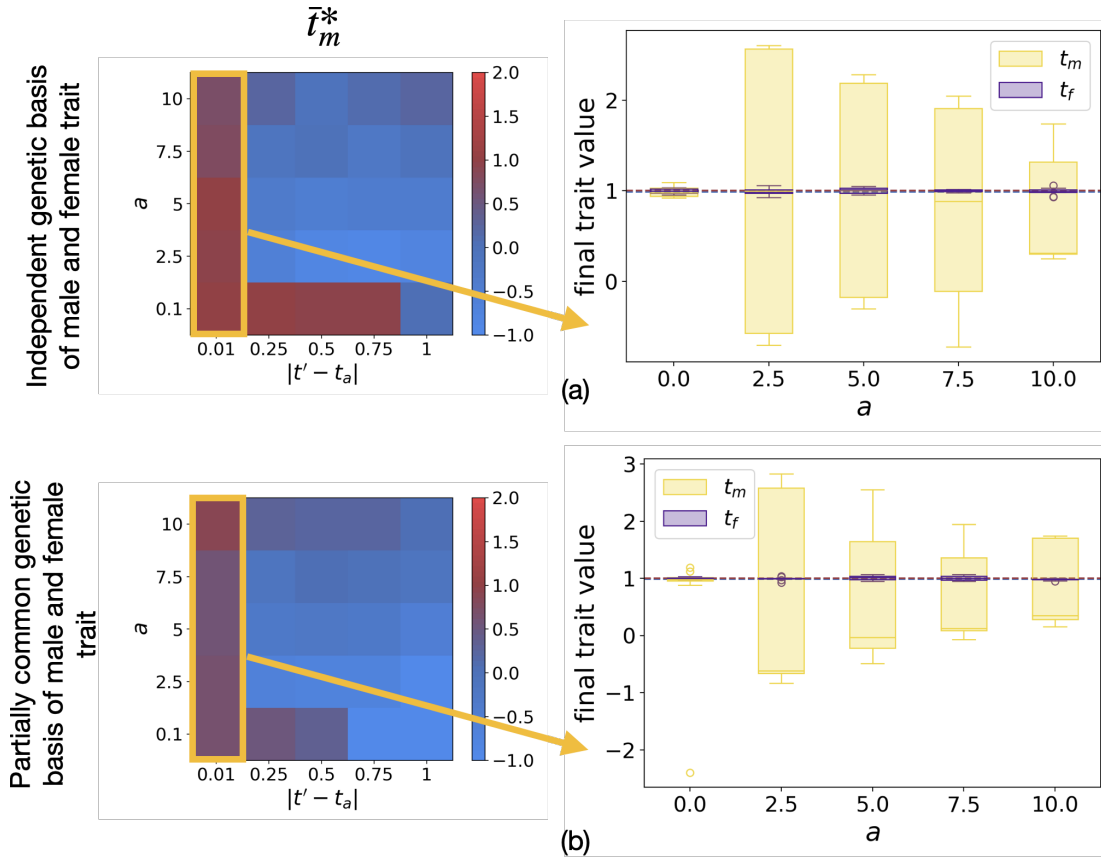


Fig. A4.16: Boxplots of final mean male (yellow) and female (purple) traits values for different female choosiness a using individual-centred simulations assuming either (a) independent genetic basis or (b) partially common genetic basis of male and female trait. We assume: (a) $r_{t_m t_f} = 0.25$, $r_{T_f P_f} = 0.25$ and (b) $r_{T_1 T_2} = 0.25$, $r_{T_2 T_3} = 0.25$, $r_{T_3 P_f} = 0.25$. We also assume: $G_0 = 0.0025$, $\mu = 0.05$, $c = 0.1$, $c_{RI} = 0.5$, $b = 5$, $d_m = d_f = 0.5$, $\lambda = 0$, $N = 100$, $\lambda' = 0.01$, $N' = 200$, $s = 0.025$, $t_a = 0.99$, $\bar{t}' = 1$. We explored 5 different values of the parameter a and we launched 10 replicate runs for each parameter set.

A4.11.2 FLM caused by sexually contrasted predation

The deterministic quantitative model shows that, when FLM is caused by sexually contrasted predation ($d_f > d_m$ and $a = 0$), sexual dimorphism always stems from the evolution of female phenotypes away from the ancestral trait, *i.e.* $|\bar{t}_f^* - t_a| > |\bar{t}_m^* - t_a|$ (see Appendix 5 and see Figure 4.2(a) for an illustration). Individual-centred simulations confirm this pattern (Figure A4.17), except when the distance between the ancestral trait and the mimetic trait is low ($|t_a - t'| = 0.01$). In this case, developmental constraints and predation promote the same trait value ($t_a \simeq t'$). The higher stabilising selection in females, caused by a higher predation pressure, implies that female trait diverge less from the ancestral trait than males (Figure A4.19).

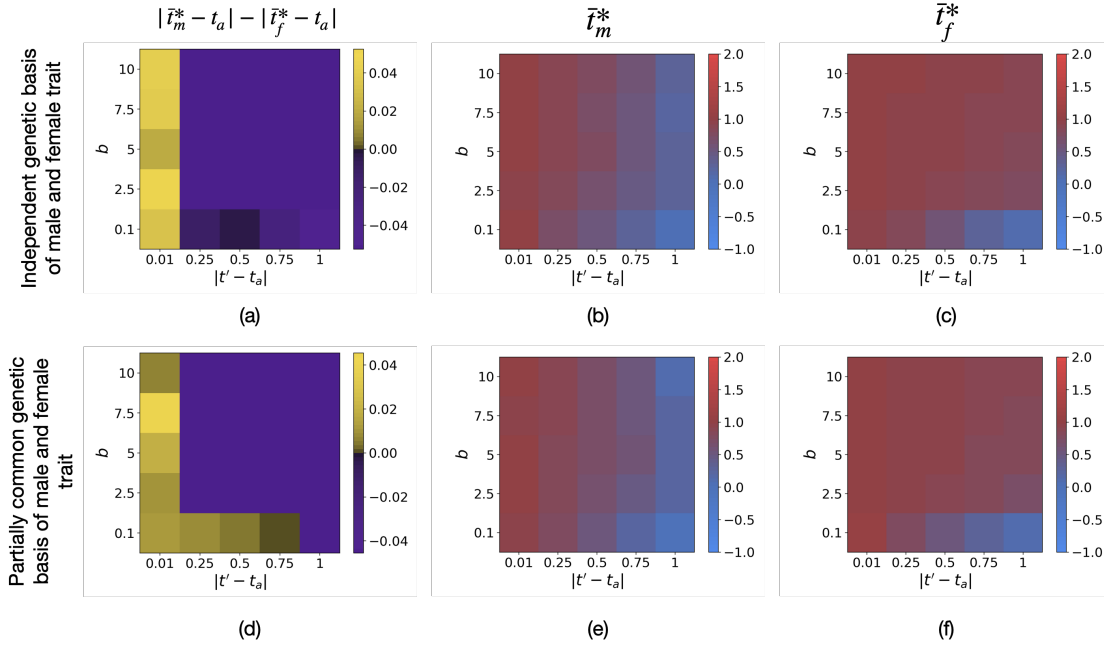


Fig. A4.17: Influence of the distance between the ancestral and the mimetic traits $|t' - t_a|$ and of predator discrimination b on (a)(d) the difference between the level of divergence in males and females $|\bar{t}_m^* - t_a| - |\bar{t}_f^* - t_a|$, (b)(e) final male trait \bar{t}_m^* and (c)(f) final female trait \bar{t}_f^* using individual-centred simulations assuming either (a)(b)(c) independent genetic basis or (d)(e)(f) partially common genetic basis of male and female trait. We assume: (a) $r_{T_m T_f} = 0.25$, $r_{T_f P_f} = 0.25$ and (b) $r_{T_1 T_2} = 0.25$, $r_{T_2 T_3} = 0.25$, $r_{T_3 P_f} = 0.25$. We also assume: $G_0 = 0.0025$, $\mu = 0.05$, $c = 0$, $a = 0$, $c_{RI} = 0$, $d_m = 0.1$, $d_f = 0.5$, $\lambda = 0$, $N = 100$, $\lambda' = 0.01$, $N' = 200$, $s = 0.1$, $\bar{t}' = 1$. We explored 5 different values of each parameter b and t_a and we launched 10 replicate runs for each parameter set.

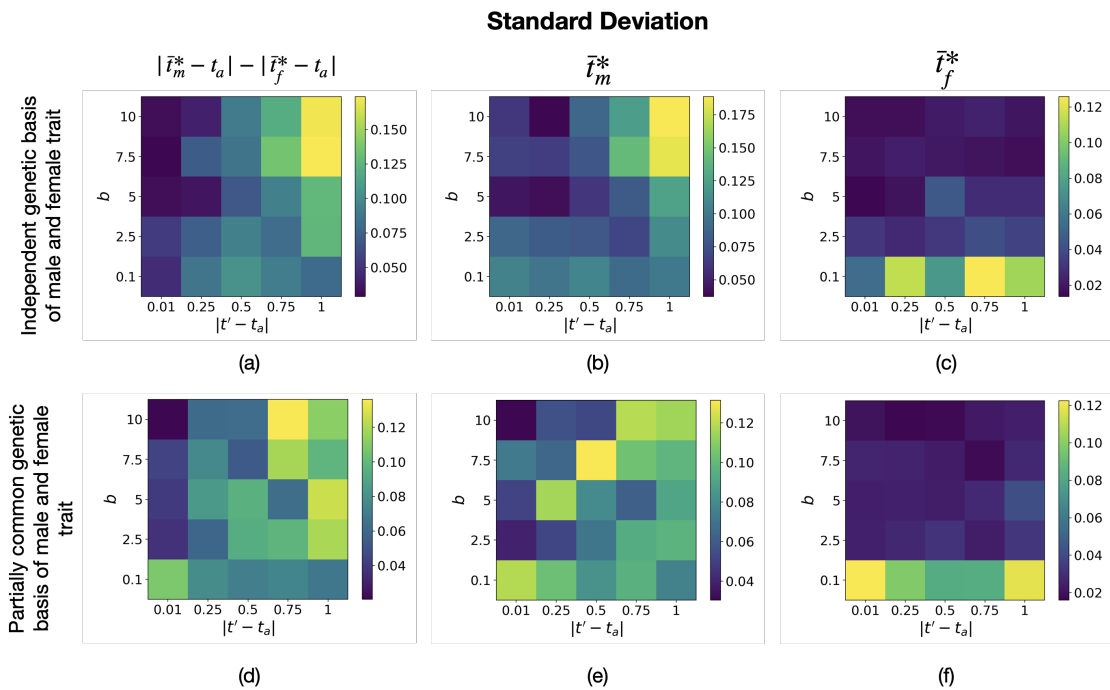


Fig. A4.18: Standard deviation associated with Figure A4.17 of (a)(d) the difference between the level of divergence in males and females $|\bar{t}_m^* - t_a| - |\bar{t}_f^* - t_a|$, (b)(e) final male trait \bar{t}_m^* and (c)(f) final female trait \bar{t}_f^* using individual-centred simulations assuming either (a)(b)(c) independent genetic basis or (d)(e)(f) partially common genetic basis of male and female trait.

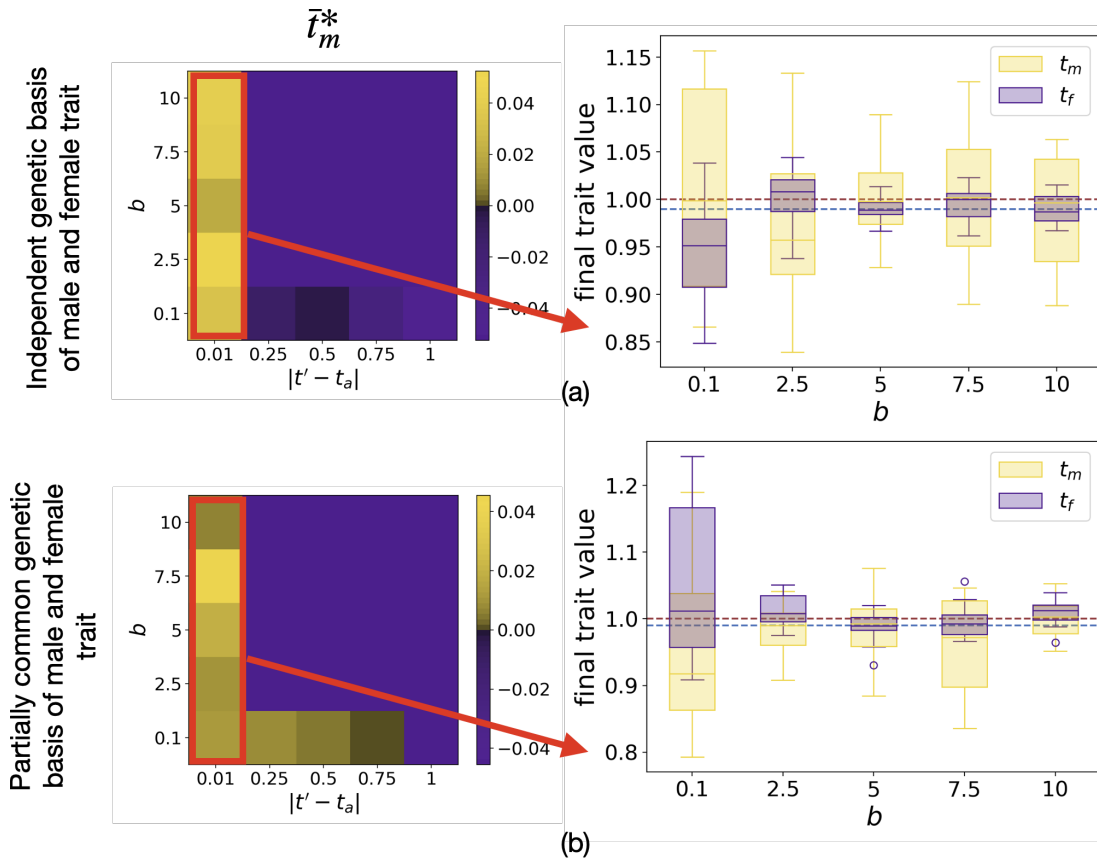


Fig. A4.19: Boxplots of final mean male (yellow) and female (purple) traits values for different female choosiness a using individual-centred simulations assuming either (a) independent genetic basis or (b) partially common genetic basis of male and female trait. We assume: (a) $r_{T_m T_f} = 0.25$, $r_{T_f P_f} = 0.25$ and (b) $r_{T_1 T_2} = 0.25$, $r_{T_2 T_3} = 0.25$, $r_{T_3 P_f} = 0.25$. We also assume: $G_0 = 0.0025$, $\mu = 0.05$, $c = 0$, $a = 0$, $c_{RI} = 0$, $d_m = 0.1$, $d_f = 0.5$, $\lambda = 0$, $N = 100$, $\lambda' = 0.01$, $N' = 200$, $s = 0.1$, $t_a = 0.99$, $\bar{t}' = 1$. We explored 5 different values of the parameter b and we launched 10 replicate runs for each parameter set.

A4.12 Additional figures: The evolution of FLM depends on defence level.

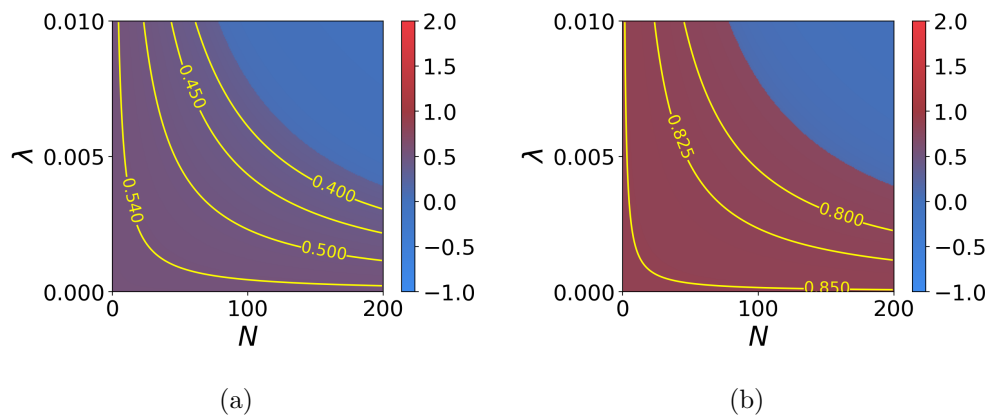


Fig. A4.20: Influence of the density N and of the individual defence level λ in the *focal* species on the equilibrium values of (a) male trait \bar{t}_m^* and (b) female trait \bar{t}_f^* when female-limited mimicry is caused by sexually contrasted predation ($d_f > d_m$, $a = 0$). Yellow lines indicate equal trait value. We assume: $G_{t_m} = G_{t_f} = G_{p_f} = 0.01$, $G_{t_m t_f} = 0.001$, $c_{RI} = 0$, $c = 0$, $a = 0$, $b = 5$, $d_m = 0.01$, $d_f = 0.05$, $\lambda' = 0.01$, $N' = 200$, $s = 0.01$, $t_a = 0$, $t' = 1$.

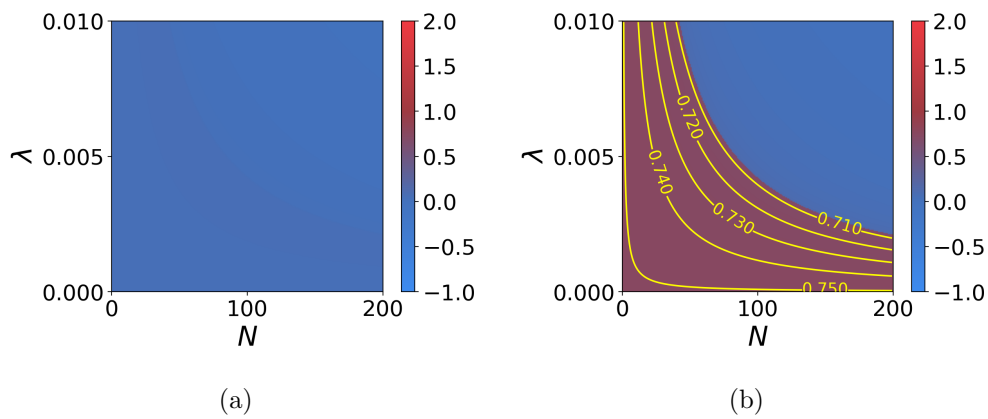


Fig. A4.21: Influence of the density N and of the individual defence level λ in the *focal* species on the equilibrium values of (a) male trait \bar{t}_m^* and (b) female trait \bar{t}_f^* when female-limited mimicry is caused by sexually contrasted predation ($d_f > d_m$, $a = 0$). Yellow lines indicate equal trait value. We assume: $G_{t_m} = G_{t_f} = G_{p_f} = 0.01$, $G_{t_m t_f} = 0.001$, $c_{RI} = 0$, $c = 0$, $a = 0$, $b = 5$, $d_m = 0.01$, $d_f = 0.05$, $\lambda' = 0.01$, $N' = 200$, $s = 0.02$, $t_a = 0$, $t' = 1$.

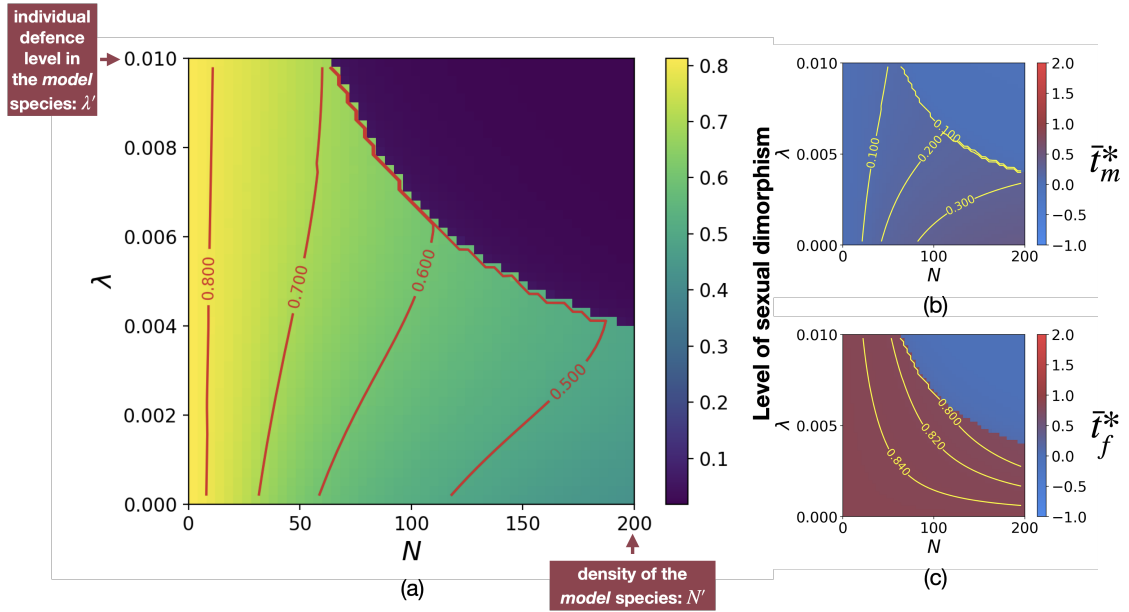


Fig. A4.22: Influence of the density N and of the individual defence level λ in the *focal* species on the equilibrium values of (a) the level of sexual dimorphism $|\bar{t}_m^* - \bar{t}_f^*|$, (b) male trait \bar{t}_m^* and (c) female trait \bar{t}_f^* when female-limited mimicry is generated by sexual selection caused by reproductive interference (c_{RI} , $a > 0$ and $d_f = d_m$). Red and yellow lines indicate equal levels of sexual dimorphism and trait value respectively. We assume: $G_{t_m} = G_{t_f} = G_{p_f} = 0.01$, $G_{t_m t_f} = 0.001$, $c_{RI} = 0.01$, $c = 0.1$, $a = 5$, $b = 5$, $d_m = d_f = 0.05$, $\lambda' = 0.01$, $N' = 200$, $s = 0.01$, $t_a = 0$, $t' = 1$.

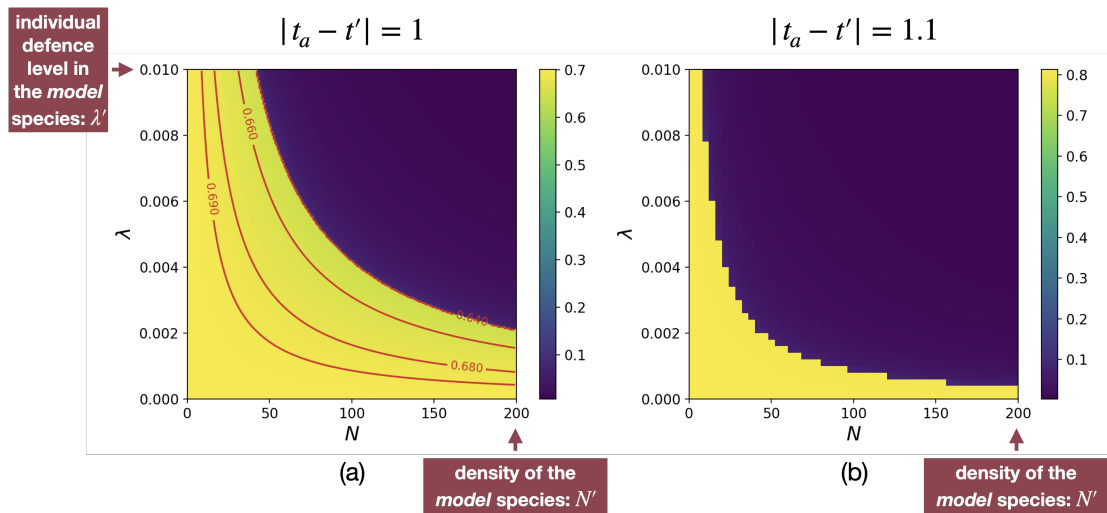


Fig. A4.23: Influence of the density N and of the individual defence level λ in the *focal* species on the equilibrium values of the level of sexual dimorphism ($|\bar{t}_m^* - \bar{t}_f^*|$) for different distances between the ancestral and the mimetic traits ((a) $|t_a - t'| = 1$ (b) $|t_a - t'| = 1.1$) when female-limited mimicry is caused by sexually contrasted predation ($d_f > d_m$, $a = 0$). Red lines indicate equal levels of sexual dimorphism. We assume: $G_{t_m} = G_{t_f} = G_{p_f} = 0.01$, $G_{t_m t_f} = 0.001$, $c_{RI} = 0$, $c = 0$, $a = 0$, $b = 5$, $d_m = 0.01$, $d_f = 0.05$, $\lambda' = 0.01$, $N' = 200$, $s = 0.02$, $t' = 1$.

A4.13 Investigation of the effect of defence level on the evolution of FLM using individual-centred simulations

A4.13.1 FLM caused by sexually contrasted predation

The deterministic quantitative model highlights that, when developmental constraints are high, the level of sexual dimorphism ($|\bar{t}_m^* - \bar{t}_f^*|$) decreases with the defence level in both males and females ($\lambda N/2$) (Figure 4.7(b)). Individual-centred simulations confirm this result (Figure A4.24).

By contrast, the deterministic quantitative model highlights that, when developmental constraints are low, the level of sexual dimorphism increases with the defence level in both males and females (Figure 4.7(a)). Individual-centred simulations confirm that, when developmental constraints are low, the level of sexual dimorphism increases with the individual defence level λ of the *focal* species (Figure A4.26). However, a discrepancy is observed for the effect of the density of the *focal* species: in this case, the level of sexual dimorphism no longer increases with with density of the *focal* species (Figure A4.26). Stochasticity of the mean male and female trait values in the population is indeed likely to increase sexual dimorphism. The amplitude of this stochastic effect is indeed reduced in population with higher density. In these larger populations, a more limited level of sexual dimorphism is observed (see figure A4.27).

A4.13.2 FLM caused by reproductive interference

Departing from the results obtained assuming predation differences between sexes, the deterministic quantitative model then shows that reproductive interference generates markedly higher sexual dimorphism for low values of population density in the *focal* species (Figure 4.8(a)). The individual-centred simulations are in line

with this result: a low value of the population density in the *focal* species ($N = 50$) leads to the evolution of high level of sexual dimorphism (Figure A4.28).

Using the deterministic quantitative model, mimicry toward the sympatric defended *model* species is no longer promoted in either sexes, when the level of defence within the *focal* species is high (Figures A4.20, A4.21 and 4.8(b)(c)) leading to sexual monomorphism. This result is observed under both selective hypotheses. The distance between the ancestral and the mimetic traits $|t' - t_a|$ limits mimicry in both sexes (Figure A4.23), highlighting the important role of the initial advantage and disadvantage of mimicry. Using individual-centred simulations, we nevertheless observed that male and female traits can get closer to the mimetic trait by stochasticity, enabling mimicry to be promoted, when the level of defence within the *focal* species is high (Figures A4.24, A4.26 and A4.28).

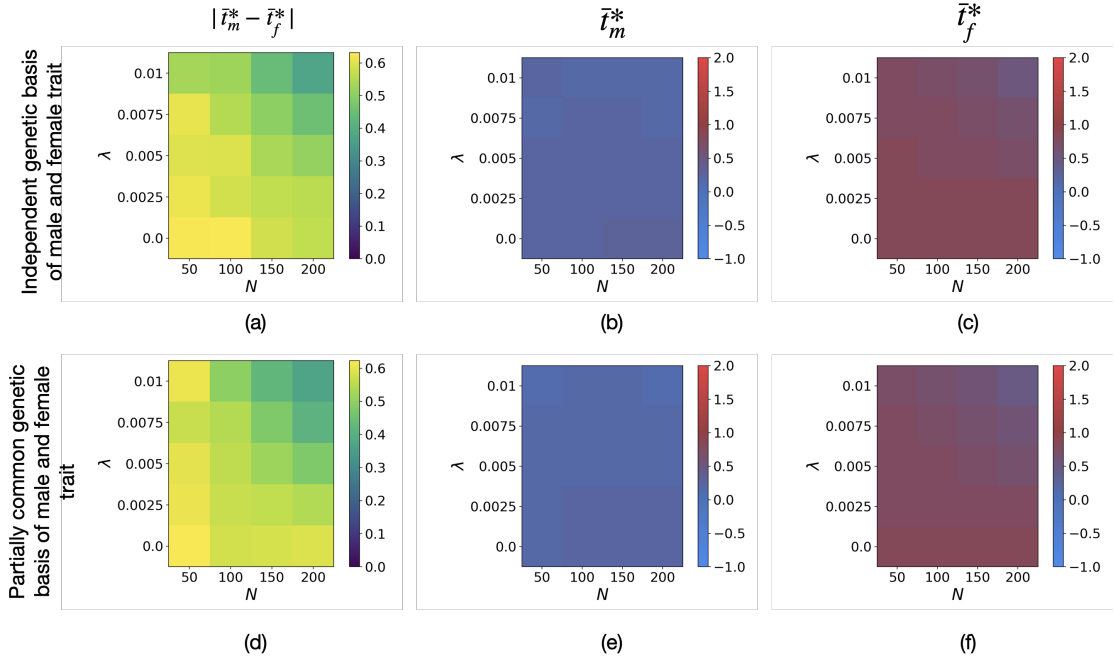


Fig. A4.24: Influence of the density N and of the individual defence level λ in the *focal* species on the equilibrium values of (a)(d) the level of sexual dimorphism $|\bar{t}_m^* - \bar{t}_f^*|$, (b)(e) male trait \bar{t}_m^* and (c)(f) female trait \bar{t}_f^* when selective constraints are high using individual-centred simulations assuming either (a)(b)(c) independent genetic basis or (d)(e)(f) partially common genetic basis of male and female trait. We assume: (a) $r_{T_m T_f} = 0.25$, $r_{T_f P_f} = 0.25$ and (b) $r_{T_1 T_2} = 0.25$, $r_{T_2 T_3} = 0.25$, $r_{T_3 P_f} = 0.25$. We also assume: $G_0 = 0.0025$, $\mu = 0.05$, $c = 0$, $a = 0$, $c_{RI} = 0$, $b = 5$, $d_m = 0.1$, $d_f = 0.5$, $\lambda' = 0.01$, $N' = 200$, $s = 0.1$, $t_a = 0$, $\bar{t}' = 1$. We explored respectively 4 and 5 different values of the parameters N and λ and we launched 100 replicate runs for each parameter set.

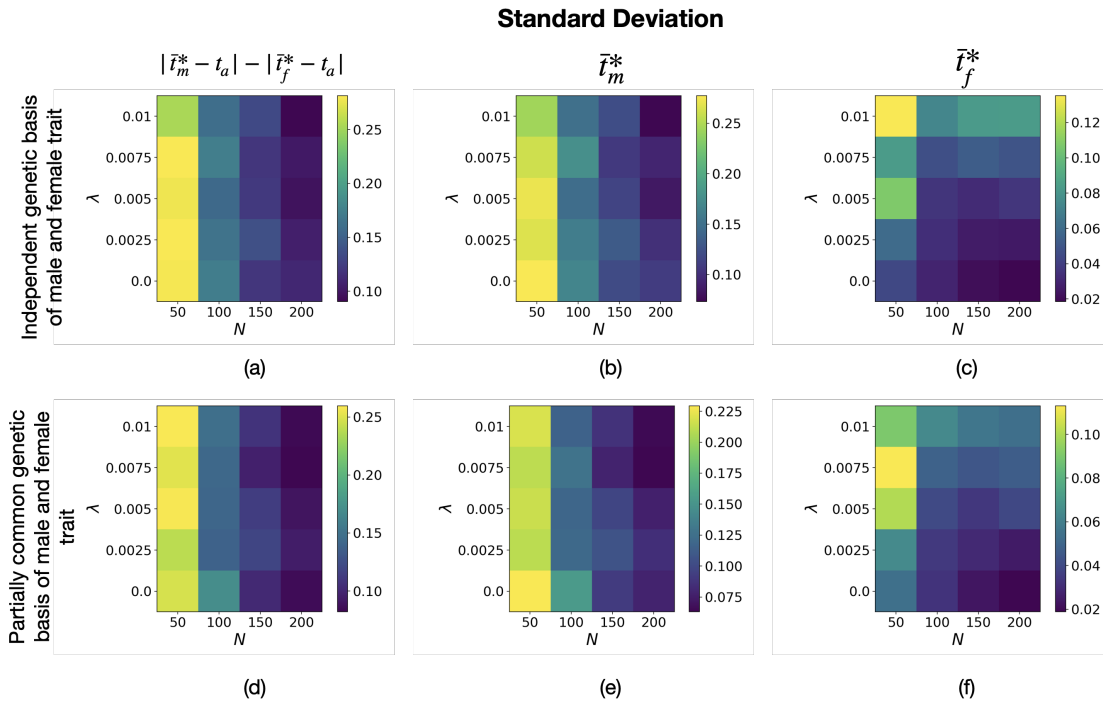


Fig. A4.25: Standard deviation associated with Figure A4.24 of (a)(d) the level of sexual dimorphism $|\bar{t}_m^* - \bar{t}_f^*|$, (b)(e) final male trait \bar{t}_m^* and (c)(f) final female trait \bar{t}_f^* when selective constraints are high using individual-centred simulations assuming either (a)(b)(c) independent genetic basis or (d)(e)(f) partially common genetic basis of male and female trait.

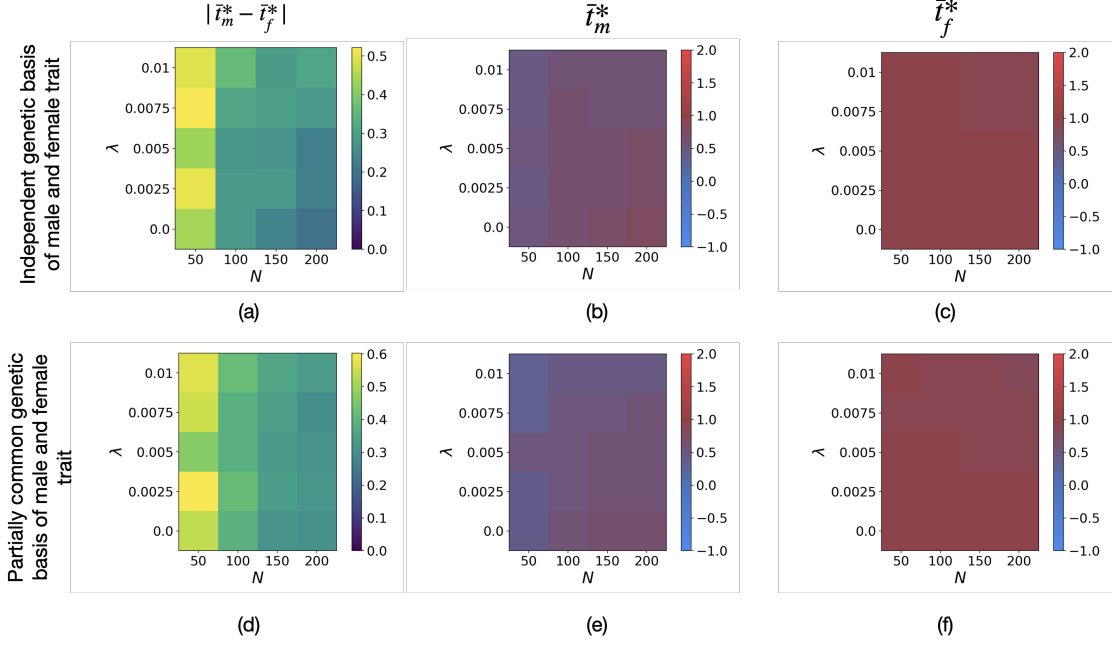


Fig. A4.26: Influence of the density N and of the individual defence level λ in the *focal* species on the equilibrium values of (a)(d) the level of sexual dimorphism $|\bar{t}_m^* - \bar{t}_f^*|$, (b)(e) male trait \bar{t}_m^* and (c)(f) female trait \bar{t}_f^* when selective constraints are low using individual-centred simulations assuming either (a)(b)(c) independent genetic basis or (d)(e)(f) partially common genetic basis of male and female trait. We assume: (a) $r_{T_m T_f} = 0.25$, $r_{T_f P_f} = 0.25$ and (b) $r_{T_1 T_2} = 0.25$, $r_{T_2 T_3} = 0.25$, $r_{T_3 P_f} = 0.25$. We also assume: $G_0 = 0.0025$, $\mu = 0.05$, $c = 0$, $a = 0$, $c_{RI} = 0$, $b = 5$, $d_m = 0.1$, $d_f = 0.5$, $\lambda' = 0.01$, $N' = 200$, $s = 0.05$, $t_a = 0$, $\bar{t}' = 1$. We explored respectively 4 and 5 different values of the parameters N and λ and we launched 100 replicate runs for each parameter set.

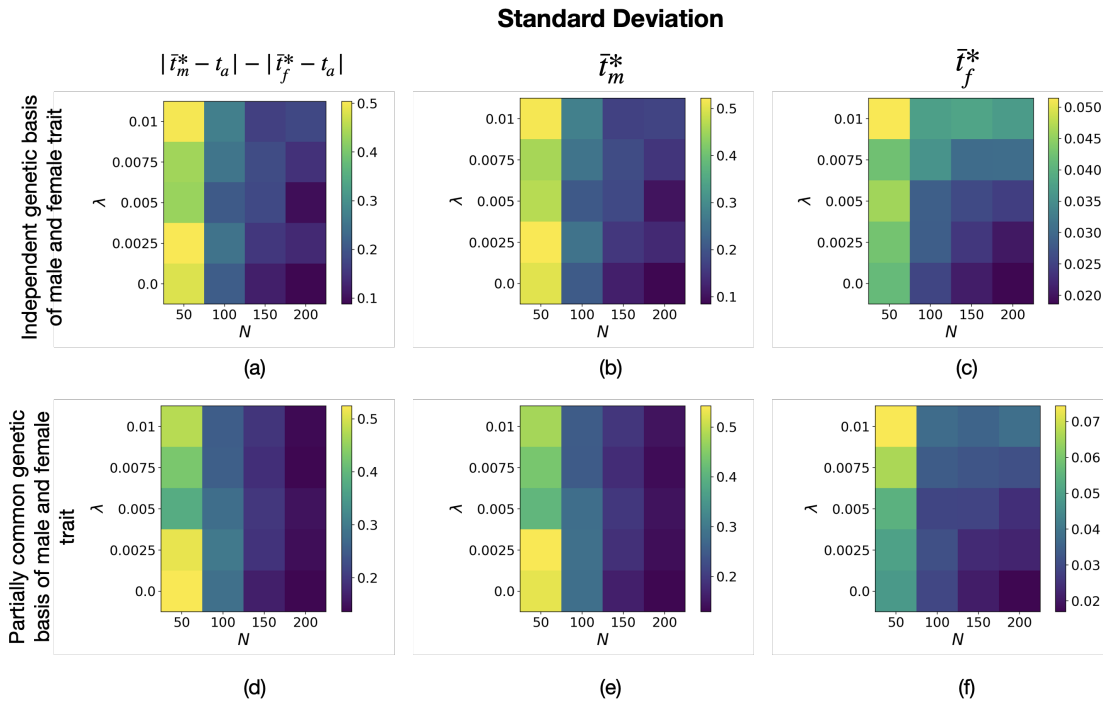


Fig. A4.27: Standard deviation associated with Figure A4.26 of (a)(d) the level of sexual dimorphism $|\bar{t}_m^* - \bar{t}_f^*|$, (b)(e) final male trait \bar{t}_m^* and (c)(f) final female trait \bar{t}_f^* when selective constraints are low using individual-centred simulations assuming either (a)(b)(c) independent genetic basis or (d)(e)(f) partially common genetic basis of male and female trait.

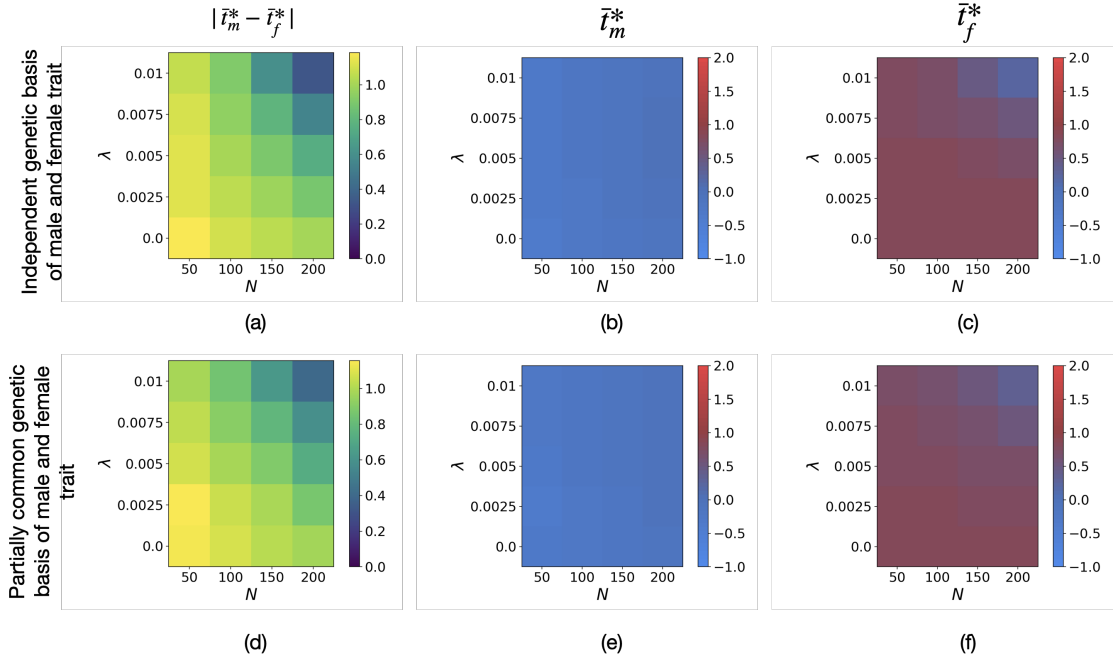


Fig. A4.28: Influence of the density N and of the individual defence level λ in the *focal* species on the equilibrium values of (a)(d) the level of sexual dimorphism $|\bar{t}_m^* - \bar{t}_f^*|$, (b)(e) male trait \bar{t}_m^* and (c)(f) female trait \bar{t}_f^* when selective constraints are high using individual-centred simulations, assuming either (a)(b)(c) independent genetic basis or (d)(e)(f) partially common genetic basis of male and female trait. We assume: (a) $r_{T_m T_f} = 0.25$, $r_{T_f P_f} = 0.25$ and (b) $r_{T_1 T_2} = 0.25$, $r_{T_2 T_3} = 0.25$, $r_{T_3 P_f} = 0.25$. We also assume: $G_0 = 0.0025$, $\mu = 0.05$, $c = 0.1$, $a = 5$, $c_{RI} = 0.5$, $b = 5$, $d_m = 0.5$, $d_f = 0.5$, $\lambda' = 0.01$, $N' = 200$, $s = 0.1$, $t_a = 0$, $\bar{t}' = 1$. We explored respectively 4 and 5 different values of the parameters N and λ and we launched 100 replicate runs for each parameter set.

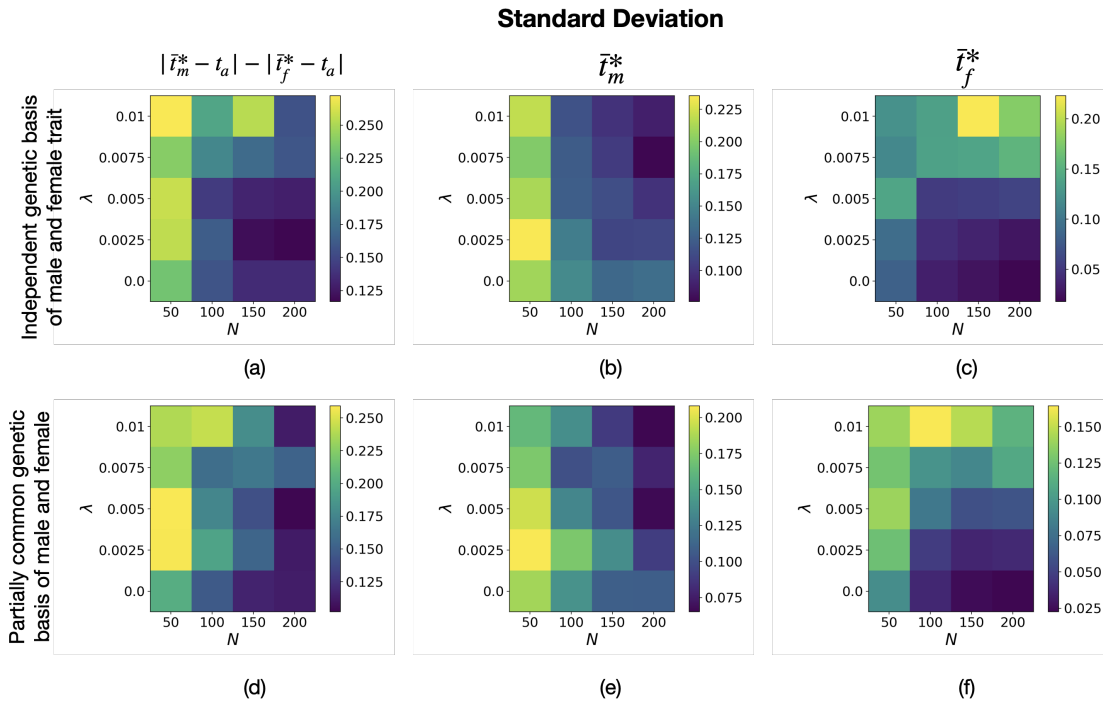


Fig. A4.29: Standard deviation associated with Figure A4.28 of (a)(d) the level of sexual dimorphism $|\bar{t}_m^* - \bar{t}_f^*|$, (b)(e) final male trait \bar{t}_m^* and (c)(f) final female trait \bar{t}_f^* when selective constraints are high, using individual-centred simulations assuming either (a)(b)(c) independent genetic basis or (d)(e)(f) partially common genetic basis of male and female trait.

Part III

Why and when are adaptive traits used in mate choice ?

I now investigate why and when traits involved in local adaptation are targeted by mate preference. Preference targeting adaptive traits can enhance offspring fitness, but we also see in Part II that such preference can lead to reproductive interference when locally adapted traits are shared between sympatric species. Preference may rather target other traits, unlinked to local adaptation, but differing between sympatric species. Multiple traits preference targeting both adaptive traits, as well as additional species recognition traits, may produce adapted offspring, without implying reproductive interference. I investigate the evolution of preference based on multiple traits, when the traits used as cues can be either neutral or submitted to shared selective pressures favoring trait similarity between sympatric species (**Chapter 5**).

CHAPTER 5

Evolution of mate preference towards multiple traits in sympatric species

Ludovic Maisonneuve, Charline Smadi and Violaine
Llaurens

Abstract

So far we studied the evolution of mate preference based on one trait, and its consequence on phenotypic distribution. However the evolutionary factors determining which and how many traits are targeted by mate choice are largely unknown. In sympatric species, trait variation is shaped by similar selective pressure, promoting similar adaptive traits in the different species. When preference targets such adaptive traits, the similarity between species induce heterospecific matings and costs for the choosy partners. The evolution of preference for different traits thus likely depends on the ecological interactions between species. Using a mathematical model, we thus study the evolution of preference towards two evolving traits shared by sympatric species and we investigate how selective regimes on traits, opportunity cost and sensory trade-off shape the evolution of preference for multiple traits. We show that the conflict between adaptation and species recognition may promote multiple traits preference targeting an adaptive trait as well as another trait relevant for species recognition. However we show that opportunity costs limit the evolution of such multiple traits preference. Because adaptation reduces phenotypic diversity, opportunity costs promotes preference based on adaptive traits rather than on traits relevant for species recognition.

Introduction

The evolution of mate preference plays a major role in the diversification of traits and species in the wild. Yet, little is known on the evolutionary factors determining the traits preferentially targeted by preferences, and especially the number of different cues used during mate choice.

Preferences are based on traits displayed by the parents, but their evolution usually depends on the indirect fitness benefit in the offspring (Neff & Pitcher, 2005). The fitness of the offspring depends not only on the intraspecific competition but also on the ecological interactions with sympatric species. When poorly-divergent species occur in sympatry, mate preferences targeting certain traits can be pro-

moted because of the reduced fitness in the hybrids (Merrill *et al.*, 2012), but also because of the reduction in costly sexual interactions with heterospecifics (Gröning & Hochkirch, 2008). The evolution of preferences may therefore strongly depend on the selection regimes acting on the targeted traits within species, but also on the distribution of these traits in other species living in sympatry. Such multifarious selection acting on the different traits displayed by males may then favor the evolution of female preferences targeting several traits. Using multiple cues may indeed improve some components of the fitness in the offspring and/or enhance recognition of conspecific males (Candolin, 2003).

Multiple traits preference may then be promoted when targeting traits associated with different components of the indirect fitness benefit (*e.g.* (Doucet & Montgomerie, 2003; Girard *et al.*, 2015; Dale & Slagsvold, 1996)). Theoretical modeling show that preference towards multiple traits providing different indirect fitness benefit can evolve (Iwasa & Pomiankowski, 1994). The evolution of preference towards multiple non-adaptive cues can occur, when these cues provide greater reproductive success in the sons (*sexy sons hypothesis*) (Pomiankowski & Iwasa, 1993), suggesting that sexual selection can also promote the evolution of preference for multiple traits. Furthermore, selection promoting species recognition also promotes the evolution of preference for multiple traits that differentiate closely related species (Hohenlohe & Arnold, 2010; Vortman *et al.*, 2013; Patten *et al.*, 2004). While several sexual and natural selection have been suggested to favor the evolution of multiple traits preference, such evolution is likely to crucially depend on trait variations and covariation within and among sympatric species. By contrast with classical 'magic' traits (Servedio *et al.*, 2011), similar traits may be promoted by natural selection in different sympatric species (*e.g.* in mimetic species, Boussens-Dumon & Llaurens (2021)), indirect fitness benefit may then induce selection on preference conflicting with species recognition (*e.g.* (Gumm & Gabor, 2005; Higgie & Blows, 2007)). For example, in the spadefoot toad, preference for mating call increases the number of eggs fertilized in choosy females but leads to reproductive interference, because of the similarity of call between sympatric species (Pfennig, 2000). Preferences targeting multiple traits may then

allow to improve both offspring fitness through the transmission of adapted alleles and species recognition. For example, in field crickets of the genus *Teleogryllus*, female targets both (1) CHCs, providing fitness benefits to their offspring (Berson & Simmons, 2019), and (2) male calling song (Hill *et al.*, 1972) that differentiate sympatric species (Moran *et al.*, 2020).

While preference based on multiple traits may be promoted by natural and sexual selection, several constraints might limit the number of traits targeted by preference. Preferences are generally associated with fixed cost generated by mate searching, and these costs might be increased when preference targets multiple traits. Theoretical studies indeed show that the joint fixed costs of preference based on different trait indeed promotes preference based on single trait providing the greatest benefit (Schluter & Price, 1993), especially when the joint fixed costs quickly increases with the strength of preference for each trait (Pomiankowski & Iwasa, 1993; Iwasa & Pomiankowski, 1994). The evolution of preference for multiple traits may also be limited by the number of available partners displaying the preferred combination of traits. Opportunity costs associated with female rejection in choosy females may then increase when the number of targeted traits grows.

The evolution of multiple traits preference may also be limited by the complex cognitive processes involved, explaining the low number of traits used in mate choice in some clades (Candolin, 2003). Multiple traits-based mate choice may thus preferentially evolve in species where multiple sensory systems allow such cognitive integration. Evolutionary trade-off are often thought to limit the evolution of multiple sensory system: the development of sensory systems is frequently associated with the regression of others (Barton *et al.*, 1995; Nummela *et al.*, 2013). Moreover, physical constraints may generate sensory trade-offs: for example, visual system model of the surfperch reveals trade-off in the performance between luminance and chromatic detection, because of the limited numbers of the different types of cones in the eyes (Cummings, 2004). Neural integration of multiple information may also be limited, generating trade-offs in the use of multiple traits in decision. In the swordtail fish *Xiphophorus pygmaeus*, females express preference for a visual and an olfactory traits when there are exposed to the variation of only one trait

within potential mate. However, when both traits vary within potential mates, females do not express preference (Crapon de Caprona & Ryan, 1990), suggesting that sensory trade-off limits the use of multiple traits in preference.

These contradictory developmental and ecological factors call for a general framework determining the evolution of preferences towards different traits shared between sympatric species, that may be either neutral or shaped by natural and sexual selection. Here, we thus use mathematical modeling to investigate the evolution of preference based on multiple traits. We study the evolution of preference towards two evolving traits (T_1 and T_2) shared by two sympatric species (A and B) aiming at identifying how selection regimes acting on the targeted traits, as well as reproductive interference between species favor preference targeting a single *vs.* multiple traits.

Method

Modelling the evolution of female preference targeting different traits

We consider two closely-related species (A & B) living in sympatry, and assume that individuals from both species display two main traits controlled by a single haploid locus (loci T_1 and T_2 respectively, with two possible alleles 0 or 1). We fix the genotypic distribution in species B and we study the evolution of traits and preference on those traits in the focal species species A .

Only females express mate preference towards the traits displayed by males, and their preference depends on their own phenotype (following the matching rule described in Kopp *et al.* (2018)): we assume assortative preference whereby preferentially mate with males displaying traits similar to their own traits (Figure 5.1). Female assortative preference can target either traits (1 and 2) displayed by the males. A preference modifier locus M controls the relative level of attention of females toward trait 1 *vs.* trait 2 during their choice expressed by males (referred

to as the preference direction γ). We assume that only two alleles can occur at locus M with different values of γ modulating the level of attention on either traits. The set of different loci is given by $\mathcal{L} = \{T_1, T_2, M\}$ and each genotype is a vector in $\mathcal{G} = \{0, 1\}^3$. We study the invasion of the mutant allele 1 associated with the value γ_m in the species A, where the allele 0, associated with the value γ_{wt} , was initially fixed.

We assumed that females can encounter and have sexual interactions with heterospecifics. Heterospecific sexual interactions lead to fitness costs but do not produce any viable offspring. The evolutionary fate of the mutant at locus M in species A may thus depend on (1) reproductive interference promoting preferences that enhance species recognition and (2) the selection regime acting on traits T_1 and T_2 , enhancing the offspring survival. We assume an infinite population and we track down the frequency of each genotype across generations in species A. We assume that a generation is composed of three steps: (1) natural selection, (2) reproduction and (3) mutation, as detailed below.

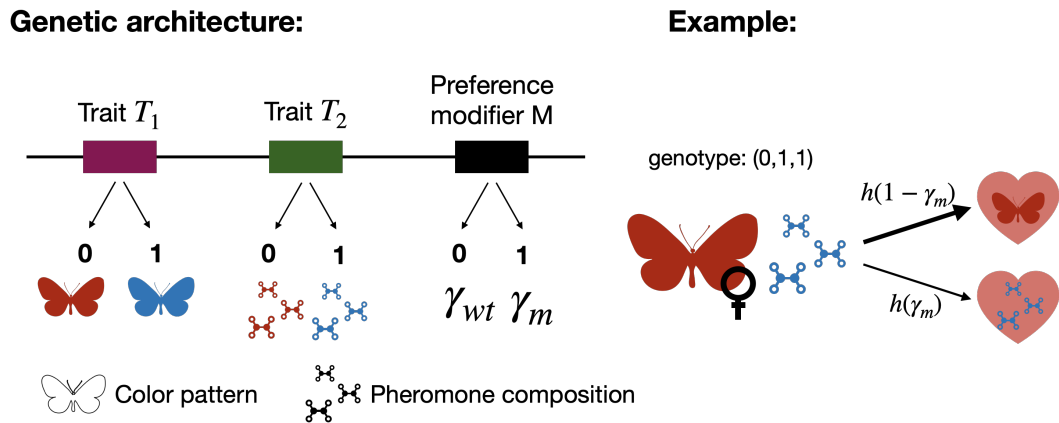


Fig. 5.1: **Genetic architecture underlying trait and preference in species A.** As an illustrative example, here we show trait 1 as wing coloration and the trait 2 as a pheromonal composition. See also an illustration of the phenotype and behavior of a female of genotype vector (1, 0, 1). We note γ as the parameter controlling the preference direction, and h as the function describing the cognitive trade-off regulating the amount of attention paid to both traits

Selection regime acting on the displayed traits

We assume that the traits T_1 and T_2 displayed by the individuals can modify their survival. We define f_i and f'_i as the frequencies of genotype $i \in \{1, 2\}$ in the focal species before and after a step of natural selection acting on survival, respectively. The resulting frequency after selection, f'_i is then given by

$$f'_i = \frac{w_i}{\bar{w}} f_i, \quad (5.1)$$

where w_i is the fitness component due to natural selection of an individual of genotype i , while \bar{w} is the average fitness component due to natural selection averaged.

$$\bar{w} = \sum_{i \in \mathcal{G}} w_i f_i, \quad (5.2)$$

where \mathcal{G} is the set of all genotypes.

We note s_1 and s_2 the selective advantages associated with allele 1 at locus T_1 and T_2 , respectively. When natural selection favors individuals with allele 0 at locus T_i , s_i is negative for $i \in \{1, 2\}$.

The fitness component due to natural selection of an individual of genotype i is thus given by:

$$w_i = (1 + (T_1)_i s_1) (1 + (T_2)_i s_2), \quad (5.3)$$

where $(T_j)_i$ is the value of trait T_j (0 or 1) of individuals of genotype i for $j \in \{1, 2\}$.

Reproductive success depending on female preference on traits displayed by males

Genotypic frequencies after reproduction in the focal species then depend on the contribution to the next generation of the different crosses between females and males of genotype j and k respectively, described by $m_{j,k}$, for all j and k in \mathcal{G} . We

note \bar{m} the mean value of this contribution across all mating pairs

$$\bar{m} = \sum_{j,k \in \mathcal{G}} f'_j f'_k m_{j,k}. \quad (5.4)$$

The frequency after reproduction of genotype i in species A is then given by

$$f''_i = \sum_{j,k \in \mathcal{G}} f'_j f'_k \frac{m_{j,k}}{\bar{m}} \beta(i, j, k), \quad (5.5)$$

where $\beta(i, j, k)$ describes the segregation of alleles during reproduction and provides the probability that a mating between a female of genotype j and a male of genotype k produces an offspring of genotype i . We assume recombination between female's and male's haplotypes, then the offspring inherits randomly from one of the two recombined haplotypes.

The contribution to the next generation of a mating of a pair then depends on the female preference towards the traits displayed by males, controlled by loci T_1 and T_2 . Assortative preference is assumed and the relative attention given by a female of genotype j to trait 2 vs. trait 1 is controlled by the preference direction parameter γ_j , determined by the allele at locus M : allele 0 is associated with γ_{wt} and allele 1 is associated with the value γ_m . The attention provided on male trait in a female of genotype j is thus given by:

$$\gamma_j = (1 - (M)_j) \gamma_{wt} + (M)_j \gamma_m, \quad (5.6)$$

where $(M)_j$ is the allele (0 or 1) at locus M in genotype j . We assume that the relative attentions to the two traits, controlled by the parameter γ are submitted to a cognitive trade-off described by the function h : attention on trait 1 and 2 are respectively given by $h(1 - \gamma)$ and $h(\gamma)$ with

$$\forall x \in [0, 1], h(x) = x^a \quad \text{and} \quad a \in [0, +\infty).$$

h is a non-decreasing function, so that attention on one trait diminishes attention

on the alternative one. Moreover, $h(0) = 0$ and $h(1) = 1$, so that in the two extreme cases, female choice relies on a single trait. The parameter a tunes the shape of the trade-off function h (see Figure A5.2):

- when $a = 1$, h is linear, leading to a **linear trade-off**, where the female attention on traits 1 (resp. 2) is proportional to $1 - \gamma$ (resp. γ) (see black curve in Figure A5.2).
- when $a < 1$, h is concave, leading to a **weak trade-off** between attention towards the two male traits. Females can thus use both traits for mate choice (see blue curve in Figure A5.2).
- when $a > 1$, h is convex leading to a **strong trade-off** in female attention between the two traits. Females focusing on one trait largely ignore the alternative trait, and intermediate values of γ lead to poor attention on both traits (see red curve in Figure A5.2).

Therefore, when a female of genotype j in species A encounters a male of genotype k , she accepts the male with probability

$$\phi(j, k) = \left(1 - \mathbb{1}_{(T_1)_j \neq (T_1)_k} \rho h(1 - \gamma_j)\right) \left(1 - \mathbb{1}_{(T_2)_j \neq (T_2)_k} \rho h(\gamma_j)\right), \quad (5.7)$$

where $\mathbb{1}_{\{\cdot\}}$ is the indicator function that returns 1 if the condition in subscript is realized and 0 otherwise. The parameter ρ quantifies the strength of assortative female preference.

During an encounter between individuals from different sexes, the probability that a female of genotype j accepts a conspecific male is then given by (Otto *et al.*, 2008):

$$T(j) = \sum_{k \in \mathcal{G}} \underbrace{\frac{N}{N + \tilde{N}} f'_k}_{\text{probability of encountering a conspecific male of genotype } k} \underbrace{\phi(j, k)}_{\text{probability of accepting a conspecific male of genotype } k}, \quad (5.8)$$

where N and \tilde{N} are the densities of species A and B respectively.

A female of genotype j may also accept an heterospecific male with probability

$$T_{RI}(j) = \sum_{k \in \mathcal{G}} \underbrace{\frac{\tilde{N}}{N + \tilde{N}} \tilde{f}_k}_{\text{probability of encountering an heterospecific male of genotype } k} \underbrace{c_{RI} \phi(j, k)}_{\text{probability of accepting an heterospecific male of genotype } k}, \quad (5.9)$$

where $c_{RI} \in [0, 1]$ captures the investment of females in interspecific mating. This cost of reproductive interference incurred to the females can be reduced when female preference is also based on alternative traits differing between species, or when individuals from both species do not encounter frequently. We assume that heterospecific crosses never produce any viable offspring, and that a female engaged in such a mating cannot recover the associated fitness loss.

Knowing that a female of genotype j has mated with a conspecific male, the probability that this male is of genotype k is given by

$$\Phi(j, k) = \frac{\phi(j, k) f'_k}{\sum_{l \in \mathcal{G}} \phi(j, l) f'_l}. \quad (5.10)$$

If females only encountered one male, the proportion of crosses between a female of genotype j and a conspecific male of genotype k would be

$$\mathcal{P}^1(j, k) = f'_j T(j) \Phi(j, k). \quad (5.11)$$

However, we assume that females refusing a mating opportunity can encounter another male with probability $1 - c$. We interpret c as the cost of choosiness (similar to the coefficient c_r , referred to as relative cost of choosiness in (Otto *et al.*, 2008)). The proportion of crosses between a female of genotype j and a

conspecific male of genotype k is thus given by

$$\begin{aligned} \mathcal{P}(j, k) &= \sum_{n=0}^{+\infty} ((1 - T(j) - T_{RI}(j)) (1 - c))^n \mathcal{P}^1(j, k) \\ &= \frac{\mathcal{P}^1(j, k)}{c + (1 - c)(T(j) + T_{RI}(j))}, \end{aligned} \quad (5.12)$$

where $((1 - T(j) - T_{RI}(j)) (1 - c))^n$ is the probability that a female of genotype j rejects the n males she first encounters and then encounters an $(n + 1)$ -th male.

The contribution to the next generation of a mating between a female of genotype j and a male of genotype k is thus given by

$$m_{j,k} = \frac{T(j)}{c + (1 - c)(T(j) + T_{RI}(j))} \frac{\phi(j, k)}{\sum_l f_l^T \phi(j, l)}. \quad (5.13)$$

Mutation

We assume that mutations can occur at loci T_1, T_2 within offspring. We assume that with probability $u_{0 \rightarrow 1}^{T_i}$ (resp. $u_{1 \rightarrow 0}^{T_i}$) allele 0 (resp. 1) mutates into allele 1 (resp. 0) at locus $T_i, i \in \{1, 2\}$.

All variables and parameters used in the model are summed up in Table A5.1.

Model exploration

Using QLE analysis to determine the evolutionary stable preference direction

We perform a Quasi-Linkage Equilibrium (QLE) analysis allowing to estimate the change of allele frequency at each locus. QLE analysis assumes that selection is weak and that recombination is strong compared to selection. In line with this hypothesis, we assume that $s_1, s_2, \rho, c_{RI}, c$ are of order ε with ε low and that the recombination rates are of order 1. We also assume that mutation rates are of

order ε . The QLE analysis is performed using Wolfram Mathematica 12.0 and all the details of the analytical results are presented in Appendix A5.1.

The QLE analysis allows to numerically estimate the evolutionary stable value of γ . The mutant is introduced at frequency P_M^0 . We assume that the mutations at locus M have a low effect *i.e.* the difference γ_{wt} and γ_m is small (but see Appendix 1 for mutations with high effect). We consider:

- Evolutionary stable γ : value of γ_{wt} preventing the invasion of any other mutation of small effect at locus M .
- Repulsor: value of γ_{wt} enabling the invasion of other mutations of small effect at locus M .

We assume that once a mutant increases in frequency after its introduction it replaces the wild type allele in the population. Then the preference direction γ in the population tends to one of the evolutionary stable value refer as equilibrium value γ^* .

In these QLE analyses, we generally assume that ancestral preference equally targets both traits ($\gamma_0 = 1/2$). However, the evolutionary stable direction of preference γ^* may depend on the ancestral value γ_0 , we thus study the dependence to ancestral preference direction assuming the three different selective regimes detailed below, and summarized our findings in the Appendix (see Figures A5.3, A5.6 and A5.8).

In all these three cases, we also study the effects of the shape of the trade-off function h (through the parameter a) and of opportunity costs (through the parameter c) on equilibrium preference direction.

Selection regimes promoting the evolution of multiple trait preference

We applied the QLE analysis method described above to specifically investigate three main selective regimes and to test their respective effects on the evolution of multiple traits preference in females.

(a) Preference enhancing offspring fitness

First, we consider that both trait provide an indirect fitness benefit due to natural selection ($s_1 > 0$ and $s_2 > 0$). To explicitly investigate whether preference would be based on multiple traits or on the trait providing the strongest indirect fitness benefit, we assume that natural selection acts more intensely on trait T_1 than on T_2 (*i.e.* $s_1 > s_2$). We assume no cost generated by heterospecific interactions ($c_{RI} = 0$), but still hypothesize complete inviability in the hybrids.

(b) Preference enhancing species recognition

We then assume that heterospecific interactions generate costly reproductive interference between sympatric species ($c_{RI} = 0.01$) and investigate how selection promoting reproductive isolation impacts the evolution of multiple traits preference. When assuming reproductive interference costs, the advantage gained from a choice based on given trait crucially depends on the phenotypic distribution of this trait in the two sympatric species. We then consider that in species A, because of mutations, trait value 1 is common at both traits with the frequency of trait value 1 higher at trait T_1 than at trait T_2 ($u_{0 \rightarrow 1}^{T_1} = 0.003$, $u_{1 \rightarrow 0}^{T_1} = 0.001$, $u_{0 \rightarrow 1}^{T_2} = 0.002$ and $u_{1 \rightarrow 0}^{T_2} = 0.001$). We also explored the impact of different phenotypic distributions in species B in the evolution of preferences in species A. We focus only on the impact of reproductive interference on the evolution of preference and therefore assume that neither trait T_1 nor T_2 are submitted to natural selection ($s_1 = s_2 = 0$).

(c) Preference enhancing both offspring fitness and species recognition

Finally, we test whether multiple trait preference can be promoted when one trait is submitted to a natural selection in both sympatric species, therefore also promoting preference towards an alternative trait neutral from selection, that may enhance species recognition. We then assume a natural selection regime promoting the same trait value 1 at T_1 in both species. We thus assume that natural selection favors trait values 1 ($s_1 > 0$) in species A and that trait value 1 is fixed ($\tilde{P}_{T_1} = 1$) in species B. We then assume costs generated by reproductive interference ($c_{RI} > 0$), so that preferences based on T_1 are likely be costly. We then assume that both species are easily distinguishable based on trait T_2 . We thus assume that the frequency of allele 0 at trait T_2 , is higher in species A, whereas allele 1 is more common in species B ($\tilde{P}_{T_1} = 0.6$). We investigate several strengths of natural selection favoring allele 1 at trait T_1 (s_1), as well as several strengths of reproductive interference (c_{RI}). Because the proportion of maladapted trait value 0 at T_1 increases the advantage of choosing adapted trait value 1, we investigate the effect of different mutation rates at locus T_1 , assuming a symmetrical mutation rate ($u_{0 \rightarrow 1}^{T_1} = u_{1 \rightarrow 0}^{T_1}$).

Results

We investigate the evolution of multiple traits preference in females by studying the invasion of a mutant at a modifier locus M , determining the attention paid to either traits (T_1 and T_2) displayed in males. We applied a QLE approach to determine the equilibrium level of attention paid to either traits γ^* , depending on the shape a of the cognitive trade-off limiting the attention on both traits simultaneously (see methods).

Which traits indicate 'good genes' ?

We first assume no costly heterospecific interaction and test the effect of natural selection acting on both traits (T_1 and T_2) on the evolution of female preference.

Female preference towards the two traits can be promoted because of the positive effects generated on the fitness of their offspring when they carry the adapted alleles. Furthermore, preference may also be promoted by sexual selection, because females have an advantage to produce 'sexy offspring' (see Equation (A5.10)). By contrast with previous model (Pomiankowski & Iwasa, 1993), our model show that sexual selection alone can not promotes drive the evolution of multiple traits preference (see Appendix A5.2).

When assuming natural selection on the traits ($s_1 > 0$ and $s_2 > 0$), our model does predict the evolution of multiple trait preference. Assuming that ancestral preference equally target both traits ($\gamma^0 = 1/2$), the fitness benefit gained by the offspring displaying adapted alleles of females carrying a mutant allele at the preference at the modifier locus M promotes the evolution of multiple preference. To specifically study the evolution of preference towards several traits in this 'good genes' hypothesis, we consider that natural selection acts more intensely on T_1 ($s_1 > s_2$), and determine the condition favouring the evolution of preference on both traits. Assuming a weak cognitive trade-off (low a) and opportunity costs (low c), the evolutionary stable preference is based on both traits, with more attention on trait T_1 under stronger selection (see hatched area in Figure 5.2 (a)). This preference leads to the production of offspring with adapted alleles at both traits. However, stronger cognitive trade-off and opportunity costs prevent the evolution of such multiple traits preference (Figure 5.2 (a)). Interestingly, linear trade-off ($\log(a) = 0$) leads to preference uniquely based on the trait under stronger selection (Figure 5.2 (a)). A weaker trade-off than linear trade-off is thus a necessary condition for the evolution of multiple traits preference, when both traits are under natural selection.

When assuming a strong trade-off, the evolution of preference also tightly depends on the ancestral preference value (γ^0) (Figure A5.3). When the preference initially targets the trait T_2 ($\gamma^0 \simeq 1$), the evolution of female preference favours more attention towards the mildly selected trait T_2 (see Figure A5.4). This is probably due to the strong sexual selection initially promoting preference on T_2 : when trait T_2 is ancestrally targeted by preference, it provides an indirect fitness benefit

due to the production of 'sexy son'. This sexual selection promoting preference targeting T_2 conflicts with the natural selection, promoting preference targeting T_1 . Moreover, when assuming a strong cognitive trade-off, preference based on both traits leads to poor attention towards both traits, thus creating a fitness valley limiting the switch of female attention from one trait toward the alternative ones. When female choice is ancestrally mainly based on trait T_2 , therefore creating positive sexual selection favouring preference on T_2 , the positive selection on T_1 is not powerful enough to cross this fitness valley, and the evolution towards attention to the trait T_1 is not observed. However, the cross of this fitness valley is facilitated when mutations have a larger effect size (see figure A5.5).

Which traits participate to reinforcement ?

We then investigate whether reinforcement of species barriers promoted by reproductive interference may promote the evolution of multiple traits preference. We assume costly reproductive interference ($c_{RI} = 0.01$), and that both traits are not under natural selection ($s_1 = s_2 = 0$). We assume that trait value 1 is common at both traits in species A, whereas trait value 0 is common at both traits in species B, so that both traits are relevant cues for species recognition. Similarly to the natural selection regime explored above (hypothesis (a)), we assumed a higher frequency of trait value 1 in trait T_1 than at trait T_2 , making T_1 the best cue for species recognition. Similarly to the results obtained for hypothesis (a), multiple traits preference can evolve when the cognitive trade-off and the opportunity costs are weak (Figure 5.2 (b)).

When assuming that heterospecific mating attempts may happen, the advantage gained from a choice based on a given trait crucially depends on the phenotypic distribution of this trait in the two sympatric species (see Equation (A5.6)). We then explored different phenotypic distributions in species B, to investigate the effect of heterospecific mating on the evolution of the targeting of the trait by females.

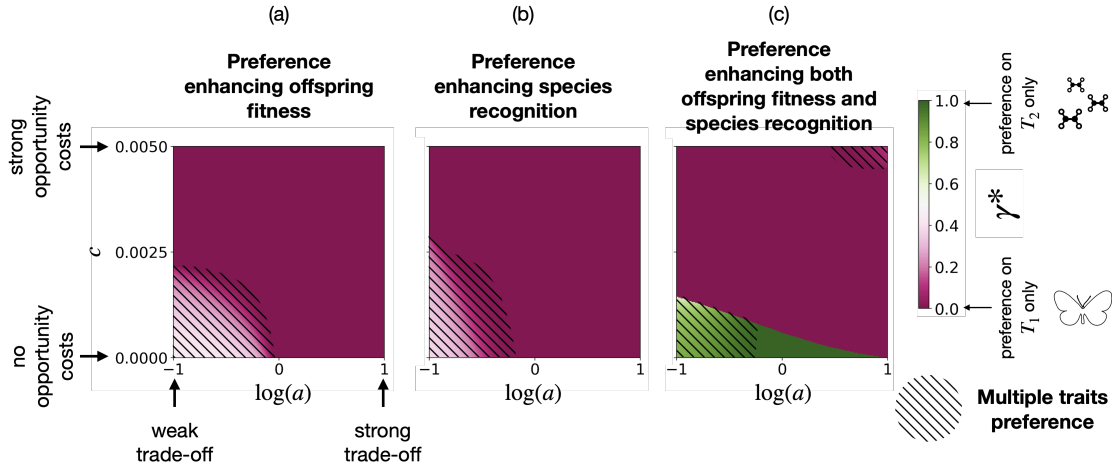


Fig. 5.2: Evolution of female preferences, depending on three different selection regime. The three plot investigates the effect of the cognitive trade-off function a and on cost of choosiness c on the equilibrium preference direction γ^* , for these 3 selective regimes. Hatched area indicates parameter combinations where multiple traits preference is observed at equilibrium ($0 < \gamma^* < 1$). In species A, mutation and natural selection promotes trait value 1 at both traits ($u_{0 \rightarrow 1}^{T_1} = 0.003$, $u_{1 \rightarrow 0}^{T_1} = 0.001$, $u_{0 \rightarrow 1}^{T_2} = 0.002$, $u_{1 \rightarrow 0}^{T_2} = 0.001$, $s_1 \geq 0$ and $s_2 \geq 0$). We assume: (a) that both traits are under natural selection, with stronger selection on T_1 than T_2 ($s_1 = 0.02$ and $s_2 = 0.01$), (b) reproductive interference ($c_{RI} = 0.05$) and that both trait may allow species recognition ($\tilde{P}_{T_1} = \tilde{P}_{T_2} = 0$) (c) reproductive interference ($c_{RI} = 0.05$), that trait T_1 is under natural selection ($s_1 = 0.02$) and that trait T_2 may allow species recognition ($\tilde{P}_{T_2} = 0.4$). Ancestrally preference equally targets both trait ($\gamma_0 = 1/2$). By default we assume: $P_{T_1}^0 = P_{T_2}^0 = 0.5$, $P_M^0 = 0.01$, $\tilde{P}_{T_1} = \tilde{P}_{T_2} = 1$, $s_1 = s_2 = 0$, $\rho = 0.01$, $c_{RI} = 0$, $N = \tilde{N} = 10$. Note that the dependence of these results to the ancestral value γ_0 is detailed in Figure A5.3.

When species differ in the distribution of both traits preferences based on both traits then become advantageous, leading to multiple traits preference (Figure 5.3). Else single trait preference based on the trait that differentiate the most conspecific and heterospecific evolve. The parameter space where females choose only on trait T_1 is wider because this trait is more likely to differentiate species as the frequency of trait value 1 is higher at trait T_1 than at trait T_2 .

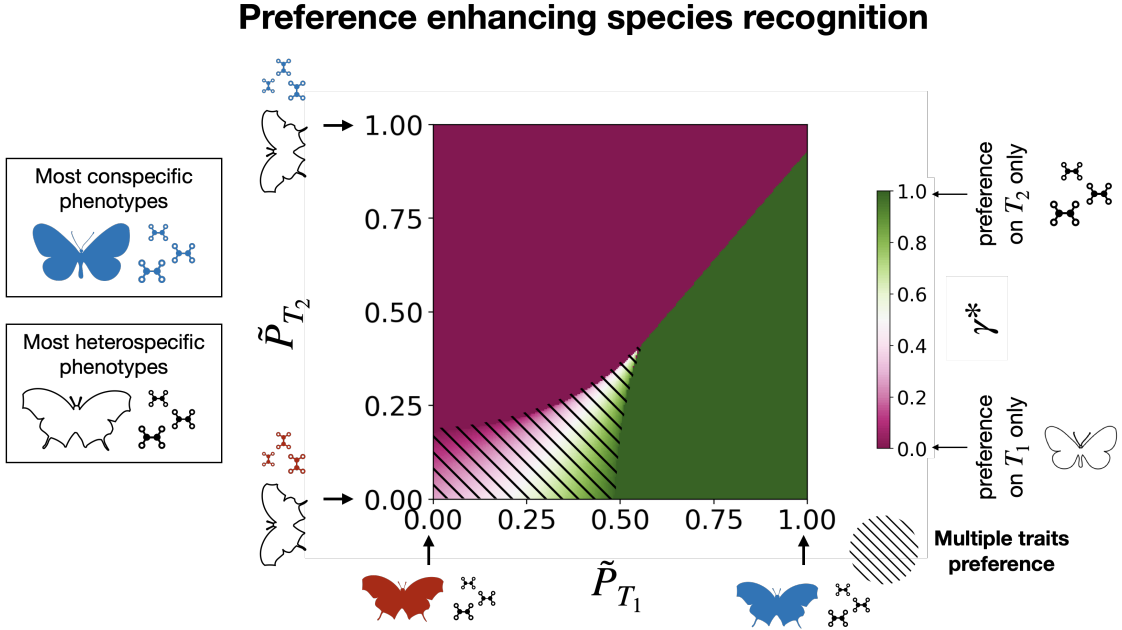


Fig. 5.3: **Equilibrium preference direction γ^* depending on the phenotypic distributions in species B (\tilde{P}_{T_1} and \tilde{P}_{T_2}).** Hatched area indicates parameter combinations where multiple traits preference is observed at equilibrium ($0 < \gamma^* < 1$). In species A, mutations promote trait value 1 at both traits ($u_{0 \rightarrow 1}^{T_1} = 0.003$, $u_{1 \rightarrow 0}^{T_1} = 0.001$, $u_{0 \rightarrow 1}^{T_2} = 0.002$, $u_{1 \rightarrow 0}^{T_2} = 0.001$). Ancestrally, preference equally targets both trait ($\gamma_0 = 1/2$). We assume: $P_{T_1}^0 = P_{T_2}^0 = 0.5$, $P_M^0 = 0.01$, $s_1 = s_2 = 0$, $\rho = 0.01$, $c = 0.001$, $c_{RI} = 0.05$, $a = e^{-1}$, $N = \tilde{N} = 10$. Note that the dependence of these results to the ancestral value γ_0 is detailed in Figure A5.6.

Connecting 'good genes' and reinforcement theory

We explore the evolution of multiple traits preference that may allow producing fitted offspring, while enhancing species recognition. We thus assume that the trait T_1 is under natural selection, leading to resemblance to species B (*e.g.* modeling sympatric species where the same trait allow local adaptation in both species): we assume that natural selection favors trait values 1 ($s_1 > 0$) in species A and that trait value 1 is fixed ($\tilde{P}_{T_1} = 1$) in species B. In contrast, the trait T_2 is not submitted to natural selection, but is a relevant cue for species recognition: we assume that the frequency of allele 1 is higher in species A, whereas allele 0 is more common in species B ($\tilde{P}_{T_1} = 0.4$).

Weak trade-off and opportunity costs allow the evolution of multiple traits preference mainly based on the neutral trait allowing species recognition (T_2) (Figure 5.2 (c)). Opportunity costs then promote preference based on trait under natural selection T_1 (Figure 5.2 (c)). Indeed natural selection acting on trait T_1 reduces phenotypic diversity in the focal species and therefore also reduces opportunity costs associated with preference based on the trait T_1 in this species (see Equation (A5.9)). Thus high mutation rate at trait T_1 , leading to high phenotypic diversity, limits preference based on trait under natural selection T_1 (Figure A5.7). Increasing values of the cognitive trade-off promotes choice on the the trait T_2 (Figure 5.2 (c)), because it provides a better fitness benefit (Note that this fitness benefit depends on our assumptions on the relative levels of strength of natural selection on T_1 and of reproductive interference, see below). However, when opportunity costs increases, an increase of trade-off then leads preference to target only targeting the trait under natural selection (T_1) (Figure 5.2 (c)). Trade-off promotes preference mainly based on one trait, however preference mainly based on neutral trait leads to stronger opportunity cost because of the higher phenotypic diversity in the neutral trait (T_2), while natural selection on the trait T_1 strongly limit intra-specific diversity. Then strong trade-off, in interaction with opportunity costs, promotes preference targeting only the naturally selected trait T_1 .

Very strong trade-off and opportunity costs surprisingly promote multiple traits preference (Figure 5.2 (c)). Due to the important trade-off, this preference leads to poor attention on both traits, resulting in almost random mating, that limits opportunity costs.

We then investigate the impact of the strength of natural selection favoring allele 1 at trait T_1 (s_1) and the strength of reproductive interference (c_{RI}) on the evolutionary stable preference direction. As expected natural selection (resp. reproductive interference) promotes preference based on the naturally selected trait T_1 (reps. the trait allowing species recognition T_2) (Figure 5.4). Without opportunity costs ($c = 0$), natural selection promotes multiple traits preference, whereas reproductive interference leads to preference targeting T_2 only. Because we assume complete inviability in the hybrids, with strong reproductive interference, females

prioritize species recognition.

Opportunity costs ($c = 0.001$) allow only the evolution of multiple traits preferences that mainly target the neutral trait. Multiple traits preferences mainly targeting the naturally selected trait would reduce the phenotypic diversity at trait T_1 , *via* sexual selection. Thus such preferences would, by reducing opportunity costs, strongly advantage preference targeting T_1 and then promotes the single trait preference targeting the trait T_1 .

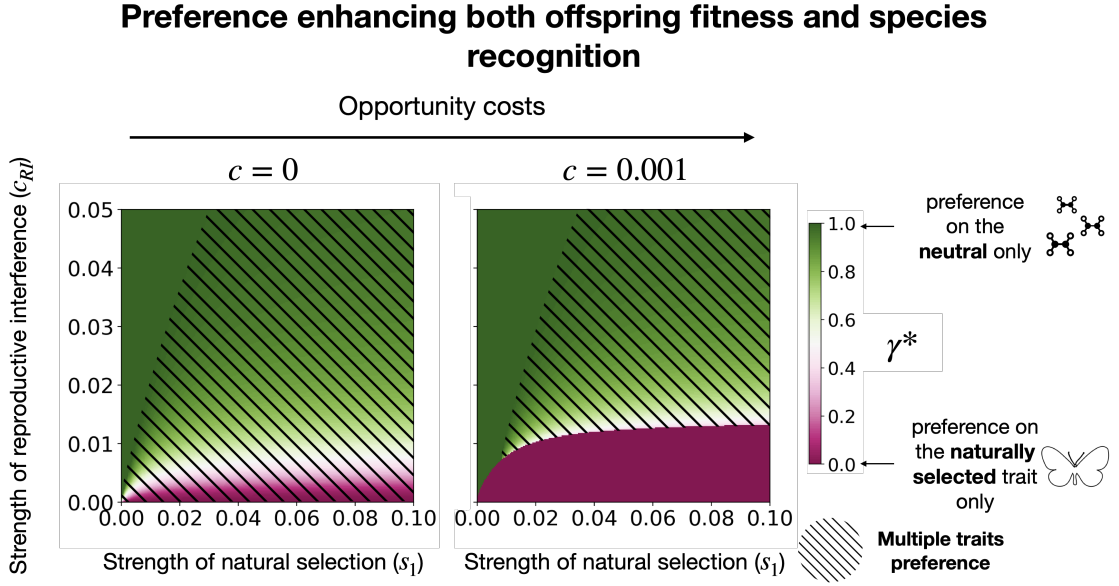


Fig. 5.4: **Evolution of preference direction γ^* , depending on the strength natural selection acting on trait T_1 (s_1) and the strength of reproductive interference (c_{RI}), for different cost of choosiness (c).** We assume (a) $c = 0$ and (b) $c = 0.001$. Hatched area indicates parameter combinations where multiple traits preference is observed at equilibrium ($0 < \gamma^* < 1$). Ancestrally, preference equally targets both trait ($\gamma_0 = 1/2$). We assume: $P_{T_1}^0 = P_{T_2}^0 = 0.5$, $P_M^0 = 0.01$, $\tilde{P}_{T_1} = 1$, $\tilde{P}_{T_2} = 0.4$, $s_2 = 0$, $\rho = 0.01$, $a = e^{-1}$, $N = \tilde{N} = 10$, $u_{0 \rightarrow 1}^{T_1} = 0.003$, $u_{1 \rightarrow 0}^{T_1} = 0.001$, $u_{0 \rightarrow 1}^{T_2} = 0.002$, $u_{1 \rightarrow 0}^{T_2} = 0.001$. Note that the dependence to γ_0 is detailed in Figure A5.8.

Altogether our results show how natural and sexual selection, sensory trade-off and ancestral preference shape the evolution of female preference toward different traits displayed by males.

Discussion

Mate preferences have been extensively studied in the light of the 'good genes' hypothesis (Puurttinen *et al.*, 2009) or in the context on reinforcement (Servedio & Noor, 2003). By jointly considering (1) the selection regimes acting on the targeted traits within species, as well as (2) interactions with other species living in sympatry, our theoretical study provides a general framework reconciling these research fields.

We thus focused on natural selection regime shared between sympatric species promoting species similarity, increasing risks of reproductive interference. Our approach thus drastically differ from classical studies on reinforcement, focusing on 'magic traits', submitted to disruptive selection between species (Servedio *et al.*, 2011). Because 'magic traits' are honest signals of both local adaptation and of species identity, there is no antagonistic selection regimes that may promote the evolution of multiple trait preferences in this case.

Our results show that opportunity costs play a key role in the evolution of multiple trait preference. In our model, the opportunity costs promotes preference based on naturally selected traits rather than on traits allowing species recognition. As natural selection erodes phenotypic diversity, preference based on traits allowing species recognition leads to stronger opportunity cost, promoting preference targeting the naturally selected traits. However, the low level of variations are usually observed in locally adapted traits prevent positive selection on these traits: because there is hardly any 'maladapted' variants, there is no longer selection to avoid it. Our model highlights that female preference may then preferentially target traits that differ from other species (Figure A5.7). For example in *Heliconius* butterflies, wing pattern is under selection because predators associated locally abundant wing patterns with unpalatability, leading to the fixation of a local wing pattern within and between species. In some of these mimetic species, female preference targets chemical cues differentiating sympatric species. (González-Rojas *et al.*, 2020).

In our model, species recognition traits are neutral. However constraints act on

trait display, depending notably on the detectability of the displayed trait. We assume that choosers perceived all trait values equally. However, increased trait detectability may induce costs: for example, the conspicuousness of a trait display increase parasitism and predation risks (Zuk & Kolluru, 1998). Increasing costs of sexual trait conspicuousness may theoretically promotes the light display of several traits (Johnstone, 1995a), therefore promoting preference multiple towards multiple cryptic traits.

Our results highlight how indirect fitness benefit and/or reproductive interference can promotes female preference for multiple traits. Our model highlights that the evolution of multiple traits occur only when the cognitive trade-off is weak. The evolution of multiple trait preference is therefore probably more likely to emergence in species where complex neural processes do occur. Nevertheless, several alternative decision mechanisms may reduce this cognitive trade-off. For example sequential/hierarchical mate preference, whereby targeted traits are process in a hierarchical order, efficiently produce decision, even considering a large number of traits (Gigerenzer *et al.*, 1999). Sequential mate preference is frequently observed (*e.g.* (Shine & Mason, 2001; Eddy *et al.*, 2012; Gray, 2022)) and may allow the evolution of multiple traits preference. Sequential mate choice may emerge because some trait are visible at long-distance (such as color or calls), whereas others are perceived only at short distances (such as oviposition site guarded by males or male-emitted pheromones) (*e.g.* (Candolin & Reynolds, 2001; López & Martín, 2001; Mérot *et al.*, 2015)).

The distance at which different traits are perceived may play a key role in reproductive isolation (Moran *et al.*, 2020). Females deceived by short-distance trait of the heterospecific males may have already spent time and energy or may need to deploy substantial efforts to avoid heterospecific mating. Therefore, females may still suffer from increased costs associated to reproductive interference, even if they eventually manage to avoid mating with heterospecific males (Gröning & Hochkirch, 2008). Therefore reproductive interfere may promote preference targeting long-distance trait that may reduce efficiently heterospecific interactions.

Reproductive isolation between species also depends on the niche of individuals of both species. Mating occurs between individuals sharing the same niche leading to niche-based assortative mating. Niche segregation may play a key role in the evolution of reproductive isolation. In two teafrogs species, differing by their mating call (Park *et al.*, 2013), different spatial and temporal segregation in calling and resting places during breeding period increases reproductive isolation (Borzée *et al.*, 2016). As well as sequential mate preference, niche segregation may efficiently participate to reproductive isolation without generating trade-off with preference for other traits. Niche segregation limit opportunity costs because there is no need to sample a species recognition trait, whereas sequential mate preference increase sampling time.

Our study shows how natural and sexual selection may promote multiple traits preference in sympatric species. Our study highlights the importance of understanding trade-off between preference targeting different trait whereas opportunity costs to understand what trait are targeted by preference.

Conclusion

We study the direction of preference towards two evolving traits shared by sympatric species. We consider selection regimes acting on traits that increase similarity with heterospecific individuals, leading to costly sexual interactions. We study how selective regimes on traits, heterospecific interactions, opportunity costs and sensory trade-off shape the evolution of preference for multiple traits. Weak opportunity costs and sensory trade-off allow the evolution of multiple traits preference enhancing offspring fitness and/or species recognition. Our main result is that that opportunity costs promote preference based on adaptive traits rather than on traits relevant for species recognition. Because adaptation reduces the number of trait values, preference based on adaptive traits hardly suffer from opportunity costs. Then opportunity costs may limit multiple traits preference enhancing both offspring fitness and species recognition.

Acknowledgments

The authors would like to thank the ANR SUPERGENE (ANR-18-CE02-0019) for funding the PhD of LM, and the Emergence program from Paris city council for supporting the team of VL. This work was also supported by the Chair “Modélisation Mathématique et Biodiversité” of VEOLIA- Ecole Polytechnique-MNHN-F.X.

Appendix

A5.1 QLE analysis

A5.1.1 Evolution of mating traits under natural and sexual selection

First, we explored the relative effects of natural and sexual selections on the evolution of traits in species A. Following the QLE approach, the change of allele 1 frequency at T_i , for $i \in \{1, 2\}$, after one generation in this species is given by:

$$\Delta P_{T_i} = G_{T_i} \overbrace{\left(s_i + \bar{\rho}_i \left(P_{T_i} - \frac{1}{2} \right) \right)}^{\text{natural and sexual selections}} + \overbrace{(1 - P_{T_i})u_{0 \rightarrow 1}^{T_i} - P_{T_i}u_{1 \rightarrow 0}^{T_i}}^{\text{action of mutations}} + O(\varepsilon^2), \quad (\text{A5.1})$$

where G_I is the genetic diversity at locus $I \in \{T_1, T_2, M\}$ given by

$$G_I = P_I(1 - P_I), \quad (\text{A5.2})$$

and $\bar{\rho}_1$ and $\bar{\rho}_2$ are the average strengths of preference on traits T_1 and T_2 respectively in the population

$$\bar{\rho}_1 = \rho((1 - P_M)h(1 - \gamma_{wt}) + P_M h(1 - \gamma_m)), \quad (\text{A5.3})$$

$$\bar{\rho}_2 = \rho((1 - P_M)h(\gamma_{wt}) + P_M h(\gamma_m)). \quad (\text{A5.4})$$

While the action of natural selection simply depends on the advantage of trait value 1 due to natural selection s_i , the effect of sexual selection is modulated by the average strength of preference on trait T_1 in the population $\bar{\rho}_i$. Sexual selection promotes (resp. disfavors) allele 1 when this allele is the most common (resp. rare) in the population *i.e.* when $P_{T_1} > 1/2$ (resp. $P_{T_1} < 1/2$) generating a positive frequency-dependent selection. The assortative mate preference assumed implies that most females display the most common trait and seek for males exhibiting

this trait. The most frequently displayed trait allele is therefore associated with an enhanced reproductive success. An enhanced attention of females towards one out of the two male traits then results in a reduction of the polymorphism for this trait more targeted by sexual selection.

A5.1.2 Evolution of mutants modifying the trait used by females for mate choice

The traits targeted by preference in species A can be shared with species B. This is even more likely when these traits are submitted to similar natural selection pressures in both sympatric species, enhancing a similar frequencies of traits. The natural selection exerted on the traits in both species might therefore strongly affect the risk of heterospecific mate choice. We thus investigate the evolution of the focus of female preference on either trait in species A, depending on the natural selection exerted on either trait. We thus study the invasion of a mutant at locus M associated with the value γ_m , differing from the value γ_{wt} associated with the ancestral allele. Under the QLE approximation, the allele frequency variation at the preference locus can be divided into three terms, denoted $\Delta^{\text{dir-RI}}$, $\Delta^{\text{dir-c}}$ and $\Delta^{\text{ind}}P_M$, reflecting the effect of direct selection due to reproductive interference and opportunity costs and indirect selection, on the change of the mutant frequency ΔP_M respectively.

$$\Delta P_M = \Delta^{\text{dir-RI}}P_M + \Delta^{\text{dir-c}}P_M + \Delta^{\text{ind}}P_M + O(\varepsilon^3). \quad (\text{A5.5})$$

Reproductive interference promotes preference targeting the trait leading to strongest species recognition.

The effect of reproductive interference on the change of mutant frequency is given by

$$\Delta^{\text{dir-RI}} P_M = G_{MCRI} \frac{\tilde{N}}{N} \left(\delta\rho_1 \left(P_{T_1} - \frac{1}{2} \right) \left(P_{T_1} - \tilde{P}_{T_1} \right) + \delta\rho_2 \left(P_{T_2} - \frac{1}{2} \right) \left(P_{T_2} - \tilde{P}_{T_2} \right) \right), \quad (\text{A5.6})$$

where \tilde{P}_{T_1} and \tilde{P}_{T_2} are the frequencies of allele 1 at loci T_1 and T_2 respectively in heterospecific. $\delta\rho_1$ and $\delta\rho_2$ quantify the effect of the mutant allele on the preference on trait T_1 and T_2 respectively compared to the wild type allele

$$\delta\rho_1 = \rho (h(1 - \gamma_m) - h(1 - \gamma_{wt})), \quad (\text{A5.7})$$

$$\delta\rho_2 = \rho (h(\gamma_m) - h(\gamma_{wt})). \quad (\text{A5.8})$$

For instance when $\delta\rho_2 > 0$ the mutant allele leads to more attention on trait T_2 than the wild type allele. Note that h is an increasing function: $\delta\rho_1$ and $\delta\rho_2$ thus have opposite signs, *i.e.* when mutant allele increases female attention on one trait, it also decreases female attention on the other trait.

As expected, the effect of reproductive interference mainly depends on density ratio between species A and B, \tilde{N}/N : the probability that a female encounters an heterospecific male increases with \tilde{N}/N . Selection caused by reproductive interference also increases with the strength of preference ρ , because the stronger preferences are, the more females with preference leading to heterospecific rejection avoid heterospecific mates. This leads to a greater fitness difference between females with different preferences intensifying selection, due to reproductive interference.

Reproductive interference promotes preference on the trait allowing more accurate species recognition. Selection due to reproductive interference depends then on relative phenotypic frequencies in both species. Preference on a trait leads to

increased intraspecific matings than expected under random mating, when the targeted trait is more common within the species A than within species B. The higher the difference in trait frequencies between species, the stronger species recognition is. However, natural selection favors resemblance on the selected trait between species A and B and thus leads to similar cost of reproductive interference than expected under random mating. By contrast, when traits are neutral, phenotypic distributions within the two species can be more different. Preference based on trait may either increase or decrease species recognition compared to random mating. Females are more attracted by heterospecifics when the most common preferred trait value is more common within heterospecifics. Therefore in some cases focusing on neutral traits may be worst for species recognition than naturally selected trait.

Sympatry with other species intensifies opportunity costs

Preference allows to reject heterospecific males but also leads to the rejection of conspecific males. After rejecting a male, a female has a probability c of not encountering another male leading to an opportunity cost. The effect of these opportunity costs on change of mutant frequency is given by

$$\Delta^{\text{dir-c}} P_M = -G_M c \frac{N + \tilde{N}}{N} (\delta\rho_1 G_{T_1} + \delta\rho_2 G_{T_2}). \quad (\text{A5.9})$$

The fate of a mutant depends on trait polymorphism and on its effect on the attention towards either male traits. Limited polymorphism in a male trait indeed reduces opportunity costs, associated with female choice based on that trait. Because we assume assortative mating, most females have and prefer the most abundant trait value leading to low opportunity cost. Since natural selection reduces polymorphism at the male adaptive trait, opportunity costs may promote female preference towards trait under stronger natural selection.

Surprisingly, selection due to opportunity costs increases with the proportion of heterospecifics. When a female rejects a conspecific male, she has to wait to

encounter another conspecific male to produce offspring and avoid opportunity cost. However, the more there are heterospecifics, the more females will encounter heterospecific males before encountering a conspecific male, making the rejection of a conspecific more dramatic when conspecific males are rare. The effect of opportunity costs is thus proportional to the average number of males that females will encounter until she encounters a conspecific $(N + \tilde{N})/N$.

Indirect selection promotes preference on the trait providing the strongest indirect fitness benefit

The mutant at locus M does not only directly change the fitness because it modifies reproductive interference and opportunity costs, but also because it can be associated with different alleles at the traits loci T_1 and T_2 in the offspring, leading to contrasted indirect fitness benefits. Within offspring, the mutant allele at locus M becomes associated with the preferred alleles at trait T_1 or T_2 . Therefore selection on the traits T_1 and T_2 can indirectly affect the frequency of the mutant at locus M . The term describing the effect of indirect selection on mutant alleles at locus M is given by

$$\Delta^{\text{ind}}P_M = \underbrace{D_{T_1M}^*}_{\text{genetic association between } T_1 \text{ and } M} \underbrace{\left(s_1 + \bar{\rho}_1(P_{T_1} - \frac{1}{2})\right)}_{\text{direct selection on } T_1} + \underbrace{D_{T_2M}^*}_{\text{genetic association between } T_2 \text{ and } M} \underbrace{\left(s_2 + \bar{\rho}_2(P_{T_2} - \frac{1}{2})\right)}_{\text{direct selection on } T_2}, \quad (\text{A5.10})$$

where $D_{T_1M}^*$ (resp. $D_{T_2M}^*$) is the genetic association between the mutant allele at locus M and allele 1 at locus T_1 (resp. T_2), see (A5.11). When the mutant is associated with a trait value, direct selection on this trait indirectly affects change of mutant frequency.

The genetic association between the mutant at locus M and the trait T_i , for $i \in$

$\{1, 2\}$, is given by

$$D_{T_i M}^* = G_{T_i} G_M \delta \rho_i \left(P_{T_i} - \frac{1}{2} \right) + O(\varepsilon^2). \quad (\text{A5.11})$$

When the mutant leads to more attention on T_i ($\delta \rho_i > 0$), the mutant becomes associated with the most common allele at T_i . Because of assortative female preference, when one trait value is common, females mostly prefer this trait. This generates a tighter association between preference and trait alleles. Accordingly, when the mutant leads to less attention on T_i ($\delta \rho_i < 0$), it is associated with the rarest allele. As trait alleles promoted by natural selection are more common, indirect selection promotes preference towards the trait under stronger selection. This selection includes natural and sexual selections, highlighting the importance of the ancestral value of γ in the population which determines the strength of sexual selection acting on each trait.

A5.2 Preference enhancing offspring 'sexiness'

We consider the case where the indirect fitness benefit provided by each trait is exclusively due to production of 'sexy son'. We then assume no natural selection and no reproductive interference ($s_1 = s_2 = c_{RI} = 0$). Because opportunity costs may depend on the distribution of trait values at each trait we assume that mutations promote a more balanced proportion of trait values on T_2 ($u_{0 \rightarrow 1}^{T_2} = 0.002$ and $u_{1 \rightarrow 0}^{T_2} = 0.001$) than on T_1 ($u_{0 \rightarrow 1}^{T_1} = 0.003$ and $u_{1 \rightarrow 0}^{T_1} = 0.001$).

Without opportunity costs ($c = 0$), multiple traits preference evolve only for very weak trade-off ($\log(a) \simeq -1$) (Figure A5.1). With subsequent opportunity costs, the evolution of preference depends on the shape of the trade-off:

- With strong trade-off ($\log(a) > 0$), the opportunity costs surprisingly promote preference based on both traits. This preference leads to poor attention on both traits, leading to an almost random mating that limits opportunity

costs. This result is observed because we assume fixed strength of level preference (ρ). Considering an evolving strength of level preference, the high opportunity costs would promote no preference ($\rho = 0$).

- By contrast, with weak trade-off ($\log(a) < 0$), opportunity costs favor attention only on trait T_1 . Females with preference on both traits suffer from high opportunity costs, because they are likely to refuse a large number of males and may therefore have a decreased reproductive success. Females then choose on the trait with the lower phenotypic diversity limiting opportunity costs.

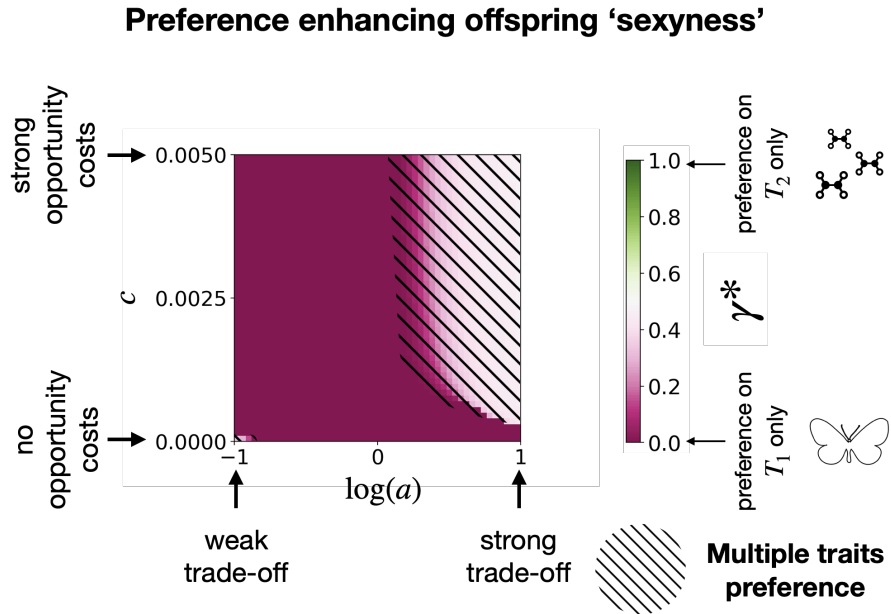


Fig. A5.1: **Equilibrium preference direction γ^* depending on $\log(a)$ where a tunes the shape of the trade-off function and on cost of choosiness (c).** Hatched area indicates parameter combinations where multiple traits preference is observed at equilibrium ($0 < \gamma^* < 1$). In species A mutations promotes higher phenotypic diversity at trait T_2 ($u_{0 \rightarrow 1}^{T_1} = 0.003$, $u_{1 \rightarrow 0}^{T_1} = 0.001$, $u_{0 \rightarrow 1}^{T_2} = 0.002$, $u_{1 \rightarrow 0}^{T_2} = 0.001$). Ancestrally preference equally targets both trait ($\gamma_0 = 1/2$). We assume: $P_{T_1}^0 = P_{T_2}^0 = 0.5$, $P_M^0 = 0.01$, $\tilde{P}_{T_1} = \tilde{P}_{T_2} = 1$, $s_1 = s_2 = 0$, $\rho = 0.01$, $c_{RI} = 0$, $N = \tilde{N} = 10$, .

A5.3 Table and Figures

Abbreviation	Description
\mathcal{L}	Set of different loci for the <i>matching rule</i> model: $\mathcal{L} = \{T_1, T_2, M\}$ and for the <i>preference/trait</i> model $\mathcal{L} = \{T_1, P_1, T_2, P_2, M\}$.
\mathcal{G}	Set of different genotypes for the <i>matching rule</i> model: $\mathcal{G} = \{0, 1\}^3$ and for the <i>preference/trait</i> model $\mathcal{G} = \{0, 1\}^5$.
f_i/\tilde{f}_i	Frequency of genotype i in species A or B.
P_I/\tilde{P}_I	Frequency of allele 1 at locus I , for $I \in \mathcal{L}$, in species A or B.
N/\tilde{N}	Density of species A/B.
G_I	Genetic diversity at locus I in species A, $G_I = P_I(1 - P_I)$ for $I \in \mathcal{L}$.
$(I)_i$	Allele at locus I of the genotype i for $(I, i) \in \mathcal{L} \times \mathcal{G}$.
$D_{\mathcal{I}}$	Genetic association between alleles at loci in \mathcal{I} : $D_{\mathcal{I}} = \sum_{i \in \mathcal{G}} f_i \prod_{I \in \mathcal{I}} (P_I - (I)_i)$ for $\mathcal{I} \subset \mathcal{L}$.
$f'_i/f''_i/f'''_i$	Frequency of genotype i in species a after natural selection/reproduction/mutation.
s_n	Selective advantage of allele 1 at locus T_n , $n \in \{0, 1\}$.
γ_i	Preference direction.
h	Trade-off function determining the relative focus of females on either trait displayed by males.
a	Trade-off parameter tuning the shape of the function h
ρ	Strength of female preference.
c_{RI}	Strength of reproductive interference.
c	Cost of choosiness.
$u_{0 \rightarrow 1}^I/u_{1 \rightarrow 0}^I$	Mutation rate of allele 0/1 towards 1/0 at locus $I \in \mathcal{L}$.

Table A5.1: Description of variables and parameters used in the model.

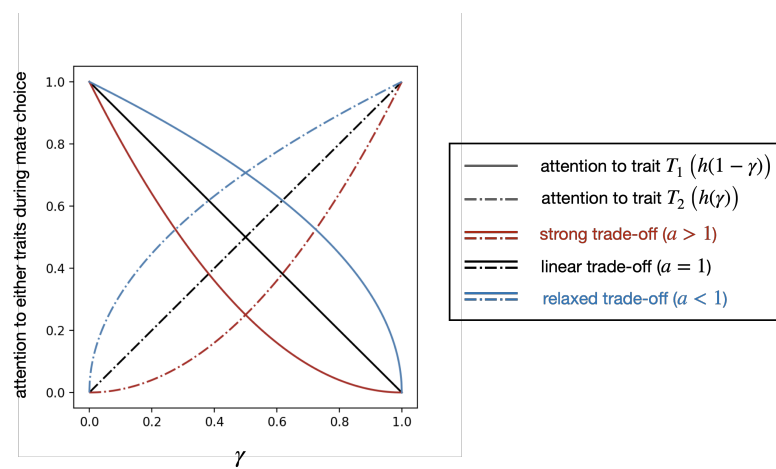


Fig. A5.2: Attention paid by females to either traits displayed by males during assortative mate choice, depending on the preference direction parameter γ controlled by the locus M , for different shapes of the trade-off function h . Blue, red and black lines indicate concave, convex and linear trade-off functions respectively.

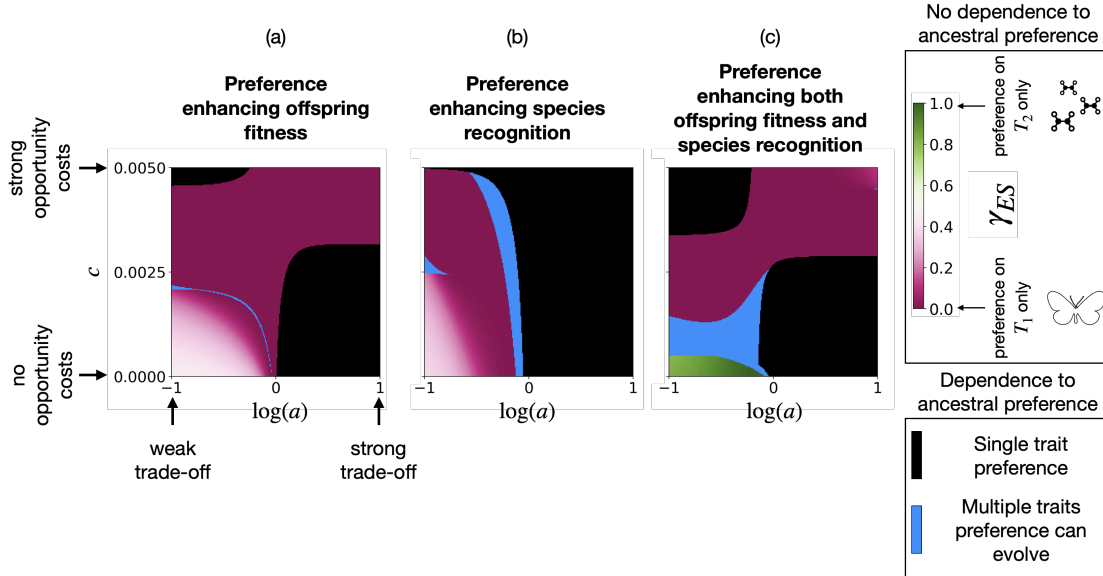


Fig. A5.3: Evolutionary stable preference, depending on three different selection regime. The three plot investigates the effect of the cognitive trade-off function a and on cost of choosiness c on the evolutionary stable preference, for these 3 selective regimes. Shades of color indicates the unique value γ_{ES} . Black and blue area indicates parameter spaces with several values γ_{ES} . In black area only single trait preferences are evolutionary stable. In blue area at least one γ_{ES} value corresponds to multiple trait preference. In species A mutations and natural selection promotes trait value 1 at both traits in species A ($u_{0 \rightarrow 1}^{T_1} = 0.003$, $u_{1 \rightarrow 0}^{T_1} = 0.001$, $u_{0 \rightarrow 1}^{T_2} = 0.002$, $u_{1 \rightarrow 0}^{T_2} = 0.001$, $s_1 \geq 0$ and $s_2 \geq 0$). We assume: (a) that both traits are under natural selection ($s_1 = 0.02$ and $s_2 = 0.01$), (b) reproductive interference ($c_{RI} = 0.05$) and that both trait may allow species recognition ($\tilde{P}_{T_1} = \tilde{P}_{T_2} = 0$) (c) reproductive interference ($c_{RI} = 0.05$), that trait T_1 is under natural selection ($s_1 = 0.02$) and that trait T_2 allowing species recognition ($\tilde{P}_{T_2} = 0.4$). By default we assume: $P_{T_1}^0 = P_{T_2}^0 = 0.5$, $P_M^0 = 0.01$, $\tilde{P}_{T_1} = \tilde{P}_{T_2} = 1$, $s_1 = s_2 = 0$, $\rho = 0.01$, $c_{RI} = 0$, $N = \tilde{N} = 10$, .

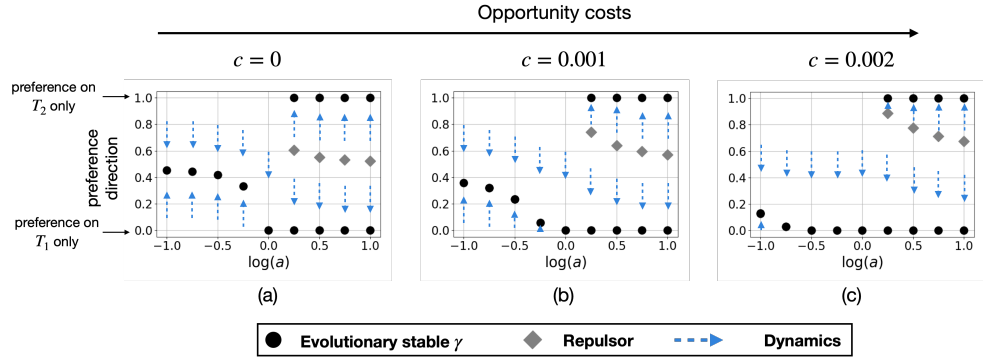


Fig. A5.4: **Evolutionary stable value of γ depending on $\log(a)$ where a tunes the shape of the trade-off function for different values of cost of choosiness (c).** Black dots represent evolutionary stable γ , grey squares represent repulsors and blue arrows represent dynamics (see Method part). We assume (a) $c = 0$, (b) $c = 0.001$ and (c) $c = 0.002$. We also assume: $P_{T_1}^0 = P_{T_2}^0 = 0.5$, $P_M^0 = 0.01$, $\tilde{P}_{T_1} = 1 = \tilde{P}_{T_2} = 0$, $s_1 = 0.02$, $s_2 = 0.01$, $\rho = 0.01$, $c_{RI} = 0$, $N = \tilde{N} = 10$, $u_{0 \rightarrow 1}^{T_1} = 0.003$, $u_{1 \rightarrow 0}^{T_1} = 0.001$, $u_{0 \rightarrow 1}^{T_2} = 0.002$, $u_{1 \rightarrow 0}^{T_2} = 0.001$.

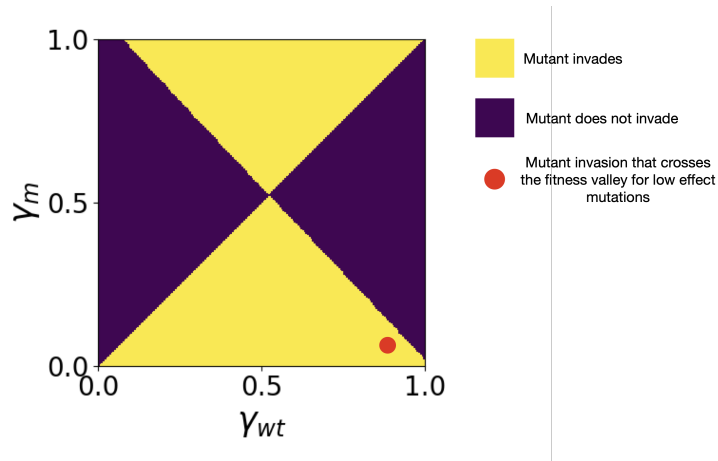


Fig. A5.5: **Invasion graph.** Red dot shows the invasion of the mutant with high effect mutation. We assume: $\log(a) = 1$, $P_{T_1}^0 = P_{T_2}^0 = 0.5$, $\tilde{P}_{T_1} = \tilde{P}_{T_2} = 1$, $s_1 = 0.02$, $s_2 = 0.01$, $\rho = 0.01$, $c = 0$, $c_{RI} = 0$, $N = \tilde{N} = 10$, $u_{0 \rightarrow 1}^{T_1} = 0.003$, $u_{1 \rightarrow 0}^{T_1} = 0.001$, $u_{0 \rightarrow 1}^{T_2} = 0.002$, $u_{1 \rightarrow 0}^{T_2} = 0.001$.

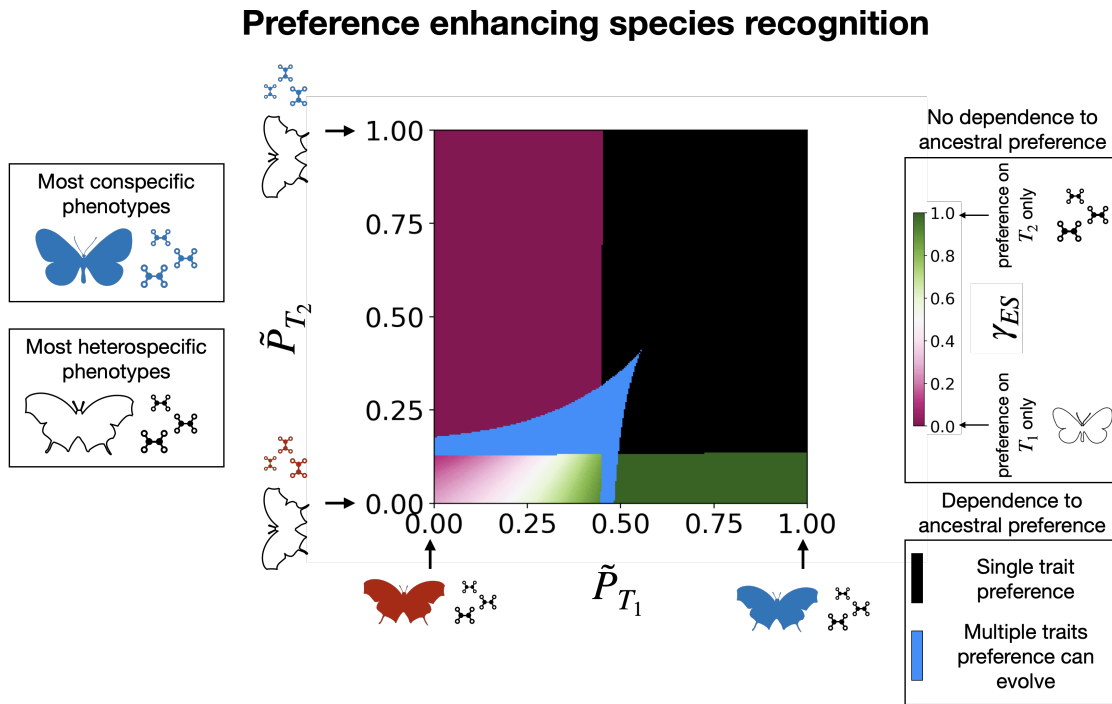


Fig. A5.6: **Evolutionary stable preference direction γ_{ES} depending on the phenotypic distributions in species B (\tilde{P}_{T_1} and \tilde{P}_{T_2}).** Shades of color indicates the unique value γ_{ES} . Black and blue area indicates parameter spaces with several values γ_{ES} . In black area only single trait preferences are evolutionary stable. In blue area at least one γ_{ES} value corresponds to multiple trait preference. In species A mutations promote trait value 1 at both traits in species A ($u_{0 \rightarrow 1}^{T_1} = 0.003$, $u_{1 \rightarrow 0}^{T_1} = 0.001$, $u_{0 \rightarrow 1}^{T_2} = 0.002$, $u_{1 \rightarrow 0}^{T_2} = 0.001$). We assume: $P_{T_1}^0 = P_{T_2}^0 = 0.5$, $P_M^0 = 0.01$, $s_1 = s_2 = 0$, $\rho = 0.01$, $c = 0.001$, $c_{RI} = 0.05$, $a = e^{-1}$, $N = \tilde{N} = 10$.

Preference enhancing both offspring fitness and species recognition

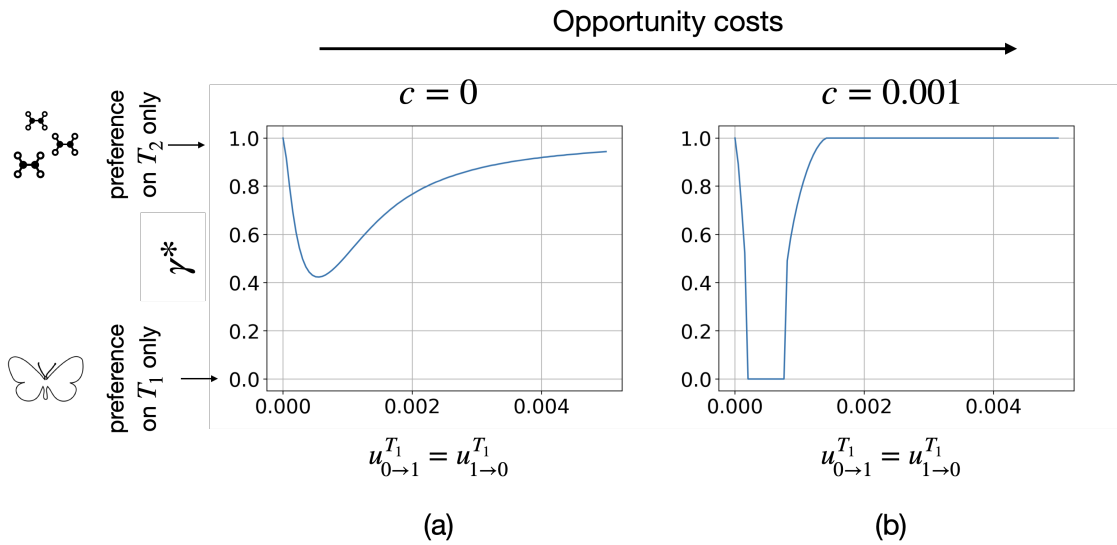


Fig. A5.7: **Equilibrium preference direction γ^* depending on mutation rates at locus T_1 ($u_{0 \rightarrow 1}^{T_1} = u_{1 \rightarrow 0}^{T_1}$) for different cost of choosiness (c).** We assume (a) $c = 0$ and (b) $c = 0.001$. Ancestrally preference equally targets both trait ($\gamma_0 = 1/2$). We assume: $P_{T_1}^0 = P_{T_2}^0 = 0.5$, $P_M^0 = 0.01$, $\tilde{P}_{T_1} = \tilde{P}_{T_2} = 1$, $s_1 = s_2 = 0$, $\rho = 0.01$, $a = e^{-1}$, $c_{RI} = 0$, $N = \tilde{N} = 10$, $u_{0 \rightarrow 1}^{T_2} = 0.002$, $u_{1 \rightarrow 0}^{T_2} = 0.001$.

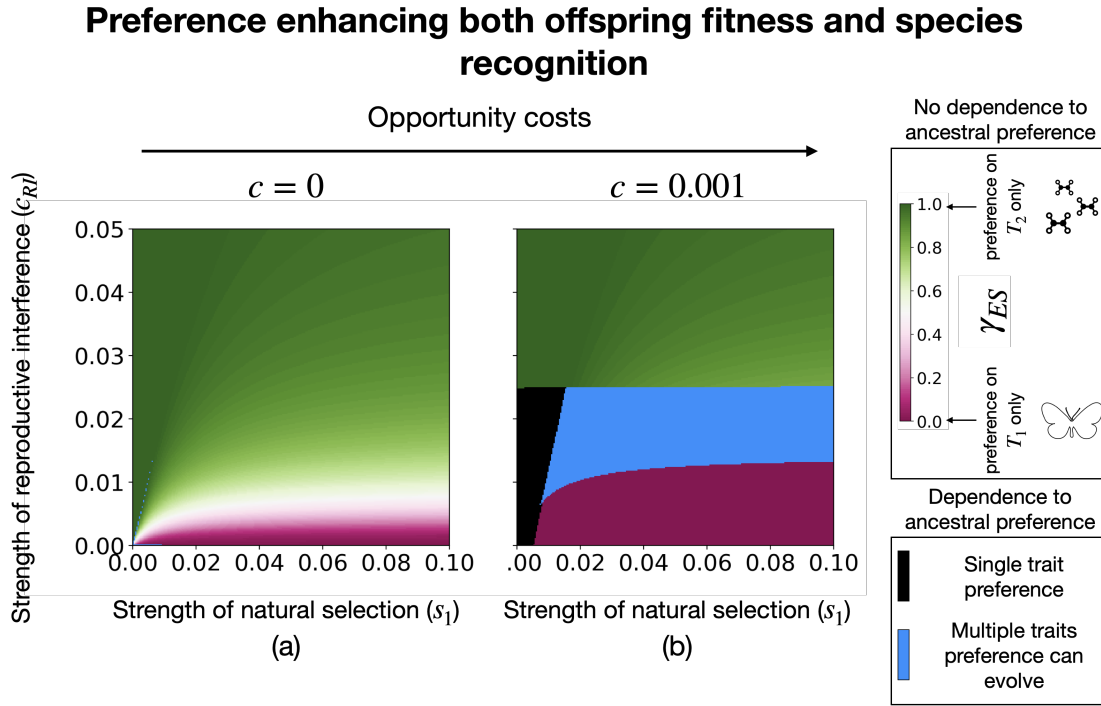


Fig. A5.8: **Evolutionary stable preference direction γ_{ES} depending on natural selection acting on trait T_1 (s_1) and the strength of reproductive interference (c_{RI}) for different cost of choosiness (c).** We assume (a) $c = 0$ and (b) $c = 0.001$. Shades of color indicates the unique value γ_{ES} . Black and blue area indicates parameter spaces with several values γ_{ES} . In black area only single trait preferences are evolutionary stable. In blue area at least one γ_{ES} value corresponds to multiple trait preference. We assume: $P_{T_1}^0 = P_{T_2}^0 = 0.5$, $P_M^0 = 0.01$, $\tilde{P}_{T_1} = 1$, $\tilde{P}_{T_2} = 0.4$, $s_2 = 0$, $\rho = 0.01$, $a = e^{-1}$, $N = \tilde{N} = 10$, $u_{0 \rightarrow 1}^{T_1} = 0.003$, $u_{1 \rightarrow 0}^{T_1} = 0.001$, $u_{0 \rightarrow 1}^{T_2} = 0.002$, $u_{1 \rightarrow 0}^{T_2} = 0.001$.

CHAPTER FIVE

Discussion

Overview of the thesis results

This thesis has explored the evolution of preference for unusual traits, and identified original mechanisms involved in the evolution of preference targets. Mate preference for locally adaptive traits may be particularly advantageous because it enhances offspring fitness in the local environment. However, mate preference can target maladaptive traits limiting adaptation. In this thesis, I focused on two mechanisms limiting the evolution of preference for adaptive traits.

First, I focused on the evolution of disassortative mating based on warning trait, observed within polymorphic mimetic butterfly *Heliconius numata*. In this species, local adaptation of warning trait and migration may have likely promoted the formation of a supergene, controlling warning trait variations. However, the supergene in *Heliconius numata* has also captured and/or accumulated deleterious genetic mutations. In **chapter 1**, I showed that the deleterious genetic mutations associated with the supergene can promote the evolution of disassortative mating, despite the positive frequency-dependent selection acting on warning trait. I also identified how genetic architecture of mate preference can favor the emergence of such disassortative mating behaviors. In **chapter 2**, I showed that polymorphic loci where the alleles carrying genetic deleterious mutations are dominant, promote the evolution of disassortative mating. Disassortative mating generates sexual selection, which disadvantages heterozygotes at the mating trait locus, limiting the evolution of disassortative preferences. Yet, the genetic architecture of polymorphic traits, such as inversions, reduces the negative sexual selection feedback, as well as opportunity costs associated with disassortative mating. My results highlighted the key role of genetic architecture of mating traits and preferences in the evolution of mate preference.

Second, I focused on how species interaction may limit the evolution of preference towards locally adaptive traits. The positive frequency-dependent selection exerted by predators promotes the convergence of warning traits between sympatric species. However, warning traits are also involved in mate recognition, so that trait convergence might result in heterospecific courtship and mating. In **chapter 3**, I

showed that such reproductive interference promotes preferences for non-mimetic males, because these preferences reduce interactions with heterospecifics. Such preference partially or totally limits the evolution of mimicry, promoting either imperfect mimicry or complete divergence of traits between sympatric species. I highlighted the importance of (1) female and predator discrimination capacities, as well as (2) of historical constraints limiting the warning trait evolution, in the evolution of either imperfect-mimetic or non-mimetic warning traits. In **chapter 4**, I proposed that reproductive interference, by promoting female preference for non-mimetic males, explain the female-limited mimicry observed in some butterfly species. My results highlight how mate preference may limit adaptation to the local environment, and how ecological interaction between species may disturb the adaptive process, occurring within species.

Third, I investigated which traits mate preferences are likely to target. In **chapter 5**, I showed that the conflict between adaptation and species recognition may promote multiple traits preference, targeting an adaptive trait as well as other traits relevant for species recognition. However, I showed that opportunity costs limit the evolution of such multiple traits preference. Because adaptation reduces phenotypic diversity, opportunity costs promote preference based on adaptive traits rather than on traits relevant for species recognition.

In my thesis, I started by studying the evolution of disassortative mating. Then I studied the evolution of reproductive character displacement in mimetic species. Reproductive character displacement is often studied in a context of reinforcement, where it generates an assortative mating leading to reproductive isolation between different populations. All along my thesis, I thus had a reflexion about these two concepts of assortative and disassortative mating in a context of adaptation and speciation. I then decided to write an opinion paper on these concepts, to provide a critical review on these evolutionary mechanisms.

Is Disassortative mating widespread ?

While assortative mating is described in many traits and in a large variety of taxa, disassortative mating is generally thought to be restricted to a handful of emblematic examples. Here we provide an alternative view, showing that disassortative preferences might actually be quite common in nature and play a substantial role in both trait and species diversification.

Disassortative mating occurs when individuals with dissimilar phenotypes mate more often than expected under random mating (Burley, 1983; Hedrick, 2016) (see Box 2). Disassortative mating is then generally described as a characteristic of a population, rather than as an individual. Alternatively, disassortative preference can be defined as an individual preference trait, where a chooser tends to prefer mates, dissimilar from himself, compared with a random choice.

Classical examples of disassortative mating

Numerous examples of disassortative mating are reported in polymorphic populations. Disassortative preference prevents selfing in plants and in fungi, *via* system of self-incompatibility (*i.e.* heterostyly Li *et al.* (2016) and S-alleles Hiscock & McInnis (2003) in plants, mating types in fungi Billiard *et al.* (2011)). By contrast with such examples of disassortative mating based self-incompatibility system, disassortative mating may also be non-strict, where matings preferentially happen between individuals with different phenotypes. Disassortative mating is also documented cases at the MHC loci in animals, where individuals show preference for genotypes different from their own (Kamiya *et al.*, 2014). MHC genes are involved in specific recognition of pathogens, and host-pathogens interactions classically generate negative frequency dependent selection and/or heterozygote advantage (recognition of a larger range of pathogens) (Piertney & Oliver, 2006). Such balancing selection regimes are thought to promote disassortative mating at MHC loci (Slade & McCallum, 1992; Penn & Potts, 1999; Ihara & Feldman, 2003).

Disassortative mating also targets a chromosomal inversion in seaweed flies (Day & Butlin, 1987) (potentially through preference based on cuticular hydrocarbon Enge *et al.* (2021)), chirality in snails (Schilthuizen *et al.*, 2007) but is frequently observed based on coloration (*e.g.* in tropical butterflies (Chouteau *et al.*, 2017), in arctic skuas (Bengtson & Owen, 1973), in white throated sparrows (Throneycroft, 1975; Tuttle *et al.*, 2016), in feral pigeons (Johnston & Johnson, 1989), and in wolves (Hedrick *et al.*, 2016)). Such disassortative mating is often associated with heterozygote advantage (Jay *et al.*, 2021; Butlin *et al.*, 1984; Mérot *et al.*, 2020; Horton *et al.*, 2013) at the mating trait. This type of disassortative mating is adaptive, in the sense that a phenotypic dissimilarity within a mated pairs increases individuals fitness, because it enhances offspring fitness (see Box 2).

Box 2: Definitions

Disassortative mating: when mating occurs in a population more often between individuals with dissimilar phenotype than expected under random mating.

Disassortative preference: individual preference where the chooser tends to prefer mates dissimilar from himself as compared with random preference.

Adaptive disassortative mating/preference: disassortative mating/preference where the phenotypic dissimilarity within a mated pairs increases individuals fitness.

Incidental disassortative mating/preference: disassortative mating/preference arising from a conflict between adaptation and mate preference.

Adaptation towards the local environment: selective process enhancing individuals fitness in a given environment. Here, we assume adaptation linked to natural selection, thus excluding sexual selection.

Conflict between adaptation and mate preference: arise when mate preference targets non-adaptive traits, so that sexual selection and adaptation promote different trait values.

Unknown examples of disassortative mating

Disassortative mating is often assumed to be rare in natural populations. However, we may overlook some cases fitting with the definition of disassortative mating. Under the definition of disassortative mating (Box 2), disassortative mating may be involved in the evolution of sexual dimorphism.

Disassortative mating involved in sexual dimorphism

The sexual selection model is one popular explanation for the evolution of sexual dimorphism (Hedrick & Temeles, 1989). Darwin indeed suggested that sexual selection, *via* female choice, promotes the evolution of divergent phenotype in males, whereas females keep the ancestral phenotype (Darwin, 1871). This model of sexual dimorphism evolution implies that sexual selection favors males that are more dissimilar from females than the average of males, driving the evolution of a dissimilar male phenotype (see figure 9 for an illustration). Females then mate more often with more dissimilar males than expected under random mating, fitting the definition of disassortative mating (Burley, 1983; Hedrick, 2016). This model of sexual dimorphism evolution can thus be viewed as a case of disassortative mating. In sexually dimorphic species, several experimental studies (reviewed in (Hedrick & Temeles, 1989)) measured sexual selection in males, resulting from females preference, that may have underlain the evolution of sexual dimorphism, suggesting that such disassortative mating may be common in natural population.

Reproductive interference may promote disassortative mating

Disassortative mating targeting neutral trait may also arise because of reproductive interference with other species. Reproductive interference, *i.e.* costly sexual interaction between sympatric species, may also be a major force promoting preference for locally maladapted traits (see Box 3). Reproductive interference may

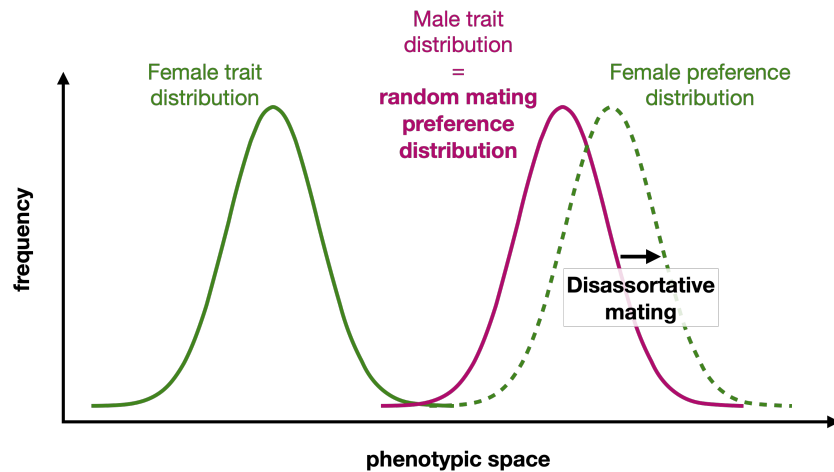


Fig. 9: Illustration of disassortative female preference leading to the evolution of sexual dimorphism. The green and pink solid lines are respectively the distribution of female and male trait. Under random mating the distribution of preference is equal to the distribution of male trait. The dashed green line is the distribution of female preference.

cause reproductive character displacement (Gröning & Hochkirch, 2008; Kyogoku, 2015): the process by which a mating trait shared between two species becomes more dissimilar in sympatric than in allopatric populations because of the negative selection against heterospecific interactions (Brown & Wilson, 1956). Theoretical studies have investigated how the evolution of female preference may promote reproductive character displacement in males (McPeck & Gavrillets, 2006; Yamaguchi & Iwasa, 2013): reproductive interference is predicted to favor the divergence between female preference and trait displayed by heterospecifics, because such preference reduces mating attempts with heterospecifics, and therefore promotes the divergence of reproductive traits between conspecific and heterospecific males, through sexual selection.

Such disassortative mating, by targeting trait values at the limit of trait distribution, may be an agent of trait evolution, by generating directional sexual selection. For instance, in two of the three fruit fly species of the genus *Blepharoneura* that court on the same host plant, a morphometric analysis reveals sexual dimorphism in wing shape where males, but not females, from the two different species differ in

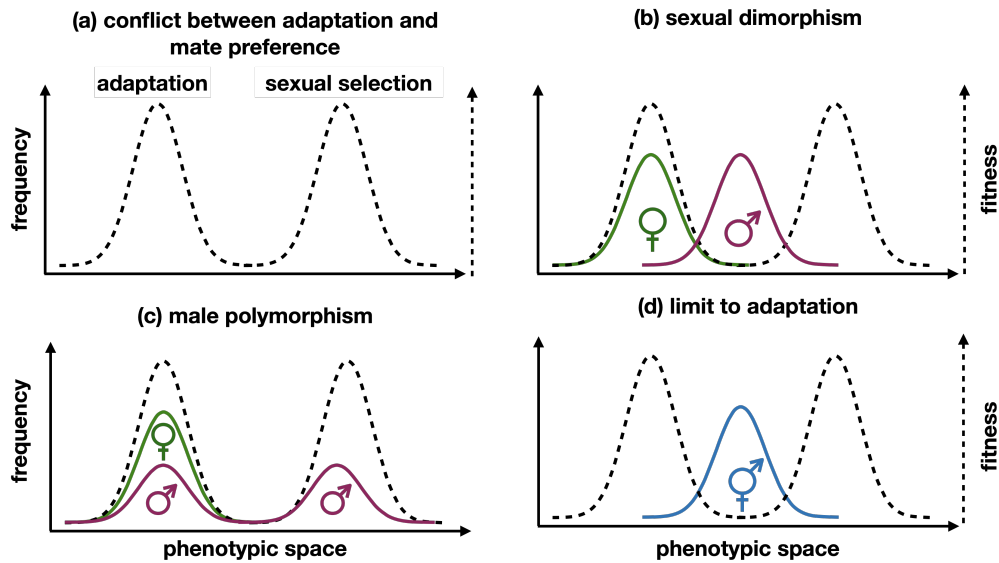


Fig. 10: Illustration of (a) a conflict between adaptation and female preference. Such conflict may either (b) promotes sexual dimorphism, (c) promotes male dimorphism or (d) limits adaptation in both sexes. Dashed lines represent fitness variation due to adaptation and sexual selection. Solid lines represent trait distribution. The blue solid line means that male and female traits have the same distribution. Purple and green solid lines are male and female trait distributions respectively.

wing shape (Marsteller *et al.*, 2009). In the mexican spadefoot toads *Spea multiplicata*, the level of sexual size dimorphism increases with the proportion of species from the same genus *Spea bombifrons* living in sympatry (Pfennig & Pfennig, 2005) suggesting a link between species interaction and sexual dimorphism. Here again, females may mate more often with more dissimilar males than expected under random mating, also fitting with the definition of disassortative mating (Burley, 1983; Hedrick, 2016).

Box 3: When choosing a trait locally adapted increases the risks of reproductive interference

Because sympatric species face a similar environment, natural selection may promote similar adaptive traits in different sympatric species. Therefore, preferences for these adaptive traits may lead to costly courtship and mating with heterospecifics. For example, in the fruit fly *Drosophila serrata*, female preference based on cuticular hydrocarbons (CHCs) increases offspring fitness (Hine *et al.*, 2002). However, such preference leads to reproductive interference with the species *Drosophila birchii*, promoting reproductive character displacement of CHCs in sympatric population of *Drosophila serrata* (Higgie *et al.*, 2000; Higgie & Blows, 2007). The sharp change of CHCs between allopatric and sympatric natural population may indicate a strong selection against the displaced CHCs in allopatric populations (Higgie & Blows, 2007), suggesting that reproductive interference may limit preference for adaptive traits. Such conflict is also observed in the spadefoot toad *Spea multiplicata* where female preference for mating call leads to an increasing number of fertilized eggs, but may lead to reproductive interference as the preferred call resembles the call of heterospecifics (Pfennig, 2000). In sympatric population, females prefer a call that differs from heterospecifics, but this preference reduces female fertility, suggesting a strong reproductive interference in natural populations. Conflict between reproductive interference and preference for adaptive traits may be particularly important when a shared selection specifically promotes traits similarity between sympatric species. In aposematic species, warning traits advertising defense against predators are under strong selection, promoting similarity between sympatric species (mimicry) (Chazot *et al.*, 2014). Indeed, individuals displaying a common warning trait experience a reduced predation risk because predators have already associated the signal with defense (Arias *et al.*, 2016d; Chouteau *et al.*, 2016). This positive frequency-dependent selection promotes similarity between defended individuals regardless of their species (Müller, 1879). Because in defended species, preferences often target the warning trait (Jiggins *et al.*, 2001; Kronforst *et al.*, 2006; Merrill *et al.*, 2014; Naisbit *et al.*, 2001), species similarity increases the risk of reproductive interference. Empirical examples of reproductive interference in Müllerian mimetic systems have been reported (Estrada & Jiggins, 2002; Vasconcellos-Neto & Brown, 1982).

Consequence of disassortative preference on adaptation

By contrast with adaptive disassortative mating, such disassortative mating is incidental. This disassortative mating emerges because mate preference targets locally non-adaptive traits. For example, indirect fitness benefit of producing 'sexy sons', may also promote preferences for neutral or handicapping traits whereas females have a locally adaptive trait (Fisherian runaway (Fisher, 1930; Lande, 1981; Kirkpatrick, 1982)). Then sexual selection generated by such incidental disassortative mating and local adaptation may promote different trait values (see Figure A5.3 (a)), generating a conflict that may limit adaptation to the local environment. As we saw, such mating preference may drive the evolution of trait in males only, leading to the evolution of sexual dimorphism (see Figure (b)).

Female choice can generate disruptive selection on male trait, due to the conflict between local adaptation and sexual selection (see Figure (a)). Disruptive selection promotes polymorphism (Mather, 1955), and may then promote polymorphism in the male mating trait (see Figure (c)). Depending on the genetic architecture of male and female traits, such incidental disassortative mating may also limit adaptation in both sexes (see theoretical studies in mimetic system Boussens-Dumon & Llaurens (2021), Chapter 3, see Figure (d)).

Nevertheless, selective regimes promoting similar traits in sympatric species may not always promote the evolution of disassortative preference. Additional mating traits enhancing species recognition may be targeted by preference preventing conflict with adaptation (Candolin, 2003). Opportunity costs of rejecting a potential mate promote mate preference based on locally adaptive traits rather than preference based on traits enhancing species recognition (Chapitre 5). Such costs indeed increase the proportion of unpreferred potential mate in the population, and weakly impact mate preference based on locally adaptive traits because adaptation reduces phenotypic diversity. Therefore, in populations where choosers suffer from opportunity costs, reproductive interference may promote the evolution of disassortative mating.

How to measure disassortative mating ?

Why does clarifying random mating expectation matter ?

In a context of reinforcement, where species can produce hybrids, preferences underlying the evolution of reproductive character displacement would rather be described as assortative preference. This is because of one ambiguity in the definition of assortative and disassortative mating (Lewontin *et al.*, 1968; Burley, 1983; Hedrick, 2016; Bolnick & Fitzpatrick, 2007). The assortative *vs.* disassortative mating depends on the pool of potential mates considered. If two populations A and B can hybridize, random mating expectations are computed considering individuals of both populations. Then, assortative mating is detected in such divergent populations (Figure 11). By contrast, if post-zygotic isolation is complete between both populations, random mating expectations are computed among individuals within each population, and disassortative mating will be detected in each population. Also, when females from both populations keep displaying a shared ancestral trait value (for example adapted to the local environment), while reproductive character displacement happens in males only, disassortative preference is detected.

What is the right scale to define random mating ? Detecting assortative or disassortative matings allow to identify selective regimes acting on trait and preference or the existence of a structuration in the population. The assortative mating observed at the scale of both populations is relevant for understanding the evolution of reproductive isolation occurring between the two populations. The incidental disassortative mating observed at the scale of each population, informs us of preference targeting trait values at the limit of trait distribution, driving the evolution of trait in both populations. This disassortative mating may inform us of a conflict between local adaptation and mate preference.

When comparing divergent species, assortative mating is likely to be detected. Drift and local selection generate a spatial structuration of phenotypic distribution, generating incidental assortative mating (Jiang *et al.*, 2013). However, de-

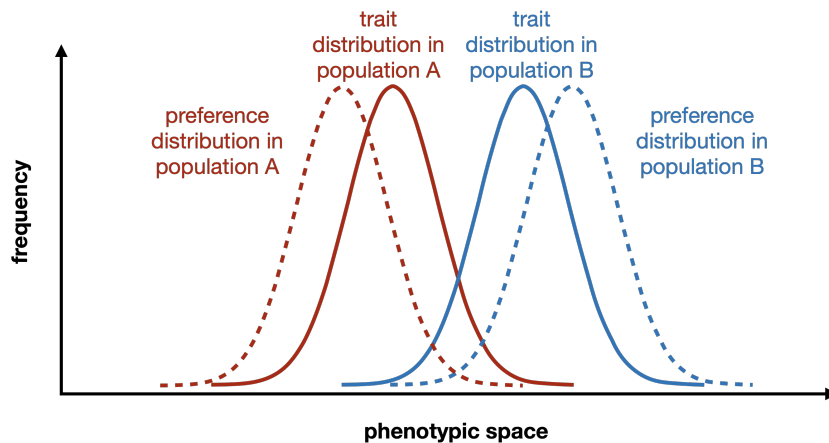


Fig. 11: Illustration of preference leading to reproduction character displacement within two populations. Solid and dashed lines are respectively the distribution of female and male trait. Red and blue represent the two different population A and B respectively.

tecting such assortative mating does not reveal a selection promoting reproductive isolation between different populations, but rather the existence of a spatial structuration. Collecting data to characterise mating preference in living organisms is difficult, so searchers merge data from different populations, which increases the estimated strength of assortative mating (see meta-analyses on size-assortative mating Rios Moura *et al.* (2021)). Rios Moura *et al.* (2021), as previous meta-analyses (Jiang *et al.*, 2013; Janicke *et al.*, 2019), found that disassortative mating is uncommon. However, these meta-analyses probably overestimate assortative mating.

Why do we underestimate disassortative mating ?

These studies rely on the Pearson's correlation coefficient r estimating the correlation between male and female phenotypes across mated pairs (Jiang *et al.*, 2013; Janicke *et al.*, 2019; Rios Moura *et al.*, 2021) and define respectively assortative and disassortative mating as a positive or a negative r coefficient.

This Pearson's correlation coefficient considers only individual belonging to mated

DISCUSSION

pairs, and ignores the trait distribution in non-reproducing individuals. Yet, the non-reproducing individuals are part to the pool of potential mates, and the avoidance of the non-reproducing individuals is the consequence of mating preference. The Pearson's correlation coefficient fails to detect disassortative matings generating directional sexual selection (see Box 4). Such disassortative matings indeed generate differences of reproductive success among potential mates, underlying directional selection. However, these differences in reproductive success may not be detected using the Pearson's correlation coefficient focusing only on mated individuals.

Box 4: Pearson's correlation coefficient does not accurately describe disassortative matings generating directional sexual selection

The discrepancy induced by the different definitions can be illustrated using a toy example of disassortative mating generating directional sexual selection. Let's assume a population of butterflies which can display two alternative wing colors, either red or blue. We assume that natural selection favors red individuals, then most individuals in the population have red wings. We assume that butterflies from this population encounter red heterospecifics, leading to reproductive interference. Such reproductive interference promotes preference for the rare blue individuals, enhancing the rate of conspecific matings (Figure 12). In this example the frequency of mating with dissimilar individuals is higher than expected under random mating, but the Pearson's correlation coefficient is null.

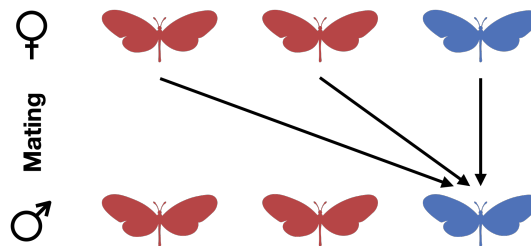


Fig. 12: Example of matings within a population. Disassortative mating may be detected or not, depending on the different definitions. According to the definition we use, disassortative mating occurs because the frequency of mating with dissimilar individuals (equals to $2/3$) is higher than expected under random mating (equals to $4/9$). However, using the Pearson's correlation coefficients, disassortative mating is not detected. Indeed the correlation between male and female phenotypes across mated pairs is null as there is no variation of phenotypes among mated males.

We think using the definition of assortative mating given by Lewontin *et al.* (1968); Burley (1983); Hedrick (2016); Bolnick & Fitzpatrick (2007), rather than the Pearson's correlation coefficient (Jiang *et al.*, 2013; Janicke *et al.*, 2019; Rios Moura *et al.*, 2021), would be more relevant to understand the evolution of mate preferences and their consequences on adaptation and speciation. Indeed, the Pearson's correlation coefficients, by ignoring the trait distribution in non-reproducing indi-

viduals, may sometimes fail to detect sexual selection.

Genetic architecture enabling the evolution of disassortative mating

So far, we questioned the claim that disassortative mating may be rare compared to assortative mating in natural populations. Such claim would also imply that the conditions enabling the evolution of assortative mating are more widespread than those enabling the evolution of disassortative mating in natural populations. Here, we review the scientific literature to uncover the conditions on genetic architecture of the mating trait and preference enabling the evolution of disassortative mating.

Genetic architecture of the mating trait

Because of the opportunity costs associated with the rejection of mating partners, the evolution of disassortative mating crucially depends on the distribution of traits in potential mates, and the genetic architecture of mating traits impacts this distribution. In classical examples of adaptive disassortative mating, a single locus controls the variation of the mating trait (*e.g.* cuticular hydrocarbon in seaweed flies (Enge *et al.*, 2021), sex organ morphology in heterostyly system Li *et al.* (2016); Kappel *et al.* (2017), plumage in the white throated sparrows Tuttle *et al.* (2016), wing color pattern in tropical butterflies Chouteau *et al.* (2017), chirality in snails Schilthuizen *et al.* (2007), protein involved in self-incompatibility in plants Hiscock & McInnis (2003), mating type in some fungi Billiard *et al.* (2011); Branco *et al.* (2018)).

Assuming a single locus genetic architecture of mating trait makes the evolution of disassortative mating limited in diploid population (Chapitre 2). Disassortative preferences rapidly become genetically associated with heterozygosity at the mating trait locus. Most individuals with disassortative preference are then heterozygote at the mating trait locus and tends to prefer homozygotes at the mating

trait locus. When disassortative mating increases, it generates sexual selection promoting homozygotes over heterozygotes, generating a selective regime impairing the fixation of disassortative mating. The generated negative sexual selection feedback limits the evolution of disassortative mating. Moreover, disassortative mating produces an excess of heterozygotes in the population. When disassortative mating is common, individuals with disassortative preference also suffer from increased opportunity costs, due to preference towards the scarce homozygotes. Because individuals chose their mate based on their phenotype, the dominance relationships at the mating trait locus that determines heterozygote phenotype, is a crucial parameter. When the rarest mating trait allele is dominant, the negative sexual selection feedback limiting the evolution of disassortative mating is reduced. Such condition also reduces opportunity costs associated with disassortative mating. Depending on the dominance relationships at the mating trait locus, strict disassortative mating can thus evolve despite the negative sexual selection feedback.

Such strict dominance interactions are generally observed between self-incompatibility S-alleles (Hatakeyama *et al.*, 1998), which is a case of strict disassortative mating. Similarly, in the white throated sparrow, where disassortative mating is almost obligate Thronycroft (1975); Tuttle *et al.* (2016). A strict dominance relationship is observed at the supergene controlling plumage variation (Tuttle *et al.*, 2016). A strict dominance of mating trait allele is also observed in the mimetic butterfly *Heliconius numata* (Jay *et al.*, 2021).

In these examples, dominant alleles are associated with recessive deleterious mutations (Llaurens *et al.*, 2009; Tuttle *et al.*, 2016; Jay *et al.*, 2021). Numerical simulations highlight that the association of recessive deleterious mutations to the dominant allele favors the evolution of disassortative mating (Chapter 2). Polymorphism at a single locus promotes the accumulative of recessive deleterious mutations, because there is limited recombination between different alleles (Berdan *et al.*, 2021). Once disassortative mating becomes common, recessive deleterious mutations accumulate mainly in dominant alleles. Recessive deleterious mutations are indeed not purged in dominant alleles, because the frequency of homozygous

with recessive alleles is low (Llaurens *et al.*, 2009). Once disassortative mating is common in the population, this accumulation of recessive deleterious mutations in dominant alleles may allow the evolution of higher levels of disassortative mating.

Disassortative mating based on MHC genotype, involved in the immune response, is also frequently reported in a wide range of species (Kamiya *et al.*, 2014). In contrast with previous examples, MHC genotype depends of a multiple alleles at several loci, reducing opportunity costs and the negative sexual selection feedback. This is consistent with the numerical analysis reported in Greenspoon & M'Gonigle (2014), showing that the evolutionarily stable level of disassortative preference targeting a MHC locus increases with the number of alleles at a MHC locus. The evolution of disassortative preference at MHC loci may be facilitated by the multiple alleles maintained by selection exerted by pathogens (de Vries, 1989). By contrast with previous examples of disassortative mating, the co-dominance of MHC alleles may promote the evolution of disassortative mating. Such co-dominance indeed increases parasite detection, generating heterozygotes advantage, promoting the evolution of MHC-based disassortative mating (Penn *et al.*, 2002).

Incidental disassortative mating underlying reproductive character displacement may be observed based on a trait displaying either discrete or continuous variation (*e.g.* chirality, either dextral or sinistral, in snail Johnson (1982) and body size in tinkerbirds (Kirschel *et al.*, 2009)). Theoretical studies show that when the mating trait displays a continuous variation, female discrimination capacities determine the level of divergence between female preference and trait displayed by heterospecifics (McPeck & Gavrillets, 2006; Yamaguchi & Iwasa, 2013). A high female discrimination can promote an imperfect similarity of mating traits between sympatric species that both (1) limit reproductive interference and (2) allow the display of adaptive trait values (Chapter 3). By contrast, when the mating trait is polymorphic, such imperfect similarity may not happen, leading more often to disassortative mating underlying reproductive character displacement.

Genetic architecture of preference

Molecular mechanisms underlying preference are largely unknown. Yet, they are key to understand how disassortative preference can evolve. Mathematical models investigating the evolution of mate preference often assume two types of genetic architectures underlying mate choice behaviour. Many models assumed matching rule, *i.e.* assumes that mate choice depends on a match between the phenotypes of the chooser and the chosen individuals (Kopp *et al.*, 2018). The matching rule, often used in mathematical models, may be rather uncommon in nature (Kopp *et al.*, 2018). Testing matching rule is hard, because it requires to manipulate the signal of the chooser, to test whether it modifies the choice (but see Hauber *et al.* (2000)). By contrast other models assumed preference allele triggering attraction or rejection towards the recognised phenotype (Kopp *et al.*, 2018). A theoretical study showed that genetic architectures of preference implying recognition of specific alleles, triggering either attraction or rejection towards the recognised phenotype, limits the evolution of disassortative mating, when the genetic basis of the preference and the mating trait are not tightly linked (Chapter 1). In this two-locus genetic architecture model, with one mating trait locus and one preference locus, recombination produces 'assortative' haplotype. For example, recombination favors the association between mating trait allele and a preference allele triggering attraction for the trait associated with the mating trait allele.

Alleles underlying disassortative mating empirically identified generally trigger rejection towards the recognised phenotype, either by mechanically preventing assortative mating because of alternative relative height difference between pistil and anthers (*e.g.* alleles at the heterostyly locus in plants (Li *et al.*, 2016)), or by molecular recognition of S-alleles provoking an incompatible reaction (*e.g.* alleles at the self-incompatibility locus (Hiscock & McInnis, 2003) in plants or at mating type loci *MAT* in fungi (Billiard *et al.*, 2011)). These molecular and morphological mechanisms allow the evolution of disassortative mating, because these rejection alleles also control the variation of the mating trait. For instance, at the *S*-locus, the gene *SCR*, controlling the proteins expressed on the pollen coat and the gene

SRK encoding the receptor located in the pistil are tightly linked (Sato *et al.*, 2002). The *S*-locus shows important structural rearrangements that limit the recombination between these two genes (Goubet *et al.*, 2012). This recombination suppression may have favored the evolution of self-incompatibility.

The genetic mechanisms involved in disassortative mating are nevertheless largely unknown in animals. The genetic basis of mate preferences are mostly documented for assortative mating behaviors. Attraction towards specific traits have been documented to trigger assortative mating in *Heliconius* butterflies (Jiggins *et al.*, 2001). The locus controlling male preference for yellow *vs.* white in *H. cydno* maps close to the gene *aristalless*, whose expression differences determine the white/yellow switch in this species (Kronforst *et al.*, 2006; Westerman *et al.*, 2018). In *H. melpomene*, a major QTL associated with preference towards red was identified in crosses between individuals displaying a red pattern and individuals with a white pattern (Merrill *et al.*, 2019). This QTL is also located close to the gene *optix* involved in the variation of red patterning in *H. melpomene*. Assortative mating in *Heliconius* thus seems to rely on alleles encoding preference for specific cues, linked with loci involved in the variation of these cues.

Models investigating the evolution of sexual dimorphism by sexual selection, or reproductive character displacement, assume genetic architecture of preference involving recognition alleles and recombination with mating trait loci (Lande & Arnold (1985); McPeck & Gavrillets (2006); Yamaguchi & Iwasa (2013), Chapter 3 and 4). By contrast with adaptive disassortative mating, the genetic architecture of preference involving recognition alleles and recombination allows the evolution of incidental disassortative mating. The reason remains unclear but the number of loci controlling variation in trait and preference may be crucial. In contrast with some classical examples of disassortative mating, these models assume continuous variation of trait and preference values controlled by a large number of loci. The MHC-genotype may be close to a quantitative trait, because there is a large number of loci (Stefan *et al.*, 2019). Furthermore, multiple alleles are maintained within each of these loci. As a result, the level of divergence between MHC haplotypes, composed of a series of alleles at the different loci, can be highly variable. The

level of divergence within a MHC-genotype might play a substantial role in the resistance to multiple pathogens (Lenz, 2011; Arora *et al.*, 2019), and might influence mate preference (Wedekind & Füre, 1997). MHC-based disassortative mating may be based on odour cues (Wedekind & Penn, 2000). The genetic architecture of MHC-based disassortative mating remains unknown, but the genetic basis of mate preference could be unlinked to MHC loci. In case of incidental disassortative preference, the fact that the phenotypic dissimilarity within a mated pair does not enhance offspring fitness could also explain why recombination allows the evolution of such preference.

Conclusion

The literature on disassortative mating has mainly focused on disassortative mating promoted by balancing selection. In this review, we highlight that disassortative mating might be more widespread than previously thought. Disassortative mating may be involved in the evolution of sexual dimorphism, driven by female preference: females keep the ancestral trait adapted to the local environment, while sexual selection promotes the evolution of a dissimilar trait in males. Contrary to classical examples, disassortative mating may generate a selection promoting trait values at the limit of trait distribution. Costly sexual interactions between sympatric species may be a major cause of such mating preference limiting local adaptation. We stress the need to consider inter-specific, in addition to intra-specific evolutionary pressures on the evolution of preference, to reconcile population genetics studies focusing on the role of mate preference on adaptation with speciation studies considering the effect of mate preference on population divergence.

BIBLIOGRAPHY

Bibliography

- Andersson, M. 1994. *Sexual selection*. Vol. 72. Princeton University Press. 10
- Arias, M., Mappes, J., Théry, M., & Llaurens, V. 2016a. Inter-species variation in unpalatability does not explain polymorphism in a mimetic species. *Evolutionary ecology*, **30**(3), 419–433. 24, 26
- Arias, M., Meichanetzoglou, A., Elias, M., Rosser, N., de Silva, D. L., Nay, B., & Llaurens, V. 2016b. Variation in cyanogenic compounds concentration within a heliconius butterfly community: does mimicry explain everything? *Bmc evolutionary biology*, **16**(1), 272. 39
- Arias, M., le Poul, Y., Chouteau, M., Boisseau, R., Rosser, N., Théry, M., & Llaurens, V. 2016c. Crossing fitness valleys: empirical estimation of a fitness landscape associated with polymorphic mimicry. *Proceedings of the royal society b: Biological sciences*, **283**(1829), 20160391. 131
- Arias, M., le Poul, Y., Chouteau, M., Boisseau, R., Rosser, N., Théry, M., & Llaurens, V. 2016d. Crossing fitness valleys: empirical estimation of a fitness landscape associated with polymorphic mimicry. *Proceedings of the royal society b: Biological sciences*, **283**(1829), 20160391. 342
- Arora, J., Pierini, F., McLaren, P. J., Carrington, M., Fellay, J., & Lenz, T. L. 2019. HLA Heterozygote Advantage against HIV-1 Is Driven by Quantitative and Qualitative Differences in HLA Allele-Specific Peptide Presentation. *Molecular biology and evolution*, **37**(3), 639–650. 353
- Aubier, T. G., & Sherratt, T. N. 2015. Diversity in müllerian mimicry: The optimal predator sampling strategy explains both local and regional polymorphism in prey. *Evolution*, **69**(11), 2831–2845. 162

BIBLIOGRAPHY

- Aubier, T. G., Kokko, H., & Joron, M. 2019. Coevolution of male and female mate choice can destabilize reproductive isolation. *Nature communications*, **10**(1), 5122. 116
- Backwell, P. R. Y., & Passmore, N. I. 1996. Time constraints and multiple choice criteria in the sampling behaviour and mate choice of the fiddler crab, *uca annulipes*. *Behavioral ecology and sociobiology*, **38**(6), 407–416. 86
- Balmford, A., Thomas, A. L. R., & Jones, I. L. 1993. Aerodynamics and the evolution of long tails in birds. *Nature*, **361**(6413), 628–631. 10
- Balogh, A. C., & Leimar, O. 2005. Müllerian mimicry: an examination of fisher’s theory of gradual evolutionary change. *Proceedings of the royal society b: Biological sciences*, **272**(1578), 2269–2275. 132, 161
- Balshine, S., Kempenaers, B., Székely, T., Kokko, H., & Johnstone, R. A. 2002. Why is mutual mate choice not the norm? operational sex ratios, sex roles and the evolution of sexually dimorphic and monomorphic signalling. *Philosophical transactions of the royal society of london. series b: Biological sciences*, **357**(1419), 319–330. 242
- Bank, C., Hermisson, J., & Kirkpatrick, M. 2012. Can reinforcement complete speciation? *Evolution*, **66**(1), 229–239. 87
- Barrett, S. C. 1990. The evolution and adaptive significance of heterostyly. *Trends in ecology & evolution*, **5**(5), 144 – 148. 86
- Barton, N. H., & Turelli, M. 1991. Natural and sexual selection on many loci. *Genetics*, **127**(1), 229–255. 86, 135, 168, 170, 215, 250, 251
- Barton, R. A., Purvis, A., & Harvey, P. H. 1995. Evolutionary radiation of visual and olfactory brain systems in primates, bats and insectivores. *Philosophical transactions of the royal society of london. series b: Biological sciences*, **348**(1326), 381–392. 19, 296

- Bates, H. W. 1862. Contributions to an insect fauna of the amazon valley (lepidoptera: Heliconidae). *Biological journal of the linnean society*, **16**(1), 41–54. 23, 211
- Baur, J., Giesen, A., Rohner, P. T., Blanckenhorn, W. U., & Schäfer, M. A. 2020. Exaggerated male forelegs are not more differentiated than wing morphology in two widespread sister species of black scavenger flies. *Journal of zoological systematics and evolutionary research*, **58**(1), 159–173. 245
- Beccaloni, G. 1997. Ecology, natural history and behaviour of ithomiine butterflies and their mimics in ecuador (lepidoptera: Nymphalidae: Ithomiinae). *Tropical lepidoptera*, **8**(01), 103–124. 131
- Beccaloni, G. W. 2008. Vertical stratification of ithomiine butterfly (Nymphalidae: Ithomiinae) mimicry complexes: the relationship between adult flight height and larval host-plant height. *Biological journal of the linnean society*, **62**(3), 313–341. 162
- Belt, T. 1874.. *The naturalist in nicaragua: A narrative of a residence at the gold mines of chontales; journeys in the savannahs and forests. with observations on animals and plants in reference to the theory of evolution of living forms.* London, J. Murray,. 28, 212, 241
- Bengtson, S.-A., & Owen, D. F. 1973. Polymorphism in the arctic skua *Stercorarius parasiticus* in iceland. *Ibis*, **115**(1), 87–92. 338
- Benitez-Vieyra, S., de Ibarra, N. H., Wertlen, A. M., & Cocucci, A. A. 2007. How to look like a mallow: evidence of floral mimicry between turneraceae and malvaceae. *Proceedings of the royal society b: Biological sciences*, **274**(1623), 2239–2248. 131
- Benson, W. W. 1972. Natural selection for mullerian mimicry in heliconius erato in costa rica. *Science*, **176**(4037), 936–939. 131, 139, 219

BIBLIOGRAPHY

- Berdan, E. L., Blanckaert, A., Butlin, R. K., & Bank, C. 2021. Deleterious mutation accumulation and the long-term fate of chromosomal inversions. *PloS genetics*, **17**(3), 1–23. 71, 349
- Berson, J. D., & Simmons, L. W. 2019. Female cuticular hydrocarbons can signal indirect fecundity benefits in an insect. *Evolution*, **73**(5), 982–989. 19, 296
- Billiard, S., López-Villavicencio, M., Devier, B., Hood, M. E., Fairhead, C., & Giraud, T. 2011. Having sex, yes, but with whom? inferences from fungi on the evolution of anisogamy and mating types. *Biological reviews*, **86**(2), 421–442. 68, 337, 348, 351
- Boggs, C. L., & Gilbert, L. E. 1979. Male contribution to egg production in butterflies: Evidence for transfer of nutrients at mating. *Science*, **206**(4414), 83–84. 242
- Bolnick, D. I., & Fitzpatrick, B. M. 2007. Sympatric speciation: Models and empirical evidence. *Annual review of ecology, evolution, and systematics*, **38**(1), 459–487. 10, 344, 347
- Borer, M., Van Noort, T., Rahier, M., & Naisbit, R. E. 2010. Positive frequency-dependent selection on warning color in alpine leaf beetles. *Evolution*, **64**(12), 3629–3633. 22
- Borzée, A., Kim, J. Y., Da Cunha, M. A. M., Lee, D., Sin, E., Oh, S., Yi, Y., & Jang, Y. 2016. Temporal and spatial differentiation in microhabitat use: Implications for reproductive isolation and ecological niche specification. *Integrative zoology*, **11**(5), 375–387. 315
- Boussens-Dumon, G., & Llaurens, V. 2021. Sex, competition and mimicry: an eco-evolutionary model reveals how ecological interactions shape the evolution of phenotypes in sympatry. *Oikos*, **in press**. 18, 134, 214, 295, 343
- Boyden, T. C. 1976. Butterfly palatability and mimicry: Experiments with ameiva lizards. *Evolution*, **30**(1), 73–81. 22

- Branco, S., Carpentier, F., Rodríguez de la Vega, R. C., Badouin, H., Snirc, A., Le Prieur, S., Coelho, M. A., de Vienne, D. M., Hartmann, F. E., Begerow, D., Hood, M. E., & Giraud, T. 2018. Multiple convergent supergene evolution events in mating-type chromosomes. *Nature communications*, **9**(1), 2000. 348
- Brennan, P. L., Clark, C. J., & Prum, R. O. 2010. Explosive eversion and functional morphology of the duck penis supports sexual conflict in waterfowl genitalia. *Proceedings of the royal society b: Biological sciences*, **277**(1686), 1309–1314. 245
- Briolat, E. S., Burdfield-Steel, E. R., Paul, S. C., Rönkä, K. H., Seymoure, B. M., Stankowich, T., & Stuckert, A. M. M. 2019. Diversity in warning coloration: selective paradox or the norm? *Biological reviews*, **94**(2), 388–414. 23, 131
- Brooks, R., & Couldrige, V. 1999. Multiple sexual ornaments coevolve with multiple mating preferences. *The american naturalist*, **154**(1), 37–45. 14, 87
- Brower, A. V. Z. 1996. Parallel race formation and the evolution of mimicry in *Heliconius* butterflies: a phylogenetic hypothesis from mitochondrial dna sequences. *Evolution*, **50**(1), 195–221. 26
- Brown, W. L., J., & Wilson, E. O. 1956. Character Displacement. *Systematic biology*, **5**(2), 49–64. 133, 340
- Brown, K. S., & Benson, W. W. 1974. Adaptive polymorphism associated with multiple müllerian mimicry in *heliconius numata* (lepid. nymph.). *Biotropica*, **6**(4), 205–228. 25
- Burley, N. 1983. The meaning of assortative mating. *Ethology and sociobiology*, **4**(4), 191–203. 337, 339, 341, 344, 347
- Butlin, R. K., Collins, P. M., & Day, T. H. 1984. The effect of larval density on an inversion polymorphism in the seaweed fly *coelopa frigida*. *Heredity*, **52**(3), 415–423. 37, 338

BIBLIOGRAPHY

- Bybee, S. M., Yuan, F., Ramstetter, M. D., Llorente-Bousquets, J., Reed, R. D., Osorio, D., & Briscoe, A. D. 2012. Uv photoreceptors and uv-yellow wing pigments in heliconius butterflies allow a color signal to serve both mimicry and intraspecific communication. *The american naturalist*, **179**(1), 38–51. 159
- Byers, D. L., & Meagher, T. R. 1992. Mate availability in small populations of plant species with homomorphic sporophytic self-incompatibility. *Heredity*, **68**(4), 353–359. 12
- Byers, J. A., & Waits, L. 2006. Good genes sexual selection in nature. *Proceedings of the national academy of sciences*, **103**(44), 16343–16345. 12, 13, 86
- Byers, J., Wiseman, P., Jones, L., & Roffe, T. 2005. A large cost of female mate sampling in pronghorn. *The american naturalist*, **166**(6), 661–668. 11, 85
- Candolin, U. 2003. The use of multiple cues in mate choice. *Biological reviews*, **78**(4), 575–595. 18, 19, 295, 296, 343
- Candolin, U., & Reynolds, J. D. 2001. Sexual signaling in the European bitterling: females learn the truth by direct inspection of the resource. *Behavioral ecology*, **12**(4), 407–411. 314
- Casselton, L. A. 2002. Mate recognition in fungi. *Heredity*, **88**(2), 142–147. 37
- Chai, P. 1996. Butterfly visual characteristics and ontogeny of responses to butterflies by a specialized tropical bird. *Biological journal of the linnean society*, **59**(1), 37–67. 22
- Chai, P., & Srygley, R. B. 1990. Predation and the flight, morphology, and temperature of neotropical rain-forest butterflies. *The american naturalist*, **135**(6), 748–765. 29, 211
- Charlesworth, D., & Charlesworth, B. 1975. Theoretical genetics of batesian mimicry ii. evolution of supergenes. *Journal of theoretical biology*, **55**(2), 305–324. 25, 26

- Chazot, N., Willmott, K. R., Santacruz Endara, P. G., Toporov, A., Hill, R. I., Jiggins, C. D., & Elias, M. 2014. Mutualistic mimicry and filtering by altitude shape the structure of andean butterfly communities. *The american naturalist*, **183**(1), 26–39. 23, 131, 157, 158, 342
- Chouteau, M., Arias, M., & Joron, M. 2016. Warning signals are under positive frequency-dependent selection in nature. *Proceedings of the national academy of sciences*, **113**(8), 2164–2169. 22, 25, 39, 44, 131, 139, 219, 342
- Chouteau, M., Llaurens, V., Piron-Prunier, F., & Joron, M. 2017. Polymorphism at a mimicry supergene maintained by opposing frequency-dependent selection pressures. *Proceedings of the national academy of sciences*, **114**(31), 8325–8329. 24, 39, 54, 88, 111, 338, 348
- Chouteau, M., Dezeure, J., Sherratt, T. N., Llaurens, V., & Joron, M. 2019. Similar predator aversion for natural prey with diverse toxicity levels. *Animal behaviour*, **153**, 49 – 59. 39
- Cisar, C. R. 1999. Mating system of the filamentous ascomycete, *glomerella cingulata*. *Current genetics*. 86
- Cortesi, F., & Cheney, K. L. 2010. Conspicuousness is correlated with toxicity in marine opisthobranchs. *Journal of evolutionary biology*, **23**(7), 1509–1518. 131
- Cotto, O., & Servedio, M. R. 2017. The roles of sexual and viability selection in the evolution of incomplete reproductive isolation: From allopatry to sympatry. *The american naturalist*, **190**(5), 680–693. 114
- Crapon de Caprona, M.-D., & Ryan, M. J. 1990. Conspecific mate recognition in swordtails, *xiphophorus nigrensis* and *x. pygmaeus* (poeciliidae): olfactory and visual cues. *Animal behaviour*, **39**(2), 290–296. 20, 159, 297
- Cummings, M. E. 2004. Modelling divergence in luminance and chromatic detection performance across measured divergence in surfperch (embiotocidae) habitats. *Vision research*, **44**(11), 1127–1145. 19, 296

BIBLIOGRAPHY

- Dale, S., & Slagsvold, T. 1996. Mate choice on multiple cues, decision rules and sampling strategies in female pied flycatchers. *Behaviour*, **133**(11/12), 903–944. 18, 295
- Dalziell, A. H., & Welbergen, J. A. 2016. Mimicry for all modalities. *Ecology letters*, **19**(6), 609–619. 132
- Darragh, K., Vanjari, S., Mann, F., Gonzalez-Rojas, M. F., Morrison, C. R., Salazar, C., Pardo-Diaz, C., Merrill, R. M., McMillan, W. O., Schulz, S., & Jiggins, C. D. 2017. Male sex pheromone components in *Heliconius* butterflies released by the androconia affect female choice. *Peerj*, **5**(Nov.), e3953. 28, 133, 159, 213, 242
- Darwin, C. 1871. *The descent of man*. J. Murray. 10, 210, 339
- Day, T. H., & Butlin. 1987. Non-random mating in natural populations of the seaweed fly, *Coelopa frigida*. *Heredity*. 37, 338
- de Cara, M., Barton, N., & Kirkpatrick, M. 2008. A model for the evolution of assortative mating. *The American Naturalist*, **171**(5), 580–596. 13, 37, 87, 92
- de Vries, R. R. P. 1989. *Biological significance of the MHC*. Dordrecht: Springer Netherlands. Pages 6–12. 114, 350
- Devries, P., Lande, R., & Murray, D. 1999. Associations of co-mimetic ithomiine butterflies on small spatial and temporal scales in a neotropical rainforest. *Biological Journal of the Linnean Society*, **67**(05), 73 – 85. 162
- Dieckmann, U. 2004. *Adaptive speciation*. Cambridge Studies in Adaptive Dynamics. Cambridge University Press. 87
- Dittrich, W., Gilbert, F., Green, P., McGregor, P., & Grewcock, D. 1993. Imperfect mimicry: a pigeon's perspective. *Proceedings of the Royal Society of London. Series B: Biological Sciences*, **251**(1332), 195–200. 157

- Doucet, S. M., & Montgomerie, R. 2003. Multiple sexual ornaments in satin bowerbirds: ultraviolet plumage and bowers signal different aspects of male quality. *Behavioral ecology*, **14**(4), 503–509. 18, 295
- Drickamer, L. C., Gowaty, P. A., & Holmes, C. M. 2000. Free female mate choice in house mice affects reproductive success and offspring viability and performance. *Animal behaviour*, **59**(2), 371 – 378. 12, 13, 86
- Eddy, S. L., Kiemiec-Tyburczy, K. M., Uyeda, J. C., & Houck, L. D. 2012. The influence of sequential male courtship behaviors on courtship success and duration in a terrestrial salamander, *Plethodon shermani*. *Ethology*, **118**(12), 1240–1250. 314
- Elias, M., Gompert, Z., Jiggins, C., & Willmott, K. 2008. Mutualistic interactions drive ecological niche convergence in a diverse butterfly community. *Plos biology*, **6**(12), 1–1. 131, 157, 158, 162
- Encinas-Viso, F., Young, A. G., & Pannell, J. R. 2020. The loss of self-incompatibility in a range expansion. *Journal of evolutionary biology*, **33**(9), 1235–1244. 12
- Enge, S., Mérot, C., Mozuraitis, R., Apšegaite, V., Bernatchez, L., Martens, G. A., Radžiute, S., Pavia, H., & Berdan, E. L. 2021. A supergene in seaweed flies modulates male traits and female perception. *bioRxiv*. 338, 348
- Estrada, C., & Jiggins, C. D. 2008. Interspecific sexual attraction because of convergence in warning colouration: is there a conflict between natural and sexual selection in mimetic species? *Journal of evolutionary biology*, **21**(3), 749–760. 27, 133, 213
- Estrada, C., & Jiggins, C. 2002. Patterns of pollen feeding and habitat preference among heliconius species. *Ecological entomology*, **27**(08), 448 – 456. 159, 242, 342
- Ewens, W. J. 1979. *Mathematical population genetics i. theoretical introduction*. Springer, New York, NY. 86

BIBLIOGRAPHY

- Falk, C. T., & Li, C. C. 1969. Negative assortative mating: exact solution to a simple model. *Genetics*, **62**(1), 215–223. 71, 88
- Faria, R., Johannesson, K., Butlin, R. K., & Westram, A. M. 2019. Evolving inversions. *Trends in ecology & evolution*. 71
- Fiedler, D., Sbeglia, G. C., Nehm, R. H., & Harms, U. 2019. How strongly does statistical reasoning influence knowledge and acceptance of evolution? *Journal of research in science teaching*, **56**(9), 1183–1206. 9
- Finkbeiner, S. D., Briscoe, A. D., & Reed, R. D. 2014. Warning signals are seductive: Relative contributions of color and pattern to predator avoidance and mate attraction in heliconius butterflies. *Evolution*, **68**(12), 3410–3420. 158
- Fisher, R. A. 1930. *The genetical theory of natural selection*,. Oxford: The Clarendon Press. 13, 14, 16, 86, 87, 343
- Flanagan, N. S., Tobler, A., Davison, A., Pybus, O. G., Kapan, D. D., Planas, S., Linares, M., Heckel, D., & McMillan, W. O. 2004. Historical demography of müllerian mimicry in the neotropical heliconius butterflies. *Proceedings of the national academy of sciences*, **101**(26), 9704–9709. 26, 132
- Ford, E. 1975. *Ecological genetics*. Springer Netherlands. 28, 211
- Franks, D. W., & Noble, J. 2004. Batesian mimics influence mimicry ring evolution. *Proceedings of the royal society of london. series b: Biological sciences*, **271**(1535), 191–196. 132
- Franks, D. W., & Sherratt, T. N. 2007. The evolution of multicomponent mimicry. *Journal of theoretical biology*, **244**(4), 631 – 639. 132, 161
- Franks, D. W., Ruxton, G. D., & Sherratt, T. N. 2009. Warning signals evolve to disengage batesian mimics. *Evolution*, **63**(1), 256–267. 162
- Fujimoto, H., Hiramatsu, T., & Takafuji, A. 1996. Reproductive interference between panonychus mori yokoyama and p. citri (mcgregor) (acari: Tetranychidae) in peach orchards. *Applied entomology and zoology*, **31**(1), 59–65. 16

- Gavrilets, S. 2004. *Fitness landscapes and the origin of species (mpb-41)*. Princeton University Press. 87
- Gavrilets, S., & Boake, C. 1998. On the evolution of premating isolation after a founder event. *The american naturalist*, **152**(5), 706–716. 92
- Gigerenzer, G., Todd, P., & Group, A. R. 1999. *Simple heuristics that make us smart*. Evolution and cognition. Oxford University Press. 314
- Gilchrist, G. W. 1990. The consequences of sexual dimorphism in body size for butterfly flight and thermoregulation. *Functional ecology*, **4**(4), 475–487. 29, 211
- Girard, M. B., Elias, D. O., & Kasumovic, M. M. 2015. Female preference for multi-modal courtship: multiple signals are important for male mating success in peacock spiders. *Proceedings of the royal society b: Biological sciences*, **282**(1820), 20152222. 18, 295
- Gomulkiewicz, R. S., & Hastings, A. 1990. Ploidy and evolution by sexual selection: a comparison of haploid and diploid female choice models near fixation equilibria. *Evolution*, **44**(4), 757–770. 87
- González-Rojas, M. F., Darragh, K., Robles, J., Linares, M., Schulz, S., McMillan, W. O., Jiggins, C. D., Pardo-Diaz, C., & Salazar, C. 2020. Chemical signals act as the main reproductive barrier between sister and mimetic *Heliconius* butterflies. *Proceedings of the royal society b: Biological sciences*, **287**(1926), 20200587. 28, 133, 159, 213, 242, 313
- Goodale, E., & Kotagama, S. W. 2006. Vocal mimicry by a passerine bird attracts other species involved in mixed-species flocks. *Animal behaviour*, **72**(2), 471 – 477. 131
- Goubet, P. M., Bergès, H., Bellec, A., Prat, E., Helmstetter, N., Mangenot, S., Gallina, S., Holl, A.-C., Fobis-Loisy, I., Vekemans, X., & Castric, V. 2012. Contrasted patterns of molecular evolution in dominant and recessive self-incompatibility haplotypes in arabidopsis. *Plos genetics*, **8**(3), 1–13. 69, 352

BIBLIOGRAPHY

- Grace, J. L., & Shaw, K. L. 2011. Coevolution of male mating signal and female preference during early lineage divergence of the hawaiian cricket, *Laupala cerasina*. *Evolution*, **65**(8), 2184–2196. 14, 87
- Gray, D. A. 2022. Sexual selection and 'species recognition'; revisited: serial processing and order-of-operations in mate choice. *Proceedings of the royal society b: Biological sciences*, **289**(1971), 20212687. 314
- Greenfield, M. D., Alem, S., Limousin, D., & Bailey, N. W. 2014. The dilemma of fisherian sexual selection: Mate choice for indirect benefits despite rarity and overall weakness of trait-preference genetic correlation. *Evolution*, **68**(12), 3524–3536. 13
- Greenspoon, P. B., & M'Gonigle, L. K. 2014. Host–parasite interactions and the evolution of nonrandom mating. *Evolution*, **68**(12), 3570–3580. 88, 114, 350
- Greenspoon, P. B., & Otto, S. P. 2009. Evolution by fisherian sexual selection in diploids. *Evolution*, **63**(4), 1076–1083. 87
- Grill, C. P., & Moore, A. 1998. Effects of a larval antipredator response and larval diet on adult phenotype in an aposematic ladybird beetle. *Oecologia*, **114**, 274–282. 132
- Gröning, J., & Hochkirch, A. 2008. Reproductive interference between animal species. *The quarterly review of biology*, **83**(10), 257–82. 16, 27, 28, 133, 140, 161, 213, 295, 314, 340
- Gumm, J. M., & Gabor, C. R. 2005. Asexuals looking for sex: conflict between species and mate-quality recognition in sailfin mollies (*poecilia latipinna*). *Behavioral ecology and sociobiology*, **58**(6), 558–565. 18, 295
- Gwynne, D. T., & Rentz, D. C. F. 1983. Beetles on the bottle: male buprestids mistake stubbies for females (coleoptera). *Australian journal of entomology*, **22**(1), 79–80. 16

- Harms, U., & Fiedler, D. 2019. *Improving student understanding of randomness and probability to support learning about evolution*. Cham: Springer International Publishing. Pages 271–283. 9
- Hatakeyama, K., Watanabe, M., Takasaki, T., Ojima, K., & Hinata, K. 1998. Dominance relationships between s-alleles in self-incompatible *brassica campestris* l. *Heredity*, **80**(2), 241–247. 349
- Hatfield, T., & Schluter, D. 1999. Ecological speciation in sticklebacks: Environment-dependent hybrid fitness. *Evolution*, **53**(3), 866–873. 16
- Hauber, M. E., Sherman, P. W., & Paprika, D. 2000. Self-referent phenotype matching in a brood parasite: the armpit effect in brown-headed cowbirds (*molothrus ater*). *Animal cognition*, **3**(2), 113–117. 22, 351
- Hedrick, A. V., & Temeles, E. J. 1989. The evolution of sexual dimorphism in animals: Hypotheses and tests. *Trends in ecology & evolution*, **4**(5), 136–138. 339
- Hedrick, P. W., Smith, D. W., & Stahler, D. R. 2016. Negative-assortative mating for color in wolves. *Evolution*, **70**(4), 757–766. 338
- Hedrick, P. 2016. Inbreeding and nonrandom mating. *Pages 249–254 of: Kliman, R. M. (ed), Encyclopedia of evolutionary biology*. Oxford: Academic Press. 337, 339, 341, 344, 347
- Heisler, I. L. 1984. A quantitative genetic model for the origin of mating preferences. *Evolution*, **38**(6), 1283–1295. 13, 86
- Heisler, I. L. 1985. Quantitative genetic models of female choice based on 'arbitrary' male characters. *Heredity*, **55**(2), 187–198. 13, 86
- Higgie, M., & Blows, M. 2007. Are traits that experience reinforcement also under sexual selection? *The american naturalist*, **170**(3), 409–420. 18, 295, 342
- Higgie, M., Chenoweth, S., & Blows, M. W. 2000. Natural selection and the reinforcement of mate recognition. *Science*, **290**(5491), 519–521. 342

BIBLIOGRAPHY

- Higginson, D. M., Miller, K. B., Segraves, K. A., & Pitnick, S. 2012. Female reproductive tract form drives the evolution of complex sperm morphology. *Proceedings of the national academy of sciences*, **109**(12), 4538–4543. 14, 87
- Hill, K. G., Loftus-Hills, J. J., & Gartside, D. F. 1972. Pre-mating isolation between the Australian field crickets *Teleogryllus commodus* and *T. oceanicus* (Orthoptera : Gryllidae). *Australian journal of zoology*, **20**(2), 153–163. 19, 296
- Hine, E., Lachish, S., Higginson, D. M., & Blows, M. W. 2002. Positive genetic correlation between female preference and offspring fitness. *Proceedings of the royal society of London. series B: Biological sciences*, **269**(1506), 2215–2219. 342
- Hines, H. M., Counterman, B. A., Papa, R., Albuquerque de Moura, P., Cardoso, M. Z., Linares, M., Mallet, J., Reed, R. D., Jiggins, C. D., Kronforst, M. R., & McMillan, W. O. 2011. Wing patterning gene redefines the mimetic history of Heliconius butterflies. *Proceedings of the national academy of sciences*, **108**(49), 19666–19671. 158
- Hinojosa, J. C., Koubínová, D., Dincă, V., Hernández-Roldán, J., Munguira, M. L., García-Barros, E., Vila, M., Alvarez, N., Mutanen, M., & Vila, R. 2020. Rapid colour shift by reproductive character displacement in Cupido butterflies. *Molecular ecology*, **29**(24), 4942–4955. 17
- Hiscock, S. J., & McInnis, S. M. 2003. Pollen recognition and rejection during the sporophytic self-incompatibility response: Brassica and beyond. *Trends in plant science*, **8**(12), 606 – 613. 12, 38, 68, 86, 337, 348, 351
- Hohenlohe, P. A., & Arnold, S. J. 2010. Dimensionality of mate choice, sexual isolation, and speciation. *Proceedings of the national academy of sciences*, **107**(38), 16583–16588. 18, 295
- Holt, R. D. 1985. Population dynamics in two-patch environments: Some anomalous consequences of an optimal habitat distribution. *Theoretical population biology*, **28**(2), 181 – 208. 45

- Horton, B. M., Hu, Y., Martin, C. L., Bunke, B. P., Matthews, B. S., Moore, I. T., Thomas, J. W., & Maney, D. L. 2013. Behavioral characterization of a white-throated sparrow homozygous for the *zal2(m)* chromosomal rearrangement. *Behavior genetics*, **43**(1), 60–70. 38, 338
- Houtman, A. M., & Falls, J. 1994. Negative assortative mating in the white-throated sparrow, *zonotrichia albicollis*: the role of mate choice and intra-sexual competition. *Animal behaviour*, **48**(2), 377–383. 38
- Howard, R. S., & Lively, C. M. 2003. Opposites attract? mate choice for parasite evasion and the evolutionary stability of sex. *Journal of evolutionary biology*, **16**(4), 681–689. 87
- Howard, R. S., & Lively, C. M. 2004. Good vs complementary genes for parasite resistance and the evolution of mate choice. *Bmc evolutionary biology*, **4**(1), 48. 87
- Huber, B., Whibley, A., Poul, Y. L., Navarro, N., Martin, A., Baxter, S., Shah, A., Gilles, B., Wirth, T., McMillan, W. O., & Joron, M. 2015. Conservatism and novelty in the genetic architecture of adaptation in *heliconi* butterflies. *Heredity*, **114**(5), 515–524. 25
- Hughes, N. K., Kelley, J. L., & Banks, P. B. 2012. Dangerous liaisons: the predation risks of receiving social signals. *Ecology letters*, **15**(11), 1326–1339. 11, 85
- Ihara, Y., & Feldman, M. W. 2003. Evolution of disassortative and assortative mating preferences based on imprinting. *Theoretical population biology*, **64**(2), 193 – 200. 87, 88, 337
- Iwasa, Y., & Pomiankowski, A. 1994. The evolution of mate preferences for multiple sexual ornaments. *Evolution*, **48**(3), 853–867. 18, 19, 295, 296
- Iwasa, Y., Pomiankowski, A., & Nee, S. 1991. The evolution of costly mate preferences ii. the “handicap” principle. *Evolution*, **45**(6), 1431–1442. 136, 137, 216, 217

BIBLIOGRAPHY

- Janicke, T., Marie-Orleach, L., Aubier, T. G., Perrier, C., & Morrow, E. H. 2019. Assortative mating in animals and its role for speciation. *The american naturalist*, **194**(6), 865–875. 85, 114, 115, 116, 345, 347
- Jay, P., Whibley, A., Frézal, L., Ángeles Rodríguez de Cara, M., Nowell, R. W., Mallet, J., Dasmahapatra, K. K., & Joron, M. 2018. Supergene evolution triggered by the introgression of a chromosomal inversion. *Current biology*, **28**(11), 1839–1845.e3. 25
- Jay, P., Chouteau, M., Whibley, A., Bastide, H., Parrinello, H., Llaurens, V., & Joron, M. 2021. Mutation load at a mimicry supergene sheds new light on the evolution of inversion polymorphisms. *Nature genetics*, **53**(3), 288–293. 27, 40, 71, 88, 107, 112, 338, 349
- Jay, P., Leroy, M., Le Poul, Y., Whibley, A., Arias, M., Chouteau, M., & Joron, M. 2022. Association mapping of colour variation in a butterfly provides evidence that a supergene locks together a cluster of adaptive loci. *Philosophical transactions of the royal society b: Biological sciences*, **377**(1856), 20210193. 25
- Jennions, M. D., Moller, A. P., & Petrie, M. 2001. Sexually selected traits and adult survival: A meta-analysis. *The quarterly review of biology*, **76**(1), 3–36. 13
- Jiang, Y., Bolnick, D. I., & Kirkpatrick, M. 2013. Assortative mating in animals. *The american naturalist*, **181**(6), E125–E138. 37, 85, 114, 115, 344, 345, 347
- Jiggins, C. D., & McMillan, W. O. 1997. The genetic basis of an adaptive radiation: Warning colour in two heliconius species. *Proceedings: Biological sciences*, **264**(1385), 1167–1175. 26
- Jiggins, C. D., Naisbit, R. E., Coe, R. L., & Mallet, J. 2001. Reproductive isolation caused by colour pattern mimicry. *Nature*, **411**(6835), 302–305. 24, 27, 28, 86, 132, 213, 342, 352

- Johnson, M. S. 1982. Polymorphism for direction of coil in *partula suturalis*: Behavioural isolation and positive frequency dependent selection. *Heredity*, **49**(2), 145–151. 350
- Johnston, R. F., & Johnson, S. G. 1989. Nonrandom Mating in Feral Pigeons. *The condor*, **91**(1), 23–29. 338
- Johnstone, R. A. 1995a. Honest advertisement of multiple qualities using multiple signals. *Journal of theoretical biology*, **177**(1), 87–94. 314
- Johnstone, R. A. 1995b. Sexual selection, honest advertisement and the handicap principle: reviewing the evidence. *Biological reviews*, **70**(1), 1–65. 245
- Joron, M., Jiggins, C. D., Papanicolaou, A., & McMillan, W. O. 2006a. Heliconius wing patterns: an evo-devo model for understanding phenotypic diversity. *Heredity*, **97**(3), 157–167. 158
- Joron, M., & Iwasa, Y. 2005. The evolution of a müllerian mimic in a spatially distributed community. *Journal of theoretical biology*, **237**(1), 87 – 103. 26, 39, 40, 45, 50, 55, 139
- Joron, M., Wynne, I. R., Lamas, G., & Mallet, J. 1999. Variable selection and the coexistence of multiple mimetic forms of the butterfly *heliconius numata*. *Evolutionary ecology*, **13**(7), 721–754. 26, 39
- Joron, M., Papa, R., Beltrán, M., Chamberlain, N., Mavárez, J., Baxter, S., Abanto, M., Bermingham, E., Humphray, S. J., Rogers, J., Beasley, H., Barlow, K., French Constant, R. H., Mallet, J., McMillan, W. O., & Jiggins, C. D. 2006b. A conserved supergene locus controls colour pattern diversity in *heliconius* butterflies. *Plos biology*, **4**(10), e303–e303. 25, 40
- Joron, M., Frezal, L., Jones, R. T., Chamberlain, N. L., Lee, S. F., Haag, C. R., Whibley, A., Becuwe, M., Baxter, S. W., Ferguson, L., Wilkinson, P. A., Salazar, C., Davidson, C., Clark, R., Quail, M. A., Beasley, H., Glithero, R., Lloyd, C., Sims, S., Jones, M. C., Rogers, J., Jiggins, C. D., & French Constant,

BIBLIOGRAPHY

- R. H. 2011. Chromosomal rearrangements maintain a polymorphic supergene controlling butterfly mimicry. *Nature*, **477**(7363), 203–206. 25, 40, 112
- Joshi, J., Prakash, A., & Kunte, K. 2017. Evolutionary assembly of communities in butterfly mimicry rings. *The american naturalist*, **189**(4), E58–E76. 24, 157, 158, 161
- Kamiya, T., O’Dwyer, K., Westerdahl, H., Senior, A., & Nakagawa, S. 2014. A quantitative review of mhc-based mating preference: the role of diversity and dissimilarity. *Molecular ecology*, **23**(21), 5151–5163. 337, 350
- Kapan, D. D. 2001. Three-butterfly system provides a field test of müllerian mimicry. *Nature*, **409**(6818), 338–340. 131
- Kappel, C., Huu, C. N., & Lenhard, M. 2017. A short story gets longer: recent insights into the molecular basis of heterostyly. *Journal of experimental botany*, **68**(21-22), 5719–5730. 348
- Karlin, S., & Feldman, M. W. 1968. Further analysis of negative assortative mating. *Genetics*, **59**(1), 117–136. 88
- Karlsson, B., & Wickman, P.-O. 1990. Increase in reproductive effort as explained by body size and resource allocation in the speckled wood butterfly, pararge aegeria (l.). *Functional ecology*, **4**(5), 609–617. 29, 211
- Katoh, M., Tatsuta, H., & Tsuji, K. 2020. Mimicry genes reduce pre-adult survival rate in papilio polytes: A possible new mechanism for maintaining female-limited polymorphism in batesian mimicry. *Journal of evolutionary biology*, **33**(10), 1487–1494. 212
- Kikuchi, D., & Pfennig, D. 2010. Predator cognition permits imperfect coral snake mimicry. *The american naturalist*, **176**(6), 830–834. 157, 244
- Kirkpatrick, M., & Barton, N. H. 1997. The strength of indirect selection on female mating preferences. *Proceedings of the national academy of sciences*, **94**(4), 1282–1286. 16

- Kirkpatrick, M. 1982. Sexual selection and the evolution of female choice. *Evolution*, **36**(1), 1–12. 13, 14, 87, 343
- Kirkpatrick, M. 2000. Reinforcement and divergence under assortative mating. *Proceedings of the royal society of london. series b: Biological sciences*, **267**(1453), 1649–1655. 87
- Kirkpatrick, M. 2010. How and why chromosome inversions evolve. *Plos biology*, **8**(9), e1000501. 26, 71
- Kirkpatrick, M., & Barton, N. 2006. Chromosome Inversions, Local Adaptation and Speciation. *Genetics*, **173**(1), 419–434. 26, 27
- Kirkpatrick, M., & Nuismer, S. L. 2004. Sexual selection can constrain sympatric speciation. *Proceedings of the royal society of london. series b: Biological sciences*, **271**(1540), 687–693. 48, 87
- Kirkpatrick, M., & Ravigné, V. 2002. Speciation by natural and sexual selection: Models and experiments. *The american naturalist*, **159**(S3), S22–S35. 16
- Kirkpatrick, M., Johnson, T., & Barton, N. 2002. General Models of Multilocus Evolution. *Genetics*, **161**(4), 1727–1750. 86, 135, 136, 168, 215, 249, 250
- Kirschel, A. N. G., Blumstein, D. T., & Smith, T. B. 2009. Character displacement of song and morphology in african tinkerbirds. *Proceedings of the national academy of sciences*, **106**(20), 8256–8261. 350
- Knapton, R. W., & Falls, J. B. 1983. Differences in parental contribution among pair types in the polymorphic white-throated sparrow. *Canadian journal of zoology*, **61**(6), 1288–1292. 112
- Komata, S., Lin, C.-P., & Sota, T. 2018. Do juvenile developmental and adult body characteristics differ among genotypes at the doublesex locus that controls female-limited batesian mimicry polymorphism in papilio memnon?: A test for the “cost of mimicry” hypothesis. *Journal of insect physiology*, **107**, 1–6. 212

BIBLIOGRAPHY

- Komata, S., Kitamura, T., & Fujiwara, H. 2020. Batesian mimicry has evolved with deleterious effects of the pleiotropic gene doublesex. *Scientific reports*, **10**(1), 21333. 212
- Kondrashov, A. S., & Shpak, M. 1998. On the origin of species by means of assortative mating. *Proceedings. biological sciences*, **265**(1412), 2273–2278. 87
- Kopp, M., & Hermisson, J. 2008. Competitive speciation and costs of choosiness. *Journal of evolutionary biology*, **21**(4), 1005–1023. 11, 85
- Kopp, M., Servedio, M. R., Mendelson, T. C., Safran, R. J., Rodríguez, R. L., Hauber, M. E., Scordato, E. C., Symes, L. B., Balakrishnan, C. N., Zonana, D. M., & van Doorn, G. S. 2018. Mechanisms of assortative mating in speciation with gene flow: Connecting theory and empirical research. *The american naturalist*, **191**(1), 1–20. 20, 21, 38, 39, 68, 87, 106, 116, 297, 351
- Krebs, R. A., & West, D. A. 1988. Female mate preference and the evolution of female-limited batesian mimicry. *Evolution*, **42**(5), 1101–1104. 28, 212
- Kronforst, M. R., Young, L. G., Kapan, D. D., McNeely, C., O’Neill, R. J., & Gilbert, L. E. 2006. Linkage of butterfly mate preference and wing color preference cue at the genomic location of wingless. *Proceedings of the national academy of sciences*, **103**(17), 6575–6580. 24, 27, 28, 69, 132, 213, 342, 352
- Kruijt, J. P., & Hogan, J. A. 1967. Social Behavior on the Lek in Black Grouse, *Lyrurus Tetrix Tetrix* (L.). *Ardea*, **55**(1-2), 204 – 240. 11, 85
- Kuang, Y., & Takeuchi, Y. 1994. Predator-prey dynamics in models of prey dispersal in two-patch environments. *Mathematical biosciences*, **120**(1), 77 – 98. 45
- Kunte, K. 2008. Mimetic butterflies support wallace’s model of sexual dimorphism. *Proceedings of the royal society b: Biological sciences*, **275**(1643), 1617–1624. 28, 211, 240

- Kunte, K. 2009. The diversity and evolution of batesian mimicry in *Papilio swallowtail* butterflies. *Evolution*, **63**(10), 2707–2716. 212, 241
- Kunte, K., Kizhakke, A. G., & Nawge, V. 2021. Evolution of mimicry rings as a window into community dynamics. *Annual review of ecology, evolution, and systematics*, **52**(1), 315–341. 160, 161
- Küpper, C., Stocks, M., Risse, J. E., dos Remedios, N., Farrell, L. L., McRae, S. B., Morgan, T. C., Karlionova, N., Pinchuk, P., Verkuil, Y. I., Kitaysky, A. S., Wingfield, J. C., Piersma, T., Zeng, K., Slate, J., Blaxter, M., Lank, D. B., & Burke, T. 2016. A supergene determines highly divergent male reproductive morphs in the ruff. *Nature genetics*, **48**(1), 79–83. 42
- Kyogoku, D. 2015. Reproductive interference: ecological and evolutionary consequences of interspecific promiscuity. *Population ecology*, **57**(2), 253–260. 133, 340
- Lamunyon, C. 1997. Increased fecundity, as a function of multiple mating, in an arctiid moth, *Utetheisa ornatrix*. *Ecological entomology*, **22**(1), 69–73. 242
- Lande, R. 1981. Models of speciation by sexual selection on polygenic traits. *Proceedings of the national academy of sciences*, **78**(6), 3721–3725. 13, 14, 15, 87, 92, 168, 250, 343
- Lande, R., & Arnold, S. J. 1985. Evolution of mating preference and sexual dimorphism. *Journal of theoretical biology*, **117**(4), 651–664. 215, 216, 218, 352
- Le Poul, Y., Whibley, A., Chouteau, M., Prunier, F., Llaurens, V., & Joron, M. 2014. Evolution of dominance mechanisms at a butterfly mimicry supergene. *Nature communications*, **5**(1), 5644. 42
- Le Roy, C., Roux, C., Authier, E., Parrinello, H., Bastide, H., Debat, V., & Llaurens, V. 2021. Convergent morphology and divergent phenology promote the coexistence of morpho butterfly species. *Nature communications*, **12**(1), 7248. 159

BIBLIOGRAPHY

- Lederhouse, R. C., & Scriber, J. M. 1996. Intrasexual selection constrains the evolution of male black swallowtail butterflies, *Papilio polyxenes*. *Evolution*, **50**(2), 717–722. 212
- Lenz, T. L. 2011. Computational prediction of mhc ii-antigen binding supports divergent allele advantage and explains trans-species polymorphism. *Evolution*, **65**(8), 2380–2390. 353
- Lev-Yadun, S. 2009. Müllerian mimicry in aposematic spiny plants. *Plant signaling & behavior*, **4**(6), 482–483. 131
- Lewontin, R., Kirk, D., & Crow, J. 1968. Selective mating, assortative mating, and inbreeding: Definitions and implications. *Eugenics quarterly*, **15**(2), 141–143. 344, 347
- Li, J., Cocker, J. M., Wright, J., Webster, M. A., McMullan, M., Dyer, S., Swarbreck, D., Caccamo, M., Oosterhout, C. v., & Gilmartin, P. M. 2016. Genetic architecture and evolution of the s locus supergene in *primula vulgaris*. *Nature plants*, **2**(12), 16188. 68, 337, 348, 351
- Lindström, L., Alatalo, R. V., & Mappes, J. 1997. Imperfect batesian mimicry—the effects of the frequency and the distastefulness of the model. *Proceedings of the royal society b: Biological sciences*, **264**(1379), 149–153. 26, 160, 243
- Llaurens, V., Billiard, S., & Joron, M. 2013. The effect of dominance on polymorphism in mülllerian mimicry. *Journal of theoretical biology*, **337**, 101 – 110. 40, 139
- Llaurens, V., Joron, M., & Théry, M. 2014. Cryptic differences in colour among mülllerian mimics: how can the visual capacities of predators and prey shape the evolution of wing colours? *Journal of evolutionary biology*, **27**(3), 531–540. 159
- Llaurens, V., Gonthier, L., & Billiard, S. 2009. The Sheltered Genetic Load Linked to the S Locus in Plants: New Insights From Theoretical and Empirical Ap-

- proaches in Sporophytic Self-Incompatibility. *Genetics*, **183**(3), 1105–1118. 12, 71, 349, 350
- Llaurens, V., Le Poul, Y., Puissant, A., Blandin, P., & Debat, V. 2021. Convergence in sympatry: Evolution of blue-banded wing pattern in morpho butterflies. *Journal of evolutionary biology*, **34**(2), 284–295. 159
- Long, E. C., Hahn, T. P., & Shapiro, A. M. 2014. Variation in wing pattern and palatability in a female-limited polymorphic mimicry system. *Ecology and evolution*, **4**(23), 4543–4552. 211
- Long, E. C., Edwards, K. F., & Shapiro, A. M. 2015. A test of fundamental questions in mimicry theory using long-term datasets. *Biological journal of the linnean society*, **116**(3), 487–494. 160, 243
- Low, X. H., & Monteiro, A. 2018. Dorsal forewing white spots of male papilio polytes(lepidoptera: Papilionidae) not maintained by female mate choice. *Journal of insect behavior*, **31**(1), 29–41. 212
- López, P., & Martín, J. 2001. Pheromonal recognition of females takes precedence over the chromatic cue in male iberian wall lizards podarcis hispanica. *Ethology*, **107**(10), 901–912. 314
- Maisonneuve, L., Chouteau, M., Joron, M., & Llaurens, V. 2021. Evolution and genetic architecture of disassortative mating at a locus under heterozygote advantage. *Evolution*, **75**(1), 149–165. 88, 116
- Mallet, J., & Barton, N. H. 1989. Strong natural selection in a warning-color hybrid zone. *Evolution*, **43**(2), 421–431. 22, 39, 131, 139, 219
- Mallet, J., & Gilbert Jr., L. E. 1995. Why are there so many mimicry rings? correlations between habitat, behaviour and mimicry in heliconius butterflies. *Biological journal of the linnean society*, **55**(2), 159–180. 131

BIBLIOGRAPHY

- Mallet, J., & Joron, M. 1999. Evolution of diversity in warning color and mimicry: Polymorphisms, shifting balance, and speciation. *Annual review of ecology and systematics*, **30**(1), 201–233. 135, 162, 214
- Marden, J. H., & Chai, P. 1991. Aerial predation and butterfly design: How palatability, mimicry, and the need for evasive flight constrain mass allocation. *The american naturalist*, **138**(1), 15–36. 29, 211
- Marsteller, S., Adams, D. C., Collyer, M. L., & Condon, M. 2009. Six cryptic species on a single species of host plant: morphometric evidence for possible reproductive character displacement. *Ecological entomology*, **34**(1), 66–73. 17, 214, 341
- Mather, K. 1955. Polymorphism as an outcome of disruptive selection. *Evolution*, **9**(1), 52–61. 343
- McClure, M., Mahrouche, L., Houssin, C., Monllor, M., Le Poul, Y., Frérot, B., Furtos, A., & Elias, M. 2019. Does divergent selection predict the evolution of mate preference and reproductive isolation in the tropical butterfly genus *Melinaea* (nymphalidae: Ithomiini)? *Journal of animal ecology*, **88**(6), 940–952. 158
- McPeck, M. A., & Gavrilets, S. 2006. The evolution of female mating preferences: Differentiation from species with promiscuous males can promotes speciation. *Evolution*, **60**(10), 1967 – 1980. 17, 133, 134, 214, 215, 340, 350, 352
- Merrill, R. M., Wallbank, R. W. R., Bull, V., Salazar, P. C. A., Mallet, J., Stevens, M., & Jiggins, C. D. 2012. Disruptive ecological selection on a mating cue. *Proceedings of the royal society b: Biological sciences*, **279**(1749), 4907–4913. 16, 295
- Merrill, R. M., Chia, A., & Nadeau, N. J. 2014. Divergent warning patterns contribute to assortative mating between incipient heliconius species. *Ecology and evolution*, **4**(7), 911–917. 24, 27, 28, 86, 132, 213, 342

- Merrill, R. M., Neggazi, S., Morrison, C. R., Crisp, R., & McMillan, W. O. 2018. Experimental manipulation of heliconius warning patterns reduces harassment of previously mated females. *bioRxiv*. 163
- Merrill, R. M., Rastas, P., Martin, S. H., Melo, M. C., Barker, S., Davey, J., McMillan, W. O., & Jiggins, C. D. 2019. Genetic dissection of assortative mating behavior. *Plos biology*, **17**(2), 1–21. 69, 352
- Miller, G. T., & Pitnick, S. 2002. Sperm-female coevolution in drosophila. *Science*, **298**(5596), 1230–1233. 14, 87
- Moran, P. A., Hunt, J., Mitchell, C., Ritchie, M. G., & Bailey, N. W. 2020. Sexual selection and population divergence iii: Interspecific and intraspecific variation in mating signals. *Journal of evolutionary biology*, **33**(7), 990–1005. 19, 296, 314
- Morris, R. L., & Reader, T. 2016. Do crab spiders perceive Batesian mimicry in hoverflies? *Behavioral ecology*, **27**(3), 920–931. 157
- Müller, F. 1879. Ituna and thyridia: a remarkable case of mimicry in butterflies. *Trans. entomol. soc. lond*, **1879**, 20–29. 22, 23, 43, 342
- Mérot, C., Frérot, B., Leppik, E., & Joron, M. 2015. Beyond magic traits: Multimodal mating cues in heliconius butterflies. *Evolution*, **69**(11), 2891–2904. 28, 133, 213, 314
- Mérot, C., Llaurens, V., Normandeau, E., Bernatchez, L., & Wellenreuther, M. 2020. Balancing selection via life-history trade-offs maintains an inversion polymorphism in a seaweed fly. *Nature communications*, **11**(1), 670. 37, 338
- Nagylaki, T. 1993. The evolution of multilocus systems under weak selection. *Genetics*, **134**(2), 627–647. 137, 217, 251
- Naisbit, R. E., Jiggins, C. D., & Mallet, J. 2001. Disruptive sexual selection against hybrids contributes to speciation between *Heliconius cydno* and *Helico-*

BIBLIOGRAPHY

- nus melpomene*. *Proceedings of the royal society of london. series b: Biological sciences*, **268**(1478), 1849–1854. 24, 27, 28, 132, 213, 342
- Neff, B. D., & Pitcher, T. E. 2005. Genetic quality and sexual selection: an integrated framework for good genes and compatible genes. *Molecular ecology*, **14**(1), 19–38. 294
- Nishida, R. 2017. *Chemical ecology of poisonous butterflies: Model or mimic? a paradox of sexual dimorphisms in müllerian mimicry*. Singapore: Springer Singapore. Pages 205–220. 215, 243
- Nishikawa, H., Iijima, T., Kajitani, R., Yamaguchi, J., Ando, T., Suzuki, Y., Sugano, S., Fujiyama, A., Kosugi, S., Hirakawa, H., Tabata, S., Ozaki, K., Morimoto, H., Ihara, K., Obara, M., Hori, H., Itoh, T., & Fujiwara, H. 2015. A genetic mechanism for female-limited batesian mimicry in papilio butterfly. *Nature genetics*, **47**(4), 405–409. 28, 211
- Noriyuki, S. 2015. Host selection in insects: reproductive interference shapes behavior of ovipositing females. *Population ecology*, **57**(2), 293–305. 17, 159
- Noriyuki, S., Osawa, N., & Nishida, T. 2011. Prey capture performance in hatchlings of two sibling harmonia ladybird species in relation to maternal investment through sibling cannibalism. *Ecological entomology*, **36**(3), 282–289. 17, 159
- Noriyuki, S., Osawa, N., & Nishida, T. 2012. Asymmetric reproductive interference between specialist and generalist predatory ladybirds. *Journal of animal ecology*, **81**(5), 1077–1085. 17, 159
- Nuismer, S. L., Otto, S. P., & Blanquart, F. 2008. When do host-parasite interactions drive the evolution of non-random mating? *Ecology letters*, **11**(9), 937–946. 88, 115
- Nummela, S., Pihlström, H., Puolamäki, K., Fortelius, M., Hemilä, S., & Reuter, T. 2013. Exploring the mammalian sensory space: co-operations and trade-offs among senses. *Journal of comparative physiology a*, **199**(12), 1077–1092. 19, 296

- O'Donald, P. 1980a. Genetic models of sexual and natural selection in monogamous organisms. *Heredity*, **44**(3), 391–415. 13, 86
- O'Donald, P. 1980b. *Genetic models of sexual selection*. Cambridge University Press. 87
- Ohsaki, N. 1995. Preferential predation of female butterflies and the evolution of batesian mimicry. *Nature*, **378**(6553), 173–175. 29, 211
- Ohsaki, N. 2005. A common mechanism explaining the evolution of female-limited and both-sex batesian mimicry in butterflies. *Journal of animal ecology*, **74**(4), 728–734. 29, 211
- Ojala, K., Lindsröm, L., & Mappes, J. 2007. Life-history constraints and warning signal expression in an arctiid moth. *Functional ecology*, **21**(6), 1162–1167. 132
- Otto, S. P., & Rosales, A. 2020. Theory in service of narratives in evolution and ecology. *The american naturalist*, **195**(2), 290–299. 8
- Otto, S. P., Servedio, M. R., & Nuismer, S. L. 2008. Frequency-dependent selection and the evolution of assortative mating. *Genetics*, **179**(4), 2091–2112. 12, 13, 20, 24, 37, 48, 49, 85, 87, 89, 90, 92, 94, 96, 99, 101, 103, 104, 106, 111, 112, 113, 114, 115, 222, 223, 301, 302
- Otto, S. P. 1991. On evolution under sexual and viability selection: a two-locus diploid model. *Evolution*, **45**(6), 1443–1457. 87
- Park, S., Jeong, G., & Jang, Y. 2013. No reproductive character displacement in male advertisement signals of *Hyla japonica* in relation to the sympatric *H. suweonensis*. *Behavioral ecology and sociobiology*, **67**(8), 1345–1355. 315
- Parker, G. 2006. Sexual conflict over mating and fertilization: an overview. *Philosophical transactions of the royal society b: Biological sciences*, **361**(1466), 235–259. 245

BIBLIOGRAPHY

- Patten, M. A., Rotenberry, J. T., & Zuk, M. 2004. Habitat selection, acoustic adaptation, and the evolution of reproductive isolation. *Evolution*, **58**(10), 2144–2155. 18, 295
- Penn, D. J., & Potts, W. K. 1999. The evolution of mating preferences and major histocompatibility complex genes. *The american naturalist*, **153**(2), 145–164. 37, 87, 337
- Penn, D. J., Damjanovich, K., & Potts, W. K. 2002. Mhc heterozygosity confers a selective advantage against multiple-strain infections. *Proceedings of the national academy of sciences*, **99**(17), 11260–11264. 350
- Petrie, M. 1994. Improved growth and survival of offspring of peacocks with more elaborate trains. *Nature*, **371**(6498), 598–599. 13, 86
- Pfennig, D. W., & Kikuchi, D. W. 2012. Competition and the evolution of imperfect mimicry. *Current zoology*, **58**(4), 608–619. 156
- Pfennig, K. S. 2000. Female spadefoot toads compromise on mate quality to ensure conspecific matings. *Behavioral ecology*, **11**(2), 220–227. 19, 295, 342
- Pfennig, K. S., & Pfennig, D. W. 2005. Character displacement as the “best of a bad situation”: fitness trade-offs resulting from selection to minimize resource and mate competition. *Evolution*, **59**(10), 2200 – 2208. 17, 214, 341
- Piertney, S. B., & Oliver, M. K. 2006. The evolutionary ecology of the major histocompatibility complex. *Heredity*, **96**(1), 7–21. 37, 87, 337
- Pomiankowski, A. 1987. The costs of choice in sexual selection. *Journal of theoretical biology*, **128**(2), 195 – 218. 11, 85
- Pomiankowski, A., & Iwasa, Y. 1993. Evolution of multiple sexual preferences by fisher’s runaway process of sexual selection. *Proceedings: Biological sciences*, **253**(1337), 173–181. 13, 18, 19, 136, 170, 217, 251, 295, 296, 307
- Price, G. R. 1970. Selection and covariance. *Nature*, **227**(5257), 520–521. 8

- Price, G. R. 1972. Extension of covariance selection mathematics. *Annals of human genetics*, **35**(4), 485–490. 8
- Prudic, K. L., Timmermann, B. N., Papaj, D. R., Ritland, D. B., & Oliver, J. C. 2019. Mimicry in viceroy butterflies is dependent on abundance of the model queen butterfly. *Communications biology*, **2**(1), 68. 243
- Pruitt, J. N., & Riechert, S. E. 2009. Male mating preference is associated with risk of pre-copulatory cannibalism in a socially polymorphic spider. *Behavioral ecology and sociobiology*, **63**(11), 1573–1580. 16, 86
- Prusa, L. A., & Hill, R. I. 2021. Umbrella of protection: spatial and temporal dynamics in a temperate butterfly Batesian mimicry system. *Biological journal of the linnean society*, 04. 160, 243, 244
- Puurttinen, M., Ketola, T., & Kotiaho, J. 2009. The good-genes and compatible-genes benefits of mate choice. *The american naturalist*, **174**(5), 741–752. 313
- Rice, S. H. 2004. *Evolutionary theory: mathematical and conceptual foundations*. Sunderland, Mass., USA: Sinauer Associates. 7, 136, 217
- Rios Moura, R., Oliveira Gonzaga, M., Silva Pinto, N., Vasconcellos-Neto, J., & Requena, G. S. 2021. Assortative mating in space and time: patterns and biases. *Ecology letters*, **24**(5), 1089–1102. 345, 347
- Rosenthal, G. G. 2017. *Mate choice : the evolution of sexual decision making from microbes to humans*. Princeton University Press. 12, 85
- Rowland, H. M., Mappes, J., Ruxton, G. D., & Speed, M. P. 2010. Mimicry between unequally defended prey can be parasitic: evidence for quasi-batesian mimicry. *Ecology letters*, **13**(12), 1494–1502. 26, 243
- Ruxton, G. D., Franks, D. W., Balogh, A. C. V., & Leimar, O. 2008. Evolutionary implications of the form of predator generalization for aposematic signals and mimicry in prey. *Evolution*, **62**(11), 2913–2921. 132

BIBLIOGRAPHY

- Ruxton, G. D., Allen, W. L., Sherratt, T. N., & Speed, M. P. 2019. *Avoiding attack: the evolutionary ecology of crypsis, aposematism, and mimicry*. Oxford University Press. 23, 211
- Sacca, G. 1964. Comparative bionomics in the genus musca. *Annual review of entomology*, **9**(1), 341–358. 12, 85
- Sanders, K., Malhotra, A., & Thorpe, R. 2006. Evidence for a müllerian mimetic radiation in asian pitvipers. *Proceedings of the royal society b: Biological sciences*, **273**(1590), 1135–1141. 131, 212
- Sasaji, H. 1998. *Natural history of the ladybirds*. 17, 159
- Sato, K., Nishio, T., Kimura, R., Kusaba, M., Suzuki, T., Hatakeyama, K., Ockendon, D. J., & Satta, Y. 2002. Coevolution of the s-locus genes srk, slg and sp11/scr in brassica oleracea and b. rapa. *Genetics*, **162**(2), 931–940. 69, 352
- Savage, J. M., & Slowinski, J. B. 1992. The colouration of the venomous coral snakes (family elapidae) and their mimics (families aniliidae and colubridae). *Biological journal of the linnean society*, **45**(3), 235–254. 131
- Savolainen, V., Anstett, M.-C., Lexer, C., Hutton, I., Clarkson, J. J., Norup, M. V., Powell, M. P., Springate, D., Salamin, N., & Baker, W. J. 2006. Sympatric speciation in palms on an oceanic island. *Nature*, **441**, 210–2013. 86
- Schemske, D. W. 1981. Floral convergence and pollinator sharing in two bee-pollinated tropical herbs. *Ecology*, **62**(4), 946–954. 131
- Schilthuizen, M., Craze, P. G., Cabanban, A. S., Davison, A., Stone, J., Gittenberger, E., & Scott, B. 2007. Sexual selection maintains whole-body chiral dimorphism in snails. *Journal of evolutionary biology*, **20**(5), 1941–1949. 338, 348
- Schluter, D., & Price, T. 1993. Honesty, perception and population divergence in sexually selected traits. *Proceedings of the royal society of london. series b: Biological sciences*, **253**(1336), 117–122. 19, 296

- Schneider, K. A., & Bürger, R. 2006. Does competitive divergence occur if assortative mating is costly? *Journal of evolutionary biology*, **19**(2), 570–588. 11, 85
- Sculfort, O., de Castro, E. C. P., Kozak, K. M., Bak, S., Elias, M., Nay, B., & Llaurens, V. 2020. Variation of chemical compounds in wild heliconiini reveals ecological factors involved in the evolution of chemical defenses in mimetic butterflies. *Ecology and evolution*, **10**(5), 2677–2694. 243
- Servedio, M. R. 2011. Limits to the evolution of assortative mating by female choice under restricted gene flow. *Proceedings: Biological sciences*, **278**(1703), 179–187. 114
- Servedio, M. R., & Lande, R. 2006. Population genetic models of male and mutual mate choice. *Evolution*, **60**(4), 674–685. 116
- Servedio, M. R., & Noor, M. A. 2003. The role of reinforcement in speciation: Theory and data. *Annual review of ecology, evolution, and systematics*, **34**(1), 339–364. 313
- Servedio, M. R., Doorn, G. S. V., Kopp, M., Frame, A. M., & Nosil, P. 2011. Magic traits in speciation: ‘magic’ but not rare? *Trends in ecology & evolution*, **26**(8), 389–397. 18, 20, 295, 313
- Servedio, M. R., Brandvain, Y., Dhole, S., Fitzpatrick, C. L., Goldberg, E. E., Stern, C. A., Van Cleve, J., & Yeh, D. J. 2014. Not just a theory—the utility of mathematical models in evolutionary biology. *Plos biology*, **12**(12), 1–5. 8
- Sheldon, B. C., Merilö, J., Qvarnström, A., Gustafsson, L., & Ellegren, H. 1997. Paternal genetic contribution to offspring condition predicted by size of male secondary sexual character. *Proceedings of the royal society of london. series b: Biological sciences*, **264**(1380), 297–302. 13, 86
- Sherratt, T. N. 2006. Spatial mosaic formation through frequency-dependent selection in müllerian mimicry complexes. *Journal of theoretical biology*, **240**(2), 165–174. 43, 44, 162

BIBLIOGRAPHY

- Sherratt, T. N. 2008. The evolution of müllerian mimicry. *Die naturwissenschaften*, **95**(8), 681–695. 23, 27, 131, 132, 214
- Shine, R., & Mason, R. T. 2001. Courting male garter snakes (*thamnophis sirtalis parietalis*) use multiple cues to identify potential mates. *Behavioral ecology and sociobiology*, **49**(6), 465–473. 314
- Slade, R. W., & McCallum, H. I. 1992. Overdominant vs. frequency-dependent selection at mhc loci. *Genetics*, **132**(3), 861–864. 87, 337
- Smith, C. C., & Mueller, U. G. 2015. Sexual transmission of beneficial microbes. *Trends in ecology & evolution*, **30**(8), 438 – 440. 16, 86
- Springer, V., & Smith-Vaniz, W. 1972. Mimetic relationships involving fishes of the family blenniidae. *Smithsonian contributions zoology*, **112**(01). 131
- Stefan, T., Matthews, L., Prada, J. M., Mair, C., Reeve, R., & Stear, M. J. 2019. Divergent Allele Advantage Provides a Quantitative Model for Maintaining Alleles with a Wide Range of Intrinsic Merits. *Genetics*, **212**(2), 553–564. 352
- Stift, M., Hunter, B. D., Shaw, B., Adam, A., Hoebe, P. N., & Mable, B. K. 2013. Inbreeding depression in self-incompatible north-american arabidopsis lyrata: disentangling genomic and s-locus-specific genetic load. *Heredity*, **110**(1), 19–28. 12
- Su, S., Lim, M., & Kunte, K. 2015. Prey from the eyes of predators: Color discriminability of aposematic and mimetic butterflies from an avian visual perspective. *Evolution*, **69**(11), 2985–2994. 211
- Symula, R., Schulte, R., & Summers, K. 2001. Molecular phylogenetic evidence for a mimetic radiation in peruvian poison frogs supports a müllerian mimicry hypothesis. *Proceedings of the royal society of london. series b: Biological sciences*, **268**(1484), 2415–2421. 132

- Takafuji, A., Kuno, E., & Fujimoto, H. 1997. Reproductive interference and its consequences for the competitive interactions between two closely related panonychus spider mites. *Experimental & applied acarology*, **21**(6), 379–391. 16
- Thibert-Plante, X., & Gavrilets, S. 2013. Evolution of mate choice and the so-called magic traits in ecological speciation. *Ecology letters*, **16**(06). 13, 37
- Thomas, J. W., Cáceres, M., Lowman, J. J., Morehouse, C. B., Short, M. E., Baldwin, E. L., Maney, D. L., & Martin, C. L. 2008. The chromosomal polymorphism linked to variation in social behavior in the white-throated sparrow (*zonotrichia albicollis*) is a complex rearrangement and suppressor of recombination. *Genetics*, **179**(3), 1455–1468. 71
- Throneycroft, H. B. 1975. A cytogenetic study of the white-throated sparrow, *zonotrichia albicollis* (gmelin). *Evolution*, **29**(4), 611–621. 38, 88, 112, 338, 349
- Timmermans, M. J. T. N., Thompson, M. J., Collins, S., & Vogler, A. P. 2017. Independent evolution of sexual dimorphism and female-limited mimicry in swallowtail butterflies (*papilio dardanus* and *papilio phorcas*). *Mol ecol*, **26**(5), 1273–1284. 212
- Tregenza, T., & Wedell, N. 2000. Genetic compatibility, mate choice and patterns of parentage: Invited review. *Molecular ecology*, **9**(8), 1013–1027. 37
- Trivers, R. 1972. *Parental investment and sexual selection*. Page 378. 17, 20, 242
- Turner, J. R. G. 1978. Why male butterflies are non-mimetic: natural selection, sexual selection, group selection, modification and sieving*. *Biological journal of the linnean society*, **10**(4), 385–432. 28, 211, 212, 241
- Turner, J. R. G. 1987. The evolutionary dynamics of batesian and muellerian mimicry: similarities and differences. *Ecological entomology*, **12**(1), 81–95. 26
- Tuttle, E., Bergland, A., Korody, M., Brewer, M., Newhouse, D., Minx, P., Stager, M., Betuel, A., Cheviron, Z., Warren, W., Gonser, R., & Balakrishnan, C. 2016.

BIBLIOGRAPHY

- Divergence and functional degradation of a sex chromosome-like supergene. *Current biology*, **26**(3), 344–350. 38, 42, 71, 88, 107, 112, 338, 348, 349
- Van Belleghem, S. M., Alicea Roman, P. A., Carbia Gutierrez, H., Counterman, B. A., & Papa, R. 2020. Perfect mimicry between *Heliconius* butterflies is constrained by genetics and development. *Proceedings of the royal society b: Biological sciences*, **287**(1931), 20201267. 29, 212
- van der Bijl, W., Zeuss, D., Chazot, N., Tunström, K., Wahlberg, N., Wiklund, C., Fitzpatrick, J. L., & Wheat, C. W. 2020. Butterfly dichromatism primarily evolved via darwin's, not wallace's, model. *Evolution letters*, **4**(6), 545–555. 211, 240
- van Veelen, M., García, J., Sabelis, M. W., & Egas, M. 2012. Group selection and inclusive fitness are not equivalent; the price equation vs. models and statistics. *Journal of theoretical biology*, **299**, 64–80. 8
- Vasconcellos-Neto, J., & Brown, K. S. 1982. Interspecific hybridization in mechanitis butterflies (ithomiinae): a novel pathway for the breakdown of isolating mechanisms. *Biotropica*, **14**, 288. 27, 133, 342
- Vekemans, X., Schierup, M. H., & Christiansen, F. B. 1998. Mate availability and fecundity selection in multi-allelic self-incompatibility systems in plants. *Evolution*, **52**(1), 19–29. 12
- Veller, C., Muralidhar, P., & Haig, D. 2020. On the logic of fisherian sexual selection*. *Evolution*, **74**(7), 1234–1245. 87
- Vortman, Y., Lotem, A., Dor, R., Lovette, I., & Safran, R. J. 2013. Multiple sexual signals and behavioral reproductive isolation in a diverging population. *The american naturalist*, **182**(4), 514–523. 18, 295
- Wagner, W. E. 2011. Chapter 6 - direct benefits and the evolution of female mating preferences: Conceptual problems, potential solutions, and a field cricket. *Advances in the Study of Behavior*, vol. 43. Academic Press. 16, 86

- Wallace, A. R. 1865. *On the phenomena of variation and geographical distribution as illustrated by the papilionidae of the malayan region. read march 17, 1864.* London,. 210
- Wang, J., Wurm, Y., Nipitwattanaphon, M., Riba-Grognuz, O., Huang, Y.-C., Shoemaker, D., & Keller, L. 2013. A y-like social chromosome causes alternative colony organization in fire ants. *Nature*, **493**(7434), 664–668. 42
- Weatherhead, P. J., & Robertson, R. J. 1979. Offspring quality and the polygyny threshold: "the sexy son hypothesis". *The american naturalist*, **113**(2), 201–208. 14
- Wedekind, C., & Fürti, S. 1997. Body odour preferences in men and women: do they aim for specific mhc combinations or simply heterozygosity? *Proceedings of the royal society of london. series b: Biological sciences*, **264**(1387), 1471–1479. 38, 353
- Wedekind, C., & Penn, D. 2000. MHC genes, body odours, and odour preferences. *Nephrology dialysis transplantation*, **15**(9), 1269–1271. 353
- Wedekind, C., Seebeck, T., Bettens, F., & Paepke, A. J. 1995. Mhc-dependent mate preferences in humans. *Proceedings of the royal society of london. series b: Biological sciences*, **260**(1359), 245–249. 37, 87
- Welch, A. M., Semlitsch, R. D., & Gerhardt, H. C. 1998. Call duration as an indicator of genetic quality in male gray tree frogs. *Science*, **280**(5371), 1928–1930. 13, 86
- Westerman, E. L., VanKuren, N. W., Massardo, D., Tenger-Trolander, A., Zhang, W., Hill, R. I., Perry, M., Bayala, E., Barr, K., Chamberlain, N., Douglas, T. E., Buerkle, N., Palmer, S. E., & Kronforst, M. R. 2018. Aristaless controls butterfly wing color variation used in mimicry and mate choice. *Current biology*, **28**(21), 3469–3474.e4. 69, 352

BIBLIOGRAPHY

- Wiklund, C., Kaitala, A., Lindfors, V., & Abenius, J. 1993. Polyandry and its effect on female reproduction in the green-veined white butterfly (*Pieris napi* L.). *Behavioral ecology and sociobiology*, **33**(1), 25–33. 242
- Willmott, K. R., Robinson Willmott, J. C., Elias, M., & Jiggins, C. D. 2017. Maintaining mimicry diversity: optimal warning colour patterns differ among microhabitats in amazonian clearwing butterflies. *Proceedings of the royal society b: Biological sciences*, **284**(1855), 20170744. 162
- Wourms, M. K., & Wasserman, F. E. 1985. Bird predation on lepidoptera and the reliability of beak-marks in determining predation pressure. *Journal of the lepidopterists' society*, **39**(4), 239–261. 29, 212
- Wright, S. 1939. The distribution of self-sterility alleles in populations. *Genetics*, **24**(4), 538–552. 37
- Yamaguchi, R., & Iwasa, Y. 2013. Reproductive character displacement by the evolution of female mate choice. *Evolutionary ecology research*, **15**(1), 25–41. 17, 133, 134, 140, 214, 215, 340, 350, 352
- Yukilevich, R. 2021. Reproductive character displacement drives diversification of male courtship songs in *Drosophila*. *The American Naturalist*, **197**(6), 690–707. 17
- Zahavi, A. 1975. Mate selection—a selection for a handicap. *Journal of theoretical biology*, **53**(1), 205 – 214. 245
- Zuk, M., & Kolluru, G. R. 1998. Exploitation of sexual signals by predators and parasitoids. *The quarterly review of biology*, **73**(4), 415–438. 10, 314

Appendix I: Evolution of conspicuousness in warning traits

Ombeline Sculfort, Ludovic Maisonneuve, Marianne Elias,
Thomas Aubier and Violaine Llaurens

Published:

Sculfort, O, Maisonneuve, L, Elias, E, Aubier, T, Llaurens, V. (2022) Uncovering the effects of Müllerian mimicry on the evolution of conspicuousness in colour patterns.

Oikos, 2022: e08680.

doi: 10.1111/oik.08680

This work is part of the PhD of Ombeline Sculfort. This work aims at uncovering the effects of Müllerian mimicry on the evolution of conspicuousness in warning traits, using a mathematical model. In this work I participated to the conceptualisation and the analysis of the mathematical model.

OIKOS

Research

Uncovering the effects of Müllerian mimicry on the evolution of conspicuousness in colour patterns

Ombeline Sculfort, Ludovic Maisonneuve, Marianne Elias, Thomas G. Aubier and Violaine Llaurens

O. Sculfort (<https://orcid.org/0000-0002-1583-824X>) ✉ (ombelinesculfort@hotmail.fr), L. Maisonneuve (<https://orcid.org/0000-0002-9556-5973>), M. Elias (<https://orcid.org/0000-0002-1250-2353>) and V. Llaurens (<https://orcid.org/0000-0003-1962-7391>), *Inst. de Systématique, Evolution, Biodiversité (ISYEB), Muséum National d'Histoire Naturelle, CNRS, Sorbonne-Univ., EPHE, Univ. des Antilles, Paris, France. OS also at: Molécules de Communication et Adaptations des Micro-organismes (MCAM), Muséum National d'Histoire Naturelle, CNRS, Paris, France and Laboratoire Ecologie, Evolution, Interactions des Systèmes Amazoniens (LEEISA), Univ. de Guyane, CNRS, IFREMER, Cayenne, France. – T. G. Aubier (<https://orcid.org/0000-0001-8543-5596>), Dept of Biology, Univ. of North Carolina, Chapel Hill, NC, USA.*

Oikos

2022: e08680

doi: 10.1111/oik.08680

Subject Editor: Marjo Saastamoinen

Editor-in-Chief: Dries Bonte

Accepted 27 March 2022



Variation in the conspicuousness of colour patterns is observed within and among defended prey species. The evolution of conspicuous colour pattern in defended species can be strongly impaired because of increased detectability by predators. Nevertheless, such evolution of the colour pattern can be favoured if changes in conspicuousness result in Müllerian mimicry with other defended prey. Here, we develop a model describing the population dynamics of a conspicuous defended prey species, and we assess the invasion conditions of derived phenotypes that differ from the ancestral phenotype by their conspicuousness. Such change in conspicuousness may then modify their level of mimicry with the local community of defended species. Derived colour pattern displayed in this focal population can therefore be either exactly similar, partially resembling or completely dissimilar to the local mimicry ring displaying the ancestral colour pattern. We assume that predation risk depends 1) on the number of individuals sharing a given colour pattern within the population, 2) on the occurrence of co-mimetic defended species and 3) on the availability of alternative edible prey. Using a combination of analytical derivations and numerical simulations, we show that colour patterns that are less conspicuous than the ancestral one are generally favoured within mimicry rings, unless reduced conspicuousness impairs mimicry. By contrast, when a mutation affecting the colour pattern leads to a shift toward a better protected mimicry ring, a more conspicuous colour pattern can be favoured. The selected aposematic pattern then depends on the local communities of defended and edible prey, as well as on the detectability, memorability and level of mimicry of the colour patterns.

Keywords: aposematism, conspicuousness, defended mimetic community, imperfect mimicry, mimicry shift, salience, theory



www.oikosjournal.org

© 2022 The Authors. Oikos published by John Wiley & Sons Ltd on behalf of Nordic Society Oikos. This is an open access article under the terms of the Creative Commons Attribution License, which permits use, distribution and reproduction in any medium, provided the original work is properly cited.

1

Introduction

The evolution of aposematic colour patterns in defended species is puzzling because conspicuousness, which determines the detectability of prey by predators, is associated with multiple costs (Ruxton 2019). Notably, prey individuals may suffer from increased attack risk by predators stemming from higher detectability of their more conspicuous colour patterns (i.e. reduced crypsis, Mappes et al. 2014, Arias et al. 2019), even if those prey are defended (Srygley and Kingsolver 1998). However, selection against conspicuous colourations can be counter-balanced by the increased resemblance of aposematic patterns to the local communities of alternative defended prey. Indeed, Müllerian mimicry, whereby different defended prey species living in sympatry share the same colour pattern, reduces the individual predation risk (Müller 1879). The protection gained by prey with a different level of conspicuousness then depends on the level of similarity of the colour pattern they displayed to the local mimicry rings, and on the generalization behaviour of predators (Kikuchi and Pfennig 2010, Merrill et al. 2012, Chouteau et al. 2016).

When a derived colour pattern with a different level of conspicuousness emerges in a prey population, it can be perceived by predators as partly or totally different from the ancestral colour pattern, thereby increasing predation risk (Greenwood et al. 1989, Lindström et al. 2001). By contrast, the evolution of conspicuousness of colour pattern within a species might be facilitated when it results in a shift to an alternative mimicry ring that increases protection against predators. Individuals with a different conspicuousness of colour pattern can therefore either 1) be perceived by predators as similar to the ancestral mimicry ring, 2) be considered by predators as more similar to an alternative mimicry ring or 3) perceived by predators as different from the signal displayed in all local mimicry ring.

A change in conspicuousness may not necessarily modify the signal recognized by predators: some other features of the colour pattern can be efficient in triggering predator memorability (Wüster et al. 2004, Valkonen et al. 2011, Barnett et al. 2016), and therefore predator avoidance learning (Dolenská et al. 2009), whatever the level of conspicuousness of the colour pattern. Alternatively, conspicuousness can be the most memorable feature of the aposematic colour pattern (Ruxton et al. 2004, Lindstedt et al. 2011, Buechel et al. 2018), such that only highly conspicuous colour pattern triggers rapid avoidance learning in predators (Aronsson and Gamberale-Stille 2009, Dell'aglio et al. 2016). Altogether, memorability, crypsis and mimicry can therefore shape the evolution of conspicuousness. The defended butterflies from the tribe Ithomiini is a striking example where those three components are likely to affect the evolution of conspicuousness. The majority of these butterflies exhibit mildly-conspicuous aposematic signals, where wings are composed of cryptic transparent parts, combined with a few coloured elements (Corral-Lopez et al. 2021). Transparency decreases detectability of Ithomiini butterflies by avian predators (Arias et al. 2019, McClure et al. 2019). Yet, mimicry among Ithomiini

species and with other Lepidoptera suggests that those mildly conspicuous colour patterns are still under selection by predation promoting their convergence, and therefore truly act as aposematic signals (Beccaloni 1997, Pinna et al. 2021). Those different selection pressures could explain the persistence of transparent cryptic wing pattern associated with some key memorable features observed in Ithomiini clear-wing species.

Traditionally, modelling studies investigating the evolution of aposematism do not consider mimetic interactions (Leimar et al. 1986, Speed and Ruxton 2005a, b, Broom et al. 2006), while those investigating the evolution and implications of mimicry generally consider all colour patterns to have the same impact on predator learning behaviour (Müller 1879, Sherratt 2006, Gompert et al. 2011, Aubier et al. 2017; but see Franks et al. 2009). Nevertheless, the composition of local communities of prey, both edible and defended, likely plays a great role in the evolution of aposematic patterns: for instance, the availability of alternative prey was shown to strongly influence the evolution of mimicry (Kokko et al. 2003, Aubier and Sherratt 2020). Here we thus investigate the evolution of conspicuousness within a species evolving in a community of edible and defended prey species. We study the interplay between protection provided by co-mimetic communities, and specific properties of the colour pattern itself, such as detectability and memorability (see Fig. 1 for an illustration). We use a mathematical modelling approach to test whether a mutation affecting the conspicuousness of the colour pattern can invade in a defended species engaged in Müllerian mimicry, depending on the effect of the mutation on 1) the phenotypic similarity to different mimicry rings, and on 2) the detectability and memorability of the derived colour pattern.

Material and methods

General model

Using ordinary differential equations, we model the population dynamics of a conspicuous defended prey species. This focal species is composed of individuals all harbouring the same level of defence and displaying a colour pattern phenotype (Fig. 1). Each individual can either display the ancestral phenotype (hereafter referred to using the subscript 'a') or the derived phenotype (referred to using the subscript 'd'). Individuals with ancestral and derived phenotypes can differ in their conspicuousness level, c_a and c_d . Variations in conspicuousness can affect the perception of the colour pattern by predators, so that the derived phenotype can be either perceived as 1) totally similar to the ancestral phenotype (perfect mimicry), 2) partially similar to the ancestral phenotype (imperfect mimicry) or 3) totally different from the ancestral phenotype. In these first two cases, the derived phenotype may also benefit from the protection provided by the presence of co-mimetic species matching the ancestral colour pattern (referred to as the 'ancestral mimicry ring'). In these

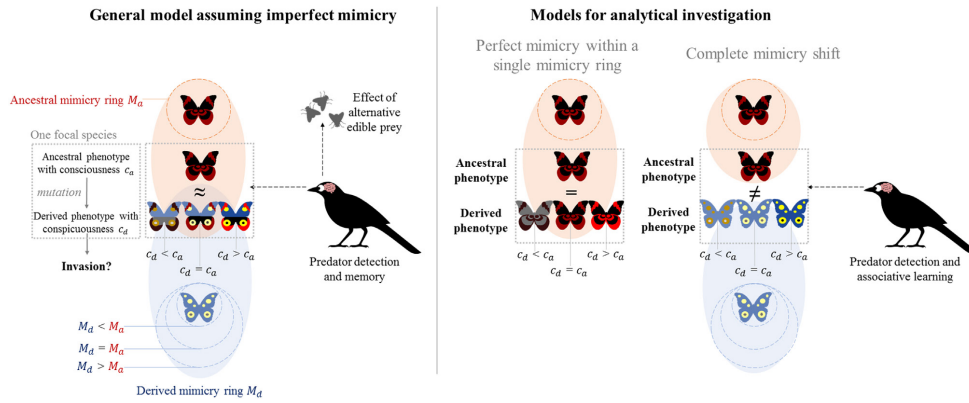


Figure 1. General scheme of our model investigating the evolution of conspicuousness of colour pattern in a population of prey involved in Müllerian mimicry. We model the population dynamics of a single focal species composed of individuals displaying either the ancestral phenotype with conspicuousness c_a or the derived phenotype with conspicuousness c_d . We test whether a mutation generating a derived phenotype with a different conspicuousness level than the ancestral phenotype can invade the population. Variation in conspicuousness can lead to different effect on the recognition of the colour patterns by the predator community. In our general model, we assume that the derived phenotype is only partially similar to the ancestral phenotypes and to the ‘ancestral mimicy ring’ displaying the ancestral colour pattern (imperfect mimicry), and we consider that alternative edible prey may alter the incentive of predators to attack cryptic prey. We also consider that the derived phenotype may match an alternative mimicy ring that we call ‘derived mimicy ring’. For analytical investigation, we consider two scenarios: 1) ‘perfect mimicry within a single mimicy ring’: both ancestral and derived phenotypes are accurate mimics to each other and to the local mimicy ring displaying the ancestral colour pattern (simplified Eq. 8), and 2) ‘complete mimicry shift’: the derived phenotype is totally dissimilar to the ancestral phenotypes and can be similar to an alternative community of defended species (simplified Eq. 9). Note that our model thus explores all possible combinations of conspicuousness and mimicry levels in the ancestral and derived phenotypes. The population dynamic of predators is not explicitly modelled, but we do consider their perception and memory capacities.

three cases, the derived phenotype may also benefit from the protection provided by an alternative mimicy ring that may look similar to the derived colour pattern (‘derived mimicy ring’; note that this terminology does not necessarily imply that this mimicy ring provides a lower protection than the ‘ancestral mimicy ring’).

Following Joron and Iwasa (2005), the changes through time in densities N_a and N_d of individuals displaying the ancestral and derived phenotypes depend on both local demography (described by the term R_a and R_d) and predation (described by the terms P_a and P_d):

$$\frac{dN_a}{dt} = R_a - P_a \tag{1}$$

$$\frac{dN_d}{dt} = R_d - P_d \tag{2}$$

Local demography

Individuals displaying the ancestral and derived phenotypes belong to the same species. As such, they share the same

baseline growth rate r , compete for the same resources and share the same carrying capacity K (see Table 1 for a summary of the notations and default values). The changes in density of individuals displaying either the ancestral or derived colour pattern due to intra-specific competition follow a logistic regulation rule, as in the previous model of mimicry described by Joron and Iwasa (2005):

$$R_a = rN_a \left(1 - \frac{N_a + N_d}{K} \right) \tag{3}$$

$$R_d = rN_d \left(1 - \frac{N_a + N_d}{K} \right) \tag{4}$$

Predation

Individuals with ancestral or derived phenotypes are characterized by their conspicuousness c_a and c_d , respectively. Their predation risk depends on their colour pattern phenotype and its associated characteristics (detectability and memorability), and on the composition of the local community of defended and edible prey. Specifically, we assume that all

APPENDIX I

Table 1. Notations before rescaling the system of equations, and default values used in our model.

Parameters and default values	Description
$N_a(t), N_d(t)$	Number of individuals displaying the ancestral or derived phenotypes at time t
c_a, c_d	Conspicuousness of the ancestral or derived phenotypes
$M_a=5000$	Reduction of the predation risk due to the ‘ancestral mimicry ring’ matching the ancestral phenotype (includes the abundance, defence, the conspicuousness and the memorability of the colour patterns carried by those species)
M_d	Reduction of the predation risk due to the ‘alternative mimicry ring’ matching the derived phenotype (includes the abundance, defence, the conspicuousness and the memorability of the colour patterns carried by those species)
$\beta_a = \beta_d = 1$	Translation parameters modulating the effect of conspicuousness on the memorability of the ancestral or derived phenotypes by predator
$u = 1$	Associative learning response by predators due to the defence levels of individuals in the focal population
$p = 0.5$	Baseline predation rate
$h = 0$	Availability of alternative edible prey modulating the predation risk applied to by cryptic phenotype in the focal defended population (with c_a or c_d equal to 0)
$l = 0$	Phenotypic distance between the ancestral and derived phenotypes that is not related to differences in conspicuousness
γ	Perceived dissimilarity between ancestral and derived phenotypes, after accounting for the generalization behaviour of predators
S	Level of similarity between ancestral or derived phenotypes; function of γ, l, c_a and c_d
$r = 10$	Baseline growth rate of the focal species
$K = 1000$	Carrying capacity of the focal species

individuals from the focal species, whatever their phenotype, have the same level of defence, which triggers the same associative learning response in predators (through parameter u). The baseline predation rate, p , on individuals with alternative and derived phenotype is also modulated by their detectability (modulated by their conspicuousness c_a and c_d), by their memorability (through parameter β_a and β_d), and by the abundance of alternative edible prey (through parameter h) and the presence of local mimicry rings matching the ancestral and derived colouration (through parameter M_a and M_d). The protection gained by individuals displaying a given phenotype is then modulated by the similarity, S , to the other individuals from the focal species (but also by the similarity to the local mimicry rings).

The predation rate for individuals displaying either the ancestral or derived phenotype is thus modelled as:

$$P_a = \frac{\text{baseline predation risk} \times \text{detectability}}{\text{degree of predator learning}} N_a \quad (5)$$

$$P_a = \frac{p \times (c_a + h)}{1 + u(\beta_a c_a N_a + S \beta_d c_d N_d) + M_a + S M_d} N_a$$

$$P_d = \frac{\text{baseline predation risk} \times \text{detectability}}{\text{degree of predator learning}} N_d \quad (6)$$

$$P_d = \frac{p \times (c_d + h)}{1 + u(S \beta_a c_a N_a + \beta_d c_d N_d) + S M_a + M_d} N_d$$

Importantly, we do not model explicitly the density of predators. Instead, we consider predation through those mortality functions, which capture how predators affect the mortality of individuals belonging to a focal species (Joron and Iwasa 2005). The important features of these mortality functions are described below (see also the Supporting information for more details).

Density-dependent predation risk

The predation risk is modelled following Joron and Iwasa (2005) and thus describes the density-dependent mortality risk incurred by any defended prey facing a natural predator community. Within this predator community, some predator individuals have already encountered the warning colour pattern and have learned to avoid it, while some other predator individuals are completely naïve (e.g. migrating individuals or juveniles) or are still learning about the warning colour pattern. As a result, the predation risk decreases as the number of individuals sharing the same colour pattern increases (Müller 1879). We thus assume that the degree of predator learning increases as the density of individuals sharing the same colour pattern increases, in Eq. 5 and 6.

Effects of conspicuousness on the predation risk

We assume that the conspicuousness of the colour pattern has two opposite effects on predation risk. On the one hand, increased conspicuousness increases the risk of being detected by predators, and therefore of being attacked (numerator terms in Eq. 5 and 6). On the other hand, increased conspicuousness makes the colour pattern easier to remember for predators, and therefore enhances protection brought by predator learning (Sherratt 2002a, Broom et al. 2006) (in the denominator terms in Eq. 5 and 6).

Depending on the type of colour pattern variation (e.g. variations in colour contrast or pattern) triggering variations in conspicuousness, the mutation affecting conspicuousness can change the memorability of the colour pattern. The effect of conspicuousness on predator learning is modulated by parameters β_a and β_d , which describe the levels of memorability induced in predators by given levels of conspicuousness (in the ancestral and derived phenotypes, respectively). Individuals with ancestral and derived phenotypes can thus differ in their levels of memorability, expressed as $\beta_a \times c_a$ and $\beta_d \times c_d$ respectively (in the denominator terms in Eq. 5 and 6). If $\beta_a = 0$ or $\beta_d = 0$, the phenotype is not memorized

even when it is conspicuous, and predator never associate the colour pattern with defence (i.e. this is not a warning colour pattern). We therefore focus on cases where $\beta_a > 0$ and $\beta_d > 0$, i.e. when an increase in conspicuousness associates with an increase in memorability (thereby triggering more rapid avoidance learning in predators and reducing predation).

Mimetic environment and shifts in mimicry ring

We consider that our focal conspicuous defended species is not isolated but instead belongs to a mimicry ring, as often observed in nature (Mallet and Gilbert 1995). To keep the model analytically tractable, we do not model explicitly the population dynamics of each species of the mimicry community, just like we did not model explicitly the predator community. Instead, we model the protection provided by the local mimicry rings, taking the form of a higher degree of predator learning of the colour patterns carried by the focal individuals (in the denominator terms in Eq. 5 and 6). Those mimicry rings can harbour either the ancestral or the derived colour pattern, through parameter M_a and M_d , respectively. Parameter M_a and M_d thus capture the protection provided by co-mimetic defended prey, and therefore account for the abundance, the level of defence, the conspicuousness and the memorability of the mean phenotype of the co-mimetic species. Note that each mimetic community could therefore be seen as a single alternative defended 'model' species. By changing the level of conspicuousness, mutations in the focal species can change the level of similarity to the ancestral mimicry ring, but it can also trigger a shift in colour pattern, resulting in a greater similarity of the derived phenotype to a different mimicry ring (providing a protection through $M_d > 0$).

Imperfect mimicry

We assume that variation in the level of conspicuousness between the ancestral and derived phenotypes can modify the level of similarity perceived by predators, thereby modulating predator generalization (Kikuchi and Pfennig 2013, Motyka et al. 2020). Mutations can thus generate derived colour patterns that are perceived as slightly different from the ancestral phenotype by the predators (i.e. imperfect mimicry). We thus model the degree of similarity $S \in [0,1]$ between the ancestral and the derived phenotypes, which affects the recognition by predators. For $S=1$, ancestral and derived phenotypes resemble each other and are perceived by predators as having the same phenotype. By contrast, for $S=0$, ancestral and derived phenotypes do not look alike and are perceived by predators as completely distinct. Following Ruxton et al. (2008), the similarity level is defined as a Gaussian generalization function:

$$S = e^{-\gamma \sqrt{(c_a - c_d)^2 + l^2}} \quad (7)$$

The parameter $\gamma \in [0; +\infty[$ describes the generalization behaviour of predators, i.e. how much they perceive phenotypic

differences. The parameter l represents the distance between the ancestral and the derived colour patterns; i.e. the phenotypic distance that is not related to differences in conspicuousness. Hence, the phenotypic similarity between derived and ancestral phenotypes, as perceived by predators, depends on differences in colour pattern (l) and differences in conspicuousness ($(c_a - c_d)^2$). In our main analysis, however, we perform our analyses with $l=0$ and we implement different values of l in supplementary analyses to investigate the effect of this parameter.

Availability of alternative prey

The availability of alternative edible prey may affect the effort of predators to seek for cryptic prey when resources are scarce. We thus introduce a parameter, h , which modulates the prey baseline mortality rate, so that even cryptic prey (with conspicuousness c_a or c_d equal to 0) can be attacked. The lack of alternative prey makes predators more motivated to search for cryptic prey, hence increasing the predation rate of cryptic prey. Therefore, the lack of alternative edible prey translates into high values of h . By contrast, a high abundance of alternative edible prey translates into low values of h .

Analytical derivations under two scenarios: 'perfect mimicry within a single mimicry ring' and 'complete mimicry shift'

We can derive analytical solutions for our system of equations, in two opposite scenarios, schematized in Fig. 1:

- 1) *Perfect mimicry within a single mimicry ring*. Ancestral and derived phenotypes differ in conspicuousness but are perceived by predators as similar colour patterns (similarity $S=1$; e.g. obtained for complete predator generalization $\gamma=0$). Thus, individuals with either ancestral or derived phenotypes belong to the same mimicry ring that provides the same protection $M_a + M_d$. Under this condition, it makes sense to consider that $M_d=0$ so that M_a alone reflects the protection provided by the ancestral mimicry ring (in the denominator term in Eq. 5 and 6). Ancestral and derived phenotypes nevertheless still differ in their conspicuousness and, in most cases, also in their memorability ($c_a \times \beta_a \neq c_d \times \beta_d$). For analytical tractability, we assume here that $h=0$.
- 2) *Complete mimicry shift*. Ancestral and derived phenotypes differ in conspicuousness and derived phenotypes display a colour pattern perceived as completely different from the ancestral one by predators (similarity $S=0$; e.g. obtained for the absence of predator generalization $\gamma \rightarrow \infty$). The ancestral and derived phenotypes are thus not generalized by predators, but the derived phenotype may match a different mimicry ring characterized by parameter M_d (in the denominator term in Eq. 6). Because ancestral and derived phenotypes are distinct colour patterns, they may also have a different associated memorability. For analytical tractability, we also assume here that $h=0$.

To derive analytically the system of equations of these two situations, we rescale all variables and parameters to baseline growth rate and carrying capacity, as follows: $n_a = N_a/K$, rescaled density of ancestral individuals; $n_d = N_d/K$, rescaled density of derived individuals; $\delta = p/r$, rescaled baseline mortality rate; $\tau = rt$ rescaled time unit; and $\lambda_a = uK\beta_a$ and $\lambda_d = uK\beta_d$ rescaled deterrence factor (as in Joron and Iwasa 2005). Note that by defining the rescaled parameters λ_a and λ_d , we combine the effects of unpalatability and memorization on the learning of the colour pattern by predators.

The dynamical system assuming ‘Perfect mimicry within a single mimicry ring’ ($b=0$, $M_d=0$ and $S=1$) then becomes:

$$\begin{aligned} \frac{dn_a}{d\tau} &= n_a(1-n_a-n_d) - \frac{\delta c_a n_a}{1+(\lambda_a c_a n_a + \lambda_d c_d n_d) + M_a} \\ \frac{dn_d}{d\tau} &= n_d(1-n_a-n_d) - \frac{\delta c_d n_d}{1+(\lambda_a c_a n_a + \lambda_d c_d n_d) + M_a} \end{aligned} \quad (8)$$

By contrast, assuming ‘Complete mimicry shift’ ($b=0$ and $S=0$), the system becomes:

$$\begin{aligned} \frac{dn_a}{d\tau} &= n_a(1-n_a-n_d) - \frac{\delta c_a n_a}{1+\lambda_a c_a n_a + M_a} \\ \frac{dn_d}{d\tau} &= n_d(1-n_a-n_d) - \frac{\delta c_d n_d}{1+\lambda_d c_d n_d + M_d} \end{aligned} \quad (9)$$

All analytical derivations are detailed in the Supporting information. We investigate analytically the evolution of conspicuousness by conducting invasion analyses on the systems of Eq. 8 and 9. We first derive the expression of the density n_a at equilibrium when the initial population is composed solely of ancestral individuals (solution of $dn_d/d\tau=0$, assuming $n_d=0$). We then determine the sign of the growth rate of the derived population, assuming that derived phenotypes are rare within a population of individuals displaying the ancestral phenotype at equilibrium (sign of $dn_d/d\tau$, assuming $n_a = n_a^*$ and $n_d \ll n_a$). If the sign of this growth rate is positive, then derived phenotypes can invade the population.

Numerical analyses

We cannot get any analytical results from the general model, in particular when we account for imperfect mimicry (i.e. for intermediate value of phenotypic similarity S to local mimicry rings, $0 < S < 1$; obtained for intermediate values of γ), or for increased predation rate on cryptic prey (for $b > 0$). In those cases, we assess the density N_a^* of the ancestral population at equilibrium numerically (reached for $t=1000$). We then infer invasion numerically by calculating the sign of the derivative dN_d/dt when $\frac{N_d}{N_a^*} = 10^{-9}$ and by assuming that the derived phenotype can invade when $dN_d/dt > 0$.

Given that invading derived phenotypes will eventually replace the ancestral phenotypes in the population (as shown numerically in the Supporting information), we can infer the equilibrium (fixation of the ancestral or derived colour pattern) from the invasion analysis.

Results

All additional analyses and supplementary figures supporting our results are described in Supporting information.

A decrease in conspicuousness is favoured within a single mimicry ring (assuming ‘perfect mimicry within a single mimicry ring’; $S=1$)

We first explore the evolution of conspicuousness when ancestral and derived phenotypes are perceived as perfectly similar by predators, and thus belong to the same mimicry ring (panels marked by a single symbol ‘*’ in Fig. 2). The derived phenotype only invades when its conspicuousness is lower than that of the ancestral phenotype: $c_d < c_a$ (analytical derivations detailed in the Supporting information).

Assuming perfect mimicry to the ancestral mimicry ring, selection therefore favours less conspicuous colour patterns. Such evolutionary process may occur via small-effect mutations modifying conspicuousness. Less conspicuous individuals are indeed less detectable while simultaneously benefiting from the protection provided by the mimicry ring, and therefore suffer less predation overall than more conspicuous individuals. Such positive selection on more cryptic derived phenotypes is likely to ultimately lead to highly cryptic colouration as the evolutionary stable strategy.

A mimicry shift can promote an increase in conspicuousness (assuming a ‘complete mimicry shift’; $S=0$)

We then explore the evolution of conspicuousness when the derived colour pattern is perceived by predators as completely distinct from the ancestral colour pattern, and perfectly matches an alternative mimicry ring (panels marked by the symbol ‘**’ in Fig. 2). This is likely to apply when the mutation leads to drastic changes in colour pattern (via a large-effect mutation) and a mimicry ring shift.

Our analytical results detailed in the Supporting information show that the level of conspicuousness under which the derived phenotypes are advantaged when introduced in the population mostly composed of individuals with the ancestral phenotype is:

$$c_d < c_a \frac{1+M_d}{1+\lambda_a c_a n_a^* + M_a} \quad (10)$$

There is thus a conspicuousness threshold value under which the derived phenotypes are advantaged. The effects of parameters on this threshold value are summarized in Fig. 3.

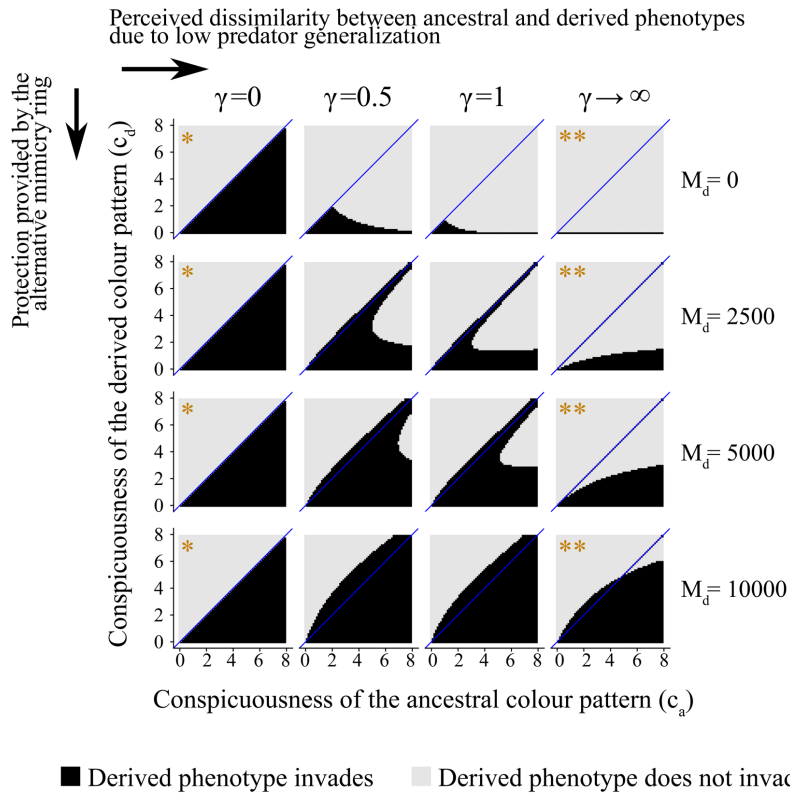


Figure 2. Evolution of conspicuousness depending on the mimetic community and on the similarity between ancestral and derived phenotypes. Inference of the evolutionary equilibrium from the invasion analysis, with ancestral and derived phenotypes having different levels of conspicuousness (c_a, c_d). We consider different values of parameter M_d , which controls the protection provided by the alternative mimicry ring, and of parameter γ , which controls the perceived dissimilarity between ancestral and derived phenotypes (the condition $\gamma \rightarrow \infty$ is obtained by assuming no similarity between phenotypes; i.e. $S=0$). Note that the ancestral mimicry ring provides a protection $M_d=5000$. The diagonal blue line represents cases where $c_a=c_d$. Colour scale indicates the sign of the derivative dN_d/dt assuming mutants are rare. Light grey represents cases where the derived phenotype does not invade ($dN_d/dt < 0$). Black represents cases where the derived phenotype invades: the derived phenotype is less conspicuous than the ancestral phenotype below the blue diagonal ($dN_d/dt > 0$ and $c_d < c_a$), and more conspicuous than the ancestral phenotype above the blue diagonal ($dN_d/dt > 0$ and $c_d > c_a$). Symbols * and ** represent situations where we assessed analytically the conditions of invasions of a derived phenotype ('perfect mimicry within a single mimicry ring', and 'complete mimicry shift', respectively). When invasion occurs, it ultimately leads to the fixation of the derived phenotype (as shown in the Supporting information with the same parameter combinations). Note that the panels on the left are all identical because protection M_d benefits to all individuals when mimicry is perfect ($\gamma=0$); an increase in M_d therefore reflects an increase in M_a . Here, $\beta_a=1$ and $b=0$. See other default values in Table 1.

Contrary to the results obtained above assuming 'perfect mimicry within a single mimicry ring', slightly less conspicuous derived phenotypes do not always invade, because of the potential costs associated with displaying a less protected alternative colour pattern (panels marked by a symbol * in Fig. 2).

Overall, less conspicuous derived phenotypes are more advantaged than more conspicuous derived phenotypes. In

particular, derived phenotypes that are completely cryptic (with $c_d=0$; because we assume here that $b=0$) always invades (because the threshold value $c_a \frac{1+M_d}{1+\lambda_a c_a n_a + M_a} > 0$), even when the derived colour pattern does not match any mimicry ring. Yet, derived phenotypes that are more conspicuous than the ancestral phenotype ($c_d > c_a$) may

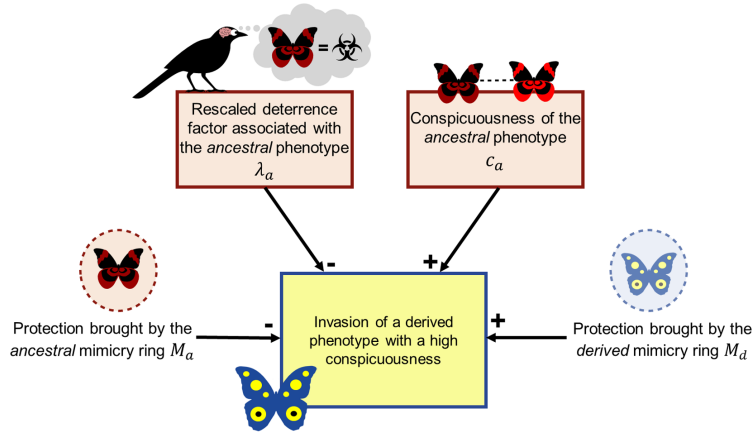


Figure 3. Effects of the parameters on the invasion of derived phenotypes, assuming a ‘complete mimicry shift’. Those effects are based on the effects of those parameters on the conspicuousness threshold $c_a \frac{1 + M_d}{1 + \lambda_a c_a n_a^* + M_a}$ (Eq. 10). See also the Supporting information. Note that the rescaled deterrence factor associated with the ancestral phenotype is expressed as $\lambda_a = uK\beta_a$. The rescaled baseline mortality rate $\delta = p/r$ has a very little effect on the invasion of the derived phenotype and is therefore not represented here.

be advantaged if the ratio shown in Eq. 10 is superior to 1, i.e. if $M_d > \lambda_a c_a n_a^* + M_a$ (area in black above the blue diagonal in the panels marked by a symbol ** in Fig. 2). Consistent with our working hypothesis, our model confirms that for a more conspicuous derived colour pattern to be positively selected, it requires that the alternative mimicry ring (M_d) provides better protection than the combination of the ancestral population ($\lambda_a c_a n_a^*$) and the other species belonging to the same mimicry ring (M_a). By contrast, when the mimicry ring matching the ancestral colour pattern provides a greater protection to ancestral individuals than does the other mimicry ring to the derived phenotype, this prevents derived colour patterns from invading (Fig. 3).

Imperfect mimicry inhibits the invasion of derived phenotypes, and is more favourable to an increase in conspicuousness

We now investigate the effect of imperfect mimicry, by focusing on intermediate similarity between ancestral and derived phenotypes; with $S \in]0,1[$ depending on the term $c_a - c_d$ (Eq. 7), assuming that perceived differences by predators only rely on conspicuousness ($l=0$ and intermediate γ). Imperfect mimicry reduces not only the positive number-dependent selection brought by the ancestral individuals of the focal species on the derived phenotype, but also the protection from the entire ancestral mimicry ring on the derived phenotype. Imperfectly mimetic derived phenotypes are more favoured when their conspicuousness is similar to that of the

ancestral phenotype, which increases their mimetic protection ($c_d \approx c_a$ for intermediate values of γ in Fig. 2, i.e. close to the blue diagonal).

When the imperfectly-mimetic derived phenotype matches an alternative mimetic community that provides strong protection (high M_d ; for intermediate values of γ in Fig. 2), the invasion of a more conspicuous derived colour pattern can occur easily when the derived conspicuousness remains similar to that of the ancestral phenotype ($c_d \approx c_a$). Imperfectly-mimetic derived phenotypes indeed benefit from resembling the ancestral phenotype while simultaneously roughly resembling another mimetic community, both reducing predation pressure. The fitness advantage associated with these jack-of-all-trade phenotypes (Sherratt 2002b) is confirmed in simulations for variable values of l , capturing the phenotypic distances that do not rely on conspicuousness and that are perceived by predators (i.e. differences in colour pattern).

Easily-memorable phenotypes that facilitate predator learning inhibit the evolution of increased conspicuousness

The invasion of a more conspicuous derived phenotype when an alternative mimetic community co-occur is then modulated by the level of memorability induced by the ancestral colour pattern displayed by the focal species. We notice that when conspicuousness strongly enhances the memorability of the colour pattern (high values of β_a ; Fig. 4), the invasion of derived colour

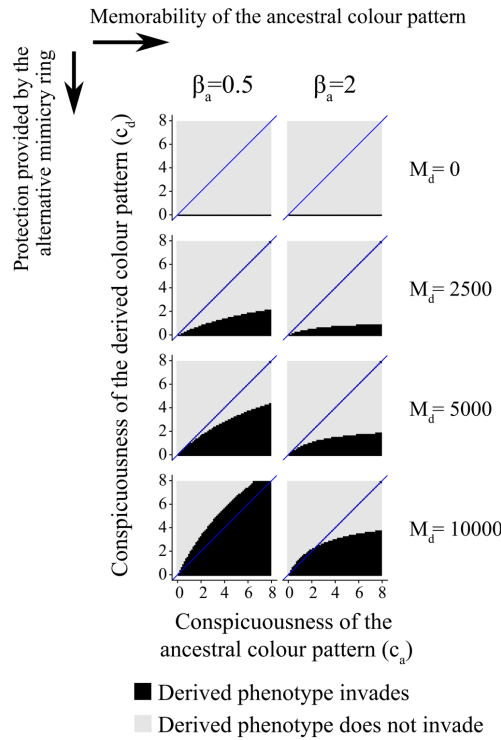


Figure 4. Evolution of conspicuousness depending on its impact on predator memorability. We consider different values of parameter β_a , which controls the effect of conspicuousness on memorability in the ancestral phenotype. See Figure 2 for more details. Here, $\gamma \rightarrow \infty$ (by setting $S=0$) and $b=0$. See other default values in Table 1.

pattern is impaired just like when the defence triggers strong predator learning (high u) (Fig. 3). These two parameters indeed tune the intensity of the number-dependent selection driven by predator avoidance-learning (strength in number; $\lambda_d = uK\beta_d$), increasing the protection incurred to the ancestral phenotype. By contrast, the memorability associated with the derived colour pattern (controlled by β_d ; note however that parameter M_d also accounts for the memorability in co-mimetic species) does not affect the invasion conditions of the derived colour pattern, because derived phenotypes are rare initially and therefore $\beta_d N_d \approx 0$.

Predation pressure and availability of alternative prey modulate selection on conspicuousness

Increased baseline predation pressure (rescaled δ) increases the range of conspicuousness values enabling the invasion of the derived phenotype: when predation rate is high, a slight

decrease in conspicuousness in the derived phenotype is favoured, despite the cost associated with the shift to a less protected mimicry ring. Nonetheless, the magnitude of this effect is very low. Therefore, a change in the abundance of alternative prey affects only weakly the evolution of conspicuousness, through a change in the baseline predation pressure.

The model also assumed that when alternative edible prey are scarce, predators have more incentive to search for cryptic prey (high values of b). In such condition, increased conspicuousness in the derived phenotype is more strongly favoured, a phenomenon enhanced by the protection provided by the derived mimicry ring (higher values of M_d , Fig. 5; but note that the conspicuous values where higher conspicuousness is favoured does not change, as highlighted in the Supporting information). Our model thus highlights that increased conspicuousness in warning patterns is likely to be favoured when the baseline predation rate on cryptic prey is high, as expected when alternative food sources for predators are scarce.

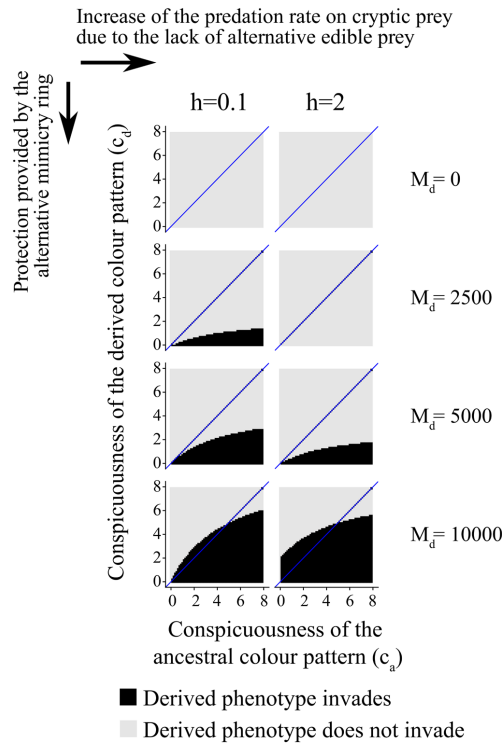


Figure 5. Evolution of conspicuousness depending on the abundance of alternative edible prey. We consider different values of parameter b , which controls the increase of the baseline predation rate on cryptic prey. See Figure 2 for more details. Here, $\gamma \rightarrow \infty$ (by setting $S=0$) and $\beta_a = 1$. See other default values in Table 1.

Discussion

Evolution toward decreasing level of conspicuousness within mimicry ring

Our model predicts that mimetic colour pattern may evolve toward reduced conspicuousness and complete crypsis within mimicry rings when mimicry is perfect (assuming ‘perfect mimicry within a single mimicry ring’ in our model). Less conspicuous individuals benefit from reduced detection by predators and therefore benefit from a lower predation rate than more conspicuous individuals. As long as the colour pattern is generalized by predators, all individuals within a mimicry ring benefit from the same reduction in predation risk, brought by the strength in number. Less conspicuous derived phenotypes act as selfish elements that may eventually replace the more conspicuous colour pattern, resulting in an increased predation risk for all members of the mimicry ring, because predator learning becomes less efficient as the mean conspicuousness decreases in the prey population. Ultimately, this would lead

to completely cryptic colour pattern that is no longer detected by predators. This result is consistent with the higher rates of shifts from aposematism to crypsis than the reverse along the phylogeny of amphibians (Arbuckle and Speed 2015).

Nevertheless, variations of conspicuousness in natural colour pattern may result in colour pattern discrimination by predators, which limits the evolution of reduced conspicuousness within mimicry rings (a feature explored in our model when we assume imperfect mimicry; for intermediate γ and $M_d = 0$ a derived phenotype that is less conspicuous than the ancestral phenotype does not necessarily invade in Fig. 2). Such colour pattern discrimination could explain the persistence of key memorable conspicuous elements associated with transparent cryptic wings observed in *Ithomiini* clearwing species and their co-mimics (Beccaloni 1997). Overall, selection pressure within mimicry rings may ultimately influence Müllerian mimetic interactions by favouring reduced detectability in some mimetic species, thereby diminishing predation risk on less noticeable mimetic prey (Arias et al. 2019).

Evolution of more conspicuous colour patterns can be promoted by mimicry shifts

Our model also highlights that a shift to more conspicuous colour patterns can be favoured when derived colour pattern matches a better-protected mimicry ring, via both perfect and imperfect mimicry. By considering the Müllerian mimetic environment in our model, we show that the conspicuousness of a colour pattern does not evolve independently from other aposematic species co-occurring in sympatry. Indeed, the evolution of conspicuousness depends on the protection provided by local defended mimetic communities, and on the presence of local edible prey communities. Here, we considered that variations in conspicuousness can result in different combinations of effects on memorability and generalization of the colour pattern. Even when assuming that conspicuousness does not associate with a direct benefit (i.e. we considered a worst-case scenario for conspicuousness invasion where crypsis is favoured), a shift to a distinct mimicry ring can still promote increased conspicuousness. Thus, our model shows that the evolution of increased conspicuousness can be promoted by natural selection exerted by predators and this prediction is in line with a previous empirical finding. For instance, the colouration of the mildly-defended viceroy butterfly *Limenitis archippus*, is thought to have evolved from a non-aposomatic ancestral pattern to an aposematic one matching the colour pattern of *Danaus* species (Platt et al. 1971, Prudic et al. 2002, Mullen 2006, Prudic and Oliver 2008). The evolution of a more conspicuous pattern could thus stem from mimicry towards the well-defended monarch butterflies living in sympatry.

In addition to mimicry, our model highlights that the evolution of conspicuousness depends on the availability of alternative prey, assuming that large amounts of palatable prey reduces the selection on aposematic signals, following Kokko et al. (2003). Models exploring the foraging behaviour of predators nevertheless suggest that their discrimination capacities depend on a more complex interplay between the profitability and colour pattern variation found in prey communities (Getty 1985). Several cognitive biases in predators, not modelled in our study, might also favour the invasion of more conspicuous warning colour patterns in defended species: biased predation (Kikuchi et al. 2020), innate memorability, direct deterrence, diet conservatism (Marples et al. 2005) or neophobia (Marples and Kelly 1999, Aubier and Sherratt 2015) have indeed been shown to promote the emergence of new warning patterns. Our study thus calls for attention to the effect of ecological interactions with other defended species, edible alternative prey, and of the diversity of colour pattern in sympatric species on the evolution of aposematism in defended species.

The effect of mimetic interaction on memorability can contribute to the evolution of mimetic colour pattern

The positive number-dependent protection gained by aposematic individuals can be modulated by the memorability of

the colour patterns, a feature that we included in our model. While our study focuses on the evolution of conspicuousness, variations in the effect of conspicuousness on predator memorability may have other important consequences for the evolution of colour patterns in mimetic communities. For instance, the high diversity of aposematic colour patterns observed within localities (Beccaloni 1997, Joron and Mallet 1998, Willmott et al. 2017, Briolat et al. 2018) could be maintained by tradeoffs between defence, memorability of the colour pattern and abundances in the different mimicry rings. In our study, we considered mimetic interactions without specifically modelling the abundance, the level of defences and the memorability of the aposematic signals of co-mimetic species. Nonetheless, our model constitutes a fundamental basis for such future theoretical research explicitly investigating the evolution of colour pattern in multiple co-mimetic species.

Conclusion

Overall, our study brings theoretical evidence that the tradeoff between detectability and memorability induced by the conspicuousness of a warning colouration influences the evolution of mimetic colour patterns in defended species. Our model shows that in a worst-case scenario, where conspicuousness does not bring any direct benefit (such as immediate deterrence), the evolution of colour pattern with increased conspicuousness can only occur when alternative edible prey are rare and when a shift to a distinct and better protected Müllerian mimicry rings occurs. Considering mimetic community therefore opens a new angle to explain the evolution of the wide diversity of colour patterns: via number-dependent selection at the community level, more conspicuous colour pattern can be favoured. Importantly, however, such mechanism at the origin of the evolution of higher conspicuousness in a species relies on the existence of conspicuousness in other species; other processes must come into play for aposematic signals to emerge in the first place. Further researches accounting for mimetic interactions and variations in memorability between warning colour pattern are needed to better understand the evolution of aposematism at the level of the prey community.

Funding – This work was supported by a grant from French National Research Agency under the LabEx ANR-10-LABX-0003-BCDiv, in the program ‘Investissements d’avenir’ number ANR-11-IDEX-0004-02, attributed to OS, by a Paris city council grant Emergence to VL. ME acknowledges funding by the French National Research Agency (ANR grant, CLEARWING, 16-CE02-0012) and by the Human Frontier Science Program (HFSP research grant RGP0014/2016). TGA was supported by a grant from the Swiss National Science Foundation and from the National Science Foundation (USA).

Conflict of interests

– We declare no competing interests.

Author contributions

Thomas G. Aubier and **Violaine Llaurens** contributed equally to this publication. **Ombeline Sculfort**: Conceptualization (equal); Data curation (equal); Formal analysis (equal); Investigation (equal); Methodology (supporting); Project administration (lead); Software (equal); Supervision (equal); Validation (equal); Visualization (equal); Writing – original draft (lead); Writing – review and editing (lead). **Ludovic Maisonneuve**: Conceptualization (equal); Formal analysis (equal); Methodology (equal); Software (equal); Validation (supporting); Writing – original draft (supporting); Writing – review and editing (supporting). **Marianne Elias**: Conceptualization (equal); Data curation (equal); Investigation (equal); Supervision (equal); Validation (equal); Visualization (equal); Writing – original draft (equal); Writing – review and editing (equal). **Thomas G. Aubier**: Conceptualization (equal); Data curation (equal); Formal analysis (lead); Investigation (equal); Methodology (lead); Software (lead); Supervision (lead); Validation (lead); Visualization (equal); Writing – original draft (equal); Writing – review and editing (equal). **Violaine Llaurens**: Conceptualization (lead); Funding acquisition (lead); Investigation (lead); Methodology (equal); Project administration (equal); Resources (equal); Supervision (lead); Validation (lead); Visualization (equal); Writing – original draft (equal); Writing – review and editing (equal).

Data availability statement

The model is implemented in C++ and the code will be available from the Dryad Digital Repository: <<https://doi.org/10.5061/dryad.cz8w9gj5m>> (Sculfort et al. 2022).

Supporting information

The Supporting information associated with this article is available with the online version.

References

- Arbuckle, K. and Speed, M. 2015. Antipredator defenses predict diversification rates. – *Proc. Natl Acad. Sci. USA* 112: 13597–13602.
- Arias, M. et al. 2019. Transparency reduces predator detection in mimetic clearwing butterflies. – *Funct. Ecol.* 33: 1110–1119.
- Aronsson, M. and Gamberale-Stille, G. 2009. Importance of internal pattern contrast and contrast against the background in aposematic signals. – *Behav. Ecol.* 20: 1356–1362.
- Aubier, T. G. and Sherratt, T. N. 2015. Diversity in Müllerian mimicry: the optimal predator sampling strategy explains both local and regional polymorphism in prey. – *Evolution* 69: 2831–2845.
- Aubier, T. G. and Sherratt, T. N. 2020. State-dependent decision-making by predators and its consequences for mimicry. – *Am. Nat.* 196: E127–E144.
- Aubier, T. G. et al. 2017. Mutualistic mimicry enhances species diversification through spatial segregation and extension of the ecological niche space. – *Evolution* 71: 826–844.
- Barnett, J. B. et al. 2016. Aposematism: balancing salience and camouflage. – *Biol. Lett.* 12: 20160335.
- Beccaloni, G. W. 1997. Ecology, natural history and behaviour of Ithomiine butterflies and their mimics in Ecuador (Lepidoptera: Nymphalidae: Ithomiinae). – *Trop. Lepid. Res.* 8: 103–124.
- Briolat, E. S. et al. 2018. Diversity in warning coloration: selective paradox or the norm? – *Biol. Rev.* 94: 388–414.
- Broom, M. et al. 2006. Evolutionarily stable defence and signalling of that defence. – *J. Theor. Biol.* 242: 32–43.
- Buechel, S. D. et al. 2018. Brain size affects performance in a reversal-learning test. – *Proc. R. Soc. B* 285: 20172031.
- Chouteau, M. et al. 2016. Warning signals are under positive frequency-dependent selection in nature. – *Proc. Natl Acad. Sci. USA* 113: 2164–2169.
- Corral-Lopez, A. et al. 2021. Field evidence for colour mimicry overshadowing morphological mimicry. – *J. Anim. Ecol.* 90: 698–709.
- Dell'aglio, D. D. et al. 2016. Avoidance of an aposematically coloured butterfly by wild birds in a tropical forest. – *Ecol. Entomol.* 41: 627–632.
- Dolenská, M. et al. 2009. What constitutes optical warning signals of ladybirds (Coleoptera: Coccinellidae) towards bird predators: colour, pattern or general look? – *Biol. J. Linn. Soc.* 98: 234–242.
- Franks, D. W. et al. 2009. Warning signals evolve to disengage batesian mimics. – *Evolution* 63: 256–267.
- Getty, T. 1985. Discriminability and the sigmoid functional response: how optimal foragers could stabilize model-mimic complexes. – *Am. Nat.* 125: 239–256.
- Gompert, Z. et al. 2011. Heterogeneity in predator micro-habitat use and the maintenance of Müllerian mimetic diversity. – *J. Theor. Biol.* 281: 39–46.
- Greenwood, J. J. D. et al. 1989. Frequency-dependent selection on aposematic prey: some experiments. – *Biol. J. Linn. Soc.* 36: 213–226.
- Joron, M. and Iwasa, Y. 2005. The evolution of a Müllerian mimic in a spatially distributed community. – *J. Theor. Biol.* 237: 87–103.
- Joron, M. and Mallet, J. 1998. Diversity in mimicry: paradox or paradigm? – *Trends Ecol. Evol.* 13: 461–466.
- Kikuchi, D. W. and Pfennig, D. W. 2010. High-model abundance may permit the gradual evolution of Batesian mimicry: an experimental test. – *Proc. R. Soc. B* 277: 1041–1048.
- Kikuchi, D. W. and Pfennig, D. W. 2013. Imperfect mimicry and the limits of natural selection. – *Q. Rev. Biol.* 88: 297–315.
- Kikuchi, D. W. et al. 2020. Biased predation could promote convergence yet maintain diversity within Müllerian mimicry rings of *Oreina* leaf beetles. – *J. Evol. Biol.* 33: 887–898.
- Kokko, H. et al. 2003. Alternative prey can change model-mimic dynamics between parasitism and mutualism: model-mimic dynamics with alternative prey. – *Ecol. Lett.* 6: 1068–1076.
- Leimar, O. et al. 1986. Evolutionary stability of aposematic coloration and prey unprofitability: a theoretical analysis. – *Am. Nat.* 128: 469–490.
- Lindstedt, C. et al. 2011. Direction and strength of selection by predators for the color of the aposematic wood tiger moth. – *Behav. Ecol.* 22: 580–587.
- Lindström, L. et al. 2001. Strong antiapostatic selection against novel rare aposematic prey. – *Proc. Natl Acad. Sci. USA* 98: 9181–9184.
- Mallet, J. and Gilbert, L. E. 1995. Why are there so many mimicry rings? Correlations between habitat, behaviour and mimicry in *Heliconius* butterflies. – *Biol. J. Linn. Soc.* 55: 159–180.

- Mappes, J. et al. 2014. Seasonal changes in predator community switch the direction of selection for prey defences. – *Nat. Commun.* 5: 5016.
- Marples, N. M. and Kelly, D. J. 1999. Neophobia and dietary conservatism: two distinct processes? – *Evol. Ecol.* 13: 641–653.
- Marples, N. M. et al. 2005. Perspective: the evolution of warning coloration is not paradoxical. – *Evolution* 59: 933–940.
- McClure, M. et al. 2019. Why has transparency evolved in aposematic butterflies? Insights from the largest radiation of aposematic butterflies, the Ithomiini. – *Proc. R. Soc. B* 286: 20182769.
- Merrill, R. M. et al. 2012. Disruptive ecological selection on a mating cue. – *Proc. R. Soc. B* 279: 4907–4913.
- Motyka, M. et al. 2020. Interactions in multi-pattern Müllerian communities support origins of new patterns, false structures, imperfect resemblance and mimetic sexual dimorphism. – *Sci. Rep.* 10: 11193.
- Mullen, S. P. 2006. Wing pattern evolution and the origins of mimicry among North American admiral butterflies (Nymphalidae: Limenitids). – *Mol. Phylogenet. Evol.* 39: 747–758.
- Müller, F. 1879. Ituna and Thyridia; a remarkable case of mimicry in butterflies (transl. by Ralph Meldola from the original German article in *Kosmos*, May 1879, 100). – *Trans. Entomol. Soc. Lond.* 1879: 20–29.
- Pinna, C. S. et al. 2021. Mimicry can drive convergence in structural and light transmission features of transparent wings in Lepidoptera. – *eLife* 10: e69080.
- Platt, A. P. et al. 1971. Demonstration of the selective advantage of mimetic limenitids butterflies presented to caged avian predators. – *Evolution* 25: 692–701.
- Prudic, K. L. and Oliver, J. C. 2008. Once a Batesian mimic, not always a Batesian mimic: mimic reverts back to ancestral phenotype when the model is absent. – *Proc. R. Soc. B* 275: 1125–1132.
- Prudic, K. L. et al. 2002. Evaluating a putative mimetic relationship between two butterflies, *Adelpha bredowii* and *Limenitis lorquini*. – *Ecol. Entomol.* 27: 68–75.
- Ruxton, G. D. 2019. Defensive coloration. – In: Choe, J. C. (ed.), *Encyclopedia of animal behavior*, 2nd edn. Academic Press, pp. 298–303.
- Ruxton, G. D. et al. 2004. Avoiding attack: the evolutionary ecology of crypsis, warning signals and mimicry. – In: *Oxford biology*. Oxford Univ. Press, p. 249.
- Ruxton, G. D. et al. 2008. Evolutionary implications of the form of predator generalization for aposematic signals and mimicry in prey. – *Evolution* 62: 2913–2921.
- Sculfort, O. et al. 2022. Data from: Uncovering the effects of Müllerian mimicry on the evolution of conspicuousness in colour patterns. – *Dryad Digital Repository*, <<https://doi.org/10.5061/dryad.cz8w9gj5m>>.
- Sherratt, T. N. 2002a. The coevolution of warning signals. – *Proc. R. Soc. B* 269: 741–746.
- Sherratt, T. N. 2002b. The evolution of imperfect mimicry. – *Behav. Ecol.* 13: 821–826.
- Sherratt, T. N. 2006. Spatial mosaic formation through frequency-dependent selection in Müllerian mimicry complexes. – *J. Theor. Biol.* 240: 165–174.
- Speed, M. P. and Ruxton, G. D. 2005a. Warning displays in spiny animals: one (more) evolutionary route to aposematism. – *Evolution* 59: 2499–2508.
- Speed, M. P. and Ruxton, G. D. 2005b. Aposematism: what should our starting point be? – *Proc. R. Soc. B* 272: 431–438.
- Srygley, R. B. and Kingsolver, J. G. 1998. Red-wing blackbird reproductive behaviour and the palatability, flight performance and morphology of temperate pierid butterflies (*Colias*, *Pieris* and *Pontia*). – *Biol. J. Linn. Soc.* 64: 41–55.
- Valkonen, J. et al. 2011. Disruption or aposematism? Significance of dorsal zigzag pattern of European vipers. – *Evol. Ecol.* 25: 1047–1063.
- Willmott, K. R. et al. 2017. Maintaining mimicry diversity: optimal warning colour patterns differ among microhabitats in Amazonian clearwing butterflies. – *Proc. R. Soc. B* 284: 20170744.
- Wüster, W. et al. 2004. Do aposematism and Batesian mimicry require bright colours? A test, using European viper markings. – *Proc. R. Soc. B* 271: 2495–2499.

On the conflict between mate preference and adaptation: a mathematical approach

Sexual preferences play a major role in the process of adaptation and speciation. While preferences for adaptive traits have been extensively studied, but various targets of preference are observed in natural populations, including attractions towards dissimilar or maladaptive traits. During my thesis, I focused on these peculiar forms of sexual preferences. I used mathematical modelling to identify the conditions for the evolution of mate preference targeting locally adaptive *vs.* maladaptive traits. I focused on the evolution of preference targeting warning traits, associated with defence against predators as a case study. Warning colorations reduce predation when they become widespread in a given environment: the local community of predators learns to associate the warning trait with defence and then avoid attacks on prey displaying them. Warning coloration are thus a relevant example of convergent evolution driven by local adaptation. Because these colorations can also be used as a cue during mate choice, they appear as a relevant trait to study the interactions between preference evolution and local selection on the preferred cue in sympatric species. First, I focused on the evolution of disassortative mating in polymorphic populations. I focused on the species *H. numata*, which display polymorphism in warning signals, controlled by a single supergene. Using numerical simulations, I studied how disassortative preferences, leading to preference on locally maladaptive phenotypes can emerge. I showed that the recessive deleterious mutations usually associated with supergenes promotes the evolution of disassortative preference (chapter 1). I also identified the genetic architecture of trait and preference allowing the evolution of disassortative preference. I then used a more general model focusing on polymorphic traits used as mating cues, to identify the conditions on dominance relationships between cues alleles and on their association with deleterious mutations allowing the evolution of disassortative mating (chapter 2). Second, I focused on the effect of reproductive interference between sympatric species on the evolution of preferences. Since local adaptation promotes trait similarity between sympatric species, preference for locally adapted traits may be impaired by reproductive interference. Using quantitative genetics models, I studied the conditions allowing the evolution of preference towards locally non-adapted traits limiting reproductive interference, and its consequences on local adaptation (chapter 3) and sexual dimorphism (chapter 4). Third, I investigated why and when mate preference targets traits involved in local adaptation rather than neutral traits that may diverge between sympatric species (chapter 5). Altogether, this thesis highlights the origin of sexual preferences and shows various conditions where disassortative or maladaptive preference can emerge. I conclude with a critical review highlighting the high prevalence of disassortative mate preference in nature and its peculiar role in the processes of adaptation and speciation.